PO Box 2345, Beijing 100023, China
Fax: +86-10-85381893
E-mail: wjg@wjgnet.com www.wjgnet.com

World J Gastroenterol 2004;10(20):2927-2930
World Journal of Gastroenterology
 ISSN 1007-9327

• ESOPHAGEAL CANCER •

Construction of pETNF-P16 plasmid and its expression properties in EC9706 cell line induced by X-ray irradiation

Cong-Mei Wu, Tian-Hua Huang, Qing-Dong Xie, De-Sheng Wu, Xiao-Hu Xu

Cong-Mei Wu, Tian-Hua Huang, Qing-Dong Xie, Research Center of Reproductive Medicine, Shantou University Medical College, Shantou 515041, Guangdong Province, China
Xiao-Hu Xu, Department of Forensic Medicine, Shantou University Medical College, Shantou 515041, Guangdong Province, China
De-Sheng Wu, Lanzhou Medical College, Lanzhou 730000, Gansu Province, China
Supported by the National Natural Science Foundation of China, No. 30210103904 and the Science and Technology Program of Guangdong Province, No.2003C30304
Correspondence to: Dr. Tian-Hua Huang, Research Center of Reproductive Medicine, Shantou University Medical College, Shantou 515041, Guangdong Province, China. thhuang@stu.edu.cn
Telephone: +86-754-8900442 **Fax:** +86-754-8557562
Received: 2003-11-17 **Accepted:** 2003-12-08

Abstract

AIM: Recombined plasmid pETNF-P16 was constructed to investigate its expression properties in esophageal squamous carcinoma cell line EC9706 induced by X-ray irradiation and the feasibility of gene-radiotherapy for esophageal carcinoma.

METHODS: Recombined plasmid pETNF-P16 was constructed and transfected into EC9706 cells with lipofectamine. ELISA, Western blot, and immunocytochemistry were performed to determine the expression properties of pETNF-P16 in EC9706 after transfection induced by X-ray irradiation.

RESULTS: Eukaryotic expression vector pETNF-P16 was successfully constructed and transfected into EC9706 cells. TNFα expressions were significantly increased in the transfected cells after different doses of X-ray irradiation than in those after 0Gy irradiation (1 192.330-2 026.518 pg/mL, P<0.05-0.01), and the TNFα expressions and P16 were significantly higher 6-48 h after 2 Gy X-ray irradiation (358.963-585.571 pg/mL, P<0.05-0.001). No P16 expression was detected in normal EC9706 cells. However, there was strong expression in the transfected and irradiation groups.

CONCLUSION: X-ray irradiation induction could significantly enhance TNFα and P16 expression in EC9706 cells transfected with pETNF-P16 plasmid. These results may provide important experimental data and therapeutic potential for gene-radiotherapy of esophageal carcinoma.

Wu CM, Huang TH, Xie QD, Wu DS, Xu XH. Construction of pETNF-P16 plasmid and its expression properties in EC9706 cell line induced by X-ray irradiation. *World J Gastroenterol* 2004; 10(20): 2927-2930
http://www.wjgnet.com/1007-9327/10/2927.asp

INTRODUCTION

Esophageal carcinoma is one of the most frequent malignant tumors. Its treatment choices include surgical resection, radiation, chemotherapy and biological therapy. However, their limitations and adverse effects influence the therapeutic results. In 1992, Wechselbaum proposed the theory of gene-radiation combination treatment, that is, to ligate the promoter with irradiation-induced function and treatment gene so as to take advantages of the combined therapeutic functions of both modalities[1].

In this study, pETNF-P16 plasmid was constructed and transfected into human esophageal cancer cell line EC9706. The expressions of TNFα and P16 in the transfected cells exposed to different doses of X-ray irradiation and the time course of the expressions after 2Gy X-ray irradiation were detected to explore the feasibility of gene-radiotherapy for esophageal carcinoma.

MATERIALS AND METHODS

Cell line and vectors

The EC9706 was maintained in Dulbecco's modified Eagle's medium (DMEM), high glucose media (Life Technologies) and generously supplemented with 100 mL/L fetal bovine serum (Hyclone Laboratories), penicillin, streptomycin and nonessential amino acids (Life Technologies). PIRES1 vector was bought from Promega-Biotec (Shanghai, Promega Corporation).

Construction of pETNF-P16 plasmid

The expression vector for TNFα and P16 was constructed as Figure 1.

Transfection

Transfection of EC9706 cells was carried out in a 6-well plate. The transfection procedure began when the cells reached 70% confluence on the surface of plate wells. Solution A was prepared by separate addition of 10 μg of pETNF-P16 or PIRES1 to 100 μL serum-free medium (SFM), and solution B by addition of 10 μL liposome to 100 μL SFM. Solutions A and B were combined at room temperature for 30 min then 0.8 mL SFM was added to the tube containing the above solutions, and then the mixture was added to rinsed cells. The medium was replaced with a fresh and complete medium after 6 h in transfection. The cells were exposed to irradiation after 36 h in transfection.

Protein determination

TNFα protein was detected using ELISA kit (Genzyme). P16 protein was studied using Western blot analysis and immunocytochemistry (P16 antibody, Boster).

Ionizing irradiation

X-rays of 180 kV and 12 mA with 0.25 mmCu and 1.08 mm Al as filter were given at a dose-rate of 0.8639 Gy/min for doses of 2-20Gy.

Statistical analysis

Student's t test was used to determine the difference between groups. P values of less than 0.05 were considered statistically significant.

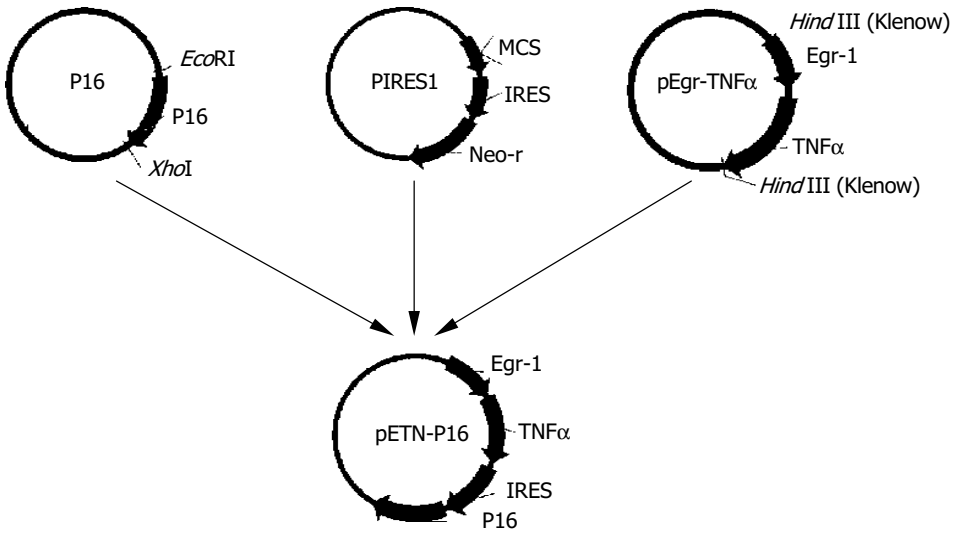

Figure 1 Construction of plasmid pETNF-P16.

RESULTS

TNFα expressions in EC9706 cells transfected with pETNF-P16 after different doses of X-irradiation

EC9706 cells transfected with pETNF-P16 received different doses of X-ray irradiation. The cells of control group were transfected with PIRES1. Eight hours after irradiation, the protein was extracted and TNFα expression was detected by ELISA.

The results showed that TNFα expression in the 2, 4, 10 Gy groups was significantly higher than that in 0 Gy group (P<0.05-0.01) (Figure 2).

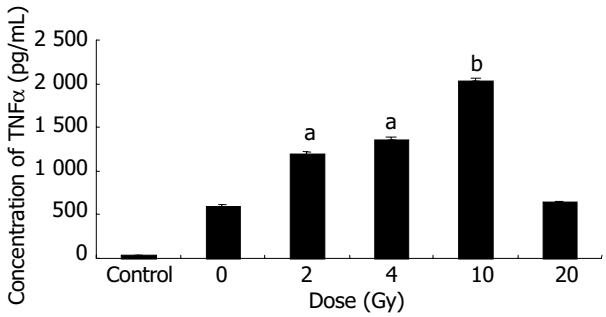

Figure 2 TNFα expression in EC9706 cells after irradiation with different doses of X-ray (mean±SD, n = 3) [a]P<0.05 [b]P<0.01 *vs* 0 Gy group.

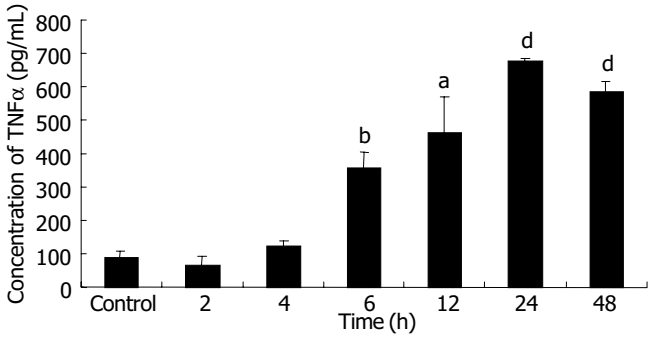

Figure 3 Expression time course of TNFα in EC9706 cells after 2 Gy of X-ray irradiation(mean±SD, n = 3). [a]P<0.05, [b]P<0.01, [d]P<0.001 *vs control* group.

TNFα and P16 expressions in EC9706 cells transfected with pETNF-P16 at different time points after 2 Gy irradiation

EC9706 cells transfected with pETNF-P16 received 2 Gy of X-ray irradiation while the control group did not receive. Proteins of TNFα and P16 were isolated at different time points after irradiation and detected by ELISA and Western blot.

ELISA results showed that TNFα expression increased from 2 to 24th, and reached the peak level at the 24[th] h, about 7.5 times of control group (P<0.01). TNFα expression in 48 h group was significantly higher than that in control group (P<0.001), but lower than that in 24 h group (P>0.05) (Figure 3).

The results of Western blot analysis showed no P16 expression in cells transfected with PIRES1 plasmid. After 2Gy X-ray irradiation, P16 expression in the cells transfected with pETNF-P16 plasmid increased between 2 h and 48 h. The expression in the control group was lower than that in 4 h to 48 h groups (Figure 4).

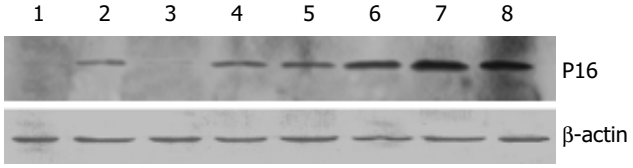

Figure 4 Expression time course of P16 in EC9706 cells after 2 Gy x-ray irradiation Lane 1: transfected with PIRES1 plasmid Lane 2: control group Lane 3: 2 h after irradiation Lane 4: 4 h after irradiation Lane 5: 6 h after irradiation Lane 6: 12 h after irradiation Lane 7: 24 h after irradiation Lane 8: 48 h after irradiation.

Immunocytochemistry

Thirty-six hours after transfected with pETNF-P16 plasmids, EC9706 cells received 2 Gy X-ray irradiation while the control group did not receive. After 24 h, anti-P16 IgG and Biotin-labeled secondary antibody were used to detect the P16 expression in treated cells. P16 protein was positive in the nucleus, cytoplasm and cellular membrane as judged by the brown color.

Immunocytochemical analysis demonstrated that all the normal EC9706 cells had no P16 expression. After transfected with pETNF-P16 plasmid, positive P16 expression in EC9706 cells was detected. Then, the transfected cells received 2 Gy X-ray irradiation and P16 expression remained positive, but morphological changes of EC9706 cells occurred.

DISCUSSION

It was reported that Egr-1 was transcriptionally induced

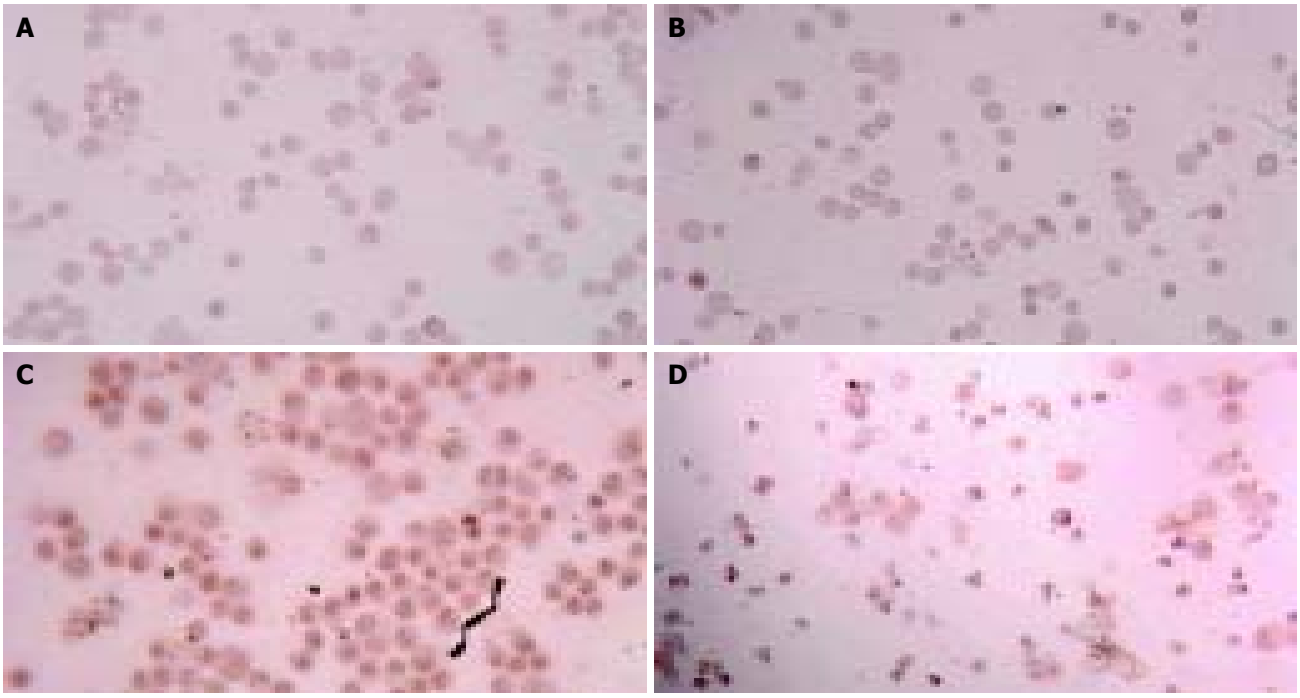

Figure 5 P16 expression in EC9706 cells transfected with pETNF-P16 plasmid after 2Gy X-ray irradiation. A: Negative control group; B: Untransfected group; C: Transfected group; D: Transfected and irradiated group.

following exposure to irradiation[2]. Sequences responsive to ionizing radiation-induced signals were determined by deletion analysis of the Egr-1 promoter. The results demonstrated that induction of Egr-1 by X-rays was conferred by serum response or CC (A/T) rGG elements. Further analysis confirmed that the region encompassing the three distal or upstream CC(A/T)rGG elements was functional in X-ray response[3-5].

Weichselbaum *et al*.[6] were forerunners in tumor gene-radiotherapy. In 1992 they put forward that ionizing radiation could be used to activate the transcription of exogenous genes encoding cytotoxic proteins, and established the techniques that might be used to target gene therapy during the treatment of human neoplasms.

Combination of gene therapy with radiation therapy could overcome some problems and side effects of either radiation or gene therapy alone, including radioresistance of some tumors and toxicities to normal tissues. Weichselbaum *et al*.[7] linked DNA sequences from the promotor region of Egr-1 to a cDNA sequence that encoded human tumor necrosis factor (TNF) alpha. Egr-TNF construction was transfected into a human cell line of hematopoietic origin, HL525 (clone 2). The latter was injected into human xenografts of the radioresistant human squamous cell carcinoma cell line SQ-20B. Animals treated with radiation and clone 2 demonstrated an improvement compared with those treated with radiation or injections of clone 2 alone. Thereafter, a variety of downstream genes were introduced to Egr-1 promoter to treat different tumors and similar results were obtained[8-10].

TNF has complex *in-vivo* anti-tumor actions and involves a series of biochemical reactions, and varies according to host metabolism. It could not only kill tumor cells directly, but also act indirectly by occluding the feeding vessels of tumors, promoting inflammation reaction of the host, stimulating cytotoxic activities of megalocytes and producing tumor-specific cytotoxic antibody. Up to now, TNF has been found to have the strongest direct tumor-killing action. However, severe side effects made the effects of systemic treatment unsatisfactory. By contrast, regional administration into the tumor had better therapeutic effects. It has been widely reported that intra-tumor TNF injection had no severe side effects on patients with malignant tumors[11-12]. We constructed pEgr-TNFα plasmid and injected it into mouse melanoma locally to induce its expression by X-ray irradiation. The results showed that pEgr-TNFα gene in combination with radiotherapy could significantly inhibit tumor and had no side effects[13].

P16 is a tumor suppressor gene product. Serrano *et al*.[14] demonstrated that P16 bound to CDK4 and inhibited the catalytic activity of CDK4/cyclin D enzymes. P16 seemed to act in a regulatory feedback circuit with CDK4, D-type cyclins and retinoblastoma protein. Overexpression of P16 gene could block cell cycle progression through the G_1-to-S phase boundary in a pRB-dependent manner[15,16]. Many P16 mutants identified from human tumors have been shown to have defects in this activity[17-19]. These suggested that the CDK4-inhibitory activity of p16 was involved in regulating cell cycle progression through the G_1/S boundary.

On the basis of anti-tumor function of TNFα and P16, we constructed pETNF-P16 plasmid and transfected EC9706 cells to investigate the expression properties of plasmid induced by X-ray irradiation. The results showed that TNFα expression in pETNF-P16-transfected cells induced by irradiation was higher than that in control group (P<0.05-0.01). Time-course studies between 6 h and 48 h after 2Gy irradiation revealed that TNFα expression in X-ray induced groups was higher than that in the control group (P<0.05-0.001). It gradually increased and peaked at the 24th h with the expression level of 7.5 times of control group (P<0.01). Immunocytochemistry showed no P16 expression in the control group, but strong expressions in the transfected and irradiated group. However, the cellular morphology was altered in the latter group and the mechanism is to be clarified.

Esophageal carcinoma still has high morbidity and mortality in China[20-22], and its treatment is still difficult[23-30]. Our work might have laid some theoretical basis for further study on esophageal cancer gene-radiotherapy, which should have promising therapeutic potential.

ACKNOWLEDGEMENTS

We are very grateful to Professor Ming-Rong Wang, Institute of Cancer, Chinese Academy of Medical Sciences for his kindness in providing us with the EC9706 cell line.

REFERENCES

1 **Weichselbaum RR**, Hallahan DE, Beckett MA, Mauceri HJ, Lee H, Sukhatme VP, Kufe DW. Gene therapy targeted by radiation preferentially radiosensitizes tumor cells. *Cancer Res* 1994; **54**: 4266-4269

2 **Christy B**, Nathans D. DNA binding site of the growth factor-inducible protein Zif268. *Proc Natl Acad Sci U S A* 1989; **86**: 8737-8741

3 **Sukhatme VP**. Early transcriptional events in cell growth: The Egr family. *J Am Soc Nephrol* 1990; **1**: 859-866

4 **Cao XM**, Koski RA, Gashler A, McKiernan M, Morris CF, Gaffney R, Hay RV, Sukhatme VP. Identification and characterization of the Egr-1gene product, a DNA-binding zinc finger protein induced by differentiation and growth signals. *Mol Cell Biol* 1990; **10**: 1931-1939

5 **Tsai-Morris CH**, Cao XM, Sukhatme VP. 5' flanking sequence and genomic structure of Egr-1, a murine mitogen inducible zinc finger encoding gene. *Nucleic Acids Res* 1988; **16**: 8835-8846

6 **Weichselbaum RR**, Kufe DW, Advani SJ, Roizman B. Molecular targeting of gene therapy and radiotherapy. *Acta Oncol* 2001; **40**: 735-738

7 **Datta R**, Taneja N, Sukhatme VP, Qureshi SA, Weichselbaum R, Kufe DW. Reactive oxygen intermediates target CC(A/T)6GG sequences to mediate activation of the early growth response 1 transcription factor gene by ionizing radiation. *Proc Natl Acad Sci U S A* 1993; **90**: 2419-2422

8 **Hanna NN**, Seetharam S, Mauceri HJ, Beckett MA, Jaskowiak NT, Salloum RM, Hari D, Dhanabal M, Ramchandran R, Kalluri R, Sukhatme VP, Kufe DW, Weichselbaum RR. Antitumor interaction of short- course endostatin and ionizing radiation. *Cancer J* 2000; **6**: 287-293

9 **Takahashi T**, Namiki Y, Ohno T. Induction of the suicide HSV-TK gene by activation of the Egr-1 promoter with radioisotopes. *Hum Gene Ther* 1997; **8**: 827-833

10 **Griscelli F**, Li H, Cheong C, Opolon P, Bennaceur Griscelli A, Vassal G, Soria J, Soria C, Lu H, Perricaudet M, Yeh P. Combined effects of radiotherapy and angiostatin gene therapy in glioma tumor model. *Proc Natl Acad Sci U S A* 2000; **97**: 6698-6703

11 **Vilcek J**, Lee TH. Tumor necrosis factor. New insights into the molecular mechanisms of its multiple actions. *J Biol Chem* 1991; **266**: 7313-7316

12 **Rothe J,** Gehr G, Loetscher H, Lesslauer W. Tumor necrosis factor receptors-structure and function. *Immunol Res* 1992; **11**: 81-90

13 **Wu CM,** Li XY, Liu SZ. Construction of pEgr.p-TNFα and its expression in NIH3T3 cells induced by ionizing irradiation. *Chin J Radiol Med Prot* 2001; **21**: 332-334

14 **Serrano M,** Hannon GJ, Beach D. A new regulatory motif in cell-cycle control causing specific inhibition of cyclin D/CDK4. *Nature* 1993; **366**: 704-707

15 **Koh J,** Enders GH, Dynlacht BD, Harlow E. Tumour-derived p16 alleles encoding proteins defective in cell-cycle inhibition. *Nature* 1995; **375**: 506-510

16 **Lukas J,** Parry D, Aagaard L, Mann DJ, Bartkova J, Strauss M, Peters G, Bartek J. Retinoblastoma-protein-dependent cell-cycle inhibition by the tumour suppressor p16. *Nature* 1995; **375**: 503-506

17 **Monzon J,** Liu L, Brill H, Goldstein AM, Tucker MA, From L, McLaughlin J, Hogg D, Lassam NJ. CDKN2A mutations in multiple primary melanomas. *N Engl J Med* 1998; **338**: 879-887

18 **Nobori T,** Miura K, Wu DJ, Lois A, Takabayashi K, Carson DA. Deletions of the cyclin-dependent kinase-4 inhibitor gene in multiple human cancers. *Nature* 1994; **368**: 753-756

19 **Soufir N,** Avril MF, Chompret A, Demenais F, Bombled J, Spatz A, Stoppa-Lyonnet D, Benard J, Bressac-de-Paillerets B. Prevalence of p16 and CDK4 germline mutations in 48 melanoma-prone families in France. The French Familial Melanoma Study Group. *Hum Mol Genet* 1998; **7**: 209-216

20 **Zhao XJ,** Li H, Chen H, Liu YX, Zhang LH, Liu SX, Feng QL. Expression of e-cadherin and beta-catenin in human esophageal squamous cell carcinoma: relationships with prognosis. *World J Gastroenterol* 2003; **9**: 225-232

21 **Heidecke CD**, Weighardt H, Feith M, Fink U, Zimmermann F, Stein HJ, Siewert JR, Holzmann B. Neoadjuvant treatment of esophageal cancer: Immunosuppression following combined radiochemotherapy. *Surgery* 2002; **132**: 495-501

22 **Tsunoo** H, Komura S, Ohishi N, Yajima H, Akiyama S, Kasai Y, Ito K, Nakao A, Yagi K. Effect of transfection with human interferon-beta gene entrapped in cationic multilamellar liposomes in combination with 5-fluorouracil on the growth of human esophageal cancer cells *in vitro*. *Anticancer Res* 2002; **22**: 1537-1543

23 **Nemoto K**, Zhao HJ, Goto T, Ogawa Y, Takai Y, Matsushita H, Takeda K, Takahashi C, Saito H, Yamada S. Radiation therapy for limited-stage small-cell esophageal cancer. *Am J Clin Oncol* 2002; **25**: 404-407

24 **Tachibana M**, Dhar DK, Kinugasa S, Yoshimura H, Fujii T, Shibakita M, Ohno S, Ueda S, Kohno H, Nagasue N. Esophageal cancer patients surviving 6 years after esophagectomy. *Langenbecks Arch Surg* 2002; **387**: 77-83

25 **Wilson KS**, Wilson AG, Dewar GJ. Curative treatment for esophageal cancer: Vancouver Island Cancer Centre experience from 1993 to 1998. *Can J Gastroenterol* 2002; **16**: 361-368

26 **Liu HH**, Yoshida M, Momma K, Oohashi K, Funada N. Detection and treatment of an asymptomatic case of early esophageal cancer using chromoendoscopy and endoscopic mucosal resection. *J Formos Med Assoc* 2002; **101**: 219-222

27 **Wang AH**, Sun CS, Li LS, Huang JY, Chen QS. Relationship of tobacco smoking, CYP1A1, GSTM1 gene polymorphism and esophageal cancer in Xi'an. *World J Gastroenterol* 2002; **8**: 49-53

28 **Muto M,** Ohtsu A, Miyata Y, Shioyama Y, Boku, N, Yoshida S. Self-expandable metallic stents for patients with recurrent esophageal carcinoma after failure of primary chemoradiotherapy. *Jpn J Clin Oncol* 2001; **31**: 270-274

29 **Yeh AM**, Mendenhall WM, Morris CG, Zlotecki RA, Desnoyers RJ, Vogel SB. Factors predictive of survival for esophageal carcinoma treated with preoperative radiotherapy with or without chemotherapy followed by surgery. *J Surg Oncol* 2003; **83**: 14-23

30 **Lew JI**, Gooding WE, Ribeiro U Jr, Safatle-Ribeiro AV, Posner MC. Long-term survival following induction chemoradiotherapy and esophagectomy for esophageal carcinoma. *Arch Surg* 2001; **136**: 737-742

Edited by Wang XL and Xu FM

PO Box 2345, Beijing 100023, China
Fax: +86-10-85381893
E-mail: wjg@wjgnet.com www.wjgnet.com

World J Gastroenterol 2004;10(20):2931-2935
World Journal of Gastroenterology
 ISSN 1007-9327

• ESOPHAGEAL CANCER •

Endoscopic survey of esophageal cancer in a high-risk area of China

Xu-Jing Lu, Zhi-Feng Chen, Cui-Lan Guo, Shao-Sen Li, Wen-Long Bai, Guo-Liang Jin,Yu-Xia Wang, Fan-Shu Meng, Feng Gao, Jun Hou

Xu-Jing Lu, Zhi-Feng Chen, Jun Hou, Hebei Cancer Institute and Fourth Affiliated Hospital of Hebei Medical University, Shijiazhuang 050011, Hebei Province, China
Cui-Lan Guo, Shao-Sen Li, Wen-Long Bai, Guo-Liang Jin, Yu-Xia Wang, Fan-Shu Meng, Feng Gao, Cixian Cancer Institute, Cixian 056500, Hebei Province, China
Supported by the National Tenth Five-Year Scientific Championship Project, No. 2001BA703B10
Correspondence to: Dr. Jun Hou, Hebei Cancer Institute, Jiankanglu 12, Hebei Medical University, Shijiazhuang 050011, Hebei Province, China. luxujing@csco.org.cn
Telephone: +86-311-6033511 **Fax:** +86-311-6077634
Received: 2003-10-09 **Accepted:** 2003-12-16

Abstract

AIM: To characterize the histological types of esophageal and cardiac mucosa by endoscopic survey of a population in a high-risk area of esophageal cancer of China.

METHODS: A selected cohort of residents in Cixian County during December 2001 and May 2002 was surveyed by using Lugol's staining, followed by computer-based statistical analysis of the data with SPSS 10.0 software.

RESULTS: Histologically, the detection rates of squamous epithelial acanthosis, squamous epithelial atrophy, and basal cell hyperplasia in the esophagus were 1.9% (38/2 013), 0.1% (3/2 013) and 0.9% (18/2 013) respectively, and those of mild, moderate, and severe esophagitis were 34.9% (703/2 013), 1.6% (33/2 013) and 0.2% (2/2 013) respectively. Mild, moderate, and severe esophageal dysplasia were detected in 8.6% (172/2 013), 7.8% (157/2 013) and 2.6% (53/2 013) respectively in the selected population, whereas *in situ* carcinoma, intramucosal carcinoma, invasive squamous carcinoma of the esophagus in 2.5% (50/2 013), 0.2% (4/2 013) and 0.7% (14/2 013) respectively. The detection rates of non-atrophic gastritis and atrophic gastritis of the cardia were 36.3% (730/2 013) and 11.5% (232/2 013) respectively, with mild and severe dysplasia of the cardia detected in 2.5% (51/2 013) and 0.8% (17/2 013), respectively, in this population; the rates of intramucosal adenocarcinoma and invasive adenocarcinoma of the cardia were 0.1% (3/2 013) and 0.8% (17/2 013) respectively. The detection rate of esophageal cancer at early stage was 79.4% (54/68). The survey rate (ratio of examined population to expected population) was 73.8% (2 013/2 725).

CONCLUSION: Histologic types of the esophageal and cardiac mucosa were characterized by endoscopic survey in a high-risk population of esophageal cancer, which may help the early detection and treatment of esophageal and cardiac cancers and dysplasia, and reduce the mortality of such malignancies.

Lu XJ, Chen ZF, Guo CL, Li SS, Bai WL, Jin GL, Wang YX, Meng FS, Gao F, Hou J. Endoscopic survey of esophageal cancer in a high-risk area of China. *World J Gastroenterol* 2004; 10(20): 2931-2935
http://www.wjgnet.com/1007-9327/10/2931.asp

INTRODUCTION

Esophageal cancer (EC) is one of the most common malignant tumors with a high incidence in such regions as China, Iran, South Africa, Uruguay, France and Italy[1], of which China has almost half of the total cases with also the highest mortality rate, the fourth leading cause of cancer-related deaths in China. According to the data derived from 1/10 sample death investigation in the whole population of China in 1990-1992, the mortality rate of esophageal cancer was 27.73/100 000 for men and 13.63/100 000 for women, which were 3.1 and 3.6 times, that reported by the World Health Organization (WHO) in 1998 respectively[2]. Some southern regions of the Taihang Mountains on the borders of Henan, Shanxi and Hebei provinces have significantly higher mortality rates of esophageal cancer. Cixian County in Hebei Province is also one of the areas with the highest mortality rate in China, where an endoscopic survey was conducted by Hebei Cancer Institute during the period between December 2001 and May 2002, and in this paper the results are reported.

MATERIALS AND METHODS

Cixian County is located at 36.30º northern latitude, 114.40º eastern longitude, on the east side of the Taihang Mountains along the Zhanghe River. It occupies an area about 1 014 square kilometers with a population of 634 470. This region contains greatly diverse geographic conditions, ranging from mountainous, hilly regions to long-stretched plains, each constituting about one-third of its total area. The climate is mainly under the influence of the warm seasonal wind from the mainland, with an annual average temperature of 18-25 ℃ and a rainfall between 600-700 mm. The dominant brown and light-colored soil yields mainly such farm products as wheat, corn, millet, rice, sweet potato and beans. Iron and coal are the main mineral resources, and the residents use coal mainly for daily cooking and heating[3].

As a key science research project sponsored by the National Tenth Five-Year Plan of China, the survey was conducted among the residents of 9 villages aged between 40 and 69 years in the hilly region of Cixian County, which is known for a higher incidence of esophageal cancer than the plain regions. The total population of the 9 villages was 12 048, and the annual incidence and mortality rate of esophageal cancer in this region during 1996-2000 were 176.0/100 000 and 126.2/100 000 respectively.

Before the survey, a county-wide conference was convened by the local government participated by the local county, countryside and village leaders and cancer prevention professionals. At the conference, special committees were set up at each of the 3 administrative levels to be responsible for the execution of the survey in the areas where they perform daily duties. After the conference, the residents in the target areas were acknowledged of the benefits of such a massive survey through a propaganda campaign. On the basis of the government record of the residents, 2 000 potential target subjects from the 9 villages were selected by the cancer prevention professionals, and two days prior to the survey, personal contacts with the subjects were made by local physicians to arrange for the details of the survey. At the

beginning of the survey, the subjects were asked to fill an epidemiological questionnaire, followed by physical examination performed by the physicians to exclude persons with serious contraindications to endoscopy. Endoscopic examinations were then performed by specialists following the procedures described by Wang *et al*.[4]. The detailed results were recorded and the biopsy specimens obtained were fixed in 80% alcohol and stained by hematoxylin-eosin (HE) for subsequent pathological diagnosis by pathologists.

Finally, the data were input into a computer to set up a survey information database and statistical analysis was performed using SPSS 10.0 software with chi-square test.

RESULTS

Survey rate

Of the totally 12 048 residents of the 9 villages, 2 992 were within the age range between 40 and 69 years, and after exclusion of 267 residents with contraindications (including 32 patients with cancer, 22 with heart diseases, 29 with cerebrovascular diseases, 55 with hypertension, 56 with other diseases, 59 already died, and 14 emigrants), the total number of subjects enrolled in this survey was 2 013 (including 973 male and 1 040 female subjects, with the male to female ratio of 0.94:1), and the survey rate was therefore 73.8% (Table 1).

Endoscopic findings of the esophagus

As shown in Table 2, the histologic detection rates of *in situ* carcinoma, intramucosal carcinoma, and invasive squamous carcinoma were 2.5% (50/2 013), 0.2% (4/2 013), and 0.7% (14/2 013), respectively; early cancerous changes were detected in 2.7% (54/2 013) of the subjects, which occupied 79.4% (54/68) of total esophageal cancer cases. Male subjects had comparable incidence of esophagitis [35.9% (349/973)] with that in female subjects [37.6% (391/1 040), $\chi^2 = 0.645$, $P = 0.422$], but had significantly higher incidence of dysplasia [23.1% (225/973) *vs* 15.1% (157/1 040) in female, $\chi^2 = 21.072$, $P = 0.000$]. The incidence of esophageal cancer did not vary significantly between the male and female subjects [3.3% (32/973) *vs* 3.5% (36/1 040), $\chi^2 = 0.001$, $P = 0.98$].

Table 3 shows that with a 5-year increase in age, the histologic incidence of esophageal cancer and dysplasia all tended to be increased from the relatively low level in the 40-year-old group to the highest in the 65-year-old group (trend $^a\chi^2 = 135.943$, $^aP = 0.000$; trend $^b\chi^2 = 182.782$, $^bP = 0.000$). The rates of esophagitis in different age groups varied significantly ($\chi^2 = 12.475$, $P = 0.029$), as well as the rates of dysplasia ($\chi^2 = 141.184$, $P = 0.000$), and esophageal cancer ($\chi^2 = 74.855$, $P = 0.000$).

Table 2 Detection rates of the histologic changes in the esophagus (%)

Type	Male (%)	Female (%)	Total (%)
Normal squamous epithelium	308 (31.7)	392 (37.7)	700 (34.8)
Squamous epithelial acanthosis	19 (2.0)	19 (1.8)	38 (1.9)
Squamous epithelial atrophy	1 (0.1)	2 (0.2)	3 (0.1)
Esophagitis			
Mild	337 (34.6)	366 (35.2)	703 (34.9)
Moderate	11 (1.1)	22 (2.1)	33 (1.6)
Severe	1 (0.1)	3 (0.3)	4 (0.2)
Dysplasia			
Mild	114 (11.7)	58 (5.6)	172 (8.6)
Moderate	82 (8.4)	75 (7.2)	157 (7.8)
Severe	29 (3.0)	24 (2.3)	53 (2.6)
In situ carcinoma	25 (2.6)	25 (2.4)	50 (2.5)
Intramucosal carcinoma	2 (0.2)	2 (0.2)	4 (0.2)
Invasive carcinoma	5 (0.5)	9 (0.9)	14 (0.7)
Others	31 (3.2)	33 (3.2)	64 (3.2)
Total	973 (100.0)	1040 (100.0)	2013 (100.0)

Endoscopic findings of the gastric cardia

The incidence of cardiac cancer was much lower than that of esophageal cancer ($\chi^2 = 26.767$, $P = 0.000$), and early cardiac cancer only occupied 15% (3/20) of cardiac cancer cases. The rates of gastritis involving the cardia were 44.5% (433/973) in male and 50.8% (529/1 040) in female subjects, showing significant difference between them ($\chi^2 = 8.159$, $P = 0.004$). The rates of dysplasia also varied significantly between them [4.9% (48/973) in male *vs* 1.9% (20/1 040) in female, $\chi^2 = 13.955$, $P = 0.000$], but not that of cardiac cancer, [1.3%(13/973) in male *vs* 0.7% (7/1 040) in female, $\chi^2 = 2.246$, $P = 0.134$], as shown in Table 4.

At a 5-year interval, the incidence of cardiac cancer and dysplasia both increased from the level in the 40-year-old group to the highest in the 65-year-old group (trend $^a\chi^2 = 84.875$, $^aP = 0.000$; trend $^b\chi^2 = 36.209$, $^bP = 0.000$, Table 5). The rates of gastritis involving the cardia and dysplasia of the cardia also varied significantly ($\chi^2 = 11.223$, $P = 0.047$; $\chi^2 = 18.901$, $P = 0.002$), as well as that of cardiac cancer ($\chi^2 = 43.351$, $P = 0.000$).

Table 1 Statistics of the residents of the 9 target villages enrolled in this survey

Village	Total population	Aged between 40-69 (yr %)	Contrain-dication	Expected population	Examined population	Survey rate (%)
Hebei Village	1 184	304 (25.7)	29	275	220	80.0
Taichen Village	1 648	412 (25.0)	39	373	287	76.9
Xichengji Village	1 682	381 (22.7)	53	328	283	86.3
Zhonghao Village	699	183 (26.2)	23	160	130	81.3
Donghao Village	1 860	494 (26.6)	26	468	208	44.4
Chejiao Village	1 618	383 (23.7)	38	345	276	80.0
Bai Village	1 679	415 (24.7)	27	388	284	73.2
Donghelan Village	1 076	271 (25.2)	17	254	208	81.9
Xihelan Village	602	149 (24.8)	15	134	117	87.3
Total	12 048	2 992 (24.8)	305	2 725	2 013	73.8

The percentages in bracket indicate the rates of the population aged 40-69 years.

Table 4 Incidence of pathological changes detected histologically in the cardia (%)

Type	Male (%)	Female (%)	Total (%)
Normal adenoepithelium	301 (31.0)	329 (31.7)	630 (31.4)
Non-atrophic gastritis	323 (33.2)	407 (39.1)	730 (36.3)
Atrophic gastritis	110 (11.3)	122 (11.7)	232 (11.5)
Dysplasia			
Mild	36 (3.7)	15 (1.4)	51 (2.5)
Severe	12 (1.2)	5 (0.5)	17 (0.8)
Intramucosal adenocarcinoma	1 (0.1)	2 (0.2)	3 (0.1)
Invasive adenocarcinoma	12 (1.2)	5 (0.5)	17 (0.8)
Others	178 (18.3)	155 (14.9)	333 (16.5)
Total	973 (100.0)	1 040 (100.0)	2 013 (100.0)

DISCUSSION

The prognosis of esophageal and cardiac cancer is the poorest among the patients with digestive carcinomas as more than 90% of them are not clinically identified until at an advanced stage, when surgery is defied due to either local tumor invading the surrounding tissues or distant metastasis, and therefore the 5-year survival rate of esophageal cancer is below 10%[5-7]. Early-stage asymptomatic esophageal cancer is basically curable with, for instance, conventional surgery and endoscopic resection, resulting in a 5-year survival rate of the patients reaching 90% or above[8-10].

For esophageal cancer prevention and treatment, a series of systematic researches including clinical, laboratory and field investigation were carried out in high-risk areas such as Linxian and Cixian counties since 1959[11-16], but at present the etiological factors have not yet been identified, and the incidence and mortality rates of esophageal cancer still remain high in those areas. A variety of detecting methods have been attempted by Chinese scientists to identify early esophageal cancer and precancerous lesions, such as exfoliative balloon cytology (EBC), occult blood bead (OBB), conventional endoscopy with

Table 3 Age-related distribution of the incidence of pathological changes in esophagus

Type	Age [yr (%)]					
	40-	45-	50-	55-	60-	65-69
Normal squamous epithelium	355 (44.8)	176 (38.4)	92 (28.6)	56 (24.9)	14 (9.4)	7 (10.4)
Squamous epithelial acanthosis	11 (1.4)	4 (0.9)	10 (3.1)	7 (3.1)	5 (3.4)	1 (1.5)
Squamous epithelial atrophy	1 (0.1)	1 (0.2)	1 (0.3)	-	-	-
Basal cell hyperplasia	6 (0.8)	6 (1.3)	3 (0.9)	1 (0.4)	2 (1.3)	-
Esophagitis						
Mild	304 (38.4)	167 (36.5)	90 (28.0)	71 (31.6)	53 (35.6)	18 (26.9)
Moderate	17 (2.1)	2 (0.4)	9 (2.8)	4 (1.8)	1 (0.7)	-
Severe	-	1 (0.2)	2 (0.6)	1 (0.4)	-	-
Dysplasia						
Mild	37 (4.7)	36 (7.9)	41 (12.7)	26 (11.6)	21 (14.1)	11 (16.4)
Moderate	19 (2.4)	30 (6.6)	43 (13.4)	26 (11.6)	26 (17.4)	13 (19.4)
Severe	12 (1.5)	12 (2.6)	12 (3.7)	6 (2.7)	9 (6.0)	2 (3.0)
In situ carcinoma	3 (0.4)	8 (1.7)	10 (3.1)	14 (6.2)	8 (5.4)	7 (10.4)
Intramucosal carcinoma	-	2 (0.4)	-	-	2 (1.3)	-
Invasive carcinoma	-	2 (0.4)	3 (0.9)	4 (1.8)	3 (2.0)	2 (3.0)
Others	27 (3.4)	11 (2.4)	6 (1.8)	9 (4.0)	5 (3.4)	6 (9.0)
Total	792 (100.0)	458 (100.0)	322 (100.0)	225 (100.0)	149 (100.0)	67 (100.0)

Table 5 Age-related distribution of detection rates of pathological changes in gastric cardia

Type	Age [yr (%)]					
	40-	45-	50-	55-	60-	65-
Normal adenoepithelium	295 (37.2)	156 (34.1)	81 (25.2)	61 (27.1)	27 (18.1)	10 (14.9)
Non-atrophic gastritis	319 (40.3)	169 (36.9)	116 (36.0)	60 (26.7)	47 (31.5)	19 (28.4)
Atrophic gastritis	90 (11.4)	45 (9.8)	38 (11.8)	34 (15.1)	14 (9.4)	11 (16.4)
Dysplasia						
Mild	13 (1.6)	8 (1.7)	10 (3.1)	8 (3.6)	8 (5.4)	4 (6.0)
Severe	-	8 (1.7)	2 (0.6)	3 (1.3)	4 (2.7)	-
Intramucosal adenocarcinoma	-	-	1 (0.3)	-	1 (0.7)	1 (1.5)
Invasive adenocarcinoma	-	1(0.2)	1 (0.3)	3 (1.3)	5 (3.4)	7 (10.4)
Others	75 (9.5)	71 (15.5)	73 (22.6)	56 (24.9)	43 (28.9)	15 (22.4)
Total	792 (100.0)	458 (100.0)	322 (100.0)	225 (100.0)	149 (100.0)	67 (100.0)

smear or biopsy, sparse hydrochloric acid preliminary screening, serum total salic acid detection (TSA), otolaryngologic examination and so forth, but all these methods are marred by certain disadvantages besides their respective advantages in the early detection of esophageal cancer and precancerous lesions[17-19].

A massive screening in the population of 126 187 in Cixian was carried out by Hebei Cancer Institute and 16 748 high risk participants aged 40 years and older were screened with exfoliative balloon cytology, the survey rate was 71.4%, resulting in the identification of 179 cases of esophageal cancer, 172 esophageal precancerous lesions, 866 stage II severe esophageal epithelial dysplasia (SEED II), 3 179 stage I severe esophageal epithelial dysplasia (SEED I) and 5 346 mild esophageal epithelium dysplasia (MEED), with the detection rates of MEED, SEED I, SEED II, esophageal precancerous lesions and esophageal cancer being 31.92%, 18.98%, 5.17%, 1.03% and 1.07%, respectively[20]. Most of the researches indicate that exfoliative balloon cytology is an effective, economic and practicable method, having higher detection rate for esophageal cancer than conventional endoscopy, but only cytological diagnosis is obtained and a further endoscopic biopsy and histopathologic confirmation are necessary. This method is now insufficient for esophageal cancer screening because of the severe discomfort and low acceptance by the target subjects.

Esophageal chromoendoscopy with multi-point biopsy and histopathologic examination has developed rapidly since 1974, which greatly increased the detection rate of esophageal cancer and precancerous lesions, and at the same time it is capable of characterizing and defining the scope of the lesions to provide guidance for treatment and follow-up, also suitable for the secondary prevention of esophageal cancer[4,21-33]. Currently the secondary prevention with early detection, early diagnosis and early treatment through chromoendoscopy survey has become the major research concern in the prevention and control of esophageal cancer.

The occurrence and development of esophageal cancer is a slow process involving multiple factors and genes and undergoing multiple stages. Prior to cancerization of the squamous esophageal epithelium, the basal cell hyperplasia or simple hyperplasia takes place and evolves into mild, moderate, severe dysplasia cells that develop, in sequence, into *in situ* carcinoma, early invasive cancer and advanced cancer[34-36]. As a part of the entire research project, a massive esophageal chromoendoscopic survey was initially conducted in the high-risk area without preliminary screening, and the high survey rate reaching 73.8% indicates that the population's compliance to the survey was high after adequate health education. The distribution of histologic types of the esophageal and cardiac mucosa in high-risk area can be accurately obtained by esophageal chromoendoscopic survey, which possesses the advantage of accurate pathologic diagnosis and differentiation of the histologic types, well defined scope of the lesions and their invasive depth.

This study will, after defining the incidences of the pathological changes of the esophageal and cardiac mucosa in the population, contribute to the early treatment of esophageal and cardiac cancer and dysplasia, increase their cure rates, and reduce the mortality of such malignancies.

REFERENCES

1 **Lu S**, Lin P, Wang G, Luo X, Wu M. Comprehensive prevention and treatment for esophageal cancer. *Chin Med J* 1999; **112**: 918-923

2 **Qiao YL**, Hou J, Yang L, He YT, Liu YY, Li LD, Li SS, Lian SY, Dong ZW. The trends and preventive strategies of esophageal cancer in high-risk areas of Taihang Mountains, China. *ZhongguoYixue Kexueyuan Xuebao* 2001; **23**: 10-14

3 **Hou J**, Lin PZ, Chen ZF, Ding ZW, Li SS, Men FS, Guo LP, He YT, Qiao CY, Duan JP, Wen DG. Field population-based blocking treatment of esophageal epithelia dysplasia. *World J Gastroenterol* 2002; **8**: 418-422

4 **Wang GQ**, Zhou MH, Cong QW, Cui HH. Lugol's solution in endoscopic diagnosis of early esophageal cancer. *Zhonghua Yixue Zazhi* 1995; **75**: 417-418

5 **Wang GQ**, Wei WQ, Hao CQ, Zhang XH, Lai SQ, Yu GX, Ju FH, Ma YH, Qiao YL, Dong ZW, Wang GQ. Minimal invasive treatment of early esophageal cancer and its precancerous lesion: endoscopic mucosal resection using transparent cap-fitted endoscope. *Zhonghua Yixue Zazhi* 2003; **83**: 306-308

6 **Liu HF**, Liu WW, Fang DC. Study of the relationship between apoptosis and proliferation in gastric carcinoma and its precancerous lesion. *Shijie Huaren Xiaohua Zazhi* 1999; **7**: 649-651

7 **Chen KN**, Xu GW. Diagnosis and treatment of esophageal cancer. *Shijie Huaren Xiaohua Zazhi* 2000; **8**: 196-202

8 **Wang GQ**, Wei WQ, Lu N, Hao CQ, Lin DM, Zhang HT, Sun YT, Qiao YL, Wang GQ, Dong ZW. Significance of screening by iodine staining of endoscopic examination in the area of high incidence of esophageal carcinoma. *Aizheng* 2003; **22**: 175-177

9 **Urba SG**, Orringer MB, Perez-Tamayo C, Bromberg J, Forastiere A. Concurrent preoperative chemotherapy and radiation therapy in localized esophageal adenocarcinoma. *Cancer* 1992; **69**: 285-291

10 **Wolfe WG**, Vaughn AL, Seigler HF, Hathorn JW, Leopold KA, Duhaylongsod FG. Survival of patients with carcinoma of the esophagus treated with combined-modality therapy. *J Thorac Cardiovasc Surg* 1993; **105**: 749-755

11 **Hu SP**, Yang HS, Shen ZY. Study on etiology of esophageal carcinoma: retrospect and prospect. *Zhongguo Aizheng Zazhi* 2001; **11**: 171-174

12 **Hou J**, Qiao CY, Meng FS, Zhang GS, He YT, Chen ZF, Liu JB, Song GH, Li SS, Hao SM, Ji HX. A case-control study on risk factor of esophageal cancer in cixian county of Hebei Province. *Zhongguo Zhongliu* 1999; **8**: 252-255

13 **Ding Z**, Gao F, Lin P. Long- term effect of treating patients with precancerous lesions of the esophagus. *Zhonghua Zhongliu Zazhi* 1999; **21**: 275-277

14 **Dawsey SM**, Fleischer DE, Wang GQ, Zhou B, Kidwell JA, Lu N, Lewin KJ, Roth MJ, Tio TL, Taylor PR. Mucosal iodine staining improves endoscopic visualization of squamous dysplasia and squamous cell carcinoma of the esophagus in Linxian, China. *Cancer* 1998; **83**: 220-231

15 **Hou J**, Yan FR. Treatment of esophageal precancerous lesion with cang dlou pill. *Zhongguo Zhongxiyi Jiehe Zazhi* 1992; **12**: 604-606

16 **Qiu SL**, Yang GR. Precursor lesions of esophageal cancer in high-risk populations in Henan Province, China. *Cancer* 1988; **62**: 551-557

17 **Lin PZ**, Chen ZF, Hou J, Liu TG, Wang JX, Ding ZW, Guo LP, Li SS, Men FS, Du CL. Chemical prevention of esophageal cancer. *Zhongguo Yixue Kexueyuan Xuebao* 1998; **20**: 413-417

18 **Cai L**, Yu SZ. A molecular epidemiologic study on gastric cancer in Changle, Fujian Province. *Shijie Huaren Xiaohua Zazhi* 1999; **7**: 652-655

19 **Hou J**, Chen ZF, He YT. Screening of esophageal cancer. *Hebei Zhigong Yixueyuan Xuebao* 2001; **18**: 32-34

20 **Hou J**, Lin PZ, Chen ZF, Wang GQ, Liu TG, Li SS, Meng FS, Du CL. A study survey of esophageal cancer in chixian of Hebei. *Zhongliu Fangzhi Yanjiu* 1998; **25**: 73-75

21 **Roth MJ**, Liu SF, Dawsey SM, Zhou B, Copeland C, Wang GQ, Solomon D, Baker SG, Giffen CA, Taylor PR. Cytologic detection of esophageal squamous cell carcinoma and precursor lesions using balloon and sponge samplers in asymptomatic adults in Linxian, China. *Cancer* 1997; **80**: 2047-2059

22 **Qin DX**, Wang GQ, Wang ZY. Double blind randomized trial on occult blood bead (OBB) and gastroscopy-pathology screening for gastro-oesophageal cancer. *Eur J Cancer Prev* 1997; **6**: 158-161

23 **Wang GQ**. 30-year experiences on early detection and treatment of esophageal cancer in high risk areas. *Zhongguo Yixue Kexueyuan Xuebao* 2001; **23**: 69-72

24 **Mitsunaga N**, Tsubouchi H. Detection of early esophageal and gastric cancers by mass screening. *Nippon Rinsho* 1996; **54**:

1415-1420

25 **Meyer V**, Burtin P, Bour B, Blanchi A, Cales P, Oberti F, Person B, Croue A, Dohn S, Benoit R, Fabiani B, Boyer J. Endoscopic detection of early esophageal cancer in a high-risk population: does Lugol staining improve videoendoscopy? *Gastrointest Endosc* 1997; **45**: 480-484

26 **Hou J**, Chen ZF, Li SS, Li ZY, Yan FR. Clinical study on treatment of esophageal precancerous lesion with Cangdouwan PILL. *Zhongguo Zhongliu Linchuang* 1996; **23**: 117-119

27 **Shimizu Y**, Tukagoshi H, Fujita M, Hosokawa M, Kato M, Asaka M. Endoscopic screening for early esophageal cancer by iodine staining in patients with other current or primary cancers. *Gastrointest Endosc* 2001; **53**: 1-5

28 **Freitag CP**, Barros SG, Kruel CD, Putten AC, Dietz J, Gruber J, Diehl AS, Meurer L, Breyer HP, Wolff F, Vidal R, Arruda CA, Luz LP, Fagundes RB, Prolla JC. Esophageal dysplasias are detected by endoscopy with Lugol in patients at risk for squamous cell carcinoma in southern Brazil. *Dis Esophagus* 1999; **12**: 191-195

29 **Misao Y**, Kumiko M, Tomoko H, Yosuke I, Nobuhiro S. Endoscopic evaluation of depth of cancer invasion in cases with superficial esophageal cancer. *Stomach And Intestine* 2001; **36**: 295-306

30 **Hiroyasu M**, Hideo S, Osamu C, Yoshifumi K. Long term prognosis of m_3,sm_1 cancer of the esophagus-comparison between EMR and radical surgery cases. *Stomach And Intestine* 2002; **37**: 53-63

31 **Junji Y**. Comparison of histological picture and ultrasonographic picture of the alimentary tract wall. *Stomach And Intestine* 2001; **36**: 276-282

32 **Tsuneo O**. Lymph nodal metastasis of m_3,sm_1 esophageal cancer. *Stomach And Intestine* 2002; **37**: 71-74

33 **Dawsey SM**, Shen Q, Nieberg RK, Liu SF, English SA, Cao J, Zhou B, Wang GQ, Lewin KJ, Liu FS, Roth MJ, Taylor PR. Studies of esophageal balloon cytology in Linxian, China. *Cancer Epidemiol Biomarkers Prev* 1997; **6**: 121-130

34 **Wang GQ**. Clinical preventive strategies to decrease incidence and death rates of esophageal cancer in high-risk areas. *Zhonghua Zhongliu Zazhi* 1999; **21**: 223

35 **Wang LD**, Zhou Q, Feng CW, Liu B, Qi YJ, Zhang YR, Gao SS, Fan ZM, Zhou Y, Yang CS, Wei JP, Zheng S. Intervention and follow-up on human esophageal precancerous lesions in Henan, northern China, a high-incidence area for esophageal cancer. *Gan To Kagaku Ryoho* 2002; **29**(Suppl 1): 159-172

36 **Wang GQ**. The trends and strategies of esophageal cancer and precancerous lesions. *Zhonghua Zhongliu Zazhi* 2002; **24**: 206

Edited by Chen WW **Proofread by** Zhu LH and Xu FM

PO Box 2345, Beijing 100023, China
Fax: +86-10-85381893
E-mail: wjg@wjgnet.com www.wjgnet.com

World J Gastroenterol 2004;10(20):2936-2939
World Journal of Gastroenterology
 ISSN 1007-9327

• GASTRIC CANCER •

Alteration of cyclin D1 in gastric carcinoma and its clinicopathologic significance

Peng Gao, Geng-Yin Zhou, Yuan Liu, Jin-Song Li, Jun-Hui Zhen, Yin-Ping Yuan

Peng Gao, Geng-Yin Zhou, Jin-Song Li, Jun-Hui Zhen, Yin-Ping Yuan, Department of Pathology, School of Medicine, Shandong University, Jinan 250012, Shandong Province, China
Yuan Liu, Qilu Hospital, Shandong University, Jinan 250012, Shandong Province, China
Supported by the National Natural Science Foundation of China, No. 30300124
Correspondence to: Peng Gao, Department of Pathology, School of Medicine, Shandong University, Jinan 250012, Shandong Province, China. gaopeng@sdu.edu.cn
Telephone: +86-531-8382045 **Fax:** +86-531-8382045
Received: 2003-11-17 **Accepted:** 2004-03-18

Abstract

AIM: To detect the genetic alteration and abnormal expression of cyclin D1 in gastric carcinoma and investigate its clinicopathologic significance in advanced gastric carcinoma.

METHODS: Proteins of cyclin D1 were detected by immunohistochemistry in 42 cases of advanced gastric carcinoma with their follow-up data available, 27 cases of early stage carcinoma, 21 cases of gastric adenoma, 22 cases of hyperplastic polyp and 20 cases of normal mucosa adjacent to adenocarcinomas. Genetic alteration of cyclin D1 was detected by Southern blot and expression of cyclin D1 mRNA was detected by PT-PCR in 42 cases of advanced gastric carcinoma.

RESULTS: Cyclin D1 protein was not expressed in normal mucosa, hyperplastic polyp and gastric adenoma, while it was only positively expressed in gastric carcinoma. The expression rate of cyclin D1 protein in early stage gastric carcinoma, advanced gastric carcinoma and lymph node metastasis was 48.1%, 47.4% and 50.0%, respectively. The amplification of cyclin D1 gene was detected in 16.6% of advanced gastric carcinomas. The overexpression of cyclin D1 mRNA was detected in 40.5% of the samples. There was no significant correlation between cyclin D1 protein expression and age, lymph-node metastasis and histological grading in patients with advanced gastric carcinoma (χ^2 = 0.038,0.059,0.241, P>0.05). Significant correlation was observed between the expression of cyclin D1 protein and the 5-year survival rate (χ^2 = 3.92, P<0.05).

CONCLUSION: Detection of cyclin D1 protein by immunohistochemistry may be useful in the diagnosis of early gastric carcinomas. Patients with positive expression of cyclin D1 protein tend to have a worse prognosis.

Gao P, Zhou GY, Liu Y, Li JS, Zhen JH, Yuan YP. Alteration of cyclin D1 in gastric carcinoma and its clinicopathologic significance. *World J Gastroenterol* 2004; 10(20): 2936-2939
http://www.wjgnet.com/1007-9327/10/2936.asp

INTRODUCTION

Hyperplasia is an essential characteristic of malignant tumors. Close attention has been paid to the role of cell-cycle regulators associated with cell proliferation in oncogenesis. Under the stimulation of proliferation signals, cells could produce early stage transcription factors such as c-*fos*, c-*jun*. These factors could bind to DNA specifically in nuclei and initiate cell cycles[1]. During the cell cycle, the progression from G1 phase to S phase (DNA synthesis phase) is essential for initiation of the cell cycle[2]. Cyclin D1, a protooncogene identified in recent years, plays a positive-regulation role in the progression[3]. The expression of cyclin D1 is an early event that is stimulated by growth factors or other mitogens .The major targets of cyclin D1-Cdk complexes are the retinoblastoma family of protein Rb[4]. Phosphorylation of Rb in mid-G_1 leads to the release of active forms of the E2F family of transcription factors. Free E2F mediates transcription of E2f-dependent genes, including DNA polymerase, thymidine kinase[5]. The role of cyclin D1 in the oncogenesis of gastric carcinoma is worth investigating[6]. So far, there are few reports about the alteration of cyclin D1 in gastric carcinoma in China. In order to understand the alteration of cyclin D1 in gastric carcinoma, the protein expression of cyclin D1 in normal mucosa, hyperplastic polyp, adenoma, early stage carcinoma and advanced carcinoma of stomach was detected by immunohistochemistry. Genetic amplification and mRNA expression of cyclin D1 in advanced gastric carcinoma were detected by Southern blot and PT-PCR. The expression of cyclin D1 was also investigated in combination with other prognostic markers in advanced gastric cancer, such as patient's age, LN metastasis, histological grade and 5-year survival rate.

MATERIALS AND METHODS

Tissue specimens

Tissues from 132 cases were collected in Qilu Hospital of Shandong University. They concluded 42 cases of advanced gastric carcinoma with their follow-up data available (among them 16 cases had lymph node metastasis), 27 cases of early stage carcinoma (among them 7 cases had carcinomas *in situ*, the other 20 cases had early infiltrating carcinomas), 21 cases of gastric adenoma, 22 cases of hyperplastic polyp, 20 cases of normal mucosa adjacent to adenocarcinomas. All samples were fixed in 40 g/L formaldehyde and embedded in paraffin for histological diagnosis and immunohistochemistry study. Fresh tissues from advanced gastric carcinoma were obtained and stored in liguid nitrogen for DNA and RNA analyses.

Immunohistochemical staining

Immunohistochemistry was performed by the labeled streptavidin biotin (LSAB) method by using vectastain Elite kit (vector, Burlingame,CA). Monoclonal antibody to cylinD1 was used at 1:100 dilution .The technique was performed as described[6] except for an antigen retrieval step. Sections were placed in plastic coplin jars containing 10 mmol/L citrate buffer and heated in microwave oven for 10 min at 675 W for antigen retrieval. A positive section produced in preparative experiments was used as positive control.

Detection of cylin D1 mRNA by reverse transcription polymerase chain reaction (RT-PCR)

Total RNA from cells was extracted by using acid guanidium-phenol-choroform as described[7] and converted to single-strand cDNA by using random 9 mers .PCR was performed by using a thermal cycler as described[8]. The sequence of primer for cylinD1 was : 5'-CTGGAGCCCGTGAAAAAGAGC-3', 5'-CTGGAGAGGAAGCGTGTGAGG-3'. A 10 μL of each mixture was analysed by electrophoresis on 20 g/L agarose gel .Each band was quantitated by gel figure analysis system (Alpha, No.IS-1220). β-actin was used as control. The sequence of primer for β-actin was: 5'-CTACAATGAGCTGCGTGTGGC-3', 5'-CAGGTCCAGACGCAGGATGGC-3'. Cyclin D1 index = cyclin D1 data /β-actin data.

Detection of genetic alteration of cyclin D1 by Southern blot

Nucleic acids were prepared by the guanidinium thyocyanate method as described[9]. Sample DNA (5 μg) was digested with restriction endonuclease *Eco*R I and fractionated by electrophoresis on 20 g/L agarose gel. The gel was denatured and DNA was transferred to nitrocellulose filters. The probe used for detection of cyclin D1 was 18-mer of oligodexoynucleotide complementary to the initial stretch of bases in cyclin D1 mRNA from -1 to +17. The probe was labeled by 32p-dcTP.The filters were prehybridized and hybridized in conditions as described[10], dried and exposed at -70 ℃ with intensifying screen for various periods of time to XAR5 Kodak films. β-actin was used as control for DNA loading amount, and normal tissue near carcinoma was used as normal control.

Statistical analysis

χ^2 test was used to evaluate the differences between two groups.

RESULTS

Expression of cyclin D1 protein in gastric carcinomas and its correlation with other prognostic fators

The cyclin D1 immunohistochemical signal was located exclusively in nuclei (Figure 1A) and variable in terms of staining intensity and the proportion of positive nuclei among the cells of an individual case. One thousand tumor cells in 10 visual fields chosen randomly were counted for each case. The case was defined as positive if the proportion of stained cells was more than 10% of the tumor cells. In 20 cases of normal mucosa, 22 cases of hyperplastic polyp and 21 cases of gastric adenoma (Figure 1A), only weak to undetectable staining was seen and no one was defined as positive. On the other hand, 13/27 (48.1%) cases of early stage gastric carcinoma (Figure 1B), 20/42 (47.6%) cases of advanced gastric carcinoma (Figure 1C), 8/16 (50.0%) cases of lymph node metastasis were defined as positive. There was no significant difference among the positive rates of them (Table 1, $P>0.05$). In the 20 cases of carcinoma with early stage infiltration, there was a good consistency of cyclin D1 expression between the *in situ* components and infiltration components. Seventeen cases showed the same immunostaining pattern in two components (85.0%). In the 16 cases of carcinoma with lymph node metastasis, 12 cases showed the same cyclin D1 immnostaining pattern in metastasis as in its primary lesion (75.0%).

Positive expression of cyclin D1 was observed in 9/24 (37.5%) patients who survived 5 years after operation. While in patients who died within 5 years, 11/18 (61.5%) cases had positive expression. There was a significant difference between the two groups (Table 1, $\chi^2 = 3.92$, $P<0.05$). No significant correlation was observed between cyclin D1 protein expression and age, lymph-node metastasis, histological grading in patients with advanced gastric carcinoma (Table 2, $\chi^2 = 0.038$, 0.059, 0.241, $P>0.05$).

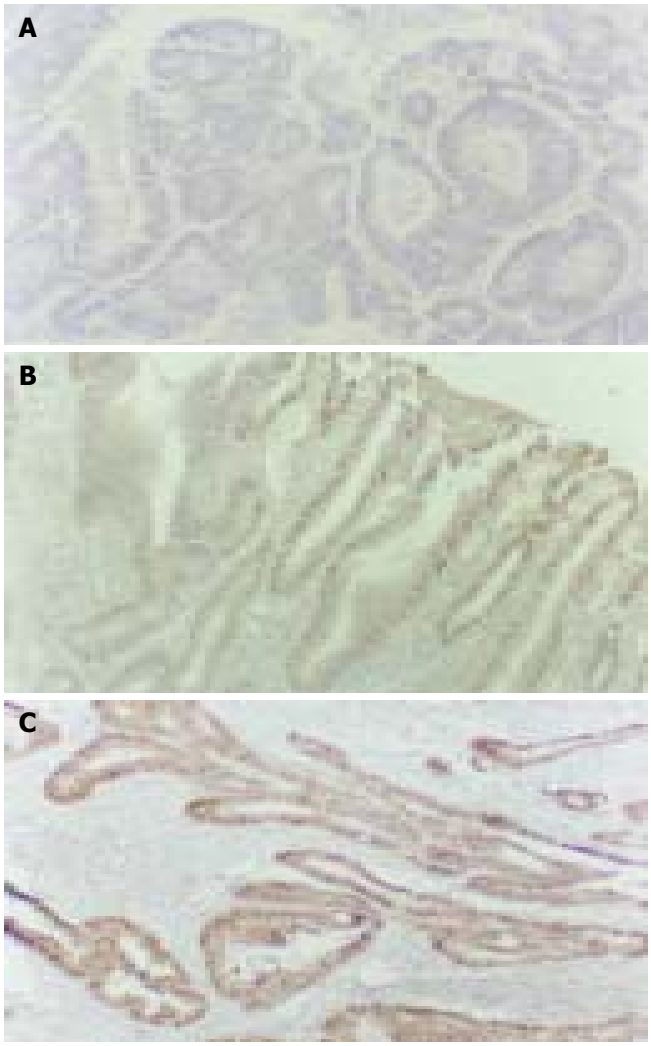

Figure 1 Expression of cyclin D1 protein. LSAB ×200. A: Gastric adenoma; B: Early stage gastric carcinoma; C: Advanced gastric carcinoma.

Table 1 Cyclin D1 expression in early stage gastric carcinoma (EC), advanced gastric carcinoma (AC) and lymph node metastasis (LNM) and five-year survival

Cyclin D1	EC	AC	LNM	5-year survival rate	
				Alive	Dead
Positive	13	20	8	9	11
Negative	14	22	8	15	7
Total	27	42	16	24	18

Table 2 Relationship between cyclin D1 expression with age, lymph node metastasis (LDM) and histological grades (HG) in patients with advanced gastric carcinoma

Cyclin D1	Age (yr)		LDM		HD		
	>60	<60	Positive	Negative	I	II	III
Positive	14	6	8	12	5	11	5
Negative	16	6	8	14	4	12	4

Abnormal expression of cyclin D1 mRNA and genetic alteration of cyclin D1 gene in advanced gastric carcinoma

The amplification products of cyclin D1 and β-actin by RT-PCR were 434 bp and 206 bp respectively. Overexpression of cyclin

D1 mRNA (Figure 2) was observed in 17/42 cases (40.5%) and all these cases showed positive expression of cyclin D1 protein.

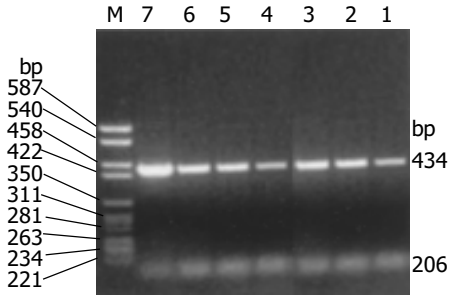

Figure 2 Overexpression of cyclin D1 mRNA detected by RT-PCR. M: marker: 1: Normal control; 3, 6, 7: Overexpression of cyclin D1 mRNA.

The level of amplification was estimated by densitometric tracing of the 4.0 kb cyclin D1 fragments of carcinomas and normal tissue. In this study, 7/42 (16.6%) cases had cyclin D1 gene amplification (2 to 4 fold), which also showed positive expression of cyclin D1 protein and overexpression of cyclin D1 mRNA. No gene rearrangement of cyclin D1 was observed in our study (Figure 3).

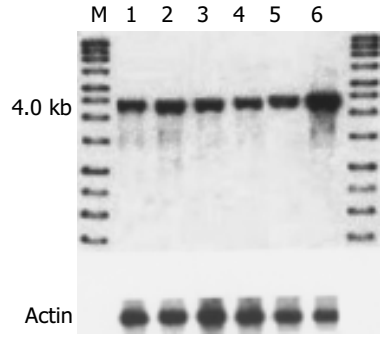

Figure 3 Genetic alteration of cyclin D1 in advanced gastric carcinoma detected by Southern blot. M: DNA marker; 1: Normal control; 6: Cyclin D1 gene amplification.

DISCUSSION

Cyclin D1 gene is located in the 11q13 region. Cyclin D1 protein consists of 295 amino acids, its function in normal cells is to regulate the progression through G1 phrase of the cell cycle in combination with CDKs by phosphorylation of pRb. In normal human tissues, the expression of cyclin D1 protein was rather low and negative by immunohistochemistry[11]. In our study, no one was positive in normal mucosa adjacent to adenocarcinomas. Negative staining was also observed in hyperplastic polyp and gastric adenoma. However, in 33/69 (47.8%) cases of gastric carcinoma, including 42 cases of advanced gastric carcinoma and 27 cases of early stage carcinoma, the expression of cyclin D1 was positive. The detection of cyclin D1 protein by immunohistochemistry is helpful in the diagnosis of early stage gastric carcinoma and could distinguish these cases from hyperplastic polyp. The expression of cell cycle regulators could be used as prognostic markers in some malignant tumors. Some studies showed that the positive expression of cyclin D1 was statistically associated with well-differentiated tumors[12]. In our study, the expression of cyclin D1 protein had no correlation with age, lymph node metastasis and histological grading of the patients. But a significant correlation was observed between cyclin D1 expression and 5-year survival rate. The patients with positive expression of cyclin D1 tended to have a worse prognosis.

Bartkora revealed a very good correlation in the expression of cyclin D1 between the *in situ* components and the invasive components of carcinoma[13]. Our results were in accordance with it. In our study, the positive rates of cyclin D1 protein in early stage carcinoma, advanced gastric carcinoma and lymph node metastases were similar, with no significant difference among them. A very high degree of consistence was found in the same section of early stage carcinoma between carcinoma *in situ* and its infiltration component (89.5%).The consistence between primary tumors and lymph node metastases in the same patient with advanced gastric carcinoma was also high (75.0%). These results suggested that positive expression of cyclin D1 protein might be an early event in gastric carcinoma pathogenesis, and it tended to maintain stable throughout the progression of infiltration and metastasis.

Genetic alteration of cyclin D1 was observed in several kinds of human tumors such as breast carcinoma[14], squamous cell carcinoma of the lung[15], endometrial carcinoma[16] and malignant gliomas[17]. Yang *et al*.[18] reported that a characteristic translocation, t (11:14) (q13; q32) involving rearrangement of cyclin D1 gene, was detected in centrocytic lymphoma and could be used in its diagnosis. In this study, cyclin D1 gene amplification accompanying positive expression of cyclin D1 protein and overexpression of cyclin D1 mRNA in advanced gastric carcinoma was observed in 7/42 (16.6%) cases. The expression rate of cyclin D1 protein (47.4%) was significantly higher than that of cyclin D1 gene amplification (16.6%). It was similar to the overexpressiom rate of cyclin D1 mRNA (42.1%). We considered that the expression of cyclin D1 protein was affected more directly by mRNA level rather than gene level. Besides gene amplification, other factors including alteration in cyclin D1 promoter or abnormal regulation by transcription factors could both up- regulate the expression of mRNA and induce more cyclin D1 protein production. The discrepancy between the expression rates of cyclin D1 mRNA and protein might be caused by stroma cells in tumor tissues, which make the overexpression rate of cyclin D1 mRNA lower.

REFERENCES

1 **Shaulian E**, Karin M. AP-1 as a regulator of cell life and death. *Nat Cell Biol* 2002; **4**: E131-E136
2 **Blagosklonny MV**, Pardee AB. The restriction point of the cell cycle. *Cell Cycle* 2002; **1**: 103-110
3 **Ortega S**, Malumbres M, Barbacid M. Cyclin D-dependent kinases, INK4 inhibitors and cancer. *Biochim Biophys Acta* 2002; **1602**: 73-87
4 **Rafferty MA**, Fenton JE, Jones AS. An overview of the role and inter-relationship of epidermal growth factor receptor, cyclin D and retinoblastoma protein on the carcinogenesis of squamous cell carcinoma of the larynx. *Clin Otolaryngol* 2001; **26**: 317-320
5 **Coqueret O**. Linking cyclins to transcriptional control. *Gene* 2002; **299**: 35-55
6 **Chen B**, Zhang XY, Zhang YJ, Zhou P, Gu Y, Fan DM. Antisense to cyclin D1 reverses the transformed phenotype of human gastric cancer cells. *World J Gastroenterol* 1999; **5**: 18-21
7 **Shoker BS,** Jarvis C, Davies MP, Iqbal M, Sibson DR, Sloane JP. Immunodetectable cyclin D(1)is associated with oestrogen receptor but not Ki67 in normal, cancerous and precancerous breast lesions. *Br J Cancer* 2001; **84**: 1064-1069
8 **Chomczynski P**, Sacchi N. Single-step method of RNA isolation by acid guanidinium thiocyanate-phenol-chloroform extraction. *Anal Biochem* 1987; **162**: 156-159
9 **Wan QH**, Qian KX, Fang SG. A simple DNA extraction and rapid specific identification technique for single cells and early embryos of two breeds of Bos taurus. *Anim Reprod Sci* 2003; **77**: 1-9

10 **Renedo M,** Martinez-Delgado B, Arranz E, Garcia M, Urioste M, Martinez-Ramirez A, Rivas C, Cigudosa JC, Benitez I. Chromosomal changes pattern and gene amplification in T cell non-Hodgkin's lymphomas. *Leukemia* 2001; **15**: 1627-1632
11 **Turner HE**, Nagy Z, Sullivan N, Esiri MM, Wass JA. Expression analysis of cyclins in pituitary adenomas and the normal pituitary gland. *Clin Endocrinol* 2000; **53**: 337-344
12 **Naidu R**, Wahab NA, Yadav MM, Kutty MK. Expression and amplification of cyclin D1 in primary breast carcinomas: relationship with histopathological types and clinico-pathological parameters. *Oncol Rep* 2002; **9**: 409-416
13 **Bartkova J**, Lukas J, Muller H, Lutzhoft D, Strauss M, Bartek J. Cyclin D1 protein expression and function in human breast cancer. *Int J Cancer* 1994; **57**: 353-361
14 **Steeg PS**, Zhou Q. Cyclins and breast cancer. *Breast Cancer Res Treat* 1998; **52**: 17-28
15 **Qiuling S**, Yuxin Z, Suhua Z, Cheng X, Shuguang L, Fengsheng H. Cyclin D1 gene polymorphism and susceptibility to lung cancer in a Chinese population. *Carcinogenesis* 2003; **24**: 1499-1503
16 **Moreno-Bueno G**, Rodriguez-Perales S, Sanchez-Estevez C, Hardisson D, Sarrio D, Prat J, Cigudosa JC, Matias-Guiu X, Palacios J. Cyclin D1 gene (CCND1) mutations in endometrial cancer. *Oncogene* 2003; **22**: 6115-6118
17 **Buschges R**, Weber RG, Actor B, Lichter P, Collins VP, Reifenberger G. Amplification and expression of cyclin D genes (CCND1, CCND2 and CCND3) in human malignant gliomas. *Brain Pathol* 1999; **9**: 435-442
18 **Yang WI,** Zukerberg LR, Motokura T, Arnold A, Harris NL. Cyclin D1 (Bcl-1, PRAD1) protein expression in low-grade B-cell lymphomas and reactive hyperplasia. *Am J Pathol* 1994; **145**: 86-96

Edited by Wang XL and Xu CT **Proofread by** Pan BR and Xu FM

PO Box 2345, Beijing 100023, China
Fax: +86-10-85381893
E-mail: wjg@wjgnet.com www.wjgnet.com

World J Gastroenterol 2004;10(20):2940-2943
World Journal of Gastroenterology
 ISSN 1007-9327

• GASTRIC CANCER •

Comparison of quality of life between urban and rural gastric cancer patients and analysis of influencing factors

Jun Tian, Zhen-Chun Chen, Bin Wu, Xin Meng

Jun Tian, Bin Wu, Xin Meng, Department of Epidemiology and Health Statistics, Fujian Medical University, Fuzhou 350004, Fujian Province, China
Zhen-Chun Chen, Fujian Cancer Hospital, Fuzhou 350014, Fujian Province, China
Correspondence to: Jun Tian, Department of Epidemiology and Health Statistics, Fujian Medical University, Fuzhou 350004, Fujian Province, China. tianjun@mail.fjmu.edu.cn
Telephone: +86-591-3569264
Received: 2003-11-18 **Accepted:** 2003-12-08

Abstract

AIM: The conception of quality of life has been widely accepted by clinic doctors. Evaluations of the treatment effect of chronic diseases have been changed to depend not only on the survival time, but also on the quality of life of the patients. Fuzhou City and Changle County are high-incidence areas of the gastric cancer in Fujian Province. The aims of this research were to compare the quality of life of urban patients with that of rural patients and analyze the factors influencing quality of life of gastric cancer patients in Fujian Province.

METHODS: The samples were drawn with cluster sampling. The urban sample consisted of 162 patients aged 25 to 75 with 143 males and 19 females. The rural sample consisted of 200 patients aged 32 to 78 with 166 males and 34 females. The patients in both the urban and rural areas were investigated, and their scores on 21 items reflecting the quality of life were measured. The methods of *t* test and stepwise regression were used to analyze the data.

RESULTS: The average total scores of quality of life of the urban patients and rural patients were 64.11 and 68.69 respectively. There was a significant difference between the means of two samples ($P = 0.0004$). Seven variables in the regression model estimated by the urban sample and 4 variables in the model by the rural sample were at the level of significance $\alpha = 0.05$. Family income, nutrition and rehabilitating exercise were selected into both the urban and rural regression models.

CONCLUSION: Most of the gastric cancer patients have poor quality of life in Fujian Province and the rural patients have lower quality of life than that of urban patients. The patients having more family income have better quality of life, and enhanced nutrition and doing rehabilitating exercise are helpful in improving the quality of life of the gastric cancer patients.

Tian J, Chen ZC, Wu B, Meng X. Comparison of quality of life between urban and rural gastric cancer patients and analysis of influencing factors. *World J Gastroenterol* 2004; 10(20): 2940-2943
http://www.wjgnet.com/1007-9327/10/2940.asp

INTRODUCTION

Along with the changes of medical pattern and health care practice, evaluations of the treatment effect of chronic diseases have been changed to depend not only on the survival time, but also on the quality of life of the patients. The quality of life of a person is his personal feeling in sections of physiology, psychology and society[1,2]. The quality of life of the cancer patients can reflect not only treatment effect but also rehabilitation effect, so it has attracted much attention since 1980. Many studies have been done regarding the quality of life of the cancer patients in western countries and Japan[3-8], and there also have been several relevant studies in China[9-11]. Another important aspect of research on the quality of life is analyzing factors influencing the quality of life. Since many factors can impact on the quality of life of the cancer patients, it is important to analyze which factors may be related to the quality of life in order to improve the quality of life of the patients. Fuzhou City and Changle County are high-incidence areas of gastric cancer in Fujian Province. Every year, there are many new cases reported in the two areas[12]. A lot of efforts have been made in prevention and treatment of gastric cancer. However, little attention has been paid to the quality of life of the gastric cancer patients and few studies have been done on how to improve the quality of life of the patients. In order to understand the levels of quality of life of the gastric cancer patients in Fujian Province, we made an epidemiological survey from May 1999 to July 1999. In this paper, we describe the levels of the quality of life of the urban patients and rural patients, compare the quality of life of the urban patients with that of the rural patients, and analyze the factors influencing the quality of life. The results of this research may be useful to doctors and nurses in the community health center to help improve the quality of life of the gastric cancer patients.

MATERIALS AND METHODS

Materials

The populations of the gastric cancer patients diagnosed between 1997 and 1998 were provided by the Tumor Registration Office of Fujian Province. The samples were drawn from the populations with cluster sampling. All of the gastric cancer patients in the urban sample were residents in Fuzhou City and diagnosed by the provincial-level hospitals. The patients in the rural sample were residents in Changle County and diagnosed by the county-level above hospitals. All of the patients in the two samples had survived for no less than one year.

Methods

The questionnaire was composed of two sections, one with 16 items related to the disease, treatment and rehabilitation of the gastric cancer patients (Table 1), and the other with 21 items related to the quality of life of the patients (Table 2). Each of the 21 items of survival quality was scored from 1 to 5 indicating the function from the worst to the best. The internal consistency and stability index, Cronbach $\alpha = 0.9866$, confirmed the reliability of the 21 items describing the quality of life. The investigators

Table 1 List of factors that may affect the quality of life of gastric cancer patients

Factor	Definition
Gender	Male 1 Female 2
Age (yr)	
Marital status	Single 1 Married 2 Divorced 3 Widowed 4
Education	Primary school 1 Middle school 2 High school 3 University 4
Family income (per capita, Yuan)	
Medical insurance	Yes 1 No 0
Clinical stage of tumor	1-4
Survival time (mo)	
Surgery	2/3 gastrectomy 1, 4/5 gastrectomy 2, total gastrectomy 3
Number of chemotherapy programs	
Time from the latest chemotherapy to the enrollment (mo)	
Treatment of traditional Chinese medicine	Yes 1 No 0
Home nursing staff	Spouse 1 Other relatives 2 Housekeepers 3 None 4
Chemotherapy	Yes 1 No 0
Enhanced nutrition	Yes 1 No 0
Rehabilitating exercise	Yes 1 No 0

visited the patient's family and asked the patient to complete the questionnaire except the contents of the disease stage and treatments which were collected from the medical records at the hospitals. The scores for the individual items shown in Table 2 were summed to produce a 'total score', representing the quality of life of each patient.

Numerical descriptive statistics were used in summarizing the total score of quality of life in urban patients and rural patients respectively, *t* test was used for testing the difference between the means of two samples and stepwise regression[13] was used for analyzing the factors influencing quality of life. SAS software package was used for all analyses[14].

Table 2 The 21 parameters of the quality of life

	Items		Items
1	Sleep	12	Knowledge of cancer
2	Range of activities	13	Mental status
3	Eating	14	Fear of disease
4	Ability of using traffic vehicles independently	15	Psychological pain
5	Ability of body movement	16	Connection with relatives and friends
6	Ability to live independently	17	Social contact
7	Housework	18	Disappointment
8	Pain	19	Confidence of fighting the disease
9	Recreational activities	20	Intellectual activities
10	Watching TV or listening to radio	21	Attitude towards treatment
11	Interest or hobby		

RESULTS

Description of samples

The urban sample consisted of 162 patients aged 25 to 75. There were 143 male and 19 female patients in the urban sample, about 88.3% and 11.7% of the urban sample size respectively. The rural sample consisted of 200 patients aged 32 to 78. There were 166 male and 34 female patients in the rural sample, about 83.0% and 17.0% of the rural sample size respectively. In the urban sample, the workers represented 42.6% and government functionaries took up 23.5%. All of the patients in the rural sample were peasants.

The quality of life

The distributions of total scores of urban patients and rural patients are shown in Table 3. Among the urban patients, the highest score was 96 and the lowest score 22, and 36.42% of the patients, the largest group, had total scores between 70 and 80 and 1.23%, the smallest group, had total scores between 90-105. Among the rural patients, the highest score was 81 and the lowest score 19, and 34.5% had total scores between 60 and 70 and none had a total score between 90-105. Table 4 shows the means and standard deviations of the total scores of the urban and rural patients. The difference of total scores between the urban and rural patients was significant ($P = 0.0004$). These results suggest that most of the gastric cancer patients had poor quality of life in Fujian Province and the qualities of life of rural patients were worse than those of urban patients.

Table 3 Distributions of total scores in urban patients and rural patients

Total score	Urban		Rural	
	n	Percentage (%)	*n*	Percentage (%)
<30	3	1.85	4	2.00
30-	3	1.85	6	3.00
40-	8	4.94	16	8.00
50-	17	10.49	54	27.00
60-	43	26.54	69	34.50
70-	59	36.42	41	20.50
80-	27	16.67	10	5.00
90-105	2	1.23	0	0.00

Table 4 Means and standard deviations of total scores in the two samples

	Number of the patients	mean	SD	95% confidence interval
Urban	162	68.69	12.98	66.69-70.69
Rural	200	64.11	11.29	62.54-65.67
		$t = 3.5885$	$P = 0.0004$	

Factors influencing the quality of life

The relationship between the total scores, also called dependent variables, and the factors shown in Table 1, also called independent variables, was analyzed by using method of stepwise regression.

Setting the level of significance $\alpha = 0.05$, we had the result

of regression analysis with urban patients (Table 5). Table 5 shows the factors influencing quality of life of gastric cancer patients and the regression coefficients. This result suggests that the factors related to the total score of urban patients were age ($P = 0.0001$), family income ($P = 0.0032$), clinical stage of the tumor ($P = 0.0375$), the time from the latest chemotherapy to the enrollment ($P = 0.0095$), home nursing staff ($P<0.0001$), enhanced nutrition ($P = 0.0431$) and rehabilitating exercise ($P = 0.0115$). As indicated by the regression coefficients, the quality of life of elder patients was worse than that of the younger ones, the patient in the early stage of gastric cancer had a better quality of life than that in the late stage and patients with a longer time period from the latest chemotherapy to the enrollment had a better quality of life than one with a shorter time period.

Table 5 Results of stepwise regression with urban patients

Variable	Regression coefficient	SEM	*t*	*P*
Age (yr)	-0.10620	0.02654	-4.00	0.0001
Family income	1.11909	0.36949	3.03	0.0032
Clinical stage of the tumor	-1.10772	0.52498	-2.11	0.0375
Time from the latest chemotherapy to the enrollment	0.09199	0.03876	2.37	0.0095
Home nursing staff	-2.98233	0.57659	-5.17	<0.0001
Enhanced nutrition	1.80669	0.88221	2.05	0.0431
Rehabilitating exercise	1.01185	0.39245	2.58	0.0115

At $\alpha = 0.05$, the results of regression analysis of the rural patients are shown in Table 6. The results suggested that the factors related to the total score of rural patients were family income ($P = 0.0193$), surgical operation ($P<0.0001$), enhanced nutrition ($P = 0.0488$) and rehabilitating exercise ($P = 0.0125$). Based on regression coefficients, patients with total gastrectomy had a worse quality of life than those with a partial gastrectomy.

Table 6 Results of stepwise regression with rural patients

Variable	Parameter estimated	SEM	*t*	*P*
Family income	1.0860	0.45974	2.36	0.0193
Surgery	-14.24462	2.77803	5.12	<0.0001
Enhanced nutrition	-2.73243	1.37834	1.98	0.0488
Rehabilitating exercise	-2.20909	0.87618	2.52	0.0125

Three factors: family income, nutrition and rehabilitating exercise, in both regression models, might be important for improving the quality of life of the gastric cancer patients. The patients having more economic incomes had a better quality of life, and increased nutrition and doing rehabilitating exercise are helpful in improving the quality of life of the gastric cancer patients.

DISCUSSION

Traditionally, the effects of treatments were evaluated by such quantitative indexes as survival rate, survival time and the volumes of tumors. The conception of quality of life is proposed, along with the changes of medical and health care practice patterns and progress of medical science. It is used to evaluate the effects of treatments for chronic diseases and cancers. The purpose of this study was to obtain the information about quality of life of gastric cancer patients in Fujian Province and explore which factors impacted on the quality of life of gastric cancer patients.

For most of gastric cancer patients, the prognosis and their qualities of life were poor since the cancers had been in advanced stages when they were diagnosed[15,16]. Our results show that most of the gastric cancer patients have low quality of life in Fujian Province, and the quality of life of rural gastric cancer patients are worse than that of urban patients. It may be that the rural patients suffered more physical and psychological pain because of their lower levels of education and economic income compared with the urban patients.

Some researchers held that patient's nutritional status played a critical role in maintaining a positive quality of life from both physical and emotional points of view[17-20]. Nutrient depletion adversely affects immune function, the patient's enjoyableness and social interactions with family and friends, which can further depress appetite[17]. Low hemoglobin levels were associated with fatigue, poor overall quality of life, and decreased ability to work. Interventions that reverse fatigue and other anemia-related symptoms should have a positive effect on quality of life[19]. Our results also showed that improved nutrition was one of the factors influencing quality of life both in rural and urban areas. This may suggest that appropriate nutritional care can help maintain the patient's body weight and protein status, reduce fatigue and improve quality of life.

Rehabilitating exercise has been thought to be a factor influencing quality of life of breast cancer patients. A review on 24 studies dealing with physical exercise and quality of life of cancer patients published between 1980 and 1997 demonstrated that physical exercise had a positive effect on quality of life including physical, functional, psychological, and emotional well-being[21-27]. In our research, rehabilitating exercise was related to quality of life of gastric cancer patients, which is consistent with previous researches. Not only can taking rehabilitating exercise improve the patient's body function, but it can also please his mood, strengthen his confidence of defeating the disease and improve his ability of contacting society.

Our results also showed that the quality of life of urban patients could be affected by the home nursing staff and rural patients affected by the surgery. The psychological status of the nursing staff may have more influence on the physiological and psychological functions of the patient. Good nutritional care for the patient requires full support from the home nursing staff[28-32]. Patients who have been given a partial gastrectomy achieved a better quality of life than those having a total gastrectomy. When the entire gastric is removed, the patients should adjust to a different eating schedule involving eating small quantities of food more frequently and high-protein foods, so the home nursing staff should be educated on providing cancer care and nutritional support. The family members should have adequate knowledge as to how to support the patient.

In summary, our data obtained by epidemiological survey show that most of the gastric cancer patients have poor quality of life in Fujian Province, and the quality of life of the rural patients are worse than that of the urban patients. The patients having more family income have better quality of life, and enhanced nutrition and doing rehabilitating exercise are helpful in improving the quality of life of the gastric cancer patients.

REFERENCES

1 **Mellette SJ**. Cancer rehabilitation. *J Natl Cancer Inst* 1993; **85**: 781-784
2 **Wang JP**, Cui JN, Chen ZG, Lin WJ, Luo J, Sun Y. Quality of life and factors that influence it among cancer patients in China. *Zhongguo Linchuang Xinlixue Zazhi* 2000; **8**: 23-26
3 **Bottomley A**. The cancer patient and quality of life. *Oncologist* 2002; **7**: 120-125
4 **Repetto L**, Ausili-Cefaro G, Gallo C, Rossi A, Manzione L. Quality of life in elderly cancer patients. *Ann Oncol* 2001; 3

(Suppl): S49-52
5 **Efficace F**, Bottomley A, van Andel G. Health related quality of life in prostate carcinoma patients: a systematic review of randomized controlled trials. *Cancer* 2003; **97**: 377-388
6 **Rustoen T**, Wiklund I, Hanestad BR, Burckhardt CS. Validity and reliability of the Norwegian version of the Ferrans and Powers Quality of Life Index. *Scand J Caring Sci* 1999; **13**: 96-101
7 **Andersen BL**. Quality of life for women with gynecologic cancer. *Curr Opin Obstet Gynecol* 1995; **7**: 69-76
8 **Arora NK**, Gustafson DH, Hawkins RP, McTavish F, Cella DF, Pingree S, Mendenhall JH, Mahvi DM. Impact of surgery and chemotherapy on the quality of life of younger women with breast carcinoma: a prospective study. *Cancer* 2001; **92**: 1288-1298
9 **Deng XL**, Wang W, Wang LS. Relationship between the Quality of life and therapeutic modalities in patients with gastric cancer. *Zhongguo Zhongliu* 2001; **10**: 78-80
10 **Tian J**, Zhang JY, Wu B, Chen JL, Chen ZC. A multifactor study on the quality of survival of aged cancer patients. *Zhonghua Laonian Yixue Zazhi* 1996; **15**: 339-342
11 **Tian J,** Wu B, Chen JL, Chen ZC, Chen JS. An influencing factors study on the quality of life of gastric carcinnoma patients. *Shuli Tongji Yu Guanli* 2000; **19**: 35-38
12 Quanguo Zhongliu Fangzhi Yanjiu Bangongshi. The cancer incidences and death rates in China (1988-1992). Bejin: *Zhongguo Yiyao Keji Chubanshe* 2001: 22-200
13 **Katz MH**. Multivariable Analysis: A Practical Guide for Clinicians. H.K.: *Science Culture Publishing House LTD* 2000: 26-45
14 **Hong N**, Hou J. SAS for Windows. Beijing: *Dianzi Gongye Chubanshe* 2001: 107-138
15 **Luo J**, Sun Y. The research on quality of life in cancer patients. *Zhongguo Zhongliu* 2001; **10**: 76-78
16 LENA-MARIE Petersson. Group rehabilitation for cancer patients: effects, patient satisfaction, utilisation and prediction of rehabilitation need. Sweden: *Tryck Medier* 2003: 14-73
17 **Small W**, Carrara R, Danford L, Logemann JA, Cella D. Quality of life and nutrition in the patient with cancer. *Oncology* 2002(Suppl): 13-14
18 **Brown J**, Byers T, Thompson K, Eldridge B, Doyle C, Williams AM. Nutrition during and after cancer treatment: A guide for informed choices by cancer survivors. *CA Cancer J Clin* 2001; **51**: 153-187
19 **Cella D**. Factors influencing quality of life in cancer patients: anemia and fatigue. *Semin Oncol* 1998; **25**(3 Suppl 7): 43-46
20 **Peltz G**. Nutrition support in cancer patients: a brief review and suggestion for standard indications criteria. *Nutr J* 2002; **1**: 1
21 **Salmon PG,** Swank AM. Exercise-based disease management guidelines for individuals with cancer: Potential applications in a high-risk mid-southern state. *J Exercise Physiol* 2002; **5**: 1-10
22 **Watson PG**. Cancer rehabilitation. The evolution of a concept. *Cancer Nurs* 1990; **13**: 2-12
23 **Courneya KS**, Friedenreich CM. Phsical exercise and quality of life following cancer diagnosis: a literature review. *Ann Behav Med* 1999; **21**: 171-179
24 **Andersen BL**. Psychological interventions for cancer patients to enhance the quality of life. *J Consult Clin Psychol* 1992; **60**: 552-568
25 **Courneya KS**, Friedenreich CM. Framework PEACE: an organizational model for examining physical exercise across the cancer experience. *Ann Behav Med* 2001; **23**: 263-272
26 **Blanchard CM**, Courneya KS, Laing D. Effects of acute exercise on state anxiety in breast cancer survivors. *Oncol Nurs Forum* 2001; **28**: 1617-1621
27 **Courneya KS**. Exercise interventions during cancer treatment: biopsychosocial outcomes. *Exerc Sport Sci Rev* 2001; **29**: 60-64
28 **Rustoen T**, Wiklund I, Hanestad BR, Moum T. Nursing intervention to increase hope and quality of life in newly diagnosed cancer patients. *Cancer Nurs* 1998; **21**: 235-245
29 **Rustoen T**, Wiklund I. Hope in newly diagnosed patients with cancer. *Cancer Nurs* 2000; **23**: 214-219
30 **Andersen BL**. Biobehavioral outcomes following psychological interventions for cancer patients. *J Consult Clin Psychol* 2002; **70**: 590-610
31 **Velikova G**, Booth L, Smith AB, Brown PM, Lynch P, Brown JM, Selby PJ. Measuring quality of life in routine oncology practice improves communication and patient well-being: a randomized controlled trial. *J Clin Oncol* 2004; **22**: 714-724
32 **Wan GJ**, Counte MA, Cella DF. The influence of personal expectations on cancer patients' reports of health-related quality of life. *Psychooncology* 1997; **6**: 1-11

Edited by Hu DK and Zhu LH **Proofread by** Chen WW and Xu FM

PO Box 2345, Beijing 100023, China
Fax: +86-10-85381893
E-mail: wjg@wjgnet.com www.wjgnet.com

World J Gastroenterol 2004;10(20):2944-2948
World Journal of Gastroenterology
 ISSN 1007-9327

• LIVER CANCER •

Down-modulation of heat shock protein 70 and up-modulation of Caspase-3 during schisandrin B-induced apoptosis in human hepatoma SMMC-7721 cells

Yi-Feng Wu, Ming-Fu Cao, Yan-Ping Gao, Fei Chen, Tao Wang, Edward P. Zumbika, Kai-Xian Qian

Yi-Feng Wu, Yan-Ping Gao, Kai-Xian Qian, College of Life Sciences, Zhejiang University, Hangzhou 310027, Zhejiang Province, China
Ming-Fu Cao, College of Life Sciences, Hangzhou Teachers college, Hangzhou 310012, Zhejiang Province, China
Fei Chen, Tao Wang, Edward P. Zumbika, School of Medicine, Zhejiang University, Hangzhou 310027, Zhejiang Province, China
Supported by the National Key Technologies Research and Development Program of China during the 10th Five-Year Plan Period, No. 2002BA760C
Correspondence to: Kai-Xian Qian, College of Life Sciences, Zhejiang University, Hangzhou 310027, Zhejiang Province, China. biocell@zju.edu.cn
Telephone: +86-571-87952761
Received: 2004-02-02 **Accepted:** 2004-02-21

Abstract

AIM: To investigate the effect of schisandrin B (Sch B) on proliferation and apoptosis of human hepatoma SMMC-7721 cells *in vitro* and regulation of Hsp70 and Caspases-3, 7, 9 expression by Sch B.

METHODS: Human hepatoma cell line SMMC-7721 was cultured and treated with Sch B at various concentrations. Growth suppression was detected with MTT colorimetric assay. Cell apoptosis was confirmed by DNA ladder detection and flow cytometric analysis. The expression of Hsp70, Caspases-3, 7, 9 were analyzed by Western blot analysis.

RESULTS: Sch B inhibited the growth of hepatoma SMMC-7721 cells in a dose-dependent manner, leading to a 50% decrease in cell number (LC50) value of 23.50 mg/L. Treatment with Sch B resulted in degradation of chromosomal DNA into small internucleosomal fragments, evidenced by the formation of a 180-200 bp DNA ladder on agarose gels. FCM analysis showed the peak areas of subdiploid at the increased concentration of Sch B. The results of Western bolt analysis showed that Hsp70 was down-regulated and Caspase-3 was up-regulated, while the activity of Caspases-7, -9 had no significant change.

CONCLUSION: Sch B is able to inhibit the proliferation of human hepatoma SMMC-7721 cells and induce apoptosis, which goes through Caspase-3-dependent and Caspase-9-independent pathway accompanied with the down-regulation of Hsp70 protein expression at an early event.

Wu YF, Cao MF, Gao YP, Chen F, Wang T, Zumbika EP, Qian KX. Down-modulation of heat shock protein 70 and up-modulation of Caspase-3 during schisandrin B-induced apoptosis in human hepatoma SMMC-7721 cells. *World J Gastroenterol* 2004; 10(20): 2944-2948
http://www.wjgnet.com/1007-9327/10/2944.asp

INTRODUCTION

Schisandrin B (Sch B, Figure 1) is a dibenzocyclooctadiene compound isolated from *Fructus Schisandrae* (FS, the fruit of *Schisandra chinensis*), an herb commonly prescribed in tonic and sedative formulae in Chinese medicine[1,2]. In clinical situations, FS was also found to produce beneficial effects on patients suffering from viral hepatitis[3]. Recently, the pharmacological profile of FS, which includes the enhancement of liver functions and inhibitory/sedative effects on the central nervous system, has been established by laboratory investigations[4-9]. We presented evidence that Sch B was able to inhibit the proliferation of human hepatoma SMMC-7721 cells and induce apoptosis *in vitro*.

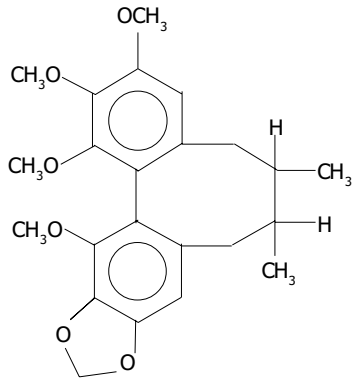

Figure 1 Chemical structure of Schisandrin B.

Apoptosis is an essential physiological process required for normal development and maintenance of tissue homeostasis[10,11]. Insufficient or excessive cell death can contribute to human diseases, including cancer, acquired immunodeficiency syndrome and some neurodegenerative disorders[12]. Although many factors are involved in apoptotic program[13-16], Caspases, a family of cysteine proteases have been shown to play a major role in the transduction of apoptotic signals and the execution of apoptosis in mammalian[17-21], which has become recognized as key components of the apoptotic machinery[22]. Most of the biochemical and morphological events of apoptosis are a direct result of Caspase-mediated cleavage of specific substrates[23,24].

Inhibition of Caspases following treatment with apoptotic stimuli has been shown to prevent some features of apoptosis. The heat shock protein 70 (Hsp70) family of proteins has been demonstrated to be a potent inhibitor of apoptosis induced by a wide range of stimuli[25,26]. It can protect against apoptosis at an early event in the apoptotic pathway. A role for Hsp70 in tumorigenesis has been suggested, based on the observations that many transformed cells have elevated levels of Hsp70 and overexpression of Hsp70 in transgenic mice results in T-cell lymphoma[27-30].

In this study, Sch B induced human hepatoma SMMC-7721 cell apoptosis was confirmed by DNA ladder detection and flow cytometric analysis. At the same time, the modulation of Hsp70 and Caspases was observed to study the mechanism of Sch B induced apoptosis in human hepatoma SMMC-7721 cells.

MATERIALS AND METHODS

Reagents

Sch B was purchased from National Institute for the Control of Pharmaceutical and Biological Products, China (NICPBP). The drug was dissolved in dimethyl sulfoxide (DMSO) at a concentration of 10 g/L. For cell treatments, the samples were further diluted in culture medium with the final DMSO concentration <5 g/L. Antibodies to Hsp70, Caspases-3, 7, 9 were purchased from Boster Biotech, China. RPMI-1640 culture medium was obtained from Gibco Co. USA. Fetal calf serum was supplied by Si-Ji-Qing Biotechnology Co. (Hangzhou, China). 96-well plates and culture bottles were purchased from Costar Co. USA. All other chemicals were purchased from Sigma Chemical (St. Louis, MO, USA).

Cell lines and culture

Human hepatoma cell line SMMC-7721 and human hepatic cell line HL-7702 were purchased from American Type Culture Collection (ATCC). Human endothelial cell line ECV-304 was obtained from Tumor Institute, Zhejiang University. Primary human fibroblast cell line was derived from fresh muscle tissues by enzymatic dissociation. Human lymphocytes were derived from umbilical blood by Ficoll-Hyaque separation method, and seeded in 96-well microplates with the concentration of phytoagglutinin (PHA). All the cell lines were grown as monolayers in RPMI1640 medium supplemented with 100 mL/L fetal calf serum and antibiotics (100 unit/mL penicillin and 100 μg/mL streptomycin), incubated at 37 ℃ in a humidified incubator containing 50 mL/L CO_2 in air.

Assay of cell proliferation

SMMC-7721 cells (100 μL of cell suspension per well) were seeded at a density of 1.5×10^5/mL in 96-well plates. Each group had three wells with a non-treated group as control. When the cells anchored to the plates, various concentrations of Sch B were added and the slides were incubated at 37 ℃ in humidified atmosphere containing 50 mL/L CO_2. When the cells described above were cultured for 48 h, 50 μL of MTT (2 mg/mL in PBS) was added to each well and cultured for another 4 h. After the supernatant was discarded, MTT formazan precipitates were dissolved in 100 μL of DMSO, shaken mechanically for 10 min and then read immediately at 570 nm in a plate reader. Cell proliferation inhibition rate (CPIR) was calculated using the following equation: CPIR = (1-average absorbance *(A)* value of experimental group/average *A* value of control group) ×100%.

Cell toxicity on primary cells or normal cell lines

HL-7702 cells, ECV-304 cells, primary human fibroblast cells, human lymphocytes (100 μL cell suspension per well) were seeded at a density of 1.0×10^5/mL in 96-well plates. Following treatment at the concentration of 10, 20, 40, 80, 160 mg/L Sch B for 24 h, cell viability was estimated by trypan blue exclusion. Six wells were measured for each concentration of test compound. All toxicity experiments were repeated at least three independent occasions.

DNA ladder demonstration

After exposed to Sch B for 12 h, SMMC-7721 cells (5×10^6/sample, both attached and detached cells) were collected and lysed with lysis buffer containing 50 mmoL Tris-HCl buffer (pH 7.5), 20 mmol/L EDTA, and 10 g/L NP-40. Then 10 g/L SDS and RNase (5 μg/mL) were added to the supernatant, and incubated at 56 ℃ for 2 h, followed by incubation with proteinase K (2.5 μg/mL) at 37 ℃ for 2 h. After the DNA was precipitated by addition of both ammonium acetate (3.3 mol/L) and ethanol (995 mL/L), it was dissolved in a gel loading buffer. DNA fragmentation was detected by electrophoresis on 15 g/L agarose gels and visualized with ethidium bromide staining.

Flow cytometric analysis

SMMC-7721 cells were seeded in culture flasks. When the cells were anchored to the plates, various concentrations (0, 10 μmol/L, 20 μmol/L, 40 μmol/L) of Sch B were added and the cells were incubated at 37 ℃ in humidified atmosphere containing 50 mL/L CO_2 for 2 d. Then each group of cells were washed with PBS, trypsinized and fixed with 700 mL/L ethanol at -20 ℃ for 30 min, and they were stained with 1.0 μg/mL propidium iodide (PI, Boehringer Mannheim, Germany). The red fluorescence of DNA-bound PI in individual cells was measured at 488 nm with an Altra flow cytometer. The results were analyzed using the ExpoII software (Beckman Coulter, USA). Ten thousand events were analyzed for each sample.

Western blotting analysis

The cells were lysed in a lysis buffer (25 mmol/L hepes, 15 g/L Triton X-100, 10 g/L sodium deoxycholate, 1 g/L SDS, 0.5 mol/L NaCl, 5 mmol/L edetic acid, 50 mmol/L NaF, 0.1 mmol/L sodium vanadate, 1 mmol/L phenylmethylsulfonyl fluoride (PMSF) and 0.1 g/L leupeptin, pH7.8) at 4 ℃ with sonication. The lysates were centrifuged at 15 000 *g* for 15 min and the concentration of the protein in each lysate was determined with Coomassie brilliant blue G-250. Loading buffer (42 mmol/L Tris-HCl, containing 100 mL/L glycerol, 23 g/L SDS, 50 g/L 2-mercaptoethanol and 0.02 g/L bromophenol blue) was then added to each lysate, which was subsequently boiled for 3 min and then electrophoresed on a SDS-polyacrylamide gel. Proteins were transferred onto a nitrocellulose filter and incubated separately with antibodies against Hsp70, Caspases-3,7,9, then labeled with peroxidase-conjugated secondary antibodies. The reactions were visualized using the enhanced chemiluminescence reagent (Sigma). The results were approved by repeating the reactions twice.

Statistical analysis

All data were expressed as mean±SD. Statistical analysis was performed by *t* test using software SPSS 11.0 for Windows. $P<0.05$ was considered statistically significant.

RESULTS

Effect of Sch B on cell proliferation

Treatment of human hepatoma SMMC-7721 cells with Sch B resulted in a dose-dependent cytotoxicity. As shown in Figure 2, Sch B-mediated cytotoxicity occurred at a concentration greater than 20 mg/L for 48 h. A significant decrease in cell number was seen in the cells treated with Sch B at 20 mg/L. The concentration of Sch B leading to a 50% decrease in cell number (LC50) was about 23.5 mg/L.

Effect of Sch B on primary cells or normal cell line toxicity

As indicated in Figure 3, Sch B had little cytocidal effect on primary human fibroblast cells and human lymphocyte cells even if at the concentration of 160 mg/L. Treatment of human HL-7702, ECV-304 with Sch B resulted in a dose-dependent cytotoxicity. But human hepatic HL-7702 cells were more resistant to the Sch B-mediated cytotoxicity than human endothelial cells, ECV-304 cells and human hepatoma SMMC-7721.

Detection of DNA fragmentation in SMMC-7721 cells treated with Sch B

As shown in Figure 4, treatment with Sch B resulted in degradation of chromosomal DNA into small internucleosomal fragments, evidenced by the formation of a 180-200 bp DNA ladder on agarose gels, hallmark of cells undergoing apoptosis. No DNA ladders were detected in the samples isolated from control cultures. These results indicated that Sch B induced an apoptotic cell death in SMMC-7721 cells.

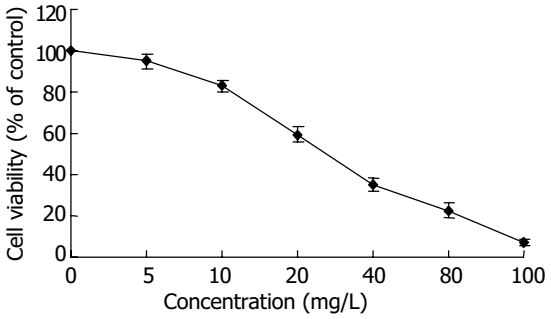

Figure 2 Inhibition rate of Sch B on proliferation of SMMC-7721 cells. Cells were incubated at concentrations of Sch B for 48 h.

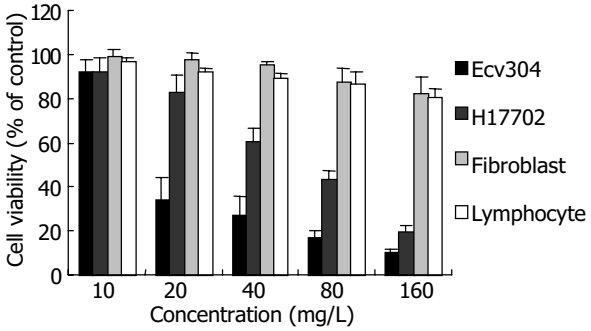

Figure 3 Cytocidal effect of Sch B on growth of human endothelial ECV-304 cells, human hepatic HL-7702 cells, primary human fibroblast cells and human lymphocyte cells. Cells were incubated at concentrations (10, 20, 40, 80, 160 mg/L) of Sch B for 48 h.

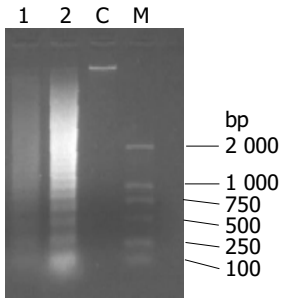

Figure 4 DNA fragmentation in SMMC-7721 cells treated with Sch B for 12 h. M: size marker; C: control culture; lane 1: 20 mg/L Sch B treatment; lane 2: 40 mg/L Sch B treatment.

Flow cytometric analysis of cell apoptosis

SMMC-7721 cells were exposed to increased concentrations of Sch B (10 mg/L, 20 mg/L, 40 mg/L) for 48 h, and the growth of the cells was analyzed using flow cytometry (Figure 5). The peak value appearing before the G1 peak is called apoptotic peak. As shown in Figure 5 and Table 1, the apoptotic peak areas and rate increased with increased concentrations of Sch B.

Table 1 Apoptosis rate of SMMC-7721 cells induced by Sch B

Sch B concentration (mg/L)	Apoptosis rate (%)
0	0.95±0.17
10	3.44±0.21[a]
20	10.73±1.17[b]
40	30.25±1.76[b]

[a]$P<0.05$, [b]$P<0.01$ *vs* control group.

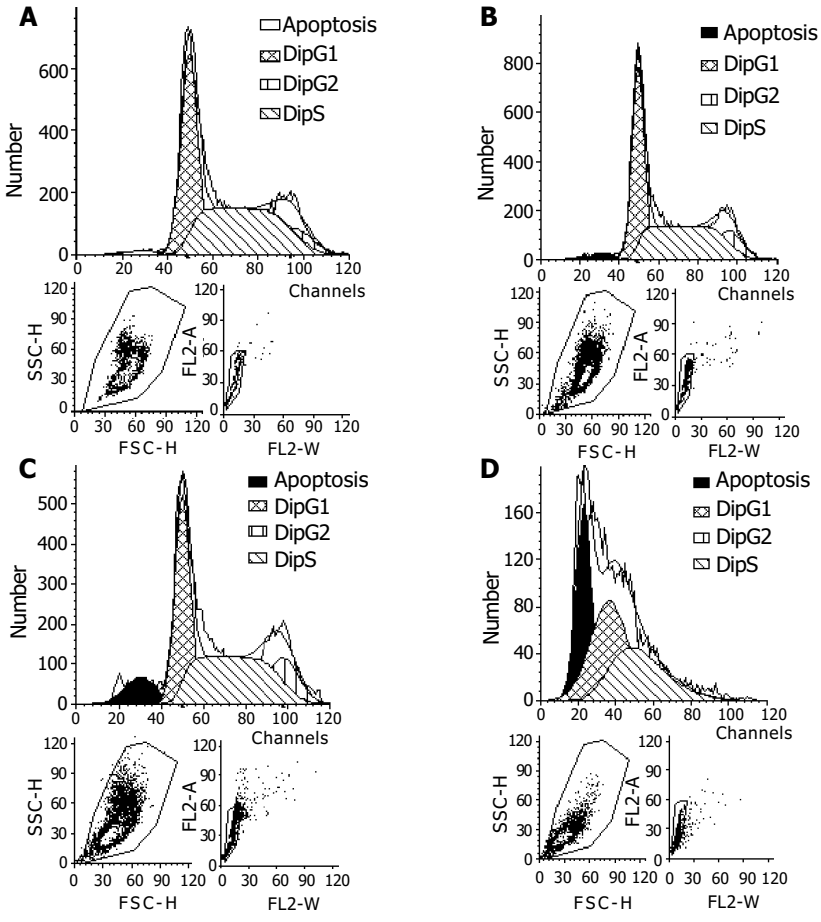

Figure 5 Cell apoptosis determined by flow cytometry. SMMC-7721 cells were treated with Sch B at various concentrations (0, 10, 20, 40 mg/L, respectively A to D) for 48 h.

Effects of Sch B on expression of Hsp70 and Caspases-3,-7,-9

Recent reports suggested that Hsp70 might help to protect cells from apoptosis at an early event in the apoptotic pathway. To elucidate whether Hsp70 was modulated during Sch B induced apoptosis, we examined the expression of Hsp70 by Western blot. Moreover, it was shown that Caspases were the main factor in the apoptotic pathway. We investigated whether Caspases were involved in inducing SMMC-7721 cell apoptosis treated with Sch B. SMMC-7721 cells treated with Sch B for 48 h were analyzed for the enzymatic activity by Western blot. The results showed that Hsp70 was down-regulated and Caspase-3 was activated, while the activity of Caspases-7,-9 had no significant change (Figure 6).

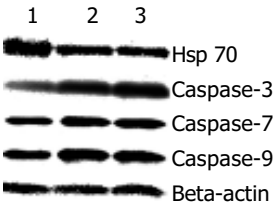

Figure 6 Effect of Sch B on expression of Hsp70, Caspases-3, -7, -9 proteins. SMMC-7721 cells were treated with Sch B for 48 h. After treatment, cell lysates were extracted, and the level of Hsp70, Caspases-3, -7, -9 proteins were analyzed by Western bolt analysis. Beta-actin was used as an internal loading control. Lane 1: control; Lane 2: 20 mg/L Sch B treatment; lane 3: 40 mg/L Sch B treatment.

DISCUSSION

After human hepatoma SMMC-7721 cells were treated at various concentrations of Sch B for 48 h, MTT colorimetric analysis showed that Sch B could significantly inhibit the proliferation of SMMC-7721 cells, with LC50 value of 23.50 mg/L. While human hepatic HL-7702 cells were more resistant to the Sch B mediated cytotoxic activity than human endothelial ECV-304 cells and human hepatoma SMMC-7721 cells. It is interesting that Sch B had an unconspicuous cytocidal effect on primary human fibroblast cells and human lymphocyte cells.

Current antineoplastic therapies, including chemotherapy and radiation-therapy, are likely to be affected by the apoptotic tendency of cells. During apoptosis, certain characteristic morphologic events, such as nuclear condensation, nuclear fragmentation, and cell shrinkage, and biochemical events, such as DNA fragmentation, would occur[31-35]. In this study, we showed that Sch B induced human hepatoma SMMC-7721 cell apoptosis was confirmed by DNA ladder and cell cycle analyses.

The commitment of cell apoptosis requires the integration of numerous inputs involving multiple signal transduction pathways. Some cellular pathways and molecular regulators/effectors of apoptosis have been identified. Many lines of evidence demonstrated that activation of Caspases is a central mechanism of apoptosis. So far, more than 15 members of Caspases have been reported in the literature, and most of them played a major role in apoptosis, participating in the initiation and execution of programmed cell death[36,37]. Based on their structure and function, Caspases are classified into two groups: initiator Caspases (such as Caspases-2,-8 and-9) and executor Caspases (such as Caspases-3, -6 and -7)[38,39]. In this study, Sch B-induced apoptosis of SMMC-7721 cells was accompanied with up-regulation of Caspase-3, but did not involve the regulation of Caspase-7 and Caspase-9 protein expression. These results suggested that Caspase-3 but not Caspase-7 was the "executors" of Sch B induced SMMC-7721 cell apoptosis that did not go through Caspase-9-dependent pathway.

Recent results indicated that Hsp70 might help to protect cells from apoptosis. Jaattela *et al*.[40] reported that Hsp70 exerted its anti-apoptotic function on downstream of Caspase-3. Creagh *et al*.[41] revealed that Hsp70 acted on upstream of the Caspases. In the presence of Hsp70, Caspase-3 was not processed or activated and the release of cytochrome C from the mitochondrial intermembrane space, a major Caspase activating mechanism, was inhibited. In this study, the down-modulation of Hsp70 was observed, indicating that Sch B could help Caspase-3 to release from the blockade of Hsp70 so as to promote human hepatoma SMMC-7721 cells to apoptosis.

In conclusion, Sch B is able to inhibit the proliferation of human hepatoma SMMC-7721 cells and induce apoptosis, which goes through Caspase-3-dependent and Caspase-9-independent pathways accompanied with the down-regulation of Hsp70 protein expression at an early event. Further investigation will focus on the identification of other signal modulations in this apoptosis pathway.

ACKNOWLEDGMENTS

The authors are grateful to Professor Shu Zheng for her help in this study.

REFERENCES

1 **Liu JH**, Ho SC, Lai TH, Liu TH, Chi PY, Wu RY. Protective effects of Chinese herbs on D-galactose-induced oxidative damage. *Methods Find Exp Clin Pharmacol* 2003; **25**: 447-452
2 **Hsieh MT**, Tsai ML, Peng WH, Wu CR. Effects of Fructus schizandrae on cycloheximide-induced amnesia in rats. *Phytother Res* 1999; **13**: 256-257
3 **Li XY**. Bioactivity of neolignans from fructus Schizandrae. *Mem Inst Oswaldo Cruz* 1991; **86**(Suppl 2): 31-37
4 **Chiu PY**, Tang MH, Mak DH, Poon MK, Ko KM. Hepatoprotective mechanism of schisandrin B: role of mitochondrial glutathione antioxidant status and heat shock proteins. *Free Radic Biol Med* 2003; **35**: 368-380
5 **Chiu PY**, Mak DH, Poon MK, Ko KM. *In vivo* antioxidant action of a lignan-enriched extract of Schisandra fruit and an anthraquinone-containing extract of Polygonum root in comparison with schisandrin B and emodin. *Planta Med* 2002; **68**: 951-956
6 **Ko KM**, Lam BY. Schisandrin B protects against tert-butylhydroperoxide induced cerebral toxicity by enhancing glutathione antioxidant status in mouse brain. *Mol Cell Biochem* 2002; **238**: 181-186
7 **Pan SY**, Han YF, Carlier PR, Pang YP, Mak DH, Lam BY, Ko KM. Schisandrin B protects against tacrine- and bis(7)-tacrine-induced hepatotoxicity and enhances cognitive function in mice. *Planta Med* 2002; **68**: 217-220
8 **Ip SP**, Yiu HY, Ko KM. Schisandrin B protects against menadione-induced hepatotoxicity by enhancing DT-diaphorase activity. *Mol Cell Biochem* 2000; **208**: 151-155
9 **Yim TK**, Ko KM. Schisandrin B protects against myocardial ischemia-reperfusion injury by enhancing myocardial glutathione antioxidant status. *Mol Cell Biochem* 1999; **196**: 151-156
10 **Souto PC**, Brito VN, Gameiro J, da Cruz-Hofling MA, Verinaud L. Programmed cell death in thymus during experimental paracoccidioidomycosis. *Med Microbiol Immunol* 2003; **192**: 225-229
11 **Hu W**, Kavanagh JJ. Anticancer therapy targeting the apoptotic pathway. *Lancet Oncol* 2003; **4**: 721-729
12 **Thompson CB**. Apoptosis in the pathogenesis and treatment of disease. *Science* 1995; **267**: 1456-1462
13 **Wajant H**, Pfizenmaier K, Scheurich P. TNF-related apoptosis inducing ligand (TRAIL) and its receptors in tumor surveillance and cancer therapy. *Apoptosis* 2002; **7**: 449-459
14 **Inoue H**, Shiraki K, Yamanaka T, Ohmori S, Sakai T, Deguchi M, Okano H, Murata K, Sugimoto K, Nakano T. Functional expression of tumor necrosis factor-related apoptosis-induc-

ing ligand in human colonic adenocarcinoma cells. *Lab Invest* 2002; **82**: 1111-1119

15 **Wei XC**, Wang XJ, Chen K, Zhang L, Liang Y, Lin XL. Killing effect of TNF-related apoptosis inducing ligand regulated by tetracycline on gastric cancer cell line NCI-N87. *World J Gastroenterol* 2001; **7**: 559-562

16 **MacFarlane M**, Harper N, Snowden RT, Dyer MJ, Barnett GA, Pringle JH, Cohen GM. Mechanisms of resistance to TRAIL-induced apoptosis in primary B cell chronic lymphocytic leukaemia. *Oncogene* 2002; **21**: 6809-6818

17 **Held J**, Schulze-Osthoff K. Potential and caveats of TRAIL in cancer therapy. *Drug Resist Updat* 2001; **4**: 243-252

18 **de Almodovar CR**, Ruiz-Ruiz C, Munoz-Pinedo C, Robledo G, Lopez-Rivas A. The differential sensitivity of Bc1-2-overexpressing human breast tumor cells to TRAIL or doxorubicin-induced apoptosis is dependent on Bc1-2 protein levels. *Oncogene* 2001; **20**: 7128-7133

19 **Ibrahim SM**, Ringel J, Schmidt C, Ringel B, Muller P, Koczan D, Thiesen HJ, Lohr M. Pancreatic adenocarcinoma cell lines show variable susceptibility to TRAIL-mediated cell death. *Pancreas* 2001; **23**: 72-79

20 **Ohshima K**, Sugihara M, Haraoka S, Suzumiya J, Kanda M, Kawasaki C, Shimazaki K, Kikuchi M. Possible immortalization of Hodgkin and Reed-Sternberg cells: telomerase expression, lengthening of telomere, and inhibition of apoptosis by NF-kappaB expression. *Leuk Lymphoma* 2001; **41**: 367-376

21 **Wall NR**, O'Connor DS, Plescia J, Pommier Y, Altieri DC. Suppression of survivin phosphorylation on Thr34 by flavopiridol enhances tumor cell apoptosis. *Cancer Res* 2003; **63**: 230-235

22 **Thornberry NA**, Lazebnik Y. Caspases: enemies within. *Science* 1998; **281**: 1312-1316

23 **Rheaume E**, Cohen LY, Uhlmann F, Lazure C, Alam A, Hurwitz J, Sekaly RP, Denis F. The large subunit of replication factor C is a substrate for Caspase-3 *in vitro* and is cleaved by a Caspase-3-like protease during Fas-mediated apoptosis. *EMBO J* 1997; **16**: 6346-6354

24 **Song Q**, Burrows SR, Smith G, Lees-Miller SP, Kumar S, Chan DW, Trapani JA, Alnemri E, Litwack G, Lu H, Moss DJ, Jackson S, Lavin MF. Interleukin-1 beta-converting enzyme-like protease cleaves DNA-dependent protein kinase in cytotoxic T cell killing. *J Exp Med* 1996; **184**: 619-626

25 **Samali A**, Cotter TG. Heat shock proteins increase resistance to apoptosis. *Exp Cell Res* 1996; **223**: 163-170

26 **Lasunskaia EB**, Fridlianskaia II, Darieva ZA, da Silva MS, Kanashiro MM, Margulis BA. Transfection of NS0 myeloma fusion partner cells with HSP70 gene results in higher hybridoma yield by improving cellular resistance to apoptosis. *Biotechnol Bioeng* 2003; **81**: 496-504

27 **Liu TS**, Musch MW, Sugi K, Walsh-Reitz MM, Ropeleski MJ, Hendrickson BA, Pothoulakis C, Lamont JT, Chang EB. Protective role of HSP72 against Clostridium difficile toxin A-induced intestinal epithelial cell dysfunction. *Am J Physiol Cell Physiol* 2003; **284**: C1073-1082

28 **Diez-Fernandez C**, Andres D, Cascales M. Attenuating effects of heat shock against TGF-beta1-induced apoptosis in cultured rat hepatocytes. *Free Radic Biol Med* 2002; **33**: 835-846

29 **Neuhofer W**, Lugmayr K, Fraek ML, Beck FX. Regulated overexpression of heat shock protein 72 protects Madin-Darby canine kidney cells from the detrimental effects of high urea concentrations. *J Am Soc Nephrol* 2001; **12**: 2565-2571

30 **Gibbons NB**, Watson RW, Coffey RN, Brady HP, Fitzpatrick JM. Heat-shock proteins inhibit induction of prostate cancer cell apoptosis. *Prostate* 2000; **45**: 58-65

31 **Mariggio MA**, Cafaggi S, Ottone M, Parodi B, Vannozzi MO, Mandys V, Viale M. Inhibition of cell growth, induction of apoptosis and mechanism of action of the novel platinum compound cis-diaminechloro-[2-(diethylamino) ethyl 4-aminobenzoate, N(4)]-chloride platinum (II) monohydrochloride monohydrate. *Invest New Drugs* 2004; **1**: 3-16

32 **Dong YG**, Chen DD, He JG, Guan YY. Effects of 15-deoxy-delta12, 14-prostaglandin J2 on cell proliferation and apoptosis in ECV304 endothelial cells. *Acta Pharmacol Sin* 2004; **1**: 47-53

33 **Liu JB**, Gao XG, Lian T, Zhao AZ, Li KZ. Apoptosis of human hepatoma HepG2 cells induced by emodin *in vitro*. *Aizheng* 2003; **22**: 1280-1283

34 **Yoo HG**, Jung SN, Hwang YS, Park JS, Kim MH, Jeong M, Ahn SJ, Ahn BW, Shin BA, Park RK, Jung YD. Involvement of NF-kappaB and Caspases in silibinin-induced apoptosis of endothelial cells. *Int J Mol Med* 2004; **13**: 81-86

35 **Eriguchi M**, Nonaka Y, Yanagie H, Yoshizaki I, Takeda Y, Sekiguchi M. A molecular biological study of anti-tumor mechanisms of an anti-cancer agent Oxaliplatin against established human gastric cancer cell lines. *Biomed Pharmacother* 2003; **57**: 412-415

36 **Dalen H**, Neuzil J. alpha-Tocopheryl succinate sensitises a T lymphoma cell line to TRAIL-induced apoptosis by suppressing NF-kappaB activation. *Br J Cancer* 2003; **88**: 153-158

37 **Biswas DK**, Martin KJ, McAlister C, Cruz AP, Graner E, Dai SC, Pardee AB. Apoptosis caused by chemotherapeutic inhibition of nuclear factor-kappaB activation. *Cancer Res* 2003; **63**: 290-295

38 **Fernandes-Alnemri T**, Litwack G, Alnemri ES. CPP32, a novel human apoptotic protein with homology to Caenorhabditis elegans cell death protein Ced-3 and mammalian interleukin-1 beta-converting enzyme. *J Biol Chem* 1994; **269**: 30761-30764

39 **Tormanen-Napankangas U**, Soini Y, Kahlos K, Kinnula V, Paakko P. Expression of Caspases-3, -6 and -8 and their relation to apoptosis in non-small cell lung carcinoma. *Int J Cancer* 2001; **93**: 192-198

40 **Jaattela M**, Wissing D, Kokholm K, Kallunki T, Egeblad M. Hsp70 exerts its anti-apoptotic function downstream of Caspase-3-like proteases. *EMBO J* 1998; **17**: 6124-6134

41 **Creagh EM**, Carmody RJ, Cotter TG. Heat shock protein 70 inhibits Caspase-dependent and -independent apoptosis in Jurkat T cells. *Exp Cell Res* 2000; **257**: 58-66

Edited by Kumar M and Wang XL **Proofread by** Xu FM

PO Box 2345, Beijing 100023, China
Fax: +86-10-85381893
E-mail: wjg@wjgnet.com www.wjgnet.com

World J Gastroenterol 2004;10(20):2949-2953
World Journal of Gastroenterology
 ISSN 1007-9327

• COLORECTAL CANCER •

Microscopic spread of low rectal cancer in regions of mesorectum: Pathologic assessment with whole-mount sections

Zhao Wang, Zong-Guang Zhou, Cun Wang, Gao-Ping Zhao, You-Dai Chen, Hong-Kai Gao, Xue-Lian Zheng, Rong Wang, Dai-Yun Chen, Wei-Ping Liu

Zhao Wang, Zong-Guang Zhou, Cun Wang, Gao-Ping Zhao, You-Dai Chen, Hong-Kai Gao, Xue-Lian Zheng, Rong Wang, Department of Gastroenterology Surgery and Institution of Digestive Surgery, West China Hospital, Sichuan University, Chengdu 610041, Sichuan Province, China
Dai-Yun Chen, Wei-Ping Liu, Department of Pathology, West China Hospital, Sichuan University, Chengdu 610041, Sichuan Province, China
Supported by the Key Project of National Outstanding Youth Foundation of China, No. 39925032 and National Natural Science Foundation of China, No. 30271283
Correspondence to: Dr. Zong-Guang Zhou, Department of Gastroenterology Surgery and Institute of Digestive Surgery, West China Hospital, Sichuan University, Chengdu 610041, Sichuan Province, China. zhou767@21cn.com
Telephone: +86-28-85422525 **Fax:** +86-28-85422484
Received: 2004-02-02 **Accepted:** 2004-02-18

Abstract

AIM: To assess the microscopic spread of low rectal cancer in mesorectum regions to provide pathological evidence for the necessity of total mesorectal excision (TME).

METHODS: A total of 62 patients with low rectal cancer underwent low anterior resection and TME, surgical specimens were sliced transversely on the serial embedded blocks at 2.5 mm interval, and stained with hematoxylin and eosin (HE). The mesorectum on whole-mount sections was divided into three regions: outer region of mesorectum (ORM), middle region of mesorectum (MRM) and inner region of mesorectum (IRM). Microscopic metastatic foci were investigated microscopically on the sections for the metastatic mesorectal regions, frequency, types, involvement of lymphatic vessels and correlation with the original rectal cancer.

RESULTS: Microscopic spread of the tumor in mesorectum and ORM was observed in 38.7% (24/62) and 25.8% (16/62) of the patients, respectively. Circumferential resection margin (CRM) with involvement of microscopic metastatic foci occurred in 6.5% (4/62) of the patients, and distal mesorectum (DMR) involved was 6.5% (4/62) with the spread extent within 3 cm of low board of the main lesions. Most (20/24) of the patients with microscopic metastasis in mesorectum were in Dukes C stage.

CONCLUSION: Results of the present study support that complete excision of the mesorectum without destruction of the ORM is essential for surgical management of low rectal cancer, an optimal DMR clearance resection margin should be no less than 4 cm, further pathologic assessment of the regions in extramesorectum in the pelvis is needed.

Wang Z, Zhou ZG, Wang C, Zhao GP, Chen YD, Gao HK, Zheng XL, Wang R, Chen DY, Liu WP. Microscopic spread of low rectal cancer in regions of mesorectum: Pathologic assessment with whole-mount sections. *World J Gastroenterol* 2004; 10(20): 2949-2953
http://www.wjgnet.com/1007-9327/10/2949.asp

INTRODUCTION

Local tumor recurrence after surgical resection of rectal cancer remains a major problem. Since Heald *et al*.[1] first reported evidence of isolated tumor deposits in the mesorectum, more authors have demonstrated that residual foci of the tumor within pelvis resulting from inadequate excision of the mesorectum were the cause of such recurrence[2,3]. Further studies revealed that remnant of microscopic tumor nodules in the mesorectum, which cannot easily be detected by imaging preoperatively or by palpation intraoperatively, other than large nodules, contributes to most of local failures[4,5].

Comparison of clinical outcomes between conventional surgery[6,7] and total mesorectal excision (TME)[1,8] showed that a proportion of microscopic tumor nodules of rectal cancer causing local pelvic collapse might settle in the outer region of mesorectum (ORM). Unfortunately, investigations on discrete tumor nodules spread in this region are rare. A comprehensive assessment of ORM in patients with low rectal cancer may provide further pathological evidence for supporting the TME procedure.

Although TME has been extensively employed as a standard procedure for surgical treatment of patients with low rectal cancer in western countries, conventional resection has been dominated in China due to little pathological information standing for TME. The present study investigated the regional spread of microscopic tumor nodules in mesorectum using whole-mount sections.

MATERIALS AND METHODS

Patients

Sixty-two consecutive patients with biopsy-proven adenocarcinoma of the rectum underwent TME at the Division of Gastroenterology Surgery of Affiliated West China Hospital of Sichuan University between November 2001 and June 2002, and specimens were examined prospectively by the same pathologist (Chen DY). Patients (30 males) had a mean age of 58 years (range, 21-78). Lesions were classified as upper or low rectal cancers based on the location of peritoneal reflection, and all diseases from our series were categorized as low rectal cancers with sigmoidoscopy preoperatively. Thirty-two patients had the lower board of primary tumors within 5 cm of anal verge, and another 30 patients had the lower board located not farther than 10 cm from anal verge and above the level of 5 cm from anal verge. None of the patients received any preoperative adjuvant therapy.

Surgical techniques

All patients were operated on by the same chief surgeon (Professor. Zhou ZG) and two assistants according to TME principles[1]. The rectum and mesorectum were mobilized as a package enveloped within the fascia properia with the preservation of autonomic nerves. Under direct vision, electrocautery was used to divide the rectosacral ligament posterior, the peritoneum posterior to the seminal vesicle in the males and the peritoneal reflection in Douglas' pouch in the females anteriorly, lateral ligaments medial to the pelvic plexus laterally. Sharp dissection

was continued down to the pelvic floor in front of Denonvilliers' fascia anteriorly and along the fascia properia posteriorly. Eventually, over 2 cm of distal clearance margin of rectal wall and over 4 cm of mesorectum were attained by transecting the rectum without stretching the bowel wall[9].

Whole-mount sections

Each specimen was straightened without stretching and pinned to a cork board, different from Quirke's method[2]. The specimens were not opened longitudinally along the antimesenteric border, and fixed in 40 g/L buffered formaldehyde for 48 h. Serial longitudinal tissue blocks were cut at 5 mm intervals from the distal portion. Each block, consisting of the full thickness of the rectal wall with the mesorectum, was fixed in 40 g/L buffered formaldehyde for another 48 h, and then embedded in paraffin. Whole-mount sections of the bowel wall and mesorectum were sliced transversely on the embedded tissue blocks in 4 μm at 2.5 mm intervals, stained with hematoxylin and eosin (HE), and examined for discrete tumor nodules microscopically (Figure 1). Circumferential resection margin (CRM) involvement was assessed in the conventional manner[10].

Parameters

The following pathological parameters were used for analysis, namely Dukes stage, differentiation grade, presence of microscopic tumor nodules, local metastasis of lymph nodes, outer region of mesorectum (ORM), distal mesorectum (DMR), CRM (involved ⩽1 mm, or clear >1 mm), and distant metastases. Microscopic metastatic nodules of rectal cancer were defined as tumor nodules ⩽1 mm in diameter, which could not be detected either preoperatively or intraoperatively. Large metastatic nodules of rectal cancer were defined as tumor nodules >5 mm in diameter, most of which could be easily detected by palpation during operation. The mesorectum on the transverse whole-mount section was divided into three regions (Figure 2).

Discrete tumor nodule spread in the mesorectum 1 mm or less away from the outermost board of CRM was recorded as involvement of CRM, and discrete tumor nodule spread in the mesorectum blow the lowest board of primary tumor was defined as involvement of DMR.

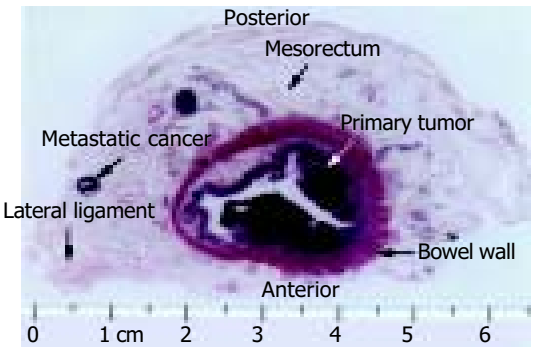

Figure 1 Illustration for regions of mesorectum.

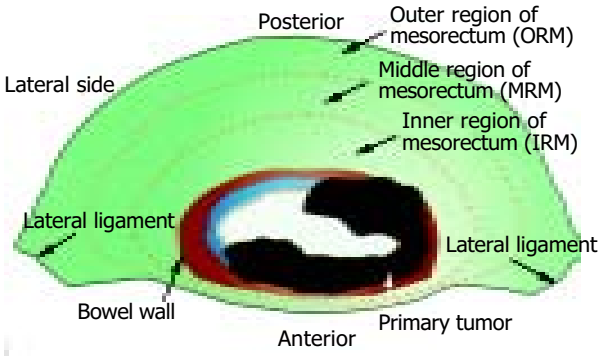

Figure 2 Transverse whole-mount sections of the specimen, HE staining, macroscopic view.

RESULTS

The clinicopathologic characteristics of the patients are summarized in Table 1. All the 62 patients underwent low anterior resection. In 52 patients (83.9%) the operation was potentially curative, while residual tumors in 2 patients (3.3%) were noticed to remain in pelvis on operation and distant metastases were observed in 8 patients (12.9%).

Table 1 Clinicopathologic characteristics of the 62 patients

Parameters	Results
Age (yr, range, mean)	20-78, 58
Sex (No. of patients)	
Male	30
Female	32
Dukes stage (No. of patients)	
A	2
B	10
C	42
D	8
Differentiation grade (No. of patients)	
High	4
Medium	34
Low	24
Distance of the primary tumor from anal verge (No. of patients)	
⩽5 cm	32
>5 cm	30
Diameter of the primary tumor (No. of patients)	
<5 cm	24
⩾5 cm	38

Microscopic spread types and involvement of mesorectum

Four types of microscopic spread of the tumor were observed in mesorectum: discrete microscopic tumor nodules, blood vessel invasion, lymphatic vessel invasion and perineural invasion (Figure 3). Microscopic spread in mesorectum was observed in 38.7% (24 of 62) of the patients (Table 2).

Table 2 Mesorectal regions with involvement of discrete tumor nodules (%)

	Involved mesorectal regions					
	MR	ORM	MRM	IRM	DMR	CRM
Tumor nodules	58.1 (36/62)	45.2 (28/62)	35.5 (22/62)	41.9 (26/62)	6.5 (4/62)	6.5 (4/62)
Microscopic tumor nodules	38.7 (24/62)	25.8 (16/62)	25.8 (16/62)	29.0 (18/62)	6.5 (4/62)	6.5 (4/62)

MR: mesorectum; ORM: outer region of mesorectum; MRM: middle region of mesorectum; IRM: inner region of mesorectum; DMR: distal mesorectum; CRM: circumferential resection margin.

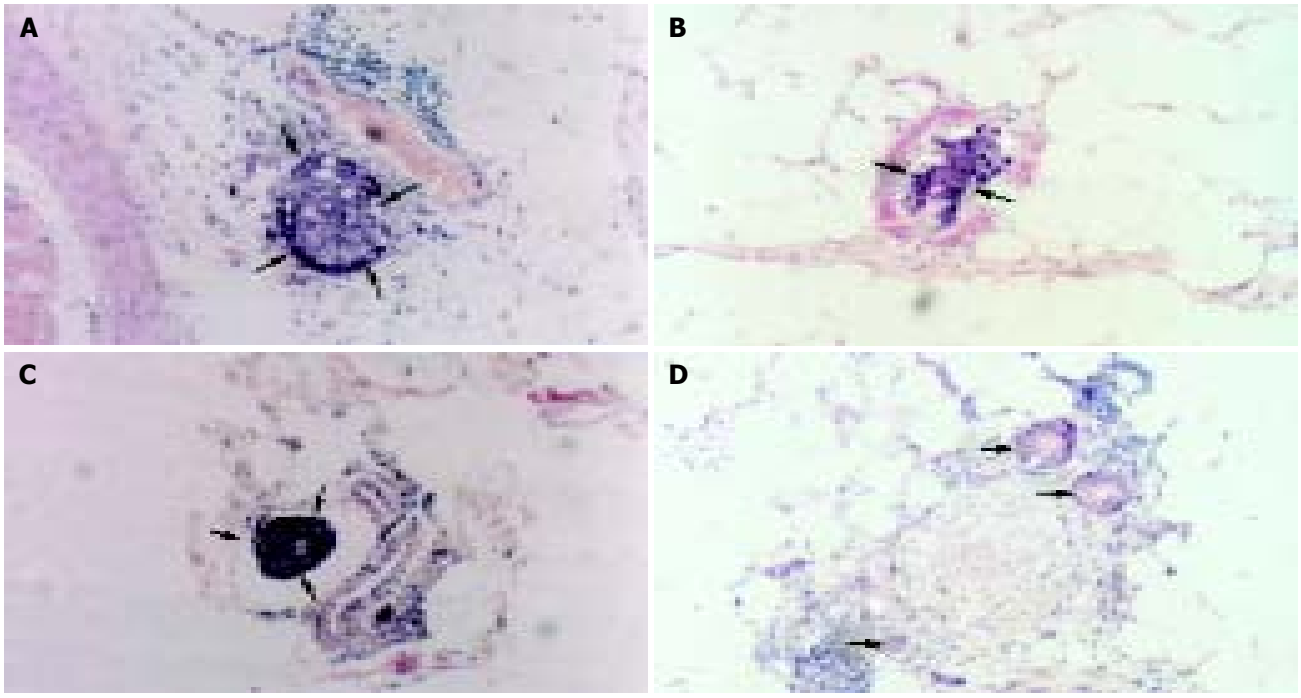

Figure 3 Spread types of microscopic tumor nodules (→) in the mesorectum, HE, ×100. A: Discrete microscopic tumor nodules; B: Blood vessel invasion; C: Lymphatic vessel invasion; D: Perineural invasion.

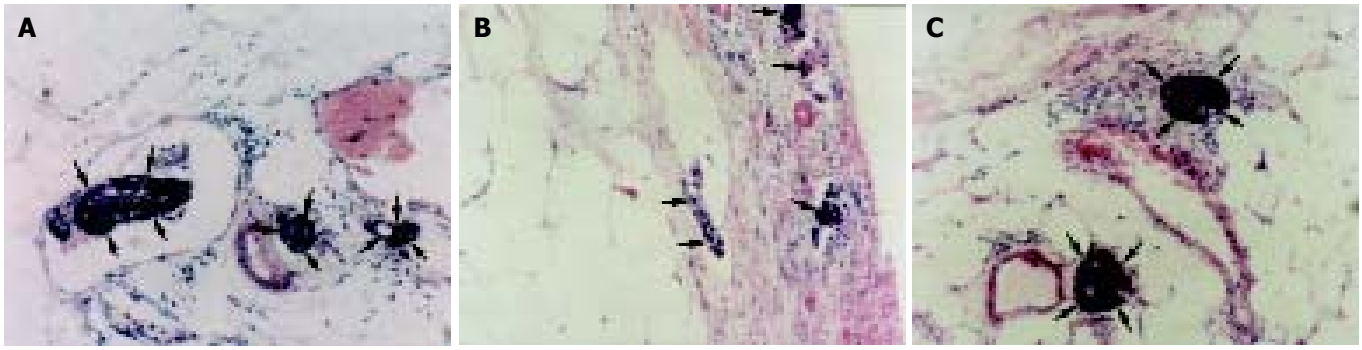

Figure 4 Microscopic tumor nodule spread (→) in outer region of the mesorectum (ORM) (4a), CRM (4b) and DMR(4c) , HE, ×100.

Microscopic spread of the tumor in outer region of mesorectum

Microscopic spread in ORM (Figure 4) occurred in 25.8% (16 of 62) of the patients (Table 2).

Microscopic spread of the tumor in circumferential resection margin

Four of 36 patients with tumor involvement of mesorectum and 2 of the 52 patients having potentially curative resections had microscopic spread in CRM.

Table 3 Mesorectal regional discrete microscopic tumor nodules involving lymph nodes or lymphatic vessels

	Involvement of MR	Involvement of ORM
L type (No. of patients)	16	14
NL type (No. of patients)	18	13

MR: mesorectum; ORM: outer region of mesorectum; L type: involving lymph nodes or lymphatic vessel; NL type: without involving lymph nodes or lymphatic vessels.

Microscopic spread of the tumor in distal mesorectum

DMR with involvement of microscopic tumor nodules was observed in 4 patients. The utmost spread was 3.0 cm or less from the low edge of primary carcinoma. The most extensive distal infiltration was seen in two cases of Dukes stage C.

Table 4 Correlation between mesorectal microscopic spread and primary tumors

Primary tumor	Spread in MR (No. of patients)	Spread in ORM (No. of patients)
Diameter: <5 cm / ⩾5 cm	10 / 14	8 / 8
Differentiation grade: high / medium / low	0 / 10 / 14	0 / 8 / 8
Dukes stage: A / B / C / D	0 / 2 / 20 / 2	0 / 2 / 12 / 2
From anal verge: ⩽5 cm / >5 cm	12 / 12	8 / 8

MR: mesorectum; ORM: outer region of mesorectum.

Microscopic spread of the tumor in mesorectal lymph nodes or lymphatic vessels

Microscopic spread nodules without involvement of lymph nodes or lymphatic vessels in mesorectum were observed in 18 patients, and such a spread in ORM was found in 13 patients (Table 3).

Correlation between regional mesorectal microscopic spread and primary tumors

Most patients (20 of 24) with mesorectal microscopic spread in

MR and 12 of 16 microscopic spreads in ORM were Dukes C stage (Table 4).

Correlation between microscopic tumor nodules and large tumor nodules

Microscopic tumor nodules coexisting with large tumor nodules were observed in 14 of 24 (58.3%) patients with microscopic spread in mesorectum.

DISCUSSION

Whole-mount sections were used to facilitate the precise and effective assessment of rectal cancer, especially in mesorectal regional spread of discontinuous microscopic tumor nodules. All whole-mount sections showed that whole morphological features of the surgical specimen enclosing the primary tumor, bowel wall and the mesorectum, could be directly observed with naked eyes and by microscopy, which enabled the investigators to obtain valuable pathological outcomes on rectal cancer[2,11].

The present study showed the incidence of discrete microscopic tumor nodules was 38.7% (24 of 62) of patients in mesorectum and 25.8% (16 of 62) of patients in ORM. The high frequency of microscopic tumor nodules in mesorectum (especial ORM) highlighted the importance of complete excision of mesorectum with fascia propria circumferentially intact for low rectal cancer. Disturbance of ORM during operation would predispose local recurrence because the undetected microscopic foci in the mesorectum, especially in ORM were easily left behind in pelvis[4,12,13]. Frequency of CRM involvement after conventional resection was reported up to 27%[2,11,14,15], compared with 6.5% after TME[16,17], which is consistent with our findings. The decrease of CRM involvement rates after TME justified the theory: the frequency of microscopic spread in ORM could be very high, and destruction of ORM which often occurred in conventional resection, could easily lead to positive CRM.

Distal mesorectal spread can be evaluated pathologically after TME, after standard resection of the rectal cancer, the DMR remained inside pelvis[18]. Frequency of discrete tumor cancer spread 3 cm or more from the primary lesions in DMR varied from 0 to 10% of the cases[4,17,19-22], and discontinuous spread in DMR could be found even up to 5 cm beyond the lower margin of the primary tumor[1,6], some patients with DMR spread had poor prognosis[21-23]. The present study showed that four cases with tumor involvement of DMR had the spread within 3 cm of primary mural tumors, with a maximum of 3.0 cm. Therefore, we support a safe DMR resection margin of no less than 4 cm for lower rectal cancer, and consider that failure to adequate excision of the involved DRM would risk in leaving behind residual microscopic cancer foci in a significant percentage of patients. The most common pattern of pelvic recurrence is extramural diseases emanating from the sacral hollow or pelvic floor, which is entirely compatible with this hypothesis[24]. But others argued that pathological evidence of DMR spread in itself did not necessarily justify total removal of DMR in all cases because the local recurrence rate and survival rate were not improved significantly even after TME[4,17].

Cawthorn[25] reported that mesorectal involvement of large tumor nodules (greater than 4 mm) was associated with significant poorer prognosis than that of small ones (less than 4 mm). However, the author cautioned that the poor prognosis might result from residual microscopic tumor nodules, which coexist with large nodules and can easily be overlooked and left behind during operation. Ueno *et al*.[13] demonstrated that large tumor nodules and microscopic tumor nodules correlated closely, and that large tumor nodules had a predicting value for existence of microscopic tumor nodules. The present study showed that 58.3% (14/24) patients with microscopic tumor foci involvement of the mesorectum had large tumor nodules (greater than 5 mm) in the mesorectum, which was lower than that reported by Ueno *et al*.

Kapiteijn *et al*. recently reported that standardized TME in combination with preoperative radiotherapy could significantly decrease the local recurrence rate in patients with rectal cancer, though its benefits in survival were not demonstrated because of a relatively short time of follow-up[26]. Other authors also concluded that preoperative radiotherapy could improve the prognosis of patients with rectal cancer[27]. In our series, no patients were treated with adjuvant therapy due to the high frequency of postoperative complications and its controversial impact on prognosis.

Extended lateral dissection beyond the extent of TME has been widely accepted in Japan as the improvement in survival rates was reported[28,29], but some argued that it had a limited advantage in prognosis and the functional problems were considerable[30,31]. Microscopic tumor nodule involvement of CRM after TME in our series suggested that a proportion of the patients had microscopic tumor spread in the extramesorectal regions in the pelvis. Further comprehensive pathological assessment of the extramesorectum is required to evaluate the curative value of TME in rectal cancer.

REFERENCES

1 **Heald RJ**, Husband EM, Ryall RD. The mesorectum in rectal cancer surgery-the clue to pelvic recurrence? *Br J Surg* 1982; **69**: 613-616

2 **Quirke P**, Durdey P, Dixon MF, Williams NS. Local recurrence of rectal adenocarcinoma due to inadequate surgical resection. Histopathological study of lateral tumour spread and surgical excision. *Lancet* 1986; **2**: 996-999

3 **Ratto C**, Ricci R, Rossi C, Morelli U, Vecchio FM, Doglietto GB. Mesorectal microfoci adversely affect the prognosis of patients with rectal cancer. *Dis Colon Rectum* 2002; **45**: 733-742

4 **Ono C**, Yoshinaga K, Enomoto M, Sugihara K. Discontinuous rectal cancer spread in the mesorectum and the optimal distal clearance margin *in situ*. *Dis Colon Rectum* 2002; **45**: 744-749

5 **Andreola S**, Leo E, Belli F, Gallino G, Sirizzotti G, Sampietro G. Adenocarcinoma of the lower third of the rectum: metastases in lymph nodes smaller than 5 mm and occult micrometastases; preliminary results on early tumor recurrence. *Ann Surg Oncol* 2001; **8**: 413-417

6 **Reynolds JV**, Joyce WP, Dolan J, Sheahan K, Hyland JM. Pathological evidence in support of total mesorectal excision in the management of rectal cancer. *Br J Surg* 1996; **83**: 1112-1115

7 **McCall JL**, Cox MR, Wattchow DA. Analysis of local recurrence rates after surgery alone for rectal cancer. *Int J Colorectal Dis* 1995; **10**: 126-132

8 **Enker WE**. Total mesorectal excision—the new golden standard of surgery for rectal cancer. *Ann Med* 1997; **29**: 127-133

9 **Zhou ZG,** Wang Z, Yu YY, Shu Y, Cheng Z, Li L, Lei WZ, Wang TC. Laparoscopic total mesorectal excision of low rectal cancer with preservation of anal sphincter: A report of 82 cases. *World J Gastroenterol* 2003; **9**: 1477-1481

10 **Quirke P**, Dixon MF. The prediction of local recurrence in rectal adenocarcinoma by histopathological examination. *Int J Colorectal Dis* 1988; **3**: 127-131

11 **Ng IO**, Luk IS, Yuen ST, Lau PW, Pritchett CJ, Ng M, Poon GP, Ho J. Surgical lateral clearance in resected rectal carcinomas. A multivariate analysis of clinicopathologic features. *Cancer* 1993; **71**: 1972-1976

12 **Paty PB**, Enker WE, Cohen AM, Lauwers GY. Treatment of rectal cancer by low anterior resection with coloanal anastomosis. *Ann Surg* 1994; **219**: 365-373

13 **Ueno H**, Mochizuki H, Tamakuma S. Prognostic significance of extranodal microscopic foci discontinuous with primary lesion in rectal cancer. *Dis Colon Rectum* 1998; **41**: 55-61

14 **Adam IJ**, Mohamdee MO, Martin IG, Scott N, Finan PJ, Johnston D, Dixon MF, Quirke P. Role of circumferential margin involvement in the local recurrence of rectal cancer. *Lancet* 1994; **344**: 707-711

15 **de Haas-Kock DF**, Baeten CG, Jager JJ, Langendijk JA, Schouten LJ, Volovics A, Arends JW. Prognostic significance of radial margins of clearance in rectal cancer. *Br J Surg* 1996; **83**: 781-785
16 **Cawthorn SJ**, Gibbs NM, Marks CG. Clearance technique for the detection of lymph nodes in colorectal cancer. *Br J Surg* 1986; **73**: 58-60
17 **Scott N**, Jackson P, al-Jaberi T, Dixon MF, Quirke P, Finan PJ. Total mesorectal excision and local recurrence: a study of tumour spread in the mesorectum distal to rectal cancer. *Br J Surg* 1995; **82**: 1031-1033
18 **McCall JL**. Total mesorectal excision: evaluating the evidence. *Aust N Z J Surg* 1997; **67**: 599-602
19 **Madsen PM**, Christiansen J. Distal intramural spread of rectal carcinomas. *Dis Colon Rectum* 1986; **29**: 279-282
20 **Williams NS**. The rationale for preservation of the anal sphincter in patients with low rectal cancer. *Br J Surg* 1984; **71**: 575-581
21 **Shirouzu K**, Isomoto H, Kakegawa T. Distal spread of rectal cancer and optimal distal margin of resection for sphincter-preserving surgery. *Cancer* 1995; **76**: 388-392
22 **Williams NS**, Dixon MF, Johnston D. Reappraisal of the 5 centimetre rule of distal excision for carcinoma of the rectum: a study of distal intramural spread and of patients' survival. *Br J Surg* 1983; **70**: 150-154
23 **Penfold JC**. A comparison of restorative resection of carcinoma of the middle third of the rectum with abdominoperineal excision. *Aust N Z J Surg* 1974; **44**: 354-356
24 **Pilipshen SJ**, Heilweil M, Quan SH, Sternberg SS, Enker WE. Patterns of pelvic recurrence following definitive resections of rectal cancer. *Cancer* 1984; **53**: 1354-1362
25 **Cawthorn SJ**, Parums DV, Gibbs NM, A'Hern RP, Caffarey SM, Broughton CI, Marks CG. Extent of mesorectal spread and involvement of lateral resection margin as prognostic factors after surgery for rectal cancer. *Lancet* 1990; **335**: 1055-1059
26 **Kapiteijn E**, Marijnen CA, Nagtegaal ID, Putter H, Steup WH, Wiggers T, Rutten HJ, Pahlman L, Glimelius B, van Krieken JH, Leer JW, van de Velde CJ. Preoperative radiotherapy combined with total mesorectal excision for resectable rectal cancer. *N Engl J Med* 2001; **345**: 638-646
27 **Camma C**, Giunta M, Fiorica F, Pagliaro L, Craxi A, Cottone M. Preoperative radiotherapy for resectable rectal cancer: A meta-analysis. *JAMA* 2000; **284**: 1008-1015
28 **Koyama Y**, Moriya Y, Hojo K. Effects of extended systematic lymphadenectomy for adenocarcinoma of the rectum-significant improvement of survival rate and decrease of local recurrence. *Jpn J Clin Oncol* 1984; **14**: 623-632
29 **Moriya Y**, Hojo K, Sawada T, Koyama Y. Significance of lateral node dissection for advanced rectal carcinoma at orbelow the peritoneal reflection. *Dis Colon Rectum* 1989; **32**: 307-315
30 **Glass RE**, Ritchie JK, Thompson HR, Mann CV. The results of surgical treatment of cancer of the rectum by radical resection and extended abdomino-iliac lymphadenectomy. *Br J Surg* 1985; **72**: 599-601
31 **Scholefield JH**, Steup WH. Surgery for rectal cancer in Japan. *Lancet* 1992; **340**: 1101

Edited by Ren SY and Wang XL **Proofread by** Xu FM

PO Box 2345, Beijing 100023, China
Fax: +86-10-85381893
E-mail: wjg@wjgnet.com www.wjgnet.com

World J Gastroenterol 2004;10(20):2954-2957
World Journal of Gastroenterology
 ISSN 1007-9327

• COLORECTAL CANCER •

Targeting cyclooxygenase-2 with sodium butyrate and NSAIDs on colorectal adenoma/carcinoma cells

Zhi-Hong Zhang, Qin Ouyang, Hua-Tian Gan

Zhi-Hong Zhang, Qin Ouyang, Hua-Tian Gan, Department of Gastroenterology, First Hospital, Western China University of Medical Sciences, Chengdu 610041, Sichuan Province, China
Supported by the Scientific Foundation of Sichuan Province, No. 174
Correspondence to: Zhi-Hong Zhang, Department of Gastroenterology, First Hospital, Western China University of Medical Sciences, Chengdu 610041, Sichuan Province, China. zhang-821@21cn.com
Telephone: +86-28-85081923
Received: 2002-07-17 **Accepted:** 2002-11-04

Abstract

AIM: The protective effects of sodium butyrate and NSAIDs (especially the highly selective COX-2 inhibitors) have attracted considerable interest recently. In this study, primary adenoma cells and HT-29 were used to investigate whether the above drugs would be effective for reducing proliferation and inducing apoptosis. Additionally, it was investigated whether NSAIDs would strengthen the effects of sodium butyrate and its possible mechanisms.

METHODS: *In vitro* primary cell culture of colorectal adenomas and HT-29 were used for this investigation. PGE_2 isolated from HT-29 cell culture supernatants was investigated by ELISA. MTT was employed to detect the anti-proliferative effects on both adenoma and HT-29 culture cells. FCM was used for apoptosis rate and cell cycle analysis. The morphology of apoptotic cells was investigated by means of electromicroscopy.

RESULTS: Sodium butyrate could stimulate the secretion of PGE_2, while NSAIDs inhibited it to below 30 pg/10^6 cells. Both butyrate and NSAIDs could inhibit cell proliferation and induce apoptosis. The effects were time- and dose-dependent ($P<0.05$). Aspirin and NS-398 could enhance the effects of sodium butyrate. The effects were stronger while sodium butyrate was used in combination with NS-398 than it was used in combination with Aspirin.

CONCLUSION: Butyrate and NSAIDs could inhibit cell proliferation and induce apoptosis respectively. NSAIDs could enhance the effects of sodium butyrate by down-regulating COX-2 expression. Selective COX-2 inhibitor is better than traditional NSAIDs.

Zhang ZH, Ouyang Q, Gan HT. Targeting cyclooxygenase-2 with sodium butyrate and NSAIDs on colorectal adenoma/carcinoma cells. *World J Gastroenterol* 2004; 10(20): 2954-2957
http://www.wjgnet.com/1007-9327/10/2954.asp

INTRODUCTION

Colorectal cancer remains the major cause of cancer-related mortality in the developed countries. With improvement in economic status, the incidence of colorectal cancer is increasing in China. Prevention of the disease is a more attractive approach to dealing with the problem than treatment of existing disease for both medical and fiscal reasons. Clinical evidences showed that removal of colorectal adenoma could attenuate 76-90% risk of colorectal cancer, but the yearly relapse rate has reached 10-15%. Therefore, the urgent task is to develop new strategies to prevent the disease. With regard to chemoprevention, butyrate sodium (sodium butyrate) and non-steroidal anti-inflammatory drugs (NSAIDs), especially selective COX-2 inhibitors have attracted more attention.

Evidences have shown that low fat and high dietary fiber diet could protect against colorectal cancer. Dietary fiber could be fermented by symbiotic bacteria in the large bowel and then a short chain fatty acid-butyrate, could be released. Clinical and laboratory studies showed that butyrate might be beneficial to the development of colorectal cancer and even in the early stage of its premalignant status[1].

NSAIDs have shown its promising role in colorectal cancer chemoprevention in recent years. Epidemic studies demonstrated that it might reduce 40-50% risk of colorectal cancer in persons who took aspirin or other NSAIDs on a regular basis[2]. The most recognized target for NSAIDs was cyclooxygenase (COX), because COX-2 showed 86% and 43% expression in colorectal adenoma and carcinoma tissues respectively[17]. Furthermore, COX-2 selective inhibitors have attracted more attention because of their minimal risk of gastrointestinal side effects.

Although the precise mechanisms are unclear, sodium butyrate and NSAIDs are involved in chemoprevention of colorectal cancer. In this study, colorectal adenoma cells and HT-29 cells were used to investigate whether the above agents were effective in reducing proliferation and inducing apoptosis, and whether NSAIDs could strengthen the effects of sodium butyrate and its possible mechanisms.

MATERIALS AND METHODS

Materials

NS-398 was a gift from Dr. W Sternson (Washington University). EGF was from Dr. Ouyang Xueshong (Hong Kong University). Sodium butyrate, aspirin, collagenaes type IV, hyaluronidase type IV were purchased from Sigma Chemical Co. Prostaglandin E_2 EIA kit was from Cayman Chemical. Arachidonic acid, insulin, FBS was from GIBIO Co.

Colorectal adenoma specimens were from resection through colonoscopy in the Endoscopic Center, First Hospital of Western China University of Medical Sciences. HT-29 was a gift from Immuno-Transplation Laboratory, First Hospital of Western China University of Medical Sciences.

Methods

Cell cultures Adenoma specimens were washed at least 10 times in PBS containing penicillin (1 000 U/mL), streptomycin (1 000 U/mL), amphotericin B (3 μg/mL). The minced tissues were digested by DMEM containing collagenaes type IV (1.5 mg/mL), hyaluronidase type IV (0.25 mg/mL) for 2 h until the tissues were dispersed into individual crypts, then they were incubated at 37 ℃, 50 mL/L CO_2 in growth medium consisting of DMEM, 50 mL/L FBS, 0.5 μg/mL insulin, 1 μg/mL hydrocortisone, 5 μg/mL transferrin, 20 ng/mL EGF, 5×10^{-9} Na_2SeO_3, 0.1 μg/mL pentagastrin, 2 mmol/L glutamine, 200 U/mL penicillin, 200 U/mL

streptomycin. The culture cells were identified as epithelial origin by immunohistochemical staining and electro microscopy (data not shown). HT-29 was cultured in standard growth condition containing DMEM, 100 g/L LBS, 200 U/mL penicillin and streptomycin.

Preparation of drugs

Sodium butyrate was dissolved in culture medium. Aspirin and NS-398 were in DMSO, and the final concentration was less than 3.3 mL/L. The drugs below were used to measure PGE_2, MTT and FCM. Sodium butyrate: 2 mmol/L, 4 mmol/L, 6 mmol/L; Aspirin: 1 mmol/L, 5 mmol/L, 10 mmol/L, 20 mmol/L; NS-398: 0.1 μmol/L, 1 μmol/L, 10 μmol/L, 50 μmol/L; 2 mmol/L Sodium butyrate+10 mmol/L Aspirin; 2 mmol/L Sodium butyrate+ 10 μmol/L NS-398. For electro microscopy, 2 mmol/L Sodium butyrate, 10 mmol/L aspirin or 10 μmol/L NS-398 was used.

Prostaglandin E_2 (PGE_2) immunoassay

HT-29 cells were seeded at a density of 1×10^6 cells/T25 flask for 48 h, and then treated with medicine for 24 h or 72 h separately. Aliquots of culture medium (1 mL) were stored at -70 ℃ until assayed (In NSAIDs treatments and control groups, an exogenous supply of 10 μmol/L AA was added to pre-treat for 30 min individually). Immunoassay was carried out according to the manufacturer's protocol. The sensitivity of the assay was 10 pg/mL.

Proliferation assays

Cell proliferation of both primary adenoma cells and HT-29 was assessed by MTT. After seeded at a density of 2×10^4 cells/well for 96 well plates with 100 μL media for 48 h, the cells were treated with medicine for 24 h or 72 h separately. At the end of incubation, the medium was removed and 20 μL MTT solution was added to each well. Then DMSO was added to each well, the optical density of each well was read on the plate reader at 570 nm.

The inhibition rate = (1- tested group optical density/the control optical density)×100%.

Flow cytometric analysis

After HT-29 cells were harvested , they were fixed in 700 mL/L ethanol overnight at 4 ℃, mixed with PI staining fluid for 20 min at 4 ℃ and then filtered. At last, the samples were examined by FCM.

Electro microscopy

The collected HT-29 cells were fixed in 30 g/L glutaraldehyde, then rinsed in 10 g/L osmium textroxide for 30 min at 4 ℃, dehydrated through a series of acetone, embedded in EPON polymerized at 60 ℃, stained with uranyl acetate and Raynold lead citrate. Finally, the sections were examined under an electron microscope.

Statistical analysis

PGE_2 expression and growth inhibition were statistically analyzed by two-way ANOVA. Comparison among the groups was analyzed by L-S-D. The apoptotic rate was analyzed by χ^2. All data were analyzed by SPSS.

RESULTS

PGE_2 production in HT-29 cells

With the increase of optical density, PGE_2 production was decreased in standard culture condition. Sodium butyrate 2 mmol/L was enough for stimulating the secretion of PGE_2 1 306 pg/10^6 cells compared with control values of 69 pg/10^6 cells in 24 h (P<0.05), but it was not time-and dose-dependent. 2 mmol/L\ 4 mmol/L\6 mmol/L sodium butyrate separately stimulated the secretion of PGE_2 1306 \1230\1385 (pg/10^6 cells). And the same concentration of sodium butyrate had no statistical differential effects in 24 h and 72 h. In contrast, NSAIDs (aspirin and NS-398) could completely inhibit PGE_2 secretion in a time-and dose-independent manner (P<0.001). After incubated for 30 min with 10 umol/L AA, PGE_2 production reached 1 470 pg/10^6 cells in control, while 1-20 mmol/L aspirin reduced the PGE_2 levels to below 30 pg/10^6 cells and 0.1-50 umol/L NS-398 reached 477 pg/10^6 cells-25 pg/10^6 cells. NS-398 was different in time- and concentration-dependence from aspirin. Sodium butyrate in combination with NSAIDs showed PGE_2 production inhibition (<30 pg/10^6 cells) (Table 1).

Sodium butyrate and NSAIDs had dose- or time-dependent anti-proliferative effects on HT-29 and adenoma cells

The anti-proliferative effects on HT-29 and adenoma cells were obvious concentration- and time- dependent (P<0.05). 2-6 mmol/L sodium butyrate after 24 h showed 4.3-12.6% on HT-29 and 5.7-11.9% on adenoma cells. They reached 23.7-62.9% and 19-30.5% after 72 h. In agreement with NS-398 and aspirin, the effect was stronger on NS-398 than on aspirin with the same concentration. 1-20 mmol/L aspirin could inhibit the cell proliferation 18.5-57.1% after 24 h and 48.5-76.6% after 72 h, while 0.1-50 μmol/L NS-398 reached 4.5-24% after 24 h and 52.2-68.5% after 72 h. The effects were more obvious on the adenoma cells. Treatment with both Sodium butyrate and NSAIDs resulted in an increase in anti-proliferative effects compared with Sodium butyrate treatment alone for HT-29, and the effects were time-dependent (Table 2).

But for adenoma cells, the results were different in repeated experiments. Only treatment with Sodium butyrate and NS-398 for 72 h showed the synergistic effects on 28.6% adenoma specimens (P<0.05).

Moreover, HT-29 cell cycle distribution was analyzed by FCM. Both Sodium butyrate and NSAIDs could arrest the cell cycle in S phase compared with the control (P<0.05), but the response to G_1/G_1 or G_2 phase was different.

Induction of apoptosis effects was dose-dependent in HT-29

Normal primary culture cells and HT-29 showed irregular polygon-appearances. The cells treated with the drugs shrank and became round, then shad from the wall and floated in the fluid. The floating cells showed blue coloration by trypan blue staining, while the attached cells were achromatical.

As expected, the dose-dependent apoptotic effects on HT-29 cells treated with Sodium butyrate or NSAIDs could be seen

Table 1 PGE_2 (pg/10^6 cells) production in HT-29 treated with Sodium butyrate and/or NSAIDs

Production of PGE2	2 mmol/L sodium butyrate	10 mmol/L aspirin	10 μmol/L NS-398	Sodium butyrate+aspirin	Sodium butyrate+NS-398
24 h	1 306±5.6	13.2±4.1	35.2±3.5	14.9±1.9	45.9±2.9
72 h	1 427±7.1	5.61±2.7	5.95±2.2	6.5±1.0	8.49±1.3

Table 2 Comparison of growth inhibition effects on HT-29 with Sodium butyrate alone or in combination with NSAIDs (%)

Time	2 mmol/L sodium butyrate	10 mmol/L aspirin	10 umol/L NS-398	Sodium butyrate+aspirin	Sodium butyrate+NS-398
24 h	4.28	55	10.2	58.3	26
72 h	23.7	72.2	63.9	81.9	70.5

Table 3 Percentage of HT-29 apoptotic cell rate (%)

	Control	Aspirin (mmol/L)			NS-398 (μmol/L)				Sodium butyrate (mmol/L)		
Concentration		1	5	10	20	0.1	1	10	50	2	4	6
Apoptotic rate	4.2±1.3	8.3±1.6	10.9±2.0	11.9±2.7	29.7±3.1	6±1.4	7.8±1.7	12.5±3.1	19.5±3.4	10.7±2.5	15.9±0.9	23.2±4.1

(P<0.05) (Table 3). Sodium butyrate with NS-398 had more preferential apoptotic effects (14.7%) compared with Sodium butyrate alone (10.7%) or Sodium butyrate in combination with aspirin (13.3%).

To confirm the induction of apoptosis, the morphological appearances of HT-29 cells were examined by elecotromicroscopy. Typical apoptotic appearances are shown in Figure 1, which included cell shrinkage, nuclear condensation, and formation of apoptotic bodies, *etc*.

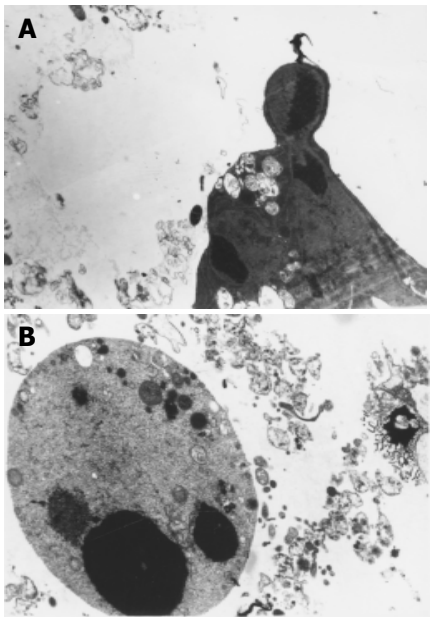

Figure 1 Morphological appearances of HT -29 cells. A: Typical appearances of apoptotic cells; B: Illustration of apoptotic bodies.

DISCUSSION

In recent years, the incidence of colorectal cancer is increasing in China. Prevention of the disease is a more attractive approach in the early stage of adenoma-cancer progression. Butyrate and NSAIDs (especially highly selective COX-2 inhibitors) have attracted considerable attention recently.

As a byproduct of carbohydrates fermented by symbiotic bacteria, butyrate has been demonstrated its important role in inhibiting cell growth and in inducing apoptosis of colorectal cancer cells *in vitro*[3]. Clinical case-control and cohort studies have shown a 40-50% reduction in colorectal cancer-related mortality in individuals taking aspirin and other NSAIDs on a regular basis compared with those not taking these agents[2]. Aspirin serves as a typical representative of classical NSAID agents. As a highly selective COX-2 inhibitor, NS-398 showed higher selective effects than others. Its IC_{50}(COX-2/COX-1) was 0.0005, while L-745, 337 was 0.003, flosulide was 0.001[4], rofecoxib was 0.0012[5]. Although the precise mechanism underlying the protective effects of NSAIDs is unclear, COX-2 could play a key role in intestinal tumorigenesis[6] and has been a widely recognized target because of its high expression in colorectal adenoma and cancer tissues[7-10]. The COX-2-dependent mechanism involving in increased angiogenesis[11-13], could reduce apoptotic susceptibility by inhibiting the cytochrome c-dependent apoptotic pathway[14]. Down-regulation of bcl_2 and CD44v6 expression and up-regulation of nm23 expression[15] could inhibit death receptor 5 expression and confer resistance to tumor necrosis factor-related apoptosis-inducing ligand (TRAIL)-induced apoptosis[16]. However, some COX-independent ways, such as lipoxgenase (LOX) another AA metabolic enzyme, could modulate sodium butyrate-induced apoptosis and cell differentiation[17]. Leukotriene (LT) D (4)/CysLT (1) R signaling could facilitate survival of colon cancer cells and LTs were accessible targets for pharmacologic treatment like COX-2[18], NF-KB/I-KB system[19]. Activated Ras and TGF-β could collaborate to increase the invasive response[20], *etc*, which have been shown to be involved in the protective mechanism. In this study, adenoma cells and HT-29 were investigated whether Sodium butyrate and aspirin/NS-398 were the effective adjuvants for the protective effects.

The relationship between PGE_2 (an AA metabolize product) and colorectal carcinogenesis is still disputed. Generally, PGE_2 could combine with the transcription factor PPARr, which activates the target gene transcription and promotes carcinogenesis[21]. PGE_2 could also increase bcl-2 expression and inhibit cell apoptosis[22] and was involved in the angiogenesis of cancers. So it has been implicated that PGE_2 inhibition is the main mechanism of anticarcinogenesis of NSAIDs. But a positive result showed that exogenous PGE_2 could not reverse the antineoplastic effects of sulindac sulfone[23]. In this study, PGE_2 production was investigated to reflect the COX-2 enzyme activity indirectly. For HT-29, Sodium butyrate could stimulate its PGE_2 secretion in a time- and dose-independent manner, suggesting that it could increase its COX-2 enzyme activity. In contrast, NSAIDs inhibited PGE_2 production. Although previous evidence displayed that the expression of COX-2 was increased by some NSAIDs and TGF-β[24], we proposed that the inhibited enzyme activity would still down-regulate the effects of NSAIDs.

Sodium butyrate could reduce cell proliferation and induce cell apoptosis in a time- and dose-dependent manner. The possible mechanism has been known to involve in a large number of parameters, including inhibition of histone deacetylase and induction of caspase-3 protease activity with a mitochondrial/cytochrome c-dependent pathway[25], enhancement of Fas-mediated apoptosis[26], inhibition of P53 expression[25]. Down-regulation of GATA-6 and up-regulation of 15-LO-1 were observed after treatment with sodium butyrate (sodium butyrate), which was also involved in stimulating cell apoptosis and cell differentiation[27]. NSAIDs had the same effects on both cell lines. This was not in a time- and dose-dependent manner. Therefore, it implied that anti-neoplastic mechanisms of NSAIDs were COX-2-dependent and COX-2-independent.

Compared with the effects on adenoma and carcinoma cells, NSAIDs had stronger inhibitory effects on carcinoma cells than on adenoma cells with MTT. Maybe the cause laid in the primarily cultured adenoma cells from different specimens, which resulted in the individual characterization of COX-2 expression and cell proliferation. Other studies gave the same conclusion that NSAIDs had stronger effects on HT-29 carcinoma cells (high COX-2 expression) than on S/KS cells (lack of COX-2 expression).

Previous studies revealed that COX-2 expression up-regulation would induce resistance to apoptosis induced by sodium butyrate. Because NSAIDs could down-regulate COX-2

expression, whether NSAIDs could sensitize the cells to the action of sodium butyrate and reduce the potential side-effects and increase the efficacy by using both drugs was investigated in this study. The data showed that NSAIDs inhibited the growth of HT-29 by sodium butyrate by down-regulating COX-2 expression. It was in agreement with the previous studies. In contrast, other studies reported that cooperation with the two agents was greatly dependent on the category of cell lines and NSAIDs, especially highly selective COX-2 inhibitors showed more preferential effects. Only HT-29 cell line was investigated in this study, so it was necessary to investigate other cell lines for more precise results. Cooperation with the two drugs could affect the two cell lines differently. The effects on HT-29 were completely shown, but only 28.6% was positive for primary adenoma specimens. The main cause depended on the adenoma samples. Additionally, treatment with NS-398 and sodium butyrate had more preferential effects than that with aspirin and sodium butyrate, suggesting that specific selective COX-2 inhibitor NS-398 had a more promising future in clinical application.

In summary, sodium butyrate and NSAIDs could inhibit the cell proliferation and induce cell apoptosis through a number of mechanisms. Combination of two kinds of agents would enhance the above effects by down-regulating COX-2 expression, which could serve as a promising chemoprevention for colorectal neoplasm.

REFERENCES

1 **Young GP,** McIntyre A, Albert V, Folino M, Muir JG, Gibson PR. Wheat bran suppresses potato starch-potentiated colorectal tumorigenesis at the aberrant crypt stage in a rat model. *Gastroenterology* 1996; **110**: 508-514

2 **Smalley WE,** DuBois RN. Colorectal cancer and nonsteroidal anti-inflammatory drugs. *Adv Pharmacol* 1997; **39**: 1-20

3 **Hernandez A,** Thomas R, Smith F, Sandberg J, Kim S, Chung DH, Evers BM. Butyrate sensitizes human colon cancer cells to TRAIL-mediated apoptosis. *Surgery* 2001; **130**: 265-272

4 **Cromlish WA**, Kennedy BP. Selective inhibition of cyclooxygenase-1 and –2 using intact insect cell assays. *Biochem Pharmacol* 1996; **52**: 1777-1785

5 **Ehrich EW,** Dallob A, De Lepeleire I, Van Hecken A, Riendeau D, Yuan W, Porras A, Wittreich J, Seibold JR, De Schepper P, Mehlisch DR, Gertz BJ. Characterization of rofecoxib as a cyclooxygenase-2 isoform inhibitor and demonstration of analgesia in the dental pain model. *Clin Pharmacol Ther* 1999; **65**: 336-347

6 **Sonoshita M,** Takaku K, Oshima M, Sugihara K, Taketo MM. Cyclooxygenase-2 expression in fibroblasts and endothelial cells of intestinal polyps. *Cancer Res* 2002; **62**: 6846-6849

7 **Eberhart CE,** Coffey RJ, Radhika A, Giardiello FM, Ferrenbach S, DuBois RN. Up-regulation of cyclooxygenase 2 gene expression in human colorectal adenomas and adenocarcinomas. *Gastroenterology* 1994; **107**: 1183-1188

8 **Takeuchi M,** Kobayashi M, Ajioka Y, Honma T, Suzuki Y, Azumaya M, Narisawa R, Hayashi S, Asakura H. Comparison of cyclo-oxygenase 2 expression in colorectal serrated adenomas to expression in tubular adenomas and hyperplastic polyps. *Int J Colorectal Dis* 2002; **17**: 144-149

9 **McEntee MF,** Cates JM, Neilsen N. Cyclooxygenase-2 expression in spontaneous intestinal neoplasia of domestic dogs. *Vet Pathol* 2002; **39**: 428-436

10 **Zhang H,** Sun XF. Overexpression of cyclooxygenase-2 correlates with advanced stages of colorectal cancer. *Am J Gastroenterol* 2002; **97**: 1037-1041

11 **Chapple KS,** Scott N, Guillou PJ, Coletta PL, Hull MA. Interstitial cell cyclooxygenase-2 expression is associated with increased angiogenesis in human sporadic colorectal adenomas. *J Pathol* 2002; **198**: 435-441

12 **Deng WG,** Saunders MA, Gilroy DW, He XZ, Yeh H, Zhu Y, Shtivelband MI, Ruan KH, Wu KK. Purification and characterization of a cyclooxygenase-2 and angiogenesis suppressing factor produced by human fibroblasts. *FASEB J* 2002; **16**: 1286-1288

13 **Cianchi F,** Cortesini C, Bechi P, Fantappie O, Messerini L, Vannacci A, Sardi I, Baroni G, Boddi V, Mazzanti R, Masini E. Up-regulation of cyclooxygenase 2 gene expression correlates with tumor angiogenesis in human colorectal cancer. *Gastroenterology* 2001; **121**: 1339-1347

14 **Sun Y,** Tang XM, Half E, Kuo MT, Sinicrope FA. Cyclooxygenase-2 overexpression reduces apoptotic susceptibility by inhibiting the cytochrome c-dependent apoptotic pathway in human colon cancer cells. *Cancer Res* 2002; **62**: 6323-6328

15 **Yu HG,** Huang JA, Yang YN, Huang H, Luo HS, Yu JP, Meier JJ, Schrader H, Bastian A, Schmidt WE, Schmitz F. The effects of acetylsalicylic acid on proliferation, apoptosis, and invasion of cyclooxygenase-2 negative colon cancer cells. *Eur J Clin Invest* 2002; **32**: 838-846

16 **Tang X,** Sun YJ, Half E, Kuo MT, Sinicrope F. Cyclooxygenase-2 overexpression inhibits death receptor 5 expression and confers resistance to tumor necrosis factor-related apoptosis-inducing ligand-induced apoptosis in human colon cancer cells. *Cancer Res* 2002; **62**: 4903-4908

17 **Ikawa H,** Kamitani H, Calvo BF, Foley JF, Eling TE. Expression of 15-lipoxygenase-1 in human colorectal cancer. *Cancer Res* 1999; **59**: 360-366

18 **Ohd JF,** Nielsen CK, Campbell J, Landberg G, Lofberg H, Sjolander A. Expression of the leukotriene D4 receptor CysLT1, COX-2, and other cell survival factors in colorectal adenocarcinomas. *Gastroenterology* 2003; **124**: 57-70

19 **Yin MJ,** Yamamoto Y, Gaynor RB. The anti-inflammatory agents aspirin and salicylate inhibit the activity of I(kappa)B kinase-β. *Nature* 1998; **396**: 77-80

20 **Roman CD,** Morrow J, Whitehead R, Beauchamp RD. Induction of cyclooxygenase-2 and invasiveness by transforming growth factor-beta (1) in immortalized mouse colonocytes expressing oncogenic Ras. *J Gastrointest Surg* 2002; **6**: 304-309

21 **Lefebvre AM,** Chen I, Desreumaux P, Najib J, Fruchart JC, Geboes K, Briggs M, Heyman R, Auwerx J. Activation of the peroxisome proliferator- activated receptor γ promotes the development of colon tumors in C57BL/6J-APCMin/+mice. *Nat Med* 1998; **4**: 1053-1057

22 **Sheng H,** Shao J, Morrow JD, Beauchamp RD, DuBois RN. Modulation of apoptosis and Bcl-2 expression by prostaglandin E2 in human colon cancer cells. *Cancer Res* 1998; **58**: 362-366

23 **Piazza GA,** Rahm AL, Krutzsch M, Sperl G, Paranka NS, Gross PH, Brendel K, Burt RW, Alberts DS, Pamukcu R. Antineoplastic drugs sulindac sulfide and sulfone inhibit cell growth by inducing apoptosis. *Cancer Res* 1995; **55**: 3110-3116

24 **Sheng H,** Shao J, O'Mahony CA, Lamps L, Albo D, Isakson PC, Berger DH, DuBois RN, Beauchamp RD. Transformation of intestinal epithelial cells by chronic TGF-β1 treatment results in downregulation of the type II TGF-β receptor and induction of cyclooxygenase-2. *Oncogene* 1999; **18**: 855-867

25 **Medina V,** Edmonds B, Young GP, James R, Appleton S, Zalewski PD. Induction of caspase-3 protease activity and apoptosis by butyrate and trichostatin A (inhibitors of histone deacetylase): dependence on protein synthesis and synergy with a mitochondrial/cytochrome c-dependent pathway. *Cancer Res* 1997; **57**: 3697-3707

26 **Bonnotte B,** Favre N, Reveneau S, Micheau O, Droin N, Garrido C, Fontana A, Chauffert B, Solary E, Martin F. Cancer cell sensitization to fas-mediated apoptosis by sodium butyrate. *Cell Death Differ* 1998; **5**: 480-487

27 **Kamitani H,** Kameda H, Kelavkar UP, Eling TE. A GATA binding site is involved in the regulation of 15-lipoxygenase-1 expression in human colorectal carcinoma cell line, caco-2. *FEBS Lett* 2000; **467**: 341-347

Edited by Wang XL and Wu XN **Proofread by** Chen WW and Xu FM

PO Box 2345, Beijing 100023, China
Fax: +86-10-85381893
E-mail: wjg@wjgnet.com www.wjgnet.com

World J Gastroenterol 2004;10(20):2958-2962
World Journal of Gastroenterology
 ISSN 1007-9327

• COLORECTAL CANCER •

A novel mouse model for colitis-associated colon carcinogenesis induced by 1,2-dimethylhydrazine and dextran sulfate sodium

Jian-Guo Wang, Dong-Fei Wang, Bing-Jian Lv, Jian-Min Si

Jian-Guo Wang, Dong-Fei Wang, Jian-Min Si, Department of Gastroenterology, Sir Run Run Shaw Hospital, Zhejiang University Medical School, Hangzhou 310016, Zhejiang Province, China
Bing-Jian Lv, Department of Pathology, Sir Run Run Shaw Hospital, Zhejiang University Medical School, Hangzhou 310016, Zhejiang Province, China
Correspondence to: Jian-Guo Wang, Department of Gastroenterology, Sir Run Run Shaw Hospital, Hangzhou 310016, Zhejiang Province, China. roshy@163.com
Telephone: +86-571-86090073 Ext. 4535
Received: 2003-12-23 **Accepted:** 2004-01-08

Abstract

AIM: To develop an efficient animal colitis-associated carcinogenesis model and to detect the expression of β-catenin and p53 in this new model.

METHODS: Dysplasia and cancer were investigated in mice pretreated with a single intraperitoneal injection of 20 mg/kg body mass of 1,2-dimethylhydrazine prior to three repetitive oral administrations of 30 g/L dextran sulfate sodium to give conditions similar to the clinically observed active and remission phases. Immunohistochemical staining of β-catenin and p53 was performed on paraffin-imbedded specimens of animals with cancer and/or dysplasia, those without dysplasia and the normal control animals.

RESULTS: At wk 11, four early-invasive adenocarcinomas and 36 dysplasia were found in 10 (90.9%) of the 11 mice that underwent 1,2-dimethylhydrazine-pretreatment with 3 cycles of 30 g/L dextran sulfate sodium-exposure. Dysplasia and/or cancer occurred as flat lesions or as dysplasia-associated lesion or mass (DALM) as observed in humans. Colorectal carcinogenesis occurred primarily on the distal portion of the large intestine. No dysplasia and/or cancer lesion was observed in the control groups with 1,2-dimethylhydrazine pretreatment or 3 cycles of 30 g/L dextran sulfate sodium exposure alone. Immunohistochemical investigation revealed that β-catenin was translocated from cell membrane to cytoplasm and/or nucleus in 100% of cases with dysplasia and neoplasm, while normal membrane staining was observed in cases without dysplasia and the normal control animals. Nuclear expression of p53 was not detected in specimens.

CONCLUSION: A single dose of procarcinogen followed by induction of chronic ulcerative colitis results in a high incidence of colorectal dysplasia and cancer. Abnormal expression of β-catenin occurs frequently in dysplasia and cancer. This novel mouse model may provide an excellent vehicle for studying colitis-related colon carcinogenesis.

Wang JG, Wang DF, Lv BJ, Si JM. A novel mouse model for colitis-associated colon carcinogenesis induced by 1,2-dimethylhydrazine and dextran sulfate sodium. *World J Gastroenterol* 2004; 10(20): 2958-2962
http://www.wjgnet.com/1007-9327/10/2958.asp

INTRODUCTION

The incidence of colorectal cancer (CRC) has been increasing in patients with ulcerative colitis (UC) and the risk of CRC increases with increased extent and duration[1-4]. The mechanisms underlying the frequent development of CRC in patients with UC are still unknown.

Through the study of animal models which do not allow experiments in humans, we could better understand the cause and mechanisms of various diseases. There are many animal ulcerative colitis models, but only a few of them are applicable to the study of dysplasia-cancer sequence. Among them, the most widely used is a mouse model with dextran sulfate sodium (DSS). DSS could be used to induce UC in mice. Acute colitis was observed by administration of 50-100 g/L DSS to mice for 4-9 d[5-8]. A chronic colitis could be induced by feeding 30-50 g/L DSS in drinking water for 7 d followed by 7-14 d of water[6,8-10]. In recent years, some researchers have described the occurrence of dysplasia and/or cancers in mice when they are subjected to repeated administration of DSS in a long term[11-13]. Before the occurrence of cancer, the features of colitis in this model were very similar to those in patients in terms of both clinical and histopathological characteristics, i.e. diarrhea, occult blood, melena, mucosal inflammatory cell infiltration, crypt abscess formation, and mucosal erosion. But this kind of models needs a long period to be established and the incidence of induced tumors is relatively low.

1,2-dimethylhydrazine (DMH) is a toxic environmental pollutant which was reported as a specific colon procarcinogen. Animal studies showed that experimental colonic tumors induced by DMH were of epithelial origin with a similar histology, morphology and anatomy to human colonic neoplasms[14]. This procarcinogen could thus provide an adequate model for studying colorectal cancer. However, mutiple treatments with DMH (20-40 mg/kg body mass) and a long-term experimental period are needed to induce large bowel neoplasms[15-17].

We present here a newly developed colitis-associated CRC mouse model in which dysplasia and cancer developed within 10 wk when mice were given a single, low dose of DMH followed by three repeated administrations of 30 g/L DSS in drinking water. We used DSS to induce recurrence-remission cycle of chronic colitis which was similar to humans and added a low dose of DMH, in order to shorten CRC development period since chronic exposure to a small amount of environmental carcinogens is also a main cause of human CRC. In addition, we found dysplasiae and cancers in this model showed positive reactivity for β-catenin, but not for p53.

MATERIALS AND METHODS

Animals

Forty-five specific pathogen-free BALB/c male mice weighing 25-30 g (Slaccas Experimental Animal Co. Ltd. Shanghai, China), 7 wk of age, were used. They were housed in plastic cages (5 or 6 mice/cage) with wood shavings under standard laboratory conditions (24±0.5 ℃ temperature, 50±10% humidity, and 12 h of light from 06.00 to 18.00). All mice were permitted free access

to a commercial diet and DSS-supplemented or normal drinking tap water in bottles at the Animal Laboratory Center of our hospital.

Study design

The design for inducing colitis-associated dysplasia and/or cancer is shown in Figure 1. At the age of 8 wk, the animals were divided into one experimental group (group A) and 3 control groups (groups B-D), 10-12 mice each group. The animals in group A were subjected to three cycles of alternating administration of distilled water containing 30 g/L synthetic dextran sulfate sodium (DSS; mol mass 5000; Wako Pure Chemical Industries, Led. Japan) for 7 d followed by distilled water for the subsequent 14 d after intraperitoneal pretreatment with 20 mg/kg 1,2-dimethylhydrazine (DMH; Sigma-Aldrich Corp. St. Louis. MO. USA). For comparison, control groups B to D received each of the treatment alone or maintained as untreated control. Three mice from group A, B, and D were sacrificed during the experiment. Fourty-two mice were anesthesized with ether and sacrificed at the age of 18 wk.

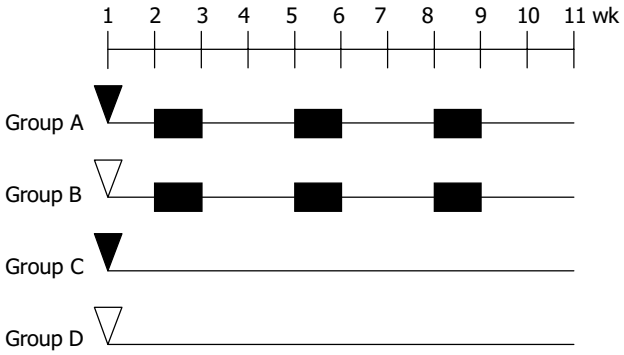

Figure 1 Experimental protocol for inducing colitis-related colon cancer in mice. ▼DMH, 20 mg/kg body mass, intraperitoneal injection; ▽ Saline 0.5 mL/mice intraperitoneal injecton; 30 g/L ■DSS in drinking water.

Observation of colitis

Changes in body weight were recorded every week throughout the experiment. Occult blood was examined on d 3 or 4 of DSS feeding, when DSS feeding was stopped, and once a week thereafter. Presence of gross blood and stool consistency were observed daily. The individuals who examined the mice were blinded as to the experimental group to which the animals belonged.

Histopathological evaluation

After death, the entire colorectum from the colocecal junction to the anal verge was examined. Their length was measured , and then the specimen was opened longitudinally and washed with saline. After colorectum was macroscopically inspected, it was immediately fixed in a 40 g/L formaldehyde buffer solution (pH 7.2).

Part of the colon was divided into three equal portions (proximal, middle and distal). Five-six pieces/portion and 14-17 pieces/colorectum were stained with hematoxylin and eosin (H&E) for histological processing.

The severity of UC of each colon was histologically graded on a scale from 0-4 and expressed using the pathological index corresponding to the following modified standard scoring system[18]: 0, normal; 1, focal inflammatory cell infiltration including polymorphonuclear leucocytes; 2, gland loss with inflammatory cell infiltration or crypt abscess formation; 3, mucosal uleration, or five or more foci of gland loss with inflammatory cell infiltration; 4, two or more areas of mucosal ulceration.

Dysplasia (low and high grades) was scored according to the criteria described by Riddell *et al*.[19]. Cancer was divided into early invasive and advanced cancer. Early invasive cancer was defined as cancer cells invading into muscularis mucosa and/or into submucosa. Advanced cancer was defined as cancer cells invading into muscularis propria or beyond.

A single experienced pathologist reviewed all cases blindly.

The evaluation of β-catenin and p53

To detect the expression of β-catenin and p53, we utilized the two step immunostaining technique. Four μm think tissue sections were dewaxed and rehydrated through changes of xylene and graded alcohol, then to water. Endogenous peroxidase activity was blocked by incubating the sections with 30 g/L hydrogen peroxidase for 15 min. Heat-mediated antigen retrieval was performed by heating the sections (immersed in 0.01 mol/L citrate buffer, pH 6.0) in a microwave oven (750 W) for 15 min. The slides were then washed with phosphate-buffered saline (PBS) before incubated with primary antibody overnight at 4 ℃. The antibody to β-catenin (Santa Cruz Biotechnology, Inc. USA) was a mouse monoclonal IgG1 antibody corresponding to amino acids 680-781 and was used at a dilution of 1:800. p53 antibody (Santa Cruz Biotechnology, Inc. USA) was a rabit polyclonal antibody that reacts with both wild-type and mutant p53 and was used at a dilution of 1:200. After washed with PBS, the slides were incubated for 30 min with the EnVision+peroxidase reagent (Zhongshan Biological Technology Co., LTD, Beijing, China). After further washed in PBS, the slides were developed with 3,3'-diaminobenzidine (DAB; Sigma-Aldrich Corp. St. Louis. MO. USA) for 5 min, and the reaction was terminated in water. The slides were then counterstained with hematoxylin, dehydrated in alcohol, and evaluated under a light microscope. Positive controls for β-catenin expression were normal human colonic epithelia. Human colonic adenocarcinoma were used as positive controls for p53 antibody. Omission of the primary antibody of β-catenin and p53 was used as a negative control.

Lesions were classified as positive for β-catenin if cytoplasmic/nuclear staining was detected (1+: ≤50% cells positive, 2+: ≥50% cell positive). Staining for p53 was considered positive if nuclear expression was detected in more than 10% of cells. Two experienced pathologists who were blinded to the specimen independently examined slides, and a high level of concordance (90%) was achieved. In case of disagreement, the slides were reviewed and a consensus view was achieved.

Statistical analysis

Statistical analysis was carried out by SPSS 11.5 for windows statistic software. Variance tests and One-way ANOVA test were used to compare the means of weight, length of large bowel in different groups, the number of neoplasms, and pathological index in different sites. $P<0.05$ was considered statistically significant.

RESULTS

Body growth, fecal examination and colorectal length

At the end of the first DSS treatment period, 75.0% (18/24) mice in groups A and B had diarrhea and occult blood or gross blood in the feces, and these signs disappeared after the mice drank distilled water for 14 d. However, during the second and third administrations of DSS, only 45.5% (10/22) and 36.4% (8/22) mice had diarrhea or occult blood, respectively.

Body growth rate was slightly lower in the mice that received 3 cycles of DSS treatment. The mean body weight of group A and B at the end of study was significantly smaller that that of

group D (P<0.05, Table 1).

Although the colorectal length was not affected by DMH-treatment alone, it was shortened by DSS treatment. The mean length of colorectum of mice in groups A and B was significantly shorter than that of mice in group D (P<0.01, Table 1).

Table 1 Body mass and colorectal length (mean±SD)

Groups	A	B	C	D
Body mass (g)	24.09±2.02[a]	25.9±2.020[a]	31.00±2.10	30.01±1.02
Colon length (cm)	8.80±0.98[b]	9.37±0.90[b]	12.21±0.94	12.66±0.73

Significantly different from group D ([a]P<0.05, [b]P<0.01).

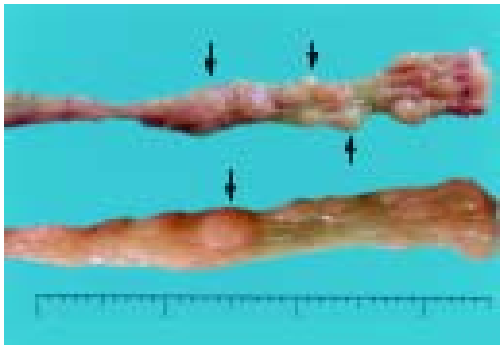

Figure 2 Induced colorectal tumors. Gross polypoid lesions are evident on the distal and middle portions of the large intestine (arrows).

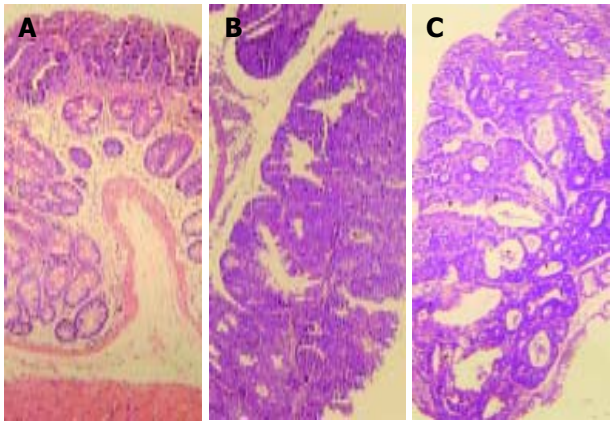

Figure 3 Histopathology showing dysplastic and cancer lesions developed in the colon of mice from group A. A: Whole-mount view of DALM with low-grade dysplasia, B: A slightly or non-elevated lesion diagnosed as high-grade dysplasia, C: whole-mount view of an early invasive cancer arising out of DALM. Hematoxylin and eosin stain. Original magnification, ×10.

Incidence and distribution of dysplasia and cancer

Group A mice that received DMH pretreatment and repeated administrations of 30 g/L DSS developed mutiple tumous in the colorectal region. Ten of 11 (90.9%) animals were detected to have at least one dysplasia and/or cancer lesion. Gross lesions were noted in 5 animals (all in group A). These lesions were dome shaped and ranged 2 to 4 mm in size, which appeared in the distal portion of the large intestine mainly, then in the middle portion, and none in the proximal part. (Table 2, Figure 2).

Most tumor tissues were tubular lesions with atypical severe cellular and structural high-grade dysplasia. A small number of lesions revealed relatively moderate dysplasia. Ten dysplasiae were categorized as low-grade dysplasia (Figure 3A), and 26 dysplasiae as high-grade dysplasia (Figure 3B), 22 out of 36 (61.1%) dysplasia lesions were DALMs. Four out of 26 tumours on the distal portion of the large intestine were confirmed to be early invasive adenocarcinomas (Figure 3C), and 3 of them arose within a DALM. No signs of tumor development were detected in control groups B to D.

Among the animals with dysplasia and/or cancer, the incidence of dysplasia and/or cancer was 15.0% (6/40), 20.0% (8/40) and 65.0% (26/40) in the proximal, middle and distal colon segments, respectively, 4 of 10 (40.0%) animals with dysplasia and/or cancer had lesions limited to only one colon segment, 3 animals (30.0%) had lesions in two different segments, and 3 animals (30.0%) had lesions in all three segments. Of the 3 animals with cancers, one had two synchronous cancers.

Pathology score/cancer relationship

The mice that received repeated administrations of 30 g/L DSS showed mild colitis regardless of DMH pretreatment. Mice in group A and B demonstrated mutiple foci of gland loss with inflammatory cell infiltration, but not many crypt abscess formations and mucosal ulcerations. Pathological scores in these two groups were statically significantly higher than those in group D (Table 2). However, there was no significant relationship between pathology scores among three portions of group A and B. This did not correlate well with the locations of CRC that developed mainly on the distal segment of colorectum.

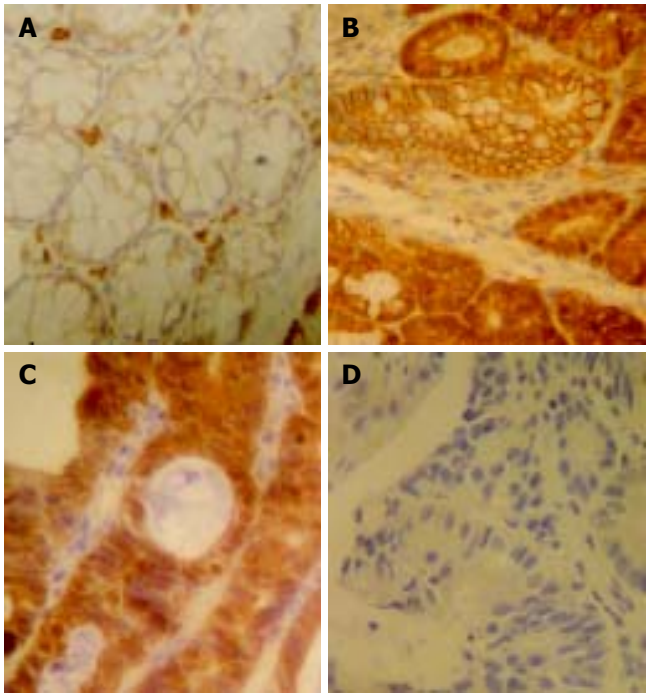

Figure 4 Immunohistochemistry of β-catenin and p53 in dysplastic lesions found in the colon of mice from group A. A: Control colon. β-catenin was expressed exclusively on the cell membrane. No cytoplasmic or nuclear staining was observed, B: Dysplasia cells expressed strong cytoplasmic and partly nuclear staining of β-catenin while other adjacent dysplastic cells showed membrane pattern of β-catenin, C: Lesions of early invasive cancer showing strong nuclear and cytoplasmic staining of β-catenin, D: No nuclear expression of p53 in lesions with high-grade dysplasia was observed. Original magnification, ×40.

β-catenin and p53 expression

Four cancers, 25 dysplasiae (10 of low-grade, 15 of high-grade), 10 negative dysplasiae and 10 control animals were studied for β-catenin and p53 expression, respectively.

In normal colon epithelial cells, β-catenin was mainly localized at the membranes of cell-cell borders (Figure 4A).

Table 2 Incidence of dysplasia/cancer and pathology score of UC (mean±SD)

Group number	Mice	Number of dysplasiae/cancers			Pathology score of UC		
		Proximal	Middle	Distal	Proximal	Middle	Distal
A	11	0.55±0.82	0.73±0.79	2.36±1.12[a]	1.82±0.40	1.72±0.46	1.82±0.40[c]
B	11	0.0±0.0	0.0±0.0	0.0±0.0	2.00±0.63	1.82±0.40	2.09±0.54[c]
C	10	0.0±0.0	0.0±0.0	0.0±0.0	0.0±0.0	0.0±0.0	0.0±0.0
D	10	0.0±0.0	0.0±0.0	0.0±0.0	0.0±0.0	0.0±0.0	0.0±0.0

[a]$P<0.05$, significantly different from proximal and middle portion of group A; [c]$P<0.05$ significantly different from group D.

Strong (2+) β-catenin expression was seen in nuclei and cytoplasms of cancer cells of 4 specimens (Figure 4C). Although the intensity was relatively weaker than that in carcinoma cells, dysplastic cells showed positivity for β-catenin in their nuclei, cytoplasms, and cell membranes (Figure 4B). The intensity was greater in high-grade dysplasiae (73.3% were 2+) than in low-grade dysplasiae (30.0% were 2+). In addition, positive reaction against β-catenin antibody was found in vascular endothelia and infiltrated inflammatory cells. However, nuclear p53 staining was not seen in tumor cells and dysplastic cells (Figure 4D).

DISCUSSION

The results of our experiment indicate that neither DMH pretreatment nor repeated administration of 3% DSS induced any tumorous lesions in the colorectum. However, their combination induced 4 invasive adenocarcinomas and 36 lesions with dysplasia in 11 mice within the relatively short term of 10 wk. Therefore, a clear synergism between the two agents was established. The histopathology of dysplasia and cancer in this model was very similar to that seen in humans. First, the animals developed dysplasia in both flat mucosa and DALM identical to that seen in humans. Second, early invasive cancer was revealed in 4 out of 40 lesions, and the data provided evidence of a dysplasia-adenocarcinoma sequence in this experimental system. Finally, the distribution of dysplasia/cancer was also similar. Colon cancers in patients with UC developed mainly on the left side of the large intestine and transverse colon. In our experiment, DMH and DSS induced colitis-related tumors dominant in the distal part of colon followed by in the middle part. In human UC, dysplasia was found in two or more segments in 42-75% of the cases and the incidence of mutiple synchronous cancers was reported to vary from 22-50%[20-22]. In the current study, the result also showed that dysplasia was present in two or more segment in 60% of the animals and the incidence of synchronous cancers was 33.3%. However, we finished the experiment in 10 wk and only induced four early invasive cancers.

β-catenin played a role in both cell adhesion and intracellular signaling[23,24]. Cytoplasmic/nuclear translocation of β-catenin was reported in human colitis-associated neoplasms[25-27] and DSS-induced CRC mice models[28,29]. In our study, we also found aberrant β-catenin expression immunohistochemical in dysplasia and cancer in mice treated with DMH and DSS. Furthermore, We noticed that cancinoma, high- and low-grade dysplasiae had different intensities and distributions of β-catenin. However, we don't know whether the translocation of β-catenin was due to loss of APC function or a direct mutation of β-catenin itself. This change might be associated with the progression from dysplasia to cancer. Our model are disimilar regarding the role of p53. Nuclear expression of p53 was a relatively early event in UC-related CRC compared with sporadic colon neoplasia[30-32]. However, in the current study, p53 immunohistochemical expression was not detected in colonic dysplasia and cancer. This findings might be due to the absence or low frequency of p53 mutations in colitis-related cancer mouse model. It is also possible that p53 mutations occurred at a later stage of cancer.

In conclusion, this study provides a novel colitis-associated mouse colon neoplasm model which features a single dose of procarcinogen followed by induction of chronic UC in a relatively short term. Futher studies on molecular mechanism or chemopreventive agents of this model may help us better understand CRC in patients with UC.

ACKNOWLEDGEMENTS

The authors wish to thank Dr. Mei Jin, Department of Pathology, Sir Run Run Shaw Hospital, Zhejiang University, Hangzhou, China, for her technical assistance in immunohistochemical analysis. We are also very grateful to Ming-Juan Jin, Department of Epidemiology and Public Health Statistics, Medical College of Zhejiang University, Hangzhou, China, for her statistical analysis.

REFERENCES

1 **Ekbom A**, Helmick C, Zack M, Adami HO. Ulcerative colitis and colorectal cancer. A population-based study. *N Engl J Med* 1990; **323**: 1228-1233
2 **Delco F,** Sonnenberg A. A decision analysis of surveillance for colorectal cancer in ulcerative colitis. *Gut* 2000; **46**: 500-506
3 **Eaden JA**, Abrams KR, Mayberry JF. The risk of colorectal cancer in ulcerative colitis: a meta-analysis. *Gut* 2001; **48**: 526-535
4 **van Hogezand RA**, Eichhorn RF, Choudry A, Veenendaal RA, Lamers CB. Malignancies in inflammatory bowel disease: fact or fiction? *Scand J Gastroenterol Suppl* 2002; **236**: 48-53
5 **Okayasu I,** Hatakeyama S, Yamada M, Ohkusa T, Inagaki Y, Nakaya R. A novel method in the induction of reliable experimental acute and chronic ulcerative colitis in mice. *Gastroenterology* 1990; **98**: 694-702
6 **Kullmann F**, Messmann H, Alt M, Gross V, Bocker T, Scholmerich J, Ruschoff J. Clinical and histopathological features of dextran sulfate sodium induced acute and chronic colitis associated with dysplasia in rats. *Int J Colorectal Dis* 2001; **16**: 238-246
7 **Aghdassi E**, Carrier J, Cullen J, Tischler M, Allard JP. Effect of iron supplementation on oxidative stress and intestinal inflammation in rats with acute colitis. *Dig Dis Sci* 2001; **46**: 1088-1094
8 **Hans W**, Scholmerich J, Gross V, Falk W. The role of the resident intestinal flora in acute and chronic dextran sulfate sodium-induced colitis in mice. *Eur J Gastroenterol Hepatol* 2000; **12**: 267-273
9 **Cooper HS**, Murthy SN, Shah RS, Sedergran DJ. Clinicopathologic study of dextran sulfate sodium experimental murine colitis. *Lab Invest* 1993; **69**: 238-249
10 **Clapper ML**, Adrian RH, Pfeiffer GR, Kido K, Everley L, Cooper HS, Murthy S. Depletion of colonic detoxication enzyme activity in mice with dextran sulphate sodium-induced colitis. *Aliment Pharmacol Ther* 1999; **13**: 389-396
11 **Okayasu I**, Yamada M, Mikami T, Yoshida T, Kanno J, Ohkusa T. Dysplasia and carcinoma development in a repeated dextran sulfate sodium-induced colitis model. *J Gastroenterol Hepatol* 2002; **17**: 1078-1083
12 **Mitamura T**, Sakamoto S, Sassa S, Suzuiki S, Kudo H, Okayasu I. The more an ulcerative colitis is repeated, the more the risk of

colorectal carcinogenesis is increased in mice. *Anticancer Res* 2002; **22**: 3955-3961

13 **Seril DN**, Liao J, Ho KL, Yang CS, Yang GY. Inhibition of chronic ulcerative colitis-associated colorectal adenocarcinoma development in a murine model by N-acetylcysteine. *Carcinogenesis* 2002; **23**: 993-1001

14 **Ma Q**, Hoper M, Anderson N, Rowlands BJ. Effect of supplemental L-arginine in a chemical-induced model of colorectal cancer. *World J Surg* 1996; **20**: 1087-1091

15 **Tsunoda A**, Shibusawa M, Tsunoda Y, Yokoyama N, Nakao K, Kusano M, Nomura N, Nagayama S, Takechi T. Antitumor effect of S-1 on DMH induced colon cancer in rats. *Anticancer Res* 1998; **18**(2A): 1137-1141

16 **Balansky R**, Gyosheva B, Ganchev G, Mircheva Z, Minkova S, Georgiev G. Inhibitory effects of freeze-dried milk fermented by selected Lactobacillus bulgaricus strains on carcinogenesis induced by 1, 2-dimethylhydrazine in rats and by diethylnitrosamine in hamsters. *Cancer Lett* 1999; **147**: 125-137

17 **Schmelz EM**, Sullards MC, Dillehay DL, Merrill AH Jr. Colonic cell proliferation and aberrant crypt foci formation are inhibited by dairy glycosphingolipids in 1, 2-dimethylhydrazine-treated CF1 mice. *J Nutr* 2000; **130**: 522-527

18 **Onderdonk AB**, Bartlett JG. Bacteriological studies of experimental ulcerative colitis. *Am J Clin Nutr* 1979; **32**: 258-265

19 **Riddell RH**, Goldman H, Ransohoff DF, Appelman HD, Fenoglio CM, Haggitt RC, Ahren C, Correa P, Hamilton SR, Morson BC, Sommers SC, Yardley JH. Dysplasia in inflammatory bowel disease: standardized classification with provisional clinical applications. *Hum Pathol* 1983; **14**: 931-968

20 **Connell WR**, Lennard-Jones JE, Williams CB, Talbot IC, Price AB, Wilkinson KH. Factors affecting the outcome of endoscopic surveillance for cancer in ulcerative colitis. *Gastroenterology* 1994; **107**: 934-944

21 **Taylor BA**, Pemberton JH, Carpenter HA, Levin KE, Schroeder KW, Welling DR, Spencer MP, Zinsmeister AR. Dysplasia in chronic ulcerative colitis: implications for colonoscopic surveillance. *Dis Colon Rectum* 1992; **35**: 950-956

22 **Vatn MH**, Elgjo K, Bergan A. Distribution of dysplasia in ulcerative colitis. *Scand J Gastroenterol* 1984; **19**: 893-895

23 **Ilyas M**, Tomlinson IP. The interactions of APC, E-cadherin and β-catenin in tumour development and progression. *J Pathol* 1997; **182**: 128-137

24 **Morin PJ**, Sparks AB, Korinek V, Barker N, Clevers H, Vogelstein B, Kinzler KW. Activation of β-catenin-Tcf signaling in colon cancer by mutations in β-catenin or APC. *Science* 1997; **275**: 1787-1790

25 **Tomlinson I**, Ilyas M, Johnson V, Davies A, Clark G, Talbot I, Bodmer W. A comparison of the genetic pathways involved in the pathogenesis of three types of colorectal cancer. *J Pathol* 1998; **184**: 148-152

26 **Brabletz T**, Jung A, Kirchner T. Beta-catenin and the morphogenesis of colorectal cancer. *Virchows Arch* 2002; **441**: 1-11

27 **Mikami T**, Mitomi H, Hara A, Yanagisawa N, Yoshida T, Tsuruta O, Okayasu I. Decreased expression of CD44, α-catenin, and deleted colon carcinoma and altered expression of β-catenin in ulcerative colitis-associated dysplasia and carcinoma, as compared with sporadic colon neoplasms. *Cancer* 2000; **89**: 733-740

28 **Cooper HS**, Murthy S, Kido K, Yoshitake H, Flanigan A. Dysplasia and cancer in the dextran sulfate sodium mouse colitis model. Relevance to colitis-associated neoplasia in the human: a study of histopathology, β-catenin and p53 expression and the role of inflammation. *Carcinogenesis* 2000; **21**: 757-768

29 **Tanaka T**, Kohno H, Suzuki R, Yamada Y, Sugie S, Mori H. A novel inflammation–related mouse colon carcinogenesis model induced by azoxymethane and dextran sodium sulfate. *Cancer Sci* 2003; **94**: 965-973

30 **Kern SE**, Redston M, Seymour AB, Caldas C, Powell SM, Kornacki S, Kinzler KW. Molecular genetic profiles of colitis associated neoplasms. *Gastroenterology* 1994; **107**: 420-428

31 **Brentnall TA**, Crispin DA, Rabinovitch PS, Haggitt RC, Rubin CE, Stevens AC, Burmer GC. Mutations in the p53 gene: an early marker of neoplastic progression in ulcerative colitis. *Gastroenterology* 1994; **107**: 369-378

32 **Ilyas M**, Talbot IC. p53 expression in ulcerative colitis: a longitudinal study. *Gut* 1995; **37**: 802-804

Edited by Ren SR and Wang XL **Proofread by** Xu FM

PO Box 2345, Beijing 100023, China
Fax: +86-10-85381893
E-mail: wjg@wjgnet.com www.wjgnet.com

World J Gastroenterol 2004;10(20):2963-2966
World Journal of Gastroenterology
 ISSN 1007-9327

• VIRAL HEPATITIS •

Impact of cigarette smoking on response to interferon therapy in chronic hepatitis C Egyptian patients

A. El-Zayadi, Osaima Selim, H. Hamdy, A. El-Tawil, Hanaa M. Badran, M. Attia, A. Saeed

A. El-Zayadi, H. Hamdy, Departments of Tropical Medicine, Ain Shams University, Cairo, Egypt
Osaima Selim, Department of Clinical Pathology, Ain Shams University, Cairo, Egypt
A. El-Tawil, Department of Pathology, Ain Shams University, Cairo, Egypt
Hanaa M. Badran, Department of Hepatology, National Liver Institute, Menoufeya, Egypt
M. Attia, Department of Hepatology and Gastroenterology, Theodor Bilharz Research Institute, Cairo, Egypt
A. Saeed, Cairo Liver Center, Giza, Egypt
Correspondence to: Professor A. El-Zayadi, Cairo Liver Center, 5 El-Gergawy St., Dokki, Giza, Egypt. clcz@tedata.net.eg
Telephone: +202-7603002 **Fax:** +202-7481900
Received: 2004-02-03 **Accepted:** 2004-03-13

Abstract

AIM: Smoking may affect adversely the response rate to interferon-α. Our objective was to verify this issue among chronic hepatitis C patients.

METHODS: Over the year 1998, 138 chronic hepatitis C male Egyptian patients presenting to Cairo Liver Center, were divided on the basis of smoking habit into: group I which comprised 38 smoker patients (>30 cigarettes/d) and group II which included 84 non-smoker patients. Irregular and mild smokers (16 patients) were excluded. Non eligible patients for interferon-α therapy were excluded from the study and comprised 3/38 (normal ALT) in group I and 22/84 in group II (normal ALT, advanced cirrhosis and thrombocytopenia). Group I was randomly allocated into 2 sub-groups: group Ia comprised 18 patients who were subjected to therapeutic phlebotomy while sub-group Ib consisted of 17 patients who had no phlebotomy. In sub-group Ia, 3 patients with normal ALT after repeated phlebotomies were excluded from the study. Interferon-α 2b 3 MU/TIW was given for 6 mo to 15 patients in group Ia, 17 patients in group Ib and 62 patients in group II. Biochemical, virological end-of- treatment and sustained responses were evaluated.

RESULTS: At the end of interferon-α treatment, ALT was normalized in 3/15 patients (20%) in group Ia and 2/17 patients (11.8%) in group Ib compared to17/62 patients (27.4%) in group II (P=0.1). Whereas 2/15 patients (13.3%) in group Ia. and 2/17 patients (11.8%) in group Ib lost viraemia compared to 13/62 patients (26%) in group II (P = 0.3). Six months later, ALT was persistently normal in 2/15 patients (13.3%) in group 1a and 1/17 patients (5.9%) in group Ib compared to 9/62 patients (14.5%) in group II (P = 0.47). Viraemia was eliminated in 1/15 patients (6.7%) in group Ia and 1/17 patients (5.9%) in group Ib compared to 7/62 patients (11.3%) in group II, but the results did not mount to statistical significance (P = 0.4).

CONCLUSION: Smokers suffering from chronic hepatitis C tend to have a lower response rate to interferon-α compared to non-smokers. Therapeutic phlebotomy improves the response rate to interferon-α therapy among this group.

El-Zayadi A, Selim O, Hamdy H, El-Tawil A, Badran HM, Attia M, Saeed A. Impact of cigarette smoking on response to interferon therapy in chronic hepatitis C Egyptian patients. *World J Gastroenterol* 2004; 10(20): 2963-2966
http://www.wjgnet.com/1007-9327/10/2963.asp

INTRODUCTION

It has been reported that cigarette smoking causes a variety of life threatening disorders such as pulmonary, cardiovascular, neoplastic, secondary polycythemia and others[1]. In addition, cigarette smoking has hepatotoxicity independent from alcoholic cirrhosis[2,3] and chronic hepatitis B virus carriers[4]. It increases the 5-year mortality rates of patients with alcoholic cirrhosis[5]. Furthermore, tobacco consumption has been associated with an increased risk of hepatocellular carcinoma (HCC) in patients with viral hepatitis[6-8]. A recent report has found that cigarette smoking was associated with increased fibrosis and histological activity in chronic hepatitis C (CHC) patients. It suggested that cigarette smoking could influence liver disease either by direct hepatotoxicity through its various constituents or secondary to erythrocytosis, immunological impact or synergistic effect with other factors such as alcohol[9].

The spectrum of liver injury in patients with CHC is broad and many factors influence the severity and progression of the lesion such as age[10], route of infection[11], genotype[12], concomitant chronic hepatitis B virus (HBV) infection[13] and others. Furthermore, many factors influence the natural history of CHC, clinical picture, and response to therapy, yet not all identified factors[12]. The adverse effects of heavy smoking particularly the response to therapy among CHC patients have been overlooked. Accordingly, we were motivated to study the impact of heavy smoking on clinical presentation, laboratory parameters and response to interferon-α (IFN-α) therapy in these patients.

MATERIALS AND METHODS

Over the year 1998, 138 CHC Egyptian male patients presenting to Cairo Liver Center for assessment of eligibility to interferon therapy were recruited. All patients met the following inclusion criteria: hepatitis C virus (HCV) antibody positive for ELISA, detectable HCV-RNA (Innolipa PCR) in serum, negative for HBsAg (Abbot ELISA), absent clinical and ultrasonographic evidence of cirrhosis, no ascites or hepatocellular carcinoma. No patient had received previous course of IFN-α therapy.

A standardized questionnaire to assess the smoking history was used[14] and accordingly all patients were divided into: smokers (group I) which consisted of 38 patients who smoked >30 cigarettes/d and non-smokers (group II) which included 84 patients who never smoked. Sixteen patients who were irregular, mild and passive smokers as well as pipe water and cigar smokers were excluded owing to difficulty in calculating smoking index. All patients in both groups were residents away from known

districts of high carbon monoxide pollution. None of the patients received drugs causing haemolysis over the preceding 6 mo period. All patients in both groups were assessed for haemoglobin, haematocrit, serum iron, and liver profile before liver biopsy. Patients who had persistently normal transaminases or had thrombocytopenia (platelet count less than 80 000/mm^3, 1 patient from group 1 and 16 patients from group 2) were considered non-eligible to interferon therapy and therefore excluded from the study.

Liver biopsy was performed using a true-cut needle to 37 patients from group I and 68 patients from group II scheduled for IFN-α therapy. All liver biopsy specimens were fixed in formalin, embedded in paraffin and routinely processed. The histological grade of disease activity and fibrosis was assessed using a reproducible scoring system[15] as follows: A 1 to A 3 for the degree of necroinflammatory activity (A 1 = mild, A3 = marked) and stage F0 to F4 for the degree of fibrosis (F0 = no fibrosis, F4 = cirrhosis). Two patients from group 1 and 6 patients from group 2 who had F4 (established cirrhosis) were also eliminated from IFN-α therapy. Iron staining using Perl's stain was done to non-cirrhotic specimen in both groups and scored according to percentage of iron stained hepatocyte.

Phlebotomy at a 2-wk interval till achieving low normal serum iron level was performed to 18 randomly allocated cases in group I patients (Ia), whereas 17 smoker patients had no phlebotomy and formed group Ib. Before undergoing phlebotomy all patients were instructed about its possible complications and all gave informed consent. None of the patients developed serious complications and all continued their schedule of phlebotomy. On serial ALT follow up, persistent normalization of ALT was observed in 3 patients in group Ia and therefore they were excluded from interferon therapy.

Thirty two smoker patients (15 from group1a and 17 from group 1b) and 62 non smoker patients from group II with persistent elevation of ALT received IFN-α therapy -3 MU TIW for 6 mo with serial evaluation of transaminases and test for HCV-RNA at the end of treatment and 6 mo later.

Statistical data was presented as mean±SD for the numeric variables. *t*-test was performed to compare both groups to each other. Response to therapy was categorized into responders and non-responders then presented into cross tables. χ^2 analysis was performed to assist the difference between the two groups. A *P* value of less than 0.05 was accepted as a level of significance.

RESULTS

Patients in group 1 had a significantly higher haemoglobin level ranging 16.1-19.1 g/dL with a mean of 16.9±0.54 g/dL compared to the patients in group 2 whose haemoglobin level ranged 13.5-16.3 g/dL with a mean of 15.3±0.59 g/dL. All patients in group 1 (100%) had a haemoglobin level exceeding 16 g/dL compared to 12/84 (14.3%) in patients of group 2.

The haematocrit level among group 1 patients ranged 56.1-61.4% with a mean of 56.3±0.86%, while group 2 patients had a haematocrit level ranging 45-55.9% with a mean of 54.8±1.16%, the difference was statistically significant ($P<0.005$). All patients in group 1 had a haematocrit value exceeding 55% compared to 14.3% of group 2 patients.

The mean serum iron level was significantly higher in group 1 (160.4±38.36 μg/dL) with a range of 100.3-283 μg/dL compared to group 2 (148.8±28.11 μg/dL) with a range of 90-194.3 μg/dL ($P<0.05$). Serum iron in 12 (31.5%) patients of group 1 was above normal level.

The mean serum uric acid level was 5.4±1.0 mg/dL in group 1 (range of 4-9 mg/dL) compared to 5.0±0.7 mg/dL (range of 3.8-6.9 mg/dL) in group 2, and the results were statistically significant ($P<0.01$).

Liver biopsy was performed to 37 patients from group 1 and 68 patients from group 2. Mild hepatitis was recorded in 10 (27%) patients of group 1 and 39 (57.4%) of group 2, whereas 17 patients (45.9%) of group 1 and 20 patients (29.4%) of group 2 had moderate hepatitis. Severe hepatitis was recorded in 8 patients (21.6%) of group 1 and 3 patients (4.4%) of group 2. Cirrhosis was recorded in 2 patients (5.4%) of group 1 and 6 patients (88%) of group 2. Iron staining using semiquantitative Perl's stain was positive with predominant periportal localization and associated steatosis in 3 (8.6%) patients of group 1 and 1 patient (1.5%) of group 2.

The end treatment biochemical response (ETBR) was reported in 5 patients (15.6%) of group 1 and 17 patients (27.4%) of group 2. Six months later only 3 patients (9.4%) of group 1 showed sustained normal ALT compared to 9 patients (14.5%) of group 2. The end treatment virological response (ETVR) was reported in 4 patients (12.5%) of group 1 and 3 patients (26%) of group 2. Six-months later, the sustained virological response (SVR) was reported in 2 patients (6.3%) of group 1 and 7 patients (11.3%) of group 2, but the differences did not reach statistical significance ($P>0.05$).

Among group I patients, ETBR in patients who had phlebotomy (group Ia) was recorded in 3 patients (20%) compared to 2 patients (11.8%) in those underwent no phlebotomy (group Ib). Two patients (13.3%) in group Ia had sustained biochemical response (SBR) compared to 1 patient (5.9%) in group 2b.

ETVR was found in 2 patients (13.3%) of group Ia compared to 2 patients (11.8%) of group Ib. SVR after 6 mo obtained in 1 patient of both groups (6.7% and 5.9%) respectively. Therefore, repeated phlebotomy increased both ETBR and SBR, but had no effect on virological responses (ETVR or SVR).

In group Ia repeated phlebotomy led to a significant decrease in mean ALT level from 167±50.3 to 112±377 IU/L ($P<0.01$).

DISCUSSION

Many studies have shown that smoking is an independent factor contributing to progression of HBV induced cirrhosis[4], alcoholic cirrhosis[1] and HCC development[6-8]. A recent French study has shown similarly that smoking favors progression to cirrhosis in chronic HCV infection independent of other co-morbid conditions[9].

The impact of smoking on various liver disorders has been extrapolated from experimental studies .It has been suggested that tobacco induced liver injury is ascribed to oxidative stress associated with lipid peroxidation[16,17]. In patients with CHC, the reduction in the concentration of hepatic, plasmatic and lymphocytic glutathione could favor the hepatotoxic effect of smoking[18]. Data from experimental studies suggest that nicotine, a major component of tobacco smoke, was rapidly absorbed through the lungs and released into circulation. Thereafter, it is mainly metabolized through the liver inducing lesions characterized by steatosis and focal or confluent necrosis[19].

A recent study demonstrated that smoking was mainly related to increased inflammatory activity but not to the stage of fibrosis[20], whereas Pessione *et al*.[9] provided evidence that smoking could worsen the degree of fibrosis in CHC independent of other co-morbid conditions. Advanced fibrosis adversely affected the response to interferon therapy[21,22], but this could not explain why smokers had lower response to interferon therapy compared to non-smokers as patients in both groups had comparable histopathological affection at entry of study. Cigarette smoking could increase generation of oxygen radicals. Chronic viral hepatitis patients who were cigarette smokers tended to have lower levels of natural anti-oxidants compared to non-smokers[23].

Smoking could induce a secondary form of polycythemia.

Smoker's polycythemia was attributable to increased carbon monoxide. The latter interfered with oxygen transport and utilization[24]. Secondary polycythemia may be associated with increased red cell turnover and subsequent rise of serum iron and tissue iron. In support of this hypothesis in our study, all smoker groups had higher hemoglobin and haematocrit compared to non-smoker group. In our study all HCV smoker patients had higher serum iron compared to HCV non-smoker patients as well.

It has long been recognized that hepatic iron overload could promote hepatic fibrosis in hereditary haemochromatosis[25]. Serum iron stores were frequently increased in patients with CHC[26]. Enhanced liver fibrosis has been reported in HCV infected patients with stainable iron in liver biopsy compared with controls with no detectable liver iron[27]. The mechanism by which iron accumulates in CHC patients has not been established but might in part be the result of iron release from damaged hepatocytes[28].

Another possible mechanism is that smoker polycythemia contributes to increased serum iron by increased cell turnover.

In support of this point of view, it was found that phlebotomy ameliorated not only symptoms related to smoker's polycythemia, but also transaminase level and resulted in persistent normalization of ALT level in 3/38 smoker patients. In our study, non-smoker patients had a better-sustained virological response rate compared to smoker patients. Although, phlebotomy resulted in a slight amelioration response rate, but results did not reach statistical significance. Many reports[29,30] showed significant improvement in serum ALT levels in interferon non-responders when they underwent iron reduction by therapeutic venesection. Three prospective, randomized controlled trials showed that iron reduction could increase the response rate to interferon therapy. While another multi-center trials showed no significant improvement in response of CHC to iron reduction treatment, although, histological improvement was documented even in patients with iron therapy alone[31].

This could be explained by other possible mechanisms such as immune alterations. Cigarette smoking may induce immune impairment by increasing apoptosis of lymphocytes, and counteracting interferon effect[32]. It was shown that tobacco smoking had a suppressive effect on human immunity as a result of decreased serum concentration of immunoglobulins and lysosyme decreased absolute number of (CD16+) NK-cells and elevated population of (CD8+) T-cytotoxic lymphocytes entailing a decrease in CD4+/CD8+ ratio[33]. Cigarette smokers exhibited impaired NK cytotoxic activity and unbalanced production of pro- and anti-inflammatory cytokines[34]. Smoking could alter immune response either directly through impairment of antigen receptor mediated signal transduction pathways leading to T cell anergy[35] or indirectly through brain immune interactions[36].

In conclusion, smokers suffering from CHC tend to have lower response to IFN-α compared to non-smokers. Therapeutic phlebotomy improves the response rate to IFN-α therapy among this group. This deserves further evaluation in prospective study. Chronic hepatitis C patients should be advised to avert smoking before embarking on interferon therapy.

REFERENCES

1 **Klatsky AL**, Armstrong MA. Alcohol smoking coffee and cirrhosis. *Am J Epidemiol* 1992; **136**: 1248-1257

2 **Corrao G**, Lepore AR, Torchio P, Valenti M, Galatola G, D'Amicis A, Arico S, di Orio F. The effect of drinking coffee and smoking cigarettes on the risk of cirrhosis associated with alcohol consumption: a case-control study. *Eur J Epidemiol* 1994; **10**: 657-664

3 **Pessione F**, Ramond MJ, Peters L, Pham BN, Batel P, Rueff B, Valla DC. Five-year survival predictive factors in patients with excessive alcohol intake and cirrhosis. Effect of alcoholic hepatitis, smoking and abstinence. *Liver Int* 2003; **23**: 45-53

4 **Yu MW**, Hsu FC, Sheen IS, Chu CM, Lin DY, Chen CJ, Liaw YF. Prospective study of hepatocellular carcinoma and liver cirrhosis in asymptomatic chronic hepatitis B virus carrier. *Am J Epidemiol* 1997; **145**: 1039-1047

5 **Mori M**, Hara M, Wada I, Hara T, Yamamoto K, Honda M, Naramoto J. Prospective study of hepatitis B and C viral infection, cigarette smoking, alcohol consumption and other factors associated with hepatocellular carcinoma risk in Japan. *Am J Epidemiol* 2000; **151**: 131-139

6 **Mukaiya M**, Nishi M, Miyake H, Hirata K. Chronic liver disease for the risk of hepatocellular carcinoma: a case control study in Japan. Etiologic association of alcohol consumption, cigarette smoking and the development of chronic liver diseases. *Hepatogastroenterology* 1998; **45**: 2328-2332

7 **Yu MW**, Chiu YH, Yang SY, Santella RM, Chern HD, Liaw YF, Chen CJ. Cytochrome P450 1A1 genetic polymorphisms and risk of hepatocellular carcinoma among chronic hepatitis B carriers. *Br J Cancer* 1999; **80**: 598-603

8 **Alberti A**, Chemello L, Benvegnu L. Natural history of hepatitis C. *J Hepatol* 1999; **31**(Suppl 1): 17-24

9 **Pessione F**, Ramond MJ, Njapoum C, Duchatelle V, Degott C, Erlinger S, Rueff B, Valla DC, Degos F. Cigarette smoking and hepatic lesions in patients with chronic hepatitis C. *Hepatology* 2001; 34: 121-125

10 **Poynard T**, Bedossa P, Opolon P. Natural history of liver fibrosis progression in patients with chronic hepatitis C. The OBSVIRC, METAVIR, CLINIVIR, and DOSVIRC groups. *Lancet* 1997; 349: 825-832

11 **Lopez-Morante A**, Saez-Royuela F, Echevarria C, Llanos C, Martin-Lorente JL, Yuguero L, Ojeda C. Influence of the transmission route and disease duration in the histopathology of chronic hepatitis C: a study of 101 patients. *Eur J Gastroenterol Hepatol* 1998; **10**: 15-19

12 **Tran TT**, Martin P. Chronic Hepatitis C. *Curr Treat Options Gastroenterol* 2001; **4**: 503-510

13 **Pontisso P**, Ruvoletto MG, Fattovich G, Chemello L, Gallorini A, Ruol A, Alberti A. Clinical and virological profiles in patients with multiple hepatitis virus infection. *Gastroenterology* 1993; **105**: 1529-1533

14 **Baum GlL**, Wolinsky E. Textbook of pulmonary disease. 5th Edn, vol 11. Boston: *Little Brown* 1994: 257

15 Intraobserver and interobserver variations in liver biopsy interpretation in patients with chronic hepatitis C. The French METAVIR Cooperative Study Group. *Hepatology* 1994; **20**(1Pt 1): 15-20

16 **Husain K**, Scott BR, Reddy SK, Somani SM. Chronic ethanol and nicotine interaction on rat tissue antioxidant defense system. *Alcohol* 2001; **25**: 89-97

17 **Watanabe K**, Eto K, Furuno K, Mori T, Kawasaki H, Gomita Y. Effect of cigarette smoke on lipid peroxidation and liver function tests in rats. *Acta Med Okayama* 1995; **49**: 271-274

18 **Barbaro G**, Di Lorenzo G, Ribersani M, Soldini M, Giancaspro G, Bellomo G, Belloni G, Grisorio B, Barbarini G. Serum ferritin and hepatic glutathione concentrations in chronic hepatitis C patients related to the hepatitis C virus genotype. *J Hepatol* 1999; **30**: 774-782

19 **Yuen ST**, Gogo AR, Luk IS, Cho CH, Ho JC, Loh TT. The effect of nicotine and its interaction with carbon tetrachloride in the rat liver. *Pharmacol Toxicol* 1995; **77**: 225-230

20 **Hezode C**, Lonjon I, Roudot-Thoraval F, Mavier JP, Pawlotsky JM, Zafrani ES, Dhumeaux D. Impact of smoking on histological liver lesions in chronic hepatitis C. *Gut* 2003; **52**: 126-129

21 **McHutchison J**. Hepatitis C therapy in treatment-naive patients. *Am J Med* 1999; **107**: 56S-61S

22 **Poynard T**, Marcellin P, Lee SS, Niederau C, Minuk GS, Ideo G, Bain V, Heathcote J, Zeuzem S, Trepo C, Albrecht J. Randomized trial of interferon alpha 2b plus ribavirin for 48 weeks or for 24 weeks versus interferon-a 2b plus placebo for 48 weeks for treatment of chronic interferon with hepatitis C virus. *Lancet* 1998; **352**: 1426-1432

23 **Yu MW**, Horng IS, Hsu KH, Chiang YC, Liaw YF, Chen CJ. Plasma selenium levels and risk of hepatocellular carcinoma among men with chronic hepatitis virus infection. *Am J Epidemiol*

1999; **150**: 367-374

24 **Panda K**, Chattopadhyay R, Chattopadhyay DJ, Chatterjee IB. Vitamin C prevents cigarette smoke-induced oxidative damage *in vivo*. *Free Radic Biol Med* 2000; **29**: 115-124

25 **Bacon BR**, Tavill AS. Haemochromatosis and the iron overload syndromes. In: Zakim B, Boyer TD, eds. Hepatology: a text book of liver disease, 3rd ed. Philadelphia: *Saunders* 1996: 1439-1489

26 **Riggio O**, Montagnese F, Fiore P, Folino S, Giambartolomei S, Gandin C, Merli M, Quinti I, Violante N, Caroli S, Senofonte O, Capocaccia L. Iron overload in patients with chronic viral hepatitis: how common is it? *Am J Gastroenterol* 1997; **92**: 1298-1301

27 **Beinker NK**, Voigt MD, Arendse M, Smit J, Stander IA, Kirsch RE. Threshold effect of liver iron content on hepatic inflammation and fibrosis in hepatitis B and C. *J Hepatol* 1996; **25**: 633-638

28 **Bonkovsky HL**, Banner BF, Rothman AL. Iron and chronic viral hepatitis. *Hepatology* 1997; **25**: 759-768

29 **Hayashi H**, Takikawa T, Nishimura N, Yano M, Isomura T, Sakamoto N. Improvement of serum aminotransferase levels after phlebotomy in patients with chronic active hepatitis C and excess hepatic iron. *Am J Gastroenterol* 1994; **89**: 986-988

30 **Piperno A**, Sampietro M, D'Alba R, Roffi L, Fargion S, Parma S, Nicoli C, Corbetta N, Pozzi M, Arosio V, Boari G, Fiorelli G. Iron stores, response to alpha- interferon therapy, and effects of iron depletion in chronic hepatitis C. *Liver* 1996; **16**: 248-254

31 **Di Bisceglie AM**, Bonkovsky HL, Chopra S, Flamm S, Reddy RK, Grace N, Killenberg P, Hunt C, Tamburro C, Tavill AS, Ferguson R, Krawitt E, Banner B, Bacon BR. Iron reduction as an adjuvant to interferon therapy in patients with chronic hepatitis C who have previously not responded to interferon: A multi-center, prospective, randomized, controlled trial. *Hepatology* 2000; **32**: 135-138

32 **Suzuki N**, Wakisaka S, Takeba Y, Mihara S, Sakane T. Effects of cigarette smoking on Fas/Fas ligand expression of human lymphocytes. *Cell Immunol* 1999; **192**: 48-53

33 **Moszczynski P**, Zabinski Z, Moszczynski P, Rutowski J, Slowinski S, Tabarowski Z. Immunological findings in cigarette smokers. *Toxic Lett* 2001; **118**: 121-127

34 **Zeidel A**, Beilin B, Yardeni I, Mayburd E, Smirnov G, Bessler H. Immune response in asymptomatic smokers. *Acta Anaesthesiol Scand* 2002; **46**: 959-964

35 **Kalra R**, Singh SP, Savage SM, Finch GL, Sopori ML. Effects of cigarette smoke on immune response: chronic exposure to cigarette smoke impairs antigen-mediated signaling in T cells and depletes IP3-sebsitive Ca(2+) stores. *J Pharmacol Exp Ther* 2000; **293**: 166-171

36 **Sopori ML**, Kozak W, Savage SM, Geng Y, Soszynski D, Kluger MJ, Perryman EK, Snow GE. Effect of nicotine on the immune system: possible regulation of immune responses by central and peripheral mechanisms. *Psychoneuroendocrinology* 1998; **23**: 189-204

Edited by Wang XL and Chen WW **Proofread by** Xu FM

PO Box 2345, Beijing 100023, China
Fax: +86-10-85381893
E-mail: wjg@wjgnet.com www.wjgnet.com

World J Gastroenterol 2004;10(20):2967-2971
World Journal of Gastroenterology
 ISSN 1007-9327

• VIRAL HEPATITIS •

siRNA-mediated inhibition of HBV replication and expression

Xiao-Nan Zhang, Wei Xiong, Jia-Dong Wang, Yun-Wen Hu, Li Xiang, Zheng-Hong Yuan

Xiao-Nan Zhang, Wei Xiong, Jia-Dong Wang, Yun-Wen Hu, Li Xiang, Zheng-Hong Yuan, Key Laboratory of Medical Molecular Virology, Ministry of Education and Health, Shanghai Medical College, Fudan University, Shanghai 200032, China
Supported by the State Basic Research Foundation of China, No. G19999054105 and Med-X Foundation of Fudan University
Correspondence to: Zheng-Hong Yuan, Key Laboratory of Medical Molecular Virology, Ministry of Education and Health, Shanghai Medical College, Fudan University, 138 Yi Xue Yuan Road Shanghai 200032, China. zhyuan@shmu.edu.cn
Telephone: +86-21-64161928 **Fax:** +86-21-64227201
Received: 2004-03-05 **Accepted:** 2004-04-13

Abstract

AIM: RNA interference (RNAi) is a newly discovered phenomenon provoked by dsRNA. The dsRNA is initially cleaved by Dicer into 21-23 nt small interfering RNA (siRNA) and can then specifically target homologous mRNA for degradation by cellular ribonucleases. RNAi has been successfully utilized to down-regulate the endogenous gene expression or suppress the replication of various pathogens in mammalian cells. In this study, we investigated whether vector-based siRNA promoted by U6 (pSilencer1.0-U6) could efficiently inhibit HBV replication in cell culture.

METHODS: pSilencer vectors with inserts targeting on different regions of HBV genome were constructed. These plasmids were co-transfected with pHBV3.8 into Huh-7 cells via lipofection and viral antigens were measured by ELISA. Viral RNA was analyzed by Northern blot. The mRNA of MxA and 2′-5′OAS was reverse transcribed and quantified by real-time PCR.

RESULTS: Vector-based siRNA could potently reduce hepatitis B virus antigen expression in transient replicative cell culture. Furthermore, Northern blot analysis showed that viral RNA was effectively degraded, thus eliminating the messengers for protein expression as well as template for reverse transcription. Real-time PCR analysis of cellular MxA and 2′-5′OAS gene expression revealed that vector-based siRNA did not provoke the interferon pathway which reassured the specificity of the vector-based RNA interference technique.

CONCLUSION: Our results indicate that RNA interference may be a potential tool to control HBV infection.

Zhang XN, Xiong W, Wang JD, Hu YW, Xiang L, Yuan ZH. siRNA-mediated inhibition of HBV replication and expression. *World J Gastroenterol* 2004; 10(20): 2967-2971
http://www.wjgnet.com/1007-9327/10/2967.asp

INTRODUCTION

Hepatitis B virus is a severe infectious pathogen causing chronic liver diseases and increasing risk of hepatocellular carcinoma[1]. Although recombinant vaccines are widely available[2], HBV infection is still a big challenge to the societies all over the world. Until now, interferon-α and nucleoside analogs, such as lamivudine, are of the few drugs capable of inhibiting HBV replication. However, interferon treatment usually results in a limited percentage of complete response and relapses generally occur without further treatment. Lamivudine, a strong inhibitor of HBV's reverse-transcriptase, has been proved to be highly effective in blocking its genome replication. Nevertheless, a significant portion of patients relapsed after cessation of treatment. With prolonged treatment, escape mutants would develop[3].

RNA interference is a newly discovered phenomenon present in almost all eukaryotes[4,5]. It is activated by dsRNA, which is subsequently cleaved by Dicer into 21-23 nt small interfering RNAs (siRNA). The siRNAs are then unwound by RISC (siRNA induced silencing complex) in the presence of ATP. The activated RISC binds to and degrades target mRNA guided by the single strand siRNA. In mammals, long dsRNA can activate protein kinase R (PKR) and RNaseL, which are key components of the interferon signaling pathway, thus causing unspecific effects, whereas 21-23 nt siRNAs are short enough to bypass them[6]. Many studies have been carried out to silence a number of RNA viruses by RNA interference, such as human immunodeficiency virus (HIV), hepatitis C virus (HCV) and poliovirus, *etc*[7-11]. As hepatitis B virus (HBV) utilizes pregenomic RNA for synthesis of viral DNA via reverse transcription, it is also an ideal candidate for RNAi. Recently, vector-based RNAi technique, which uses endogenous U6 or H1 promoter to generate small interfering RNA (siRNA) *in vivo*, has become a new and economical system to achieve gene silencing[12,13]. In this study, we investigated whether vector-based siRNA promoted by U6 (pSilencer1.0-U6) could efficiently inhibit HBV replication in cell culture.

MATERIALS AND METHODS

Materials

TRIzol reagent, Dulbecco's modified Eagle's medium (DMEM), fetal calf serum and antibiotics were from GIBCO BRL. Restriction endonucleases were supplied by MBI Fermentas. SuperScript II reverse transcriptase was from Invitrogen, Carlsbad. DNA sequence primers were synthesized by CASarray, Shanghai. pSilencer 1.0-U6 was from Ambion, Austin. HBsAg and HBeAg ELISA kit were purchased from Shanghai SIIC Kehua Biotech. pHBV3.8 plasmid encoding the whole transcript of HBV DNA (adr subtype) from the core promoter to the polyA signal region (nucleotides 1403-3215 plus 1 to 1987), was constructed as a 1.2 copy insert of the full-length HBV genome into vector pBS+ (Stratagene) via restriction enzyme *Eco*RI and *Pst*I sites (kindly provided by Professor. Yuan Wang, Institute of Biochemistry, Academia Sinica, Shanghai). After transfected into Huh-7 cells, the pHBV3.8 could express both HBV surface antigen (HBsAg) and E antigen (HBeAg), and the replication of HBV could be initiated. Plasmid pcDNA-CAT containing the chloramphenicol acetyltransferase (CAT) gene under control of the CMV promoter was co-transfected as internal control. The expression of CAT could be measured by CAT ELISA kit (Roche, Mannheim, Germany).

Cell culture and transfection

Huh-7 cell line was maintained in Dulbecco's modified Eagle's

medium supplemented with 100 mL/L fetal calf serum, 2 mmol/mL L-glutamine, 100 μg/mL penicillin and 100 units/mL streptomycin (GIBCO BRL). The cells were incubated in a humidified incubator at 37 ℃ containing 50 mL/L CO_2. Cell viability was estimated by the trypan blue dye exclusion method. Huh-7 cells were transfected using FuGENE6 cationic liposome (Roche, Mannheim, Germany), and cells were harvested 48 h and 72 h after transfection, respectively. Experiments were performed in triplicate.

Target sequence selection and insertion sequence synthesis

By aligning different subtypes of HBV genome and using the Ambion web-based software, we selected 3 regions of high conservation designated as si-HBV1, 2 and 3 to be the target sequence. The target sequence of si-HBV1 was located in S region as well as P region of the HBV genome (nt 310 to 328), si-HBV2 and 3 were both in the C region (nt 1868 to 1886 for HBV2, nt 2373 to 2391 for HBV3). si-HBV1, 2 and 3 had the siRNA sequences completely identical to the target sequence of pHBV3.8. To create pSilencer plasmids, we used the primers: 5'-TTCGCAGTCCCCAACCTCCTTCAAGAGAGGAGGTTGG GGACTGCGAATTTTTT-3' (sense) and 5'-AGCTAAAAAATT CGCAGTCCCCAACCTCCTCTCTTGAAGGAGGTTGGGGACTG CGAAGGCC-3' (antisense) for pSi-HBV1; 5'-GCCTCCAAGC TGTGCCTTGTTCAAGAGACAAGGCACAGCTTGGAGGCTTTT TT-3' (sense) and 5'AGCTAAAAAAGCCTCCAAGCTGTGCC TTGTCTCTTGAACAAGGCACAGCTTGGAGGCGGCC-3' (antisense) for pSi-HBV2; 5'-GAAGAACTCCCTCGCCTCGTT CAAGAGACGAGGCGAGGGAGTTCTTCTTTTTT-3' (sense) and 5'AGCTAAAAAAGAAGAACTCCCTCGCCTCGTCTCT TGAACGAGGCGAGGGAGTTCTTCGGCC-3' (antisense) for pSi-HBV3.

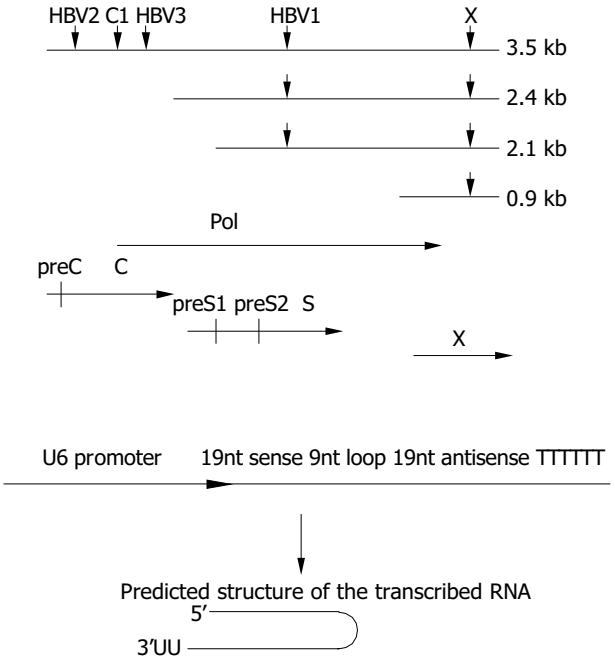

Figure 1 Design of siRNAs specific for HBV genome. A: Downward arrows show the target sites within the RNA transcripts. The HBV ORFs are shown below aligned with HBV mRNA. B: Schematic presentation of U6 promoter constructs. The inverted 19 nt sequences are separated by a 9 nt loop, transcription ends with 5Ts. The resulting shRNA (short hairpin RNA) are predicted to fold back to form a hairpin RNA.

In this study, the target sequences used by Shlomai *et al*.[14] for pSuper core1 (nt 2191 to 2209) and pSuper X (nt 1649 to 1667) were also included for comparison (Figure 1) with slight modifications to suit the DNA sequence of pHBV3.8. The oligo sequences were: 5'-AATCAGACAACTACTGTGGTTCAAGA GACCACAGTAGTTGTCTGATTTTTTTT-3' (sense) and 5'-AGCTAAAAAAAATCAGACAACTACTGTGGTCTCTTGAACC ACAGTAGTTGTCTGATTGGCC-3' (antisense) for pSi-core1; 5'-GGTCTTACATAAGAGCACTTTCAAGAGAAGTGCTCTT ATGTAAGACCTTTTTT-3' (sense) and 5'-AGCTAAAAAAG GTCTTACATAAGAGCACTTCTCTTGAAAGTGCTCTTATGTA AGACCGGCC-3' (antisense) for pSi-X.

pSi-EGFP-h was a control vector with insertion sequence targeting on EGFP gene. The synthesized oligos were: 5'-GACGTAAACGGCCACAAGTTTCAAGAGAACTTGTGG CCGTTTACGTCTTTTTT-3' (sense) and5'-AGCTAAAAAAG ACGTAAACGGCCACAAGTTCTCTTGAAACTTGTGGCCGTT TACGTCGGCC-3' (antisense).

Plasmid constructs

The oligos were annealed and cloned into *Apa*I-*Hin*dIII sites of pSilencer as described in the pSilencer 1.0 U6 manual (Ambion). All the plasmids constructed were confirmed by DNA sequencing.

Quantitiation of HBsAg and HBeAg

The HBsAg and HBeAg secreted into the culture media were measured by diagnostic ELISA kit (Shanghai SIIC Kehua Biotech).

Northern blot analysis of viral RNA

Total RNA was extracted directly from transfected cells using TRIzol reagent (Gibco BRL). After 30 min of DNaseI digestion of remaining DNA, total RNA was re-extracted by TRIzol, precipitated and dissolved in DEPC-H_2O. Ten micrograms of total RNA was electrophoresed on 10 g/L formaldehyde-agarose gel and then transferred to nylon membranes (Roche, Mannheim, Germany). After fixation at 120 ℃ for 30 min, the membrane was prehybridized for 6 h at 42 ℃ in 5×SSC, 5×Denhardt's solution, 10 g/L SDS, 50 g/L formaldehyde, 0.1 mg/mL salmon sperm DNA ,followed by hybridization with full-length HBV DNA probes labeled with [α-^{32}P] dCTP by hexamer random labeling kit (Roche, Mannheim, Germany) under the same condition of prehybridization at 42 ℃ for 16 h. After a stringent washing process at 68 ℃, the signals were detected by autoradiography, then the blots were quantified by densitometry. The 28 s and 18 s rRNA were visualized under ultraviolet light for equal loading control. The values of HBV blots were normalized by monitoring the expression of an internal control CAT by CAT ELISA (Roche, Mannheim, Germany).

Quantitative real-time PCR

Huh-7 cells in 6-well plates were transfected with 2 μg of various plasmids. After 48 h of transfection, total RNA was extracted as described above. RNA was denatured for 5 min at 65 ℃ in the presence of random hexamer, immediately cooled in ice water, then reverse transcribed using SuperScript II reverse-transcriptase according to the manufacturer's instructions. Real-time PCR (iCycler, Bio-Rad) was performed as instructed by iCycler resource guide. Reactions with no reverse transcriptase enzyme added were performed in parallel. Briefly, reactions were carried out in 25 μL volume containing 2 μL of template (cDNA or RNA), 400 nmol/L of each forward and reverse primer and 1X SybrGreenI PCR Master Mix (Roche). To quantitate cellular transcripts, dilutions of plasmids containing the human GAPDH gene were run in parallel. The experiment was performed twice. The primer sequences used included: 5'-GGTATCGTGGAAGG ACTCATGAC3' (sense) and 5'-ATGCCAGTGAGCTTCCCGT TCAGC3' (antisense) for GAPDH; 5'-GCTACACACCGTGACG GATATGG 3' (sense) and 5'-CGAGCTGGATTGGAAAGCCC3'

(antisense) for MxA; 5'-TCAGAAGAGAAGCCAACGTGA-3' (sense) and 5'-CGGAGACAGCGAGGGTAAAT-3' (antisense) for 2'-5'OAS.

RESULTS

Inhibition of HBV gene expression in transiently transfected Huh-7 cells by RNAi

pSilencer, pSi-EGFP-h and other derivatives targeting on different regions of HBV genome were co-transfected with pHBV3.8 in the ratio of 10:1 into Huh-7 cells. pcDNA-CAT was also transfected as internal control. The secreted viral antigens, HBsAg and HBeAg in the culture media were quantified 48 h and 72 h after transfection. Transfection efficiencies were standardized by measurement of CAT using CAT ELISA Kit. Compared with control vector, HBsAg and HBeAg expressions were reduced by about 60% in average when measured 48 h after transfection (Figure 2). When the antiviral effect of siRNA was assessed 72 h post-transfection, the silencing effect was still apparent, indicating the stability of the transcribed RNAi. Among all the siRNAs used, pSi-HBV1 targeting on S gene as well as P gene of HBV genome was most potent, as HBsAg and HBeAg were reduced 86% and 83% 72 h after transfection, respectively.

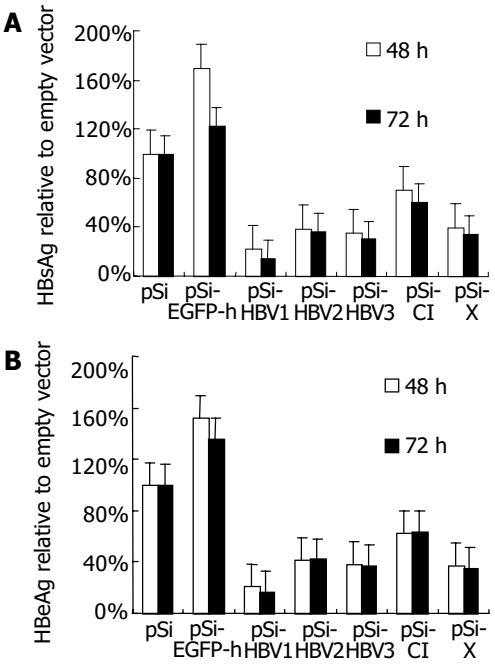

Figure 2 Effect of RNAi on HBV protein expression in transiently transfected Huh-7 cells.

Reduction of HBV viral transcripts by RNAi

To determine whether viral pregenomic RNA and other transcripts were efficiently degraded by siRNA, Northern blot assay was carried out using ^{32}P-labeled full length HBV fragment as the probe generated with a random-primed labeling kit. Compared with control vector pSi-EGFP-h, significant reduction of all the viral transcripts was observed when pSilencer vectors targeting on specific HBV RNA were used (Figure 3). Among them, pSi-HBV1 and pSi-HBV2 were much more efficient with over 90% reduction in viral RNAs.

Vector-based siRNA could not activate interferon response

To rule out the possibility that inhibition of HBV gene expression and replication by vector-based siRNA was due to the dsRNA-induced activation of IFN pathway, we compared the mRNA levels of IFN-induced genes 2'-5'OAS and MxA by quantitative real-time PCR 48 h after transfection of siRNA generating plasmids. Compared with mock-transfected Huh-7 cells, IFN induced about 10 000 and 100-fold increase in 2'-5'OAS and MxA mRNA levels, respectively. While the transfection of pSi-HBV plasmids only led to 1.67-fold and 0.71-fold (in average) induction of MxA and 2'-5'OAS, respectively, thus eliminating the non-specific effect of siRNAs (Figure 4).

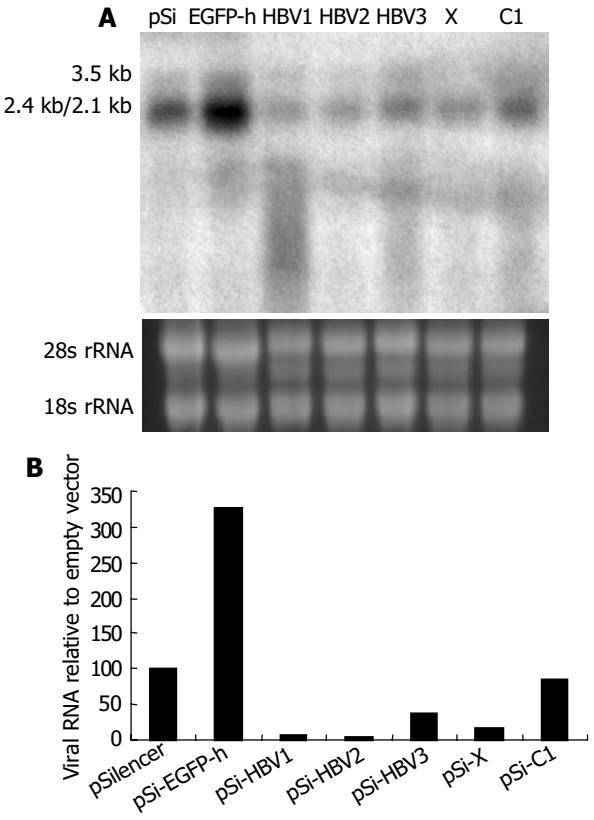

Figure 3 Effect of RNAi on HBV gene transcription detected by Northern blot. A: Northern blot experiment of HBV transcripts. The 28 s and 18s rRNAs were visualized under ultraviolet light for equal loading control. B: The hybridization signal was quantitatively evaluated by Smartview™ image analysis software (Shanghai Fu-ri Inc).

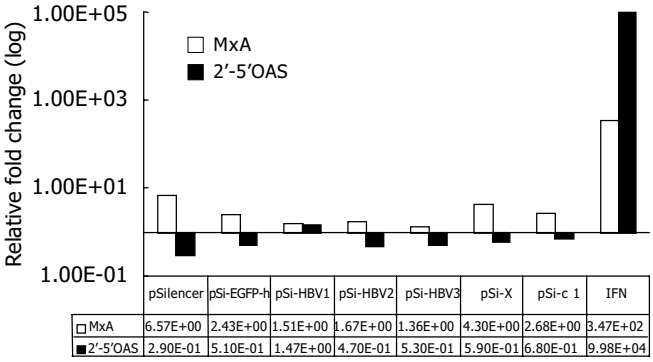

	pSilencer	pSi-EGFP-h	pSi-HBV1	pSi-HBV2	pSi-HBV3	pSi-X	pSi-c 1	IFN
MxA	6.57E+00	2.43E+00	1.51E+00	1.67E+00	1.36E+00	4.30E+00	2.68E+00	3.47E+02
2'-5'OAS	2.90E-01	5.10E-01	1.47E+00	4.70E-01	5.30E-01	5.90E-01	6.80E-01	9.98E+04

Figure 4 Effect of RNAi on IFN-induced genes. Real-time PCR quantification of MxA and 2'-5' OAS. The copy number of MxA and 2'-5'OAS were normalized with GAPDH. The relative fold induction of each gene compared with mock transfection is shown.

DISCUSSION

Numerous reports have demonstrated that RNAi can block replication of various types of mammalian viruses, including

two retroviruses, human immunodeficiency virus (HIV)[7,15-17] and Rous sarcoma virus[18]; a negative-strand RNA virus, respiratory syncytial virus (RSV)[19], two positive-stranded RNA virus, hepatitis C virus (HCV)[9,20,21] and poliovirus[10]; and a DNA virus, human papillomavirus[22]. Although HBV is a DNA virus, its replication requires a key step of reverse transcription for synthesis of viral DNA from pregenomic RNA, which is quite different from other DNA viruses. Therefore, HBV is assumed to be susceptible to siRNA not only at the level of post-transcription, but also at the level of replication.

In this study, we demonstrated that vector-based siRNA could significantly inhibit HBV antigen expression (both HBsAg and HBeAg) in hepatocytes. Furthermore, Northern blot analysis revealed that HBV pregenomic RNA and other shorter transcripts were diminished in the presence of specific siRNAs. Our results were different from a previous report[14], which demonstrated that pSuper-core1 and pSuper-core2 did not inhibit HBsAg and resulted in only a minor reduction of about 13% in the 3.5-kb transcript whereas pSuper-X reduced both HBsAg and HBcAg, and resulted in a significant reduction of about 68% at the level of all the viral transcripts. However, they were consistent with McCaffrey *et al*.[23] that siRNA targeting on the pregenomic RNA in the overlap region of the C and P open reading frames (ORF) reduced the levels of 2.4- and 2.1-kb RNAs and serum HBsAg even though it did not directly target on these RNAs. It can be assumed that HBV-specific siRNA first recognizes and degrades the corresponding sequence of viral pregenomic RNA, consequently depleting template for reverse transcription. Decreased synthesis of viral DNA then further influences the life cycle of HBV genome, especially in transcription and translation, thereby resulting in the overall inhibition of viral RNA and proteins.

Among the selected siRNAs, si-HBV1 is the most potent in inhibiting HBV replication. As si-HBV1 targeted on S region of the virus, multiple viral RNAs would be inhibited. Besides, it could also down-regulate the expression of P gene (the S ORF is within the P ORF), thus inhibiting viral replication *in trans*. These factors might explain, at least in part, why si-HBV1 has the highest efficacy.

Compared with the general nonspecific shutdown of cellular protein synthesis by double-stranded RNA (dsRNA) mediated primarily by IFN-α/β through the induction of protein kinase R (PKR) and RNaseL, the main known advantage of RNAi strategies is its high specificity on gene silencing. Attention has been paid to the potential non-specific effects of RNAi recently. Bridge *et al*.[24] found that a substantial number of siRNA vectors could trigger an interferon response. Sledz *et al*.[25] reported that transfection of siRNA resulted in interferon mediated activation of the Jak-Stat pathway and global up-regulation of IFN-stimulated genes. Although Kapadia *et al*.[20] and we did not detect the activation of known IFN-inducible pathways after transfection of siRNA or siRNA generating plasmids, the overall inhibition of viral RNAs by RNAi in our study and others still raise the possibility that RNAi may have some sequence-independent antiviral effects at certain doses. Overdose of siRNA or accumulation of unprocessed or aberrantly processed Pol III transcripts may trigger interferon response. Hence, further studies are required to optimize the dose and structure of short-haipin RNA as well as the delivery strategy to minimize the non-specific effects.

Taken together, our data show that RNAi is an attractive new strategy to inhibit the replication of hepatitis B virus. But to really apply this phenomenon to medical therapy, many problems are yet to be solved. One major problem is the selection of target sequence. Although there have been some online tools to help select the target sequence, the result is not always satisfactory. Recently, a theory has been proposed that siRNAs with relative stability at the 5' end of the sense strand, relative instability at the 5' end of the antisense strand and the cleavage site will most probably be the most effective ones[26-28]. These findings have significantly enlarged our knowledge of target selection, but the best siRNA should still be selected empirically. Therefore, a simple method of finding out the best target is urgently needed. Another major problem is how to efficiently and specifically deliver the siRNA-expressing vectors to the target cell types[29]. At present, retroviral or lentiviral vectors containing RNAi cassettes seem to be a good delivery system in carrying out gene silencing *in vivo*[30,31]. Chemically modified synthetic siRNA, which could be delivered into cells without cationic lipid carrier also holds promise for a future therapeutic agent[8]. With the advance in newly established techniques, RNAi may provide an effective therapeutic solution for HBV infection in the near future.

ACKNOWLEDGEMENTS

Wei Xiong is supported by the PhD studentship from the Ministry of Education P.R.C.

REFERENCES

1 **Tang ZY.** Hepatocellular carcinoma-Cause, treatment and metastasis. *World J Gastroenterol* 2001; **7**: 445-454
2 **Kao JH**, Chen DS. Global control of hepatitis B virus infection. *Lancet Infect Dis* 2002; **2**: 395-403
3 **Lee WM**. Hepatitis B virus infection. *N Engl J Med* 1997; **337**: 1733-1745
4 **Hannon GJ**. RNA interference. *Nature* 2002; **418**: 244-251
5 **Dykxhoorn DM,** Novina CD, Sharp PA. Killing the messenger: short RNAs that silence gene expression. *Nat Rev Mol Cell Biol* 2003; **4**: 457-467
6 **Elbashir SM**, Harborth J, Lendeckel W, Yalcin A, Weber K, Tuschl T. Duplexes of 21-nucleotide RNAs mediate RNA interference in cultured mammalian cells. *Nature* 2001; **411**: 494-498
7 **Novina CD**, Murray MF, Dykxhoorn DM, Beresford PJ, Riess J, Lee SK, Collman RG, Lieberman J, Shankar P, Sharp PA. siRNA-directed inhibition of HIV-1 infection. *Nat Med* 2002; **8**: 681-686
8 **Capodici J**, Kariko K, Weissman D. Inhibition of HIV-1 infection by small interfering RNA-mediated RNA interference. *J Immunol* 2002; **169**: 5196-5201
9 **Wilson JA**, Jayasena S, Khvorova A, Sabatinos S, Rodrigue-Gervais IG, Arya S, Sarangi F, Harris-Brandts M, Beaulieu S, Richardson CD. RNA interference blocks gene expression and RNA synthesis from hepatitis C replicons propagated in human liver cells. *Proc Natl Acad Sci U S A* 2003; **100**: 2783-2788
10 **Gitlin L**, Karelsky S, Andino R. Short interfering RNA confers intracellular antiviral immunity in human cells. *Nature* 2002; **418**: 430-434
11 **Wang QC**, Nie QH, Feng ZH. RNA interference: Antiviral weapon and beyond. *World J Gastroenterol* 2003; **9**: 1657-1661
12 **Sui G**, Soohoo C, Affar el B, Gay F, Shi Y, Forrester WC, Shi Y. A DNA vector-based RNAi technology to suppress gene expression in mammalian cells. *Proc Natl Acad Sci U S A* 2002; **99**: 5515–5520
13 **Brummelkamp TR**, Bernards R, Agami R. A system for stable expression of short interfering RNAs in mammalian cells. *Science* 2002; **296**: 550-553
14 **Shlomai A**, Shaul Y. Inhibition of hepatitis B virus expression and replication by RNA interference. *Hepatology* 2003; **37**: 764-770
15 **Jacque JM**, Triques K, Stevenson M. Modulation of HIV-1 replication by RNA interference. *Nature* 2002; **418**: 435-438
16 **Stevenson M.** Dissecting HIV-1 through RNA interference. *Nat Rev Immunol* 2003; **3**: 851-858
17 **Martinez MA,** Clotet B, Este JA. RNA interference of HIV replication. *Trends Immunol* 2002; **23**: 559-561
18 **Hu WY**, Myers CP, Kilzer JM, Pfaff SL, Bushman FD. Inhibition of retroviral pathogenesis by RNA interference. *Curr Biol* 2002; **12**: 1301-1311
19 **Bitko V**, Barik S. Phenotypic silencing of cytoplasmic genes using sequence-specific double-stranded short interfering RNA

and its application in the reverse genetics of wild type negative-strand RNA viruses. *BMC Microbiol* 2001; **1**: 34

20 **Kapadia SB**, Brideau-Andersen A, Chisari FV. Interference of hepatitis C virus RNA replication by short interfering RNAs. *Proc Natl Acad Sci U S A* 2003; **100**: 2014-2018

21 **Yokota T,** Sakamoto N, Enomoto N, Tanabe Y, Miyagishi M, Maekawa S, Yi L, Kurosaki M, Taira K, Watanabe M, Mizusawa H. Inhibition of intracellular hepatitis C virus replication by synthetic and vector-derived small interfering RNAs. *EMBO Rep* 2003; **4**: 602-608

22 **Jiang M**, Milner J. Selective silencing of viral gene expression in HPV-positive human cervical carcinoma cells treated with siRNA, a primer of RNA interference. *Oncogene* 2002; **21**: 6041-6048

23 **McCaffrey AP,** Nakai H, Pandey K, Huang Z, Salazar FH, Xu H, Wieland SF, Marion PL, Kay MA. Inhibition of hepatitis B virus in mice by RNA interference. *Nat Biotechnol* 2003; **21**: 639-644

24 **Bridge AJ**, Pebernard S, Ducraux A, Nicoulaz AL, Iggo R. Induction of an interferon response by RNAi vectors in mammalian cells. *Nat Genet* 2003; **34**: 263-264

25 **Sledz CA**, Holko M, de Veer MJ, Silverman RH, Williams BR. Activation of the interferon system by short-interfering RNAs. *Nat Cell Biol* 2003; **5**: 834-839

26 **Khvorova A**, Reynolds A, Jayasena SD. Functional siRNAs and miRNAs exhibit strand bias. *Cell* 2003; **115**: 209-216

27 **Schwarz DS**, Hutvagner G, Du T, Xu Z, Aronin N, Zamore PD. Asymmetry in the assembly of the RNAi enzyme complex. *Cell* 2003; **115**: 199-208

28 **Silva JM**, Sachidanandam R, Hannon GJ. Free energy lights the path toward more effective RNAi. *Nat Genet* 2003; **35**: 303-305

29 **Robinson R.** RNAi Therapeutics: How Likely, How Soon? *PLoS Biol* 2004; **2**: E28

30 **Brummelkamp TR**, Bernards R, Agami R. Stable suppression of tumorigenicity by virus-mediated RNA interference. *Cancer Cell* 2002; **2**: 243-247

31 **Rubinson DA**, Dillon CP, Kwiatkowski AV, Sievers C, Yang L, Kopinja J, Rooney DL, Ihrig MM, McManus MT, Gertler FB, Scott ML, Van Parijs L. A lentivirus-based system to functionally silence genes in primary mammalian cells, stem cells and transgenic mice by RNA interference. *Nat Genet* 2003; **33**: 401-406

Edited by Kumar M and Wang XL **Proofread by** Xu FM

PO Box 2345, Beijing 100023, China
Fax: +86-10-85381893
E-mail: wjg@wjgnet.com www.wjgnet.com

World J Gastroenterol 2004;10(20):2972-2978
World Journal of Gastroenterology
 ISSN 1007-9327

• VIRAL HEPATITIS •

Expression of hepatitis C virus envelope protein 2 induces apoptosis in cultured mammalian cells

Li-Xin Zhu, Jing Liu, You-Hua Xie, Yu-Ying Kong, Ye Ye, Chun-Lin Wang, Guang-Di Li, Yuan Wang

Li-Xin Zhu, Jing Liu, You-Hua Xie, Yu-Ying Kong, Ye Ye, Chun-Lin Wang, Guang-Di Li, Yuan Wang, State Key Laboratory of Molecular Biology, Institute of Biochemistry and Cell Biology, Shanghai Institutes for Biological Sciences, Chinese Academy of Sciences, Shanghai 200031, China
Supported by the National High Technology Research and Development Program of China, No. 2001AA215171
Correspondence to: Professor Yuan Wang, Institute of Biochemistry and Cell Biology, Chinese Academy of Sciences, Yueyang Road 320, Shanghai 200031, China. wangyuan@server.shcnc.ac.cn
Telephone: +86-21-54921103
Received: 2003-12-24 **Accepted:** 2004-02-13

Abstract

AIM: To explore the role of hepatitis C virus (HCV) envelope protein 2 (E2) in the induction of apoptosis.

METHODS: A carboxyterminal truncated E2 (E2-661) was transiently expressed in several cultured mammalian cell lines or stably expressed in Chinese hamster ovary (CHO) cell line. Cell proliferation was assessed by ^{3}H thymidine uptake. Apoptosis was examined by Hoechst 33258 staining, flow cytometry and DNA fragmentation analysis.

RESULTS: Reduced proliferation was readily observed in the E2-661 expressing cells. These cells manifested the typical features of apoptosis, including cell shrinkage, chromatin condensation and hypodiploid genomic DNA content. Similar apoptotic cell death was observed in an E2-661 stably expressing cell line.

CONCLUSION: HCV E2 can induce apoptosis in cultured mammalian cells.

Zhu LX, Liu J, Xie YH, Kong YY, Ye Y, Wang CL, Li GD, Wang Y. Expression of hepatitis C virus envelope protein 2 induces apoptosis in cultured mammalian cells. *World J Gastroenterol* 2004; 10(20): 2972-2978
http://www.wjgnet.com/1007-9327/10/2972.asp

INTRODUCTION

Hepatitis C virus (HCV) is the major causative agent of post-transfusion and community-acquired hepatitis. HCV has been classified in the Hepacivirus genus within the *Flaviviridae* family that includes flaviviruses, such as yellow fever and dengue viruses, and animal pestiviruses, such as bovine viral diarrhea virus (BVDV). Infection with HCV usually leads to chronic hepatitis. Although the mechanism for virus persistence is poorly understood, the high mutation rate of viral envelope proteins[1,2] and the suppression of the host immune system[3-5] are believed to contribute to the chronic infection. Analysis of peripheral blood mononuclear cells and liver biopsies from chronic patients suggested that HCV infection could induce apoptosis, which may help the virus escape the immune surveillance and causes liver injuries[6-11]. *In vitro* studies with either HCV full length RNA[12] or cDNA[13] have demonstrated that apoptosis could be induced by viral proteins. Several independent studies suggested that the viral core protein could induce apoptosis in cultured mammalian cell lines[14,15], while others using similar systems obtained different results[16-18]. Therefore, the viral molecule (s) responsible for the induction of apoptosis has not been clearly identified.

Some members in the *Flaviviridae* family, e.g. dengue and Langat viruses, could induce apoptosis during infection[19-22]. Duarte dos Santos *et al*. showed that determinants in the envelope protein of dengue type 1 virus could influence the induction of apoptosis[21]. Prikhod'ko *et al*. demonstrated that apoptosis could be induced by Langat flavivirus infection. Moreover, expression of the viral envelope protein alone was sufficient to induce apoptosis in cultured mammalian cells[22].

Since HCV envelope protein 2 (E2) displays a similar genetic organization as the envelope proteins of these viruses[23], it is possible that E2 may also induce apoptosis. It has been reported that a carboxyterminal truncated E2 (E2-661) without the transmembrane domain is properly folded in cultured mammalian cells[24,25] and has since been used in HCV studies, such as E2-CD81 binding analysis[26] and post-translational processing of E2[27]. In this study, we observed reduced cell proliferations of several cultured mammalian cell lines transiently expressing E2-661. These cells showed the typical features of apoptosis, including cell shrinkage, chromatin condensation and hypodiploid genomic DNA content. Similar apoptotic cell death was observed in an E2-661 stably expressing cell line. This is the first report that HCV E2 can induce apoptosis in cultured mammalian cells.

MATERIALS AND METHODS

Plasmid

pSecTagB/sE2 and pSecTagB/sS1E2 containing the insert of E2-661 (aa384-661 of the HCV polyprotein) coding sequence downstream to a signal sequence of Igκ and under the control of the CMV promoter (Figure 1A) were used in the study. To construct pSecTagB/sE2, E2-661 was PCR-amplified from pUC18/E (a gift from Dr. Wang *et al*.[28], Beijing University, GenBank accession# D10934) with primers 5'-GGCGTTAAGCTTAA CACCTACG TG-3' (*Hin*dIII site underlined) and 5'-CAG GAATTCTCACTCTGATCTATC-3' (*Eco*RI site underlined). The PCR product was digested with *Hin*dIII/*Eco*RI and cloned in the pSecTagB (Invitrogen). pSecTagB/sS1E2 was constructed by the insertion of a short tag derived from hepatits B virus (HBV) preS1 polypeptide (aa21-47) upstream to the E2-661 coding sequence in pSecTagB/sE2. These constructs were verified by sequencing.

Cell culture

Human liver carcinoma Huh7 and hepatoma HepG2, human cervical carcinoma HeLa and baby hamster kidney BHK-21 cell lines were grown in DMEM supplemented with 100 mL/L fetal calf serum (FCS). Chinese hamster ovary (CHO) cells were grown in DMEM/F12 (1:1) supplemented with 100 mL/L FCS. The stable E2-661 expressing cell line, CHO/sS1E2 was constructed by transfection

of CHO cells with pSecTagB/sS1E2 and selection in DMEM/F12 (1:1) medium containing 400 μg/mL Zeocin (Invitrogen)[24].

Transient expression

Expression plasmids or empty vectors were introduced into cells grown to 60% confluence with LipofectAMINE (Gibco). Transfection efficiency was monitored by co-transfection of pEGFP-C2 (Clontech) which encodes an enhanced green fluorescent protein. Two days after transfection, cells were subjected to Western blot, cell proliferation and apoptosis analysis.

Western blot analysis

Proteins were resolved on 100 g/L SDS-polyacrylamide gels and electroblotted onto nitrocellulose membranes. Membranes were blocked with 50 mL/L skimmed milk in PBS, followed by incubation with rabbit polyclonal anti-E2 antibody RE2116[29]. The blots were then incubated with horseradish peroxidase conjugated anti-rabbit IgG (Dako) and developed with SuperSignal West Pico stable peroxide solution (Pierce).

Immunofluorescence analysis

CHO and CHO/sS1E2 cells were fixed in ice-cold CMA solution (chloroform: methanol: acetone=1:2:1), incubated with anti-preS1 monoclonal antibody 125E11[30] 1 000-fold diluted in 10 g/L BSA (prepared in PBS) and followed by incubation with FITC conjugated anti-mouse IgG (Santa Cruz). Fluorescence was viewed under a fluorescence microscope.

Deglycosylation analysis

CHO and CHO/sS1E2 cells were washed twice with PBS and then harvested. Cells were lysed by boiling in the denaturing buffer provided by the manufacturer. Cell lysates were then digested with PNGase F or Endo H (NEB) for 2 h at 37 ℃. To analyze the secreted expression products, CHO and CHO/sS1E2 cells were grown in serum free OptiMEM/F12 (1:1) for 12 h. Medium was clarified by centrifugation at 20 000 *g* for 30 min at 4 ℃. Expression products were precipitated by an equal volume of ice-cold ethanol, resuspended in a small volume of PBS and subjected to Western blot analysis.

Cell proliferation analysis

Cell proliferation was measured by ^{3}H thymidine uptake according to a standard protocol[31]. Cells were incubated with 0.05 μCi ^{3}H thymidine (Amersham Pharmacia) for 4 h in complete medium with 100 mL/L FCS. Cells were then washed once with PBS and 100 mL/L trichloroacetic acid (TCA) followed by incubation in 100 mL/L TCA for 10 min at 37 ℃. After TCA was removed from the culture dishes, cells were lysed in the lysis buffer containing 0.33 mol/L NaOH and 10 g/L SDS. ^{3}H thymidine incorporation in the cell lysates was measured by liquid scintillation counting.

Apoptosis analysis

Apoptosis in stable and transient E2 expressing cells was analyzed by three methods: (1) Hoechst 33258 staining: Cells were seeded on sterile cover glasses placed in the 6-well plates the day before transfection. Two days after transfection, cells were fixed, washed twice with PBS and stained with Hoechst 33258 staining solution according to the manufacturer's instructions (Beyotime). Stained nuclei were observed under a fluorescence microscope. For the stable cell lines, similar staining procedures were performed without DNA transfection. (2) Flow cytometry: Cells were washed twice with PBS, trypsinized, and resuspended in complete medium with 100 mL/L FCS. Cells were then washed twice again with PBS and fixed with ice-cold 700 mL/L ethanol at 4 ℃ for 1 h. After the removal of ethanol, cells were incubated in PBS containing 250 μg/mL RNase A and 50 μg/mL propidium iodide (Sigma) at room templeture for 15 min, and stored in the dark at 4 ℃ until further analysis. Ten thousand cells per sample were analyzed with a FACSCalibur flow cytometer (Beckton-Dickinson). (3) DNA fragmentation: CHO and CHO/sS1E2 cells were washed twice with PBS and harvested. Cells were incubated in lysis buffer [10 mmol/L Tris, 1 mmol/L EDTA, 100 mmol/L NaCl, 5 g/L SDS, 1 μg/μL RNase A, pH8.0] at 37 ℃ for 30 min. At the end of incubation, proteinase K was added to a final concentration of 0.1mg/mL and the incubation was continued at 55 ℃ for 4 h. DNA was extracted with phenol/chloroform and precipitated with ethanol. DNA pellets were dissolved in TE buffer and analyzed on a 20 g/L agarose gel.

Statistical analysis

Statistical analysis was performed with unpaired 2-sided Student *t* test. $P<0.05$ was regarded as statistically significant.

RESULTS

Transient expression of E2-661 in mammalian cells

DNA fragments encoding aa384-661 of the HCV polyprotein (E2-661) were cloned in the expression vector pSecTagB to generate pSecTagB/sE2 and pSecTagB/sS1E2 (Figure1A). Compared to pSecTagB/sE2, E2-661 expressed by pSecTagB/sS1E2 had a small 27-aa preS1 tag located at the N-terminus to facilitate the characterization of the expression products. The above plasmids were used to transfect Huh7, HepG2, HeLa and BHK-21 cells. Cell lysates were analyzed by Western blot with anti-E2 antibody. E2-661 was detected in E2-661 transient expressing cells (Figure 1B). The expressed protein exhibited a heterogeneous pattern typical of a glycoprotein. The expression of E2-661 could also be detected in the cells (transiently) transfected with pSecTagB/sS1E2 (see below).

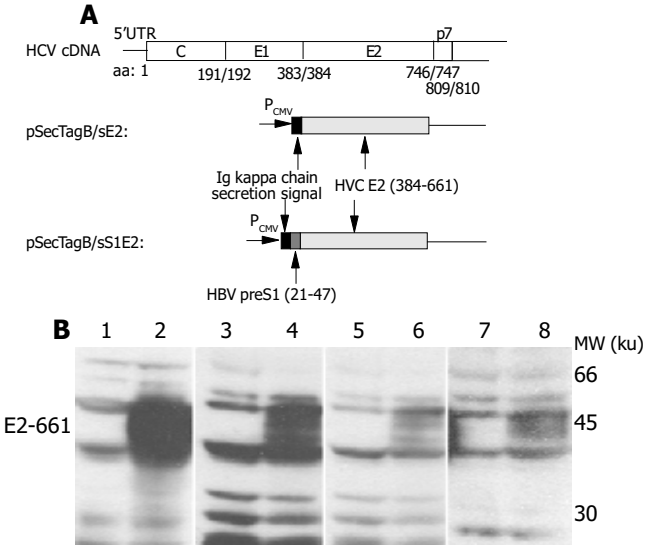

Figure 1 Transient expression of E2-661 in mammalian cells. A: Schematic representation of plasmids encoding E2-661. HBV preS1 (21-47) tag and HCV E2-661 (384-661) signal peptide are indicated. Numbers refer to amino acids of the HCV polyprotein. B: Western blot analysis of E2-661 expressed in mammalian cells with a rabbit polyclonal anti-E2 antibody RE2116. Lanes on the left of all blots were transfected with the empty vector while those on the right were transfected with pSecTagB/sE2. 1-2, BHK-21; 3-4, HeLa; 5-6, Huh7 and 7-8, HepG2. E2-661 was indicated by arrowhead.

E2 expressing cells showed reduced cell proliferation

Cells transfected with pSecTagB/sE2 showed significant cell death upon microscope observation (Figure 2A). Reduced cell

density, cell rounding and cell shrinkage were the common features of all the cell lines transfected with pSecTagB/sE2. The effect of E2 expression on the cell proliferation was further analyzed by ^{3}H thymidine uptake assay (Figure 2B). Reductions in ^{3}H incorporation were observed with all the cell lines assayed (P<0.05 for HepG2, P<0.001 for Huh7, HeLa and BHK-21). Transfection efficiencies were monitored by cotransfection with pEGFP-C2. Since a similar amount of EGFP expressing cells were observed between pSecTagB and pSecTagB/sE2 transfected cells (data not shown), the reduced cell proliferation of E2 expressing cells was not due to the transfection procedure (e.g. transfection reagent and EGFP expression). Similar results were observed with the E2 expressing plasmid pSecTagB/sS1E2 (data not shown). These results suggested that the expression of E2 was responsible for the reduction in cell proliferation.

Apoptosis induced by transient expression of E2

The reduced proliferation might be due to various reasons. To determine if apoptosis contributed to the reduced cell proliferation of E2 expressing cells, cells transfected with pSecTagB/sE2 or

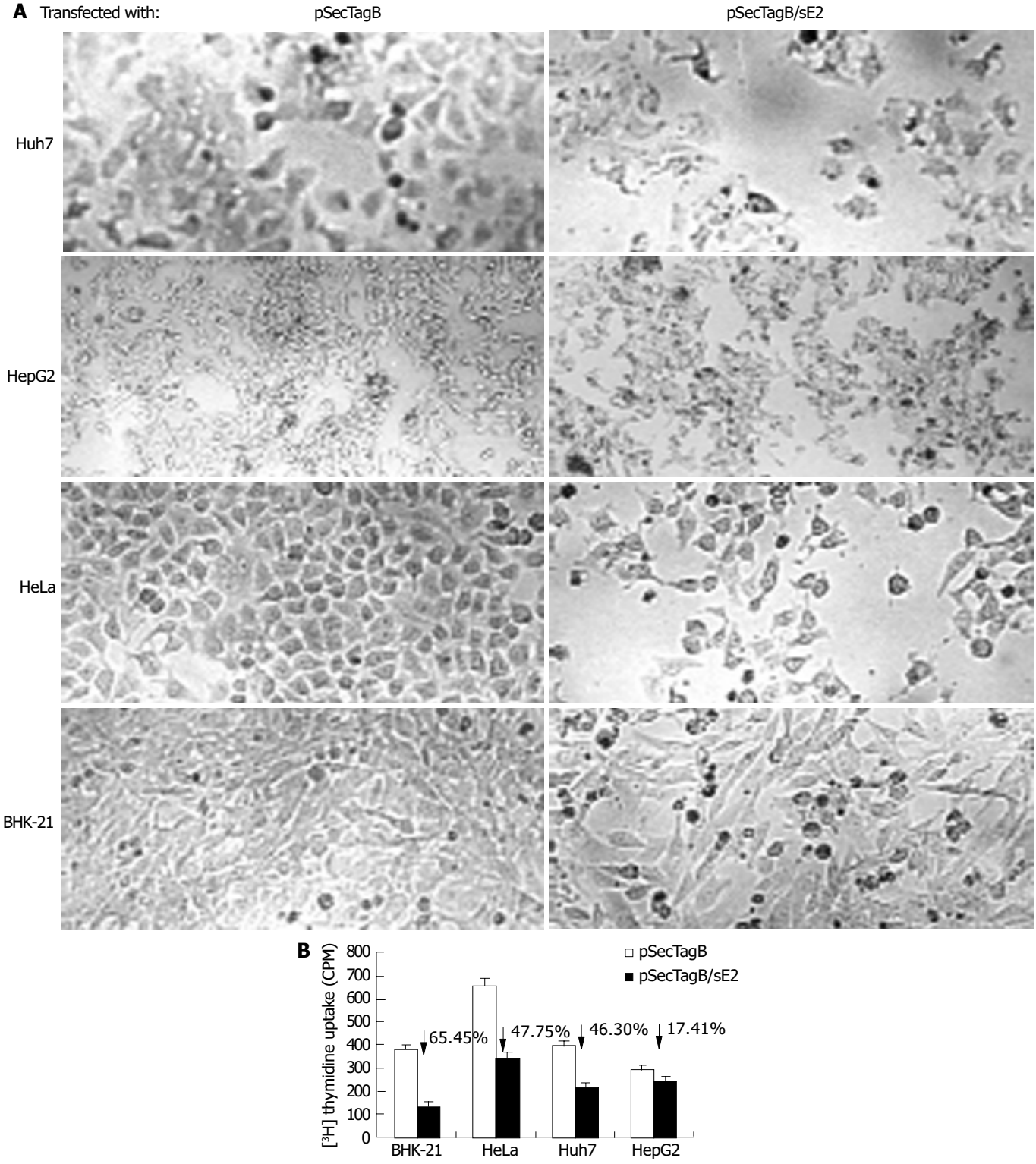

Figure 2 Reduced cell proliferation in E2 expressing cells. A: Morphology of Huh7, HepG2, HeLa, BHK-21 cells 48 h after transfection with pSecTagB or pSecTagB/sE2 (original magnification 40×). B: Reduced ^{3}H thymidine uptake by E2 expressing cells. P<0.05 betweer all the cells tested.

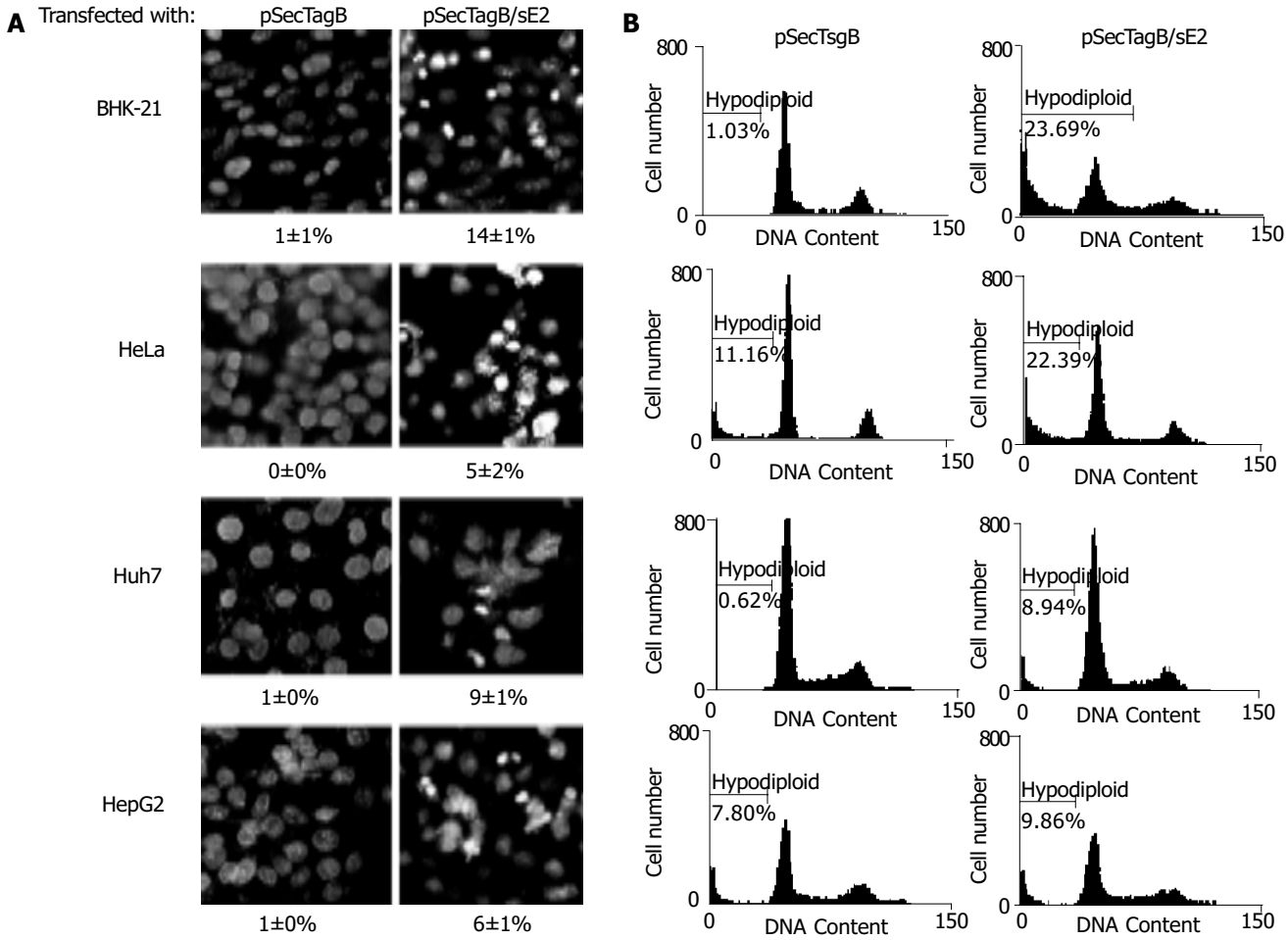

Figure 3 Apoptosis induced by transient expression of E2. A: Hoechst staining of BHK-21, HeLa, Huh7 and HepG2 cells 48 h after transfection with pSecTagB or pSecTagB/sE2. Note the bright nuclei among cells transfected with pSecTagB/sE2. Photograph is a representative experiment repeated three times (original magnification 400×). B: Flow cytometry analysis of PI stained cells 48 h after transfection with pSecTagB or pSecTagB/sE2. The percentage of cells with hypodiploid genomic DNA are indicated on each of the histogram. Results were a representative experiment repeated twice.

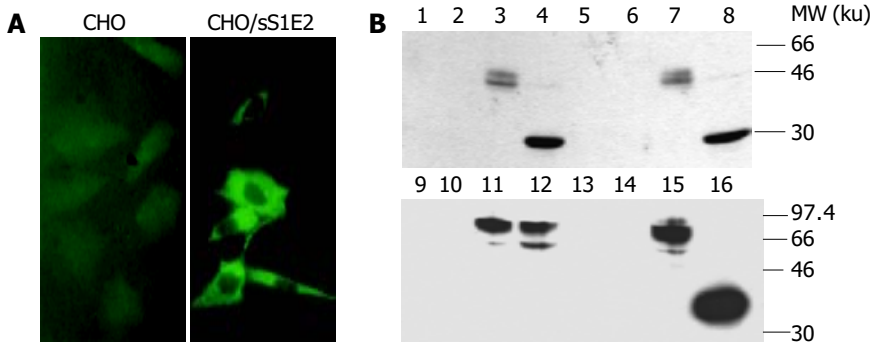

Figure 4 Expression of E2-661 in CHO/sS1E2 cells. A: Immunofluorescence of E2 in CHO/sS1E2 cells analyzed with a monoclonal anti-preS1 antibody 125E11 (original magnification 400×). B: Western blot analysis of the E2 products from CHO/sS1E2 cells. Cell lysates and proteins precipitated from culture medium were analyzed with anti-E2 polyclonal antibody RE2116 after N-glycosidase treatment. Lanes 1, 2, 5, 6: cell lysates from CHO cells; lanes 3, 4, 7, 8: cell lysates from CHO/sS1E2 cells; lanes 9, 10, 13, 14: culture medium from CHO cells; lanes 11, 12, 15, 16: culture medium from CHO/sS1E2 cells; lanes 1, 3, 9, 11: samples incubated with Endo H digestion buffer; lanes 2, 4, 10, 12: samples digested with Endo H; lanes 5, 7, 13, 15: samples incubated with PNGase F digestion buffer; lanes 6, 8, 14, 16, samples digested with PNGase F.

pSecTagB were stained with Hoechst 33258, respectively (Figure 3A). Condensed bright apoptotic nuclei were readily observed amidst the pSecTagB/sE2 transfected cells. The presence of apoptotic cells in E2 expressing cells was further confirmed by flow cytometry. Huh7, HepG2, BHK-21, HeLa cells transfected with pSecTagB/sE2 or control pSecTagB were stained with PI and analyzed by flow cytometry (Figure 3B). Hypodiploid DNA appeared in the sub-G0/G1 region, which represented dead cells. A higher percentage of dead cells was observed in all the four cell lines transfected with pSecTagB/sE2.

Apoptosis in a CHO cell line stablely expressing E2

E2 induced apoptosis was also investigated in a CHO cell line CHO/sS1E2 stably expressing E2-661. This cell line showed the expression of E2-661 as detected by indirect fluorecence assay with the monoclonal antibody against the preS1 tag (Figure 4A).

The fluorescence in CHO/sS1E2 cells suggested the localization of expressed proteins in the cytoplasm. In further characterization by Western blot analysis, cell-associated and secreted E2 proteins (from 10^5 and 10^7 cells) were detected with the E2 polyclonal antibody (Figure 4B). The cell-associated E2 protein was sensitive to Endo H (lane 4), suggesting that the glycans carried on it were ER-restricted. On the other hand, secreted E2 was resistant to Endo H (lane 12), suggesting that the glycans on this species of E2 underwent the modification by Golgi enzymes.

Similar to cells transiently transfected with pSecTagB/sE2, the morphology of CHO/sS1E2 was different from that of the original CHO cell line (Figure 5A). There were obvious differences in cell size and shape between these two cell lines. A significant number of dead cells were readily observed for CHO/sS1E2 and cells could hardly grow to 100% confluency. Similar morphology and growth curve were also observed in other CHO/sS1E2 clones (data not shown), suggesting that they are not the result of clonal selection. ^{3}H incorporation analysis showed that there was a significant reduction (72.0%, $P<0.001$) of cell proliferation for CHO/sS1E2 in comparison with CHO cells (Figure 5B).

Hoechst 33258 staining of CHO/sS1E2 showed condensed bright nuclei typical of apoptotic dead cells which reached about 14% of the total cells, while almost no apoptotic nuclei were observed in control CHO cells (Figure 6A). Flow cytometry analysis confirmed that there were a significant number of dead cells for CHO/sS1E2 (Figure 6B).

Since the cleavage of chromosomal DNA into fragments of oligonucleosomal size is a biochemical hallmark of apoptosis[32], DNA fragmentation in CHO/sS1E2 was examined by DNA laddering assay. With the freshly seeded CHO/sS1E2 cells, no obvious DNA fragmentation was observed, while clear DNA laddering in -180 bp interval was detected 48 h after cell seeding. No apoptotic DNA fragmentation was observed in CHO cells at either time points (Figure 6C).

DISCUSSION

In this study, HCV E2 was transiently expressed in several mammalian cells. All tested cells showed shrinkage in morphology and reduced cell proliferation due to the expression

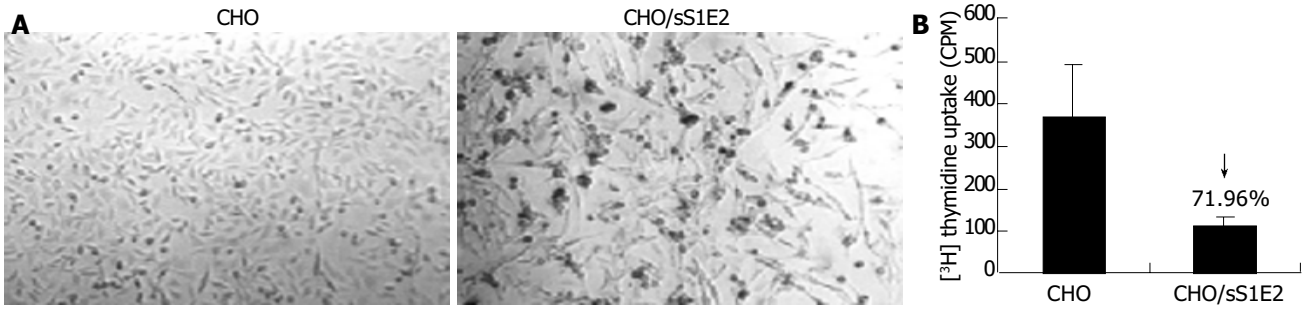

Figure 5 Reduced cell proliferation in CHO/sS1E2 cells. A: Morphology of CHO and CHO/sS1E2 cells (original magnification 40×). B: Reduced ^{3}H thymidine uptake by CHO/sS1E2 cells. CHO and CHO/sS1E2 cells were subjected to ^{3}H thymidine uptake assay 24 h after seeding. Each sample was done in quadruplicates. The differences in ^{3}H incorporation between CHO and CHO/sS1E2 cells were significant ($P<0.001$).

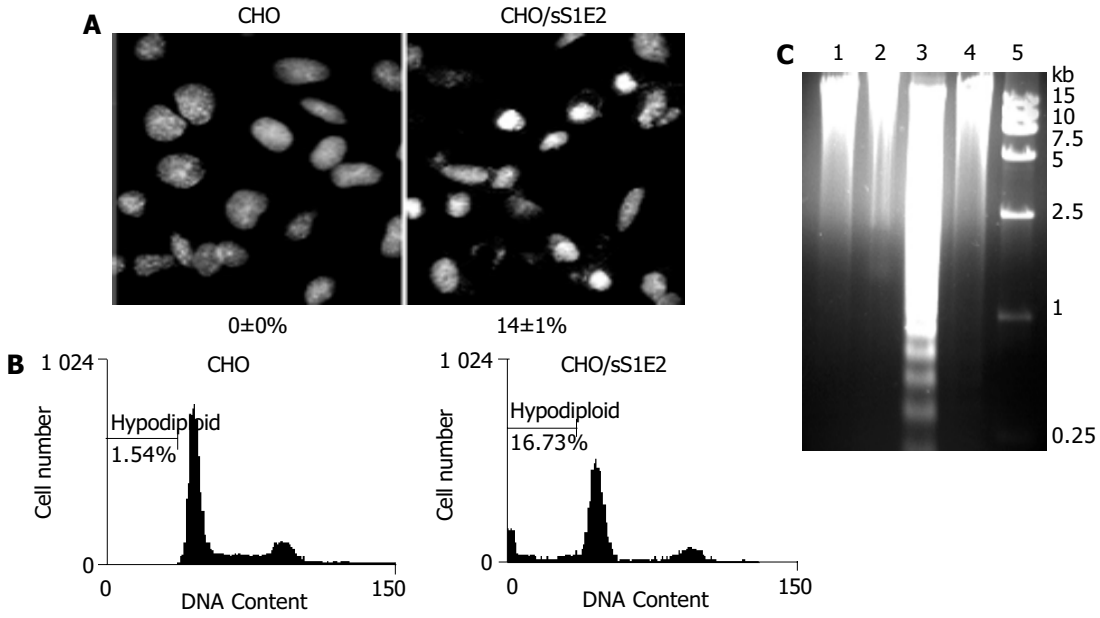

Figure 6 Apoptosis of CHO/sS1E2 cells. A: Hoechst staining of CHO and CHO/sS1E2 cells 24 h after seeding. Photograph is a representative experiment repeated three times (original magnification 400×). The percentage of condensed and fragmented nuclei is indicated at the bottom of each photo. Numbers are presented as mean±SD. B: Flow cytometry analysis of PI stained cells 24 h after seeding. The percentage of cells with hypodiploid genomic DNA is indicated on each of the histogram. Results were a representative experiment repeated twice. C: Fragmentation of CHO/sS1E2 cell DNA. Lane 1: CHO cells 48 h post-seeding; lane 2: CHO cells freshly seeded; lane 3: CHO/sS1E2 cells 48 h post-seeding; lane 4: CHO/sS1E2 cells freshly seeded; lane 5: DNA size marker.

of E2. Further evidences, such as condensed chromatin, demonstrated that apoptosis contributed, at least in part, to the cell death induced by E2. E2 induced apoptosis was also observed in a stable E2 expressing cell line CHO/sS1E2. Again there was a significant reduction in cell proliferation of CHO/sS1E2 in comparison to CHO cells. Hoechst 33258 staining, flow cytometry analysis and DNA laddering assay demonstrated that apoptosis contributed to the reduced cell proliferation. Apoptosis in CHO/sS1E2 was not due to the expression of the small preS1 tag because toxicity was not observed when preS1 was transiently expressed in cultured mammalian cells[33]. In conclusion, our results demonstrate that the expression of HCV E2 could induce apoptosis in cultured mammalian cells.

It has been reported that apoptosis is involved in the pathogenesis of hepatitis C. Immunohistochemical study suggested that the Fas system played an important role in liver injuries of viral hepatitis[34]. There is evidence that immune response (cytotoxic T lymphocyte) might be involved in the apoptosis of hepatocytes in HCV infected patients[35]. Recent studies suggested that apoptosis of hepatocytes might also be due to the cytopathic effect of viral proteins[13,14]. Our result that E2 expression induced apoptosis in cultured mammalian cells including human hepatic cells supports this hypothesis. On the other hand, E2-induced apoptosis may also partly contribute to the escape of HCV from the host immune surveillance. It awaits further investigation whether the expression of E2 can induce apoptosis in lymphocytes.

Studies of Langat flavivirus[22] demonstrated that expression of envelope (E) protein could induce apoptosis via the Caspase 3 pathway. Since HCV E2 and the E protein of Langat flavivirus share similar genetic organization and hydropathy profile[23], it is possible that E2 could induce apoptosis through a similar mechanism. Increased Fas expression observed in HCV patients[7] also suggested the involvement of the caspase-3 pathway. However, comparing the expression levels of secreted and cell-associated E2, we found that in our system, E2 was mainly cell-associated and localized in the cytoplasm. By glycosidase digestion analysis, we found that most of the cell-associated E2 were high-mannose type glycoproteins, which suggested the localization of E2 to the endoplastic reticulum (ER). Many other mammalian expression systems also showed the ER localization of the expressed HCV E2, and a large portion of them formed disulfide-linked aggregates[36-38]. The accumulation of large amount of proteins in the ER might induce ER stress and apoptosis could be triggered via the Caspase 12-mediated apoptosis pathway[39]. Further study is required for understanding the possible pathway of HCV E2 induced apoptosis.

ACKNOWLEDGEMENTS

The authors thank Professor Jia-Rui Wu for providing CHO cell line and Professor Yu Wang for the HCV cDNA for this study.

REFERENCES

1 **Bassett SE**, Thomas DL, Brasky KM, Lanford RE. Viral persistence, antibody to E1 and E2, and hypervariable region 1 sequence stability in hepatitis C virus-inoculated chimpanzees. *J Virol* 1999; **73**: 1118-1126
2 **Farci P**, Purcell RH. Clinical significance of hepatitis C virus genotypes and quasispecies. *Semin Liver Dis* 2000; **20**: 103-126
3 **Crotta S**, Stilla A, Wack A, D'Andrea A, Nuti S, D'Oro U, Mosca M, Filliponi F, Brunetto RM, Bonino F, Abrignani S, Valiante NM. Inhibition of natural killer cells through engagement of CD81 by the major hepatitis C virus envelope protein. *J Exp Med* 2002; **195**: 35-41
4 **Large MK**, Kittlesen DJ, Hahn YS. Suppression of host immune response by the core protein of hepatitis C virus: possible implications for hepatitis C virus persistence. *J Immunol* 1999; **162**: 931-938
5 **Bain C**, Fatmi A, Zoulim F, Zarski JP, Trepo C, Inchauspe G. Impaired allostimulatory function of dendritic cells in chronic hepatitis C infection. *Gastroenterology* 2001; **120**: 512-524
6 **Hiramatsu N**, Hayashi N, Katayama K, Mochizuki K, Kawanishi Y, Kasahara A, Fusamoto H, Kamada T. Immunohistochemical detection of Fas antigen in liver tissue of patients with chronic hepatitis C. *Hepatology* 1994; **19**: 1354-1359
7 **Calabrese F**, Pontisso P, Pettenazzo E, Benvegnu L, Vario A, Chemello L, Alberti A, Valente M. Liver cell apoptosis in chronic hepatitis C correlates with histological but not biochemical activity or serum HCV-RNA levels. *Hepatology* 2000; **31**: 1153-1159
8 **Emi K**, Nakamura K, Yuh K, Sugyo S, Shijo H, Kuroki M, Tamura K. Magnitude of activity in chronic hepatitis C is influenced by apoptosis of T cells responsible for hepatitis C virus. *J Gastroenterol Hepatol* 1999; **14**: 1018-1024
9 **Toubi E**, Kessel A, Goldstein L, Slobodin G, Sabo E, Shmuel Z, Zuckerman E. Enhanced peripheral T-cell apoptosis in chronic hepatitis C virus infection: association with liver disease severity. *J Hepatol* 2001; **35**: 774-780
10 **Taya N**, Torimoto Y, Shindo M, Hirai K, Hasebe C, Kohgo Y. Fas-mediated apoptosis of peripheral blood mononuclear cells in patients with hepatitis C. *Br J Haematol* 2000; **110**: 89-97
11 **Pianko S**, Patella S, Ostapowicz G, Desmond P, Sievert W. Fas-mediated hepatocyte apoptosis is increased by hepatitis C virus infection and alcohol consumption, and may be associated with hepatic fibrosis: mechanisms of liver cell injury in chronic hepatitis C virus infection. *J Viral Hepat* 2001; **8**: 406-413
12 **Kalkeri G**, Khalap N, Garry RF, Fermin CD, Dash S. Hepatitis C virus protein expression induce apoptosis in HepG2 cells. *Virology* 2001; **282**: 26-37
13 **Kalkeri G**, Khalap N, Akhter S, Garry RF, Fermin CD, Dash S. Hepatitis C viral proteins affect cell viability and membrane permeability. *Exp Mol Pathol* 2001; **71**: 194-208
14 **Zhu N**, Khoshnan A, Schneider R, Matsumoto M, Dennert G, Ware C, Lai MM. Hepatitis C virus core protein binds to the cytoplasmic domain of tumor necrosis factor (TNF) receptor 1 and enhances TNF-induced apoptosis. *J Virol* 1998; **72**: 3691-3697
15 **Honda M**, Kaneko S, Shimazaki T, Matsushita E, Kobayashi K, Ping LH, Zhang HC, Lemon SM. Hepatitis C virus core protein induces apoptosis and impairs cell-cycle regulation in stably transformed Chinese hamster ovary cells. *Hepatology* 2000; **31**: 1351-1359
16 **Marusawa H**, Hijikata M, Chiba T, Shimotohno K. Hepatitis C virus core protein inhibits Fas- and tumor necrosis factor alpha-mediated apoptosis via NF-kappaB activation. *J Virol* 1999; **73**: 4713-4720
17 **Ray RB**, Meyer K, Ray R. Suppression of apoptotic cell death by hepatitis C virus core protein. *Virology* 1996; **226**: 176-182
18 **Ray RB**, Meyer K, Steele R, Shrivastava A, Aggarwal BB, Ray R. Inhibition of tumor necrosis factor (TNF-alpha)-mediated apoptosis by hepatitis C virus core protein. *J Biol Chem* 1998; **273**: 2256-2259
19 **Despres P**, Flamand M, Ceccaldi PE, Deubel V. Human isolates of dengue type 1 virus induce apoptosis in mouse neuroblastoma cells. *J Virol* 1996; **70**: 4090-4096
20 **Avirutnan P**, Malasit P, Seliger B, Bhakdi S, Husmann M. Dengue virus infection of human endothelial cells leads to chemokine production, complement activation, and apoptosis. *J Immunol* 1998; **161**: 6338-6346
21 **Duarte dos Santos CN**, Frenkiel MP, Courageot MP, Rocha CF, Vazeille-Falcoz MC, Wien MW, Rey FA, Deubel V, Despres P. Determinants in the envelope E protein and viral RNA helicase NS3 that influence the induction of apoptosis in response to infection with dengue type 1 virus. *Virology* 2000; **274**: 292-308
22 **Prikhod'ko GG**, Prikhod'ko EA, Cohen JI, Pletnev AG. Infection with Langat Flavivirus or expression of the envelope protein induces apoptotic cell death. *Virology* 2001; **286**: 328-335
23 **Hijikata M**, Kato N, Ootsuyama Y, Nakagawa M, Shimotohno K. Gene mapping of the putative structural region of the hepatitis C virus genome by *in vitro* processing analysis. *Proc Natl Acad Sci U S A* 1991; **88**: 5547-5551
24 **Wang CL**, Zhu LX, Liu J, Zhang ZC, Wang Y, Li GD. Expression and characterization of hepatitis C Virus E2 glycoprotein

fused to hepatitis B virus preS1 (21-47) fragment in CHO cells. *Shengwuhuaxue Yu Shengwuwuli Xuebao* 2002; **34**: 400-404

25 **Michalak JP**, Wychowski C, Choukhi A, Meunier JC, Ung S, Rice CM, Dubuisson J. Characterization of truncated forms of hepatitis C virus glycoproteins. *J Gen Virol* 1997; **78**(Pt 9): 2299-2306

26 **Pileri P**, Uematsu Y, Campagnoli S, Galli G, Falugi F, Petracca R, Weiner AJ, Houghton M, Rosa D, Grandi G, Abrignani S. Binding of hepatitis C virus to CD81. *Science* 1998; **282**: 938-941

27 **Zhu LX**, Liu J, Li YC, Kong YY, Staib C, Sutter G, Wang Y, Li GD. Full-length core sequence dependent complex-type glycosylation of hepatitis C virus E2 glycoprotein. *World J Gastroenterol* 2002; **8**: 499-504

28 **Wang Y**, Okamoto H, Tsuda F, Nagayama R, Tao QM, Mishiro S. Prevalence, genotypes, and an isolate (HC-C2) of hepatitis C virus in Chinese patients with liver disease. *J Med Virol* 1993; **40**: 254-260

29 **Liu J**, Zhu L, Zhang X, Lu M, Kong Y, Wang Y, Li G. Expression, purification, immunological characterization and application of Escherichia coli-derived hepatitis C virus E2 proteins. *Biotechnol Appl Biochem* 2001; **34**(Pt 2): 109-119

30 **Yang HL**, Jin Y, Cao HT, Xu X, Li GD, Wang Y, Zhang ZC. Affinity purification of hepatitis B virus surface antigen containing preS1 region. *Shengwuhuaxue Yu Shengwuwuli Xuebao* 1996; **28**: 412-417

31 **Tolleson WH**, Melchior WB Jr, Morris SM, McGarrity LJ, Domon OE, Muskhelishvili L, James SJ, Howard PC. Apoptotic and anti-proliferative effects of fumonisin B1 in human keratinocytes, fibroblasts, esophageal epithelial cells and hepatoma cells. *Carcinogenesis* 1996; **17**: 239-249

32 **Wyllie AH**. Glucocorticoid -induced thymocyte apoptosis is associated with endogenous endonuclease activation. *Nature* 1980; **284**: 555-556

33 **Hui J**, Mancini M, Li G, Wang Y, Tiollais P, Michel ML. Immunization with a plasmid encoding a modified hepatitis B surface antigen carrying the receptor binding site for hepatocytes. *Vaccine* 1999; **17**: 1711-1718

34 **Hayashi N**, Mita E. Fas system and apoptosis in viral hepatitis. *J Gastroenterol Hepatol* 1997; **12**: S223-S226

35 **Onji M**, Kikuchi T, Kumon I, Masumoto T, Nadano S, Kajino K, Horiike N, Ohta Y. Intrahepatic lymphocyte subpopulations and HLA class I antigen expression by hepatocytes in chronic hepatitis C. *Hepatogastroenterology* 1992; **39**: 340-343

36 **Selby MJ**, Choo QL, Berger K, Kuo G, Glazer E, Eckart M, Lee C, Chien D, Kuo C, Houghton M. Expression, identification and subcellular localization of the proteins encoded by the hepatitis C viral genome. *J Gen Virol* 1993; **74**(Pt 6): 1103-1113

37 **Dubuisson J**, Hsu HH, Cheung RC, Greenberg HB, Russell DG, Rice CM. Formation and intracellular localization of hepatitis C virus envelope glycoprotein complexes expressed by recombinant vaccinia and Sindbis viruses. *J Virol* 1994; **68**: 6147-6160

38 **Dubuisson J**, Rice CM. Hepatitis C virus glycoprotein folding: disulfide bond formation and association with calnexin. *J Virol* 1996; **70**: 778-786

39 **Yoneda T**, Imaizumi K, Oono K, Yui D, Gomi F, Katayama T, Tohyama M. Activation of caspase-12, an endoplastic reticulum (ER) resident caspase, through tumor necrosis factor receptor-associated factor 2-dependent mechanism in response to the ER stress. *J Biol Chem* 2001; **276**: 13935-13940

Edited by Wang XL and Xu XQ **Proofread by** Xu FM

PO Box 2345, Beijing 100023, China
Fax: +86-10-85381893
E-mail: wjg@wjgnet.com www.wjgnet.com

World J Gastroenterol 2004;10(20):2979-2983
World Journal of Gastroenterology
 ISSN 1007-9327

• VIRAL HEPATITIS •

Construction of exogenous multiple epitopes of helper T lymphocytes and DNA immunization of its chimeric plasmid with HBV pre-S2/S gene

Wen-Jun Gao, Xiao-Mou Peng, Dong-Ying Xie, Qi-Feng Xie, Zhi-Liang Gao, Ji-Lu Yao

Wen-Jun Gao, Department of Infectious Diseases, Zhongshan People's Hospital, Zhongshan 528400, Guangdong Province, China
Xiao-Mou Peng, Dong-Ying Xie, Qi-Feng Xie, Zhi-Liang Gao, Ji-Lu Yao, Department of Infectious Diseases, Third Hospital, Sun Yat-Sen University, Guangzhou 510630, Guangdong Province, China
Supported by the National Natural Science Foundation of China, NO. 39970677 and the Science Foundation of Guangdong Province, NO. 99M04801G
Correspondence to: Xiao-Mou Peng, Department of Infectious Diseases, Third Hospital, Sun Yat-Sen University, Guangzhou 510630, Guangdong Province, China. xiaomoupeng@hotmail.com
Telephone: +86-20-85516867 Ext. 2019 **Fax:** +86-20-85515940
Received: 2004-01-01 **Accepted:** 2004-02-26

Abstract

AIM: To design and construct an exogenous multiple epitope of helper T lymphocytes (HTL), and to evaluate its effect on anti-HBs response through DNA immunization.

METHODS: Artificial HTL epitope, PADRE and four other HTL epitopes from different proteins were linked together using splicing by overlap extension to generate exogenous multiple epitopes of HTL, MTE5. pcMTE5 and pcHB were generated by cloning MTE5 and fragments of HBV pre-S2/S gene into mammalian expression plasmid pcDNA3. Four chimeric plasmids were constructed by cloning MTE5 into the region of pre-S2 gene (*Bam* HI), 5′ terminal of S gene (*Hin*cII, *Xba* I) and 3′ terminal of S gene (*Acc* I) of pcHB respectively. BALB/c mice were used in DNA immunization of the recombinant plasmids. Anti-HBs was detected using Abbott IMx AUSAB test kits.

RESULTS: The sequences of MTE5 and the 6 constructs of recombinant plasmids were confirmed to be correct by DNA sequencing. The anti-HBs response of the co-inoculation of pcHB and pcMTE5 was much higher than that of the inoculation of pcHB only (136.7±69.1 mIU/mL *vs* 27.6±17.3 mIU/mL, $P<0.01$, $t = -6.56$). Among the 4 chimeric plasmids, only the plasmid in which MTE5 was inserted into the pre-S2 region had good anti-HBs response (57.54±7.68 mIU/mL), and had no significant difference compared with those of pcHB and the co-inoculation of pcHB and pcMTE5.

CONCLUSION: Exogenous multiple epitopes of HTL had immune enhancement when they were co-inoculated with pre-S2/S gene or inoculated in the chimeric form at a proper site of pre-S2/S gene of HBV. It might suggest that it was possible to improve hepatitis B vaccine using exogenous multiple epitopes of HTL. The antibody responses were very low using DNA immunization in the study. Thus, the immune enhancement effect of exogenous multiple epitopes of HTL has to be confirmed and the effect on overcoming the drawback of the polymorphism of HLA II antigens should also be evaluated after these chimeric plasmids are expressed in mammalian cell lines.

Gao WJ, Peng XM, Xie DY, Xie QF, Gao ZL, Yao JL. Construction of exogenous multiple epitopes of helper T lymphocytes and DNA immunization of its chimeric plasmid with HBV pre-S2/S gene. *World J Gastroenterol* 2004; 10 (20): 2979-2983
http://www.wjgnet.com/1007-9327/10/2979.asp

INTRODUCTION

There are more than 300 millions of HBsAg carriers all over the world. Most of them have active infection of hepatitis B virus. Chronic hepatitis B virus infection may cause significant incidence of chronic hepatitis, cirrhosis, and hepatocellular carcinoma[1,2]. Hepatitis B vaccine inoculation is an important measure for prevention of HBV infection. Considerable variability exists, however, in response to hepatitis B vaccines, and 5-10% of healthy young adults demonstrate no or inadequate responses following a standard vaccination schedule[3-8]. The frequency of non- and low-responders is up to 40-50% in vaccined subjects with depressed immune responses, such as patients on maintenance hemodialysis. Only some of the non- or low-responders to hepatitis B vaccine are responsive to the novel recombinant triple antigen hepatitis B vaccine (pre-S1/S2 and HBsAg)[9]. These non- or low-responders usually carry specific type of class II human leukocyte antigens (HLA II antigens), such as DRB1*3, DRB1*7, DQB1*20 or DPB1*1101[10-13]. The antigen presentation is blocked because these HLA II antigen molecules on the surface of helper T lymphocytes (HTL) cannot combine efficiently with the epitope of HTL on the vaccine protein, hepatitis B surface antigen (HBsAg)[14,15]. Adding exogenous multiple epitopes of HTL, which can combine with much more types of HLA II antigens to hepatitis B vaccine may be a good way to solve this problem. Conducting HTL epitopes from tetanus toxoids (aa73-99, aa830-845) and artificial epitopes of PADRE into HBsAg can enhance the immunogenicity of HbsAg[16,17]. Adding exogenous HTL epitopes to HBsAg can let natural non-responder mice respond to HbsAg[18]. These data suggest that it is possible to use exogenous HTL epitopes to improve hepatitis B vaccine. For these reasons, an exogenous multiple epitope of HTL, MTE5, consisting of five HTL epitopes from different origins was designed and constructed. Its effect on anti-HBs response was evaluated through DNA immunization after it was inserted in different loci of HBV pre-S2/S gene.

MATERIALS AND METHODS

Reagents

pTZ19U-HBV containing double copies of HBV DNA (adw) was a gift from professor Zhi-Min Huang, Sun Yat-Sen University. T4 DNA ligase and pfu DNA polymerase were purchased form Promega Company (USA). DNA gel extraction kits and plasmid isolation kits were purchased from Qiagen Company (German). Polyclonal antibodies of anti-HBs and LSAB test kit for immunohistochemistry were purchased form DAKO Company (USA). Primers and oligonucleotide fragments shown in Table 1 were synthesized in Bioasia Biological Engineering Company (Shanghai, China).

Table 1 Primers and oligonucleotide fragments used in mte5 splicing and construction of eukaryotic expression plasmids

	Sequences (5'→3')
F1	ATGGCTAAAA CCATCGCCTA TGATGAAGAA GCTCGTCGTG GTCTGGAACG TGGTCTGAAT GCCTCCGAT
F2	GTCCAGGCAG CAACGAATTT AGCTCCCTGC AGCCAGTGTC CAGGCAGAAC ATCGGAGGCA TTCAGACCA
F3	AATTCGTTGC TGCCTGGACC CTGAAAGCTG CCGCTGGAAG ACACGTTGTT ATCGATAAGA GCTTCGGAA
F4	TTCGGTGATT CCGATAAACT TGGAATTAGC TTTGATGTAC TGCTGAGGGC TTCCAAGGCT CTTATCGAT M`TE-
MTE-P1	TCGGATCCCA TGGCTAAAAC CATCGCC
MTE-P2	GCTCTAGACT TTCGGTGATT CCGATAA
HBV-P1	CCTAAGCTTA TGCAGTGGAA CTCCACT
HBV-P2	TGGAATTCCT TAAATGTATA CCCAGAG
Bam-1	TCGGATCCCA TGGCTAAAAC CATCGCC
Bam-2	GCGGATCCCT TTCGGTGATT CCGATAA
Hinc-1	TCGTTGACAA TGGCTAAAAC CATCGCC
Hinc-2	GCGTTGACAA TTCGGTGATT CCGATAA
Xba-1	TCTCTAGACA TGGCTAAAAC CATCGCC
Xba-2	GCTCTAGACT TTCGGTGATT CCGATAA
Acc-1	TCGTATACAT GGCTAAAACC ATCGCCT
Acc-2	CGCGTATACT TCGGTGATTC CGATAAA

Animal

Eight to 12 week-old female inbred BALB/c mice were obtained from Guangzhou Traditional Chinese Medicine University.

MTE5 splicing and cloning MTE5 was designed to consist of HTL epitopes from heat shock protein 65 of *mycobacterium tuberculosis* (aa1-20), E2 polyprotein of *rubella* virus (aa54-65), artificial epitope (PADRE), heat shock protein 60 of *chlamydia trachomatis* (aa35-48) and tetanus toxoid (aa830-843). These epitopes were translated into a 219-bp fragment of DNA sequence. Then, it was synthesized in four oligonucleotide fragments, which were linked together at last using splicing by overlap extension[19,20]. The oligonucleotide fragments F1 and F2, F3 and F4 were spliced by PCR respectively at first. Their purified products were spliced together again to generate MTE5. The construct of pUMTE5 was generated by cloning MTE5 into plasmid pUC18 at the site between restriction endonucleases *Bam* HI and *Xba* I. pcMTE5 then was obtained by sub-cloning MTE5 from pUMTE5 into mammalian expression plasmid, pcDNA3. The sequence of MTE5 in pcMTE5 was confirmed using automatic DNA sequencing in Bioasia Biological Engineering Company.

HBV pre-S2/S gene cloning Pre-S2/S fragment of HBV was obtained using pTZ19U-HBV as template, and HBV-P1 and HBV-P2 as primers. The purified product was then cloned into pUC18 at the site between the restriction endonucleases *Hind* III and *Eco* RI to generate recombinant plasmid pUHB. pcHB was constructed by sub-cloning the fragment of HBV pre-S2/S gene into pcDNA3. pcHB was denominated after its sequence was confirmed by automatic DNA sequencing.

Construction of chimeric plasmids of MTE5 and HBV pre-S2/S gene MTE5 was designed to insert into the region of pre-S2 gene (*Bam* HI), 5' terminal of S gene (*Hinc* II, *Xba* I) and 3' terminal of S gene (*Acc* I) respectively. All the inserting sites were far from the α determinant to avoid deceasing the antigenicity of HBsAg. In order to obtain these chimeric plasmids, four fragments of MTE5 with different types of restriction endonuclease site in its two terminals were generated through PCR with different primers at first. Then four chimeric plasmids, pcHB-MTEB, pcHB-MTEH, pcHB-MTEX and pcHB-MTEA were constructed by cloning MTE5 into pUHB at first since pcDNA3 had some similar restriction endonuclease sites of its own, and then by sub-cloning the chimeric fragment of MTE5 and pre-S2/S into pcDNA3. The sequences of these recombinant plasmids were confirmed by automatic DNA sequencing.

Large-scale DNA preparation, DNA immunization Large-scale plasmid DNA of recombinant plasmids was prepared using Qiagen's Max-Prep kits. Plasmid DNA of pcDNA3 was used as control. Plasmid DNA was adjusted to 1 μg/mL in normal saline. Seventy BLBA/c mice were randomly divided into 8 groups. Every mouse was injected a total 100 μL of plasmid DNA which was distributed over five different sites into the anterior tibialis muscle 5 d after the injection of an equal volume of 2 g/L Bupivacaine. Boost injection was carried out every 3 wk for 3 times with an equal amount of plasmid DNA. Four weeks after the last boost injection, all mice were put to death for serum.

Detecting anti-HBs in serum Anti-HBs in serum was detected using AUSAB kits (Abbott Laboratory, USA). The tests were carried out following the manufacturer's instructions.

Pathological examination and HBsAg detection in muscle cell Pathological examination and HBsAg detection using immunohistochemistry in the mouse muscle of inoculation site from all groups were carried out after the samples were routinely embedded by paraffin in our laboratory. The muscles from the opposite leg were used as negative controls.

Statistical analysis For anti-HBs level, geometric mean titer (GMT) for each group was calculated at first. Then Student-Newman-Keuls-q was used for statistical analysis. For positive rate, Fisher's exact probability analysis was used. SPSS 10.0 for Windows was used for all statistical analyses.

RESULTS

MTE5 splicing and cloning

The theoretical products of the first and second round splicing were 120 bp and 219 bp, respectively. The actual products shown in Figure 1 were same as the design. Restriction fragment length polymorphism (RFLP) analysis was used to identify the positive clones after the 219-bp fragment was inserted into pUC18 to generate recombinant plasmid pUMTE5, which is shown in Figure 2. Two correct clones were selected by DNA sequencing among 13 positive clones of pUMTE5. The rest clones usually carried deletions or mismatches in the region longer than 50 bp of the synthesized oligonucleotide fragments, which implied that the synthesized DNA oligonucleotide fragment longer than 50 bp would not be reliable. The DNA sequence and amino acid sequence of MTE5 are shown in Figure 3. MTE5 was successfully cloned into pcDNA3 to generate pcMTE5 at last.

HBV pre-S2/S gene cloning

The theoretical base pair number of PCR products of HBV pre-S2/S fragment was about 847 bp. It was cloned into pUC18 to

generate recombinant plasmid pUHB. Then, the fragment of pre-S2/S was sub-cloned into pcDNA3 to generate recombinant plasmid pcHB. RFLP analysis was used to identify the positive clones of pcHB, which is shown in Figure 4A. After its sequence was confirmed by DNA sequencing, the recombinant plasmid was denominated as pcHB.

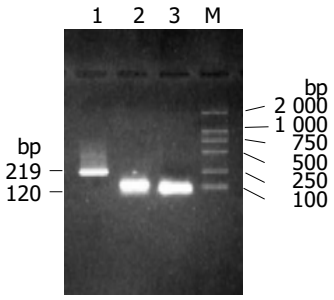

Figure 1 Electrophoresis of ultimate product of MTE5 and its middle oligonucleotide fragments. Lane 1: Ultimate product of MTE5; Lanes 2 and 3: The middle oligonucleotide fragments of MTE5; Lane M: DNA marker.

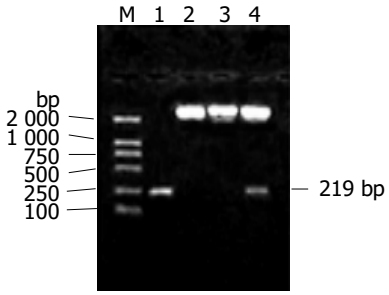

Figure 2 RFLP analysis of recombinant plasmid pUMTE5. Lane M: DNA marker; Lane 1: Splicing product of MTE5; Lanes 2 and 3: Plasmid pUC18 and recombinant plasmid pUMTE5 digested with restriction endonuclease *Xba* I; Lane 4: Recombinant plasmid pUMTE5 digested with restriction endonucleases *Xba* I and *Bam* HI.

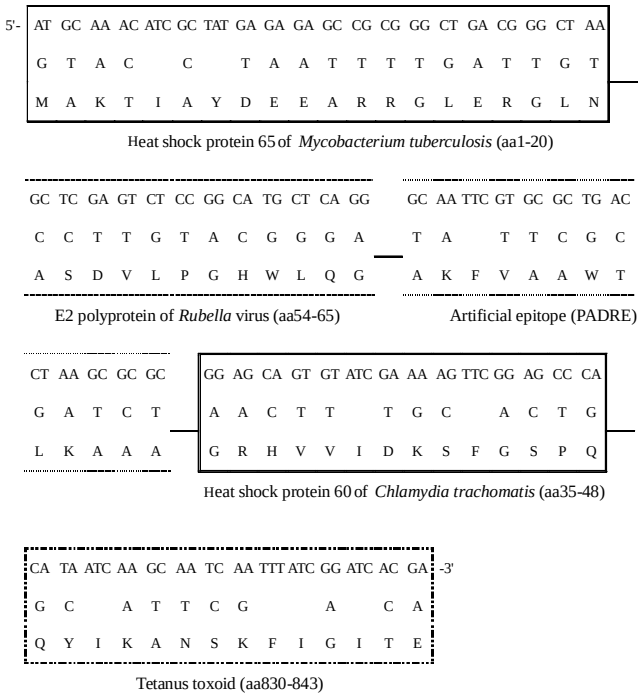

Figure 3 DNA and amino acid sequences of MTE5.

Construction of chimeric plasmids of MTE5 and HBV pre-S2/S gene

Four fragments of MTE5 with different types of restriction endonuclease site in its two terminals were successfully obtained by PCR. They were cloned into pUHB to generate their recombinant plasmids at first. The chimeric fragments of MTE5 and pre-S2/S were sub-cloned into pcDNA3 to generate their mammalian expression plasmids at last. RFLP analysis was used to identify positive clones. The results of RFLP analysis of the recombinant plasmid pcHB-MTEX with MTE5 inserted in site of *Xba* I is shown in Figure 4B as an example. The sequence of all chimeric plasmids was confirmed to be correct by DNA sequencing.

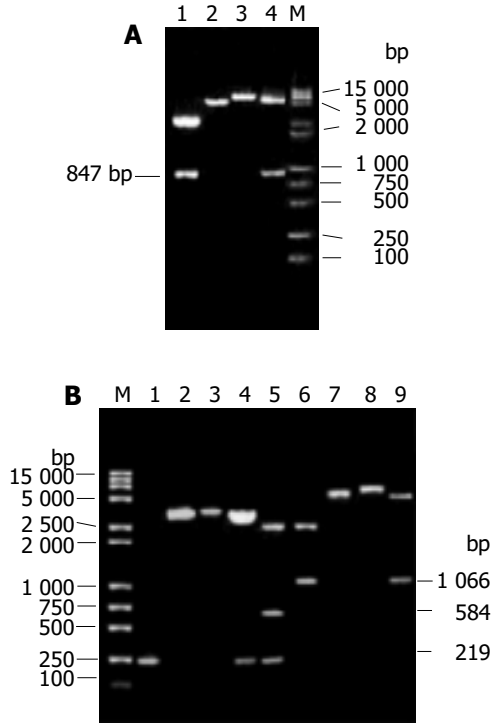

Figure 4 A: RFLP analysis of recombinant plasmid pcHB and chimeric plasimd pcHB-MTEX. Lane 1: Recombinant plasmid pUHB digested with restriction endonucleases *Hin*d III and *Eco* RI; Lanes 2 and 3: Plasmid pcDNA3 and recombinant plasmid pcHB digested with restriction endonuclease *Hin*d III; Lane 4: Recombinant plasmid pcHB digested with restriction endonucleases *Hin*d III and *Eco* RI; Lane M: DNA marker. B: RFLP analysis of the chimeric plasmid pcHB-MTEX. Lane M: DNA marker; Lane 1: MTE5; Lanes 2 and 3: Recombinant plasmid pUHB and pUHB-MTEX digested with restriction endonuclease *Eco* RI; Lane 4: Recombinant plasmid pUHB-MTEX digested with restriction endonuclease *Xba* I; Lane 5: recombinant plasmid pUHB-MTEX digested with restriction endonucleases *Xba* I and *Eco* RI; Lane 6: Recombinant plasmid pUHB-MTEX digested with restriction endonucleases *Hin*d III and *Eco* RI; Lanes 7 and 8: Recombinant plasmid pcHB and pcHB-MTEX digested with restriction endonuclease *Eco* RI; Lane 9: Recombinant plasmid pcHB-MTEX digested with restriction endonucleases *Hin*d III and *Eco* RI.

Anti-HBs responses

All mice were alive after the inoculation schedule was finished. The anti-HBs levels are shown in Table 2. The anti-HBs level was negative in groups of normal saline and plasmid pcDNA3. The anti-HBs response to co-inoculation of pcHB and pcMTE5 was much higher than that to inoculation of pcHB only (136.7±69.1 mIU/mL *vs* 27.6±17.3 mIU/mL, the positive rate was 8/10 *vs* 6/10, $P<0.01$, $t = -6.56$). Among the 4 chimeric plasmids, only pcHB-MTE-B with MTE5 inserted into pre-S2 region had a good anti-HBs response, which was 57.54±7.68 mIU/mL, and

slightly higher than that of pcHB, and lower than that of the co-inoculation of pcHB and pcMTE5. However, the difference was not statistically significant (P>0.05).

Table 2 Effect of MTE5 on anti-HBs response of HBV pre-S2/S gene

Group	Anti-HBs		Enhancement
	Positive ratio	MIU/L (GMT±SE)	
Empty control	0/5	-	-
PcDNA3	0/5	-	-
PcHB	6/10	27.60±17.3	-
PcHB/pcMTE5	8/10	136.70±69.1[b]	4.95
PcHB-MTEB	7/10	57.540±7.68	2.09
PcHB-MTEX	0/10	-	-
PcHB-MTEH	1/10	1.50	-
PcHB-MTEA	0/10	-	-

GMT: Geometric mean titer; Enhancement: GMT ratio of given group to pcHB, immune enhancement was considered when the ratio was larger than 1. "-" means ant-HBs negative or the enhancement could not be detected. [b]P<0.01, t = -6.56 *vs* pcHB group.

Histological findings and HBsAg in mouse muscle cells

Compared with the control groups and the sample from the opposite leg, all experimental groups had obvious inflammation cell filtration in the inoculation sites and HBsAg expression in muscle cells with disassembling and rupture. HBsAg was prominently expressed in cytoplasm of cells. Some cells had membrane expressions simultaneously. The positive signal of HBsAg was usually expressed in cytoplasm, and inflammation was more obvious in non- or low-anti-HBs response groups of chimeric plasmids.

DISCUSSION

The simple way for a given protein to obtain exogenous multiple epitopes was to link them to a higher molecular weight protein. The immune responses were not always good enough because of the interfering effects of immune responses of the carrying protein[21]. The spliced exogenous multiple epitopes of HTL used in this study, however, might not have immune responses of its own, and were thus preferable. The exogenous multiple epitopes of HTL, MTE5, constructed in this study consisted of 2 universal HTL epitopes and 3 unique HTL epitopes. Two universal epitopes of tetanus toxoid (aa830-843) and artificial epitope PADRE were both effective for 95% individuals of the population[22-26]. They might cover more individuals when used together. Three unique epitopes from *Mycobacterium tuberculosis* (aa1-20), E2 polyprotein of *rubella* virus (aa54-65) and heat shock protein 60 of *Chlamydia trachomatis* (aa35-48) were selected for HLA-DRB1*3, HLA-DRB1*7 and HLA-DR4 respectively[27-29]. They could improve the anti-HBs responses of hepatitis B vaccine in individuals who carried these types of HLA II antigens. Thus, the overall response rate of HB vaccine in population could rise dramatically. During the course of splicing, many deletions or mismatches were found in the spliced sequences, especially in the region of synthesized oligonucleotide fragments longer than 50 bp. It implied that synthesized DNA oligonucleotide fragments shorter than 50 bp would be preferable.

A satisfactory ant-HBs response was obtained when MTE5 and pre-S2/S were co-inoculated through DNA immunization, suggesting that MTE5 had immune enhancement. Among the 4 chimeric plasmids, only the recombinant plasmid with MTE5 inserted into the region of pre-S2 had a detectable anti-HBs response, suggesting that the insertion location of MTE5 was critical for anti-HBs response. The insertion was far from the a antigen determinant of HBsAg. Thus, the non-response cause of the rest chimeric plasmids was not clear. HBsAg could be detected in muscle cells at the inoculation site, suggesting that the construction of recombinant plasmids was successful. HBsAg positive signals were mainly located in cytoplasm, suggesting that the poor anti-HBs response might result in failure to secret the large particles like HBsAg[30-32].

The chimeric plasmid of pcHB-MTEB had an equal or better anti-HBs response as comparing with that of pcHB, and might be a good candidate for new hepatitis B vaccine in further research. DNA immunization is a simple and quick way to evaluate recombinant plasmids. The response rate of recombinant plasmids, however, was very low in this study. A considerable portion of mice did not develop anti-HBs at all. Its reason is not clear. It might be the nature of DNA immunization because this phenomenon also occurred in other researches[31]. The exact value should be evaluated after purified recombinant protein is obtained through mammalian expression. The effect on overcoming the drawback of the polymorphism of HLA II antigens should also be evaluated in the future.

REFERENCES

1 **Liaw YF**. Management of patients with chronic hepatitis B. *J Gastroenterol Hepatol* 2002; **17**: 406-408
2 **Block TM**, Mehta AS, Fimmel CJ, Jordan R. Molecular viral oncology of hepatocellular carcinoma. *Oncogene* 2003; **22**: 5093-5107
3 **Das K**, Gupta RK, Kumar V, Kar P. Immunogenicity and reactogenicity of a recombinant hepatitis B vaccine in subjects over age of forty years and response of a booster dose among nonresponders. *World J Gastroenterol* 2003; **9**: 1132-1134
4 **Kubba AK**, Taylor P, Graneek B, Strobel S. Non-responders to hepatitis B vaccination: a review. *Commun Dis Public Health* 2003; **6**: 106-112
5 **van Zonneveld M**, van Nunen AB, Niesters HG, de Man RA, Schalm SW, Janssen HL. Lamivudine treatment during pregnancy to prevent perinatal transmission of hepatitis B virus infection. *J Viral Hepat* 2003; **10**: 294-297
6 **Wang J**, Zhu Q, Zhang X. Effect of delivery mode on maternal-infant transmission of hepatitis B virus by immunoprophylaxis. *Chin Med J* 2002; **115**: 1510-1512
7 **Kao JH**, Chen DS. Global control of hepatitis B virus infection. *Lancet Infect Dis* 2002; **2**: 395-403
8 **Tsebe KV**, Burnett RJ, Hlungwani NP, Sibara MM, Venter PA, Mphahlele MJ. The first five years of universal hepatitis B vaccination in South Africa: evidence for elimination of HBsAg carriage in under 5-year-olds. *Vaccine* 2001; **19**: 3919-3926
9 **Page M**, Jones CD, Bailey C. A novel, recombinant triple antigen hepatitis B vaccine (Hepacare). *Intervirology* 2001; **44**: 88-97
10 **Thio CL**, Thomas DL, Karacki P, Gao X, Marti D, Kaslow RA, Goedert JJ, Hilgartner M, Strathdee SA, Duggal P, O'Brien SJ, Astemborski J, Carrington M. Comprehensive analysis of class I and class II HLA antigens and chronic hepatitis B virus infection. *J Virol* 2003; **77**: 12083-12087
11 **Hohler T**, Reuss E, Evers N, Dietrich E, Rittner C, Freitag CM, Vollmar J, Schneider PM, Fimmers R. Differential genetic determination of immune responsiveness to hepatitis B surface antigen and to hepatitis A virus: a vaccination study in twins. *Lancet* 2002; **360**: 991-995
12 **Desombere I**, Willems A, Leroux-Roels G. Response to hepatitis B vaccine: multiple HLA genes are involved. *Tissue Antigens* 1998; **51**: 593-604
13 **Watanabe H**, Matsushita S, Kamikawaji N, Hirayama K, Okumura M, Sasazuki T. Immunoe suppression gene on HLA-Bw54- DR4- Drw53 haplotype controls nonresponsiveness in human to hepatitis B surface antigen via CD8+ suppressor T cells. *Hum Immunol* 1988; **22**: 9-17
14 **Hohler T**, Meyer CU, Notghi A, Stradmann-Bellinghausen B, Schneider PM, Starke R, Zepp F, Sanger R, Clemens R, Meyer zum Buschenfelde KH, Rittner C. The influence of major histo-

compatibility complex class II genes and T-cell Vbeta repertoire on response to immunization with HBsAg. *Hum Immunol* 1998; **59**: 212-218

15 **Mineta M**, Tanimura M, Tana T, Yssel H, Kashiwagi S, Sasazuki T. Contribution of HLA class I and class II alleles to the regulation of antibody production to hepatitis B surface antigen in humans. *Int Immunol* 1996; **8**: 525-531

16 **Chengalvala MV**, Bhat RA, Bhat BM, Vernon SK, Lubeck MD. Enhanced immunogenicity of hepatitis B surface antigen by insertion of a helper T cell epitope from tetanus toxoid. *Vaccine* 1999; **17**: 1035-1041

17 **Peng XM**, Xie DY, Gu L, Huang YS, Gao ZL, Yao JL. Effect of exogenous epitopes of helper T lymphocyte on humoral immunity of HBV S gene DNA immunity. *Zhonghua Yixue Zazhi* 2003; **83**: 232-236

18 **Hervas-Stubbs S**, Berasain C, Golvano JJ, Lasarte JJ, Prieto I, Sarobe P, Prieto J, Borras-Cuesta F. Overcoming class II-linked non-responsiveness to hepatitis B vaccine. *Vaccine* 1994; **12**: 867-871

19 **Horton RM**, Hunt HD, Ho SN, Pullen JK, Pease LR. Engineering hybrid genes without the use of restriction enzymes: gene splicing by overlap extension. *Gene* 1989; **77**: 61-68

20 **An LL**, Whitton JL. A multivalent minigene vaccine, containing B-cell, cytotoxic T-lymphocyte, and Th epitopes from several microbes, induces appropriate responses *in vivo* and confers protection against more than one pathogen. *J Virol* 1997; **71**: 2292-2302

21 **Barzu S**, Arondel J, Guillot S, Sansonetti PJ, Phalipon A. Immunogenicity of IpaC-hybrid proteins expressed in the Shigella flexneri 2a vaccine candidate SC602. *Infect Immun* 1998; **66**: 77-82

22 **Panina-Bordignon P**, Tan A, Termijtelen A, Demotz S, Corradin G, Lanzavecchia A. Universally immunogenic T cell epitopes: promiscuous binding to human MHC class II and promiscuous recognition by T cells. *Eur J Immunol* 1989; **19**: 2237-2242

23 **Boitel B**, Blank U, Mege D, Corradin G, Sidney J, Sette A, Acuto O. Strong similarities in antigen fine specificity among DRB1*1302-restricted tetanus toxin tt830-843-specific TCRs in spite of highly heterogeneous CDR3. *J Immunol* 1995; **154**: 3245-3255

24 **Valmori D**, Sabbatini A, Lanzavecchia A, Corradin G, Matricardi PM. Functional analysis of two tetanus toxin universal T cell epitopes in their interaction with DR1101 and DR1104 alleles. *J Immunol* 1994; **152**: 2921-2929

25 **Franke ED**, Hoffman SL, Sacci JB Jr, Wang R, Charoenvit Y, Appella E, Chesnut R, Alexander J, Del Guercio MF, Sette A. Pan DR binding sequence provides T-cell help for induction of protective antibodies against Plasmodium yoelii sporozoites. *Vaccine* 1999; **17**: 1201-1205

26 **Alexander J**, Sidney J, Southwood S, Ruppert J, Oseroff C, Maewal A, Snoke K, Serra HM, Kubo RT, Sette A, Grey HW. Development of high potency universal DR-restricted helper epitopes by modification of high affinity DR-blocking peptides. *Immunity* 1994; **1**: 751-761

27 **Young SP**, Epstein E, Potter V. Determinant capture by MHC class II DR3 during processing of mycobacteria leprae 65kD heat shock protein by human B cells. *Hum Immunol* 1998; **59**: 259-264

28 **Ou D**, Chong P, Choi Y, McVeigh P, Jefferies WA, Koloitis G, Tingle AJ, Gillam S. Identification of T-cell epitopes on E2 protein of rubella virus, as recognized by human T-cell lines and clones. *J Virol* 1992; **66**: 6788-6793

29 **Deane KH**, Jecock RM, Pearce JH, Gaston JS. Identification and characterization of a DR4-restricted T cell epitope within chlamydia heat shock protein 60. *Clin Exp Immunol* 1997; **109**: 439-445

30 **Davis HL**, Michel ML, Whalen RG. DNA-based immunization induces continuous secretion of hepatitis B surface antigen and high levels of circulating antibody. *Hum Mol Genet* 1993; **2**: 1847-1851

31 **Geissler M**, Tokushige K, Chante CC, Zurawski VR Jr, Wands JR. Cellular and humoral immune response to hepatitis B virus structural proteins in mice after DNA-based immunization. *Gastroenterology* 1997; **112**: 1307-1320

32 **Geissler M**, Schirmbeck R, Reimann J, Blum HE, Wands JR. Cytokine and hepatitis B virus DNA co-immunizations enhance cellular and humoral immune responses to the middle but not to the large hepatitis B virus surface antigen in mice. *Hepatology* 1998; **28**: 202-210

Edited by Wang XL and Chen WW **Proofread by** Xu FM

PO Box 2345, Beijing 100023, China
Fax: +86-10-85381893
E-mail: wjg@wjgnet.com www.wjgnet.com

World J Gastroenterol 2004;10(20):2984-2988
World Journal of Gastroenterology
 ISSN 1007-9327

• VIRAL HEPATITIS •

Effect of artificial liver support system on patients with severe viral hepatitis: A study of four hundred cases

Lan-Juan Li, Qian Yang, Jian-Rong Huang, Xiao-Wei Xu, Yue-Mei Chen, Su-Zhen Fu

Lan-Juan Li, Qian Yang, Jian-Rong Huang, Xiao-Wei Xu, Yue-Mei Chen, Su-Zhen Fu, Department of Infectious Diseases, First Hospital, College of Medicine, Zhejiang University, Hangzhou 310003, Zhejiang Province, China
Supported by the National High Technology Research and Development Program of China (863 Program), No. 2003AA205015 and the Major Science Foundation of Zhejiang Province, No. 021107689 and No. 021103126 and the Health Foundation of Zhejiang Province, No. 2003A031
Correspondence to: Dr. Lan-Juan Li, Department of Infectious Disease, First Hospital, College of Medicine, Zhejiang University, 79 Qingchun Road, Hangzhou 310003, Zhejiang Province, China. ljli@zjwst.gov.cn
Telephone: +86-571-87236759 **Fax:** +86-571-87236755
Received: 2004-01-10 **Accepted:** 2004-03-02

Abstract

AIM: To assess the effect of artificial liver support system (ALSS) on patients with severe viral hepatitis, who were divided into treatment group and control group.

METHODS: Four hundred in-hospital patients enrolled during 1995-2003 who received ALSS therapy were studied as the treatment group. Four hundred in-hospital patients enrolled during 1986-1994 who received other medical therapies served as the control group. The methods of ALSS used included plasma exchange, hemoperfusion, hemofiltration, continuous hemodiafiltration (CHDF). The effect of ALSS treatment was studied in patients at different stages of the disease.

RESULTS: The cure rate of acute and subacute severe hepatitis in the treatment group was 78.9% (30/38), and was 11.9% (5/42) in the control group. The improved rate of chronic severe hepatitis in the treatment group was 43.4% (157/362), and was 15.4% (55/358) in the control group. We found that patients treated with ALSS in the early or middle stage of the disease had much higher survival rates than patients in the end stage of the disease.

CONCLUSION: ALSS is an effective and safe therapy for severe viral hepatitis.

Li LJ, Yang Q, Huang JR, Xu XW, Chen YM, Fu SZ. Effect of artificial liver support system on patients with severe viral hepatitis: A study of four hundred cases. *World J Gastroenterol* 2004; 10(20): 2984-2988
http://www.wjgnet.com/1007-9327/10/2984.asp

INTRODUCTION

Severe viral hepatitis is the main cause of hepatic failure in China because of the great population of hepatitis B patients, which is different from the Western countries where drugs or alcohol usually is the major cause. Despite a combination of all available treatments, the mortality of hepatic failure is more than 70%[1,2].

It is believed that damaged liver has the ability to regenerate and restore normal function of metabolism, synthesis and biotransformation. Liver transplantation remains the only effective therapeutic modality for chronic patients in end-stage[3-5]. There is also a need to develop a liver support system that can serve as a bridge to transplantation[6,7], so that patients can be supported until a liver becomes available or the condition of patients is improved. ALSS has been used to treat hepatic failure and has significantly decreased the mortality[8-11].

We designed an artificial liver support system for severe hepatitis patients. In this report, we described 400 patients with hepatic failure treated with ALSS in our hospital. Data such as concentrations of endotoxin and blood HBV, and serum amino acid spectrum were recorded. The effect of ALSS treatment was also compared in patients at different stages of the disease.

MATERIALS AND METHODS

The treatment group consisting of 400 viral severe hepatitis patients was treated with ALSS at the First Hospital of College of Medicine, Zhejiang University during 1995 to 2003. Two hundred and ninety-five were males and 105 were females. The age ranged from 20 to 64 years, with an average of 34.3±16.5 years. The control group consisting of 400 viral severe hepatitis patients was treated in Department of Internal Medicine at the same hospital during 1986 to 1994, of them 273 were males and 127 were females. The age ranged from 19 to 68 years, with an average of 32.5±18.8 years.

The patients were diagnosed according to the criteria established in the 1995 National Infectious Disease Meeting in Beijing[12]. Type A hepatitis was diagnosed by the identification of HAV-RNA and/or IgM anti-HAV. The diagnosis of hepatitis B was based on positive HBsAg. Acute type B hepatitis was diagnosed by the presence of HBsAg and/or IgM anti-HBc antibody. Three patients among them were negative for HBsAg but had positive IgM anti-HBc and they were diagnosed as type B hepatitis. All were positive for HBV DNA by PCR. An acute exacerbation of HB in a HBV carrier was diagnosed by a history of known HBsAg positivity for more than 6 mo, the presence of HBV-DNA and a markedly elevated IgG anti-HBc level. Type C hepatitis was diagnosed by the presence of either HCV RNA or anti-HCV antibody. Type B+D hepatitis was diagnosed by the presence of HBsAg and HDV-RNA. Type E hepatitis was diagnosed by the identification of IgM anti- HEV antibody.

Three types of severe viral hepatitis have been found in our country: acute, subacute and chronic severe hepatitis. Violent symptoms of acute severe hepatitis occurred within 10 d after the appearance of clinical manifestations, including malignant jaundice, hepatic encephlophathy (above phase II) and prolonged prothrombin time (PTA<40%). These patients were usually accompanied with shrinking live dullness, rapidly rising blood bilirubin (TB>171 μmol/L) and obvious abnormal liver functions. Subacute severe hepatitis patients were those who had prolonged prothrombin time (PTA<40%) after the occurrence of manifestations for more than 10 d, and meanwhile, they had any one of the following symptoms, namely hepatic encephlophathy (above phase II^{0}), rapid rising of blood bilirubin (blood TB more than 171 μmol/L within several days), severe damage of liver functions, extremely fatigue, loss of appetite,

nausea, abdominal distention or hydroperitoneum, sometimes with a tendency to bleed. Chronic severe hepatitis was clinically similar to acute or subacute severe hepatitis, but was distinguished by a known history of HBV carriage, chronic hepatitis or cirrhosis, or by the results of imaging, endoscopy or biopsy showing the existence of chronic hepatitis. Subacute and chronic severe hepatitis was classified into early, middle and end stages. Symptoms of the early stage included fulminant liver failure but without hepatic encephalopathy or ascites. The serum level of bilirubin (TB) was above 171 μmol/L, while the prothrombin time rate (PTA) was less than 40%. Liver biopsy was also taken into account when available. In addition, patients in the middle stage had hepatic encephalopathy (II°above), ascites, or a tendency to bleed with a PTA≤30%. End stage patients had severe complications such as hepatorenal syndrome, infection, hepatoencephalopathy (II°above), electrolytic disturbance, with a PTA≤20%.

In the treatment group there were 38 cases of acute or subacute severe hepatitis (6 type A, 8 type A+B, 5 type B+E, 17 type B, 2 type E), while the other 362 were cases of chronic severe hepatitis (310 type B, 18 type A+B, 14 type C, 12 type B+D, 7 type B+E, 1 type B+C+D). The average prothrombin time of the patients on admission was 31.8±7.2 s (the normal was 12 s). Sixty-eight cases were treated with ALSS in the early stage, 186 in the middle stage and 146 in the end stage. In the control group there were 42 cases of acute or subacute severe hepatitis (8 type A, 9 type A+B, 3 type B+E,20 type B,1 type E, 1 type B+C+D), while the other 358 were cases of chronic severe hepatitis (313 type B,16 type A+B,10 type C,13 type B+D,5 type B+E,1 type B+C+D) (Table 1). The average prothrombin time of the patients in control group on admission was 30.9±8.4 s. Seventy-four patients were diagnosed as early stage, 168 cases as middle stage and 158 as end stage acute or subacute severe hepatitis, respectively. There were no significant differences in sex, ages, etiology and conditions between two groups.

Table 1 Types of severe hepatitis in two groups

Types	Treatment group		Control group	
	Acute and subacute	Chronic	Acute and subacute	Chronic
A	6	0	8	0
B	17	310	20	313
C	0	14	0	10
E	2	0	1	0
B+D	0	12	0	13
A+B	8	18	9	16
B+E	5	7	3	5
B+C+D	0	1	1	1
Total	38	362	42	358

The methods of ALSS included plasma exchange, hemoperfusion, hemofiltration, continuous hemodiafiltration (CHDF). We chose therapy based on the condition of patients. The ALSS treatment room was thoroughly sterilized by UV light before each treatment. The external circulation system and the separator were connected under sterile condition, washed with 0.9% saline solution at 38 ℃ to remove the micro bubbles in the line, and then filled with 2 mg/500 mL heparin saline solution. The main parts of ALSS were 160-200 g activated carbon absorber, membrane plasma separator, bilirubin absorbent, dialyser, *etc*. Plasma exchange was performed by using a membrane separation method marketed as Plasmacure PS-06 (Kuraray Co., Japan) (Figure 1). Fresh frozen plasma (FFP) was supplied by the Hangzhou Blood Center, Chinese Red Cross. Filtration was performed at a flow rate of 4-6 liters/h using a bicarbonate buffer, pH 7.4, having a potassium concentration of 4.0 mmol/L. The volume of substitution fluid was adjusted over a range of 6-30 L, depending on the patient's response (Figure 3). Dialysis was performed concurrently at a flow rate of 500 mL/min using a conventional acetate buffer.

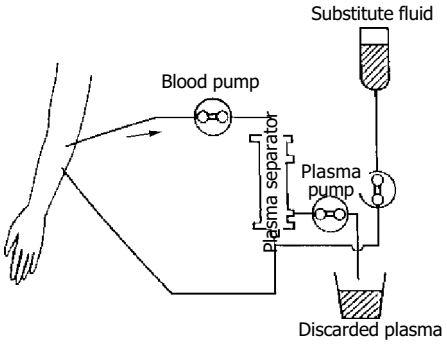

Figure 1 Circuit diagram of plasma exchange.

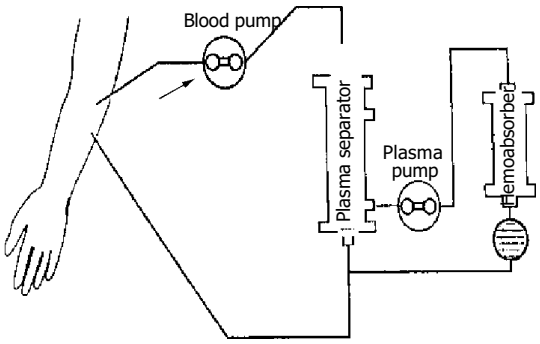

Figure 2 Circuit diagram of plasmapheresis plus plasma absorption. Special absorbers could be used to treat patients with hyperbilirubinemia or hepatic encephalopathy such as bilirubin and carbon absorbers.

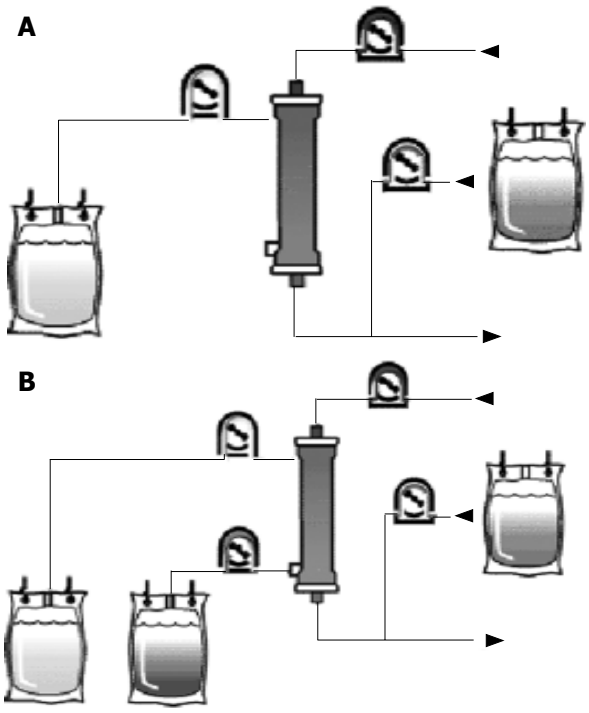

Figure 3 Continuous hemofiltration and hemodiafiltration with aid of a blood pump. A: Continuous hemofiltration with aid of a blood pump; B: Continuous hemodiafiltration with aid of a blood pump.

Before ALSS therapy, blood access was established with a double-lumen catheter inserted into the patient's jugular or femoral vein, and heparin was then used to block the catheter after each session. The circuit diagrams for plasma exchange and perfusion are shown in Figures 1, 2. During each session of ALSS therapy which was lasted for 4-6 h, the total volume of exchanged plasma was about 3 500 mL, and the exchange rate of plasma was 25-30 mL/min. A total of 3 000-4 500 mL of fresh frozen plasma and its substitute fluid, and 20-40 g albumin were supplied. The flow rate of blood was adjusted to 60-130 mL/min, and blood pressure and pulse were recorded continuously during treatment. Prophylactic antibiotics were used before and after therapy. Five mg dexamethasone and 10-20 mg heparin were injected routinely before therapy. During the session, the prothrombin time was tested constantly to allow the dose of heparin to be adjusted. A total of 10-108 mg heparin was used for each session. At the end of each ALSS treatment heparin was neutralized by injection of 10-50 mg of protamine sulphate. ALSS therapy was carried out two or three times in the first or second week, then one time each week till the patient's condition was stable.

Liver function and endotoxin levels were monitored during the therapy. Amino acid spectra were determined for 25 subjects by auto amino acid analyzing system, performed at the Analyzing Center of the Second Medical University in Shanghai. Endotoxin level was measured by quantitative Azo color test. HBV-DNA concentration in 10 cases was measured by chiron branched chain DNA assay, performed at the Virus Center of Luebrek Medical University, Germany.

Statistical analysis

All data were presented as mean±SE. The data were analyzed by SPSS 10.0. The Student's *t* test or Fischer's exact test was used to determine the level of significance between groups. A *P*-value <0.05 was considered statistically significant.

RESULTS

Nearly 90% patients experienced an improvement in symptoms such as fatigue or abdominal distention after each treatment. Results of liver function tests improved significantly in all subjects. The serum ALT, AST and TBA levels declined significantly ($P<0.001$), the level of serum bilirubin decreased from 511.36±192.81 μmol/L to 257.38±123.48 μmol/L ($P<0.001$), while the prothrombin time decreased from 31.8±7.2 s to 23.6±6.8 s (Table 2). The serum endotoxin levels before therapy in all hepatic failure patients were above the upper limit of normal which was 40 ng/L. After ALSS therapy, serum endotoxin levels declined from 58.2±12.3 ng/L to 32.4±7.8 ng/L ($P<0.001$). In the 10 patients tested, the HBV-DNA concentration declined from an average of 2 588±1 534 copies/mL to 1 815±620 copies/mL ($P<0.05$) as a result of ALSS therapy. The serum level of aromatic amino acids (AAA), such as methionine, tyrosine, phenylalanine, cysteine, arginine, especially methionine declined significantly ($P<0.05$) in 25 subjects. Meanwhile, the ratio of branched-chain amino acid/aromatic amino acid (BCAA/AAA) increased significantly ($P<0.05$) (Table 3). No significant difference in TNF, rIL-2R and IL-2 levels before and after the ALSS treatment was observed (Table 4). There was no disturbance of electrolytes after ALSS therapy.

Seventeen candidates for orthotopic liver transplantation (OLT) received 2-3 runs of ALSS and were "bridged" successfully to OLT. After OLT, ALSS was used to replace liver function in non-function period. Twelve of 17 patients were completely recovered and 3 died of infection, acute rejection and abdominal bleeding.

Among the 38 patients with acute or subacute severe hepatitis treated with ALSS 3-5 times, 30 of them (78.9%) survived for at least half a year but 8 ied in 1 mo. One hundred and fifty-seven of 362 patients with chronic severe hepatitis were cured or greatly improved, 107 patients were discharged as their own will, and 98 patients died in the next 3 onths, so the cure rate was 43.4%. In the control group, the cure rate of acute and subacute severe hepatitis was 11.9% (5/42), while cure and improved rate of chronic severe hepatitis was only 15.4% (55/358) (Table 5). There were significantly differences in the cure rate between two groups ($P<0.001$). More importantly, in the treatment group, the cure rate of patients in early or middle stage (76.5% and 61.8%, respectively) was much higher than that those in end-stage (13.7%, Table 6).

Table 2 Result of liver function test before and after ALSS therapy (mean±SE)

Liver function	Pre-treatment	Post-treatment	*P*
ALT (U/L)	123.35±281.32	53.15±94.21	<0.001
AST (U/L)	126.84±115.25	63.71±58.45	<0.001
ALP (U/L)	127.97±66.74	81.45±39.62	<0.001
TBil (μmol/L)	511.36±192.81	257.38±123.48	<0.001
ChE (U/L)	2 572.58±2 236.95	3 119.24±1 812.62	0.001
γ-GT (U/L)	42.38±53.85	20.91±25.58	<0.001
TBA (μmol/L)	256.36±48.69	119.42±49.37	<0.001
PT (s)	31.8±7.2	23.6±6.8	<0.001

Table 3 Serum amino acid levels in 25 cases before and after the first ALSS therapy (mean±SE)

	Pre-therapy (μmol/L)	After therapy (μmol/L)
Cys	65.63±41.40	53.74±26.86[a]
Phe	94.78±62.00	80.92±40.75[a]
Ala	256.51±123.73	267.84±138.32
Gly	194.89±83.43	212.50±106.07
Glu	118.50±89.65	116.85±91.26
Gln	494.16±218.91	515.84±208.81
Met	185.85±142.33	149.91±134.16[b]
Arg	170.44±231.69	143.18±175.92[a]
Lys	220.72±168.05	190.29±136.28
Tyr	121.98±82.82	104.44±59.94[a]
Leu	73.73±58.81	78.17±43.74
Orn	113.99±94.58	92.84±52.93
Tau	46.41±27.34	43.51±32.90
Ser	123.78±64.83	122.22±61.29
Thr	165.60±83.34	152.94±83.42
Asp	16.22±10.72	13.38±7.87
Asn	59.40±46.09	64.52±49.46
Val	121.69±75.01	126.35±68.72
Ile	44.86±36.61	46.29±25.88
His	96.18±73.85	87.86±51.56
BCAA/AAA	1.18±0.39	1.52±0.77[a]

[a]$P<0.05$; [b]$P<0.001$ *vs* pre-therapy group.

Table 4 Endotoxin, TNF, rIL-2R, IL-2 in patients with hepatic failure before and after ALSS therapy (mean±SE)

	Pre-treatment	Post-treatment	*P*
Endotoxin (ng/L)	58.2±12.3	32.4±7.8	<0.005
TNF (ng/L)	3.4±1.2	3.2±1.2	>0.05
rIL-2R (U/mL)	1 040.1±309.2	951.0±285.6	>0.05
IL-2 (ng/mL)	20.1±1.9	9.7±1.8	>0.05

Complications occurred during ALSS therapy included skin rash, hypotension, blood coagulation in perfusion apparatus,

Table 5 Prognosis of ALSS treatment group and control group

	ALSS treatment group				Control group			
	Acute and subacute severe hepatitis		Chronic severe hepatitis		Acute and subacute severe hepatitis		Chronic severe hepatitis	
	Cases	Ratio (%)	Cases	Ratio (%)	Cases	Ratio (%)	Cases	Ratio (%)
Cured	30	78.9	157	43.4	5	11.9	55	15.4
Discharged as their own will	2	5.3	107	29.6	16	38.1	122	34.0
Died	6	15.8	98	27.0	21	50.0	181	50.6
Total	38	100	362	100	42	100	358	100

infection, hyperkalemia, and local bleeding (Figure 4). All patients recovered after management of these complications, except one patient who died of intracranial bleeding.

Table 6 Outcome of patients in different stages after ALSS treatment

Stages	Cured		Discharged		Died		Total
	Cases	%	Cases	%	Cases	%	
Early stage	52	76.5	9	13.2	7	10.3	68
Middle stage	115	61.8	34	18.3	37	19.9	186
End stage	20	13.7	68	46.6	58	39.7	146
Total	187	46.8	111	27.8	102	25.5	400

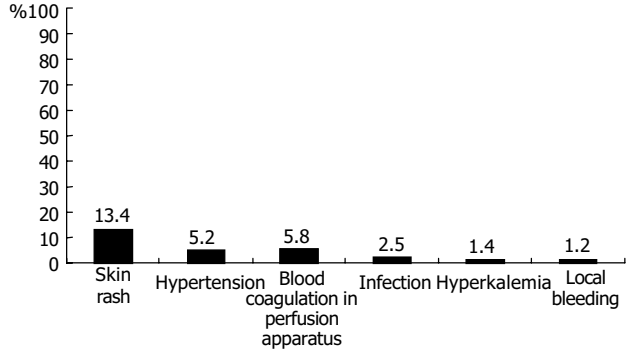

Figure 4 Incidence rate of complications of ALSS therapy.

DISCUSSION

In acute liver failure, the liver parenchyma injured by viral, toxic, or some other insults failed to function sufficiently. Temporary support of normal liver function would promote the damaged liver to restore its normal function. Artificial liver support system could serve this purpose. Moreover, when the liver lost its ability to function normally, then an artificial liver support system might be used as a "bridge" to liver transplantation[6,7]. Although various liver assistant devices have been introduced during the past 40 years, a complete artificial liver system that can support patients with severe hepatic failure till the damaged liver restores its normal function has not yet been developed[8].

We modified the artificial liver support system for treatment of patients with severe hepatic failure. We substituted the usual 50 g activated carbon absorber with 160-200 g one to remove toxic substances of intermediate molecular weight from blood. The 160-200 g carbon absorber proved to be appropriate, as a larger carbon absorber might destroy blood cells and cause side effects. The bilirubin absorbent could absorb excess bilirubin from the plasma, so that the cleaned plasma could be retransmitted to patients directly. The membrane plasma separator could separate and discard plasma containing toxic substances, and supply normal fresh plasma containing albumin and coagulation factors for patients. The volume exchanged utilizing this method was about 3 500 mL each time, much more than that utilizing traditional centrifugation methods, which exchanged only 800-1 000 mL each time. Continuous hemodiafiltration (CHDF) could eliminate middle and small molecular toxic substances, and keep the balance of internal environment[13]. These methods were used in different combinations based on the symptoms of patients (Figures 1-3). For example, when patients had hepatic encephalopathy, we performed plasma exchange in combination with plasma perfusion. For patients with hepatorenal syndrome, we chose plasma exchange and hemodialysis or hemofiltration or CHDF. For those with hyperbilirubinemia, plasma bilirubin absorption in combination with hemoperfusion was used. When the balance of water or electrolytes was disturbed, we used plasma exchange and hemofiltration or CHDF. Sometimes, more than three methods were used together for one patient. In addition, we carefully adjusted the dose of heparin and protamine according to PT, and maintained fluid balance to decrease complications such as bleeding, hemolysis, hypotension. This was crucial to decrease the mortality of hepatic failure.

Changes in the spectrum of amino acids might be another benefit of ALSS therapy. It has been shown that the concentration of aromatic amino acids (AAA) was increased in patients with fulminant hepatitis failure[14,15]. Moreover, the concentration of methionine was a sensitive indicator of liver injury because methionine was released while liver necrosis[16]. Methionine was toxic to the central nervous system, and one of the main causes of hepatic encephalopathy[17]. After ALSS therapy, the serum level of aromatic amino acids, especially methionine declined and the ratio of BCAA/AAA was significantly increased.

In this study, we found that the cure rate of treatment group was significantly higher than that of the control group, indicating that ALSS is an effective therapy in treating patients with severe hepatitis. We also compared the efficiency of ALSS therapy in different stages of severe liver disease and concluded that the cure rate of early or middle stage severe hepatitis was much higher than that of end stage severe hepatitis (76.5%, 61.8% *vs* 13.7%, respectively). It is possible that ALSS may provide a favorable internal environment for hepatocytes to regenerate and restore normal function in patients at early or middle stage. However, there was massive necrosis of hepatocytes in hepatitis patients at end stage, and liver regeneration was not sufficient to recover liver function. Our data suggested that ALSS therapy might be an effective method to treat hepatitis patients at early stages.

Liver transplantation could provide good results in the treatment of hepatic failure, with a 5-year survival rate of 60%[6,18]. However, its use has been greatly limited because of the lack of sufficient liver donors. Therefore, a system that can serve as a "bridge" to eventual OLT would greatly extend the survival rate[19,20]. Based on our data, the artificial liver support system could serve as an effective "bridge" to OLT. Plasmapheresis was also beneficial, as the levels of coagulation factors and albumin could be increased by several plasma exchanges[19]. Hemoperfusion was effective in improving the neurologic status

of patients with hepatic failure[8,21]. Hemodialysis, hemofiltration or CHDF could correct the disturbance of water or electrolytes of patients[13,22]. So ALSS could improve the condition of patients until a donor liver was available. Complications of the transplantation included acid-base imbalance, hyperbilirubinemia, disturbance of electrolytes, dysfunction of blood coagulation, acute rejection, *etc*.[23]. ALSS treatment could improve the internal environment to support patients in pre- and post-transplantation periods. In addition ALSS could therefore improve the result of OLT in patients with severe liver disease. Further appropriately controlled trials are being initiated to confirm this observation.

REFERENCES

1 **Shakil AO**, Kramer D, Mazariegos GV, Fung JJ, Rakela J. Acute liver failure: clinical features,outcome analysis, and applicability of prognostic criteria. *Liver Transpl* 2000; **6**: 163-169
2 **Mas A**, Rodes J. Fulminant hepatic failure. *Lancet* 1997; **349**: 1081-1085
3 **Ostapowicz G**, Lee WM. Acute hepatic failure: a western perspective. *J Gastroenterol Hepatol* 2000; **15**: 480-488
4 **van Hoek B**, de Boer J, Boudjema K, Williams R, Corsmit O, Terpstra OT. Auxiliary versus orthotopic liver transplantation for acute liver failure. EURALT Study Group. European Auxiliary Liver Transplant Registry. *J Hepatol* 1999; **30**: 699-705
5 **Miwa S**, Hashikura Y, Mita A, Kubota T, Chisuwa H, Nakazawa Y, Ikegami T, Terada M, Miyagawa S, Kawasaki S. Living-related liver transplantation for patients with fulminant and subfulminant hepatic failure. *Hepatology* 1999; **30**: 1521-1526
6 **Amy L**. Friedman. Why bioartificial liver support remains the holy grail. *ASAIO J* 1998; **44**: 241-243
7 **Abouna GM**, Ganguly PK, Hamdy HM, Jabur SS, Tweed WA, Costa G. Extracorporeal liver perfusion system for successful hepatic support pending liver regeneration or liver transplantation: a pre-clinical controlled trial. *Transplantation* 1999; **67**: 1576-1583
8 **Uchino J**, Matsushita M. Strategies for the rescue of patients with liver failure. *ASAIO J* 1994; **40**: 74-77
9 **Lanjuan L**, Qian Y, Jianrong H, Xiaowei X, Yuemei C, Yagang C, Weihang M, Zhi C, Suzhen F. Severe hepatitis treated with an artificial liver support system. *Int J Artif Organs* 2001; **24**: 297-303
10 **Sussman NL**, Gislason GT, Conlin CA, Kelly JH. The hepatix extracorporeal liver assist device: initial clinical experience. *Artif Organs* 1994; **18**: 390-396
11 **Li L**, Yang Q, Huang J, Xu X, Chen Y, Chen Y, Ma W, Chen Z, Fu S. Treatment of hepatic failure with artificial liver support system. *Chin Med J* 2001; **114**: 941-945
12 **Si CW**, Zhang H, Wang BE. Prevention and cure project of viral hepatitis. Revised Statement 5th National Infectious Disease Meeting, Beijing, 1995. *Zhonghua Chuanranbing Zazhi* 1995; **13**: 241-247
13 **Sadahiro T**, Hirasawa H, Oda S, Shiga H, Nakanishi K, Kitamura N, Hirano T. Usefulness of plasma exchange plus continuous hemodiafiltration to reduce adverse effects associated with plasma exchange in patients with acute liver failure. *Crit Care Med* 2001; **29**: 1386-1392
14 **Kato A**, Suzuki K, Sato S. Imbalance of amino acid metabolism in fulminant hepatitis and its management. *Nippon Rinsho* 1992; **50**: 1599-1603
15 **Takahashi Y**. Evaluation of the special therapies in fulminant viral hepatitis –a multi-institution study. *Nippon Shokakibyo Gakkai Zasshi* 1995; **92**: 7-18
16 **Higashi T**. Impaired metabolism of methionine in severe liver diseases: I. Clinical and pathophysiological significance of elevated serum methionine levels. *Gastroenterol Jpn* 1982; **17**: 117-124
17 **Toborek M**, Kopieczna-Grzebieniak E, Drozdz M, Wieczorek M. Increased lipid peroxidation and antioxidant activity in methionine induced hepatitis in rabbits. *Nutrition* 1996; 12: 534-537
18 **Goss JA**, Shackleton CR, Maggard M, Swenson K, Seu P, McDiarmid SV, Busuttil RW. Liver transplantation for fulminant hepatic failure in the pediatric patient. *Arch Surg* 1998; **133**: 839-846
19 **Agishi T**, Nakagawa Y, Teraoka S, Kubo K, Nakazato S, Ota K. Plasma exchange as a rescue strategy for hepatic failure. *ASAIO J* 1994; **40**: 77-79
20 **Larsen FS**, Hansen BA, Jorgensen LG, Secher NH, Bondesen S, Linkis P, Hjortrup A, Kirkegaard P, Agerlin N, Kondrup J. Cerebral blood flow velocity during high volume plasmapheresis in fulminant hepatic failure. *Int J Artif Organs* 1994; **17**: 353-361
21 **Ash SR**. Hemodiabsorption in the treatment of acute hepatic failure. *ASAIO J* 1994; **40**: 80-82
22 **Kaplan AA**, Epstein M. Extracorporeal blood purification in the management of patients with hepatic failure. *Semin Nephrol* 1997; **17**: 576
23 **Zhu XF**, Chen GH, He XS, Lu MQ, Wang GD, Cai CJ, Yang Y, Huang JF. Liver transplantation and artificial liver support in fulminant hepatic failure. *World J Gastroenterol* 2001; **7**: 566-568

Edited by Wang XL **Proofread by** Chen WW and Xu FM

PO Box 2345, Beijing 100023, China
Fax: +86-10-85381893
E-mail: wjg@wjgnet.com www.wjgnet.com

World J Gastroenterol 2004;10(20):2989-2993
World Journal of Gastroenterology
 ISSN 1007-9327

• VIRAL HEPATITIS •

Yeast expression and DNA immunization of hepatitis B virus S gene with second-loop deletion of α determinant region

Hui Hu, Xiao-Mou Peng, Yang-Su Huang, Lin Gu, Qi-Feng Xie, Zhi-Liang Gao

Hui Hu, Xiao-Mou Peng, Yang-Su Huang, Lin Gu, Qi-Feng Xie, Zhi-Liang Gao, Department of Infectious Diseases, the Third Affiliated Hospital, Sun Yat-Sen University, Guangzhou 510630, Guangdong Province, China
Supported by the National Natural Science Foundation of China, No. 39970677 and the Science Foundation of Guangdong Province, No. 99M04801G
Correspondence to: Xiao-Mou Peng, Department of Infectious Diseases, the Third Affiliated Hospital, Sun Yat-Sen University, Guangzhou 510630, Guangdong Province, China. xiaomoupeng@hotmail.com
Telephone: +86-20-85516867 Ext. 2019 **Fax:** +86-20-85515940
Received: 2004-03-23 **Accepted:** 2004-04-13

Abstract

AIM: Immune escape mutations of HBV often occur in the dominant epitope, the second-loop of the a determinant of hepatitis B surface antigen (HBsAg). To let the hosts respond to the subdominant epitopes in HBsAg may be an effective way to decrease the prevalence of immune escape mutants. For this reason, a man-made clone of HBV S gene with the second-loop deletion was constructed. Its antigenicity was evaluated by yeast expression analysis and DNA immunization in mice.

METHODS: HBV S gene with deleted second-loop, amino acids from 139 to 145, was generated using splicing by overlap extension. HBV deleted S gene was then cloned into the yeast expression vector pPIC9 and the mammalian expression vector pcDNA3 to generate pHB-SDY and pHB-SD, respectively. The complete S gene was cloned into the same vectors as controls. The deleted recombinant HBsAg expressed in yeasts was detected using Abbott IMx HBsAg test kits, enzyme-linked immunoadsorbent assay (ELISA) and immune dot blotting to evaluate its antigenicity *in vitro*. The anti-HBs responses to DNA immunization in BALB/c mice were detected using Abbott IMx AUSAB test kits to evaluate the antigenicity of that recombinant protein *in vivo*.

RESULTS: Both deleted and complete HBsAg were successfully expressed in yeasts. They were intracellular expressions. The deleted HBsAg could not be detected by ELISA, in which the monoclonal anti-HBs against the α determinant was used, but could be detected by Abbott IMx and immune dot blotting, in which multiple monoclonal anti-HBs and polyclonal anti-HBs were used, respectively. The activity of the deleted HBsAg detected by Abbott IMx was much lower than that of complete HBsAg (the ratio of sample value/cut off value, 106±26.7 *vs* 1 814.4±776.3, $P<0.01$, $t = 5.02$). The anti-HBs response of pHB-SD to DNA immunization was lower than that of complete HBV S gene vector pHB (the positive rate 2/10 *vs* 6/10, 4.56±3.52 mIU/mL *vs* 27.60±17.3 mIU/mL, $P = 0.02$, $t = 2.7$).

CONCLUSIONS: HBsAg with deleted second-loop of the α determinant still has antigenicity, and can also raise weak anti-HBs response in mice to DNA immunization, suggesting that it is possible to develop a subdominant vaccine for preventing infections of immune escape mutants of HBV.

Hu H, Peng XM, Huang YS, Gu L, Xie QF, Gao ZL. Yeast expression and DNA immunization of hepatitis B virus S gene with second-loop deletion of α determinant region. *World J Gastroenterol* 2004; 10(20): 2989-2993
http://www.wjgnet.com/1007-9327/10/2989.asp

INTRODUCTION

The prevalence of hepatitis B virus (HBV) is still high in some areas of the world[1,2]. Universal inoculation of hepatitis B vaccine helps to sharply decrease the prevalence of HBsAg carriers from about 10% to 2% among the urban children in China[3]. However, there are about 5-10% of healthy individuals demonstrating no or inadequate responses following a standard vaccination schedule[4,5]. A portion of these non-responders may be with a breakthrough infection of immune escape mutants[6,7]. The escape mutant infections were also frequently occurred in liver transplant recipients under hepatitis B immunoglobulin prophylaxis[8,9]. The prevalence of the mutants, usually as occult HBV infections, will progressively increase in the future since certain mutants are stable enough to be horizontally transmittable[10,11] and have a potential to be transmitted through blood transfusion because of escaping the routine screening assays. The second-loop from aa139 to aa147 of the α determinant of HBsAg is the dominant epitope. The escape mutants usually have mutations in this region, including K141E, P142S, D144E and G145R[8,9,12-16], though there are mutations in the rest part of HBsAg[17,18], and induce an altered immunity against the second-loop so that the mutants can escape vaccine-raised antibodies or rabbit polyclonal antibodies to some extent[19,20]. Fortunately, recent researches suggested that weak epitopes, such as subdominant epitopes, might not be escaped[21,22]. To let hosts respond to subdominant epitopes or to both dominant and subdominant epitopes may be an effective way for the prevention of escape mutant infections. For these reasons, a man-made clone of HBV S gene with the second-loop deletion of the α determinant region was constructed in order to destroy the dominant epitope and let the subdominant epitopes be responded by the hosts. The antigenicity of that deleted S gene was evaluated by means of yeast expression analysis and DNA immunization in mice.

MATERIALS AND METHODS

Reagents

pTZ19U-HBV containing double copies of HBV DNA (adw) was presented from professor Zhi-Min Huang, Zhongshan University, Guangzhou, China. pcDNA3 and pPIC9 were purchased from Invitrogen Company (the United States of America). T4 DNA ligase and pfu DNA polymerase were purchased from Promega Company (the United States of America). DNA gel extraction kits and plasmid isolation kits were purchased from Qiagen Company (Germany). Primers shown in Table 1 were synthesized by Bioasia Biological

Table 1 Primers used in construction of eukaryotic expression vectors

Name	Sequences (5'→3')
HBS-SD1	TCC AAG CTT ATG GGA TCC GAG AAC ATC ACA TCA GGA TTC
HBS-SD2	GCA ACA TGA GGG AAA CAT AG
HBS-SD3	TCT ATG TTT CCC TCA TGT TGC AAT TGC ACC TGT ATT CCC ATC
HBS-SD4	TCC GAA TTC TTT TGT TAG GGT TTA AAT GTA TAC C
HBPIC9-1	CCG GAA TTC GAC GAT GAC GAT AAG GAG AAC ATC ACA TCA GGA TTC
HBPIC9-2	CAA CGC GGC CGC TTA AAT GTA TAC CCA GAG AC

Engineering Company (Shanghai, China). ELISA HBsAg kit was purchased from Zhongshan Biological Engineering Company (Guangdong, China). Abbott IMx HBsAg and AUSAB test kits were purchased from Abbott Laboratory (the United States of America). Sheep polyclonal anti-HBs and labeled streptavidin biotin detecting kit were purchased from DAKO Company (the United States).

Animal

Eight to twelve week-old inbred BALB/c female mice were obtained from Guangzhou Traditional Chinese Medicine University.

Construction of HB-SD and HB-SDY fragments

HB-SD was the fragment of HBV S gene with deletion of seven amino acid residues from 139 to 145 of the second-loop of the α determinant. In order to construct HB-SD, Two fragments of HBV S gene from codon 1 to codon 138 and from codon 146 to codon 226 were obtained by polymerase chain reaction (PCR) using HBS-SD1/HBS-SD2 and HBS-SD3/HBS-SD4 as primers, respectively, and pTZ19U-HBV as template. The fragments were then connected using splicing by overlap extension after the PCR products were run on 20 g/L agarose gel and a given band was extracted using DNA gel extraction kit[23]. HB-SD was obtained at last by purifying the spliced products. HB-SDY was obtained by PCR using HB-SD as template and HBSPIC9-1/HBSPIC9-2 as primers. The control fragments of complete HBV S gene were obtained using pTZ19U-HBV as template, and HBS-SD1/HBS-SD4 or HBSPIC9-1/HBSPIC9-2 as primers.

Construction of recombinant vector pHB-SDY and pHB-SD

For construction of pHB-SDY, the fragments of HB-SD and pPIC9 were digested by restriction endonucleases *Eco*RI and *Not* I, respectively. For construction of pHB-SD, the fragment of HB-SD was digested by restriction endonucleases *Hin*d III and *Eco* RI, respectively as well as pcDNA3. Digested DNA fragment and vector DNA were ligated using T4 DNA ligase after purification. Plasmid DNA was obtained after *Escherichia coli* was transformed by ligated products. Candidate recombinant plasmids were selecteds by restriction fragment length polymorphism (RFLP) analysis and automatic DNA sequencing by Bioasia Biological Engineering Company. Control vectors pHB and pHBY were generated using the control fragments of complete HBV S gene in the same way.

Expression of pHB-SDY in yeast

The recombinant vector DNA of pHB-SDY and pHBY was prepared from transformed bacteria using Qiagen's Max-Prep kits. Yeast cells from a single colony of *Pichia pastoris* GS115 strain were cultivated using YPD culture. Vector DNA was transformed into yeast cells by lithium chloride transformation method. Transformants were grown on minimal dextrose and minimal methanol plates to screen Mut^+ and Mut^S phenotypes. PCR using AOX1 primers was utilized to screen integrants. Mut^S strain was cultivated in BMGY culture and induced using 5 mL/L methanol. Protein expression of the supernatants and cell pellets was analyzed by Coomassie-stained SDS-PAGE, ELISA, Abbott IMx and immune dot blotting assay. ELISA and IMx tests were carried out as the manufacturer's protocol. Immune dot blotting was carried out using sheep polyclonal anti-HBs as first antibody and LSAB kit to demonstrate the results.

DNA immunization analysis of pHB-SD

Large scale plasmid DNA of recombinant plasmids pHB-SD and pHB was prepared using Qiagen's Max-Prep kits. Plasmid DNA of pcDNA3 was also prepared to be used as control. Plasmid DNA was adjusted to 1 μg/μL in normal saline. Thirty BLBA/c mice were randomly divided into 4 groups. Each mouse was injected 100 μL of plasmid DNA which was distributed over five different sites into the anterior tibialis muscle 5 d after the injection of an equal volume of 2 g/L bupivacaine. Boost injection was carried out 3 times every 3 wk with equal amount of plasmid DNA. Four weeks after the last boost injection, all mice were put to death for serum. Anti-HBs in serum was detected using Abbott AUSAB kits.

Statistical analysis

For anti-HBs level, geometric mean titer (GMT) for each group was calculated at first. Then Student-Newman-Keuls-q was used for statistical analysis. For positive rate, Fisher exact probability analysis was used. SPSS 10.0 for Windows was used for all statistical analysis. $P<0.05$ was considered statistically significant.

RESULTS

Construction of HB-SD and HB-SDY

Two fragments for constructing HB-SD fragment (Figure 1) were successfully obtained with base pair number as expected. The base pair number of spliced HB-SD fragment (Figure 1) was just a little smaller than that of HB fragment (Figure 1), which was the PCR fragment of complete HBV S gene with 711 bp in length. That was conformed to the fact that HB-SD fragment was only 21 bp smaller than HB fragment. HBY and HB-SDY fragments are shown in Figure 1. Their base pair numbers were the same as designed.

Construction of pHB-SD and pHB-SDY

HB-SD fragment was inserted into the vector of pcDNA3 between restriction endonucleases *Hin*d III and *Eco*RI. When recombinant plasmids were digested with the two restriction endonucleases, the molecular weight of the small restriction fragment was the same as that of HB-SD (Figure 2). After its sequence was confirmed by DNA sequencing, the recombinant plasmid was denominated as pHB-SD. The HB fragment was cloned into the same vector to obtain a recombinant plasmid of pHB as control. HB-SDY fragment was inserted into the vector of pPIC9 between restriction endonucleases *Eco* RI and *Not* I. The digested fragment shown in Figure 2 was the same as designed in base pair numbers. The recombinant vector was denominated as pHB-SDY after its sequence was confirmed by DNA sequencing. HBY fragment was cloned into the pPIC9 to obtain recombinant vector of pHBY as control.

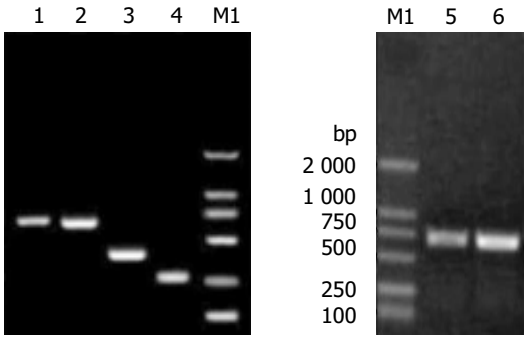

Figure 1 Electrophoresis of the fragments of HBV S gene. Lane 1: HB fragment of complete HBV S gene; Lane 2: HB-SD fragment with the second-loop deletion of the α determinant; Lane 3: DNA fragment of HBV S gene from codon 1 to codon 138; Lane 4: DNA fragment of HBV S gene from codon 146 to codon 226; Lane 5: HBY fragments; Lane 6: HB-SDY fragments; Lane M1: DNA marker.

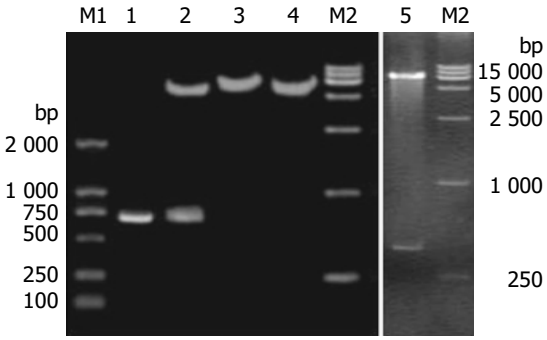

Figure 2 RFLP analysis of recombinant vectors of pHB-SD and pHB-SDY. Lane M1: DNA marker; Lane 1: HB-SD fragment; Lane 2: pHB-SD candidate digested by restriction endonuclease *Hind* III and *Eco* RI; Lane 3: pHB-SD candidate digested by restriction endonuclease *Bam* HI; Lane 4: pcDNA3 digested by restriction endonuclease *Bam* HI; Lane 5: pHB-SDY candidate digested by restriction endonuclease *Not* I and *Eco* RI; Lane M2: DNA marker.

Expression of recombinant plasmid pHB-SDY in yeast

Mut^S transformants for pHB-SDY and its control pHBY were successfully selected though growing on plates of minimal dextrose and minimal methanol. The integrant screening results of transformants are shown in Figure 3. The PCR product of Mut$^+$ transformants without gene of interest was 2.2 kb (Figure 3A). The PCR product of pPIC9 alone was 492 bp (Figure 3A). The PCR products of integrants of pHBY and pHB-SDY were 1 200 bp and 1 179 bp respectively. These transformants shown in Figure 3A were recombinants with the genes of interest, and belonged to Mut^s transformants since they had no bands of wild-type *AOX1* gene. The results of Coomassie-stained SDS-PAGE analysis of the protein expression of Mut^s transformants with pHBY and pHB-SDY are shown in Figure 3B. No recombinant protein was visible. The results of HBsAg antigenicity detection using ELISA and immune dot blotting are shown in Figure 4. The expression of transformants with pHBY was intracellular. The recombinant protein of pHB-SDY could not be detected by ELISA, and only weakly demonstrated by immune dot blotting assay. The IMx results are shown in Table 2. The ratio of sample value/cut off value of pHB-SDY was much lower than that of pHBY (P<0.01, t = 5.02).

DNA immunization

All mice were alive after the inoculation schedule was finished. The anti-HBs levels are shown in Table 2. The anti-HBs was negative in groups of normal saline and plasmid pcDNA3. The positive rate of anti-HBs was 2/10 in pHB-SD group and 6/10 in pHB group. The amount of anti-HBs induced in groups of HBV S gene with deleted second-loop of the α determinant was less than that in the complete HBV S gene groups (P = 0.02, t = 2.7).

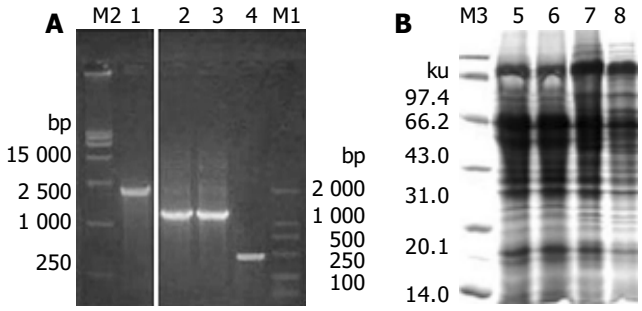

Figure 3 Screening integrants and SDS-PAGE analysis. A: Screening integrants using PCR with *AOX1* primers. Lane M2: DNA marker; Lane 1: PCR products of Mut$^+$ transformant without gene of interest; Lane 2: PCR products of Mut^s transformants with pHBY; Lane 3: PCR products of Mut^s transformants with pHB-SDY; Lane 4: PCR products of pPIC9 alone. Lane M1 were DNA markers. B: Coomassie-stained SDS-PAGE analysis of the recombinant proteins of pHB-SDY and pHBY. Lane M3: protein marker; Lane 5: cell lysate supernatants of yeast alone; Lane 6: yeast transformed with pPIC9; Lane 7: yeast transformed with pHBY; Lane 8: yeast transformed with pHB-SDY.

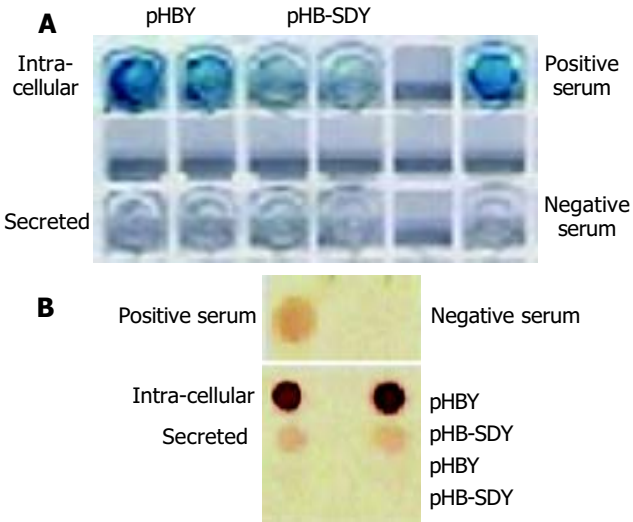

Figure 4 Antigenicity analysis of recombinant proteins using ELISA and immune dot blotting assay. (A) ELISA, (B) immune dot blotting assay.

Table 2 Antigenicity of HBsAg with second-loop deletion of α determinant

Groups	HBsAg titer by IMx S/CO value	Anti-HBs responses in DNA immunization	
		Positive rate	mIU/L (GMT±SE)
Empty control	-	0/5	-
pcDNA3	-	0/5	-
pHB	1 589±234.5[b]	6/10	27.60±17.3[c]
pHB-SD	106±26.8	2/10	4.56±3.52

S/CO: the ratio of sample against cut off value. GMT: geometric mean titer. [b]P<0.01, t = 5.02 *vs* groups of pHB-SD; [c]P = 0.02, t = 2.7 *vs* groups of pHB-SD.

DISCUSSION

The hosts usually do not respond to the subdominant epitopes in both vaccinated individuals and patients because of the dominant negative mechanism. Since they usually have no escape mutations and are not tolerant in patients, the subdominant epitopes have been widely used to overcome immunological tolerance in the fields of tumor and chronic infections[24-27]. Many subdominant epitopes were successfully responded by the hosts with chronic infections or tumor carrying patients[24-29]. However, the most data were limited in CD8+ cells or cytotoxic T lymphocytes. There are few such literatures about the epitopes of B lymphocytes. As a protective antigen, HBsAg is of great significance for prevention of HBV infection. It has been confirmed that there are more than three B-lymphocyte epitopes in HBsAg. The second-loop of α determinant is the strongest one among them[30]. It is the dominant epitope, and the rest ones are the subdominant epitopes.

To completely destroy the dominant epitope may be able to eliminate the dominant negative mechanism, and let the subdominant epitopes be responded by the hosts. In our study even after deletion of the second-loop of HBsAg α determinant, the recombinant protein expressed in yeasts still had a weak antigenicity. Though it escaped the monoclonal anti-HBs derived from the α determinant, the recombinant protein might react with polyclonal anti-HBs or monoclonal anti-HBs derived from other parts of HBsAg because it could be detected by immune dot blotting and Abbott IMx kits, in which the demonstrating antibodies consisted of monoclonal anti-HBs derived from α determinant and the rest part of HBsAg[31]. These results are similar to that of the α determinant variants that could be detected by monoclonal antibody from the rest part of HBsAg too[22]. Mammalian expression vector with deleted HBV S gene could raise a weak anti-HBs response to DNA immunization. It was not sure that this anti-HBs was protective. However, it might be able to react with HBV particles since the anti-HBs derived from the first-loop of the α determinant of HBsAg could be accessible on native HBsAg[21]. These suggested that it was possible to develop a subdominant vaccine for the prevention of immune escape mutant infections of HBV.

The response rate of recombinant plasmids was very low in our study. It might be the nature of DNA immunization because this phenomenon also occurred in researches of other scientists[32]. The deleted HBV S gene was successfully expressed in yeasts. However, the expression conditions need to be improved. The exact value of deleted HBsAg should be evaluated after purified recombinant proteins are obtained in the future. The effect of anti-HBs raised by subdominant epitopes of HBsAg on the infectivity of HBV should also be evaluated in the future.

HBsAg with deleted second-loop of the α determinant still has antigenicity, and can also raise weak anti-HBs response in mice to DNA immunization, suggesting that it is possible to develop a subdominant vaccine for preventing infections of immune escape mutants of HBV.

REFERENCES

1 **Kao JH**, Chen DS. Global control of hepatitis B virus infection. *Lancet Infect Dis* 2002; **2**: 395-403

2 **Huang P**, Ye G, Zhong J, Sha Q. Assessment of current epidemiological status of viral hepatitis in Guangdong Province, China. *Southeast Asian J Trop Med Public Health* 2002; **33**: 832-836

3 **Kane MA**. Global control of primary hepatocellular carcinoma with hepatitis B vaccine: the contributions of research in Taiwan. *Cancer Epidemiol Biomarkers Prev* 2003; **12**: 2-3

4 **Tao Q**, Feng B. Prevention and therapy of hepatitis B. *Chin Med J* 1999; **112**: 942-946

5 **Andre FE**, Zuckerman AJ. Review: protective efficacy of hepatitis B vaccines in neonates. *J Med Virol* 1994; **44**: 144-151

6 **He C**, Nomura F, Itoga S, Isobe K, Nakai T. Prevalence of vaccine-induced escape mutants of hepatitis B virus in the adult population in China: a prospective study in 176 restaurant employees. *J Gastroenterol Hepatol* 2001; **16**: 1373-1377

7 **Jeantet D**, Chemin I, Mandrand B, Zoulim F, Trepo C, Kay A. Characterization of two hepatitis B virus populations isolated from a hepatitis B surface antigen-negative patient. *Hepatology* 2002; **35**: 1215-1224

8 **Kim KH**, Lee KH, Chang HY, Ahn SH, Tong S, Yoon YJ, Seong BL, Kim SI, Han KH. Evolution of hepatitis B virus sequence from a liver transplant recipient with rapid breakthrough despite hepatitis B immune globulin prophylaxis and lamivudine therapy. *J Med Virol* 2003; **71**: 367-375

9 **Poovorawan Y**, Theamboonlers A, Chongsrisawat V, Sanpavat S. Molecular analysis of the a determinant of HBsAg in children of HBeAg-positive mothers upon failure of postexposure prophylaxis. *Int J Infect Dis* 1998; **2**: 216-220

10 **Levicnik-Stezinar S**. Hepatitis B surface antigen escape mutant in a first time blood donor potentially missed by a routine screening assay. *Clin Lab* 2004; **50**: 49-51

11 **Chakravarty R**, Neogi M, Roychowdhury S, Panda CK. Presence of hepatitis B surface antigen mutant G145R DNA in the peripheral blood leukocytes of the family members of an asymptomatic carrier and evidence of its horizontal transmission. *Virus Res* 2002; **90**: 133-141

12 **Thakur V**, Kazim SN, Guptan RC, Malhotra V, Sarin SK. Molecular epidemiology and transmission of hepatitis B virus in close family contacts of HBV-related chronic liver disease patients. *J Med Virol* 2003; **70**: 520-528

13 **Cooreman MP**, Leroux-Roels G, Paulij WP. Vaccine- and hepatitis B immune globulin-induced escape mutations of hepatitis B virus surface antigen. *J Biomed Sci* 2001; **8**: 237-247

14 **Koyanagi T**, Nakamuta M, Sakai H, Sugimoto R, Enjoji M, Koto K, Iwamoto H, Kumazawa T, Mukaide M, Nawata H. Analysis of HBs antigen negative variant of hepatitis B virus: unique substitutions, Glu129 to Asp and Gly145 to Ala in the surface antigen gene. *Med Sci Monit* 2000; **6**: 1165-1169

15 **Hou J**, Wang Z, Cheng J, Lin Y, Lau GK, Sun J, Zhou F, Waters J, Karayiannis P, Luo K. Prevalence of naturally occurring surface gene variants of hepatitis B virus in nonimmunized surface antigen-negative Chinese carriers. *Hepatology* 2001; **34**: 1027-1034

16 **Karthigesu VD**, Allison LM, Fortuin M, Mendy M, Whittle HC, Howard CR. A novel hepatitis B virus variant in the sera of immunized children. *J Gen Virol* 1994; **75**(Pt 2): 443-448

17 **Chen HB**, Fang DX, Li FQ, Jing HY, Tan WG, Li SQ. A novel hepatitis B virus mutant with A-to-G at nt551 in the surface antigen gene. *World J Gastroenterol* 2003; **9**: 304-308

18 **Komatsu H**, Fujisawa T, Sogo T, Isozaki A, Inui A, Sekine I, Kobata M, Ogawa Y. Acute self-limiting hepatitis B after immunoprophylaxis failure in an infant. *J Med Virol* 2002; **66**: 28-33

19 **Shizuma T**, Hasegawa K, Ishikawa K, Naritomi T, Iizuka A, Kanai N, Ogawa M, Torii N, Joh R, Hayashi N. Molecular analysis of antigenicity and immunogenicity of a vaccine-induced escape mutant of hepatitis B virus. *J Gastroenterol* 2003; **38**: 244-253

20 **Oon CJ**, Chen WN, Goh KT, Mesenas S, Ng HS, Chiang G, Tan C, Koh S, Teng SW, Toh I, Moh MC, Goo KS, Tan K, Leong AL, Tan GS. Molecular characterization of hepatitis B virus surface antigen mutants in Singapore patients with hepatocellular carcinoma and hepatitis B virus carriers negative for HBsAg but positive for anti-HBs and anti-HBc. *J Gastroenterol Hepatol* 2002; **17**(Suppl): S491-S496

21 **Ijaz S**, Ferns RB, Tedder RS. A 'first loop' linear epitope accessible on native hepatitis B surface antigen that persists in the face of 'second loop' immune escape. *J Gen Viral* 2003; **84**(Pt 2): 269-275

22 **Jolivet-Reynaud C**, Lesenechal M, O'Donnell B, Becquart L, Foussadier A, Forge F, Battail-Poirot N, Lacoux X, Carman W, Jolivet M. Localization of hepatitis B surface antigen epitopes present on variants and specifically recognised by anti-hepatitis B surface antigen monoclonal antibodies. *J Med Virol* 2001; **65**: 241-249

23 **Horton RM**, Hunt HD, Ho SN, Pullen JK, Pease LR. Engineering hybrid genes without the use of restriction enzymes: gene splicing by overlap extension. *Gene* 1989; **77**: 61-68
24 **Marastoni M**, Bazzaro M, Micheletti F, Gavioli R, Tomatis R. Peptide analogues of a subdominant epitope expressed in ebv-associated tumors: synthesis and immunological activity. *J Med Chem* 2001; **44**: 2370-2373
25 **Hudrisier D**, Riond J, Gairin JE. Molecular and functional dissection of the H-2Db-restricted subdominant cytotoxic T-cell response to lymphocytic choriomeningitis virus. *J Virol* 2001; **75**: 2468-2471
26 **Barouch DH**, Craiu A, Santra S, Egan MA, Schmitz JE, Kuroda MJ, Fu TM, Nam JH, Wyatt LS, Lifton MA, Krivulka GR, Nickerson CE, Lord CI, Moss B, Lewis MG, Hirsch VM, Shiver JW, Letvin NL. Elicitation of high-frequency cytotoxic T-lymphocyte responses against both dominant and subdominant simian-human immunodeficiency virus epitopes by DNA vaccination of rhesus monkeys. *J Virol* 2001; **75**: 2462-2467
27 **Nelson D**, Bundell C, Robinson B. *In vivo* cross-presentation of a soluble protein antigen: kinetics, distribution, and generation of effector CTL recognizing dominant and subdominant epitopes. *J Immunol* 2000; **165**: 6123-6132
28 **Tourdot S**, Oukka M, Manuguerra JC, Magafa V, Vergnon I, Riche N, Bruley-Rosset M, Cordopatis P, Kosmatopoulos K. Chimeric peptides: a new approach to enhancing the immunogenicity of peptides with low MHC class I affinity: application in antiviral vaccination. *J Immunol* 1997; **159**: 2391-2398
29 **Chengalvala MV**, Bhat RA, Bhat BM, Vernon SK, Lubeck MD. Enhanced immunogenicity of hepatitis B surface antigen by insertion of a helper T cell epitope from tetanus toxoid. *Vaccine* 1999; **17**: 1035-1041
30 **Maillard P**, Pillot J. At least three epitopes are recognized by the human repertoire in the hepatitis B virus group a antigen inducing protection; possible consequences for seroprevention and serodiagnosis. *Res Virol* 1998; **149**: 153-161
31 **Shah DO**, Coleman P, Chen J, Peterson B, Dimarco A, Stewart J. The detection of recombinant hepatitis B surface antigen from “vaccine escape mutants” in two HBsAg immunoassays. *Clin Lab* 2000; **46**: 161-163
32 **Geissler M**, Tokushige K, Chante CC, Zurawski VR Jr, Wands JR. Cellular and humoral immune response to hepatitis B virus structural proteins in mice after DNA-based immunization. *Gastroenterology* 1997; **12**: 1307-1320

Edited by Kumar M and Wang XL **Proofread by** Xu FM

PO Box 2345, Beijing 100023, China
Fax: +86-10-85381893
E-mail: wjg@wjgnet.com www.wjgnet.com

World J Gastroenterol 2004;10(20):2994-2996
World Journal of Gastroenterology
 ISSN 1007-9327

Prominent role of γ-glutamyl-transpeptidase on the growth of *Helicobacter pylori*

Min Gong, Bow Ho

Min Gong, Bow Ho, Department of Microbiology, Faculty of Medicine, National University of Singapore, Singapore 117597, Republic of Singapore
Supported by NMRC Grant No. 0415/2000. Gong Min is a National University of Singapore research scholar
Correspondence to: Bow Ho, Department of Microbiology, Faculty of Medicine, National University of Singapore, Science Drive 2, Singapore 117597, Republic of Singapore. michob@nus.edu.sg
Telephone: +65-68743672 **Fax:** +65-67766872
Received: 2003-10-10 **Accepted:** 2003-12-03

Abstract

AIM: γ-glutamyl transpeptidase (GGT) has been reported as a virulence and colonizing factor of *Helicobacter pylori* (*H pylori*). This study examined the effect of GGT on the growth of *H pylori*.

METHODS: Standard *H pylori* strain NCTC 11637 and 4 clinical isolates with different levels of GGT activity as measured by an enzymatic assay were used in this study. Growth inhibition and stimulation studies were carried out by culturing *H pylori* in brain heart infusion broth supplemented with specific GGT inhibitor (L-serine sodium borate complex, SBC) or enhancer (glutathione together with glycyl-glycine), respectively. The growth profiles of *H pylori* were determined based on viable bacterial count at time interval.

RESULTS: Growth was more profuse for *H pylori* isolates with higher GGT activity than those present with lower GGT activity. However, in the presence of SBC, growth of *H pylori* was retarded in a dose dependent manner ($P = 0.034$). In contrast, higher growth rate was observed when GGT activity was enhanced in the presence of glutathione and glycyl-glycine.

CONCLUSION: Higher GGT activity provides an advantage to the growth of *H pylori in vitro*. Inhibition of GGT activity by SBC resulted in growth retardation. The study shows that GGT plays an important role on the growth of *H pylori*.

Gong M, Ho B. Prominent role of γ-glutamyl-transpeptidase on the growth of *Helicobacter pylori*. *World J Gastroenterol* 2004; 10(20): 2994-2996
http://www.wjgnet.com/1007-9327/10/2994.asp

INTRODUCTION

Helicobacter pylori (*H pylori*) is a gram-negative spiral bacterium that causes chronic infection of the human stomach in adults[1-5] as well as children[6]. The chronic *H pylori* infection may lead to peptic ulceration[7-9] and may be a potential risk factor for gastric carcinoma[10-12].

The exact mechanism on how *H pylori* promotes gastric neoplasia is not known but is hypothesized to have occurred through the production of reactive oxygen species leading to oxidative stress and DNA damage in gastric epithelial cells[13-15]. The level of reduced form of the tripeptide thiol, glutathione (GSH), one of the major endogenous defense mechanisms against oxidative stress, was shown to be decreased in gastric mucosal after *H pylori* infection[16,17]. Furthermore, it has been well established that GGT plays a major role in glutathione metabolism. This enzyme catalyses transpeptidation reaction in which a γ-glutamyl moiety is transferred from γ-glutamyl compounds, such as glutathione, a non-protein sulphydryl molecule, to amino acids. In addition, GGT can use γ-glutamyl peptides as substrates in the reciprocal hydrolysis reaction, thus playing a role in the synthesis of glutathione[18,19].

It has been reported that GGT activity could be inhibited by the presence of inhibitors like L-serine sodium borate complex (SBC)[20] and acivicin[21]. Although acivicin is a more effective GGT inhibitor, it is nonspecific and inhibits a number of glutamine amino-transferase[21]. In contrast, SBC is a highly specific GGT inhibitor but substantially higher concentration of SBC as compared to acivicin is needed for an effective inhibition of GGT activity[20].

GGT being a constitutive enzyme of *H pylori* was shown to participate in the colonization of *H pylori* in Swiss specific pathogen-free mice[22]. However, a later study using a different animal model demonstrated that GGT was not essential for colonization but acted as a virulence factor[23]. The present study examined the effect of GGT on *H pylori* growth *in vitro* in the presence of GGT inhibitor as well as enhancer.

MATERIALS AND METHODS

Bacterial strains and culture conditions

A standard *H pylori* strain NCTC 11 637 and 4 clinical isolates with different levels of GGT activity were used in this study. Strains 712 and 1 018 showed high GGT activity (>1 U/mg protein) while strains 1 082 and 888 had low GGT activity (<0.4 U/mg protein).

H pylori was grown for 3 d at 37 ℃ on chocolate blood agar containing 40 g/L blood agar base No.2 (Oxoid) and 50 mL/L horse blood (Gibco) in a humidified incubator (Forma Scientific) supplied with 50 mL/L CO_2.[24] The bacterial cells were harvested and washed with PBS buffer (pH 7.4) to give a suspension of ca. 5×10^7 CFU/mL ($A_{600} = 0.2$) in either PBS or brain heart infusion (BHI, Gibco) broth.

Inhibitory effect of SBC on H pylori GGT activity

A bacterial population of 3 d old 10^7 CFU/mL *H pylori* NCTC 11 637 was incubated in BHI broth containing various concentrations (2-10 mmol/L) of SBC (Sigma) at 37 ℃ for 30 min. GGT activity of *H pylori* cells was then measured by an enzymatic assay as described by Meister *et al*.[25].

Growth inhibition and stimulation studies

H pylori NCTC 11 637 was suspended in fresh BHI broth at a final cell concentration of approximately 5×10^5 CFU per ml. For growth inhibition study, appropriate volumes of filter-sterilized (pore size, 0.2 μm; Nalgene sterile syringe filter) SBC stock solution (100 mmol/L) were added to sterile BHI broth to provide final concentrations of SBC in BHI in the range of 2-10 mmol/L. For growth stimulation study, filter-sterilized glycyl-glycine

(Sigma) and GSH (Sigma) were added to BHI broth at a final concentration of 1 mmol/L and 0.1 mmol/L, respectively.

Growth inhibition and stimulation curves were constructed based on viable bacterial count at different time interval.

Growth of various H pylori strains that expressed different levels of GGT activity

Two strains each with high GGT activity (strains 1 018 and 712) and low GGT activity (strains 1 082 and 888) were grown in BHI broth at 37 ℃ over a period of 3 wk. The bacterial populations of the various strains were enumerated at time interval.

Statistical analysis

Data was analyzed using one-way ANOVA test (SPSS). A value of $P \leqslant 0.05$ was considered statistically significant.

RESULTS

SBC inhibits GGT activity of H pylori

Figure 1 shows that *H pylori* strain NCTC 11 637 GGT activity was inhibited in a dose dependent manner upon exposure to a range of SBC concentrations (2-10 mmol/L) for 30 min at 37 ℃, where >90% GGT activity was inhibited by ⩾4 mmol/L SBC. The maximum inhibitory effect of 96% of GGT activity was achieved at the concentration of 10 mmol/L SBC.

Effect of GGT on H pylori growth

Since SBC has inhibitory effect on *H pylori* GGT activity, *H pylori* NCTC 11 637 was cultured in BHI broth supplemented with different concentrations of SBC (2-10 mmol/L). Figure 2 shows that the *H pylori* cultured in the presence of various concentrations of SBC (2-10 mmol/L) over 3 wk displayed marked inhibition on the growth of *H pylori* in a dose dependent manner (ANOVA, $P = 0.034$). *A* > 99% decrease in viability of the bacterial population was observed within 72 h after culturing *H pylori* in the presence of 10 mmol/L SBC. In contrast, *H pylori* proliferated at twice the normal growth rate in the presence of GSH and glycyl-glycine with increased GGT activity as compared to the control. And this acceleration in growth lasted over a period of more then two weeks. Similar growth profile was observed with another *H pylori* strain SS1 (data not shown).

Growth of different H pylori strains

Growth of the four *H pylori* strains with disparate GGT activities was followed over a period of 3 wk. Figure 3 shows that *H pylori* isolates with higher GGT activity (strains 1 018 and 712) grew better and more abundant than those with lower GGT activity (strains 1 082 and 888) by 10-100 folds depending on the age of culture. However, all 4 cultures showed similar growth rate at 3 wk-old.

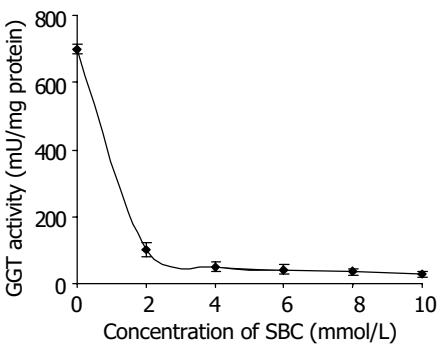

Figure 1 Inhibitory effect of SBC on *H pylori* GGT activity Inhibition of 85%, 92%, 94%, 95% and 96% were obtained by incubating *H pylori* in 2, 4, 6, 8 and 10 mmol/L SBC, respectively at 37 ℃ for 30 min.

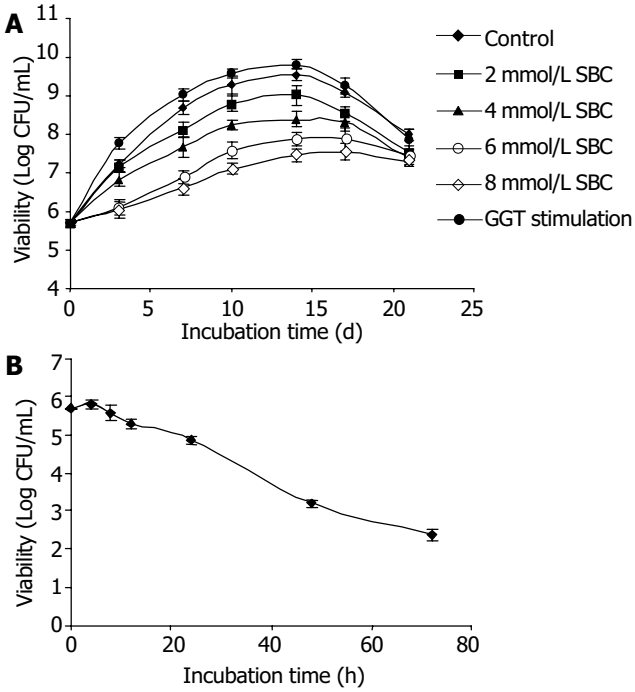

Figure 2 Effect of GGT on the growth of *H pylori*. *H pylori* strain NCTC 11 637 was cultured microaerobically in BHI broth medium supplemented with 10% fetal bovine serum at 37 ℃ and in the presence of either different concentration of GGT inhibitor or stimulator. A: Effect of 2 mmol/L (■square), 4 mmol/L (▲triangle), 6 mmol/L (×cross), 8 mmol/L (* star) SBC and GGT stimulation (0.1 mol/L GSH+1 mol/L glycyl-glycine, ●circle) on NCTC 11 637 over 21 d. Control (◆diamond). B: Effect of 10 mmol/L SBC on NCTC 11 637 over 72 h. Viability was determined continuously at time intervals. (CFU: colony-forming units).

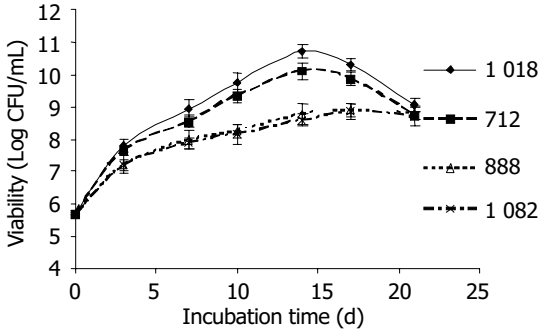

Figure 3 Growth of 4 *H pylori* strains with different levels of GGT activity *H pylori* strains 1 018 and 712 expressed high GGT activity (>1 U/mg protein) while strains 888 and 1 082 produced low GGT activity (<0.4 U/mg protein). *H pylori* strains 1 018 (diamond), 712 (■ square), 888 (△triangle), and 1 082 (×cross) were cultured in BHI medium microaerobically over 3 wk. Viability was determined continuously at time intervals.

DISCUSSION

Inhibition of GGT activity by SBC was caused by competition with respect to γ-glutamyl substrate, and it was suggested that a serine-borate complex is formed which may bind to the active site of the enzyme by interacting with a carbohydrate residue of the enzyme[20]. Although acivicin is 20 times more effective in inhibiting GGT activity as compared to SBC (data not shown), it was not used for the growth inhibition study because it is a non-specific GGT inhibitor[21]. In this study, more than 90% of GGT activity was suppressed by 4 mmol/L SBC. Inhibition of

GGT activity by SBC resulted in retarding the growth of *H pylori* in a dose dependent manner indicating that GGT is an essential enzyme in the growth of *H pylori*. In contrast, when physiological concentration of GSH and glycyl-glycine[26,27] were supplemented into the culture medium, growth of *H pylori* was accelerated by more than tow folds. The results show that the growth of *H pylori* was enhanced under GGT stimulation condition demonstrating the possibility of such event in *in vivo* situation.

In this study, it is interesting to note that *H pylori* with higher GGT activity (>1 U/mg protein) grows better than those with lower GGT activity (<0.4 U/mg protein). However, in the presence of SBC, a specific GGT inhibitor, the growth of *H pylori* was shown to be retarded. This finding that GGT is vital for the growth of *H pylori* could possibly explain why there was a reduction in the recovery of GGT isogenic mutant in the postinfected mice in the *in vivo* study carried out by McGovern *et al*.[23], while no *ggt* mutant *H pylori* were recovered in the animal model of Chevalier *et al*.[22]. The explanation supports the role of GGT activity in the ability of *H pylori* to proliferate in *in vivo* condition. However, the variation could also be due to the difference in animal model as suggested by McGovern *et al*.[23], or owing to strain difference in terms of the level of GGT activity expressed as demonstrated in this study.

It has been reported that GGT plays a significant role in *H pylori*-mediated apoptosis[28]. It was therefore suggested that *H pylori* induces apoptosis by GGT and that the bacteria gain essential nutrients from the apoptotic cells, thus establishing a permanent colony *in vivo*[28,29]. The results of earlier studies[22,23,28] indicated that GGT is an important enzyme for the growth and survival of *H pylori in vivo* while our findings that growth of *H pylori* is relative to the level of bacterial GGT activity and that higher GGT activity favors its growth *in vitro*. It is therefore proposed that GGT has a vital and prominent role to play on the growth of *H pylori*.

REFERENCES

1 **Israel DA,** Peek RM. Pathogenesis of *Helicobacter pylori*-induced gastric inflammation. *Aliment Pharmacol Ther* 2001; **15**: 1271-1290

2 **Sanders MK**, Peura DA. *Helicobacter pylori*-Associated Diseases. *Curr Gastroenterol Rep* 2002; **4**: 448-454

3 **Min K,** Hong SM, Kim KR, Ro JY, Park MJ, Kim JS, Kim JM, Jung HC, Yu E. Intramucosal *Helicobacter pylori* in the human and murine stomach: its relationship to the inflammatory reaction in human *Helicobacter pylori* gastritis. *Pathol Res Pract* 2003; **199**: 1-8

4 **Shibata K**, Moriyama M, Fukushima T, Une H, Miyazaki M, Yamaguchi N. Relation of *Helicobacter pylori* infection and lifestyle to the risk of chronic atrophic gastritis: a cross-sectional study in Japan. *J Epidemiol* 2002; **12**: 105-111

5 **Cave DR.** Chronic gastritis and *Helicobacter pylori*. *Semin Gastrointest Dis* 200; **12**: 196-202

6 **Ng BL**, Quak SH, Aw M, Goh KT, Ho B. Immune responses to differentiated forms of *Helicobacter pylori* in children with Epigastric pain. *Clin Diagn Lab Immunol* 2003 ; **10**: 866-869

7 **Lai YC**, Wang TH, Huang SH, Yang SS, Wu CH, Chen TK, Lee CL. Density of *Helicobacter pylori* may affect the efficacy of eradication therapy and ulcer healing in patients with active duodenal ulcers. *World J Gastroenterol* 2003; **9**: 1537-1540

8 **Nomura AM**, Perez-Perez GI, Lee J, Stemmermann G, Blaser MJ. Relation between *Helicobacter pylori cagA* status and risk of peptic ulcer disease. *Am J Epidemiol* 2002; **155**: 1054-1059

9 **Stack WA**, Atherton JC, Hawkey GM, Logan RF, Hawkey CJ. Interactions between *Helicobacter pylori* and other risk factors for peptic ulcer bleeding. *Aliment Pharmacol Ther* 2002; **16**: 497-506

10 **Dawsey SM**, Mark SD, Taylor PR, Limburg PJ. Gastric cancer and *H pylori*. *Gut* 2002; **51**: 457-458

11 **Blaser MJ.** Linking *Helicobacter pylori* to gastric cancer. *Nat Med* 2000; **6**: 376-377

12 **Takahashi S.** Long-term *Helicobacter pylori* infection and the development of atrophic gastritis and gastric cancer in Japan. *J Gastroenterol* 2002; **37**(Suppl 13): 24-27

13 **Davies GR**, Simmonds NJ, Stevens TR, Sheaff MT, Banatvala N, Laurenson IF, Blake DR, Rampton DS. *Helicobacter pylori* stimu-lates antral mucosal reactive oxygen metabolite production *in vivo*. *Gut* 1994; **35**: 179-185

14 **Obst B**, Wagner S, Sewing KF, Beil W. *Helicobacter pylori* causes DNA damage in gastric epithelial cells. *Carcinogenesis* 2000; **21**: 1111-1115

15 **Farinati F**, Cardin R, Degan P, Rugge M, Mario FD, Bonvicini P, Naccarato R. Oxidative DNA damage accumulation in gastric carcinogenesis. *Gut* 1998; **42**: 351-356

16 **Beil W**, Obst B, Sewing KF, Wagner S. *Helicobacter pylori* reduces intracellular glutathione in gastric epithelial cells. *Dig Dis Sci* 2000; **45**: 1769-1773

17 **Shirin H**, Pinto JT, Liu LU, Merzianu M, Sordillo EM, Moss SF. *Helicobacter pylori* decreases gastric mucosal glutathione. *Cancer Letters* 2001; **164**: 127-133

18 **Meister A**, Anderson ME. Glutathione. *Annu Rev Biochem* 1983; **52**: 711-760

19 **Tate SS**, Meister A. γ-glutamyl transpeptidase catalytic, structural and functional aspects. *Mol Cell Biochem* 1981; **39**: 357-368

20 **Tate SS**, Meister A. Serine-borate complex as a transition-state inhibitor of γ-glutamyl transpeptidase. *Proc Natl Acad Sci U S A* 1978; **75**: 4806-4809

21 **Anderson ME,** Meister A. Inhibition of γ-glutamyl transpeptidase and glutathionuria produced by γ-glutamyl amino acids. *Proc Natl Acad Sci U S A* 1986; **83**: 5029-5032

22 **Chevalier C**, Thiberge JM, Ferrero RL, Labigne A. Essential role of *Helicobacter pylori* γ-glutamyl transpeptidase for the colonization of the gastric mucosa of mice. *Mol Microbiol* 1999; **31**: 1359-1372

23 **McGovern KJ**, Blanchard TG, Gutierrez JA, Czinn SJ, Krakowka S, Youngman P. γ-glutamyltransferase is a *Helicobacter pylori* virulence factor but is not essential for colonization. *Infect Immun* 2001; **69**: 4168-4173

24 **Zheng PY**, Hua J, Yeoh KG, Ho B. Association of peptic ulcer with increased expression of Lewis antigens but not *cagA*, *iceA*, and *vacA* in *Helicobacter pylori* isolates in an Asian population. *Gut* 2000; **47**: 18-22

25 **Meister A**, Tate SS, Griffith OW. γ-Glutamyl transpeptidase. *Methods Enzymol* 1981; **77**: 237-253

26 **Tate SS**, Meister A. γ-Glutamyl transpeptidase from kidney. *Meth Enzymol* 1985; **113**: 400-419

27 **Paroni R**, Vecchi ED, Cighetti G, Arcelloni C, Fermo I, Grossi A, Bonini P. HPLC with o-phthalaldehyde precolumn derivatization to measure total, oxidized, and and protein-bound glutathione in blood, plasma, and tissue. *Clin Chem* 1995; **41**: 448-454

28 **Shibayama K**, Kamachi K, Nagata N, Yagi T, Nada T, Doi Y, Shibata N, Yokoyama K, Yamane K, Kato H, Iinuma Y, Arakawa Y. A novel apoptosis-inducing protein from *Helicobacter pylori*. *Mol Microbiol* 2003; **47**: 443-451

29 **Shibayama K**, Doi Y, Shibata N, Yagi T, Nada T, Iinuma Y, Arakawa Y. Apoptotic signaling pathway activated by *Helicobacter pylori* infection and increase of apoptosis-inducing activity under serumstarved conditions. *Infect Immun* 2001; **69**: 3181-3189

Edited by Wang XL **Proofread by** Xu FM

PO Box 2345, Beijing 100023, China
Fax: +86-10-85381893
E-mail: wjg@wjgnet.com www.wjgnet.com

World J Gastroenterol 2004;10(20):2997-3000
World Journal of Gastroenterology
 ISSN 1007-9327

Detection of anti-*Helicobacter pylori* antibodies in serum and duodenal fluid in peptic gastroduodenal disease

Angelo Locatelli, Wilson Roberto Catapani, Claudio Rufino Gomes Junior, Claudilene Battistin Paula Silva, Jaques Waisberg

Angelo Locatelli, Wilson Roberto Catapani, Claudio Rufino Gomes Junior, Claudilene Battistin Paula Silva, Jaques Waisberg, Department of Surgery, ABC Faculty of Medicine, Avenida Principe de Gales 821, Santo Andre, Sao Paulo, 09060-650, Brazil
Correspondence to: Dr. Jaques Waisberg, Rua das Figueiras 550, apto.134, Santo Andre - Sao Paulo 09080-300, Brazil. jaqueswaisberg@uol.com.br
Telephone: +55-11-44362461 **Fax:** +55-11-44362160
Received: 2004-02-20 **Accepted:** 2004-03-13

Abstract

AIM: To study the diagnosis of *Helicobacter pylori* (*H pylori*) infection through the determination of serum levels of anti-*H pylori* IgG and IgA antibodies, and the levels of anti-*H pylori* IgA antibodies in duodenal fluid.

METHODS: Data were collected from 93 patients submitted to upper digestive endoscopy due to dyspeptic symptoms. The patients were either negative (group A) or positive (group B) to *H pylori* by means of both histological detection and urease tests. Before endoscopy, peripheral blood was collected for the investigation of anti-*H pylori* IgG and IgA antibodies. To perform the urease test, biopsies were obtained from the gastric antrum. For the histological evaluation, biopsies were collected from the gastric antrum (greater and lesser curvatures) and the gastric body. Following this, duodenal fluid was collected from the first and second portions of the duodenum. For the serological assaying of anti–*H pylori* IgG and IgA, and anti-*H pylori* IgA in duodenal fluids, the ELISA method was utilized.

RESULTS: The concentration of serum IgG showed sensitivity of 64.0%, specificity of 83.7%, positive predictive value of 82.0%, negative predictive value of 66.6% and accuracy of 73.1% for the diagnosis of *H pylori* infection. For the same purpose, serum IgA showed sensitivity of 72.0%, specificity of 65.9%, positive predictive value of 72.0%, negative predictive value of 67.4% and accuracy of 69.8%. If the serological tests were considered together, i.e. when both were positive or negative, the accuracy was 80.0%, sensitivity was 86.6%, specificity was 74.2%, positive predictive value was 74.2% and negative predictive value was 86.6%. When values obtained in the test for detecting IgA in the duodenal fluid were analyzed, no significant difference (P = 0.43) was observed between the values obtained from patients with or without *H pylori* infection.

CONCLUSION: The results of serum IgG and IgA tests for *H pylori* detection when used simultaneously, are more efficient in accuracy, sensitivity and negative predictive value, than those when used alone. The concentration of IgA antibodies in duodenal fluid is not useful in identifying patients with or without *H pylori*.

Locatelli A, Catapani WR, Junior GCR, Silva CBP, Waisberg J. Detection of anti-*Helicobacter pylori* antibodies in serum and duodenal fluid in peptic gastroduodenal disease. *World J Gastroenterol* 2004; 10(20): 2997-3000
http://www.wjgnet.com/1007-9327/10/2997.asp

INTRODUCTION

Knowledge about peptic ulcers has changed profoundly since Warren and Marshall[1] managed to cultivate *Helicobacter pylori* (*H pylori*) from gastric biopsies. This raised great interest in the study of how it colonized the upper gastrointestinal tract and more specifically, in its direct relationship with peptic disease[1-3].

In epidemiological studies, serum tests could offer high sensitivity and specificity[4]. Serum assaying of anti-*H pylori* IgG and IgA antibodies could be used for the determination of prevalence of acute and chronic infections[5-7]. In general, the serum levels of anti-*H pylori* IgG antibodies were increased in the presence of infection and could be used as a marker. On the other hand, anti-*H pylori* IgA antibodies were less appropriate for this purpose[8,9], nevertheless serological findings of anti-*H pylori* IgA antibodies in symptomatic patients might have significant clinical values for the diagnosis of infection, especially if the patient was seronegative for IgG[10].

In treatment of peptic diseases among *H pylori*-infected patients, local immune responses of the host, as well as the inherent factors of the microorganism, such as the presence of cytotoxin-associated gene A (cagA) were important[11,12]. Few studies have analyzed the effect of local immune response on diseases induced by *H pylori*[13,14].

H pylori infection could result in a major increase in cells secreting IgA in human gastroduodenal mucosa[15,16] and usually induce high serum levels of anti-*H pylori* antibodies. Moreover, significant concentrations of antibodies were demonstrated in saliva, gastric fluid and feces[17]. Despite the antibody response, this microorganism has been rarely eliminated from the stomach and when it was not treated adequately the infection generally persisted in the rest of an individual's life[18].

However, the use of serological tests based on the determination of serum levels of anti-*H pylori* IgG and IgA antibodies to clinically diagnose *H pylori* infection has not yet been fully clarified[5,7,10,16].

The objective of the present study was to analyze the use of serum levels of anti-*H pylori* IgG and IgA antibodies, and the levels of anti-*H pylori* IgA antibodies in duodenal fluid for the diagnosis of *H pylori* infection.

MATERIALS AND METHODS

Patients

Examinations were done on 93 patients with peptic symptoms from November 2000 to September 2001.

The inclusion criteria were: adult patients with a normal endoscopic examination or showing a peptic disease[19,20]. The followings were considered to be exclusion criteria: presence of malignant disease of the upper digestive tract, previous gastrectomy, use of hormonal or non-hormonal anti-inflammatory medications, proton pump inhibitors, histamine H_2 receptor

blockers or antibiotics or antacids over the past twelve months, previous treatment for the elimination of *H pylori* over the past twelve months, presence of intestinal inflammatory disease or immunodeficiency of any nature, and pediatric age.

The patients (n = 93) were divided into two groups. Group A (n = 43) that had urease test and was histology negative for *H pylori*, and group B (n = 50) that had urease test and was histology positive for *H pylori*. These criteria (patients simultaneously positive or negative in histological and urease tests) were used for diagnosis of *H pylori*. In group A, 22 (51.2%) patients were males and 21 (48.8%) were females, the mean age was 34.77±12.89 years (range: 17 to 71 years). In group B, 25 (50.0%) patients were males and 25 (50.0%) were females, the mean age was 41.6±14.6 years (range: 21 to 71 years).

Methods

Endoscopic examination, biopsies of gastric mucosa and sampling of duodenal fluid To perform urease test, two biopsies were obtained from the gastric antrum (greater and lesser curvatures) at least 2 cm from the pylorus. For the histological analysis, four biopsies were collected, two of which from the gastric antrum (greater and lesser curvatures), and two of which from the gastric body on the anterior and posterior walls. Following this, a minimum of 2 mL of secreted duodenal fluid was collected from the first and second portions of the duodenum.

Processing of biopsy material The material collected from the gastric biopsies was placed in flasks containing 40 g/L buffered formaldehyde for fixation and then sent for histological examination. Slides were stained with hematoxylin and eosin and the modified Giemsa method (1% Lugol's solution and 25 g/L gentian violet solution). The four biopsy fragments removed from the gastric antrum were placed in flasks containing urease medium (Probac, Sao Paulo, Brazil), with 2 mL of solution in each. The flasks were maintained at 37 ℃ and read by the main author 6 and 12 h later.

Determination of serum levels of anti-*H pylori* IgG and IgA and anti-*H pylori* IgA in duodenal fluid Before endoscopy, peripheral blood was collected to determine the serum levels of anti-*H pylori* IgG and IgA. Two-milliliter aliquots from duodenal fluid were diluted with distilled water until a final volume of 10 mL was reached. This solution was centrifuged at 1 500 r/min for 10 min and the supernatant was stored at -20 ℃.

ELISA method (Accubind®, Monobind, Inc., Costa Mesa, California, USA) was used to determine the levels of serum anti-*H pylori* IgG and IgA and anti-*H pylori* IgA in the duodenal fluid. The serum samples were diluted to 1/100 while the samples of duodenal fluids were diluted to 1/1 000. Other steps were performed according to the instructions of manufacturer.

For both the anti-*H pylori* IgG and IgA serum antibodies, optical density values greater than 20 U/mL were considered as positive results. For the anti-*H pylori* IgA antibodies in the duodenal fluid, no reference optical density value for a positive or negative test was available. Thus, a receiver operating characteristic (ROC) curve was constructed, taking the results obtained in ELISA test *versus* the gold standard.

Statistical analysis

Statistical analysis was performed by the Mann-Whitney, Fisher's exact and Kruskal-Wallis tests. The ROC curve was constructed in order to assess the sensitivity and specificity of anti-*H pylori* IgA assays in the duodenal fluid at different cutoff levels. An alpha value less than or equal to 5% was adopted for rejection of the null hypothesis. The results were expressed as mean±SD to illustrate the distribution of variables.

RESULTS

Findings of endoscopic and histological examination

The findings of endoscopic and histological examination were gastritis alone in 32 (34.4%) patients, gastritis in association with duodenal peptic ulcer and/or moderate to severe enanthematic or erosive bulboduodenitis in 18 (19.4%), gastritis in association with hiatal hernia and/or esophagitis in 16 (17.2%), gastritis and slight bulboduodenitis in 11 (11.8%), gastritis in association with gastric ulcer and duodenal ulcer simultaneously in 4 (4.3%) and gastritis and gastric polyps in one (1.0%). Eleven (11.8%) patients presented normal endoscopic and histological examination of the gastric mucosa.

Value of serum tests for diagnosis of H pylori infection

The sensitivity, specificity, positive and negative predictive values and accuracy of the serum tests for anti-*H pylori* IgG and IgA were analyzed in relation to the gold standard. The accuracy of serum IgG levels was 73.1%, the sensitivity was 64.0%, specificity was 83.7%, positive predictive value was 82.0% and negative predictive value was 66.6%. With regard to serum IgA levels, the accuracy was 69.8%, sensitivity was 72.0%, specificity was 65.9%, positive predictive value was 72.0% and negative predictive value was 67.4%. If the serological tests were considered together, i.e. when both were positive or negative in comparison with the gold standard (Table 1), the accuracy was 80.0%, sensitivity was 86.6%, specificity was 74.2%, positive predictive value was 74.2% and negative predictive value was 86.6%.

Table 1 Frequency of patients positive or negative for serum anti-*H pylori* IgG, positive or negative for serum anti-*H pylori* IgA and negative or positive simultaneously for serum anti-*H pylori* IgG and IgA in comparison to the gold standard

	IgG (+) *n*	IgG (-) *n*	IgA (+) *n*	IgA (-) *n*	IgG and IgA (+)[f] *n*	IgG and IgA (-)[f] *n*
Histology and urease (+)	32[b]	18[b]	36[d]	14[d]	26[f]	4[f]
Histology and urease (-)	7	36	14	29	9	26

n: Number of patients; [b]P<0.0001, [d]P = 0.0002, [f]P<0.0001 *vs* histology and urease (-) group.

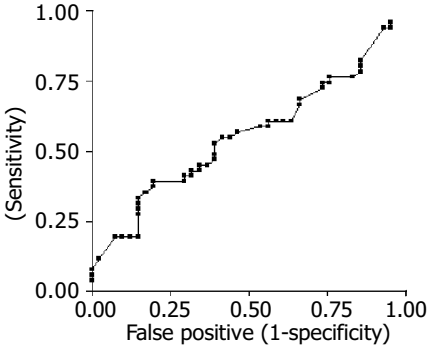

Figure 1 Sensitivity and specificity of anti-*H pylori* IgA in duodenal fluid for diagnosis of infection determined by ROC curve.

Compared with the frequencies of individuals with positive or negative results in the serological test for identifying anti-*H pylori* IgG and IgA antibodies, the serological tests were efficient in the diagnosis of the presence or absence of *H pylori* infection. The difference in the frequencies of positive and negative test results between the groups was highly significant (Table 1). With regard to the ELISA serological tests for anti-*H pylori* IgG and IgA considered together (Table 1), the difference between the frequencies of patients in each group was highly

significant ($P<0.0001$).

In comparison between the values obtained in the ELISA tests in patients positive or negative for *H pylori*, the difference was significant in relation to anti-*H pylori* serological IgA and IgG.

Value of anti-H pylori IgA antibodies in duodenal fluid for diagnosis of H pylori infection

Sensitivity, specificity and false positive ratio for IgA in the duodenal fluid were defined by the ROC curve at different cutoff levels, as compared to the gold standard (Figure 1).

When values obtained in the ELISA test for determination of anti-*H pylori* IgA antibodies in the duodenal fluids were analyzed, no significant difference ($P = 0.43$) was observed between the patients with or without *H pylori* infection.

DISCUSSION

Martin-de-Argila *et al*.[21] concluded that ELISA serum test for the detection of anti-*H pylori* IgA and IgG antibodies was sensitive and specific and should preferentially be utilized in population-based studies. Peura[22] found that the sensitivity and specificity of ELISA test ranged from 75% to 95%. Perez-Perez *et al*.[23], examined the detection of anti-*H pylori* IgA and IgG in serological samples from patients with positive cultures for *H pylori* and a histological diagnosis of gastritis, and verified that tests using both antibodies simultaneously had a sensitivity of 93.1% and a specificity of 94.4%. In our study, if the serological tests were considered together, the sensitivity was 86.6% and specificity was 74.2%. A possible explanation for this difference could be the different methods utilized as the gold standard. Indeed, the *H pylori* culture method performed by those authors could possibly have revealed smaller quantities of bacteria in the gastric mucosa. With few bacteria in the mucosa, the urease test and histology could give a false negative result.

Our results also pointed to an increased sensitivity when both anti-*H pylori* IgG and IgA were considered together, in relation to IgG or IgA alone, but the improvement in specificity occurred only in relation to IgA, and it was reduced in comparison with IgG alone. The association between IgG and IgA resulted in a marked improvement of the negative predictive value in comparison with the two assays alone, but did not offer advantages in relation to the positive predictive value.

Certainly, other variables than these might be responsible for the differences observed between the various studies, such as the severity and staging of peptic disease and the different strains of microorganism might also play a role. Strains with cytotoxin-associated gene A (cagA) exhibited more intense immunological responses[11,16,23,24].

Watanabe *et al*.[14], found that patients who presented high titers of anti-*H pylori* IgA in the gastric secretion presented a lower degree of neutrophilic infiltration on histological examination. These results suggest that anti-*H pylori* IgA antibodies have a protective function, even though this is insufficient to completely eliminate the organism.

In the present study, when the titers of anti-*H pylori* IgA in the duodenal fluid in patients with and without *H pylori* were analyzed, no significant difference was found in these values. The ROC curve, constructed using the values obtained from the determination of duodenal anti-*H pylori* IgA, compared to the gold standard, showed that the levels of this immunoglobulin in the duodenal fluid presented high sensitivity and low specificity, or even the opposite, depending on the cutoff level considered. Thus, if a cutoff level of 1.0 is adopted, it can be predicted that an individual will be negative for *H pylori* if the anti-*H pylori* IgA values in the duodenal fluid are below this reference level (sensitivity 82.4%). However, at this cutoff level, individuals with anti-*H pylori* IgA above this value will be at increased risk of being considered as false positive, i.e. with a specificity of 14.5%, the number of false positives will reach 85.4%.

Crabtree *et al*.[24], using ELISA method, evaluated the local immunological response of anti-*H pylori* IgA and IgG antibodies in patients with duodenitis. These authors observed that the local immunological response of anti-*H pylori* IgA antibodies was greater than that of anti-*H pylori* IgG antibodies. They also noted that there was a direct relationship between the titers of anti-*H pylori* antibodies and the severity of the inflammatory process found, or in other words, the more severe the duodenitis, the higher the levels of local antibodies and especially those of IgA. However, their investigation into these antibodies was done by evaluating the supernatant material from *in vitro* culture of biopsies taken from the first and second portions of the duodenum. In our study, duodenal fluid was collected from these same locations for investigating the anti-*H pylori* IgA antibodies. Often, studies performed *in vitro* could not be directly correlated with *in vivo* results because of the absence of other conditions frequently encountered *in vivo*, such as the presence of proteolytic enzymes in the intestine that could change the concentration of secreted IgA, although this immunoglobulin is very resistant to the action of these enzymes[14]. Our results expressed the concentration of IgA in the duodenal fluid, but the total amount of IgA in this fluid was unknown, because the quantity of fluid in the first and second portions of the duodenum varied between patients. Crabtree *et al*, studied anti-*H pylori* antibodies in the duodenal mucosa, and observed notable differences in antibody concentrations between the first and second portions of the duodenum. These authors observed that, in the second portion of the duodenum, the concentrations of anti-*H pylori* IgA and IgG antibodies were lower than those in the first portion. This could have had a decisive influence on our results, since the duodenal fluid presented a greater volume in the second portion of the duodenum and it was often difficult to obtain samples of duodenal fluid from the first portion.

In conclusion, the results from the present investigation demonstrate that anti-*H pylori* IgA and IgG serum immunoglobulins are useful in distinguishing between patients with and without *H pylori* infection, whereas the concentration of anti-*H pylori* IgA in the duodenal fluid is not useful in identification of infected or uninfected patients.

REFERENCES

1 **Warren JR**, Marshall BJ. Unidentified curved bacilli on gastric epithelium in active chronic gastritis. *Lancet* 1983; **1**: 1273-1275

2 **Olbe L**, Fandriks L, Hamlet A, Svennerholm AM, Thoreson AC. Mechanisms involved in *Helicobacter pylori* induced duodenal ulcer disease: an overview. *World J Gastroenterol* 2000; **6**: 619-623

3 **Svennerholm AM**, Quiding-Järbrink M. Priming and expression of immune responses in the gastric mucosa. *Microbes Infect* 2003; **5**: 731-739

4 **Jensen AK**, Andersen LP, Wachmann CH. Evaluation of eight commercial kits for *Helicobacter pylori* IgG antibody detection. *APMIS* 1993; **101**: 795-801

5 **Andersen LP**, Rosenstock SJ, Bonnevie O, Jorgensen T. Seroprevalence of immunoglobulin G, M and A antibodies to *Helicobacter pylori* in an unselected Danish population. *Am J Epidemiol* 1996; **143**: 1157-1164

6 **Morris A**, Nicholson G. Ingestion of *Campylobacter pyloridis* causes gastritis and raised fasting gastric pH. *Am J Gastroenterol* 1987; **82**: 192-199

7 **Sobala GM**, Crabtree JE, Dixon MF, Schorah CJ, Taylor JD, Rathbone BJ, Heatley RV, Axon AT. Acute *Helicobacter pylori* infection: clinical features, local and systemic immune response, gastric mucosal histology, and gastric juice ascorbic acid concentrations. *Gut* 1991; **32**: 1415-1418

8 **Andersen LP**, Kiilerick S, Pedersen G, Thoreson AC, Jorgensen F, Rath J, Larsen NE, Borup O, Krogfelt K, Scheibel J, Rune S. An analysis of seven different methods to diagnose *Helicobacter pylori* infections. *Scand J Gastroenterol* 1998; **33**: 24-30
9 **Kosunen TU**, Höök J, Rautelin HI, Myllylä G. Age-dependent increase of *Campylobacter pylori* antibodies in blood donors. *Scand J Gastroenterol* 1989; **24**: 110-114
10 **Jaskowski TD**, Martins TB, Hill HR, Litwin CM. Immunoglobulin A antibodies to *Helicobacter pylori*. *J Clin Microbiol* 1997; **35**: 2999-3000
11 **Rathbone BJ**, Wyatt JI, Worsley BW, Shires SE, Trejdosiewicz LK, Heatley RV, Losowsky MS. Systemic and local antibody responses to gastric Campylobacter pyloridis in non-ulcer dyspepsia. *Gut* 1986; **27**: 642-647
12 **Atalay C**, Atalay G, Altinok M. Serum Helicobacter pylori IgG and IgA levels in patients with gastric cancer. *Neoplasma* 2003; **50**: 185-190
13 **Doweck J**, Quintana C, Barrios A, Monastra L, Lopetegui G, Zerbo O, Schenone L, Giordano A, Valero J, Kogan Z, Bartellini MA, Corti R. Evaluation of sensitivity, specificity and predictive value of six qualitative serological methods for the detection of *Helicobacter pylori* antibodies. *Acta Gastroenterol Latinoam* 1997; **27**: 259-261
14 **Watanabe T**, Goto H, Arisawa T, Hase S, Niwa Y, Hayakawa T, Asai J. Relationship between local immune response to *Helicobacter pylori* and the diversity of disease: investigation of *H pylori*-specific IgA in gastric juice. *J Gastroenterol Hepatol* 1997; **12**: 660-665
15 **Mattsson A**, Quiding-Järbrink M, Lönroth H, Hamlet A, Ahlstedt I, Svennerholm A. Antibody-secreting cells in the stomachs of symptomatic and asymptomatic *Helicobacter pylori*-infected subjects. *Infect Immun* 1998; **66**: 2705-2712
16 **Xia HHX**, Talley NJ, Blum AL, O'Morain CA, Stolte M, Bolling-Sternevald E, Mitchell HM. Clinical and pathological implications of IgG antibody responses to Helicobacter pylori and its virulence factors in non-ulcer dyspepsia. *Aliment Pharmacol Ther* 2003; **17**: 935-943
17 **Wyatt JI**, Rathbone BJ. Immune response of the gastric mucosa to *Campylobacter pylori*. *Scand J Gastroenterol Suppl* 1988; **142**: 44-49
18 **Luzza F**, Imeneo M, Maletta M, Monteleone G, Doldo P, Biancone L, Pallone F. Isotypic analysis of specific antibody response in serum, saliva, gastric and rectal homogenates of *Helicobacter pylori*-infected patients. *FEMS Immunol Med Microbiol* 1995; **10**: 285-288
19 **Dixon MF**, Genta RM, Yardley JH, Correa P. Classification and grading of gastritis. The updated Sydney System. International Workshop on the Histopathology of Gastritis, Houston 1994. *Am J Surg Pathol* 1996; **20**: 1161-1181
20 **Garza-González E**, Bosques-Padilla FJ, Tijerina-Menchaca R, Flores-Gutiérrez JP, Maldonado-Garza HJ, Pérez-Pérez GI. Comparison of endoscopy-based and serum-based methods for the diagnosis of *Helicobacter pylori*. *Can J Gastroenterol* 2003; **17**: 101-106
21 **Martín-de-Argila C**, Boixeda D, Cantón R, Valdezate S, Mir N, De Rafael L, Gisbert JP, Baquero F. Usefulness of the combined IgG and IgA antibody determinations for serodiagnosis of *Helicobacter pylori* infection. *Eur J Gastroenterol Hepatol* 1997; **9**: 1191-1196
22 **Peura DA**. *Helicobacter pylori*: a diagnostic dilemma and a dilemma of diagnosis. *Gastroenterology* 1995; **109**: 313-315
23 **Perez-Perez GI**, Dworkin BM, Chodos JE, Blaser MJ. *Campylobacter pylori* antibodies in humans. *Ann Intern Med* 1988; **109**: 11-17
24 **Crabtree JE**, Shallcross TM, Wyatt JI, Taylor JD, Heatley RV, Rathbone BJ, Losowsky MS. Mucosal humoral immune response to *Helicobacter pylori* in patients with duodenitis. *Dig Dis Sci* 1991; **36**: 1266-1273

Edited by Wang XL **Proofread by** Chen WW and Xu FM

PO Box 2345, Beijing 100023, China
Fax: +86-10-85381893
E-mail: wjg@wjgnet.com www.wjgnet.com

World J Gastroenterol 2004;10(20):3001-3005
World Journal of Gastroenterology
 ISSN 1007-9327

• BASIC RESEARCH •

Relationship between focal adhesion kinase and hepatic stellate cell proliferation during rat hepatic fibrogenesis

Hui-Qing Jiang, Xiao-Lan Zhang, Li Liu, Chang-Chun Yang

Hui-Qing Jiang, Xiao-Lan Zhang, Li Liu, Department of Gastroenterology, The Second Hospital of Hebei Medical University, Shijiazhuang 050000, Hebei Province, China
Chang-Chun Yang, Department of Medicine, the Armed Police Hospital of Hebei Province, Shijiazhuang 050081, Hebei Province, China
Supported by the Natural Science Foundation of Hebei Province, No. 301361
Correspondence to: Professor Hui-Qing Jiang, Department of Gastroenterology, The Second Hospital of Hebei Medical University, Shijiazhuang 050000, Hebei Province, China. huiqingj@heinfo.net
Telephone: +86-311-7222951
Received: 2003-08-23 **Accepted:** 2003-09-05

Abstract

AIM: To investigate the dynamic expression of focal adhesion kinase (FAK) protein and FAK mRNA in fibrotic rat liver tissue, and the relationship between FAK and hepatic stellate cell (HSC) proliferation.

METHODS: Rat hepatic fibrosis was induced by bile duct ligation (BDL). Histopathological changes were evaluated by hematoxylin and eosin staining, and by Masson's trichrome method. FAK mRNA in the rat livers was determined by reverse transcription-polymerase chain reaction (RT-PCR), and the distributions of FAK were assessed immunohistochemistrically. The number of activated HSCs was quantified after alpha smooth muscle actin (α-SMA) staining.

RESULTS: With the development of hepatic fibrosis, the positively stained cells of α-SMA increased obviously, which were mainly resided in the portal ducts, fiber septa and perisinuses accompanied with proliferating bile ducts. The positively stained areas of the rat livers in model groups 1 to 4 wk after ligation of common bile duct (12.88±2.63%, 22.65±2.16%, 27.45±1.86%, 35.25±2.34%, respectively) were significantly larger than those in the control group (5.88±1.46%) (P<0.01). The positive staining for FAK significantly increased, which was mainly situated in portal ducts, fiber septa and around the bile ducts, vascular endothelial cells and perisinusoidal cells. The expression of FAK was positively correlated with α-SMA expression (r = 0.963, P<0.05). FAK mRNA expression was obviously up-regulated in the model groups compared to the control group.

CONCLUSION: These data suggest that expressions of FAK protein and mRNA are greatly increased in fibrotic rat livers, which may play an important role in HSC proliferation and hepatic fibrogenesis.

Jiang HQ, Zhang XL, Liu L, Yang CC. Relationship between focal adhesion kinase and hepatic stellate cell proliferation during rat hepatic fibrogenesis. *World J Gastroenterol* 2004; 10(20): 3001-3005
http://www.wjgnet.com/1007-9327/10/3001.asp

INTRODUCTION

Focal adhesion kinase (FAK) is a cytoplasmic protein tyrosine kinase that has been implicated to play an important role in integrin-mediated signal transduction pathways. Furthermore, some lines of evidence indicate FAK as a point of convergence of other signaling pathways. The *in vitro* expression of FAK and its level of phosphorylation appear to be related to several physiological phenomena, including cell adhesion, spreading, migration, cytoskeleton organization, proliferation and apoptosis[1-3]. It has been accepted that hepatic stellate cells (HSCs) represent the pivot of fibrotic process[4-9]. In healthy livers, HSCs are perisinusoidal mesenchymal elements with characteristic intracytoplasmatic lipid droplets rich in retinyl esters. In contrast, in chronic liver injury, HSCs undergo a process of activation from the resting fat-storing phenotype towards a myofibroblast-like phenotype[10].

Current evidence indicates that activated HSCs are responsible for the majority of extracellular matrix protein depositions in liver fibrosis[11]. Although a recent study has focused on the roles of FAK in cultured cells[12], little is known about its regulation *in vivo* or its relevance to HSC proliferation. In addition, it is not known whether FAK is up-regulated in response to liver injury by bile duct ligation (BDL). To assess whether FAK was associated with fibrogenesis or the survival of HSCs in biliary fibrosis, we investigated the expression of FAK in liver tissues from rats with BDL-induced biliary fibrosis using immunohistochemistry and reverse transcription-polymerase chain reaction (RT-PCR), we also used immunohistochemistry method to examine the expression of α-smooth muscle actin (α-SMA) as a marker of activated HSCs.

MATERIALS AND METHODS

Reagents

Monoclonal antibodies against FAK and α-SMA were products of Santa Cruz Biotech Inc. Streptavidin peroxidase (SP) immunohistochemical kit was purchased from Zhongshan Biological Technology Co. (Beijing). Trizol reagent was obtained from Life Technologies, Inc (USA). One tube RT-PCR kit was from Promega Co (USA). Primers for rat FAK and β-actin were designed by ourselves in accordance with gene sequence in GeneBank, synthesized and purified by Bao Biological Engineering Co. (Dalian). All other reagents were analytically pure.

Animal model and experimental protocol

A total of 80 adult male Sprague-Dawley rats weighing 350-400 g were purchased from the Experimental Animal Center of Hebei Medical University (Clearing Grade, Certificate No. 04057). All rats were housed in plastic cages and allowed free access to food and water. For the purpose of this study, rats were randomly divided into eight groups (ten rats in each group) as follows: Control group (sham-operated group), with BDL for 2 h, 6 h, 2 d, 1 wk, 2 wk, 3 wk and 4 wk, respectively. The rats were subjected to laparotomy with their common bile ducts completely ligated while they were intraperitoneally injected with ketamine hydrochloride at a dose of 100 mg/kg[13]. Under deep anaesthesia, the peritoneal cavity was opened and the common bile duct

was double-ligated with 3-0 silk and cut between the ligatures. Control animals underwent a sham operation that consisted of exposure but not ligation of the common bile duct. At various intervals postoperation, animals were anaesthetised and the livers were harvested. Liver tissue specimens were routinely fixed in 40 g/L phosphate-buffered formaldehyde and embedded in paraffin. Some liver tissue specimens were used for light microscopy and immunohistochemistry using anti α-SMA and FAK, while others were snap-frozen in liquid nitrogen and stored at -80 ℃ for RNA analysis. In addition, control livers were harvested 4 wk after sham operation.

Histopathology

For light microscopic examination, liver specimens were routinely fixed overnight in 40 g/L phosphate-buffered formaldehyde, embedded in paraffin. Tissue sections (5-μm thick) were stained with haematoxylin and eosin (HE) for morphological evaluation and Masson's trichrome for assessment of fibrosis.

Immunohistochemical detection of α-SMA and FAK

All immunohistochemical studies using the streptavidin-peroxidase technique were performed on 5-μm thick sections of paraformaldehyde-fixed and paraffin-embedded liver block tissue mounted on APES-coated slides. Slides were deparaffinised in xylene, and rehydrated in graded ethanol. Endogenous peroxidase activity was quenched with a 30 mL/L hydrogen peroxide solution in methanol at room temperature for 30 min, followed by rinsing in pH 6.0 phosphate-buffered saline (PBS). After antigen retrieval in a water bath set in a 10 mmol/L citrate buffer (pH 6.0) at 94 ℃ for 8 min, 10 min, respectively, the slides were immediately cooled for 20 min at room temperature. Non-specific binding sites were blocked by incubation with washing buffer containing 100 mL/L normal goat serum at 37 ℃ for 30 min. Sectionsrnight at 4 ℃ with a mouse monoclonal antibody directed against α-SMA or FAK at a dilution of 1:100. The secondary antibody bindings were localized using a biotin conjugated rabbit anti-mouse IgG (1:100 dilution), followed by incubation with streptavidin-peroxidase complex (1:200 dilution). Peroxidase conjugates were subsequently visualised using diaminobenzidine (DAB) solution in hydrogen peroxide as a chromogen yielding a brown reaction product. Sections were then counterstained in Mayer's hematoxylin and mounted over cover slips. All incubations were performed in a moist chamber. Furthermore, between each incubation step, the slides were washed three times with PBS for 5 min. To ensure antibody specificity, negative control samples were processed in parallel under the same conditions but with omission of the first antibody, which was replaced by an equal volume of PBS. The α-SMA-positive parenchyma and the FAK-positive parenchyma were measured by a video-image analysis system and expressed as a percentage of area occupied by the signal.

RNA extraction and RT -PCR assay

Expression of FAK mRNA was evaluated with RT-PCR. Total RNA from liver specimens (100 mg) was isolated using a monophasic solution of phenol and guanidine thiocyanate (Trizol), precipitated in ethanol and resuspended in sterile RNAase-free water for storage at -80 ℃ until use, as recommended by the suppliers. Total RNA was quantified spectrometrically at 260 nm, and the quality of isolated RNA was analysed on agarose gels under standard conditions. One-step RT-PCR was performed according to the manufacturer's instructions. Two micrograms of RNA was added to each reaction and RT-PCR was routinely performed using 5 units of AMV reverse transcriptase, 5 units of *Tfl* DNA polymerase, 10 pmoL of each oligonucleotide primer, 10 pmoL of dNTP mix and 25 mmol/L $MgSO_4$ in a final reaction volume of 50 μL. Primer sequences were as follows: FAK, forward 5'-ACT TGG ACG CTG TAT TGG AG-3' and reverse 5'-CTG TTG CCT GCT TTC TGG AT-3', fragment length 833 bp; β-actin, forward 5'- AGC TGA GAG GGA AAT CGT GCG -3' and reverse 5'- GTG CCA CCA GAC AGC ACT GTG -3', fragment length 300 bp. RT-PCR was performed in the following steps: reverse transcription was performed at 41 ℃ for 45 min, pre-denaturation at 94 ℃ for 2 min; then amplification was performed in a thermal controller for 35 cycles (denaturation at 94 ℃ for 40 s, annealing at 52 ℃ for 1 min and extension at 72 ℃ for 1.5 min), and a final extension at 72 ℃ for 10 min after the last cycle. A 10 μL of the PCR products was analyzed on 15 g/L agarose gel containing ethidium bromide with TAE buffer at 80 V for 40 min and photographed under UV illumination. The band intensities were quantified by densitometry. FAK/β-actin quotient indicated the relative expression of FAK. Experiments were performed at least three times with similar results.

Statistical analysis

The data were expressed as mean±SD. The mean values were compared by using analysis of variance, followed by the Student-Newman-Keuls test if the former was significant. The correlation between the expressions of FAK and α-SMA was analyzed for statistical significance by the simple linear regression analysis. *P* values less than 0.05 were considered statistically significant.

RESULTS

Histology of progressive fibrotic liver injury

In accordance with previous reports[13], a marked liver fibrosis was apparently observed in the SD rats after BDL. In the present study, the results of HE and Masson's trichrome staining confirmed spotted (or scattered) perivenular degeneration of hepatocytes, an increase in the inflammatory infiltrates in the necrotic areas and bile ductular proliferation in the portal triads after 1 wk of BDL. After 2 wk of BDL, all rats showed expanded portal tracts with fibrous tissues, portal-to-portal fibrous bridging, nodular transformation and widespread proliferating bile ductules that extended into the parenchyma in places without clear-cut cirrhosis. After BDL for 3-4 wk, the animals developed severe fibrosis associated with proliferating bile ducts that formed a continuous meshwork of connective tissues with complete distortion of lobular architecture, whereas there was no notable histological abnormality or evidence of stainable collagen in any of the shamly operated control livers (Figure 1A-D).

Identification of proliferating and activated HSC

Since α-SMA was expressed in activated HSCs, immunostaining for this protein was used to detect and quantify the numbers of activated HSCs. *A* weak staining for α-SMA positive cells in the shamly operated control livers was observed in vascular smooth muscle cells and sinusoids. With the development of hepatic fibrosis, the positive stainings for α-SMA were greatly increased in the cells of portal ducts, fibrotic septa, perisinuses and around the proliferated bile ducts. The positively stained areas of the rat livers in model groups 1 to 4 wk after ligation of common bile duct (12.88±2.63%, 22.65±2.16%, 27.45±1.86%, 35.25±2.34%, respectively) were significantly larger than that in control group (5.88±1.46%) ($P<0.01$, Figure 2 A-C).

Distribution of FAK protein in common bile duct ligated rat liver

To explore the distribution of FAK, the sections of rat livers in sham operation and BDL groups were immunostained using specific monoclonal anti-FAK antibody. In the sections from sham operation group, expression of FAK was found in vascular smooth muscle cells and perisinusoidal cells. In contrast, the positive staining of BDL rat liver was obviously visible in and

around α-SMA-positive areas, which were prevailingly detected in portal ducts, fibrotic septa, perisinusoidal cells and cells around the bile ducts as well as vascular endothelial cells. The positive areas of the rat livers in model groups 1 to 4 wk after ligation of common bile duct (13.05±1.32%, 18.43±2.18%, 23.45±2.73%, 31.00±2.77%, respectively) were significantly larger than that in control group (3.98±1.27%) (P<0.01, Figure 3A-C).

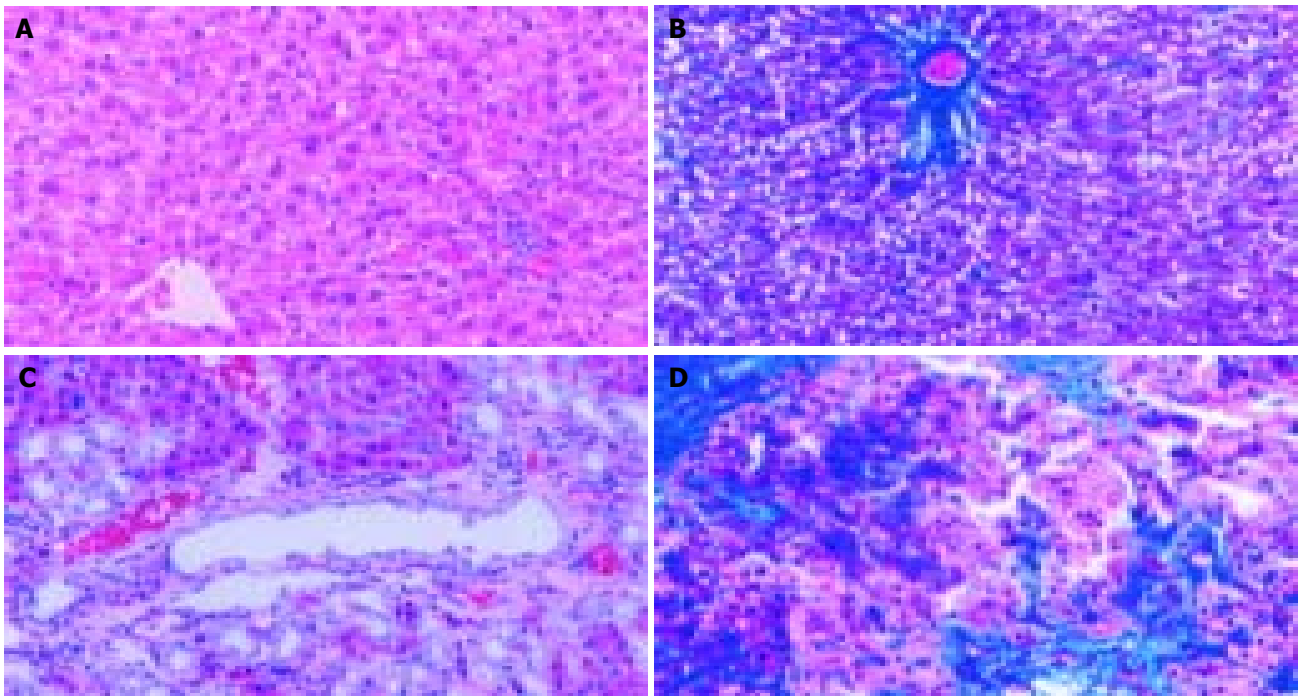

Figure 1 Histopathological changes in liver tissue (100×) A: Normal hepatic lobular architecture in sham operation group (HE); B: Few ECM deposition in sham operation group (Massson trichome); C: Extensive ductular proliferation and ECM deposition 4 wk after BDL (HE); D: Extensive connective tissue deposition 4 wk after BDL (Massson trichome).

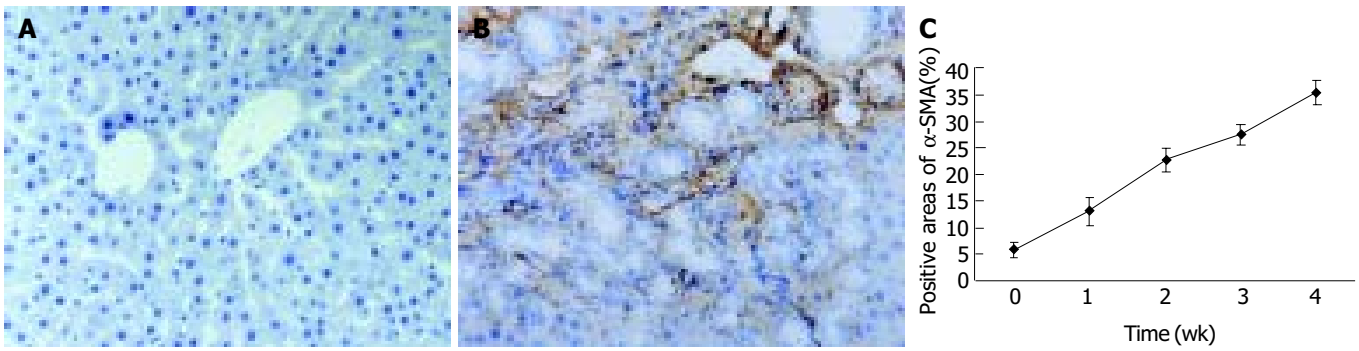

Figure 2 α-SMA protein expression in liver tissue stained by immunohistochemistry (SP 200×) A: Few α-SMA expressions in sham operation group; B: Positive cells of α-SMA resided in portal ducts, fiber septa, perisinuses and around proliferated bile ducts after 2 wk BDL; C: Positively stained areas of α-SMA expression in model groups 1 to 4 wk after common bile duct ligation.

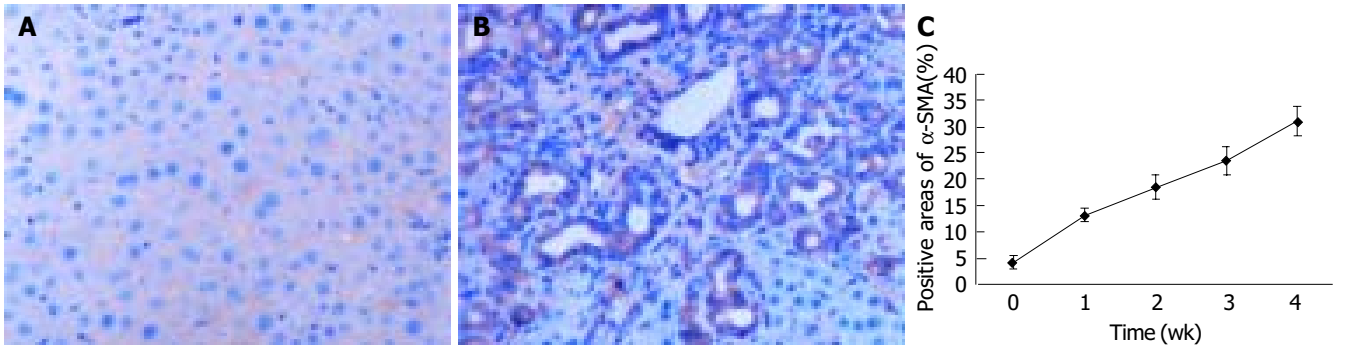

Figure 3 FAK protein expression in liver tissue stained by immunohistochemistry (SP 200×) A: FAK protein expression in sham operation group; B: FAK protein expression 2 wk after BDL; C: Time course of FAK expression in hepatic fibrogenesis stained by immunohistochemistry.

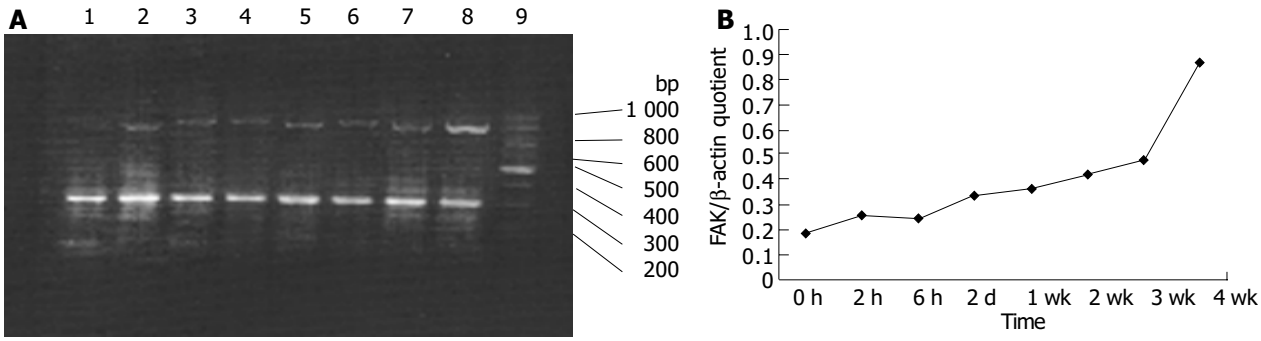

Figure 4 RT-PCR analysis of mRNA encoding FAK in hepatic fibrogenesis A: RT-PCR analysis of mRNA encoding FAK in hepatic fibrogenesis at different time points. Lane 1: sham operation group; lane 2: BDL 2 h; lane 3: BDL 6 h; lane 4: BDL 2 d; lane 5: BDL 1 wk; lane 6: BDL 2 wk; lane 7: BDL 3 wk; lane 8: BDL 4 wk; lane 9: Marker B: Band intensities were quantified by densitometry. FAK/β-actin quotient indicated the relative expression of FAK.

FAK mRNA expression in common bile duct ligated rat livers

Although it was shown that FAK protein was produced by liver tissues *in vivo*, it was not clear whether the FAK mRNA level under fibrogenic response was increased *in vivo*. Therefore, we investigated the production of FAK mRNA in the liver. RT-PCR results revealed faint bands for FAK mRNA in the sham operation group, whereas obvious and specific bands for FAK mRNA in fibrotic liver of BDL groups. Moreover, FAK mRNA expression was initially up-regulated and reached the peak level 4 wk after BDL. The levels housekeeping gene, β-actin, did not show any significant differences between normal and BDL rat liver tissues (Figure 4A, B).

Correlation between FAK and α-SMA

Immunohistochemistry experiments were performed to analyze whether FAK protein distribution was correlated with α-SMA between sham operation group and BDL group. The results indicated that FAK was positively correlated with α-SMA (r =0.963, P<0.05).

DISCUSSION

HSCs, a principal cellular source of extracellular matrix during chronic liver injury, undergo a transition into α-SMA-expressing myofibroblast-like cells in response to injury. Furthermore, HSC activation is associated with stellate cell proliferation, increased contractility, enhanced matrix production, and expression of a number of fibrogenic and proliferative cytokines and their cognate receptors. Therefore, HSCs could play a pivotal role in cellular and molecular events that lead to fibrosis[14-17]. As above, expressing α-SMA is one of the characteristics of activated HSCs. Cassiman *et al*.[18] and α-SMA-positive cells mainly reside in the portal triads and fibrotic septa accompanied with proliferating bile ducts. Namely,α-SMA-positive cells was coincident with collagen deposition. The results of the present study verified that the positive cells of α-SMA, which mainly reside in portal ducts, fibrotic septa, perisinuses and around the proliferated bile ducts, were greatly increased with the development of hepatic fibrosis compared with sham operation group. Thus, our results are consistent with the others mentioned above.

Various factors and signal transduction pathways have been shown to regulate the activation and proliferation of HSCs[8,9,19-21]. However, the mechanism by which *in vivo* factors impact HSC activation is not clear as yet. To better understand the mechanism by which FAK is generated in liver tissues might influence HSC activation, proliferation, and hepatic fibrogenesis, we performed the current research.

FAK, a 125 kD molecule, is a cytoplasmic nonreceptor tyrosine kinase that has been shown to play a key role in the regulation of cell adhesion, spreading, migration, cytoskeleton organization, proliferation and apoptosis. Furthermore, some lines of evidence has indicated FAK is a point of convergence of many signaling pathways[22]. The co-localization of FAK with integrins in focal adhesion plaque (FAP) is a trigger for cell adhesion-dependent activation of FAK signals[22]. Subsequently, its autophosphorylation at Tyr397 in the N-terminal domain is prerequisite, which may initiate a number of signaling pathways. Among them, RAS-dependent mitogen-activated protein kinase (MAPK) pathway is the clearest. It has been found that the RAS-RAF-MEK (ERK kinase)-ERK (extracellular signal-regulated kinase) pathway is involved in many cellular behaviors[22,23], such as proliferation, apoptosis. FAK knockout mice showed extensive mesodermal defects and embryonic death[24]. Moreover, the monoclonal antibody specific for FAK microinjected into fibroblasts could inhibit FAK activity and give rise to apoptosis of fibroblasts[25]. The results presented herein demonstrated that FAK protein was obviously expressed in portal ducts, fibrotic septa, perisinusoidal cells in BDL rat livers, which was in accordance was the distribution α-SMA-positive loci. In addition, FAK mRNA expression was also elevated with the progression of hepatic fibrosis. Importantly, FAK protein distribution was positively correlated with α-SMA. So, we suggested that activation of FAK in BDL rat liver tissues might activate downstream signal molecules, which could modulate gene expression of HSCs and give rise to hepatic fibrosis.

To date, the mechanism of FAK elevation during hepatic fibrogenesis remains unknown. But increasing *in vitro* evidence supports that HSCs are a major cell source of FAK. First, extracellular matrix components, including collagen and fibronectin could activate FAK in HSCs via integrin signal pathway[26-28]. Second, cytokines such as platelet derived growth factor (PDGF), endothelin (ET), insulin-like growth factor-1 (IGF-1) and tumor necrosis factor (TNF), could increase the production of FAK[29]. Third, reactive oxygen species (ROS) like H_2O_2 could also elevate the expression of FAK[30,31]. In contrast, antioxidants such as Salvia Miltiorrhiza, might have opposite effects on FAK expression in HSCs[32,33].

In conclusion, FAK-mediated activation of HSCs can result in hepatic fibrogenesis. Inhibition of FAK activity by various methods would be expected to attenuate liver fibrosis and, therefore, deserve further study.

REFERENCES

1 **Taylor JM**, Mack CP, Nolan K, Regan CP, Owens GK, Parsons JT. Selective expression of an endogenous inhibitor of FAK regulates proliferation and migration of vascular smooth muscle cells. *Mol Cell Biol* 2001; **21**: 1565-1572

2 **Sonoda Y**, Matsumoto Y, Funakoshi M, Yamamoto D, Hanks

SK, Kasahara T. Anti-apoptotic role of focal adhesion kinase (FAK). Induction of inhibitor-of-apoptosis proteins and apoptosis suppression by the overexpression of FAK in a human leukemic cell line, HL-60. *J Biol Chem* 2000; **275**: 16309-16315

3 **Almeida EA**, Ilic D, Han Q, Hauck CR, Jin F, Kawakatsu H, Schlaepfer DD, Damsky CH. Matrix survival signaling: from fibronectin via focal adhesion kinase to c-Jun NH(2)-terminal kinase. *J Cell Biol* 2000; **149**: 741-754

4 **Jiang HQ,** Zhang XL. Progress in the study of pathogenesis in hepatic fibrosis. *Shijie Huaren Xiaohua Zazhi* 2000; **8**: 687-689

5 **Gressner AM.** The cell biology of liver fibrogenesis - an imbalance of proliferation, growth arrest and apoptosis of myofibroblasts. *Cell Tissue Res* 1998; **292**: 447-452

6 **Friedman SL.** Molecular mechanisms of hepatic fibrosis and principles of therapy. *J Gastroenterol* 1997; **32**: 424-430

7 **Friedman SL.** Cytokines and fibrogenesis. *Semin Liver Dis* 1999; **19**: 129-140

8 **Pinzani M**, Marra F, Carloni V. Signal transduction in hepatic stellate cells. *Liver* 1998; **18**: 2-13

9 **Huang GC**, Zhang JS. Signal transduction in activated hepatic stellate cells. *Shijie Huaren Xiaohua Zazhi* 2001; **9**: 1056-1060

10 **Iredale JR.** Hepatic stellate cell behavior during resolution of liver injury. *Semin Liver Dis* 2001; **21**: 427-436

11 **Benyon RC**, Arthur MJ. Extracellular matrix degradation and the role of hepatic stellate cells. *Semin Liver Dis* 2001; **21**: 373-384

12 **Su JM,** Gui L, Zhou YP, Zha XL. Expression of focal adhesion kinase and alpha5 and beta1 integrins in carcinomas and its clinical significance. *World J Gastroenterol* 2002, **8**: 613-618

13 **Liu H**, Song D, Lee SS. Role of heme oxygenase-carbon monoxide pathway in pathogenesis of cirrhotic cardiomyopathy in the rat. *Am J Physiol Gastrointest Liver Physiol* 2001; **280**: G68-G74

14 **Iredale JP**, Benyon RC, Pickering J, McCullen M, Northrop M, Pawley S, Hovell C, Arthur MJ. Mechanisms of spontaneous resolution of rat liver fibrosis. Hepatic stellate cell apoptosis and reduced hepatic expression of metalloproteinase inhibitors. *J Clin Invest* 1998; **102**: 538-549

15 **Issa R**, Williams E, Trim N, Kendall T, Arthur MJ, Reichen J, Benyon RC, Iredale JP. Apoptosis of hepatic stellate cells: involvement in resolution of biliary fibrosis and regulation by soluble growth factors. *Gut* 2001; **48**: 548-557

16 **Cales P.** Apoptosis and liver fibrosis: antifibrotic strategies. *Biomed Pharmacother* 1998; **52**: 259-263

17 **Greenwel P**, Dominguez-Rosales JA, Mavi G, Rivas-Estilla AM, Rojkind M. Hydrogen peroxide: a link between acetaldehyde-elicited α1 (I) collagen gene up-regulation and oxidative stress in mouse hepatic stellate cells. *Hepatology* 2000; **31**: 109-116

18 **Cassiman D**, Libbrecht L, Desmet V, Denef C, Roskams T. Hepatic stellate cell/myofibroblast subpopulations in fibrotic human and rat livers. *J Hepatol* 2002; **36**: 200-209

19 **Ramm GA**, Carr SC, Bridle KR, Li L, Britton RS, Crawford DH, Vogler CA, Bacon BR, Tracy TF. Morphology of liver repair following cholestatic liver injury: resolution of ductal hyperplasia, matrix deposition and regression of myofibroblasts. *Liver* 2000; **20**: 387-396

20 **Zhang XL**, Jiang HQ. Intracellular signal transduction pathway of integrin and hepatic stellate cell behavior. *Zhongguo Bingli Shengli Zazhi* 2003; **18**: 987-991

21 **Svegliati-Baroni G,** Ridolfi F, Di Sario A, Saccomanno S, Bendia E, Benedetti A, Greenwel P. Intracellular signaling pathways involved in acetaldehyde-induced collagen and fibronectin gene expression in human hepatic stellate cells. *Hepatology* 2001; **33**: 1130-1140

22 **Guan JL**. Role of focal adhesion kinase in integrin signaling. *Int J Biochem Cell Biol* 1997; **29**: 1085-1096

23 **Zhao JH,** Guan JL. Role of focal adhesion kinase in signaling by the extracellular matrix. *Prog Mol Subcell Biol* 2000; **25**: 37-55

24 **Schaller MD**. Biochemical signals and biological responses elicited by the focal adhesion kinase. *Biochim Biophys Acta* 2001; **1540**: 1-21

25 **Hungerford JE**, Compton MT, Matter ML, Hoffstrom BG, Otey CA. Inhibition of pp125FAK in cultured fibroblasts results in apoptosis. *J Cell Biol* 1996; **135**: 1383-1390

26 **Boudreau NJ**, Jones PL. Extracellular matrix and integrin signalling: the shape of things to come. *Biochem J* 1999; **339**(Pt 3): 481-488

27 **Zhang XL,** Jiang HQ, Liu L, Bai Y, Song M. Effects of Arg-Gly-Asp-Ser tetrapeptide on integrin signaling and apoptosis in hepatic stellate cells. *Zhonghua Ganzangbing Zazhi* 2003; **11**: 479-482

28 **Iwamoto H**, Sakai H, Tada S, Nakamuta M, Nawata H. Induction of apoptosis in rat hepatic stellate cells by disruption of integrin-mediated cell adhesion. *J Lab Clin Med* 1999; **134**: 83-89

29 **Carloni V,** Pinzani M, Giusti S, Romanelli RG, Parola M, Bellomo G, Failli P, Hamilton AD, Sebti SM, Laffi G, Gentilini P. Tyrosine phosphorylation of focal adhesion kinase by PDGF is dependent on ras in human hepatic stellate cells. *Hepatology* 2000; **31**: 131-140

30 **Jiang HQ**, Zhang XL, Liu L. Induction of apoptosis with Salvia miltiorrhiza monomer IH764-3 via downregulating focal adhesion kinase in H_2O_2-stimulated hepatic stellate cells. *Zhongguo Bingli Shengli Zazhi* 2003; **19**: 18-21

31 **Liu L**, Jiang HQ, Zhang XL. The effect and mechanism of Salvia miltiorrhiza monomer IH764-3 on proliferation and collagen of hepatic stellate cells stimulated by H_2O_2. *Zhongguo Yingyong Shengli Zazhi* 2003; **19**: 78-81

32 **Zhang XL**, Jiang HQ, Liu L, Zhao DQ. The apoptosis-inducing role of Salvia miltiorrhiza monomer IH764-3 in hepatic stellate cells. *Zhonghua Neike Zazhi* 2002; **41**: 166-167

33 **Zhao DQ,** Jiang HQ, Xiu HM, Zhang XL, Yao XX. Effects of IH764-3 on proliferation and apoptosis of HSCs. *Zhonghua Ganzangbing Zazhi* 2002; **10**: 265-274

Edited by Kumar M and Wang XL **Proofread by** Xu FM

PO Box 2345, Beijing 100023, China
Fax: +86-10-85381893
E-mail: wjg@wjgnet.com www.wjgnet.com

World J Gastroenterol 2004;10(20):3006-3010
World Journal of Gastroenterology
 ISSN 1007-9327

• BASIC RESEARCH •

Gene expression profile in liver of hB1F transgenic mice

Shui-Liang Wang, Hua Yang, You-Hua Xie, Yuan Wang, Jian-Zhong Li, Long Wang, Zhu-Gang Wang, Ji-Liang Fu

Shui-Liang Wang, Hua Yang, Jian-Zhong Li, Ji-Liang Fu, Department of Medical Genetics, Second Military Medical University, Shanghai 200433, China
Shui-Liang Wang, PLA Certer for Laboratory Medicine, Fuzhou General Hospital, Fuzhou 350025, Fujian Province, China
You-Hua Xie, Yuan Wang, State Key Laboratory for Molecular Biology, Institute of Biochemistry and Cell Biology, Shanghai Institutes for Biological Sciences, Chinese Academy of Sciences, Shanghai 200031, China
Long Wang, Zhu-Gang Wang, Ji-Liang Fu, Shanghai Nanfang Research Center for Model Organisms, Shanghai 201203, China
Supported by the National Natural Science Foundation of China, No.39830360; the National "863" High Technology Research and Development Program of China, No.2001AA221261; the Qi Ming Xing Program from Shanghai Science and Technology Committee, No. 01QA14046
Correspondence to: Professor Ji-Liang Fu, Department of Medical Genetics, Second Military Medical University, 800 Xiangyin Road, Shanghai 200433, China. jlfu@guomai.sh.cn
Telephone: +86-21-25070027 **Fax:** +86-21-25070027
Received: 2003-10-15 **Accepted:** 2003-12-08

Abstract

AIM: To analyze the tissue morphologic phenotype and liver gene expression profile of hB1F transgenic mice.

METHODS: Transgene expression was analyzed with RT-PCR and Western blotting. For one of the transgenic mouse lines, tissue expression pattern of the transgene was also examined with immunochemical methods. Pathological analysis was used to examine the tissue morphologic phenotype of established transgenic mice. The liver gene expression profile of transgenic mice was analyzed with microchip, and some of the differentially expressed genes were verified with RT-PCR.

RESULTS: The expressions of hB1F were shown in livers from 6 of 7 transgenic mouse lines. The overexpression of hB1F transgene did not cause pathological changes. Expressions of three genes were up-regulated, while down-regulation was observed for 25 genes.

CONCLUSION: The overexpression of hB1F transgene may cause changes of gene expression profiles in the liver of transgenic mice.

Wang SL, Yang H, Xie YH, Wang Y, Li JZ, Wang L, Wang ZG, Fu JL. Gene expression profile in liver of hB1F transgenic mice. *World J Gastroenterol* 2004; 10(20): 3006-3010
http://www.wjgnet.com/1007-9327/10/3006.asp

INTRODUCTION

Human hepatitis B virus enhancer II B1 binding factor (hB1F, also known as LRH-1, hFTF, CPF) belongs to the *fushi tarazu* factor 1 (FTZ-F1) nuclear receptor subfamily, which was formally designated as NR5A2[1-3]. Like other FsTZ-F1 receptors, hB1F contains a particular FTZ-F1 box which is located at the C-terminus of the DNA-binding domain (DBD) and binds to the response element as monomer[1]. The biological function of hB1F is just being unveiled. It has been reported that hB1F and/or its rodent homologs play an important role in regulating the liver-specific expression of several genes[4,5]. Recent findings pinpoint hB1F as a critical transcription regulator in bile acid biosynthesis[2,6,7], cholesterol homeostasis[8-10], sex hormone biosynthesis[11-13], and lipid metabolism[14].

To facilitate the study on the function of hB1F, we have established 7 transgenic mouse lineages carrying hB1F transgene[15]. In this study, we analyzed the expression of the transgene in livers of these transgenic mouse lines with RT-PCR and Western blotting. Tissue expression pattern of the transgene in one of the transgenic mouse lines was also examined with immunochemical methods. The results of pathological analysis demonstrated that the overexpression of hB1F transgene did not cause pathological changes. We then analyzed the gene expression profile in the liver of transgenic mice with microchip and found that the expression of 3 genes was up-regulated while the expression of 25 genes was down-regulated. Some of the differentially expressed genes were verified with RT-PCR. The expression of farnesyl pyrophosphate synthase, a key enzyme in cholesterol biosynthesis, was inhibited in hB1F transgenic mice.

MATERIALS AND METHODS

Animals

C57 mice were maintained by Shanghai Nanfang Research Center for Model Organisms (SNRCMO). hB1F transgenic mice were produced in SNRCMO, maintained and bred in the Laboratory Animal Center of the Second Military Medical University.

Expression of the transgene

Total RNA was isolated from tissues with the TRIzol reagent (Invitrogen) according to the manufacturer's instructions. Semiquantitative RT-PCR reactions were performed with primer pair sets 5'-CCGACAAGTGGTACATGGAA-3' and 5'-CTGCTGCGGG TAGTTACA CA-3' for hB1F cDNA, and 5'-AACTTTGGCATTGTGGAAGG-3' and 5'-TGTGAGGGAG ATGCTCAGTG-3' for mouse glyceraldehyde-3-phosphate dehydrogenase (GAPDH) cDNA, which resulted in the generation of 300 bp and 600 bp products, respectively. PCR reactions were performed 30 cycles at 94 ℃ for 1 min, at 57 ℃ for 1 min, and at 72 ℃ for 1 min. PCR products were electrophoresed on 15 g/L agarose gels.

For Western blotting, protein samples from tissues were prepared according to the protocol from Santa Cruz Biotechnology, Inc. Each protein sample (50 μg) was electrophoresed on 100 g/L SDS-polyacrylamide gel and transferred to PVDF membrane. Membranes were blocked with 50 g/L non-fat milk in Tween-TBS (TBST) overnight at 4 ℃ and incubated with the anti-Flag antibody (Sigma) at a dilution of 1:500 in TBST for 2 h at room temperature. Membranes were washed three times with TBST and incubated with a horseradish peroxidase-conjugated anti-mouse IgG at a dilution of 1:2 000 at room temperature for 1 h. Immunodetection was carried out with an enhanced chemiluminescence kit (Amersham Pharmacia Biotech) according to the manufacturer's instructions.

Immunochemistry and pathological analysis

Tissue samples were fixed in 10% (vol/vol) neutral formalin,

embedded in paraffin, and sectioned for staining. Immunohistochemistry was performed on deparaffinized sections. Tissue sections were permeabilized with 3 g/L Triton X-100 in PBS for 30 min. After washed with PBS, sections were saturated for 30 min at room temperature with PBS containing 50 mL/L milk and then incubated for 1 h at room temperature with the anti-Flag antibody (1/250 dilution). This incubation was followed by five washes for 5 min in PBS-10 mL/L milk and then incubated with a sheep anti-mouse IgG (1/100 dilution) in PBS-milk for 1 h at room temperature. Sections were then washed five times for 5 min in PBS and coverslipped with 500 mL/L glycerol in PBS and examined under a microscope and photographed. Immunochemistry and pathological analyses were carrried out at the Department of Pathology, Changhai Hospital of the Second Military Medical University.

Microchip analysis of gene expression profile change

RNAs were isolated from livers of two male transgenic mice (TGM-4) and a male C57 mouse. Expressions of 8, 315 genes of the mice were analyzed by using BiostarM-80s cDNA arrays (Biostar genechip Inc., Shanghai, China). Control C57 mouse liver cDNA was labeled with fluorescence Cy3 and TGM-4 liver cDNA was labeled with fluorescence Cy5. Cy3 intensity values were adjusted to Cy3* by multiplying a normalization coefficient. The ratios of Cy5/Cy3* were calculated and genes were identified as either up-regulated when the ratio >2, or down-regulated when the ratio <0.5.

Semi-quantitative RT-PCR analysis

Primers used in PCR for CBG gene were 5'-TGTCGTCGCTGCA CTTAATC-3' and 5'-AGCACATTCCCTTCATCCAG-3', and for FPPS gene 5'-GGCCATGTGGATCT TGGTAG-3' and 5'-GAGGAGAGGCTCGTAGCAGA-3', which resulted in generations of 255 bp and 301 bp products, respectively. The cycling parameters were at 94 ℃ for 5 min, followed by 30 cycles at 94 ℃ for 1 min, at 57 ℃ for 1 min, and at 72 ℃ for 1 min. The PCR products were separated on 1.5% agarose gels. Signals were quantified by density analysis of the digital images using Alpha image software (Alpha Co., Ltd).

Statistical analysis

Differences in CBG and FPPS mRNA expressions (comparing CBG/GAPDH or FPPS/GAPDH ratios) were analyzed using one-way ANOVA and by the Student-Newman- Keuls multiple range test.

RESULTS

Transgene expression in livers of transgenic mice

Since the liver is the main organ that expresses hB1F which is involved in the regulation of the liver-specific expression of several important genes, the overexpression of hB1F transgene in mouse liver may serve as an *in vivo* model to study the function of hB1F in liver. We examined the expression of hB1F transgene in livers of seven transgenic mouse lines. RT-PCR results showed that except TGM-2, six out of seven transgenic mouse lines examined had expression of the transgene (Figure 1). Western blot results demonstated the expression of the transgene was found in livers of all lines with a relatively higher expression in lines TGM-3, TGM-6, and TGM-7 (Figure 2).

Morpholgy of TGM tissues

Pathological analysis was performed to examine whether the

Table 1 Genes up- or down-regulated in liver of TGM-4

Gene	Ratio 1	Ratio 2	Average Ratio	GenBank ID
Down-regulated: Trypsin 4	0.279	0.355	0.317	NM_011646
PAS Ser/Thr kinase	0.223	0.412	0.318	NM_080850
Elongation of very long chain fatty acids-like 3	0.274	0.402	0.338	NM_007703
4933406J07Rik RIKEN cDNA	0.363	0.352	0.358	AK016694
Similar to hypothetical protein MGC3169 clone MGC:25675	0.367	0.372	0.369	BC014728
Farnesyl pyrophosphate synthase	0.328	0.419	0.374	AF309508
Similar to hypothetical protein DKFZp434G2226 clone MGC:27627	0.422	0.328	0.375	BC016095
T cell immunoglobulin mucin-3	0.333	0.434	0.384	AF450241
Malate dehydrogenase mitochondrial	0.419	0.350	0.385	NM_008617
1810009A17Rik RIKEN cDNA	0.362	0.430	0.396	AK007392
Tetratricopeptide repeat domain	0.386	0.412	0.399	NM_009441
1810007A24Rik RIKEN cDNA	0.342	0.461	0.402	NM_026925
1810015P03Rik RIKEN cDNA	0.371	0.432	0.402	NM_025458
4930563E19Rik RIKEN cDNA	0.424	0.394	0.406	AK016201
1700030E05Rik RIKEN cDNA	0.400	0.422	0.411	BC017608
2700007P21Rik RIKEN cDNA	0.364	0.458	0.411	AK012215
Capping protein alpha 3	0.455	0.383	0.419	NM_007605
Trefoil factor 1	0.378	0.464	0.421	NM_009362
Ketohexokinase	0.447	0.444	0.446	NM_008439
Mus musculus cDNA	0.429	0.467	0.448	AV079172
Amylase 1 salivary	0.430	0.470	0.450	NM_007446
Elastase 2	0.495	0.448	0.472	NM_007919
Transient receptor protein 2	0.446	0.499	0.472	NM_011644
Clone IMAGE:3587716	0.491	0.458	0.474	BC012849
Heavy polypeptide 8 skeletal muscle	0.486	0.489	0.488	M12289
Up-regulated:				
602390464F1 Mus musculus cDNA	2.097	2.512	2.305	BG293529
Corticosteroid binding globulin	2.154	2.577	2.366	NM_007618
602843872F1 Mus musculus cDNA	3.259	2.292	2.775	BG974154

expression of hB1F transgene might cause any pathological changes in tissues of the transgenic mice. As shown in Figure 3, no obvious pathological change was observed in all tissues from the transgenic mouse line TGM-4. Therefore, as far as the tissues were examined, the expression of hB1F transgene did not result in pathological consequences in TGM-4. Similar results were obtained with other lines (data not shown).

Gene expression profile in livers of TGM-4

Microchip analysis was perfomed to investigate whether the gene expression profile of the host mice might be altered in the transgenic lines due to the expression of hB1F transgene. The gene expression profiles of cells from the livers of two independent TGM-4 mice were compared with that of the non-transgenic control mouse. Figure 4 represents a visual demonstration of the comparison of gene expression profiles between TGM-4 and C57. The expressions of 28 genes in the livers of TGM-4 mice were found to have changed compared with the C57 control mouse. Among them, 25 genes were down-regulated and 3 genes were up-regulated (Table 1).

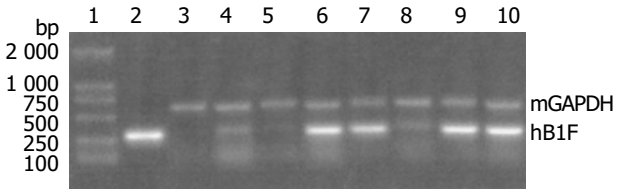

Figure 1 Semi-quantitative RT-PCR results of transgene expression in livers of TGMs lane 1: DNA molecular weight marker DL2 000 (Takara Inc.); lane 2: Positive control, pcDNA3-hB1F; lane 3: Negative control, liver of C57 mouse; lanes 4-10: livers of different lines of transgenic mice, TGM-1 to 7.

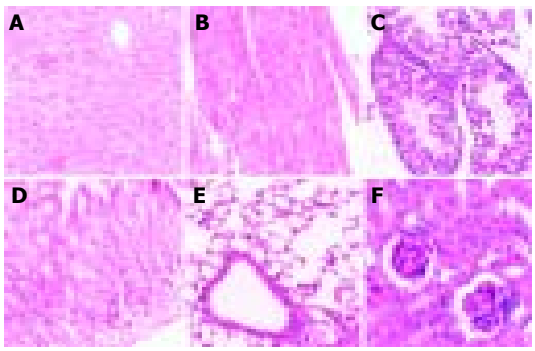

Figure 3 Morphology of TGM-4 tissues A: liver; B: heart; C: testicle; D: stomach; E: lung; F: kidney.

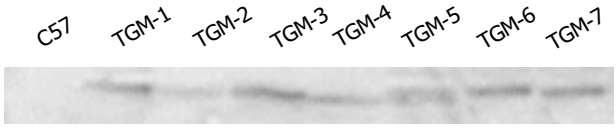

Figure 2 Western blot analysis of hB1F transgene expression in livers of TGMs.

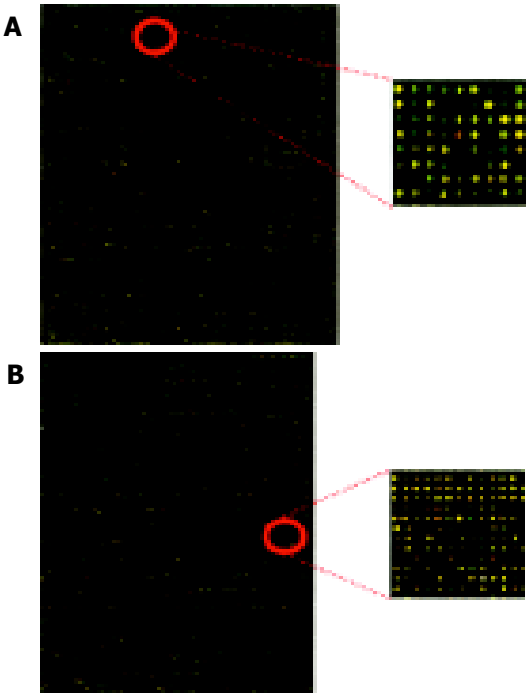

Figure 4 Visual demonstration of gene expression profiles between C57 control mouse and hB1F TGM4 A. chip 1; B. chip 2. Red signals stand for the up-regulated genes and green ones for the down-regulated genes. Yellow signals stand for non-differentially expressed genes.

RT-PCR analysis of diffentially expressed genes

Based on the results of the microchip analysis, some of the differentially expressed genes including corticosteroid-binding globulin (CBG) and farnesyl pyrophosphate synthase (FPPS) were subjected to further analysis. Semi-quantitative RT-PCR was performed with samples used in the microchip analysis and also with additional samples from other transgenic lines, TGM-1, TGM-3, TGM-6, and TGM-7. The corticosteroid binding globulin (serine/cysteine proteinase inhibitor) gene was up-regulated in the liver of TGM-4 (Figure 5) and the farnesyl

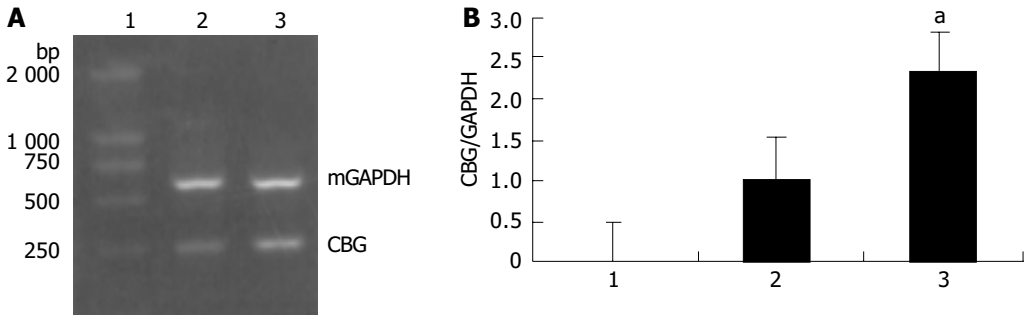

Figure 5 Semi-quantitative RT-PCR results of CBG expression in livers of TGM-4 and C57 control mouse. A: lane 1: DNA molecular weight marker DL2 000; lane 2: C57 control mouse; lane 3: TGM-4. B: The ratio of CBG / GAPDH was caclutated for each sample and used as an indication for the relative expression of CBG. The average value for the control was taken as 1. RT-PCR was repeated three times and the results were presented as mean±SE. Statistical significance was subjected to one-way ANOVA and Student-Newman-Keuls multiple range test. $^{a}P<0.05$ *vs* control.

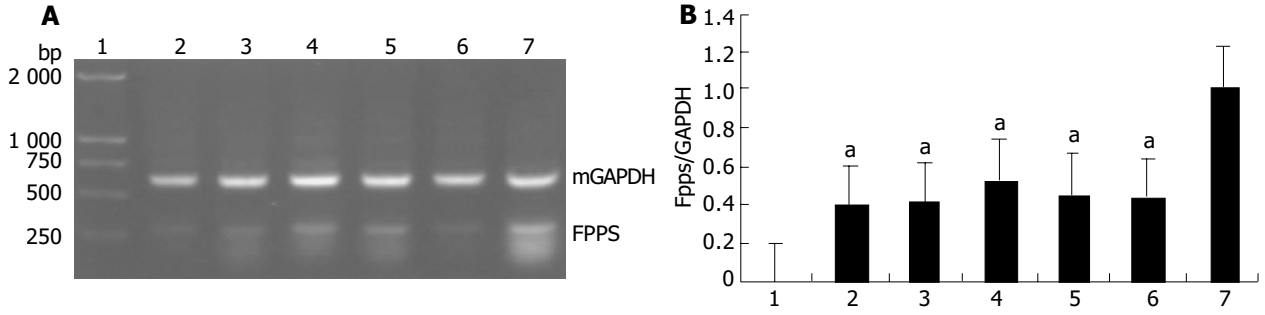

Figure 6 Semi-quantitative RT-PCR results of FPPS expression in livers of TGMs and C57 control mouse. A: lane 1: DNA molecular weight marker DL2000; lane 2: TGM-1; lane 3: TGM-3; lane 4: TGM-4; lane 5: TGM-6; lane 6: TGM-7; lane 7: C57 control mouse. B: The ratio of FPPS/GAPDH was caclutated for each sample and used as an indication for the relative expression of FPPS. The average value for the control was taken as 1. RT-PCR was repeated three times and results were presented as mean±SE. Statistical significance was subjected to one-way ANOVA and Student-Newman-Keuls multiple range test. $^aP<0.05$ *vs* control.

pyrophosphate synthase gene was down-regulated in all transgenic mouse lines (Figure 6). These results were well consistent with the microchip analysis data.

DISCUSSION

In this report, we verified the expression of hB1F transgene in several transgenic lines we have constructed previously. Results from RT-PCR and Western blotting analysis indicated that hB1F transgene was expressed in livers of all transgenic lines but with different expression levels. Besides liver, the transgene was also expressed in other organs such as stomach and testis (data not shown). The tissue expression pattern of hB1F transgene was expected since the transcription of thet ransgene was under the control of the CMV early promoter which has a relative broad tissue expression range. Although hB1F was thought previously to be present mainly in liver and pancreas, recent data revealed that it could be expressed in many types of tissues, such as intestine[10,16], ovary[17], adrenal gland[12], and preadipocytes[11,18]. Therefore, the transgenic lines established and verified in this study would provide a valuable animal model for studying the function of hB1F in multiple tissues.

Given that hB1F plays an important role in cholesterol homeostasis and bile acid biosynthesis, it is somewhat unexpected that no discernable pathological changes resulting from the overexpression of hB1F transgene have occurred in these transgenic lines. It is possible that the overexpression of hB1F might negatively feedback on the expression of the endogenous mouse counterpart of hB1F, mLRH-1. It remains to determine whether the expression of the enodgeous mLRH-1 changes in cells overexpressing hB1F. On the other hand, it is apparent from the microchip analysis that the expression of some genes were altered in livers of these transgenic lines. Since disturbance to metabolic pathways such as the cholesterol homeostasis might require a long incubation time before any pathological phenotypes could be observed, it is necessary to perform a long term follow-up investigation on the possible pathological changes.

Among the genes identified to exhibit altered expressions in hB1F transgenic mice, the gene that encodes the farnesyl pyrophosphate synthase (FPPS) is the most interesting one. FPPS could catalyse the formation of farnesyl pyrophosphate (FPP) through the condensation of dimethylallyl pyrophosphate with two molecules of isopentenyl pyrophosphate. FPP is a key cellular intermediate for the biosynthesis of isoprenoids and a precursor of cholesterol, steroid hormones, dolichols, haem A and ubiquinone. Furthermore, it has been found that FPP and its derivative geranylgeranyl pyrophosphate are involved in prenylation, a post-translational modification of a variety of cellular proteins that influence their proper cellular localizations and biological functions[19]. The semi-quantitative RT-PCR results confirmed the down-regulated expression of FPPS in all transgenic lines, suggesting that inhibition of the expression of FPPS has a general effect on hB1F transgenic mice, unrelated to other reasons such as the position effect due to the integration of the transgene. Given the complexity of the regulatory network for the cholesterol homeostasis, it is still early to speculate on the molecular mechanism underlying the inhibition of expression of FPPS in hB1F transgenic mice. Whether hB1F directly or indirectly inhibits the expression of FPPS awaits future study.

REFERENCES

1 **Li M,** Xie YH, Kong YY, Wu X, Zhu L, Wang Y. Cloning and characterization of a novel human hepatocyte transcription factor, hB1F, which binds and activates enhancer II of hepatitis B virus. *J Biol Chem* 1998; **273**: 29022-29031

2 **Nitta M,** Ku S, Brown C, Okamoto AY, Shan B. CPF: an orphan nuclear receptor that regulates liver-specific expression of the human cholesterol 7alpha-hydroxylase gene. *Proc Natl Acad Sci U S A* 1999; **96**: 6660-6665

3 Nuclear Receptors Nomenclature Committee. A unified nomenclature system for the nuclear receptor superfamily. *Cell* 1999; **97**: 161-163

4 **Galarneau L,** Pare JF, Allard D, Hamel D, Levesque L, Tugwood JD, Green S, Belanger L. The alpha1-fetoprotein locus is activated by a nuclear receptor of the Drosophila FTZ-F1 family. *Mol Cell Biol* 1996; **16**: 3853-3865

5 **Pare JF,** Roy S, Galarneau L, Belanger L. The mouse fetoprotein transcription factor (FTF) gene promoter is regulated by three GATA elements with tandem E box and Nkx motifs, and FTF in turn activates the Hnf3beta, Hnf4alpha, and Hnf1alpha gene promoters. *J Biol Chem* 2001; **276**: 13136-13144

6 **Goodwin B,** Jones SA, Price RR, Watson MA, McKee DD, Moore LB, Galardi C, Wilson JG, Lewis MC, Roth ME, Maloney PR, Willson TM, Kliewer SA. A regulatory cascade of the nuclear receptors FXR, SHP-1, and LRH-1 represses bile acid biosynthesis. *Mol Cell* 2000; **6**: 517-526

7 **Lu TT,** Makishima M, Repa JJ, Schoonjans K, Kerr TA, Auwerx J, Mangelsdorf DJ. Molecular basis for feedback regulation of bile acid synthesis by nuclear receptors. *Mol Cell* 2000; **6**: 507-515

8 **Luo Y,** Liang CP, Tall AR. The orphan nuclear receptor LRH-1 potentiates the sterol-mediated induction of the human CETP gene by liver X receptor. *J Biol Chem* 2001; **276**: 24767-24773

9 **Schoonjans K**, Annicotte JS, Huby T, Botrugno OA, Fayard E, Ueda Y, Chapman J, Auwerx J. Liver receptor homolog 1 controls the expression of the scavenger receptor class B type I. *EMBO Rep* 2002; **3**: 1181-1187

10 **Inokuchi A,** Hinoshita E, Iwamoto Y, Kohno K, Kuwano M, Uchiumi T. Enhanced expression of the human multidrug resistance protein 3 by bile salt in human enterocytes: A transcriptional control of a plausible bile acid transporter. *J Biol Chem* 2001; **276**: 46822-46829

11 **Clyne CD,** Speed CJ, Zhou J, Simpson ER. Liver receptor homologue-1 (LRH-1) regulates expression of aromatase in preadipocytes. *J Biol Chem* 2002; **277**: 20591-20597
12 **Wang ZN,** Bassett M, Rainey WE. Liver receptor homologue-1 is expressed in the adrenal and can regulate transcription of 11 beta-hydroxylase. *J Mol Endocrinol* 2001; **27**: 255-258
13 **Sirianni R,** Seely JB, Attia G, Stocco DM, Carr BR, Pezzi V, Rainey WE. Liver receptor homologue-1 is expressed in human steroidogenic tissues and activates transcription of genes encoding steroidogenic enzymes. *J Endocrinol* 2002; **174**: R13-17
14 **Fayard E,** Schoonjans K, Annicotte JS, Auwerx J. Liver receptor homolog 1 controls the expression of carboxyl ester lipase. *J Biol Chem* 2003; **278**: 35725-35731
15 **Wang SL,** Yang H, Xie YH, Wang Y, Li JZ, Wang L, Wang ZG, Fu JL. Establishment of transgenic mice carrying the gene of human nuclear receptor NR5A2 (hB1F). *World J Gastroenterol* 2003; **6**: 1333-1336
16 **Rausa FM,** Galarneau L, Belanger L, Costa RH. The nuclear receptor fetoprotein transcription factor is coexpressed with its target gene HNF-3beta in the developing murine liver, intestine and pancreas. *Mech Dev* 1999; **89**: 185-188
17 **Falender AE,** Lanz R, Malenfant D, Belanger L, Richards JS. Differential expression of steroidogenic factor-1 and FTF/LRH-1 in the rodent ovary. *Endocrinology* 2003; **144**: 3598-3610
18 **Iwaki M,** Matsuda M, Maeda N, Funahashi T, Matsuzawa Y, Makishima M, Shimomura I. Induction of adiponectin, a fat-derived antidiabetic and antiatherogenic factor, by nuclear receptors. *Diabetes* 2003; **52**: 1655-1663
19 **Zhang FL,** Casey PJ. Protein prenylation: molecular mechanisms and functional consequences. *Annu Rev Biochem* 1996; **65**: 241-269

Edited by Wang XL **Proofread by** Xu FM

PO Box 2345, Beijing 100023, China
Fax: +86-10-85381893
E-mail: wjg@wjgnet.com www.wjgnet.com

World J Gastroenterol 2004;10(20):3011-3015
World Journal of Gastroenterology
 ISSN 1007-9327

• BASIC RESEARCH •

Anti-tumor effect of *pEgr-IFNγ* gene-radiotherapy in B16 melanoma-bearing mice

Cong-Mei Wu, Xiu-Yi Li, Tian-Hua Huang

Cong-Mei Wu, Tian-Hua Huang, Research Center of Reproductive Medicine, Shantou University Medical College (SUMC), Shantou 515041, Guangdong Province, China
Xiu-Yi Li, The Ministry of Public Health Radiobiology Research Unit of Jilin University, Changchun 130021, Jilin Province, China
Supported by the National Natural Science Fundation of China, No. 39970229
Correspondence to: Dr. Cong-Mei Wu, Research Center of Reproductive Medicine, Shantou University Medical College, Shantou 515041, Guangdong Province, China. cmwu@stu.edu.cn
Telephone: +86-754-8900442 **Fax:** +86-754-8557562
Received: 2003-12-10 **Accepted:** 2004-03-02

Abstract

AIM: To construct a *pEgr-IFNγ* plasmid and to investigate its expression properties of interferon-γ (INF-γ) induced by irradiation and the effect of gene-radiotherapy on the growth of melanoma.

METHODS: A recombined plasmid, *pEgr-IFNγ*, was constructed and transfected into B16 cell line with lipofectamine. The expression properties of *pEgr-IFNγ* were investigated by ELISA. Then, a B16 melanoma-bearing model was established in mice, and the plasmid was injected into the tumor tissue. The tumor received 20 Gy X-ray irradiation 36 h after injection, and IFN-γ expression was detected from the tumor tissue. A tumor growth curve at different time points was determined.

RESULTS: The eukaryotic expression vector, *pEgr-IFNγ,* was successfully constructed and transfected into B16 cells. IFN-γ expression was significantly increased in transfected cells after X-ray irradiation in comparison with 0 Gy group (77.73-94.60 pg/mL, P<0.05-0.001), and was significantly higher at 4 h and 6 h than that of control group after 2 Gy X-ray irradiation (78.90-90.00 pg/mL, P<0.01-0.001). When the transfected cells were given 2 Gy irradiation 5 times at an interval of 24 h, IFN-γ expression decreased in a time-dependent manner. From d 3 to d 15 after IFNγ gene-radiotherapy, the tumor growth was significantly slower than that after irradiation or gene therapy alone.

CONCLUSION: The anti-tumor effect of pEgr-IFNγ gene-radiotherapy is better than that of genetherapy or radiotherapy alone for melanoma. These results may establish an important experimental basis for gene-radiotherapy of cancer.

Wu CM, Li XY, Huang TH. Anti-tumor effect of *pEgr-IFNγ* gene-radiotherapy in B16 melanoma-bearing mice. *World J Gastroenterol* 2004; 10(20): 3011-3015
http://www.wjgnet.com/1007-9327/10/3011.asp

INTRODUCTION

Radiotherapy is one of the treatments for cancer. However, its therapeutic effect is still unsatisfactory, and thus new therapeutic strategy must be adopted. Gene therapy in combination with radiotherapy is one of the most important advances[1-4]. The introduction of Egr-1 promoter induced by irradiation has provided a possible approach to this combination therapy[5-6].

IFNγ is the first cytokine produced by gene engineering and used for treatment of carcinoma, and has anti-tumor effects. Its antitumor mechanism includes direct inhibition of tumor cell proliferation, and indirect action by activating cytotoxic activities[7-18]. In the present study we constructed the pEgr-IFNγ plasmid by connecting IFNγ cDNA to Egr-1 promoter to investigate its expression properties in B16 cells and its antitumor effect in mice.

MATERIALS AND METHODS

Construction of pEgr-IFNγ Plasmid

The expression vector for pEgr-IFNγ is shown in Figure 1.

Cell line and transfection

B16 cell line was cultured in MH Radiobiology Research Unit of Jilin University and maintained in RPMI 1640 (Life Technologies) with 100 mL/L fetal bovine serum (Hyclone Laboratories), L-glutamine, 100 μg/mL of streptomycin, and 100 U/mL of penicillin. The cell line was incubated at 37 ℃ in 50 mL/L CO_2.

B16 cells were transfected in a 6-well plate when the cells reached 70% confluence. Solution A was prepared by addition of 10 μg of pEgr-IFNγ or pcDNA3.1$^+$ to 100 μL serum-free medium (SFM), and solution B by addition of 10 μL liposome to 100 μL SFM. Solutions A and B were mixed at room temperature for 30 min, then mixed with 0.8 mL SFM, the mixture was added to the rinsed cells. The medium was replaced with fresh and complete medium 6 h after transfection.

Protein determination

Supernatants from different groups were collected for detection of the IFNγ expression with ELISA kit (Genzyme).

Establishment of B16 melanoma-bearing model

Adult female Kunming mice were provided by the Experimental Animal Center of Jilin University, with an average weight of 18±2 g.

A melanoma-bearing model was established by subcutaneous injection at right hind limb with 0.1 mL B16 cells (5×10^6 /mL), 10 d later, tumor tissue received multi-focus injection of plasmids packaged with liposome (20 μg plasmid and 0.1 mL liposome per mouse) for the experimental groups.

Tumor size was measured. Then, tumor volume (V) was calculated according to the formula: $V\ (mm^3) = L\times W^2/2$, where, L: the longest diameter of tumor; W: the diameter at right angles on the largest horizontal section. Tumor growth rate (f) was the ratio of the volume at different time points over the initial volume (V_0).

Ionizing irradiation

X-rays of 200 kV and 10 mA with 0.5 mm copper and 1.0 mm aluminum filter were given at a dose-rate of 0.8639 Gy/min for a total dose of 2--20 Gy.

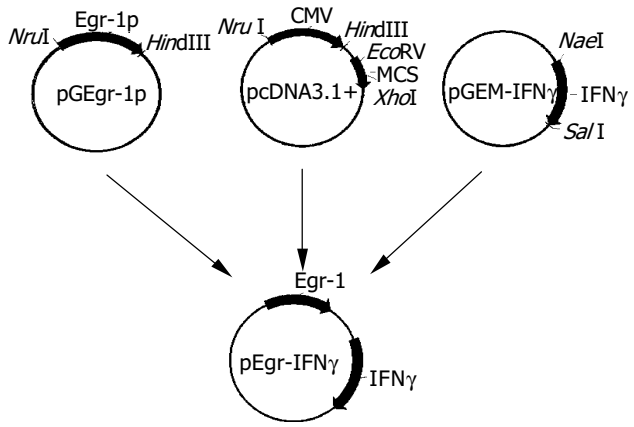

Figure 1 Construction of plasmid pEgr-IFNγ.

B16 cells were seeded in a 6-well plate and randomly divided into different groups. The experiment groups received X-ray irradiation of various doses or at different time points, control groups received sham irradiation simultaneously.

Mice bearing B16 xenografts ($n = 40$) were randomly divided into five groups: control group, 20 Gy group, pcDNA3.1+20 Gy group, pEgr-IFNγ group and pEgr-IFNγ+20 Gy group. Thirty-six hours before irradiation, melanoma tissue was injected with plasmids or buffer at 5 separate sites. Tumor beds were given 20 Gy X-ray irradiation. Animals of 20 Gy group, pcDNA3.1+20 Gy group and pEgr-IFNγ+20 Gy group were shielded with lead except for the tumor-bearing hind limb, animals in the other 2 groups were given sham-irradiation at the same time. Tumors were measured and recorded as previously described.

RT-PCR

Total RNA were extracted from EC9706 cells and tumor tissue for RT-PCR. GAPDH was used as an internal reference. Primers were as follows: GAPDH, forward primer 5'-TGCACCACCAAC TGCTTAGC -3' and reverse one 5'-GGCATGGACTGTGG TCATGAG-3', mouse IFNγcDNA, forward primer 5'-GATCCT TTGGACCCTCTG ACTT-3' and reverse one 5'-AGACAGTGA TAAACTATAAATGAGCG-3'.

RT-PCR was performed as following: denaturation at 95 ℃ for 3 min, 30 cycles at 95 ℃ for 45 s, at 56 ℃ for 45 s, at 72 ℃ for 40 s and extension at 72 ℃ for 10 min.

Statistical analysis

Student's *t* test was used to determine comparability between groups. *P* values less than 0.05 were considered statistically significant.

RESULTS

B16 cell line transfected with pEgr-IFNγ plasmid

Pre- and post-transfection of B16 cells are shown in Figure 2.

IFNγ expressions in B16 cells transfected with pEgr-IFNγ after different doses of X-irradiation

After transfection B16 cells received different doses of X-ray irradiation. The cells of control group were transfected with pcDNA3.1$^+$ plasmid. Six hours after irradiation IFNγ expression and mRNA level were detected.

The results showed that IFNγ expression in 2-20 Gy groups was significantly higher than that in 0 Gy group (P<0.05-0.01) (Figure 3).

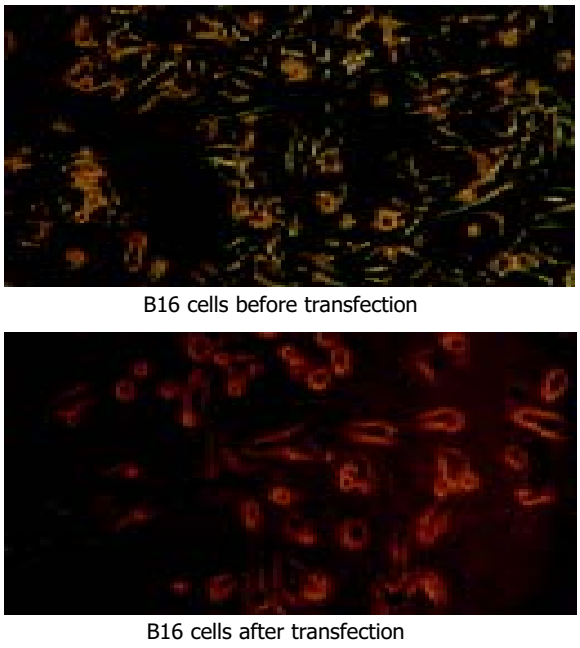

Figure 2 Pre- and post-transfection of B16 cells.

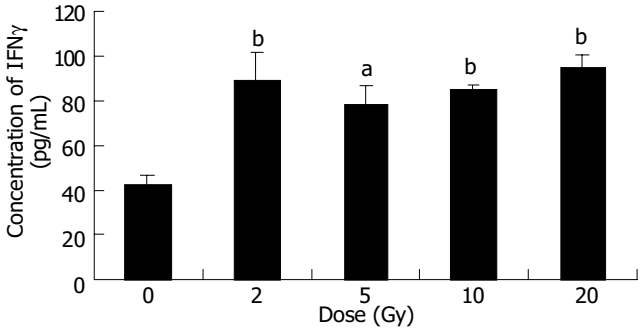

Figure 3 Expression of IFNγ in B16 cells after different doses X-ray irradiation. (mean±SD, $n = 3$) ^aP<0.05 and ^bP<0.01 *vs* 0 Gy group.

After irradiation IFNγ mRNA could be detected in B16 cells (Figure 4). The level of IFNγ mRNA was compared with that of GAPDH, and their ratios are shown in Table 1. The IFNγ mRNA levels in 2-20 Gy groups were higher than that of 0 Gy group.

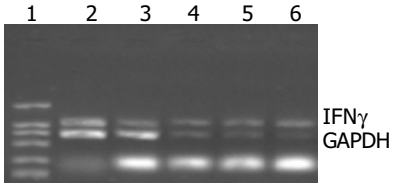

Figure 4 IFNγ mRNA level in B16 cells after different doses of X-ray irradiation. Lane 1: DL2000 Marker; Lane 2: 0 Gy group; Lane 3: 2 Gy group; Lane 4: 5 Gy group; Lane 5: 10 Gy group; Lane 6: 20 Gy group.

IFNγ expressions in B16 cells transfected with pEgr-IFNγ at different time points after 2Gy irradiation

After transfection B16 cells received 2 Gy of X-ray irradiation while the control group received sham irradiation. IFNγ protein was detected at different time points after irradiation. ELISA results showed that the IFNγ expression increased with time from 2 h to 6 h in a time-dependent manner, and peaked at 6 h, about 1.8 times of that in control group (P<0.001). However,

from 8 h to 48 h post-radiation IFNγ expressions were not significantly different from that in control group (Figure 5).

Table 1 IFNγ mRNA level in B16 cells after irradiation with different doses

Dose (Gy)	Ratio of IFNγ mRNA level
0	0.819
2	0.972
5	1.347
10	1.950
20	2.144

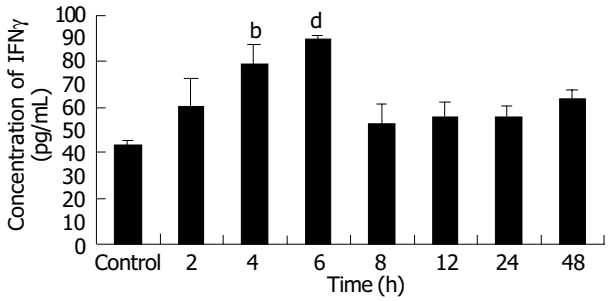

Figure 5 Expression time course of IFNγ in B16 cells after 2 Gy X-ray irradiation (mean±SD, n = 3) ^{b}P<0.01 and ^{d}P<0.001 *vs* control group.

Expression of IFNγ in B16 cells at different time points after X-ray irradiation

After transfection B16 cells received 2 Gy irradiation while the control group received sham irradiation. IFNγ expression was detected 6 h later. Irradiation and detection were repeated 5 times at an interval of 24 h.

The result showed that the IFNγ expression after the first irradiation was the highest, then decreased in a time-dependent manner. The expressions after the first 2 times of irradiation were higher than that in control group (P<0.01-0.001) (Figure 6).

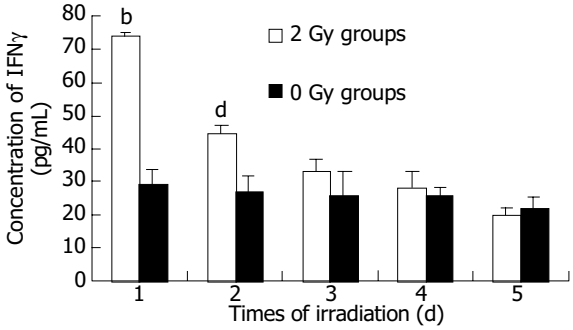

Figure 6 Expression of IFNγ in B16 cells at different time points after X-ray irradiation (mean±SD, n = 3) ^{b}P<0.01 and ^{d}P<0.001 *vs* 0 Gy groups.

Effect of gene-radiotherapy on tumor growth

Melanoma-bearing mice of different groups were shown in Figure 7.

Tumor growth rate of pEgr-IFNγ group was significantly slower than that of control group (P<0.001) between 6 d and 15 d after irradiation (Table 2), so was pEgr-IFNγ plus 20 Gy group compared with control and 20 Gy groups between 3 d and 15 d after irradiation (P<0.001).

Table 2 Tumor growth rate after gene-radiotherapy (mean±SD, n = 8)

Group	f (V/V_0) on days after irradiation				
	3 d	6 d	9 d	2 d	15 d
Control	1.23±0.37	3.11±1.5	12.29±4.83	20.21±7.62	22.80±8.50
20 Gy	1.57±0.19	2.34±0.40	3.28±0.68^{b}	4.18±0.66^{b}	6.18±1.40^{b}
PcDNA3.1+20 Gy	1.86±0.54	1.67±0.40^{ad}	2.26±0.50^{bd}	2.86±0.58^{bd}	5.19±0.66^{b}
PEgr-IFNγ	1.38±0.23	1.76±0.56^{b}	2.61±0.75^{b}	5.23±0.98^{b}	8.03±2.14^{b}
PEgr-IFNγ+20 Gy	0.48±0.10^{bf}	0.34±0.11^{bf}	0.38±0.14^{bf}	0.43±0.11^{bf}	0.35±0.10^{bf}

^{a}P<0.05, ^{b}P<0.001 *vs* control group; ^{d}P<0.01, ^{f}P<0.001 *vs* 20 Gy group.

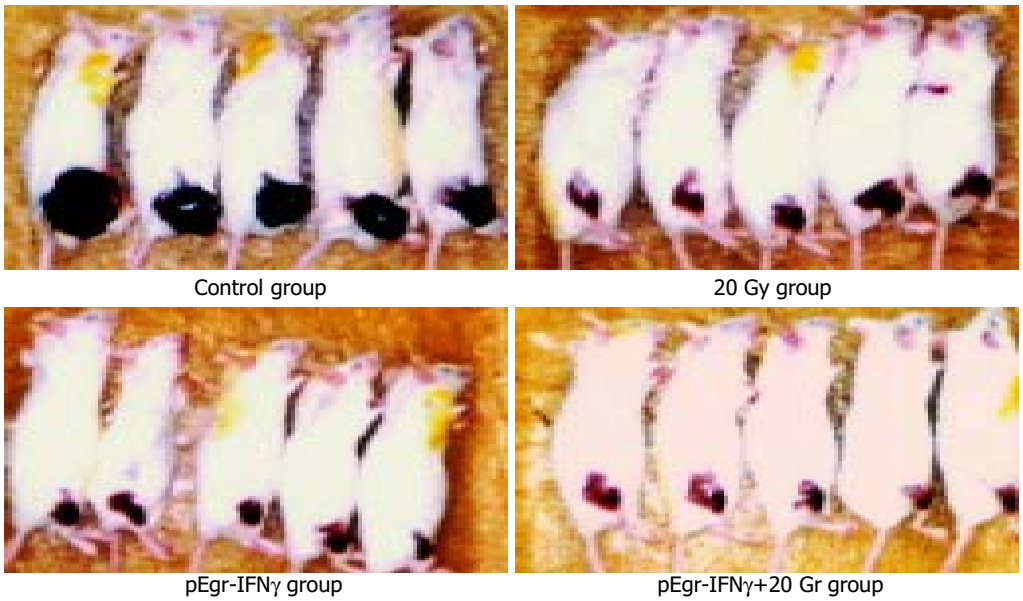

Figure 7 Melanoma-bearing mice 15 d after treatment.

RT-PCR analysis of IFNγ in tumor tissue

Melanoma-bearing mice were injected with plasmids, and the tumor received 20 Gy X-ray irradiation, 3 d later total RNA from tumor tissue was extracted for RT-PCR.

GAPDH bands were shown in all groups, but IFNγ cDNA bands were shown only in pEgr-IFNγ and pEgr-IFNγ+20 Gy groups (Figure 8).

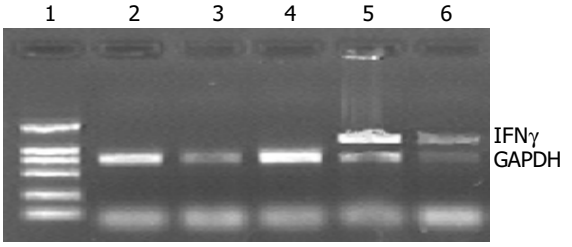

Figure 8 RT-PCR analysis of intratumor IFNγ. Lane 1: DL2000 Marker; Lane 2: control; Lane 3: 20 Gy; Lane 4: pcDNA3.1+20 Gy; Lane 5: pEgr-IFNγ; Lane 6: pEgr-IFNγ+20 Gy.

DISCUSSION

In 1992 Weichselbaum put forward the new therapeutic strategy that took advantage of the dual tumor-killing effects of genetherapy and radiotherapy, namely, to choose certain exogenous genes that could be activated by irradiation and then transcript some cytotoxic proteins to kill the tumor cells. They also established the techniques that might be used for target gene therapy of carcinomas[19-25].

It had been reported that Egr-1 was transcriptionally induced by exposure to irradiation, and its induction by irradiation was conferred by serum response or CC (A/T) rGG elements in its promoter region[26-30]. Based on this finding, we firstly connected IFNγ cDNA with Egr-1 promoter to construct pEgr-IFNγ plasmid to investigate the expression properties in B16 melanoma cells. Furthermore, a melanoma model was established by subcutaneous injection of B16 cells, and then plasmids were injected to observe its antitumor effect *in vivo*.

Firstly, B16 cells transfected with pEgr-IFNγ received different doses of X-ray irradiation and the IFNγ expression was detected. The results showed that the IFNγ expression level in B16 cells post-transfection induced by irradiation was higher than that of sham-irradiation group (P<0.05-0.01). Time-course studies revealed that IFNγ expression reached its peak at 6 h after 2Gy irradiation, and the maximal level was 1.8 times of that in control group (P<0.01). Furthermore, after repeated irradiation the IFNγ expression in B16 cells post-transfection reached the peak level just after the first irradiation, and then decreased in time-dependent manner. All of these demonstrated that pEgr-IFNγ plasmid could enhance IFNγ expression.

Secondly, the results of *in vivo* experiments showed that the proliferation of melanoma was significantly inhibited in pEgr-IFNγ group in comparison with control group between 6 and 15 d after irradiation (P<0.001). So was pEgr-IFNγ gene-radiotherapy group compared with control and 20 Gy groups between 3 and 15 d after irradiation (P<0.001). IFNγ expression was detected in melanoma tissue having receivied injection of pEgr-IFNγ plasmid. These results demonstrated that injection of pEgr-IFNγ improved antitumor effect, and combined pEgr-IFNγ and irradiation showed the most optimal effect.

This study combined pEgr-IFNγ plasmid and irradiation, and demonstrated much more enhanced antitumor efficacy than either one in the melanoma model. It was very easy to administer directly the plasmid into melanoma tissue, and therapeutic dose could also be administered as required. The tumor could be effectively exposed to radiation with external beam or intratumoral sources, or both, to enhance local IFNγ expression and boost local tumor control. Increased IFNγ levels might elicit systemic mediators, such as cytokines and matrix proteinases, which target occult distant metastases and thereby further enhance the therapeutic ratio. The absence of systemic toxicities with intratumoral administration of IFNγ supports the safe addition of pEgr-IFNγ gene radiotherapy to current antitumor protocols.

REFERENCES

1 **Weichselbaum RR**, Hallahan DE, Beckett MA, Mauceri HJ, Lee H, Sukhatme VP, Kufe DW. Gene therapy targeted by radiation preferentially radiosensitizes tumor cells. *Cancer Res* 1994; **54**: 4266-4269

2 **Liu XF**, Zou SQ, Qiu FZ. Construction of HCV-core gene vector and its expression in cholangiocarcinoma. *World J Gastroenterol* 2002; **8**: 135-138

3 **Gou WJ**, Yu EX, Liu LM, Li J, Chen Z, Lin JH, Meng ZQ, Feng Y. Comparison between chemoembolization combined with radiotherapy and chemoembolization alone for large hepatocellular carcinoma. *World J Gastroenterol* 2003; **9**: 1697-1701

4 **Ido A,** Uto H, Moriuchi A, Nagata K, Onaga Y, Onaga M, Hori T, Hirono S, Hayashi K, Tamaoki T, Tsubouchi H. Gene therapy targeting for hepatocellular carcinoma: selective and enhanced suicide gene expression regulated by a hypoxia-inducible enhancer linked to a human alpha-fetoprotein promoter. *Cancer Res* 2001; **61**: 3016-3021

5 **Datta R**, Rubin E, Sukhatme V, Qureshi S, Hallahan D, Weichselbaum RR, Kufe DW. Ionizing radiation activates transcription of the EGR1 gene via CArG elements. *Proc Natl Acad Sci U S A* 1992; **89**: 10149-10153

6 **Tsai Morris CH**, Cao XM, Sukhatme VP. 5' flanking sequence and genomic structure of Egr-1, a murine mitogen inducible zinc finger encoding gene. *Nucleic Acids Res* 1988; **16**: 8835-8846

7 **Lokshin A**, Mayotte JE, Levitt ML. Mechanism of interferon beta-induced squamous differentiation and programmed cell death in human non-small-cell lung cancer cell lines. *J Natl Cancer Inst* 1995; **87**: 206-212

8 **Shiau AL,** Lin CY, Tzai TS, Wu CL. Postoperative immunogene therapy of murine bladder tumor by *in vivo* administration of retroviruses expressing mouse interferon-gamma. *Cancer Gene Ther* 2001; **8**: 73-81

9 **Siesjo P**, Visse E, Sjogren HO. Cure of established, intracerebral rat gliomas induced by therapeutic immunizations with tumor cells and purified APC or adjuvant IFN-gamma treatment. *J Immunother Emphasis Tumor Immunol* 1996; **19**: 334-345

10 **Saleh M**, Jonas NK, Wiegmans A, Stylli SS. The treatment of established intracranial tumors by in situ retroviral IFN-gamma transfer. *Gene Ther* 2000; **7**: 1715-1724

11 **Li XM**, Chopra RK, Chou TY, Schofield BH, Wills Karp M, Huang SK. Mucosal IFN-gamma gene transfer inhibits pulmonary allergic responses in mice. *J Immunol* 1996; **157**: 3216-3219

12 **Fujinami K**, Ikeda I, Miura T, Kondo I. Combination therapy with 5-fluorouracil (5-FU), cisplatin (CDDP) and interferon alpha-2B (IFN alpha-2B) for advanced renal cell carcinoma. *Gan To Kagaku Ryoho* 1996; **23**: 1689-1691

13 **Yeow WS**, Lawson CM, Beilharz MW. Antiviral activities of individual murine IFN-alpha subtypes *in vivo*: intramuscular injection of IFN expression constructs reduces cytomegalovirus replication. *J Immunol* 1998; **160**: 2932-2939

14 **Ahn EY**, Pan G, Vickers SM, McDonald JM. IFN-gammaupregulates apoptosis-related molecules and enhances Fas-mediated apoptosis in human cholangiocarcinoma. *Int J Cancer* 2002; **1**: 445-451

15 **Blanck G**. Components of the IFN-gamma signaling pathway in tumorigenesis. *Arch Immunol Ther Exp* 2002; **50**: 151-158

16 **Nayak SK**, McCallister T, Han LJ, Gangavalli R, Barber J, Dillman RO. Transduction of human renal carcinoma cells with human gamma-interferon gene via retroviral vector. *Cancer Gene Ther* 1996; **3**: 143-150

17 **Tada H**, Maron DJ, Choi EA, Barsoum J, Lei H, Xie Q, Liu W, Ellis L, Moscioni AD, Tazelaar J, Fawell S, Qin X, Propert KJ, Davis A, Fraker DL, Wilson JM, Spitz FR. Systemic IFN-beta

gene therapy results in long-term survival in mice with established colorectal liver metastases. *J Clin Invest* 2001; **108**: 83-95

18 **Paradis TJ**, Floyd E, Burkwit J, Cole SH, Brunson B, Elliott E, Gilman S, Gladue RP. The anti-tumor activity of anti-CTLA-4 is mediated through its induction of IFN gamma. *Cancer Immunol Immunother* 2001; **50**: 125-133

19 **Weichselbaum RR**, Hallahan DE, Sukhatme VP, Kufe DW. Gene therapy targeted by ionizing radiation. *Int J Radiat Oncol Biol Phys* 1992; **24**: 565-567

20 **Weichselbaum RR**, Kufe DW, Advani SJ, Roizman B. Molecular targeting of gene therapy and radiotherapy. *Acta Oncol* 2001; **40**: 735-738

21 **Khodarev NN**, Park JO, Yu J, Gupta N, Nodzenski E, Roizman B, Weichselbaum RR. Dose-dependent and independent temporal patterns of gene responses to ionizing radiation in normal and tumor cells and tumor xenografts. *Proc Natl Acad Sci U S A* 2001; **98**: 12665-12670

22 **Gupta VK**, Park JO, Jaskowiak NT, Mauceri HJ, Seetharam S, Weichselbaum RR, Posner MC. Combined gene therapy and ionizing radiation is a novel approach to treat human esophageal adenocarcinoma. *Ann Surg Oncol* 2002; **9**: 500-504

23 **Hanna NN**, Seetharam S, Mauceri HJ, Beckett MA, Jaskowiak NT, Salloum RM, Hari D, Dhanabal M, Ramchandran R, Kalluri R, Sukhatme VP, Kufe DW, Weichselbaum RR. Antitumor interaction of short- course endostatin and ionizing radiation. *Cancer J* 2000; **6**: 287-293

24 **Takahashi T**, Namiki Y, Ohno T. Induction of the suicide HSV-TK gene by activation of the Egr-1 promoter with radioisotopes. *Hum Gene Ther* 1997; **8**: 827-833

25 **Griscelli F**, Li H, Cheong C, Opolon P, Bennaceur- Griscelli A, Vassal G, Soria J, Soria C, Lu H, Perricaudet M, Yeh P. Combined effects of radiotherapy and angiostatin gene therapy in glioma tumor model. *Proc Natl Acad Sci U S A* 2000; **97**: 6698-6703

26 **Christy B**, Nathans D. DNA binding site of the growth factor-inducible protein Zif268. *Proc Natl Acad Sci U S A* 1989; **86**: 8737-8741

27 **Seyfert VL**, Sukhatme VP, Monroe JG. Differential expression of a zinc finger-encoding gene in response to positive versus negative signaling through receptor immunoglobulin in murine B lymphocytes. *Mol Cell Biol* 1989; **9**: 2083-2088

28 **Joseph LJ**, Le-Beau MM, Jamieson GA Jr, Acharya S, Shows TB, Rowley JD, Sukhatme VP. Molecular cloning, sequencing, and mapping of EGR2, a human early growth response gene encoding a protein with “zinc-binding finger” structure. *Proc Natl Acad Sci U S A* 1988; **85**: 7164-7168

29 **Sukhatme VP**. Early transcriptional events in cell growth: the Egr family. *J Am Soc Nephrol* 1990; **1**: 859-866

30 **Cao XM**, Koski RA, Gashler A, McKiernan M, Morris, CF, Gaffney R, Hay RV, Sukhatme VP. Identification and characterization of the Egr-1gene product, a DNA-binding zinc finger protein induced by differentiation and growth signals. *Mol Cell Biol* 1990; **10**: 1931-1939

Edited by Ren SY and Wang XL **Proofread by** Xu FM

PO Box 2345, Beijing 100023, China
Fax: +86-10-85381893
E-mail: wjg@wjgnet.com www.wjgnet.com

World J Gastroenterol 2004;10(20):3016-3020
World Journal of Gastroenterology
 ISSN 1007-9327

• BASIC RESEARCH •

Differentiation of rat marrow mesenchymal stem cells into pancreatic islet beta-cells

Li-Bo Chen, Xiao-Bing Jiang, Lian Yang

Li-Bo Chen, Xiao-Bing Jiang, Lian Yang, Department of Surgery, Union Hospital of Huazhong University of Science and Technology, Wuhan 430022, Hubei Province, China
Supported by the National Natural Science Foundation of China, No. 30170911
Correspondence to: Dr. Li-Bo Chen, Department of Surgery, Union Hospital of Huazhong University of Science and Technology, Wuhan 430022, Hubei Province, China. libo_chen@hotmail.com
Telephone: +86-27-85726301 **Fax:** +86-27-85776343
Received: 2003-12-10 **Accepted:** 2004-02-01

Abstract

AIM: To explore the possibility of marrow mesenchymal stem cells (MSC) *in vitro* differentiating into functional islet-like cells and to test the diabetes therapeutic potency of Islet-like cells.

METHODS: Rat MSCs were isolated from Wistar rats and cultured. Passaged MSCs were induced to differentiate into islet-like cells under following conditions: pre-induction with L-DMEM including 10 mmol/L nicotinamide+1 mmol/L β-mercaptoethanol+200 mL/L fetal calf serum (FSC) for 24 h, followed by induction with serum free H-DMEM solution including 10 mmol/L nicotinamide+1 mmol/L,β-mercaptoethanol for 10 h. Differentiated cells were observed under inverse microscopy, insulin and nestin expressed in differentiated cells were detected with immunocytochemistry. Insulin excreted from differentiated cells was tested with radioimmunoassay. Rat diabetic models were made to test *in vivo* function of differentiated MSCs.

RESULTS: Typical islet –like clustered cells were observed. Insulin mRNA and protein expressions were positive in differentiated cells, and nestin could be detected in pre-differentiated cells. Insulin excreted from differentiated MSCs (446.93±102.28 IU/L) was much higher than that from pre-differentiated MSCs (2.45±0.81 IU/L (P<0.01). Injected differentiated MSCs cells could down-regulate glucose level in diabetic rats.

CONCLUSION: Islet-like functional cells can be differentiated from marrow mesenchymal stem cells, which may be a new procedure for clinical diabetes stem -cell therapy, these cells can control blood glucose level in diabetic rats. MSCs may play an important role in diabetes therapy by islet differentiation and transplantation.

Chen LB, Jiang XB, Yang L. Differentiation of rat marrow mesenchymal stem cells into pancreatic islet beta-cells. *World J Gastroenterol* 2004; 10(20): 3016-3020
http://www.wjgnet.com/1007-9327/10/3016.asp

INTRODUCTION

Diabetic mellitus (DM), one of the leading causes of morbidity and mortality in many countries, is caused by an absolute insulin deficiency due to the destruction of insulin secreting pancreatic cells (type 1 DM) or by a relative insulin deficiency due to decreased insulin sensitivity, usually observed in overweight individuals (type 2 DM). In both types of the disease, an inadequate mass of functional islet cells is the major determinant for the onset of hyperglycemia and the development of overt diabetes. Islet transplantation has recently been shown to restore normoglycemia in type 1 DM[1]. However, a limited supply of human islet tissues prevents this therapy from being used in patients with type 1 DM. Alternatively, much effort has been made to increase β cell mass by stimulating endogenous regeneration of islets or *in vitro* differentiated islet-like cells[2-5]. Multipotent stem cells have been described within pancreatic islets and in nonendocrine compartments of the pancreas[6-12], and these cells have the capacity of differentiating into pancreatic islet-like structures. Furthermore, cells that do not reside within the pancreas, such as embryonic stem cells(ESC), hepatic oval cells, cells within spleen, have been differentiated into pancreatic endocrine hormone-producing cells *in vitro* and *in vivo*[13-21]. However, despite their differentiating potency, differentiation of various stem cells into islet cells has two major obstacles preventing clinical application: One is that these stem cells do not originate from DM patients, transplanting them would unavoidably be rejected by DM recipients. The other is that the source is not enough to provide abundant stem cells. The current article reports a potential means to generate insulin-producing cells, islet differentiation from bone marrow-derived stem cells. We suggest that cells within the adult bone marrow (mesenchymal stem cells MSC) are capable of differentiating into functional pancreatic β cell phenotypes.

MATERIALS AND METHODS

Materials

Wistar rats were bought from Animal Center, Tongji Medical College. All procedure was accordant with animal experiment guideline of the university. Cell culture medium L-DMEM (4.5 mmol/L glucose), H-DMEM (23 mmol/L glucose) and fetal calf serum (FCS) were bought from GIBCO Co. Nicotinamide, β-mercaptoethanol, B27 were from Sigma Co. Anti-nestin, anti-insulin monoclonal antibodies were bought from Santa Cruz Co. RT-PCR kit and primers were purchased from GIBCO Co. Radioimmunoassay (RIA) kit was purchased from Beijing North Biotechnology Co.

Differentiation of rat marrow mesenchymal stem cells into functional islet β cells

Bone marrow was isolated from femoral bone under aseptic condition and dispersed into single cell suspension, L-DMEM cells were cultured in a density of 1×10^9/L at 37 ℃, 50 mL/L CO_2 for 48 h. Suspended cells were disposed and adherent cells were cultured in L-DMEM with 200 mL/L FCS for about 10 d, culture medium was changed at 3-d intervals. These cells were digested with 2.5 g/L trypse and passed for 2-3 generations when the confluence reached 70-90%. Then, cells with 70-80% confluence were induced to differentiate into functional pancreatic cells. Cells were pre-induced with 10 mmol/L nicotinamide and 1 mmol/L

β-mercaptoethanol in L-DMEM for 24 h, and re-induced with 10 mmol/L nicatinomide and 1 mmol/L Mercaptoethanol in serum-free H-DMEM for another 10 h. Cells induced without nicotinamide or β-mercaptoethanol were used as controls.

Function assessment of differentiated cells

Cell morphology changes were investigated under converted microscope. Insulin-1 mRNA or protein expression was detected with immunocyto-chemical procedure and reverse transcription polymerase chain reaction (RT-PCR), and insulin level in culture suspension secreted from differentiated cells was detected with radio-immunological assay (RIA).

RT-PCR

Total RNA from 5×10^6 pre-treated or post-treated MSC cells was isolated according to a Qiagen protocol including DNase treatment. Reverse transcription was carried out using the Superscript protocol. Taq-man RT-PCR was performed using the Master Mix (Applied Biosystems). Insulin-1 primers were designed using the primer express program (Applied Biosystems) according to gene bank sequences. The following primers were used for Insulin-1: forward: 5'-GGGGAACGTGGT TTCTTCTA-3', backward: 5'-TAGACGAGGGAGATGGTTGA CC-3'. 35 cycles of 94 ℃×30 s, 55 ℃×30 s, 72 ℃×30 s were performed and the PCR product for Insulin-1 was 187 bp. GAPDH was used as internal control with the following primers: forward: TGGTATCGTGGAAGGACTCATGA. backward: ATGCCAGTGAGCTTCCCGTTCAGC. Products were tested with 15 g/L gel electrophoresis.

Immunohistochemistry

Cells adherent to slides were fixed with 40 g/L para-formaldehyde. After washed, the slides were incubated with a biotin-goat anti- rat insulin or nestin monoclonal antibodies (Santa Cruz Co, USA) diluted 1:200 in 50 mL/L normal goat serum for 20 min at room temperature. Immuno-reactive cells were visualized using the Vectastain Elite ABC Kit (Vector Labs, USA) with 3'3 diaminobenzidine tetrachloride (DAB) (Boehringer-Mannheim) as the chromogen. All sections were counterstained with hematoxylin.

Radioimmunoassay

The amounts of immunoreactive insulin in supernatants secreted from differentiated cells 48 h after treatment and cells 24 h before treatment were determined by RIA using a commercially available RIA kit according to the manufacturer's instructions. Briefly, to each polypropylene RIA tube 100 μL each of anti-Insulin, ^{125}I- insulin, and insulin or the samples were added. Immune complexes were precipitated 24 h later with 1 mL of 160 mL/L polyethylene glycol solution, and a gamma counter was used to determine the radioactivity in the precipitates. There was no nonspecific interference of the assay with the components of the samples. Determinations were carried out in triplicate and the means and standard deviations were obtained.

Primitive glucose controling role of differentiated MSCs on STZ-diabetic rats

Diabetic animal models were made according to the standard procedure with modifications. Briefly, 10 Wistar rats (weighting about 200 grams) were intravenously injected with 50 mg/L streptozotocin (STZ) from caudal veins, and glucose levels were tested 1 week later with Roche ACCU-CHEK glucose tester. Two rats died and were excluded. After stable hyperglycemia level was achieved, 3 animals were subcutaneously injected with 5×10^6 differentiated cells, while 2 others received the same amount of un-differentiated cells, the remaining 1 did not receive any cells. One week after cell injection, animal glucose level was recorded.

Statistical analysis

Data were analyzed with Student's *t* test, $P<0.05$ was considered statistically significant.

RESULTS

Morphological changes of MSC differentiation

Under inversed microscope, undifferentiated MSCs were typical of adherent spindle and fibrocyte- like. However, under differentiation, these spindle-like cells changed rapidly into round or oval types with confluence. These cells were abundant in endocrinal granules, similar to those differentiated islet cells from ES cells. These grape-like cells lasted for at least 2 wk. Some cells changed into neuron-like cells with typical processes.

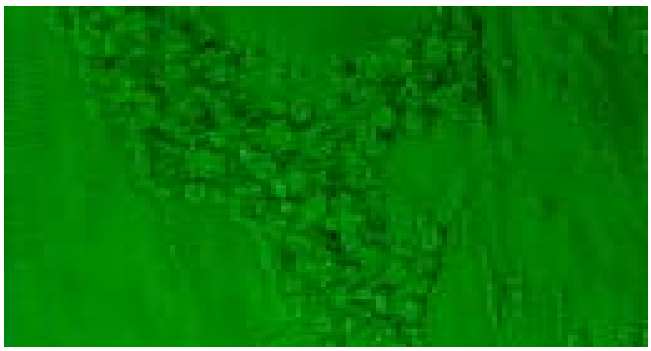

Figure 1 Islet-like grape-shaped cells isolated from marrow mesenchymal stem cells.

Insulin-1 transcription in differentiated cells

To assess insulin-1 mRNA expression in differentiated cells, RT-PCR was applied on MSCs shortly after bone marrow isolation (Neg), 24 h before nicotinamide and β-mercaptoethanol treatment (Pre), 48 h (Islet1) and 1week after Nicotinamide and β-mercaptoethanol treatment (Islet2). There were no pre-differentiated MSCs (Figure 2). However, 48 h after treatment, insulin-1 mRNA transcription could be detected and continued for at least 1 wk. Since we did not observe any pancreatic islet-like cells in control group, RT-PCR was not performed on this group of cells.

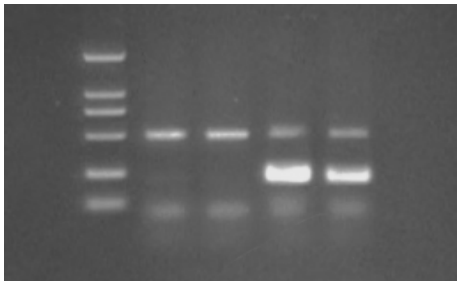

Figure 2 Insulin transcription in pre-differentiated MSCs shown in RT-PCR. Neg: MSCs undifferentiated; Pre: MSCs 24 h before differentiation; Islet1: cells 24 h after differentiation; Islet2: cells 1w after differentiation.

Insulin and nestin protein expression in different stages of MSCs

Immunocytochemistry was performed to test insulin or nestin protein expressions in MSCs. Insulin could be observed obviously in those grape-like cells (Islet-like), and in unchanged spindle-like cells not positively stained. Nestin was regarded

as an important pre-marker for islet cell differentiation, and its expression was tested. Immunocytochemistry showed nestin positivity in pre-differentiated spindle-like cells (Figure 4), while no nestin positivity in differentiated islet-like cells.

To further clarify the function of these differentiated cells, RIA was used to assess the insulin excretion from these cells in 6 independent cell cultures. As shown in Table 1, pre-differentiated MSCs seldom secreted insulin into their supernatant if any. However, 48 h after differentiation, these islet-like cells produced much insulin and secreted insulin in extra-cellular medium.

Figure 3 Insulin staining for islet -like cells. Strong brown staining indicates insulin positivity in differentiatly arranged grape shape cells.

Figure 4 Positive nestin in pre-differentiated MSCs.

Table 1 Insulin excretion changes in pre- and differentiated MSCs (RIA) (IU / L)

Group	Insulin excretion in pre-treated MSCs	Insulin excretion in treated islet-like cells
1	1.67	410.79
2	2.53	383.21
3	1.53	465.81
4	3.36	308.28
5	2.20	516.45
6	3.40	597.02

In supernatant of pre-differentiated MSC cells, there was no obvious insulin excretion (2.45±0.81 IU/L). Forty-eight h after differentiation, cells excreted more insulin into supernatant, the insulin level was as high as 446.93±102.28 IU/L (t = 10.65 ^{b}P<0.01).

To test if these MSC-differentiated islet-like cells could exert glucose-controlling function, 6 diabetic Wistar rat models were included. Each of 3 rats was administered subcutaneously 5×10^{6} differentiated cells, 2 received similar un-differentiated MSCs injection, while the last one received none. Glucose levels of these 6 rats at different times are shown in Table 2. Although lack of statistical analysis, it could be suggested that MSC-differentiated islet-like cells could change diabetic glucose level.

Table 2 Blood glucose level (mmol/L) changes in STZ-diabetic rats

Types of cells injected	Glucose level 24 h before injection	Glucose level 1 w after injection
Islet1	>33.3	25.4
Islet2	>33.3	21.4
Islet3	25.3	19.7
MSC1	>33.3	>33.3
MSC2	28.9	29.7
Non	>33.3	>33.3

Islet1, Islet1, Islet3: different STZ-diabetic rats received islet cell injection; MSC1, MSC2: STZ-diabetic rats received undifferentiated MSC injection; Non: STZ-diabetic rats did not receive cell injection.

DISCUSSION

Multipotent stem cells within pancreas and outside could develop into insulin-secreting islet cells[7-21]. However, differentiation of various stem cells into islet cells has two major obstacles preventing clinical application. As these stem cells do not originate from DM patients, these cells transplanted would be rejected by DM recipients. The source is not enough to provide abundant stem cells.

Bone marrow mesenchymal cells (MSC) reside in bone marrow and are multipotent, and can differentiate into lineages of mesenchymal tissues, such as bone, cartilage, fat, tendon, muscle, adipocytes, chondrocytes, osteocytes[22-24]. MSCs could differentiate into endodermal and epidermal cells, such as vascular endothelial cells, neurocytes, lung cells and hepatocytes[25-27]. MSCs as differentiation donors are of advantages compared with other stem cells as ESC or stem cells from organs. MSCs are of great multiplication potency. Cell-doubling time is 48-72 h, and cells could be expanded in culture for more than 60 doublings[28]. Functional cells differentiated from MSCs transplanted into MSC donors (autologous transplantation) would not cause any rejection.

Differentiation of MSCs into functional pancreatic islet cells is not yet reported. Ianus *et al*.[29] reported, using a CRE-LoxP system, bone marrow from male mice with an enhanced green fluorescent protein (GFP) replacing insulin expression was transplanted into lethally irradiated recipient female mice. After 4-6 wk, recipient mice revealed both Y chromosome and GFP positivity in pancreatic islets. These GFP positive cells expressed insulin, glucose transporter-2 and other islet β cell related markers. Cells from bone marrow were able to differentiate into islet cells. MSCs could differentiate into hepatocytes[25,27], precursor cells of hepatocytes could differentiate into pancreatic islet cells, adult hepatic stem cells could trans-differentiate into pancreatic endocrine hormone-producing cells[19,20]. These reports indicated that, MSCs had the capacity of differentiating into pancreatic islet cells.

We found that MSCs could successfully differentiate into pancreatic islet β-like cells. These cells were morphologically similar to pancreatic islet cells. More importantly, they could also transcript, translate and excrete insulin. Cells were injected subcutaneously into NOD rat models, although lack of statistical data, these MSC-derived cells could regulate NOD blood glucose level. Nestin was regarded as a marker of precursors of pancreatic islet cells[10,14]. In our study, nestin was also positive in pre-pancreatic islet MSCs, suggesting that MSCs could differentiate into islet cells. High glucose concentration was considered as a potent inducer for pancreatic islet differentiation. Nicotinamide was used to preserve islet viability and function through poly

(ADP-ribose) polymerase (PARP)[30], β-mercaptoethanol was commonly used as a neurocyte inducer. In our primary experiment, high glucose alone could not effectively induce MSC to differentiate into islet-like cells. After nicotinamide was added, they could effectively transform MSCs into islet-like cells. This may imply that nicotinamide could be an effective inducer, or it could protect differentiated cells from dying or transforming into other cell types. β-mercaptoethanol increased the potency of nicotinamide in our experiment. Considering nestin expression in pre-differentiated MSCs, MSCs might differentiate into pancreatic islet-like cells through intermediate neurocyte stage. We did not test the insulin secretion based on the number of cells, the increased insulin in supernatant might be mainly from increased insulin excretion by islet-like cells.

Bone marrow stem cells are non-endodermal cells with no immediate relationship to putative pancreatic stem cells that are resident in tissues of endodermal origin or developmental neuro-endocrine stem cells derived from the endoderm. Alternatively, stem cells in bone marrow may be derived from sites of endodermal origin. Regardless of their germ layer of origin, these cells represent multi-potent cells mediated by circulating signals, and can be recruited to neuro-endocrine compartments of the pancreas. Once homing of these cells to pancreatic islets has occurred, local cell-cell interaction as well as paracrine factors may initiate differentiation.

There was an argument[31] that Islet-like cells differentiated from ESC were falsely insulin positive from insulin-uptake. These insulin-positive cells which do not transcript insulin mRNA, are TUNEL+. Bone marrow cells could also fuse with other cells and adopt the phenotypes of these cells[32,33]. However, cell differentiation in our report was not the case. Islet cells expressed insulin at both mRNA and protein levels, the excreting insulin level was far more higher than that in culture media and that of pre-differentiated cells. Further more, these MSCs-derived cells could down-regulate glucose level in diabetic rats.

In conclusion, MSCs can differentiate into functional pancreatic islet-like cells *in vitro*. If human MSCs, especially MSCs from diabetes patients themselves can be isolated, proliferated, differentiated into functional pancreatic islet-like cells, and transplanted back into their donors (autologous transplantation), their high proliferation potency and rejection avoidance will provide one promising therapy for diabetes.

REFERENCES

1 **Shapiro AM**, Lakey JR, Ryan EA, Korbutt GS, Toth E, Warnock GL, Kneteman NM, Rajotte RV. Islet transplantation in seven patients with type 1 diabetes mellitus using a glucocorticoid-free immunosuppressive regimen. *N Engl J Med* 2000; **343**: 230–238

2 **Bonner-Weir S**, Taneja M, Weir GC, Tatarkiewicz K, Song KH, Sharma A, O'Neil JJ. *In vitro* cultivation of human islets from expanded ductal tissue. *Proc Natl Acad Sci U S A* 2000; **97**: 7999–8004

3 **Abraham EJ**, Leech CA, Lin JC, Zulewski H, Habener JF. Insulinotropic hormone glucagon-like peptide-1 differentiation of human pancreatic islet-derived progenitor cells into insulin-producing cells. *Endocrinology* 2002; **143**: 3152-3161

4 **Schmied BM**, Ulrich A, Matsuzaki H, Ding X, Ricordi C, Weide L, Moyer MP, Batra SK, Adrian TE, Pour PM. Transdifferentiation of human islet cells in a long-term culture. *Pancreas* 2001; **23**: 157-171

5 **Lipsett M**, Finegood DT. Beta-cell neogenesis during prolonged hyperglycemia in rats. *Diabetes* 2002; **51**: 1834–1841

6 **Ramiya VK**, Maraist M, Arfors KE, Schatz DA, Peck AB, Cornelius JG. Reversal of insulin-dependent diabetes using islets generated *in vitro* from pancreatic stem cells. *Nat Med* 2000; **6**: 278–282

7 **Schwitzgebel VM**, Scheel DW, Conners JR, Kalamaras J, Lee JE, Anderson DJ, Sussel L, Johnson JD, German MS. Expression of neurogenin3 reveals an islet cell precursor population in the pancreas. *Development* 2000; **127**: 3533-3542

8 **Jensen J**, Heller RS, Funder-Nielsen T, Pedersen EE, Lindsell C, Weinmaster G, Madsen OD, Serup P. Independent development of pancreatic alpha- and beta-cells from neurogenin3-expressing precursors: a role for the notch pathway in repression of premature differentiation. *Diabetes* 2000; **49**: 163-176

9 **Guz Y**, Nasir I, Teitelman G. Regeneration of pancreatic beta cells from intra-islet precursor cells in an experimental model of diabetes. *Endocrinology* 2001; **142**: 4956–4968

10 **Zulewski H**, Abraham EJ, Gerlach MJ, Daniel PB, Moritz W, Muller B, Vallejo M, Thomas MK, Habener JF. Multipotential nestin-positive stem cells isolated from adult pancreatic islets differentiate *ex vivo* into pancreatic endocrine, exocrine, and hepatic phenotypes. *Diabetes* 2001; **50**: 521-533

11 **Gao R**, Ustinov J, Pulkkinen MA, Lundin K, Korsgren O, Otonkoski T. Characterization of endocrine progenitor cells and critical factors for their differentiation in human adult pancreatic cell culture. *Diabetes* 2003; **52**: 2007-2015

12 **Hardikar AA**, Marcus-Samuels B, Geras-Raaka E, Raaka BM, Gershengorn MC. Human pancreatic precursor cells secrete FGF2 to stimulate clustering into hormone-expressing islet-like cell aggregates. *Proc Natl Acad Sci U S A* 2003; **100**: 7117-7122

13 **Soria B**, Roche E, Berna G, Leon-Quinto T, Reig JA, Martin F. Insulin-secreting cells derived from embryonic stem cells normalize glycemia in streptozotocin-induced diabetic mice. *Diabetes* 2000; **49**: 157–162

14 **Lumelsky N**, Blondel O, Laeng P, Velasco I, Ravin R, McKay R. Differentiation of embryonic stem cells to insulin-secreting structures similar to pancreatic islets. *Science* 2001; **292**: 1389-1394

15 **Assady S**, Maor G, Amit M, Itskovitz-Eldor J, Skorecki KL, Tzukerman M. Insulin production by human embryonic stem cells. *Diabetes* 2001; **50**: 1691-1697

16 **Hori Y**, Rulifson IC, Tsai BC, Heit JJ, Cahoy JD, Kim SK. Growth inhibitors promote differentiation of insulin-producing tissue from embryonic stem cells. *Proc Natl Acad Sci U S A* 2002; **99**: 16105-16110

17 **Shiroi A**, Yoshikawa M, Yokota H, Fukui H, Ishizaka S, Tatsumi K, Takahashi Y. Identification of insulin-producing cells derived from embryonic stem cells by zinc-chelating dithizone. *Stem Cells* 2002; **20**: 284-292

18 **Kim D**, Gu Y, Ishii M, Fujimiya M, Qi M, Nakamura N, Yoshikawa T, Sumi S, Inoue K. *In vivo* functioning and transplantable mature pancreatic islet-like cell clusters differentiated from embryonic stem cell. *Pancreas* 2003; **27**: E34-E41

19 **Deutsch G**, Jung J, Zheng M, Lora J, Zaret KS. A bipotential precursor population for pancreas and liver within the embryonic endoderm. *Development* 2001; **128**: 871-881

20 **Yang L**, Li S, Hatch H, Ahrens K, Cornelius JG, Petersen BE, Peck AB. *In vitro* trans-differentiation of adult hepatic stem cells into pancreatic endocrine hormon producing cells. *Proc Natl Acad Sci U S A* 2002; **99**: 8078–8083

21 **Kodama S**, Kuhtreiber W, Fujimura S, Dale EA, Faustman DL. Islet regeneration during the reversal of autoimmune diabetes in NOD mice. *Science* 2003; **302**: 1223-1227

22 **Pittenger MF**, Mackay AM, Beck SC, Jaiswal RK, Douglas R, Mosca JD, Moorman MA, Simonetti DW, Craig S, Marshak DR. Multilineage potential of adult human mesenchymal stem cells. *Science* 1999; **284**: 143-147

23 **Krause DS**, Theise ND, Collector MI, Henegariu O, Hwang S, Gardner R, Neutzel S, Sharkis SJ. Multi-organ, Multi-lineage engraftment by a single bone marrow-derived stem cells. *Cell* 2001; **105**: 369-377

24 **Jiang Y,** Jahagirdar BN, Reinhardt RL, Schwartz RE, Keene CD, Ortiz-Gonzalez XR, Reyes M, Lenvik T, Lund T, Blackstad M, Du J, Aldrich S, Lisberg A, Low WC, Largaespada DA, Verfaillie CM. Pluripotency of mesenchymal stem cells derived from adult marrow. *Nature* 2002; **418**: 41-49

25 **Petersen BE**, Bowen WC, Patrene KD, Mars WM, Sullivan

AK, Murase N, Boggs SS, Greenberger JS, Goff JP. Bone marrow as a potential source of hepatic oval cells. *Science* 1999; **284**: 1168-1170

26 **Davani S**, Marandin A, Mersin N, Royer B, Kantelip B, Herve P, Etievent JP, Kantelip JP. Mesenchymal progenitor cells differentiate into an endothelial phenotype, enhance vascular density, and improve heart function in a rat cellular cardiomyoplasty model. *Circulation* 2003; **108**(Suppl 1): II253-258

27 **Schwartz RE**, Reyes M, Koodie L, Jiang Y, Blackstad M, Lund T, Lenvik T, Johnson S, Hu WS, Verfaillie CM. Multipotent adult progenitor cells from bone marrow differentiate into functional hepatocyte-like cells. *J Clin Invest* 2002; **109**: 1291-1302

28 **Reyes M**, Lund T, Lenvik T, Aguiar D, Koodie L, Verfaillie CM. Purification and *ex vivo* expansion of postnatal human marrow mesodermal progenitor cells. *Blood* 2001; **98**: 2615-2625

29 **Ianus A**, Holz GG, Theise ND, Hussain MA. *In vivo* derivation of glucose- competent pancreatic endocrine cells from bone marrow without evidence of cell fusion. *J Clin Invest* 2003; **111:** 843-850

30 **Kolb H,** Burkart V. Nicotinamide in type 1 diabetes. Mechanism of action revisited. *Diabetes Care* 1999; **22**(Suppl 2): B16-20

31 **Rajagopal J**, Anderson WJ, Kume S, Martinez OI, Melton DA. Insulin staining of ES cells progeny from insulin uptake. *Science* 2003; **299**: 363

32 **Terada N**, Hamazaki T, Oka M, Hoki M, Mastalerz DM, Nakano Y, Meyer EM, Morel L, Petersen BE, Scott EW. Bone marrow cells adopt the phenotype of other cells by spontaneous cell fusion. *Nature* 2000; **416**: 542-545

33 **Spees JL**, Olson SD, Ylostalo J, Lynch PJ, Smith J, Perry A, Peister A, Wang MY, Prockop DJ. Differentiation, cell fusion, and nuclear fusion during *ex vivo* repair of epithelium by human adult stem cells from bone marrow stroma. *Proc Natl Acad Sci U S A* 2003; **100**: 2397-2402

Edited by Wang XL and Ren SR **Proofread by** Xu FM

PO Box 2345, Beijing 100023, China
Fax: +86-10-85381893
E-mail: wjg@wjgnet.com www.wjgnet.com

World J Gastroenterol 2004;10(20):3021-3025
World Journal of Gastroenterology
 ISSN 1007-9327

• BASIC RESEARCH •

Adenoviral transfer of human interleukin-10 gene in lethal pancreatitis

Zi-Qian Chen, Yao-Qing Tang, Yi Zhang, Zhi-Hong Jiang, En-Qiang Mao, Wei-Guo Zou, Ruo-Qing Lei, Tian-Quan Han, Sheng-Dao Zhang

Zi-Qian Chen, Yao-Qing Tang, Yi Zhang, Zhi-Hong Jiang, En-Qiang Mao, Ruo-Qing Lei, Tian-Quan Han, Sheng-Dao Zhang, Department of Surgery, Ruijin Hospital, Shanghai Second Medical University, Shanghai 200025, China
Wei-Guo Zou, Institute of Biochemistry and Cell Biology, Shanghai Institute for Biological Sciences, Chinese Academy of Sciences, Shanghai 200031, China
Supported by Science and Technology Committee of Shanghai Municipal Government, No. 00419019
Correspondence to: Sheng-Dao Zhang, Department of Surgery, Affiliated Ruijin Hospital, Shanghai Second Medical University, Shanghai 200025, China. chenziq@hotmail.com
Telephone: +86-21-64370045 Ext. 611002
Received: 2004-01-15 **Accepted:** 2004-02-24

Abstract

AIM: To evaluate the therapeutic effect of adenoviral-vector-delivered human interleukin-10 (hIL-10) gene on severe acute pancreatitis (SAP) rats.

METHODS: Healthy Sprague-Dawley (SD) rats were intraperitoneally injected with adenoviral IL-10 gene (AdvhIL-10), empty vector (Adv0) or PBS solution. Blood, liver, pancreas and lung were harvested on the second day to examine hIL-10 level by ELISA and serum amylase by enzymatic assay. A SAP model was induced by retrograde injection of sodium taurocholate through pancreatic duct. SAP rats were then administered with AdvhIL-10, Adv0 and PBS solution by a single intraperitoneal injection 20 min after SAP induction. In addition to serum amylase assay, levels of hIL-10 and tumor necrosis factor-α (TNF-α) were detected by RT-PCR, ELISA and histological study. The mortality rate was studied and analyzed by Kaplan–Meier and log rank analysis.

RESULTS: The levels of hIL-10 in the pancreas, liver and lung of healthy rats increased significantly after AdvhIL-10 injection (1.42 ng/g in liver, 0.91 ng/g in pancreas); while there was no significant change of hIL-10 in the other two control groups. The concentration of hIL-10 was increased significantly in the SAP rats after AdvhIL-10 injection (1.68 ng/g in liver, 1.12 ng/g in pancreas) compared to the other two SAP groups with blank vector or PBS treatment ($P<0.05$). The serum amylase levels remained normal in the AdvhIL-10 transfected healthy rats. However, the serum amylase level was significantly elevated in the other two control SAP rats. In contrast, serum amylase was down-regulated in the AdvhIL-10 treated SAP groups. The TNF-α expression in the AdvhIL-10 treated SAP rats was significantly lower compared to the other two control SAP groups. The pathohistological changes in the AdvhIL-10 treated group were better than those in the other two control groups. Furthermore, the mortality of the AdvhIL-10 treated group was significantly reduced compared to the other two control groups ($P<0.05$).

CONCLUSION: Adenoviral hIL-10 gene can significantly attenuate the severity of SAP rats, and can be used in the treatment of acute inflammation process.

Chen ZQ, Tang YQ, Zhang Y, Jiang ZH, Mao EQ, Zou WG, Lei RQ, Han TQ, Zhang SD. Adenoviral transfer of human interleukin-10 gene in lethal pancreatitis. *World J Gastroenterol* 2004; 10(20): 3021-3025
http://www.wjgnet.com/1007-9327/10/3021.asp

INTRODUCTION

The pathogenesis of severe acute pancreatitis (SAP) is complicated. Studies have indicated that the explosive production and release of pro-inflammatory cytokines play an important role in its pathogenesis. There is evidence that TNF-α and interleukin-1 (IL-1) are very important inflammatory cytokines in this process[1,2]. Although pro-inflammatory cytokines are necessary for protecting against inflammation in the early phase, uncontrolled and adverse inflammatory effects of the systemic cytokine response could also be harmful. Thus, inhibiting the synthesis of pro-inflammatory cytokines and altering the balance between pro- and anti- inflammatory cytokines might significantly affect the severity of pancreatitis and the survival rate[3,4]. IL-10 is a major anti-inflammatory cytokine. It has been shown to be down-regulated the expression of TNF and other inflammatory cytokines from activated macrophages. IL-10 could block the release of oxygen free radicals and nitrogen oxide. In consequence[5], it could decrease the mortality[6-8]. These findings suggested that administration of IL-10 could be useful in blocking these pro-inflammatory cytokines during the initiation of acute pancreatitis.

Gene therapy as a novel drug delivery system to express proteins in individual tissues has been used in inflammatory diseases[9]. The use of deficient adenovirus vectors might be a useful tool for this gene therapy due to its high infectious activity and high protein expression ability. Gene therapy has been proposed in many inflammation diseases to produce anti-inflammatory cytokines at local sites[10,11]. However, transfection of SAP rats with an adenoviral vector has not been previously reported.

In this paper, we reported a successful gene therapy for SAP rats. Our experiments showed that human IL-10 expression in tissues could block the development of SAP and improve the survival rate. The results suggest a novel potential therapeutic approach for the treatment of patients with acute pancreatitis.

MATERIALS AND METHODS

Materials

Adenovirus expression system (Adenoviral Gateway Expression Kit, 293A Cell Line, Gateway LR Clonase Enzyme Mix, Lipofectamine 2000) and TRIzol reagent were provided by Invitrogen (San Diego, CA). pcDNA3IL-10 plasmid was generously donated by professor XY Liu (Shanghai Institute for Biological Sciences, Chinese Academy of Sciences, Shanghai, China). Restriction enzyme (*Hin*dIII, *Eco*RI, *Bam*HI, *Sal*I) was obtained from Promega (Madison, Wi, USA). Sodium taurocholate was purchased from Sigma Chemical Company

(St Louis, MO). Amylase enzyme assay kits were obtained from Shanghai Kehua-Hualing Diagnosis Kit Co (Shanghai, China). An ELISA kit specific for human IL-10 was purchased from Diaclone Research International (BESANÇON Cedex, French).

Adenoviral vectors

Human IL-10 cDNA was cloned into the *Bam*HI and *Eco*RI sites of pEntr 1A vector. Then the IL-10 cDNA was moved into the adenoviral destination vector from pEntr 1A vector by Gateway LR Clonase. The recombinant E1 deleted type 5 adenoviral vector encode hIL-10 under the transcriptional control of the cytomegalovirus promoter and contained the bGHp(A) sequence. Adenovirus hIL-10 vector was transfected into 293A human embryonic kidney cell line with Lipofectamine 2000. After transfection, cells were fed with fresh DMEM solution until the onset of cytopathic effect. Viruses were propagated in the 293A and purified by ultra centrifugation through two caesium chloride gradients. The titer of adenoviral vectors was determined by plaque assay on 293A cells. Viral stocks were aliquoted and stored in 100 mL/L glycerol at -80 ℃ until use.

Adenovirus IL-10 gene transfection into healthy rats

Sprague-Dawley (SD) rats were purchased from Shanghai BK Experimental Animal Company (Shanghai, China) and maintained in filter-top cages under specific pathogen-free conditions. The Animal Study Ethics Committee of Shanghai Second Medical University approved all experiments. The experiments were conducted in 6-7 week-old male rats, weighing 170-180 g. Adult healthy male SD rats (n = 20) were given a single intraperitoneal injection of adenovirus PBS solution containing 10^{10} pfu of the AdvhIL-10. All injections were performed with a sterile 25-gauge needle in the left lower quadrant of the abdomen. Rats were anesthetized using sodium pentobarbital (40 mg/kg injection, intraperitoneal) and killed 24, 48, 96, and 168 h after transfection. Blood samples were obtained from the celiac artery. The samples were separated and stored at -70 ℃ for determination of amylase. Pancreas, liver and lung were immediately dissected from their attachments and divided for isolation of total RNA and total protein. some samples were fixed in 40 g/L buffered formaldehyde for histopathological test. PBS control group (n = 5) received an intraperitoneal injection of PBS solution, and the empty vector control group (n = 5) was given a single intraperitoneal injection of empty vector (Adv0) containing 10^{10} pfu viruses. Tissues of both control groups were harvested 24 h later as previously described.

Adenovirus IL-10 gene therapy in SAP rats

SD rats (n = 80) were randomly divided into four groups: normal, AdvhIL-10, Adv0, and PBS groups. After laparotomy, SAP model was induced through injection of 0.5 mL of 30 g/L sodium taurocholate via the pancreatic duct. Twenty minutes after sodium taurocholate injection, AdvhIL-10 group received 0.5 mL single intraperitoneal injection of AdvhIL-10 containing 10^{10} pfu of AdvhIL-10. Two control groups received 0.5 mL single intraperitoneal injection of Adv0 (containing 10^{10} pfu viruses) or PBS solution, respectively. In each group, 5 rats were sacrificed by dislocation of the cervical vertebra 24 and 48 h after induction of SAP, respectively. Blood samples were obtained as previously described for determination of amylase. Pancreas, liver, and lungs were harvested as previously described and prepared for RT-PCR, ELISA, and histopathological test. Mortality was observed among the rats 7 d after the initiation of pancreatitis.

Assay

Serum amylase levels were measured at 37 ℃ by an enzymatic assay using a Beckman nucleic acid and protein analyzer DU 640 (BECKMAN, USA) standardized for these rat proteins. All serum samples were assayed in duplicate, and the results were averaged at the end of the experiment. Rat TNF-α, hIL-10 levels in the homogenates were determined using commercially available enzyme-linked immunosorbent assay (ELISA) kits from Diaclone Research International.

IL-10 and TNF-α mRNA expression

Total RNA was extracted from homogenized liver, pancreas, and lung with TRIzol reagent following the manufacturer's instructions. Aliquots of 5 μg of total RNA were reverse-transcribed by using a first-strand cDNA synthesis kit (Promega A3500). The cDNA was then amplified by polymerase chain reaction using primers specific for hIL-10 or TNF-α with β-actin primers serving as controls. The primer sequences and sizes of amplification products were as follows: hIL-10 sense, 5'- GAGCG, GATCC, ATGAA, GTGGG, TAACC, TTTC-3'; antisense, 5'- ATACG, AATTC, CTGCA, GCGGC, CGCCA, CT-3' (540 base pairs); TNF sense, 5'-TGCCT, CAGCC, TCTTC, TCATT-3'; antisense, 5'-ACACC, CATTC, CCTTC, ACAGA-3' (446 base pairs); β-actin sense, 5'-TTGTA, ACCAA, CCTGGG, ACGAT, ATGG-3'; antisense, 5'-TGGAA, GACTC, CTCCC, AGGTA-3' (515 base pairs). Following an initial denaturation at 94 ℃ for 5 min, the samples were amplified by 27 cycles of denaturation at 94 ℃ for 40 s, annealing at 58 ℃ for 50 s, extension at 72 ℃ for 90 s, and ended by extension at 72 ℃ for 15 min. The PCR reaction products were separated on 20 g/L agarose gels. Photo-micrographs of ethidium bromide stained gels were taken. Relative mRNA levels of hIL-10, TNF-α and β-actin were determined by computer-assisted densitometric scanning.

Histopathological analysis

Pancreas samples were fixed in 40 g/L buffered formaldehyde and embedded in paraffin.Then the samples were cut into 5 μm thick sections,and stained with haematoxylin and eosin for light microscropic examination. Histological assessment was performed by an investigator blinded to the treatment group. The severity of pancreatitis was determined by the degree of edema, hemorrhage, inflammation and necrosis[11].

Statistical analysis

Results were expressed as mean±SD. Differences between groups were compared by two-way ANOVA. P<0.05 was considered statistically significant. Mortality was assessed by Kaplan-Meier and log rank analysis. All data processing was done with a statistical program, SPSS 11.0.

RESULTS

hIL-10 levels in pancreas, liver, and lung at 24 h post- transfection in healthy rats

Twenty-four h after transfection, The normal and two control groups did not show hIL-10 protein expression.

hIL-10 protein was effectively measured in healthy rats after AdvhIL-10 administration. The hIL-10 level in pancreas, liver, and lung increased and reached its peak at 24 h post-transfection, then decreased gradually 4 d after transfection. The hIL-10 level in the tissues was undetectable 7 d post-transfection, and was the highest in the liver among the three observed organs (Figure 1A).

Serum amylase levels and histological changes in healthy rats

There were no significant differences in serum amylase level among the rats effectively transfected with AdvIL-10 and Adv0 and PBS treated rats in the duration of the experiment (Figure 6, P>0.05). In addition, no detectable histology alternation of the pancreas, liver, and lungs was observed in the transfected rats.

Panceatic edema, hyperemia, exudation and necrosis were not detected. These findings indicated that adenovirus gene transfer could be performed safely.

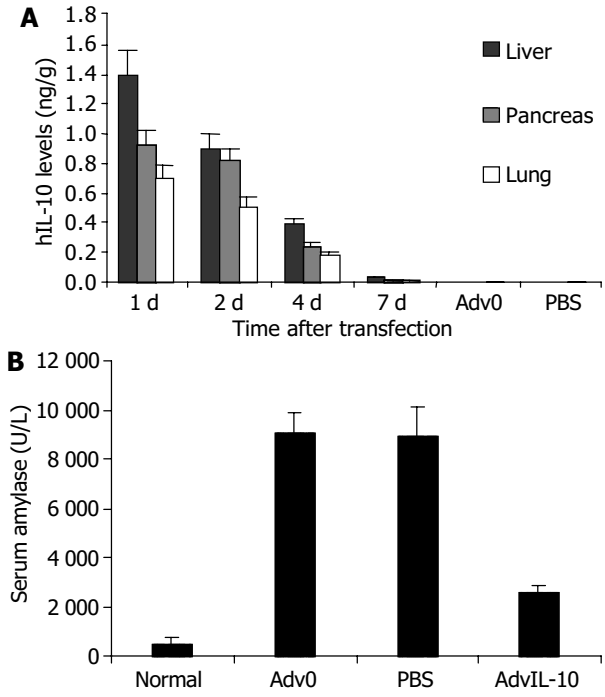

Figure 1 hIL-10 levels and serum amylase levels in pancreas, liver, and lung after adminstration of AdvIL-10, Adv0, and PBS in healthy and SAP rats. A: hIL-10 levels in pancreas, liver and lung after administration of AdvIL-10, Adv-0 and PBS in healthy rats. B: Serum amylase levels in pancreas, liver and lung after administration of AdvIL-10, Adv-0 and PBS in SAP rats.

Serum amylase in SAP rats

The SAP rats treated with Adv0 and PBS showed a significant increase in serum amylase level compared to normal rats (P<0.05). Transfection with AdvhIL-10 after induction of pancreatitis decreased the severity of SAP, as evidenced by markedly attenuated amylase production compared to the two control SAP groups (Figure 1B, P<0.05).

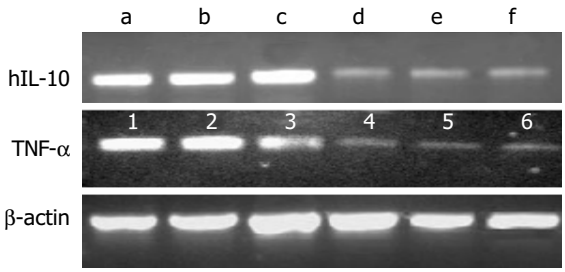

Figure 2 Expression of IL-10 and TNF-α in SAP rat tissues 24 h post- transfection with AdvhIL-10 and PBS. Lanes a, b and c: IL-10 expression in liver, pancreas, and lung, respectively, in AdvIL-10 treated SAP rats; Lanes d, e and f: IL-10 expression in liver, pancreas, and lung, respectively, in the PBS treated SAP rats; Lanes 1, 2, and 3: TNF-α expression in liver, pancreas, and lung, respectively, in PBS treated SAP rats; Lanes 4, 5, and 6: TNF-α expression in liver, pancreas, and lung, respectively, in AdvIL-10 treaed SAP rats. β-actin served as control.

IL-10 and TNF-α mRNA expression in SAP rats

HIL-10 mRNA was strongly expressed in the AdvhIL-10 treated pancreatitis rats 24 h post-tranfection. The levels of hIL-10 in pancreas, liver, and lung did not show significant difference. A weak expression of hIL-10 was observed in Adv0 and PBS treated pancreatitis rats 24 h post-tranfection. TNF-α gene in the normal rats was not detected. The expression of TNF-α gene was significantly higher in the pancreatitis rats treated with Adv0 and PBS than that in those treated with AdvhIL-10 (P<0.05, Figure 2). In the AdvhIL-10 group, the level of TNF-α gene was moderate in pancreas and weak in the liver and lung (Figure 3).

Levels of hIL-10 and TNF-α proteins in SAP rats

The levels of IL-10 in pancreas, liver and lung in the AdvhIL-10 group were markedly higher than those in the two control groups 24 and 48 h post-transfection (P<0.05). No significant difference was observed between the two control groups (Figure 3A). In normal rats, TNF-α expression was undetectable. Twenty-four h after induction of pancreatitis, TNF-α level was significantly higher in Adv0 and PBS groups than that in AdvIL-10 group (P<0.05, Figure 3B).

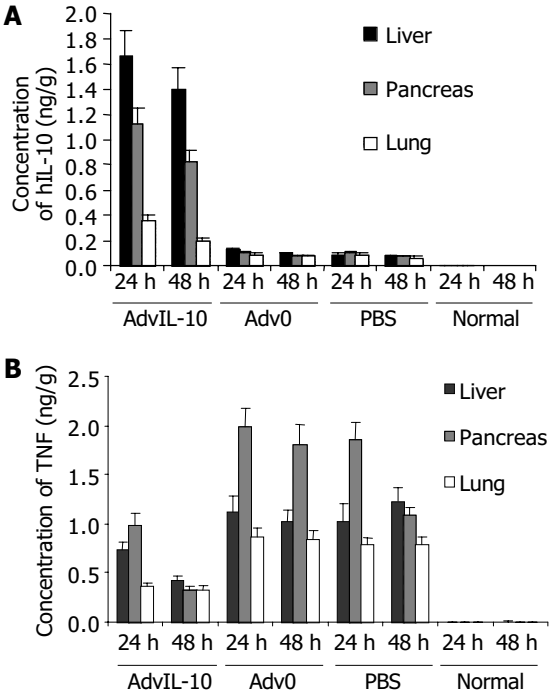

Figure 3 hIL-10 and TNF-α levels in liver, pancreas, and lungs of SAP rats after treatment with AdvIL-10, Adv0, and PBS. A: hIL-10 levels in liver, pancreas and lungs of SAP rats after treatment with AdvIL-10, Adv-0 and PBS. B: TNF-α levels in liver, pancreas and lungs of SAP rats after treatment with Adv-10, Adv-0 and PBS.

Histopathological changes

Hematoxylin and eosin-stained sections of pancreas from pancreatitis rats treated with Adv0 and PBS showed an increase in inflammation, hemorrhage, and necrosis after injection of sodium taurocholate. The histological changes in the AdvIL-10 treated pancreatitis rats were mild compared with the control groups. Most of the pathological parameters of pancreatic injury were significantly decreased in pancreatitis rats transfected with AdvIL-10 gene compared to the pancreatitis rats treated with Adv0 and PBS (P<0.05, Table 1, Figure 4).

Mortality

No significant difference in mortality was observed between the two control SAP groups within 7 d after SAP inducetion, 90% of the rats were died in the Adv0 and PBS treated groups, while only 20% of the rats were died in the AdvIL-10 gene therapy group (Figure 5).

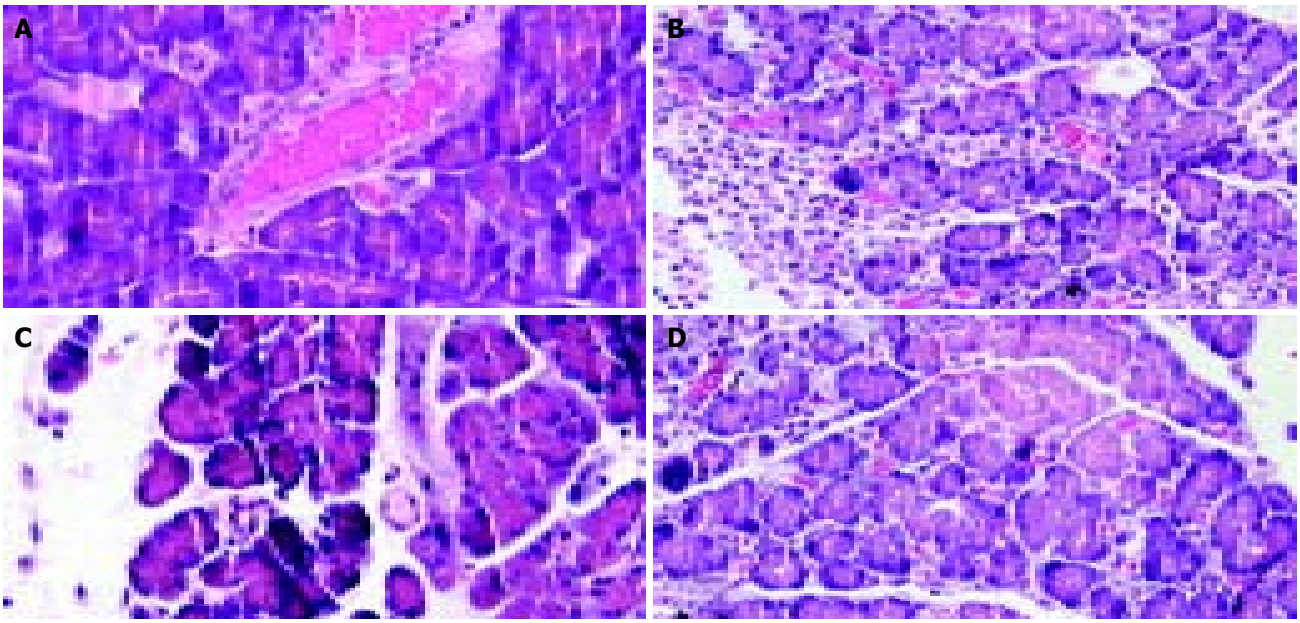

Figure 4 Histological sections of rat pancreas (HE, 200×). A: Normal rat pancreas; B: Severe necrotizing acute pancreatitis with hemorrhage and necrosis 24 h after induction with sodium taurocholate; C: Acute pancreatitis in rats treated with AdvhIL-10; D: Acute pancreatitis in rats treated with PBS (the pathology changes in the Adv0 group were completely the same as PBS group).

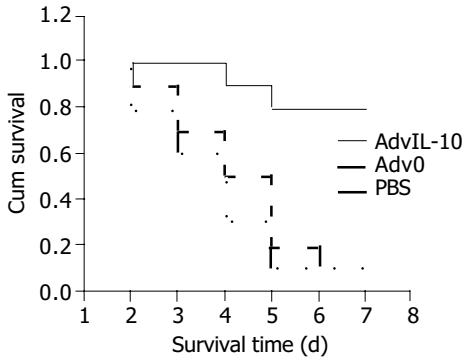

Figure 5 Survival rate of SAP rats after treatment.

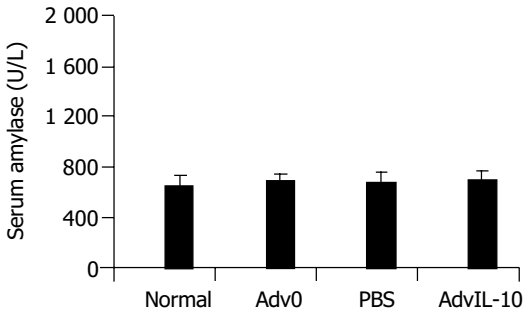

Figure 6 Serum amylase levels in heathy rats 24 h after transfection with Adv0, PBS and AdvIL-10.

Table1 Histological scores of pancreas from rats with SAP (mean±SD)

	Normal	PBS (or Adv0)	hIL-10 transfected
Edema	0±0	2.26±0.13	1.74±0.13
Necrosis	0±0	2.56±0.21	0.51±0.13
Inflammation	0±0	3.43±0.14	0.46±0.14
Hemorrhage	0±0	2.31±0.17	0.13±0.11

DISCUSSION

IL-10 gene therapy has been widely explored for the treatment of many diseases, including intestinal transplantation immune regulation, bronchiolitis, endotoxemia, and rheumatoid arthritis[12-15]. In the present report, we explored the tissue levels, distribution, and biological responses of hIL-10 mediated by adenoviral vectors in healthy and pancreatitis rats. Adenovirus vector has many advantages. Adenovirus genomes did not integrate into the host cell chromosome and had a high efficiency gene transfer than cationic liposome regardless of the proliferative state of tissues. Although the duration of gene expression was short, the level of therapeutic gene expression was much higher [16]. Adenoviral vectors could bind to cell surface integrins and gain entry by receptor mediated endocytosis using receptors such as Coxsackie virus and adenovirus receptor[17]. Thus, adenoviral vector could offer the opportunity to target specific tissues for highly local expression, owing to special tropism for pulmonary epithelial cells, hepatocytes, and pancreatic epithelial cells[18-20]. Expression of adenoviral vector was rapid, protein appearance usually occurred within hours and peak concentration appeared within 1-2 d after adenoviral administration[21]. Furthermore, adenovirus vectors could be prepared at a much higher titre.

Norman James[22] reported that with very few exceptions, cytokines were not constitutively produced. The results of our experiment is consistent with Norman James's results. We explored the use of adenovirus based gene therapy to deliver hIL-10 gene intraperitoneally to healthy and pancreatitis rats. Tissue hIL-10 protein was highly produced 24, 48 h after AdvhIL-10 was injected into peritoneal cavity of healthy rats. The current study demonstrated that the current adenovirus delivery system could offer a highly efficient transfection and well-correlated tissue accummulation. We also found that highly efficient transfection with AdvhIL-10 did not result in an increase in amylase and lipase or any alteration in pancreatic histopathology. Therefore, adenoviral vector mediated hIL-10 gene delivery in healthy rats was well tolerable and safe. In SAP rats, AdvhIL-10 attenuated the release of serum amylase and decreased histologic injury significantly. In addition, the action of TNF-α could also be diminished by IL-10. The important factor of our experiment was the increase of survival rate resulted from adenoviral vector mediated hIL-10 gene delivery in rats with lethal acute pancreatitis. These results are consistent with several previous reports on adenoviral vector-mediated gene therapy in pancreatitis and acute lung inflammation[9,23,24].

There is sufficient evidence (immunological, pathophysiological, and biochemical) that SAP is a systemic rather than a local critical condition. The severity of the process varied from a limited local inflammation of the pancreas to a systemic multiorgan failure. SAP was characterised by enzyme activation, interstitial edema, hemorrhage and necrosis[25]. Many pro- and anti- inflammation cytokines are involved in the initiation of acute pancreatitis. IL-10, produced by TH2 cells, macrophages, stellate cells and hepatocytes, has been reported to play an important role in inflammatory diseases[26]. It has been reported the deficiency of IL-10 gene could prompte colitis and fibrosis probably by its failure in inhibiting the overproduction of tumor growth factor-β_1 and TNF[27,28]. The later is secreted by macrophages and can enhance inflammation in a local site. In animals, IL-10 is endogenously released during inflammatory diseases, and its blockade could result in higher elevations of TNF as well as more severe histologic injury[10]. Production of large quantities of exogenous IL-10 in local sites of inflammation could change the balance of pro- and anti- inflammation cytokines and block the production and release of TNF and other pro-inflammation cytokines. IL-10 adminstration could improve of local and systemic conditions. In the current study, exogenous hIL-10 was found to be able to inhibit the progress of acute pancreatitis in rats. Similar results were also reported by previous studies[10,11].

The time to administrate AdvIL-10 seems to be very important, since it takes time to transfect and express protein. Thus, early administration of AdvIL-10 might block the induction of TNF and IL-1[5]. Kato *et al*. reported that the time to administratie hIL-10 should be in the early period of sepsis. In the current study, hIL-10 gene was administrated 20 min after the induction of SAP, and the highest level of IL-10 protein was observed 24 h after adminstration, which was very similar to a previous study by Denham *et al*.[10].

In conclusion, human genes can be effectively transfected into rat pancreas, livers, and lungs using a adenoviral vector-mediated delivery system. Transfection of hIL-10 gene can decrease the severity of pancreatitis and improve the survival rate. As gene therapy is becoming a more acceptable method of treatment, it is anticipated that adenovirus-based gene therapy will become available as a drug delivery system. Cytokine modulating therapies, like IL-10, represent an attractive therapeutic approach for the treatment of acute pancreatitis patients in clinic.

REFERENCES

1 **Viedma JA**, Perez-Mateo M, Dominguez JE, Carballo F. Role of C-reactive protein and phospholipase A. *Gut* 1992; **33**: 1264-1267
2 **Grewal HP**, Mohey el Din A, Gaber L, Kotb M, Gaber AO. Amelioration of the physiologic and biochemical changes of acute pancreatitis using an anti-TNF alpha polyclonal antibody. *Am J Surg* 1994; **167**: 214-218
3 **Walley KR**, Lukacs NW, Standiford TJ, Strieter RM, Kunkel SL. Balance of inflammatory cytokines related to severity and mortality of murinesepsis. *Infect Immun* 1996; **64**: 4733-4738
4 **Weiss YG,** Deutschman CS. Modulation of gene expression in critical illness: a new millennium or a brave new world? *Crit Care Med* 2000; **28**: 3078-3079
5 **Rongione AJ**, Kusske AM, Kwan K, Ashley SW, Reber HA, McFadden DW. Interleukin 10 reduces the severity of acute pancreatitis in rats. *Gastroenterology* 1997; **112**: 960-967
6 **Gazzinelli RT**, Oswald IP, James SL, Sher A. IL-10 inhibits parasite killing and nitrogen oxide production by IFN-gamma-activated macrophages. *J Immunol* 1992; **148**: 1792-1796
7 **Pradier O**, Gerard C, Delvaux A, Lybin M, Abramowicz D, Capel P, Velu T, Goldman M. Interleukin-10 inhibits the induction of monocyte procoagulant activity by bacterial lipopolysaccharide. *Eur J Immunol* 1993; **23**: 2700-2703
8 **Howard M**, Muchamuel T, Andrade S, Menon S. Interleukin 10 protects mice from lethal endotoxemia. *J Exp Med* 1993; **177**: 1205-1208
9 **Minter RM**, Ferry MA, Murday ME, Tannahill CL, Bahjat FR, Oberholzer C, Oberholzer A, LaFace D, Hutchins B, Wen S, Shinoda J, Copeland EM 3rd, Moldawer LL. Adenoviral delivery of human and viral IL-10 in murine sepsis. *J Immunol* 2001; **167**: 1053-1059
10 **Denham W**, Denham D, Yang J, Carter G, MacKay S, Moldawer LL, Carey LC, Norman J. Transient human gene therapy: a ovel cytokine regulatory strategr for experimental pancreatitis. *Ann Surg* 1998; **227**: 812-820
11 **Zou WG**, Wang DS, Lang MF, Jin DY, Xu DH, Zheng ZC, Wu ZH, Liu XY. Human interleukin 10 gene therapy decreases the severity and mortality of lethal pancreatitis in rats. *J Surg Res* 2002; **103**: 121-126
12 **Zhu M**, Wei MF, Liu F, Shi HF, Wang G. Interleukin-10 modified dendritic cells induce allo-hyporesponsiveness and prolong small intestine allograft survival. *World J Gastroenterol* 2003; **9**: 2509-2512
13 **Boehler A**, Chamberlain D, Xing Z, Slutsky AS, Jordana M, Gauldie J, Liu M, Keshavjee S. Adenovirus-mediated interleukin-10 gene transfer inhibits post-transplant fibrous airway obliteration in an animal model of bronchiolitis obliterans. *Hum Gene Ther* 1998; **9**: 541-551
14 **Xing Z**, Ohkawara Y, Jordana M, Graham FL, Gauldie J. Adenoviral vector-mediated interleukin-10 expression *in vivo*: intramuscular gene transfer inhibits cytokine responses in endotoxemia. *Gene Ther* 1997; **4**: 140-149
15 **Whalen JD**, Lechman EL, Carlos CA, Weiss K, Kovesdi I, Glorioso JC, Robbins PD, Evans CH. Adenoviral transfer of the viral IL-10 gene periarticularly to mouse paws suppresses development of collagen-induced arthritis in both injected and uninjected paws. *J Immunol* 1999; **162**: 3625-3632
16 **Wickham TJ**. Targeting adenovirus. *Gene Therapy* 2000; **7**: 110-114
17 **Bergelson JM**, Cunningham JA, Droguett G, Kurt-Jones EA, Krithivas A, Hong JS, Horwitz MS, Crowell RL, Finberg RW. Isolation of a common receptor for Coxsackie B viruses and adenoviruses 2 and 5. *Science* 1997; **275**: 1320-1323
18 **Crystal RG**. The gene as the drug. *Nat Med* 1995; **1**: 15-17
19 **Worgall S**, Wolff G, Falck-Pedersen E, Crystal RG. Innate immune mechanisms dominate elimination of adenoviral vectors following *in vivo* administration. *Hum Gene Ther* 1997; **8**: 37-44
20 **Weber M**, Deng S, Kucher T, Shaked A, Ketchum RJ, Brayman KL. Adenoviral transfection of isolated pancreatic islets: a study of programmed cell death (apoptosis) and islet function. *J Surg Res* 1997; **69**: 23-32
21 **Minter RM**, Rectenwald JE, Fukuzuka K, Tannahill CL, La Face D, Tsai V, Ahmed I, Hutchins E, Moyer R, Copeland EM 3rd, Moldawer LL. TNF-alpha receptor signaling and IL-10 gene therapy regulate the innate and humoral immune responses to recombinant adenovirus in the lung. *J Immunol* 2000; **164**: 443-451
22 **Norman J**. The role of cytokines in the pathogenesis of acute pancreatitis. *Am J Surg* 1998; **175**: 76-83
23 **Van Laethem JL**, Marchant A, Delvaux A, Goldman M, Robberecht P, Velu T, Deviere J. Interleukin 10 prevents necrosis in murine experimental acute pancreatitis. *Gastroenterology* 1995; **108**: 1917-1922
24 **Minter RM**, Ferry MA, Rectenwald JE, Bahjat FR, Oberholzer A, Oberholzer C, La Face D, Tsai V, Ahmed CM, Hutchins B, Copeland EM 3rd, Ginsberg HS, Moldawer LL. Extended lung expression and increased tissue localization of viral IL-10 with adenoviral gene therapy. *Proc Natl Acad Sci U S A* 2001; **98**: 277-282
25 **Jungermann J**, Lerch MM, Weidenbach H, Lutz MP, Kruger B, Adler G. Dissassembly of rat pancreatic acinar cytoskeleton during supramaximal secretagogue stimulation. *Am J physiol* 1995: G328-338
26 **De Vries JE**. Immunosuppressive and anti-inflammatory properties of interleukin 10. *Ann Med* 1995; **27**: 537-541
27 **Lindsay JO**, Ciesielski CJ, Scheinin T, Hodgson HJ, Brennan FM. The prevention and treatment of murine colitis using gene therapy with adenoviral vectors encoding IL-10. *J Immunol* 2001; **166**: 7625-7633
28 **Thompson K**, Maltby J, Fallowfield J, McAulay M, Millward-Sadler H, Sheron N. Interleukin-10 expression and function in experimental murine liver inflammation and fibrosis. *Hepatology* 1998; **28**: 1597-1606

Edited by Kumar M and Wang XL **Proofread by** Xu FM

PO Box 2345, Beijing 100023, China
Fax: +86-10-85381893
E-mail: wjg@wjgnet.com www.wjgnet.com

World J Gastroenterol 2004;10(20):3026-3033
World Journal of Gastroenterology
 ISSN 1007-9327

• BASIC RESEARCH •

Changes of inflammation-associated cytokine expressions during early phase of experimental endotoxic shock in macaques

Xiao-Hui Ji, Ke-Yi Sun, Yan-Hong Feng, Guo-Qing Yin

Xiao-Hui Ji, Ke-Yi Sun, Department of Microbiology and Immunology, Nanjing Medical University, Nanjing 210029, Jiangsu Province, China
Yan-Hong Feng, Guo-Qing Yin, Department of Infectious Diseases, Second Hospital of Medical College, Southeast University, Nanjing 210003, Jiangsu Province, China
Supported by the Foundation of the Municipal Government of Nanjing, No. ZKG9809 and Health Bureau of Jiangsu Province, No. TS9904
Correspondence to: Xiao-Hui Ji, Department of Microbiology and Immunology, Nanjing Medical University, 140 Hanzhong Road, Nanjing 210029, Jiangsu Province, China. immune@njmu.edu.cn
Telephone: +86-25-86862654 **Fax:** +86-25-86862655
Received: 2003-11-12 **Accepted:** 2003-12-22

Abstract

AIM: To study changes of inflammation-associated cytokine expressions during early phase of endotoxic shock in macague.

METHODS: Experiments were performed in *Macaque mulatta* treated with LPS 2.8 mg/kg in shock model group or with normal saline in control group. Blood samples were collected before, or 60 min, or 120 min after LPS injection, respectively. Liver and spleen tissues were obtained at 120 min after LPS injection. The plasma levels of TNF-α, IL-1 β, IL-10 and IL-12P40 were determined by double-antibody sandwich ELISA with antibodies against human cytokines. The mRNA levels of TNF-α, IL-1 β, and IL-18 in peripheral blood mononuclear cells (PBMCs), liver and spleen were examined by real-time fluorescence semi-quantitative RT-PCR with the primers based on human genes.

RESULTS: Mean systemic arterial pressure (MAP), systemic vascular resistance index (SVRI) and left ventricular work index (LVWI) of macaques were significant declined in shock model group on average 60 min after LPS injection. The plasma levels of TNF-α and IL-10 were significantly increased 60 min after LPS injection and then decreased. The plasma levels of IL-1 β and IL-12P40 were significantly increased at 120 min after LPS injection. The mRNA levels of TNF-α and IL-1 β were significantly increased 60 min after LPS stimulation in PBMCs and 120 min after LPS stimulation in livers. The mRNA level of IL-18 was significantly increased 120 min after LPS stimulation in PBMCs and livers. But in spleen, only TNF-α mRNA level in LPS group was significantly higher 120 min after LPS stimulation, compared with that in control group.

CONCLUSION: An endotoxic shock model of *Macaque mulatta* was successfully established. Both antibodies for ELISA and PCR primers based on human cytokine assays were successfully applied to detect macaque cytokines. In the model, inflammatory cytokines, such as TNF-α, IL-1 β, IL-12 and IL-18 as well as anti-inflammation cytokine IL-10, were released at very early phase of endotoxic shock within 120 min after LPS injection. PBMCs and liver cells might be the important sources of these cytokines.

Ji XH, Sun KY, Feng YH, Yin GQ. Changes of inflammation-associated cytokine expressions during early phase of experimental endotoxic shock in macaques. *World J Gastroenterol* 2004; 10(20): 3026-3033
http://www.wjgnet.com/1007-9327/10/3026.asp

INTRODUCTION

Endotoxin-induced shock mostly occurs during serious infection with Gram-negative bacteria. Lipopolysaccharide (LPS), residing in the outer membrane of all Gram-negative bacteria and being the major component of Gram-negative bacteria cell walls and the toxic component of endotoxin, is considered as an important initiating factor of the Gram-negative septic syndrome in human. Gram-negative sepsis has aroused great concern in clinic because of its high mortality. But LPS is not the direct causative factor. It is well known that LPS activates immunocytes, such as monocyte-macrophage and lymphocyte, and induces these cells to excessively release a series of potent inflammatory cytokines, including TNF- α, IL-1 β, IL-6, IL-8 and IL-18. It is the excessive cytokines, such as TNF- α, IL-1 β, IL-6 and IL-18, that result in high fever, hypotension, vascular endothelial cell damage and disseminated intravascular coagulation, blood capillary leak syndrome, and multiple organ failure. On the other hand, in patients with primary liver injury, such as viral hepatitis, LPS plays an important role in intestinal endotoxemia, which in turn induces secondary liver injury and liver failure[1]. New therapeutic concepts for the treatment of endotoxic shock or endotoxemia with anti-inflammatory cytokines have been developed. Although knowledge about the changes of inflammation-associated cytokines during endotoxemia and endotoxic shock has been well addressed, the change pattern of inflammatory cytokines just during the early phase of endotoxemia and endotoxic shock is still not clear and worth working on, because it can help the selection of new therapeutic targets. The therapies in early phase are more effective.

The aim of the present study was to investigate the changes of TNF- α, IL-1 β IL-10, IL-12 and IL-18 expressions during early phase (within 120 min) of endotoxic shock in macaques.

MATERIALS AND METHODS

Animals

Totally 25 macaques (*Macaca mulatta*) of 5-8 years old, weighing 4.8-9.2 kg (6.17±1.1 kg), were obtained from Shanghai Laboratory Animal Center, Chinese Academy of Sciences. All animal studies were carried out in accordance with the institutional regulations concerning animal experimentation of the Ministry of Health of China. The animals were housed at 10-25 ℃ with light, around 8-10 h per day for, at least, a week before experiment. One of 25 macaques was used in preliminary experiment for the optimal dose of LPS at which hypotension and shock should be induced. The other 24 macaques were divided into two groups: 19 in LPS group and 5 in normal saline (NS) group.

Agents

LPS, derived from *E. coli* O127: B8 and prepared by phenol

extraction, was purchased from Sigma Co. (Saint Louis, USA). ELISA kits for detecting human TNF- α, IL-1 β, IL-10 and IL-12 P40/ P70 were from Pharmingen (San Diego, USA). TriZol RNA extraction kit was from Gibco (Grand Island, USA). Moloney murine leukemia virus (M-MLV) reverse transcriptase, RNase inhibitor, PCR kit and PGEM-T vector were all from Promega (Shanghai, China). PCR product purification kit was from Boehringer Mannheim Co. (Mannheim, Germany). Plasmid DNA extraction kit was from Scientz Bio Co. (Shanghai, China).

PCR primers

In order to determine the mRNA expression levels of inflammatory cytokines by RT-PCR, some pairs of primers based on specific sequences published previously were used. These primers, synthesized in ShengGong Biotech Co. (Shanghai, China), are shown in Table1.

Establishment of endotoxic shock model

In the pilot experiment, one macaque was used to find out optimal dose of LPS. Intravenous injection of LPS of 2.8 mg/kg resulted in reduction of mean arterial pressure (MAP) from 17.55 to 10.80 kPa. This dosage was applied to establish macaque model of endotoxic shock in this experiments. After being fasted overnight, macaques were anesthetized with ketamine (15 mg/kg, intramuscularly), then they were mechanically ventilated with a ventilator (SERVE900c, Siemens- Elama) through trachea intubator. Tidal volume was set at 12 mL/kg and the respiratory rate at 20 beat/min during experiment. A value of 5 cm H_2O (1 cm H_2O = 0.098 kPa) of positive end-expiratory pressure was applied to maintain end-expiratory lung volume. Anesthesia was maintained with repeated intravenous injection of sodium γ-hydroxybutyl acid (200 mg/kg·h) and intramuscular injection of fentanylicitras (a bolus of 6 μg/kg·30 min). A pulmonary artery catheter was placed in the jugular vein for detecting hemodynamic parameters by thermodilution (Siemens,). After percutaneous puncture, the catheter was introduced into the femoral artery and forwarded into the abdominal aorta for measuring blood pressure. Nineteen animals in the shock group were given a dose of 2.8 mg/kg LPS i.v., while 5 animals in the control group were given 1 mL/kg normal saline. Occurrences of endotoxic shock were confirmed by reduction of MAP by 30% and by other hemodynamic changes, such as the reduction of systemic vascular resistance index (SVRI) or left ventricular work index (LVWI), in LPS group. It took 60 min on average to establish shock after LPS injection. Venous blood of 18 animals in LPS group and 5 animals in NS control group were collected at 0, 60 and 120 min after LPS or NS injection for detection of inflammation-associated cytokines. Then, the macaques were sacrificed for detecting myocardial damages in another sub-study of this project. At the same time, a small portion of liver and spleen tissues were sliced and stored at -80 ℃ after being rapidly frozen in liquid nitrogen for mRNA assays.

Blood processing

Blood from the macaques, anticoagulated with EDTA-Na_2, were centrifuged, at 1 500 r/min×10 min, to separate plasma from cells. The plasma were stored at -20 ℃ for cytokines detection. The sedimentary cells were resuspended with Hanks' solution and the cell suspension was centrifuged with Ficoll-Hypaque lymphocyte separating medium, at 2 000 r/min×20 min, to get peripheral blood mononuclear cells (PBMCs). After being rapidly frozen in liquid nitrogen, PBMCs from the macaques were stored at -80 ℃ for mRNA assays.

Plasma cytokines detection

The levels of TNF-α, IL-1 β, IL-10 and IL-12P40/P70 in plasma were determined by double-antibodies sandwich ELISA using the kits. The assays were performed according to the kit protocol.

Test for intracellular cytokine mRNA

PBMCs of 10^6 and liver or spleen tissue of 0.1 g were used to extract total cytoplasmic RNA according to the TriZol method. The total RNA was converted to complementary DNA (cDNA) by a reverse transcription step with M-MLV reverse transcriptase, OligodT primer, RNase inhibitor and dNTPs. Using the cDNA, specific primers, SYBR-Green I and PCR kit, a series of real-time semi-quantitative PCR were performed with a DNA amplifier (PE5700) to determine levels of mRNA coding for TNF- α, IL-1 β and IL-18, as well as β-actin which was used in the assay as an internal control, in PBMCs, liver and spleen. cDNA samples were amplified for 40 cycles: denaturation at 94 ℃ for 30 s, annealing at 60 ℃ for 60 s and extension at 68 ℃ for 120 s. The ratio of fluorescence intensity of cytokine-specific product to that of the internal control product represents relative levels of cytokine mRNA expression. After PCR, the products were cloned into PGEM-T vector, which was then used to transform JM109 *E. coli*. The plasmid DNAs of positive clones were extracted for sequencing.

Statistical analysis

All results were expressed as mean±SD. The significances of differences between LPS shock group and NS control group were evaluated by *t*-test. Testing standard was set at $\alpha = 0.05$. $P<0.05$ indicates a significant difference, and $P<0.01$ indicates a remarkably significant difference.

RESULTS

Change of TNF-α within 120 min after LPS administration

Plasma concentration of TNF-α in LPS group increased earlier and was significantly higher than that in NS group at 60 min after LPS administration, then decreased to a level similar to that in NS group. This result is shown in Figure 1A. The dynamics for TNF-α mRNA expression by PBMCs in LPS group was similar to that for plasma TNF-α concentration. The result is shown in Figure 1B.

Table 1 PCR primer sequences for TNF-α , IL-1 β and IL-18 detection

Cytokine	Primer	Sequence	Reference
Human TNF- α	upstream	TCA CAG GGC AAT GAT CCC AAA GTA GAC CTG C	[2,3]
	downstream	ATG AGC ACT GAA AGC ATG ATC	
Human IL-1 β	upstream	TTA GGA AGA CAC AAA TTG CAT GGT GAA	[2,3]
	downstream	ATG GCA GAA GTA CCT GAG CTC	
Human IL-18	upstream	GCT TGA ATC TAA ATT ATC AGT C	[4]
	downstream	GAA GAT TCA AAT TGC ATC TTA T	
Human β-actin	upstream	TTC CAG CCT TCC TTC CTG G	[5]
	downstream	TTG CGC TCA GGA GGA GCA AT	

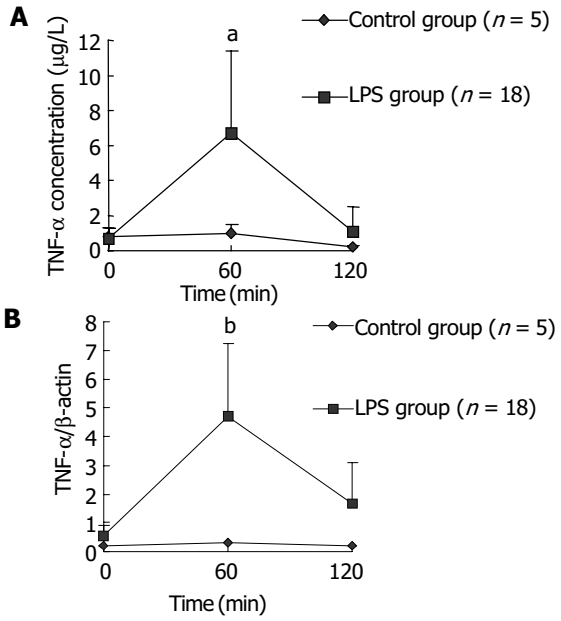

Figure 1 Kinetics curves for TNF-α expression in macaque plasma (A) and. PBMCs (B) within 120 min after LPS administration. [a]*P*<0.05 *vs* control group; [b]*P*<0.01 *vs* control group.

The expression levels of TNF-α mRNA in liver and spleen in LPS group were remarkably higher than those in NS control group at 120 min after LPS challenge. The results were presented in Figure 2.

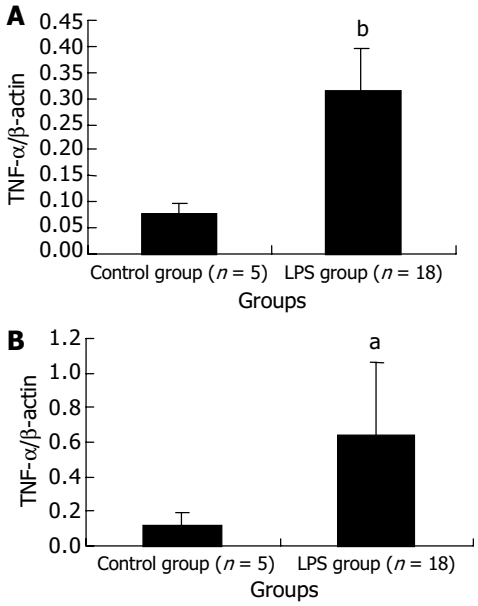

Figure 2 Transcript levels of TNF-α mRNA in liver (A) and spleen (B) at 120 min after LPS administration. [a]*P*<0.05 *vs* control group, [b]*P*<0.01 *vs* control group.

Change of IL-1 β within 120 min after LPS administration

The plasma IL-1 β level in LPS group began to rise at 60 min after LPS challenge and was significantly higher at 120 min after LPS challenge, compared with that in NS control group. Whereas the IL-1 β transcription level in PBMCs rose earlier than plasma IL-1 β level. The transcription level of IL-1 β in PBMCs of LPS group was significantly higher than that in control group at 60 min after LPS injection, and then dropped to a level similar to that in control group after another 60 min. Figure 3 shows the changes of plasma level and transcription level of IL-1 β within 120 min after LPS injection.

The transcript level of IL-1 β mRNA in the liver of LPS group remarkably increased at 120 min after LPS administration. But the level in the spleen did not show a significant increase. These results are shown in Figure 4.

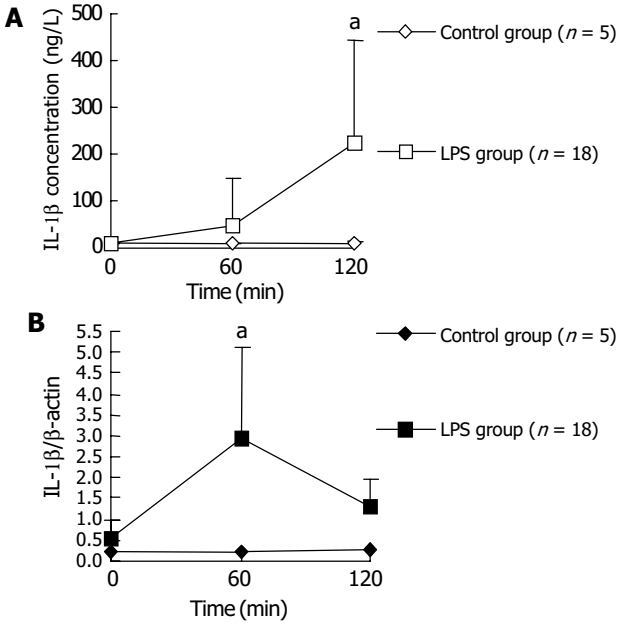

Figure 3 Dynamics of IL-1 β expression in macaque plasma (A) and PBMCs (B) within 120 min after LPS challenge. [a]*P*<0.05 *vs* control group.

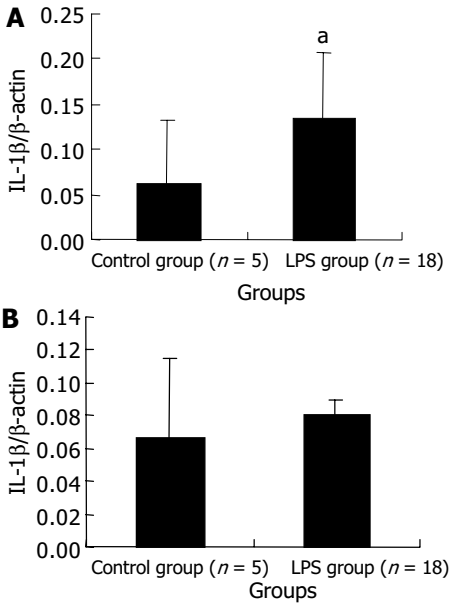

Figure 4 Transcript levels of IL-1 β mRNA in liver(A) and spleen(B) at 120 min after LPS administration. [a]*P*<0.05 *vs* control group.

Changes of IL-18 mRNA expression in PBMCs, liver and spleen within 120 min after LPS administration

The expression level of IL-18 mRNA in PBMCs gradually increased with LPS challenge and a statistical significance could be found at 120 min after LPS challenge. The results are presented in Figure 5. Data in Figure 6 indicate at 120 min after LPS challenge, the expression levels of IL-18 mRNA in LPS group were significantly higher in liver cells, not in spleen cells, compared with those in control group after NS injection.

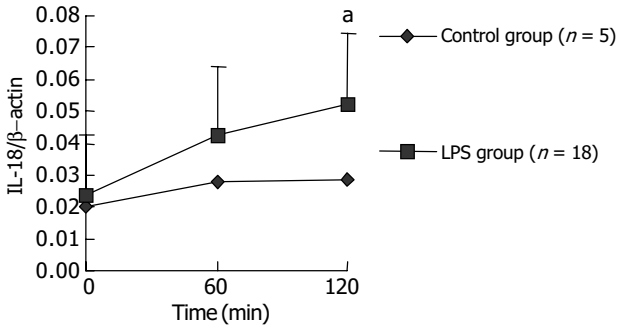

Figure 5 The change of IL-18 mRNA transcript level in PBMCs within 120 min after LPS challenge. $^aP<0.05$ *vs* control group.

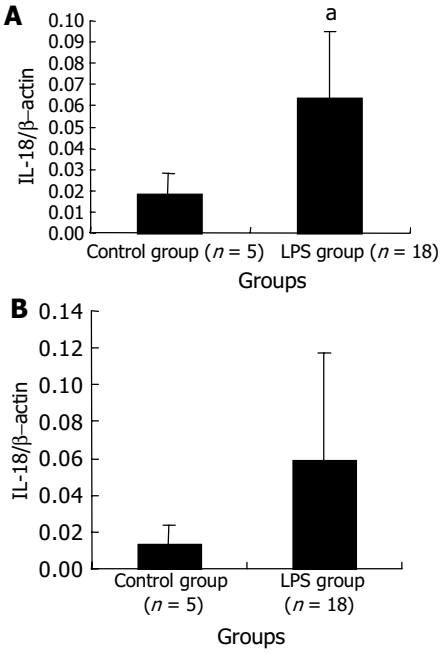

Figure 6 The levels of IL-18 mRNA transcript in liver (A) and spleen (B) at 120 min after LPS challenge. $^aP<0.05$ *vs* control group.

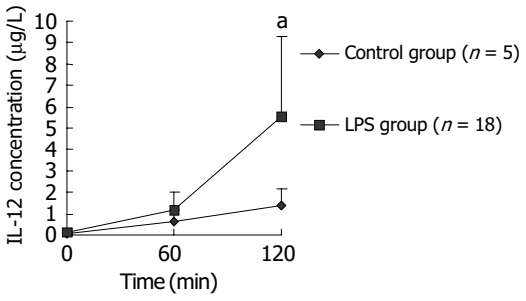

Figure 7 Change of plasma IL-12 levels within 120 min after LPS challenge. $^aP<0.05$ *vs* control group.

Change of plasma IL-12 levels within 120 min after LPS challenge

Sixty minutes after LPS challenge, plasma IL-12P40/P70 level of macaques in LPS group gradually rose and was significantly higher than that in control group at 120 min after LPS challenge. Data are supplied in Figure 7.

Change of plasma IL-10 levels within 120 min after LPS administration

Immediately after LPS administration, plasma IL-10 level of macaques in LPS group increased slightly, and showed a statistically significant rise at 60 min after LPS injection, compared with control group. Thereafter the level gradually declined to normal level. The results are shown in Figure 8.

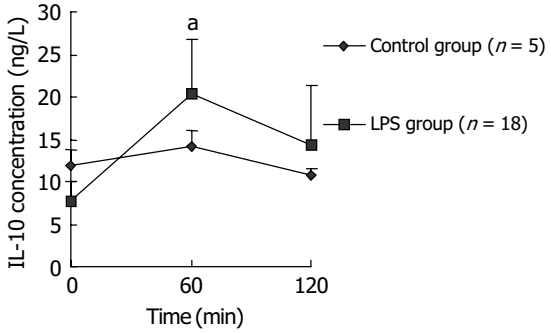

Figure 8 Change of plasma IL-10 level within 120 min after LPS injection. $^aP<0.05$ *vs* control group.

DISCUSSION

Endotoxic shock model

A series of endotoxic shock animal models have been established for studies. *Macaque Mulatta* belongs to primate animals. The physiological functions and anatomical features are similar among primates, including humans. Therefore, it is important to study primate model of endotoxic shock in order to understand septic shock in human. In the present study, an endotoxic shock model of macaque was established to study about changes of inflammation-associated cytokines during early phase of endotoxic shock.

In human volunteers, an intravenous injection with endotoxin bolus of 2-4 ng/kg caused pyrexia, cytokine release and mild decline of MAP[6,7]. In non-human primate, however, LPS sensitivities were quite different: chimpanzee shared the sensitivity of human to LPS, while baboons and rhesus macaques were insensitive to LPS like rodents[8,9]. Chimpanzee is too precious to be commonly used in research, baboon and macaque are used as primate model more commonly. The injection bolus of LPS of 10-20 mg/kg, or continuous infusion of LPS of 10 mg/(kg·h) was applied in several studies with rhesus macaques[10,11]. A bolus injection of LPS 3.0 mg/kg for *Macaque mulatta* model had been reported previously by Hajek[12]. In the present study, we successfully established an endotoxic shock model of *Macaque mulatta*, which was proved by the decline of MAP, SVRI and LVWI. The LPS dose we used was 2.8 mg/kg and consistent with the previous report in *Macaque mulatta* model[12].

Methodology of detection for macaque cytokines

Unfortunately, no standard and commercial ELISA kits for detection of macaque cytokines are available. Nevertheless, it is reasonable to try application of human cytokine kits to detect macaque cytokines, because there is a high homology in genome between human and primate animals such as macaque[2] and it was reported that IL-2 receptor on the surface of rhesus monkey cells reacted with antibody against human IL-2 receptor[13] and IL-1, IL-2 and TNF-α from monkey cells could bind to antibodies against human IL-1, IL-2 and TNF-α in ELISA[13,14]. In this experiment, we tried to use ELISA kits for detection human cytokines to determine the levels of TNF-α, IL-1 β, IL-12P40/P70 and IL-10 of *Macaque mulatta* and successfully obtained useful data.

Similarly, we used the primers based on human TNF-α, IL-1 β, IL-18 and β-actin genes to amplify the cDNA segments of macaque TNF-α, IL-1 β, IL-18 and β-actin by RT-PCR methods and successfully obtained the expected products such as 702-bp segment of TNF-α, 810-bp segment of IL-1 β, 341-bp segment of IL-18 and 225-bp segment of β-actin (Figure 9). The PCR products from one macaque were sequenced for homology comparison with human homologue. The results indicated that the identity of TNF-α or IL-18 gene segment between macaque and human was 97%, IL-1 β was 93% (Figure 10).

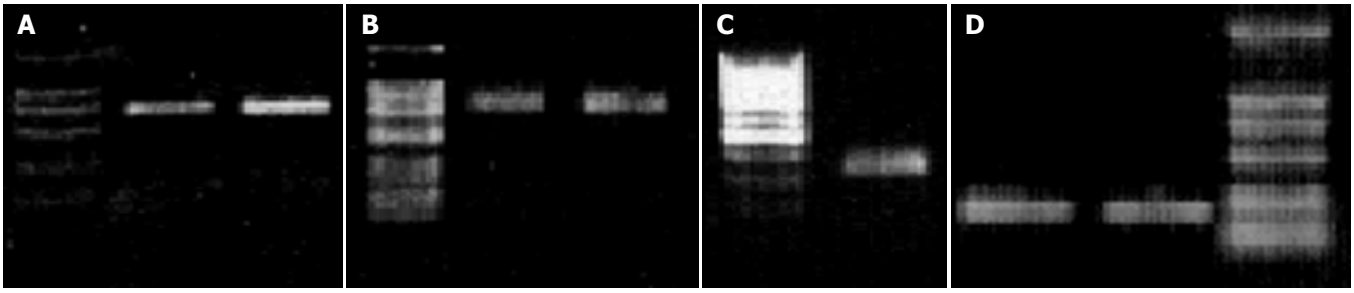

Figure 9 Identification of amplified products by RT-PCR with the method of agarose gel electrophoresis. A: 702 bp from TNF-α gene; B: 810 bp from IL-1 β gene; C: 341 bp from IL-18 gene; D: 225 bp from β-actin gene.

```
Query: 9    gggcaatgatcccaaagtagacctgcccagactcggcaaagtcgagatagtcgggcagat 68
             ||||||||||||||||||||||||||||||||||||||||||||||||||||||||| |||
Sbjct: 849  gggcaatgatcccaaagtagacctgcccagactcggcaaagtcgagatagtcgggccgat 790
Query: 69   tgatctcagcgctgagtcgatcacccttctccagctgaaagacccctcctaggtagatgg 128
             |||||||||||||||||| |||||||||||||||| |||||||||| || |||||||
Sbjct: 789  tgatctcagcgctgagtcggtcacccttctccagctggaagacccctcccagatagatgg 730
Query: 129  gctcgtaccagggcttggcctcagccccctctggagtctccctctggcaggggctcttga 188
             |||| |||||||||||||||||||||||||| |||||||||||||||||||||||||
Sbjct: 729  gctcataccagggcttggcctcagccccctctggggtctccctctggcaggggctcttga 670
Query: 189  tggcagagaggaggttgaccttggtctggtaggagacggcgatgcggctgatggtgtggg 248
             ||||||||||||||||||||||||||||||||||||||||||||||||||||||||||
Sbjct: 669  tggcagagaggaggttgaccttggtctggtaggagacggcgatgcggctgatggtgtggg 610
Query: 249  tgaggagcacatggttggaggggcagccttggcccttgaagaggacctgggagtagatga 308
             ||||||||||||||| ||||||||||||||||||||||||||||||||||||||||||
Sbjct: 609  tgaggagcacatgggtggaggggcagccttggcccttgaagaggacctgggagtagatga 550
Query: 309  ggtacaggccttctgatggcaccaccagctggttatctgtcagctccacgccattggcca 368
             |||||||||| |||||||||||||||||||||||| ||||||||||||||||||||||
Sbjct: 549  ggtacaggccctctgatggcaccaccagctggttatctctcagctccacgccattggcca 490
Query: 369  ggagggcattggcccggcggttcagccactggagctgcccctcagcttgagggtttgcta 428
             ||||||||||||||||||||||||||||||||||||||||||||||||||||||||||
Sbjct: 489  ggagggcattggcccggcggttcagccactggagctgcccctcagcttgagggtttgcta 430
Query: 429  caacatgggctacaggcttgtcacttggggttcgagaagatgatctgactgcctgagcca 488
             |||||||||||||||||||||||| |||||||||||||||||||||||||||| ||||
Sbjct: 429  caacatgggctacaggcttgtcactcggggttcgagaagatgatctgactgcctgggcca 370
Query: 489  gagggctgattagagaggggtccttggggaactcttccctctgggggccgatcactccaa 548
             |||||||||||||||| ||||| ||||||||||||||||||||||||||||||||||
Sbjct: 369  gagggctgattagagaggtccctggggaactcttccctctgggggccgatcactccaa 310
Query: 549  agtgcagcagacagaagagcgtggtggcgcctgccacgagcaggaaggagaagaggctga 608
             |||||||||| |||||||||||||||||||||||| |||||||||||||||||||||
Sbjct: 309  agtgcagcaggcagaagagcgtggtggcgcctgccacgatcaggaaggagaagaggctga 250
Query: 609  ggaaccagcaccgcctggagccctggggccccgctgtcttcctggggagcgcctcctcgg 668
             ||||| |||||||||||||||||||||||| |||||||| ||||||||||||||||||
Sbjct: 249  ggaacaagcaccgcctggagccctggggccccctgtcttcttggggagcgcctcctcgg 190
Query: 669  ccagctccacgtcccggatcatgctttcagtgctcat 705
             |||||||||||||||||||||||||||||||||||||
Sbjct: 189  ccagctccacgtcccggatcatgctttcagtgctcat 153

Query: 33   tttaggaagacacaaattgcatggtgaagtcagttatatcctggccacctctggtccctc 92
             |||||||||||||||||||||||||||||||||||||||||||||||| ||| |||||||||
Sbjct: 868  tttaggaagacacaaattgcatggtgaagtcagttatatcctggccgcctttggtccctc 809
Query: 93   ccaagaagacgggcatgttttccgcttgagaggtgctgacgtaccagttggggaattggg 152
             ||| |||||||||||||||| |||||||||||||| |||||||||||||| ||||
Sbjct: 808  ccaggaagacgggcatgttttctgcttgagaggtgctgatgtaccagttggggaactggg 749
Query: 153  cagactcgaattccagcttgttattgatttctatcttgttgaagacaaatcgcttttcca 212
             |||||||| ||||||||||||||||||||||||||||||||||||||||||||||||||
Sbjct: 748  cagactcaaattccagcttgttattgatttctatcttgttgaagacaaatcgcttttcca 689
Query: 213  tcttcttctttgggtagtttttgggatctacactctccagctgtagcgtgggcttatcat 272
             |||||||||||||||| |||||||||||||||||||||||| ||||||||||||||
Sbjct: 688  tcttcttctttgggtaatttttgggatctacactctccagctgtagagtgggcttatcat 629
```

Figure 10 Differences of cDNA fragments from TNF-α (A), IL-1 β (B) and IL-18 (C) gene between macaque and human according to GenBank.

Semi-quantitative analysis of mRNA based on RT-PCR can be completed by using β-actin mRNA as an internal standard and by densitometry of product electrophoresis band scanned or product dot hybridized with specific probe. The relative index (RI) of mRNA is calculated using a formula as RI = density scan value of specific product/density scan value of internal control. Here, RI may represent the relative level of specific mRNA. In the present study, we also used β-actin mRNA as an internal control. In order to increase detection sensitivity, we used SYBR-Green I, a kind of fluorescence stain for ds-DNA, in the quantitative analysis. Moreover, a two step strategy of reverse transcription first and then PCR was applied to ensure the consistency of amplification efficiency between cytokine and control mRNA. On the other hand, a real-time PCR was performed to find the cycle number of exponential phase of target DNA. Because the cycle number of exponential phase of cellular target DNA is different from that of primer-dimer DNA, it is possible to exclude primer-dimer interference with target DNA quantitative analysis when the product of cellular target DNA is collected within its exponential phase. In our experiment,

the cycle numbers of exponential phase of cellular target DNA were all less than 40, while that of primer-dimer was far more than 40. So the PCR was carried out for 40 cycles.

Expression changes of inflammation-associated cytokines during early phase of endotoxic shock model of macaques

TNF-α is one of the most important inflammatory cytokines and has a lot of cellular origins such as monocyte-macrophages, lymphocytes and endotheliocytes. The present study demonstrated the level of plasma TNF-α peaked at 60 min after LPS injection and then gradually decreased. The change of mRNA expression level in PBMCs was nearly synchronous, which indicated PBMCs were one of main sources of plasma TNF-α. After LPS challenge, expression levels of TNF-α mRNA both in liver and in spleen increased, suggesting that liver and spleen were also the sources of plasma TNF-α. TNF-α releases firstly during infection or inflammatory reaction. In endotoxic shock models of rats, rabbits and monkeys, plasma TNF-α levels were reported to increase at 30 min after LPS injection and reach the peak about 60-120 min after LPS injection[15], which was in great agreement with our results. Kupffer cells in liver were an important source of TNF-α. It was reported in endotoxin-induced liver injury model of mice, there were two expression peaks of TNF-α mRNA in liver, one happened within 2 h after LPS injection and the other happened 5 h after LPS injection. The first peak, during which TNF-α was derived from LPS-activated kupffer cells, was not as high as the second one. The second peak was induced by other inflammatory cytokines such as INF-γ and IL-18, and was the main factor inducing liver injury[16]. In the present experiment, the increase of TNF-α mRNA in liver at 120 min after LPS injection should be the first peak. We found the expression level of TNF-α mRNA in spleen cells also increased after LPS injection. There are few studies on TNF-α production by spleen in endotoxic shock models, which needs more investigations.

IL-1 β, produced by activated monocyte-macrophages, is also an important inflammatory cytokine that is released early. Leturcq[17] reported that the peak of plasma IL-1 β level in endotoxic shock model of cynomolgus monkeys appeared at 2 h after LPS stimulation which was slightly later than that of plasma TNF-α. This is similar to our result. We observed that IL-1 β plasma level increased in 2 h after LPS injection, but later than TNF-α level did. The fact that expression level of IL-1 β mRNA in PBMCs increased significantly at 60 min after LPS injection and quite earlier than plasma level suggested that PBMCs were the main source of circulating IL-1 β. PBMCs synthesized and released IL-1 β firstly and IL-1 β accumulated in plasma sequentially. The liver cells were also one of IL-1 β sources, but spleen cells the not.

IL-18, produced mainly by kupffer cells and other macrophages, is another important inflammatory factor. IL-18 activates cytokine network of liver and inflammatory reaction. By inducing INF-γ, IL-18 causes the second peak of TNF-α and sequential increase of FasL which induces apoptosis of liver cells[16-18]. IL-18 was found to be expressed basically in fresh-separated human PBMCs and to increase significantly in 1 h after LPS stimulation[4]. In LPS-induced acute liver injury model in Propionibacterium acnes-primed INF-γ-deficient mice , IL-18 was found to show a basic expression in liver followed by a remarkably increased expression within 2 h after stimulation with Propionibacterium acnes and LPS[19]. In this study, we found in endotoxic shock model of macaques, IL-18 mRNA expression in PBMCs began to increase after LPS stimulation and showed a statistically significant increase 2 h later. We also demonstrated a significant increase of IL-18 transcription in liver cells after LPS stimulation. These discoveries in macaque models were not reported here before.

IL-12, produced mainly by macrophages, kupffer cells and dendritic cells, activates neutrophilic granulocytes and promotes release of inflammatory cytokines such as INF-γ, TNF-α *etc*.[20,21], while inhibits the release of anti-inflammation cytokines such as IL-10[22]. So, IL-12 is also closely related to inflammatory responses. Reports about the change of IL-12 expression in endotoxic shock was quite few except for Tsuji's work, in which plasma IL-12 level of acute liver injury model mice was reported to reach a peak within 3 h after LPS stimulation, following the first peak of TNF-α[19]. In Trinchieri's opinion, the observation of dynamics of inflammatory cytokines in above model mice suggested that the order of activation for these cytokines was: the first peak of TNF-α, IL-12, IL-18, INF-γ, the second peak of TNF-α and FasL[23]. Our observation indicated in macaque mulatta, the plasma IL-12 concentration significantly increased in 120 min after LPS stimulation. To our knowledge, there were few reports about IL-12 dynamics in endotoxic shock primate model. Our results in macaque were compatible with Trinchieri's description.

IL-10, originated from Th1, Tr (regulator) or Th3 cells and B lymphocytes as well as monocyte-macrophages, is an anti-inflammation cytokine, inhibiting the release of inflammation cytokines such as TNF-α, IL-1 β, IL-6, IL-8, IL-12 and IL-18[24,25]. It is one of the cytokines produced very early after LPS injection in mice model, like TNF-α. Dynamics curves showed two peaks of plasma IL-10 in mice model: plasma IL-10 level reached the first peak in 1-5 h after LPS injection and then declined; the second peak appeared in 8-12 h after LPS injection. Plasma IL-10 originated from kupffer cells in liver during the first peak, while it originated from peripheral blood lymphocytes during the second peak[26]. The amount of IL-10 in the first peak during early phase of endotoxic shock was not enough to suppress the increases of inflammatory cytokines and hence effectively stop inflammation. So it is necessary to use exogenous recombinant IL-10 as a therapeutics in early phase of endotoxic shock to interrupt the chain release of inflammatory cytokines and to stop shock development[27]. In the present study, we observed IL-10 level in shock model of macaques increased slightly, and significantly in 60 min after LPS injection and formed a smaller peak, and about 60 min later it returned nearly to the value of control group. Our result in macaque model was quite consistent with that in mouse model. The rise of IL-10 level we observed in early phase of endotoxic shock in macaque models should correspond to the first peak.

It is necessary to mention Kupffer cells for understanding the dynamics of inflammatory cytokine release induced by LPS. LPS is the main activator of Kupffer cells, while Kupffer cells are the major source of inflammatory cytokines, such as TNF-α, IL-12 and IL-18, which are produced in response to LPS. TNF-α is the key factor in systemic inflammation (for example, endotoxic shock and septic syndrome), and it is Kupffer cells that are the major source of TNF-α in the liver. So Kupffer cells play an important role in systemic inflammatory reaction caused by Gram-negative bacteria. On the other hand, Kupffer cells are the main scavengers of LPS and also play an important role in removing circulatory LPS and relieving the stimulation and injury caused by LPS[28].

REFERENCES

1 **Han DW.** Intestinal endotoxemia as a pathogenetic mechanism in liver failure. *World J Gastroenterol* 2002; **8**: 961-965

2 **Villinger F**, Brar SS, Mayne A, Chikkala N, Ansari AA. Comparative sequence analysis of cytokine genes from human and nonhuman primates. *J Immunol* 1995; **155**: 3946-3954

3 **Benveniste O**, Vaslin B, Villinger F, Le Grand R, Ansari AA, Dormont D. Cytokine mRNA levels in unmanipulatedlex and *in vitro* stimulated monkey PBMCs using a semi-quantitative RT-PCR and high sensitivity fluorescence-based detection

strategy. *Cytokine* 1996; **8**: 32-41
4 **Puren AJ**, Fantuzzi G, Dinarello CA. Gene expression, synthesis, and secretion of interleukin18 and interleukin1β are differentially regulated in human blood mononuclear cells and mouse spleen cells. *Proc Natl Acad Sci U S A* 1999; **96**: 2256-2261
5 **Takebe Y**, Seiki M, Fujisawa J, Hoy P, Yokota K, Arai K, Yoshida M, Arai N. SR alpha promoter: an efficient and versatile mammalian cDNA expression system composed of the simian virus 40 early promoter and the R-U5 segment of human T-cell leukemia virus type 1 long terminal repeat. *Mol Cell Biol* 1988; **8**: 466-472
6 **Pernerstorfer T**, Schmid R, Bieglmayer C, Eichler HG, Kapiotis S, Jilma B. Acetaminophen has greater antipyretic efficacy than aspirin in endotoxemia: a randomized, double-blind, placebo-controlled trial. *Clin Pharmacol Ther* 1999; **66**: 51-57
7 **Boujoukos AJ**, Martich GD, Supinski E, Suffredini AF. Compartmentalization of the acute cytokine response in humans after intravenous endotoxin administration. *J Appl Physiol* 1993; **74**: 3027-3033
8 **Redl H**, Bahrami S, Schlag G, Traber DL. Clinical detection of LPS and animal models of endotoxemia. *Immunobiology* 1993; **187**: 330-345
9 **Harper PL**, Taylor FB, DeLa Cadena RA, Courtney M, Colman RW, Carrell RW. Recombinant antitrypsin pittsburgh undergoes proteolytic cleavage during E. coli sepsis and fails to prevent the associated coagulopathy in a primate model. *Thromb Haemost* 1998; **80**: 816-821
10 **Richman AV**, Okulski EG, Balis JU. New Concepts in the pathogenesis of acute tubular necrosis associated with sepsis. *Ann Clin Lab Sci* 1981; **11**: 211-219
11 **Premaratne S**, May ML, Nakasone CK, McNamara JJ. Pharmacokinetics of endotoxin in a rhesus macaque septics shock model. *J Surg Res* 1995; **59:** 428-432
12 **Hajek M**, Trcka V, Vanecek M, Helfert I, Misak J. A model of experimental endotoxin shock in monkeys and its therapeutic control. *Z Exp Chir* 1978; **11**: 317-321
13 **Schmitt DA**. *In vitro* interleukin-1 and 2 production and interleukin 2 receptor expression in the rhesus monkey. *Life Sci* 1996; **59**: 931-937
14 **Verdier F**, Aujoulat M, Condevaux F, Descotes J. Determination of lymphocyte subsets and cytokine levels in cynomolgus monkeys. *Toxicology* 1995; **105**: 81-90
15 **Carvalho GL**, Wakabayashi G, Shimazu M, Karahashi T, Yoshida M, Yamamoto S, Matsushima K, Mukaida N, Clark BD, Takabayashi T, Brandt CT, Kitajima M. Anti-interleukin-8 monoclonal antibody reduces free radical production and improves hemodynamics and survival rate in endotoxic shock in rabbits. *Surgery* 1997; **122**: 60-68
16 **Tsutsui H**, Matsui K, Kawada N, Hyodo Y, Hayashi N, Okamura H, Higashino K, Nakanishi K. IL-18 accounts for both TNF-α–and Fas ligand-mediated hepatotoxic pathways in endotoxin-induced liver injury in mice. *J Immunol* 1997; **159**: 3961-3967
17 **Leturcq DJ**, Moriarty AM, Talbott G, Winn RK, Martin TR, Ulevitch RJ. Antibodies against CD14 protect primates from endotoxin-induced shock. *J Clin Invest* 1996; **98**: 1533-1538
18 **Puren AJ,** Fantuzzi G, Gu Y, Su SM, Dinarello CA. Interleukin-18 (IFNγ–inducing factor) induces IL-8 and IL-1 β via TNFα production from non-CD14+ human blood mononuclear cells. *J Clin Invest* 1998; **101**: 711-721
19 **Tsuji H**, Mukaida N, Harada A, Kaneko S, Matsushita E, Nakanuma Y, Tsutsui H, Okamura H, Nakanishi K, Tagawa Y, Iwakura Y, Kobayashi K, Matsushima K. Alleviation of lipopolysaccharide-induced acute liver injury in *Propionibacterium acnes*-primed IFN-γ-deficient mice by a concomitant reduction of TNF-α, IL-12, and IL-18 production. *J Immunol* 1999; **162**: 1049-1055
20 **Trinchieri G**. Interleukin-12: a proinflammatory cytokine with immunoregulatory functions that brdge innate resistance and antigen-specific adaptive immunity. *Annu Rev Immunol* 1995; **13**: 251-276
21 **Carson WE**, Yu H, Dierksheide J, Pfeffer K, Bouchard P, Clark R, Durbin J, Baldwin AS, Peschon J, Johnson PR, Ku G, Baumann H, Caligiuri MA. A fatal cytokine-induced systemic inflammatory response reveals a critical role for NK cells. *J Immunol* 1999; **162**: 4943-4951
22 **Marshall JD**, Secrist H, Dekruyff RH, Wolf SF, Umetsu DT. IL-12 inhibits the production of IL-4 and IL-10 in allergen-specific human CD4+ T lymphocytes. *J Immunol* 1995; **155**: 111-117
23 **Trinchieri G**. Immunobiology of interleukin-12. *Immunol Res* 1998; **17**: 269-278
24 **Nemeth ZH**, Hasko G, Vizi ES. Pyrrolidine dithiocarbamate augments IL-10, inhibits TNF-alpha, MIP-1alpha, IL-12, and nitric oxide production and protects from the lethal effect of endotoxin. *Shock* 1998; **10**: 49-53
25 **Marshall JD**, Aste-Amezaga M, Chehimi SS, Murphy M, Olsen H, Trinchieri G. Regulation of human IL-18 mRNA expression. *Clin Immunol* 1999; **90**: 15-21
26 **Barsig J**, Kusters S, Vogt K, Volk HD, Tiegs G, Wendel A. Lipopolysaccharide-induced interleukin-10 in mice: role of endogenous tumor necrosis factor-α. *Eur J Immunol* 1995; **25**: 2888-2893
27 **Howard M**, Muchamuel T, Andrade S, Menon S. Interleukin 10 protects mice from lethal endotoxemia. *J Exp Med* 1993; **177**: 1205-1208
28 **Terpstra V,** van Amersfoort ES, van Velzen AG, Kuiper J, van Berkel TJ. Hepatic and extrahepatic scavenger receptors: function in relation to disease. *Arterioscler Thromb Vasc Biol* 2000; **20**: 1860-1872

Edited by Zhu LH **Proofread by** Chen WW and Xu FM

PO Box 2345, Beijing 100023, China
Fax: +86-10-85381893
E-mail: wjg@wjgnet.com www.wjgnet.com

World J Gastroenterol 2004;10(20):3034-3038
World Journal of Gastroenterology
 ISSN 1007-9327

• CLINICAL RESEARCH •

Diagnostic role of secretin-enhanced MRCP in patients with unsuccessful ERCP

László Czakó, Tamás Takács, Zita Morvay, László Csernay, János Lonovics

László Czakó, Tamás Takács, János Lonovics, First Department of Medicine, University of Szeged, Szeged, Hungary
Zita Morvay, László Csernay, International Medical Center, Szeged, Hungary
Supported by the ETT 5K503 and the Hungarian Academy of Sciences, BÖ 5/2003
Correspondence to: Dr. László Czakó, First Department of Medicine, University of Szeged, Szeged, PO Box 469, H-6701, Hungary. czal@in1st.szote.u-szeged.hu
Telephone: +36-62-545201 **Fax:** +36-62-545185
Received: 2004-02-20 **Accepted:** 2004-04-06

Abstract

AIM: To evaluate the value of MR cholangiopancreatography (MRCP) in patients in whom endoscopic retrograde cholangiopancreatography (ERCP) was unsuccessfully performed by experts in a tertiary center.

METHODS: From January 2000 to June 2003, 22 patients fulfilled the inclusion criteria. The indications for ERCP were obstructive jaundice (n = 9), abnormal liver enzymes (n = 8), suspected chronic pancreatitis (n = 2), recurrent acute pancreatitis (n = 2), or suspected pancreatic cancer (n = 1). The reasons for the ERCP failure were the postsurgical anatomy (n = 7), duodenal stenosis (n = 3), duodenal diverticulum (n = 2), and technical failure (n = 10). MRCP images were evaluated before and 5 and 10 min after i.v. administration of 0.5 IU/kg secretin.

RESULTS: The MRCP images were diagnosed in all 21 patients. Five patients gave normal MR findings and required no further intervention. MRCP revealed abnormalities (primary sclerosing cholangitis, chronic pancreatitis, cholangitis, cholecystolithiasis or common bile duct dilation) in 10 patients, who were followed up clinically. Four patients subsequently underwent laparotomy (hepaticojejunostomy in consequence of common bile duct stenosis caused by unresectable pancreatic cancer; hepaticotomy+Kehr drainage because of insufficient biliary-enteric anastomosis; choledochojejunostomy, gastrojejunostomy and cysto-Wirsungo gastrostomy because of chronic pancreatitis, or choledochojejunostomy because of common bile duct stenosis caused by chronic pancreatitis). Three patients participated in therapeutic percutaneous transhepatic drainage. The indications were choledocholithiasis with choledochojejunostomy, insufficient biliary-enteric anastomosis, or cholangiocarcinoma.

CONCLUSION: MRCP can assist the diagnosis and management of patients in whom ERCP is not possible.

Czakó L, Takács T, Morvay Z, Csernay L, Lonovics J. Diagnostic role of secretin-enhanced MRCP in patients with unsuccessful ERCP. *World J Gastroenterol* 2004; 10(20): 3034-3038
http://www.wjgnet.com/1007-9327/10/3034.asp

INTRODUCTION

The most sensitive diagnostic modality in suspected biliopancreatic diseases is endoscopic retrograde cholangiopancreatography (ERCP)[1-4]. However, the success rate of the examination mainly depends on the experience of the endoscopist, and does not exceed 95-98% even in the largest specialized centers. Previous operations (Billroth II, Roux-en-Y or biliary-enteric anatomy), duodenal stenosis, or duodenal diverticulum make cannulation of the ducts difficult or even impossible, and increase the risk of complications[5-7]. If ERCP fails, intravenous (iv) or percutaneous transhepatic cholangiography (PTC) is the alternative method. Since the diagnostic accuracy of iv cholangiography is very low, it is no longer used. PTC is invasive, may be associated with severe complications, and can successfully be applied if the intrahepatic biliary tree is dilated. PTC and iv cholangiography are both unable to visualize the pancreatic duct[8-10]. There is clearly a need for a noninvasive, sensitive and specific diagnostic modality for patients with suspected biliopancreatic disease if ERCP fails[11]. Magnetic resonance cholangiopancreatography (MRCP) is a new noninvasive diagnostic modality capable of producing high-quality images of the pancreatobiliary tree. It has been emphasized that its sensitivity (81-100%), specificity (94-98%), positive (86-93%) and negative (94-98%) predictive values and diagnostic accuracy (94-97%) are as high as those of ERCP, which makes MRCP a promising alternative to diagnostic ERCP[12-16]. Moreover, MRCP has the following advantages over ERCP. It is noninvasive, there are no complication, no radiation, no need for any contrast agent. It causes less discomfort for the patients, and can provide useful information on the parenchymatous organs in this region in combination with conventional cross-sectional MR sequences.

The aim of our study was to assess the value of MRCP in the management of patients with biliopancreatic diseases in whom ERCP was failed.

MATERIALS AND METHODS

Between January 2000 and June 2003 a prospective study was conducted. Twenty-two patients were enrolled, in whom ERCP performed by experts at our endoscopic unit failed to adequately visualize the clinically relevant duct(s). Failure meant two unsuccessful ERCP attempts by precut papillotomy with a needle knife when the ducts were not cannulated with the conventional approach. There were 10 males and 12 females, with a mean age of 51.2 years, range 24-82 years. The indications for ERCP were obstructive jaundice (n = 9), abnormal liver enzymes (n = 8), suspected chronic pancreatitis (n = 2), recurrent acute pancreatitis (n = 2), or suspected pancreatic cancer (n = 1). The reasons for the ERCP failure were the postsurgical anatomy (n = 7), duodenal stenosis (n = 3), duodenal diverticulum (n = 2), or technical failure (n = 10) (Table 1). All patients gave their informed consent after receiving a detailed explanation of the complete examination procedure.

MRCP

All patients underwent MR imaging (Signa Horizon LX 1.0 T-Scanner, General Electric, USA). T1-weighted and T2-weighted

axial plane fast spoiled gradient (FSPGR) images were acquired. These images were used to evaluate the liver and pancreas parenchyma and also to plan the MRCP data collection. The heavily T2-weighted MRCP images were taken in two sets. With a single shot technique, one 30.0-70.0-mm-thick slice was first acquired at TR 5 000 ms, TE 500 ms, with a 320×320 matrix and 40×36 FOV. In the second set, 9-13 thin (5.0 mm) slices with a 2-mm gap were taken from the same region. The breath-hold technique was used for all sequences. "Dualflex" flexible body coil was applied. MRCP images were evaluated before and 5 and 10 min after the iv administration of 0.5 IU/kg secretin (Secretolin, Hoechst, Frankfurt am Main, Germany)[17]. The administration of secretin induced the secretion of bile and pancreatic juice. Consequently, the ductal filling was increased, and the visualization of the biliary and pancreatic ducts and the image quality were therefore improved[18].

RESULTS

The MRCP images were of diagnostic quality in all but 1 patient. MRCP furnished normal findings in 5 cases and revealed abnormalities in 17 patients (Table 1). Conservative medical treatment was applied in 10 cases. MRCP demonstrated mild bile duct dilation caused by chronic pancreatitis in 3 patients. Since they were mainly asymptomatic, surgical intervention was not indicated. Primary sclerosing cholangitis was indicated by MRCP in 3 patients, the cholestasis was improved after treatment with ursodeoxycholic acid. Gallbladder stones were found in an 82-year-old female patient, operation was not recommended because of her age. In a 77-year-old female patient who had previously undergone choledochoduodenostomy, the extrahepatic biliary tree exhibited caliber changes. This finding was considered to correspond to cholangitis, the abnormal liver function was normalized by antibiotic therapy. In 2 patients with previous cholecystectomy and abnormal liver enzymes, MRCP revealed mild extrahepatic bile duct dilation (postcholecystectomy syndrome?). The liver function normalized without treatment in 1 patient, and in response to ursodeoxycholic acid treatment in the other (Table 1).

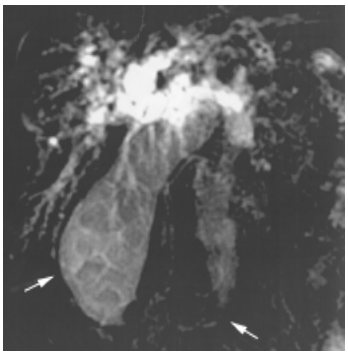

Figure 1 MRCP of a 78-year-old female patient. The common bile duct is dilated with a stricture at the level of the papilla of Vateri (open arrow), with multiple stones in the gallbladder (solid arrow). The Wirsung duct is not visible.

Seven patients required therapeutic interventions. Four of these 7 patients underwent surgery. The indication for operation was based on the MRCP findings, which were confirmed at surgery in 3 of the 4 cases. In 1 patient (No. 10, Figure 1), MRCP revealed only the site, but not the cause of the bile duct obstruction. This patient was referred to the endoscopy unit because of obstructive jaundice. MRCP demonstrated a prepapillary common bile duct obstruction. The Wirsung duct was not visible. These findings, the clinical picture and the result of duodenoscopy led to a suspicion of pancreatic head carcinoma. The patient was operated on, and the surgery confirmed the suspicion. Curative resection was not possible because of the local invasiveness of the tumor, bilio-enteric anastomosis was performed.

Figure 2 MRCP of a 58-year-old female patient in whom ERCP failed because of a previous Billroth II resection. The intrahepatic biliary tree is markedly dilated with stones (open arrows), and the choledochojejunostomy anastomosis is narrowed (solid arrow). The patient underwent hepaticotomy and Kehr drainage.

In 1 patient in whom ERCP was failed because of a previous Billroth II resection, MRCP demonstrated a stricture of the choledochojejunostomy anastomosis as the cause of a bile duct obstruction (No. 1, Figure 2). The intrahepatic biliary tree was markedly dilated and contained secondary stones. The patient subsequently underwent hepaticotomy and Kehr drainage.

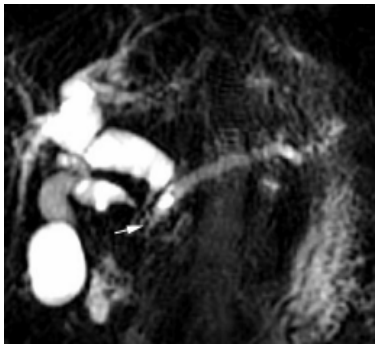

Figure 3 MRCP of a 63-year-old male patient in whom ERCP failed because of duodenal stenosis. The calcified pancreatic head obstructs the Wirsung duct and the common bile duct (arrow) with an upstream dilation, causing the "double duct sign". The intrahepatic biliary tree and the cystic duct are also dilated. The patient underwent choledochojejunostomy, gastrojejunostomy and Wirsungogastrostomy.

In a patient with chronic pancreatitis, whose disease was not followed up regularly, ERCP was indicated because of obstructive jaundice, but it failed in consequence of duodenal stenosis. MRCP showed obstruction of the Wirsung duct and the common bile duct by the calcified pancreatic head, with an upstream dilation in both ducts, causing the "double duct sign" (No. 11, Figure 3). The intrahepatic biliary tree and the cystic duct were also dilated. The patient underwent choledochojejunostomy, gastrojejunostomy and Wirsungo gastrostomy. Similarly, in a patient with chronic pancreatitis in whom a previous Billroth II resection precluded ERCP, MRCP demonstrated an intrapancreatic bile duct obstruction. Choledochoenterostomy was performed (No. 19).

In 3 patients of advanced age in a moribund physical status, the bile duct obstruction was treated with percutaneous transhepatic drainage (PTD). MRCP indicated common bile duct stones in a patient who had previously undergone choledochojejunostomy

Table 1 Indications for ERCP, reasons for ERCP failure, MRCP findings, and management of patients

Patient	Indication for ERCP	Reason for ERCP failure	MRCP findings	Management of patients
1	Obstructive jaundice	Billroth II anatomy (choledochojejunostomy anatomy)	stricture of choledochojejunostomy	hepaticotomy +Kehr drainage
2	Obstructive jaundice	Billroth II anatomy (choledochojejunostomy anatomy)	cholangitis	antibiotic treatment
3	Obstructive jaundice	choledochojejunostomy anatomy	choledocholithiasis	PTD
4	Obstructive jaundice	Roux and Y anatomy hepaticojejunostomy anatomy	stricture of hepaticojejunostomy	PTD
5	Cholestasis biliary pancreatitis	technical	cholecystolithiasis	follow-up
6	Cholestasis	technical	mild CBD dilatation	follow-up
7	Suspected pancreatic cancer	duodenal stenosis	chronic pancreatitis	follow-up
8	Obstructive jaundice	technical	cholangiocarcinoma	PTD
9	Cholestasis	technical	PSC	follow-up
10	Obstructive jaundice	technical	distal stricture of CBD	hepaticojejunostomy unresectable pancreas carcinoma
11	Obstructive jaundice chronic pancreatitis	duodenal stenosis	"double duct sign"	choledochojejunostomy gastrojejunostomy Wirsungogastrostomy
12	Obstructive jaundice chronic pancreatitis	technical	intrapancreatic stricture of CBD, chronic pancreatitis	follow-up
13	Cholestasis	technical (choledocho-duodenostomy anatomy)	normal	follow-up
14	Cholestasis	duodenal diverticulum	PSC	follow-up
15	Cholestasis	technical	PSC	follow-up
16	Obstructive jaundice	duodenal diverticulum	normal	follow-up
17	Recurrent pancreatitis	technical	normal	follow-up
18	Recurrent pancreatitis	technical	normal	follow-up
19	Obstructive jaundice	Billroth II anatomy	intrapancreatic stricture of CBD, chronic pancreatitis	choledochoenterostomy cholecystectomy
20	Cholestasis	technical	mild CBD dilation	follow-up
21	Obstructive jaundice	duodenal stenosis	intrapancreatic stricture of CBD, chronic pancreatitis	follow-up
22	Cholestasis	Billroth II anatomy	normal	follow-up

CBD: common bile duct; PSC: primary sclerosing cholangitis; PTD: percutan transhepatic drainage.

(No. 3), another with a hepaticojejunostomy anastomotic stricture (No. 4) and one with prepapillary cholangiocarcinoma (No. 8, Figure 4). These findings were confirmed by PTC and the patients subsequently underwent biliary drainage.

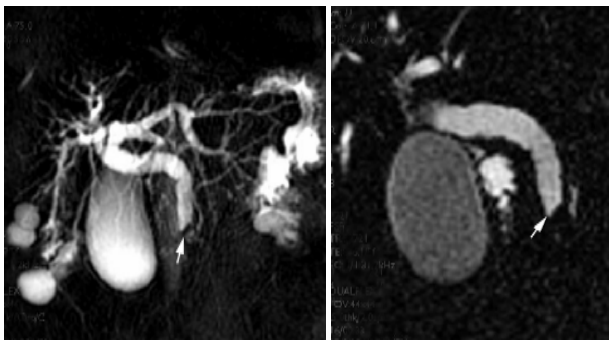

Figure 4 Normal Wirsung duct and bilateral renal cysts in an 81-year-old female patient. The intraluminal focus with low signal intensity in the distal common bile duct (arrow) proved to be cholangiocarcinoma. The biliary tree is dilated. With regard to her age and physical status, the patient underwent biliary stent implantation to ensure bile flow.

DISCUSSION

ERCP is the most sensitive and specific technique currently available for visualization of the biliary tree and pancreatic duct. Beside the establishment of a diagnosis, this examination at the same time offers therapeutic options. However, ERCP is invasive, and may be associated with complications, and patients who undergo ERCP need sedation. Another disadvantage is that it affords no information on extraductal lesions, and does not opacify the obstructed segment in the event of total duct obstruction. It was unsuccessful in 3-10% of the cases, even in the largest endoscopic centers[5-7]. Inexperience of the endoscopist and anatomic factors such as previous gastroenteroanastomosis, duodenal stenosis, or periampullary diverticulum might lead to higher rates of unsuccessful ERCP[19,20]. When the papilla of Vater is in the visual field of the duodenoscope, but conventional cannulation fail, precut papillotomy could be performed with a needle knife, and cannulation could subsequently be achieved. However, precut papillotomy could increase the frequency and severity of complications as compared with conventional ERCP (6-12% *vs* 1-5%)[21,22]. Iv cholangiography or PTC examinations are the alternative choices for visualization of the biliary tree. However, iv cholangiography has been no longer used, because its

diagnostic accuracy was limited[8]. PTC is a sensitive method of detecting biliary abnormalities, but it was invasive, might be associated with severe complications, and could successfully be applied if the intrahepatic biliary tree was dilated. In addition, neither PTC nor iv cholangiography was able to visualize the pancreatic duct[9,10].

The need for a safe and noninvasive technique for examination of the biliary tree and pancreatic duct resulted in the development of MRCP. A number of studies have demonstrated that the sensitivity, specificity, positive and negative predictive values and diagnostic accuracy of MRCP in the detection of biliopancreatic diseases are as high as those of ERCP[12-16]. Despite these data, the actual role of MRCP in the diagnostic work-up of patients with suspected biliopancreatic disease is not clear. Besides its advantages, MRCP has certain drawbacks. Most importantly, it does not allow simultaneous therapeutic intervention. While ERCP offers a therapeutic option in the same session after the diagnosis is made (papillotomy, removal of choledocholithiasis, stenting of a biliary stricture, *etc*.), MRCP yields only the diagnosis. Clips, stents, pneumobilia, hemobilia and ascites might result in artifacts and impede interpretation of the MRCP image. Despite the new technological advances in MR imaging, its resolution has remained behind that of ERCP[23].

In the present study we assessed the value of MRCP in the management of patients in whom ERCP was unsuccessful. MRCP prevented an invasive procedure in 15 of 22 cases and guided therapy in the remaining 7. Ten patients were treated conservatively. They did not require further diagnostic examinations or therapeutic interventions; they were asymptomatic or responded well to the medical therapy during the follow-up. In 7 patients, therapeutic intervention was indicated by the MRCP findings. The information provided by MRCP was sufficient for the decision-making, and a further diagnostic work-up was required in only 1 patient. This patient (No. 10) was referred to the endoscopy unit because of obstructive jaundice. Duodenoscopy revealed an enlarged papilla of Vater with an irregular surface, which was suspicious of malignancy. Cannulation of the biliary or the pancreatic duct was impossible, even after precut papillotomy. The histological examination of the biopsy specimens taken from the papilla indicated no malignancy. MRCP demonstrated a dilated biliary tree with a severe prepapillary stricture (Figure 1). The pancreas was not separated well from its surroundings in the conventional axial plane MR images, because of the lack of peripancreatic fatty tissue. The Wirsung duct was not depicted or could not be identified among the fluid-filled bowels, despite the use of secretin. The evaluation of the MR images was hampered by the technical artifacts. These findings and the clinical picture together suggested pancreatic head carcinoma. The patient was operated on. The surgery confirmed the suspicion, but a curative resection was impossible as a result of the local invasiveness of the tumor. Biliary-enteric anastomosis was performed.

The sensitivity, specificity, positive and negative predictive values and diagnostic accuracy of MR imaging in the detection of pancreatic cancer were at least as high as those of computer tomography or ERCP[24,25]. The combination of conventional MR imaging with MRCP and MR angiography could increase the accuracy in the diagnosis, the staging of pancreatic malignancies and the assessment of respectability[26-29]. With this combined MR imaging technique, the biliary tree and pancreatic duct with the surrounding vessels and parenchymatous organs could be depicted in one examination, which makes it cost-effective. In our case, the poor quality of the MR imaging with significant amount of artifacts might explain why it was unable to diagnose the cause of the biliary obstruction.

Four patients underwent surgery without further diagnostic examinations. In 3 cases the diagnosis made by MR was confirmed by the surgical findings. In 1 case (No. 10), the MR revealed only the site, but not the cause (i.e. pancreatic cancer) of the bile duct obstruction, which was diagnosed during the operation. In 3 patients, surgery was not recommended because of their moribund physical status. PTC was performed and in each case confirmed the results of MRCP. These patients subsequently underwent biliary drainage.

Seven out of 22 patients required intervention after MRCP. This points the major drawbacks of MRCP. It is unable to combine therapy with diagnosis. It could be argued that the 3 patients with obstructive jaundice who required PTC and PTD after MRCP might have better served by proceeding to this modality directly. However, the fact that MRCP is noninvasive is a powerful point in its favor. It can identify those patients where therapeutic intervention is needed.

Our results suggest that MRCP is a feasible and valuable diagnostic modality in patients in whom ERCP fails. MRCP facilitates the management of these patients. It differentiates patients who require invasive therapy from those who can be treated conservatively, and provides information necessary for the planning of surgical or radiological interventions.

REFERENCES

1 **Pasanen PA**, Partanen KP, Pikkarainen PH, Alhava EM, Janatuinen EK, Pirinen AE. A comparison of ultrasound, computed tomography and endoscopic retrograde cholangiopancreatography in the differential diagnosis of benign and malignant jaundice and cholestasis. *Eur J Surg* 1993; **159:** 23-29

2 **Ponchon T,** Pilleul F. Diagnostic ERCP. *Endoscopy* 2002; **34:** 29-42

3 **Baron TH,** Fleischer DE. Past, present, and future of endoscopic retrograde cholangiopancreatography: perspectives on the National Institutes of Health consensus conference. *Mayo Clin Proc* 2002; **77:** 407-412

4 NIH State of Science Conference on ERCP. 2002-01-14-16. Available from: URL: http://consensus.nih.gov

5 **Bilbao MK,** Dotter CT, Lee TG, Katon RM. Complications of endoscopic retrograde cholangiopancreatography (ERCP). A study of 10 000 cases. *Gastroenterology* 1976; **70:** 314-320

6 **Choudari CP,** Sherman S, Fogel EL, Phillips S, Kochell A, Flueckiger J, Lehman GA. Success of ERCP at a referral center after a previously unsuccessful attempt. *Gastrointest Endosc* 2000; **52:** 478-483

7 **Loperfido S,** Angelini G, Benedetti G, Chilovi F, Costan F, De Berardinis F, De Bernardin M, Ederle A, Fina P, Fratton A. Major early complications from diagnostic and therapeutic ERCP: a prospective multicenter study. *Gastrointest Endosc* 1998; **48:** 1-10

8 **Tham TC,** Collins JS, Watson RG, Ellis PK, McIlrath EM. Diagnosis of common bile duct stones by intravenous cholangiography: prediction by ultrasound and liver function tests compared with endoscopic retrograde cholangiography. *Gastrointest Endosc* 1996; **44:** 158-163

9 **Ott DJ,** Gelfand DW. Complications of gastrointestinal radiologic procedures: II. Complications related to biliary tract studies. *Gastrointest Radiol* 1981; **6:** 47-56

10 **Harbin WP,** Mueller PR, Ferrucci JT Jr. Transhepatic cholangiography: complicatons and use patterns of the fine-needle technique: a multi-institu tional surveg. *Radiology* 1980; **135:** 15-22

11 **Soto JA,** Yucel EK, Barish MA, Chuttani R, Ferrucci JT. MR cholangiopancreatography after unsuccessful or incomplete ERCP. *Radiology* 1996; **199:** 91-98

12 **Lomanto D,** Pavone P, Laghi A, Panebianco V, Mazzocchi P, Fiocca F, Lezoche E, Passariello R, Speranza V. Magnetic resonance-cholangiopancreatography in the diagnosis of biliopancreatic diseases. *Am J Surg* 1997; **174:** 33-38

13 **Coakley FV,** Schwartz LH. Magnetic resonance cholangiopancreatography. *J Magn Reson Imaging* 1999; **9:** 157-162

14 **Takehara Y.** Can MRCP replace ERCP? *J Magn Reson Imaging*

1998; **8:** 517-534

15 **Soto JA,** Barish MA, Yucel EK**,** Siegenberg D, Ferrucci JT, Chuttani R. Magnetic resonance cholangiography: comparison with endoscopic retrograde cholangiopancreatography. *Gastroenterology* 1996; **110:** 589-597

16 **Sahai AV,** Devonshire D, Yeoh KG, Kay C, Feldman D, Willner I, Farber J, Patel R, Tamasky PR, Cunningham JT, Trus T, Hawes RH, Cotton PB. The decision-making value of magnetic resonance cholangiopancreatography in patients seen in a referral center for suspected biliary and pancreatic disease. *Am J Gastroenterol* 2001; **96:** 2074-2080

17 **Czako L,** Endes J, Takacs T, Boda K, Lonovics J. Evaluation of pancreatic exocrine function by secretin-enhanced magnetic resonance cholangiopancreatography. *Pancreas* 2001; **23:** 323-328

18 **Hellerhoff KJ,** Helmberger H 3rd, Rosch T, Settles MR, Link TM, Rummeny EJ. Dynamic MR pancreatography after secretin administration: image quality and diagnostic accuracy. *Am J Raentgenol* 2002; **179:** 121-129

19 **Nicaise N,** Pellet O, Metens T, Deviere J, Braude P, Struyven J, Matos C. Magnetic resonance cholangiopancreatography: interest of IV secretin administration in the evaluation of pancreatic ducts. *Eur Radiol* 1998; **8:** 16-22

20 **Mosca S.** How can we reduce complication rates and enhance success rates in Billroth II patients during endoscopic retrograde cholangiopancreatography? *Endoscopy* 2000; **32:** 589-590

21 **Rollhauser C,** Al-Kawas FH. Endoscopic access to the papilla of Vater for endoscopic retrograde cholangiopancreatography in patients with Billroth II or Roux-en-Y gastrojejunoanastomosis. *Gastrointest Endosc* 1997; **46:** 581-582

22 **Larkin CJ,** Huibregtse K. Precut sphincterotomy: indications, pitfalls, and complications. *Curr Gastroenterol Rep* 2001; **3:** 147-153

23 **Keogan MT,** Edelman RR. Technologicl advances in abdominal MR imaging. *Radiology* 2001; **220:** 310-320

24 **Adamek HE,** Albert J, Breer H, Weitz M, Schilling D, Riemann JF. Pancreatic cancer detection with magnetic resonance cholangiopancreatography and endoscopic retrograde cholangiopancreatography: a prospective controlled study. *Lancet* 2000; **356:** 190-193

25 **Ichikawa T,** Haradome H, Hachiya J, Nitatori T, Ohtomo K, Kinoshita T, Araki T. Pancreatic ductal adenocarcinoma: Preoperative assessment with helical CT versus dynamic MR imaging. *Radiology* 1997; **202:** 655-662

26 **Catalano C,** Pavone P, Laghi A, Panebianco V, Scipioni A, Fanelli F, Brillo R, Passariello R. Pancreatic adenocarcinoma: combination of MR imaging, MR angiography and MR cholangiopancreatography for the diagnosis and assessment of resectability. *Eur Radiol* 1998; **8:** 428-434

27 **Adamek HE,** Breer H, Karschkes T, Albert J, Riemann JF. Magnetic resonance imaging in gastroenterology: time to say goodbye to all that endoscopy? *Endoscopy* 2000; **32:** 406-410

28 **Mitchell RM,** Byrne MF, Baillie J. Pancreatitis. *Lancet* 2003; **361:** 1447-1455

29 **Kay CL.** Which test to replace diagnostic ERCP – MRCP or EUS? *Endoscopy* 2003; **35:** 426-428

Edited by Wang XL **Proofread by** Chen WW and Xu FM

PO Box 2345, Beijing 100023, China
Fax: +86-10-85381893
E-mail: wjg@wjgnet.com www.wjgnet.com

World J Gastroenterol 2004;10(20):3039-3043
World Journal of Gastroenterology
 ISSN 1007-9327

• BRIEF REPORTS •

Autonomic and sensory nerve dysfunction in primary biliary cirrhosis

Katalin Keresztes, Ildikó Istenes, Aniko Folhoffer, Peter L Lakatos, Andrea Horvath, Timea Csak, Peter Varga, Peter Kempler, Ferenc Szalay

Katalin Keresztes, Ildikó Istenes, Aniko Folhoffer, Peter L Lakatos, Andrea Horvath, Timea Csak, Peter Varga, Peter Kempler, Ferenc Szalay, 1st Department of Medicine, Semmelweis University, Budapest, Hungary
Correspondence to: Professor Ferenc Szalay, MD, PhD, 1st Department of Medicine, Semmelweis University, Koranyi S. 2/A, H-1083 Budapest, Hungary. szalay@bel1.sote.hu
Telephone: +36-1-210-1007 **Fax:** +36-1-210-1007
Received: 2004-01-10 **Accepted:** 2004-04-14

Abstract

AIM: Cardiovascular autonomic and peripheral sensory neuropathy is a known complication of chronic alcoholic and non-alcoholic liver diseases. We aimed to assess the prevalence and risk factors for peripheral sensory nerve and autonomic dysfunction using sensitive methods in patients with primary biliary cirrhosis (PBC).

METHODS: Twenty-four AMA M2 positive female patients with clinical, biochemical and histological evidence of PBC and 20 age matched healthy female subjects were studied. Five standard cardiovascular reflex tests and 24-h heart rate variability (HRV) analysis were performed to define autonomic function. Peripheral sensory nerve function on median and peroneal nerves was characterized by current perception threshold (CPT), measured by a neuroselective diagnostic stimulator (Neurotron, Baltimore, MD).

RESULTS: Fourteen of 24 patients (58%) had at least one abnormal cardiovascular reflex test and thirteen (54%) had peripheral sensory neuropathy. Lower heart rate response to deep breathing ($P = 0.001$), standing ($P = 0.03$) and Valsalva manoeuvre ($P = 0.01$), and more profound decrease of blood pressure after standing ($P = 0.03$) was found in PBC patients than in controls. As a novel finding we proved that both time domain and frequency domain parameters of 24-h HRV were significantly reduced in PBC patients compared to controls. Each patient had at least one abnormal parameter of HRV. Lower CPT values indicated hyperaesthesia as a characteristic feature at peroneal nerve testing at three frequencies (2000 Hz: $P = 0.005$; 250 Hz: $P = 0.002$; 5 Hz: $P = 0.004$) in PBC compared to controls. Correlation of autonomic dysfunction with the severity and duration of the disease was observed. Lower total power of HRV correlated with lower CPT values at median nerve testing at 250 Hz ($P = 0.0001$) and at 5 Hz ($P = 0.002$), as well as with those at peroneal nerve testing at 2000 Hz ($P = 0.01$).

CONCLUSION: Autonomic and sensory nerve dysfunctions are frequent in PBC. Twenty-four-hour HRV analysis is more sensitive than standard cardiovascular tests for detecting of both parasympathetic and sympathetic impairments. Our novel data suggest that hyperaesthesia is a characteristic feature of peripheral sensory neuropathy and might contribute to itching in PBC. Autonomic dysfunction is related to the duration and severity of PBC.

Keresztes K, Istenes I, Folhoffer A, Lakatos PL, Horvath A, Csak T, Varga P, Kempler P, Szalay F. Autonomic and sensory nerve dysfunction in primary biliary cirrhosis. *World J Gastroenterol* 2004; 10(20): 3039-3043
http://www.wjgnet.com/1007-9327/10/3039.asp

INTRODUCTION

Autonomic neuropathy (AN) is frequent complication of both alcoholic and non-alcoholic chronic liver diseases[1]. Cardiovascular AN represents a serious complication as it carries a 5-fold risk of mortality in patients with chronic liver diseases[2]. In a 10-mo long follow-up study in patients awaiting for liver transplantation the mortality was significantly higher in patients with AN (27%) compared to those without AN (0%), suggesting that AN should be taken into consideration for early liver transplantation in patients with advanced liver disease[3]. Up to now the precise explanation of increased mortality associated with AN has not been identified. Beside the most severe complications of AN-silent myocardial ischaemia and infarction, cardiorespiratory arrest, major arrhythmias[4] -the attenuation of circadian variation of blood pressure and heart rate may contribute to the higher death rate[5,6]. Prolongation of the QT-interval is also involved in the poor prognosis of AN accompanying chronic liver disease [7,8]. Autonomic neuropathy may also be regarded as a potential etiologic factor of hyperdynamic circulation and portal hypertension[9].

Recently, attention has been focused on the importance of 24-h heart rate variability (HRV). It has been confirmed that HRV is a strong and independent predictor of mortality after an acute myocardial infarction[10]. Time and frequency domain analysis of HRV proved to be a reliable, noninvasive tool to provide quantitative information on cardiovascular autonomic function differentiated into vagal and sympathetic components[11]. Additionally, assessment of HRV is a sensitive method for early detection of autonomic neuropathy even if the standard cardiovascular reflex tests are normal[12]. Depressed HRV has been described not only in cardiovascular disorders, but also in chronic liver diseases[5,13-15]. Although autonomic and sensory neuropathy is known as a common extrahepatic manifestation in chronic liver diseases[1,3,7,13], there are only few data on risk factors of neuropathy in PBC[16,17].

The aim of our study was to assess the frequency and predisposing factors of autonomic and peripheral sensory neuropathy in PBC.

MATERIALS AND METHODS

Patients

Twenty-four female patients with PBC (mean age: 60.4±7.1 years; range: 45-73 years) from the Hepatological Outpatient Unit of Semmelweis University, Budapest and 20 age-matched healthy female controls (mean age: 59.3±6.8 years; range: 44-72 years) were recruited for this cross sectional study. The diagnosis of PBC was based on characteristic clinical and laboratory data, AMA M2 positivity and liver biopsy. The severity of liver disease was assessed by histologic classification. Stage I: 2, stage II: 5, stage III: 12 and stage IV: 5 patients. Full medical history was taken, followed by thorough physical and neurologic

examination in each patient and control. Patients were only included if they were normotensive, ie. no history of hypertension, and at the time of inclusion visiting office blood pressure <140/90 mmHg calculated by the mean of three measurements using Korotkov's technique and no evidence of disease known to affect autonomic function (e.g. other hepatic disease, cardiovascular, kidney, endocrinologic, neurologic and psychiatric disorders including alcoholism). None was taking any antihypertensive drugs or other medications, apart from ursodeoxycholic acid, vitamin D and calcium supplementation[18], and none had ascites. The healthy controls were recruited from the staff of our institution and their family members. Every participant was asked to refrain from consuming caffeine and alcoholic beverages, and tobacco products 12 h before autonomic testing.

Methods

The autonomic function was explored by the *five standard cardiovascular reflex tests*[19]. Heart rate tests (heart rate responses to deep breathing, the 30/15 ratio and the Valsalva ratio) mainly reflect parasympathetic function while blood pressure responses to sustained handgrip and standing primarily allow the assessment of sympathetic integrity. Patients with at least one abnormal or two borderline cardiovascular tests were considered to have autonomic neuropathy. The same research assistant using a computerized ECG-recording-analyzing system developed by Innomed Inc, Budapest, Hungary, performed all reflex tests.

Two channel 24-h ECG recordings were done by CardioTens equipment (Meditech, Budapest, Hungary). This device complies with the requirements of the British Hypertension Society and the Association for the Advancement of Medical Instrumentation protocols. Automatic filters were used to continuously restore baseline and filter background and muscle noise. Analysis of stored data was done by Medibase software. The recording was also edited using visual control and manual corrections were made to omit ectopic beats, arrhythmic events and noise effects and only normal-to-normal beats (NN intervals) were used for further analysis. Ratio of normal beats to total number of beats was >95% in both groups.

To characterize 24-h *HRV*, time domain and frequency domain methods were used. Since there were several parameters cited in the literature to assess HRV, we selected a limited number of parameters according to the recommendations of the European Society of Cardiology and the North American Society of Pacing and Electrophysiology[11]. Statistical time domain parameters could be calculated from either the direct measurements of NN intervals or from the differences between NN intervals. The following parameters were calculated from direct measurements of NN intervals: standard deviation of all NN (SDNN) intervals reflecting all the cyclic components responsible for variability and standard deviation of the averages of NN (SDANN) intervals in all 5-min segments of the entire recording, an estimate of the changes in heart rate due to cycles longer than 5 min.

Statistical time domain parameters deriving from NN interval differences are RMSSD and pNN50. RMSSD (the square root of the mean of the sum of the squares of differences between adjacent NN intervals) is an estimate of short-term components of HRV. PNN50 (the proportion of adjacent NN intervals differ by more than 50 ms) was considered to reflect the vagal tone of the heart.

A simple geometric time domain parameter, HRV triangular index (HRVTI) was also computed. HRVTI is the integral of the density distribution (the number of all NN intervals) divided by the maximum of the density distribution. HRVTI represents overall HRV.

In the frequency domain analysis (power spectral density analysis) of heart period oscillations low- (0.04-0.15 Hz) and high- (0.15-0.4 Hz) frequency bands of the power (i.e. variance) spectrum (power distribution as function of frequency) was performed. The following frequency domain measures were computed: TP (total power: variance of all NN intervals), LF (power in the low frequency range) which is under both sympathetic and parasympathetic influences, HF (power in the high frequency range) which is an acknowledged measure of the parasympathetic (i.e. vagal) modulations.

Peripheral sensory function was characterized by the evaluation of the current perception threshold (CPT) with a neuroselective diagnostic stimulator (Neurotron, Baltimore, MD, USA), which permits transcutaneous testing at three sinusoidal frequencies (2000 Hz, 250 Hz and 5 Hz). The intensity of the stimulating current was changed within the range from 0.01 to 9.99 mA. The neurometer is the first instrument designed for the overall assessment of all types of sensory fibres. As demonstrated by the results of comparative trials conducted earlier[20], CPT values measured during high frequency stimulation correlated best with tests of large fibre function and low frequency CPT values correlated with tests of small fibre function. Median and peroneal nerves (digital branches) were studied.

The Local Regional Committee of Science and Research Ethics approved the study. Written informed consent was obtained.

Statistical analysis

All analyses were performed using Statistica Software. Data are expressed as mean±SD and were compared between groups by Student's *t*-test. Correlations between variables were analysed by partial correlation coefficient calculation adjusted for age. $P<0.05$ was regarded as statistically significant.

RESULTS

Autonomic function

Using standard cardiovascular tests[18], 14 PBC patients (58%) had at least one abnormal autonomic function test. Among these patients parasympathetic neuropathy was found in 8 (57.1%) patients, sympathetic nerve dysfunction was observed in 2 patients, and 4 subjects had both parasympathetic and sympathetic damage.

As a novel finding we proved that both time domain and frequency domain parameters of HRV were significantly reduced in PBC patients compared to controls. Each patient had at least one abnormal parameter of HRV.

Results of cardiovascular reflex tests and HRV parameters are presented in Table 1. The heart rate response to deep breathing ($P = 0.001$), as well as to standing ($P = 0.03$) and Valsalva manoeuvre ($P = 0.01$) was significantly lower in PBC patients than in age matched control subjects. A more profound decrease of systolic blood pressure after standing ($P = 0.03$) was found in patients compared to healthy controls. By HRV analysis most of the time-domain indices were significantly lower in patients than in controls (PNN50: $P = 0.0008$; HRVTI: $P = 0.004$; RMSSD: $P = 0.006$ and SDNN: $P = 0.015$). PBC patients also showed significantly lower total power ($P = 0.0001$), power of LF band ($P = 0.00007$) and of HF band ($P = 0.004$).

Peripheral sensory nerve function

At least one abnormal sensory parameter was detected in 13 patients (54%), of whom 12 had hyperaesthetic type, and only one had hypoaesthetic type sensory nerve dysfunction. Among patients with sensory neuropathy the lower extremities were affected in all 13 patients, while 3 patients had abnormal CPT values at upper extremities testing. Lower CPT values, indicating hyperaesthesia, were found in PBC patients compared with age matched controls at peroneal nerve testing at all three frequencies ($P<0.01$) as well as at median nerve testing at 250 Hz ($P = 0.03$). The CPT values of patients and controls are shown in Table 2.

Table 1 Results of cardiovascular reflex tests and 24-h heart rate variability (HRV) parameters in patients with PBC and age matched healthy controls

	Patients with PBC (n = 24)	Age-matched controls (n = 20)	P value
Cardiovascular reflex tests			
Deep breathing test (beats / min)	11.3 (4.4)	17.5 (6.6)	0.001
30 / 15 ratio	1.18 (0.1)	1.29 (0.2)	0.03
Valsalva ratio	1.32 (0.1)	1.48 (0.2)	0.01
Orthostatic test (mmHg)	-7.1 (8.6)	-1.5 (3.7)	0.03
Handgrip test (mmHg)	20.4 (8.1)	22.3 (4.4)	NS
Time domain parameters of HRV			
SDNN (ms)	119 (42)	151 (37)	0.015
SDANN (ms)	142 (102)	165 (66)	NS
RMSSD (ms)	23 (10)	38 (22)	0.006
PNN50 (%)	2.4 (4)	11 (10)	0.0008
HRVTI	28 (8)	38 (13)	0.004
Frequency domain parameters of HRV			
TP (ms^2)	1506 (701)	4032 (2787)	0.0001
LF (ms^2)	299 (176)	1213 (977)	0.00007
HF (ms^2)	150 (148)	525 (565)	0.004

Table 2 Current perception threshold (CPT) values in PBC patients and controls at median and peroneal nerve testing at three different frequencies

	Patients with PBC (n = 24)	Age-matched controls (n = 20)	P value
CPT (mA)-Median nerve			
2000 Hz	2.45 (0.75)	2.94 (0.87)	0.076
250 Hz	0.81 (0.33)	1.10 (0.46)	0.030
5 Hz	0.42 (0.23)	0.50 (0.17)	0.242
CPT (mA)-Peroneal nerve			
2000 Hz	2.91 (0.71)	3.61 (0.66)	0.005
250 Hz	1.01 (0.39)	1.40 (0.26)	0.002
5 Hz	0.68 (0.40)	1.06 (0.28)	0.004

Associations of autonomic function with clinical and biochemical characteristics

After adjustment for age, the longer duration of the disease was associated with less prominent increase of diastolic blood pressure during sustained handgrip test (r = -0.52, P = 0.01). Duration of the disease also correlated with reduced SDNN and SDANN (r = 0.47 and r = -0.45, P<0.05, for both). The severity of PBC (stage) was found to negatively correlate with lower HRVTI (r = -0.6, P = 0.01) and lower SDANN (r = -0.49, P = 0.04) as well.

Partial correlation analysis revealed that lower prothrombin activity was associated with lower heart rate response to standing (r = 0.79, P = 0.006) as well as to deep breathing (r = 0.63, P = 0.04). The serum albumin positively correlated with SDNN and HRVTI (r = 0.47 and 0.57, P<0.05, for both). Serum AST and ALT levels negatively correlated with SDNN (r = -0.54, P = 0.01, for both). Positive correlations of SDNN (r = 0.62, P = 0.004) and Valsalva ratio (r = 0.51, P = 0.02) with serum trigliceride levels were found. These relationships remained significant after age adjustment.

Correlations of peripheral sensory nerve function with clinical and chemical characteristics

Negative correlations of serum ALT with CPT values at median nerve testing at 250 HZ (r = -0.56, P = 0.005) as well as with CPT at peroneal (r = -0.48, P = 0.03) and median nerve (r = -0.45, P = 0.02) at 5 Hz were revealed. AST and ALP levels were inversely related to CPT values at peroneal nerve testing at all three frequencies, as well as to those at median nerve testing at 250 Hz and 5 Hz. An inverse relationship was also found between serum bilirubin levels and CPT values at median nerve testing at 5 Hz (r = -0.43, P = 0.04). None of these relationships was altered by adjustment for age.

Interestingly no correlation was found between peripheral sensory nerve function and duration and severity of PBC. Furthermore, no association was found between sensory nerve function and serum lipid levels, prothrombin activity and serum albumin levels.

Associations between autonomic and peripheral sensory nerve function

Reduced total power was associated with lower CPT values testing median nerve at 250 Hz (r = 0.69, P = 0.0001), and at 5 Hz (r = 0.62, P = 0.002), as well as with those testing peroneal nerve at 2000 Hz (r = 0.53, P = 0.01). HF-power was positively related to CPT values at peroneal nerve testing at 2000 Hz (r = 0.51, P = 0.01), LF-power correlated positively with CPT values testing median nerve at 250 (r = 0.53, P = 0.01), as well as at 5 Hz (r = 0.47, P = 0.03). A significant positive correlation was observed between the SDNN and the CPT values testing the median nerve at 2000 Hz (r = 0.60, P = 0.003), as well as at 250 Hz (r = 0.53, P = 0.01) and at 5 Hz (r = 0.50, P = 0.02). Lower SDANN values were associated with lower CPT values at the median nerve at 2000 Hz (r = 0.52, P = 0.01). The PNN50 values correlated positively with CPT values testing the peroneal nerve at 2000 Hz (r = 0.50, P = 0.02) and the beat-to-beat variation was also positively related to CPT values at the peroneal nerve at 250 Hz (r = 0.47, P = 0.02), even after adjustment for age.

DISCUSSION

Somatic neuropathy accompanying advanced stage primary biliary cirrhosis, was described as early as 1964 by Walker and Thomas[21]. In the last two decades, autonomic neuropathy has been found as a common complication of this type of liver disease[1,16,17,22]. The poor prognosis of neuropathy has been widely known even in chronic liver diseases, primarily as regards the impairment of autonomic functions[2,3]. During the 4-year follow-up study of Hendrickse *et al*., mortality was 30% among patients with autonomic neuropathy and 6% in those without AN[2]. As suggested by the description of clinical features, the prognosis of sensory neuropathy was rather poor. In their 14-year follow-up study conducted on diabetic patients, Coppini *et al.* showed that sensory neuropathy was an independent predictor for mortality[23].

There are only few studies on the prevalence of autonomic and sensory neuropathy in PBC, and the characteristics of the study population have a strong impact on prevalence data. Nevertheless, our data are consistent with previous findings showing that autonomic and sensory neuropathy were frequent complications in patients with PBC[1,16,17].

Sensory neuropathy has also been found as a common complication in chronic liver diseases, yet there are no data on its prognostic importance.

Although many studies have been published on autonomic and sensory neuropathy in chronic liver diseases, some of the results were conflicting. To our knowledge this is the first study in PBC conducted on the evaluation of autonomic function assessed both by the standard cardiovascular reflex tests and by 24-h HRV analysis. HRV analysis could indicate the synchronic impairment of the parasympathetic and sympathetic systems in PBC. To date only one systematic study has assessed the factors that predispose to autonomic and sensory nerve dysfunction in PBC[17], but in their study the autonomic function was only evaluated by the standard tests. We confirmed previous data showing that autonomic dysfunction was related to the severity of liver damage[1,14,15,24], contrary to Oliver[25] who did not show similar results. As a novel finding not only the severity, but also the duration of PBC was related to autonomic dysregulation. It would be worthy to investigate neuropathy in asymptomatic PBC population[26]. We have also found a close correlation between decreased serum albumin and prothrombin activity with the autonomic dysfunction, which differed from the data of Lazzeri *et al*.[5], but these results were consistent with two other studies[3,15]. Moreover, in our study the serum AST and ALT levels were inversely related to the autonomic function. The markers of cholestasis did not correlate with the autonomic function, in keeping with the data of Coelho[15]. An interesting finding in our study was that lower serum trigliceride level was associated with impaired autonomic function. This is of interest, since PBC related somatic neuropathy was originally attributed to lipid deposition[21]. Later, however, no significant association of hyperlipidaemia with autonomic and sensory neuropathy was demonstrated[17], which is consistent with our data regarding the serum cholesterol level.

Sensory impairment might involve both large myelinated fibres and small sensory fibres as demonstrated by Kempler[16]. These data are consistent with the present results showing abnormal CPT values at all types of sensory fibres, testing both median and peroneal nerves. Abnormal CPT values were more frequent on the lower extremities, which were in accordance with previous observations that longer fibres were damaged earlier[27]. The present data extended previous results by analysing which type of sensory nerve dysfunction was specific for PBC. Our data provide the first evidence that hyperesthaesia is a feature of peripheral sensory neuropathy in PBC. In this phase of neuropathy the degeneration and regeneration of non-myelinated small fibres occur concomitantly. These processes were inaccesible to earlier methods for sensory testing, but the neurometer could permit the detection of this early phase of sensory nerve impairment[28]. Evaluating the current perception threshold by neurometer seems a simple and comprehensive way of assessing even early abnormalities of peripheral sensory nerve function in patients with PBC. Recent studies have demonstrated that itching, a characteristic symptom in PBC, could be evoked by activation of peripheral unmyelinated C-fibers[29,30]. In our study, patients with hyperaesthaesia at 5 Hz had itching. Considering that 5 Hz CPT values demonstrate the unmyelinated C-fibre function, our results support the possible role for unmyelinated C-fibre damage in hyperaesthaesia in the pathogenesis of pruritus in PBC.

Serum bilirubin and albumin were found to be associated with peripheral nerve function in the only one study published on correlation of sensory nerve dysfunction in PBC[17]. Our results confirmed these data regarding serum bilirubin, but not serum albumin. Moreover, in our study not only elevated serum bilirubin, but higher serum AST, ALT and ALP were also related to lower CPT values.

Our results were consistent with those of Hendrickse[17], showing that peripheral sensory nerve function correlates with cardiovascular autonomic function in patients with PBC. Prospective studies are required to evaluate the prognostic importance of sensory neuropathy in PBC.

In summary, autonomic and sensory nerve dysfunctions are frequent complications in patients with PBC and seem to be mutually related. The novel findings of reduced time and frequency domain parameters of 24-h HRV analysis indicate the synchronic impairment of parasympathetic and sympathetic systems. HRV analysis is more sensitive than standard cardiovascular tests for detecting autonomic neuropathy. This study provides the first evidence that hyperaesthesia involving all types of fibres is characteristic for sensory neuropathy in PBC. Hyperaesthaesia of unmyelinated fibres might partly be responsible for itching, a characteristic symptom in PBC. Our data suggest that autonomic neuropathy is related to the severity and duration of liver disease as well as to the markers of hepatocellular dysfunction.

REFERENCES

1 **Szalay F**, Marton A, Keresztes K, Hermanyi ZS, Kempler P. Neuropathy as an extrahepatic manifestation of chronic liver diseases. *Scand J Gastroenterol* 1998; **228**(Suppl): 130-132

2 **Hendrickse MT**, Thuluvath PJ, Triger DR. The natural history of autonomic neuropathy in chronic liver disease. *Lancet* 1992; **339**: 1462-1464

3 **Fleckenstein JF**, Frank S, Thuluvath PJ. Presence of autonomic neuropathy is a poor prognostic indicator in patients with advanced liver disease. *Hepatology* 1996; **23**: 471-475

4 **Valensi P.** Diabetic autonomic neuropathy: what are the risks? *Diabetes Metab* 1998; **24**(Suppl 3): 66-72

5 **Lazzeri C**, La Villa G, Laffi G, Vecchiarino S, Gambilonghi F, Gentilini P, Franchi F. Autonomic regulation of heart rate and QT interval in nonalcoholic cirrhosis with ascites. *Digestion* 1997; **58**: 580-586

6 **Moller S**, Winberg N, Henriksen JH. Noninvasive 24-hour ambulatory arterial blood pressure monitoring in cirrhosis. *Hepatology* 1995; **22**: 88-95

7 **Kempler P**, Varadi A, Szalay F. Autonomic neuropathy and prolongation of QT-interval in liver disease. *Lancet* 1992; **340**: 318

8 **Fischberger SB**, Pittman NS, Rossi AF. Prolongation of the QT interval in children with liver failure. *Clin Cardiol* 1999; **22**: 658-660

9 **Kempler P**, Toth T, Szalay F. May autonomic neuropathy play a role in the development of hyperdinamic circulation and portal hypertension in chronic liver diseases? (Hypothesis). In: Aquino AV, Picdad FF, Sulit YQM (eds). *23rd Congress of the International Society of Internal Medicine Monduzzi Editore Bologna Italy* 1996: 251-254

10 **La Rovere MT**, Bigger JT, Marcus FI, Mortara A, Schwartz PJ. Baroreflex sensitivity and heart-rate variability in prediction of total cardiac mortality after myocardial infarction ATRAMI (Autonomic Tone and Reflexes After Myocardial Infarction) Investigators. *Lancet* 1998; **351**: 478-484
11 No author guideline: Heart rate variability: standards of measurement, physiological interpretation, and clinical use. Task Force of the European Society of Cardiology and the North American Society of Pacing and Electrophysiology. *Circulation* 1996; **93**: 1043-1065
12 **Barron SA**, Rogovski Z, Kanter Y, Hemli Y. Parasympathetic autonomic neuropathy in diabetes mellitus: the heart is denervated more often than the pupil. *Electromyogr Clin Neorophysiol* 1994; **34**: 467-469
13 **Dillon JF**, Plevris JN, Nolan J, Ewing DJ, Neilson JM, Bouchier IA, Hayes PC. Autonomic function in cirrhosis assessed by cardiovascular reflex tests and 24-hour heart rate variability. *Am J Gastroenterol* 1994; **89**: 1544-1547
14 **Fleisher LA,** Fleckenstein JF, Frand SM, Thuluvath PJ. Heart rate variability as a predictor of autonomic dysfunction in patients awaiting liver transplantation. *Dig Dis Sci* 2000; **45**: 340-344
15 **Coelho L**, Saraiva S, Guimaraes H, Freitas D, Providencia LA. Autonomic function in chronic liver disease assessed by Heart Rate Variability Study. *Rev Port Cardiol* 2001; **20**: 25-36
16 **Kempler P**, Varadi A, Kadar E, Szalay F. Autonomic and peripheral neuropathy in primary biliary cirrhosis:evidence of small sensory fibre damage and prolongation of the QT interval. *J Hepatol* 1994; **21**: 1150-1151
17 **Hendrickse MT**, Triger DR. Autonomic and peripheral neuropathy in primary biliary cirrhosis. *J Hepatol* 1993; **19**: 401-407
18 **Szalay F**. Treatment of primary biliary cirrhosis. *J Physiol Paris* 2001; **95**: 407-412
19 **Ewing DJ**, Martyn CN, Young RJ, Clarke BF. The value of cardiovascular autonomic function tests: 10 years experience in diabetes. *Diabetes Care* 1985; **8**: 491-498
20 **Pitei DL**, Watkins PJ, Stevens MJ, Edmonds ME. The value of the NEUROMETER® CPT in assessing diabetic neuropathy by measurement of the current perception threshold. *Diabetic Med* 1994; **11**: 872-876
21 **Walker JG,** Thomas PK. Xanthomatosus neuropathy in primary biliary cirrhosis. *Tijdschr Gastroenterol* 1964; **48**: 84-86
22 **Thuluvath PJ**, Triger DR. Autonomic neuropathy and chronic liver disease. *Q J Med* 1989; **72**: 737-747
23 **Coppini DV**, Bowtell PA, Weng C, Young PJ, Sönksen PH. Showing neuropathy is related to increased mortality in diabetic patients – a survival analysis using an accelerated failure time model. *J Clin Epidemiol* 2000; **53**: 519-523
24 **Bajaj BK**, Agarwal MP, Ram BK. Autonomic neuropathy in patients with hepatic cirrhosis. *Postgrad Med J* 2003; **79**: 408-411
25 **Oliver MI**, Miralles R, Rubies-Prat J, Navarro X, Espadaler JM, Sola R, Andreu M. Autonomic dysfunction in patients with non-alcoholic chronic liver disease. *J Hepatol* 1997; **26**: 1242-1248
26 **Jiang XH**, Zhong RQ, Fan XY, Hu Y, An F, Sun JW, Kong XT. Characterization of M2 antibodies in asymptomatic Chinese population. *World J Gastroenterol* 2003; **9**: 2128-2131
27 **Oh SJ.** Clinical Electromyelography: Nerve conduction studies. In: Oh SJ ed. Nerve conduction in polyneuropathies. *Baltimore William Wilkins* 1993: 579-591
28 **Kempler P.** Neurometer. In: Kempler P ed. Neuropathies. Pathomechanism, clinical presentation, diagnosis therapy. *Budapest Springer* 2002: 74-76
29 **Bergasa NV**. Pruritus and fatigue in primary biliary cirrhosis. *Clin Liver Dis* 2003; **7**: 879-900
30 **Stander S**, Steinhoff M, Schmelz M, Weisshaar E, Metze D, Luger T. Neurophysiology of pruritus: cutaneous elicitation of itch. *Arch Dermatol* 2003; **139**: 1463-1470

Edited by Wang XL **Proofread by** Chen WW and Xu FM

PO Box 2345, Beijing 100023, China
Fax: +86-10-85381893
E-mail: wjg@wjgnet.com www.wjgnet.com

World J Gastroenterol 2004;10(20):3044-3047
World Journal of Gastroenterology
 ISSN 1007-9327

• BRIEF REPORTS •

Expression of mucins and E-cadherin in gastric carcinoma and their clinical significance

Hong-Kai Zhang, Qiu-Min Zhang, Tie-Hua Zhao, Yuan-Yuan Li, Yong-Fen Yi

Hong-Kai Zhang, **Tie-Hua Zhao,** Department of Pathology, Fuxing Hospital, Capital University of Medical Sciences, Beijing 100038, China
Qiu-Min Zhang, Shenzhen Nanling Hospital, Shenzhen 518123, Guangdong Province, China
Yuan-Yuan Li, **Yong-Fen Yi,** Department of Pathology, Chongqing Medical University, Chongqing 400016, China
Supported by the Science Reserch Foundation of the Health Bureau of Chongqing Municipality, No.2000-48
Correspondence to: Dr. Yong-Fen Yi, Department of Pathology, Chongqing Medical University, Chongqing 400016, China. yiyongfen1953@yahoo.com.cn
Telephone: +86-23-68485789
Received: 2004-01-02 **Accepted:** 2004-02-12

Abstract

AIM: To investigate the expression of three types of mucin (MUC1, MUC2, MUC5AC) and E-cadherin in human gastric carcinomas and their clinical significance.

METHODS: Ninety-four gastric cancer specimens were classified according to WHO criteria and detected by immunohistochemical assay of expression of mucins and E-cadherin.

RESULTS: The positive expression rates of MUC1, MUC2, MUC5AC and E-cadherin were 82% (77/94), 84% (79/94), 40% (38/94) and 56% (53/94) respectively. MUC1 expression was significantly correlated with the types of cancer (the positive rates of MUC1 in well and moderately differentiated tubular adenocarcinoma, poorly differentiated adenocarcinoma, signet-ring cell carcinoma and mucinous carcinoma were 91%, 87%, 71%, 71%, respectively, $P<0.05$), age of patients (the positive rates of it among the people who are younger than 40 years, between 40-60 years and over 60 year were 74%, 81%, 89%, $P<0.05$), lymph nodes involvement (the positive rates in the non-interfered group and the interfered group were 78%, 85%, $P<0.05$) and tumor size (the positive rates in the tumors with the size less than 3 cm, 3-6 cm and larger than 6 cm were 69%, 92%, 69%, $P<0.05$); MUC2 expression was significantly associated with types of cancers and had the strongest expression in mucinous carcinomas (the positive rates of MUC2 in well and moderately differentiated tubular adenocarcinoma, poorly differentiated adenocarcinoma, signet-ring cell carcinoma and mucinous carcinoma were 94%, 70%, 81%, 100%, $P<0.05$), but it had no obvious relation to age, gender, tumor location, lymph nodes involvement, depth of invasion and metastasis to extra-gastric organs ($P>0.05$); MUC5AC expression was not related to any of the characteristics investigated except that it had relation to gender, whereas MUC5AC showed the tendency to higher expression in less invasive lesions and lower expression in advanced stage cancers ($P>0.05$); No significant difference was found for E-cadherin expression. There were strong positive relationships between the expression of MUC1 and E-cadherin, MUC2 and E-cadherin, MUC1 and MUC2 ($R = 0.33$, $R = 0.22$, $R = 0.32$, respectively, $P<0.05$). According to the COX proportional hazards model, older patients, involvement of lymph nodes, different types of gastric cancer and MUC2 expression were significantly associated with poorer outcome of gastric carcinoma patients ($\beta = 0.08$, $\beta = 3.94$, $\beta = 1.33$, $\beta = 0.75$, respectively, $P<0.05$).

CONCLUSION: MUC1 and MUC2 are good markers of different types of gastric cancer. MUC2 is especially a good marker of mucinous carcinoma. MUC1, MUC2 may interfere with the function of E-cadherin in gastric carcinomas, and have synergic effect on progression of gastric cancers.

Zhang HK, Zhang QM, Zhao TH, Li YY, Yi YF. Expression of mucins and E-cadherin in gastric carcinoma and their clinical significance. *World J Gastroenterol* 2004; 10(20): 3044-3047
http://www.wjgnet.com/1007-9327/10/3044.asp

INTRODUCTION

Mucins, the high molecular weight glycoproteins that contain oligosaccharides, are the major components of the mucous gel covering the surface of epithelial tissue. Their main functions are thought to be lubrication and protection of the epithelial surface[1,2]. To date, at least thirteen mucins have been found[3].

MUC1, an epithelial mucin glycoprotein, is highly expressed in lactating mammary glands[4]. Under pathological conditions, such as colon adnenocarcinoma and pancreas adnenocarcinoma or stomach adnenocarcinoma, MUC1 would change its expression fashion and rate[5]. MUC2, a gel-forming mucin, highly expresses in normal intestinal tissues and has no expression in normal gastric mucosa. However, it had *de novo* expression in stomach when the mucosa underwent metaplasia and carcinoma[6]. MUC5AC, a gastric type mucin in gastric cardia and body mucosa, is decreased when the tissue has cancers[7]. E-cadherin is a calcium-dependent cell-cell adhesion molecule and its expression decreases in the carcinoma tissues thus contributing to cancer progression and correlate with patients' prognosis[8].

Despite many studies have been done in gastric carcinoma tissue, the results are still in contradiction. Some reported that MUC1 could well predict the patients' prognosis, while others thought not. MUC2 showed the same result[9,10]. MUC5AC is a relatively less studied molecule, and its expression decreases in advanced cancers than in early cancers[11]. Study on E-cadherin also remains contradictory[12,13]. What's more, few studies have been done about their relationships, especially between E-cadherin and the mucins. The present study was designed to provide some useful information on these molecules.

MATERIALS AND METHODS

Materials

Ninety-four patients with gastric adenocarcinomas confirmed pathologically and underwent gastrectomy in our hospital from January 1989 to December 2000 were Systemically selected for the study. Patients' age, gender, tumor location, depth of invasion, local lymph nodes involvement, metastasis, tumor size were all obtained from the original records. Specimens were

histologically classified according to WHO criteria by two experienced pathologists . Among these subjects, there were 33 moderately and highly-differentiated tubular carcinomas, 23 poorly differentiated adenocarcinomas, 31 signet-ring cell carcinomas and 7 mucinous carcinomas. There were 64 male and 30 female patients with a mean age of 52.1±12.1 years (range 25-75 years). The mean tumor size was 4.5±2.0 cm in diameter (range 1-10 cm). A total of 48 patients provided full information during follow-up.

Reagents and methods

Antibodies against MUC1, MUC2 and MUC5AC were purchased from Shenzhen Jingmei Biotechnology, Inc., and the antibody against E-cadherin was from Fujian Maixin Co, Ltd. All the 94 formalin-fixed, paraffin-embedded specimens were sliced sequentially with a thickness of 4 μm. According to the protocol, these tissue sections were dewaxed, rehydrated, incubated with 30 mL/L hydrogen peroxide in methanol for 30 min to block endogenous peroxidase, and then washed with PBS (phosphate buffered saline, pH 7.4). After that, they were incubated with non-immunized horse serum for 30 min at room temperature, washed again, and incubated with the specific antibodies overnight at 4 ℃ or 1 h at 37 ℃. They were washed again, incubated with the secondary antibody (Biotin labeled goat anti-rabbit antibody) and streptavidin-biotin peroxidase for 30 min separately, visualized with 3,3'-diaminobenzidine tetra-hydrochloride and H_2O_2, counterstained with haematoxylin. Primary antibodies were replaced with PBS buffer as negative control.

In order to obtain a more precise relation between mucins and the clinical indicators, a semiquantitative analysis was performed to evaluate positively stained cells in carcinoma tissues as +++, ++, + or -. We examined 10 fields of each cancerous tissue at high magnification (×400) and scored the intensity of color as 0 for non-stained,1 for the color of yellow, 2 for brown-yellow, 3 for brown; the rate of positive cell was judged as negative (0) if it was less than 5%, 1 for 5-25%, 2 for 26-50%, 3 for over 50%. The mean intensity scores were multiplied by the rate scores. Negative group (-) was defined when the result was 0, 1-3 was mild-positive (+), 4-5 was moderate-positive (++) and equal or greater than 6 was strong positive (+++).

Statistical analysis

χ^2 test, the hazards proportional analysis (COX) and the correlation analysis were used to determine differences between groups using SPSS 10.0 software. Statistical significance was established at $P<0.05$.

RESULTS

Expression and distribution of MUC1, MUC2, MUC5AC and E-cadherin

The positivity rate of MUC1 was 82% in the cancerous tissues. It expressed in the cytoplasm diffusely or stained on the membrane of the cells. There were significant differences in its expression among different types of the cancer ($P<0.05$) with the highest expression rate in well and moderately differentiated tubular

Table 1 protein expression in gastric carcinoma

	n	MUC1				MUC2				MUC5AC				E-cadherin			
		-	+	++	+++	-	+	++	+++	-	+	++	+++	-	+	++	+++
Types of cancer			$P = 0.005$				$P = 0.001$				NS				NS		
WMDTA	33	3	2	3	25	2	3	7	21	21	6	0	6	10	8	5	10
PDA	23	3	11	2	7	7	6	5	5	15	4	1	3	11	5	3	4
SRCC	31	9	10	2	10	6	9	10	6	14		5	8	15	8	4	4
MC	7	2	1	0	4	0	0	0	7	6	0	0	1	5	2	0	0
Age(yr)			$P = 0.03$				NS				NS				NS		
⩽40	19	5	4	2	8	3	6	5	5	12	2	2	3	10	7	1	1
>40, ⩽60	48	9	18	1	20	10	9	10	19	26	10	3	9	20	9	8	11
>60	27	3	2	4	18	3	2	7	15	18	2	1	6	11	7	3	6
Sex			NS				NS				$P = 0.02$				NS		
male	64	13	14	4	33	10	10	14	30	42	5	3	14	28	17	7	12
female	30	4	10	3	13	6	7	8	9	14	9	3	4	13	6	5	6
Location			NS				NS				NS				NS		
Upper 1/3	13	0	4	1	8	1	2	0	10	12	0	0	1	3	4	1	5
Middle 1/3	23	6	6	0	11	4	3	6	10	12	3	2	6	11	7	2	3
Lower 1/3	58	11	14	6	27	11	12	16	19	32	11	4	11	27	12	9	10
Invasion			NS				NS				NS				NS		
within mucosa & sub-mucosa	7	2	1	0	4	3	2	0	2	5	0	0	2	4	1	0	2
Muscular layer	19	5	7	1	6	5	4	6	4	9	1	3	6	9	3	5	2
Serosa	68	10	16	6	36	8	11	16	33	42	13	3	10	28	19	7	14
Metastasis to LN			$P = 0.031$				NS				NS				NS		
No	40	9	14	10	7	9	9	11	11	25	4	3	8	20	8	5	7
Yes	54	8	10	7	29	7	8	11	28	31	10	3	10	21	15	7	11
Metastasis to other organs			NS				NS				NS				NS		
No	70	14	19	7	30	13	12	18	27	42	7	5	16	32	19	8	11
Yes	24	3	5	0	16	3	5	4	12	14	7	1	2	9	4	4	7
Tumor size (cm)			$P = 0.044$				NS				NS				NS		
⩽3	29	9	4	4	12	9	6	6	8	17	5	0	7	12	7	3	7
3-6	52	4	17	3	28	5	10	15	22	29	9	5	9	20	15	6	11
>6	13	4	3	0	6	2	1	1	9	10	0	1	2	9	1	3	0

NS: no significant difference; WMDTA: well and moderately differentiated tubular adenocarcinoma; PDA: Poorly differentiated adenocarcinoma; SRCC: Signet-ring cell; MC: mucinous carcinoma; LN: lymph node.

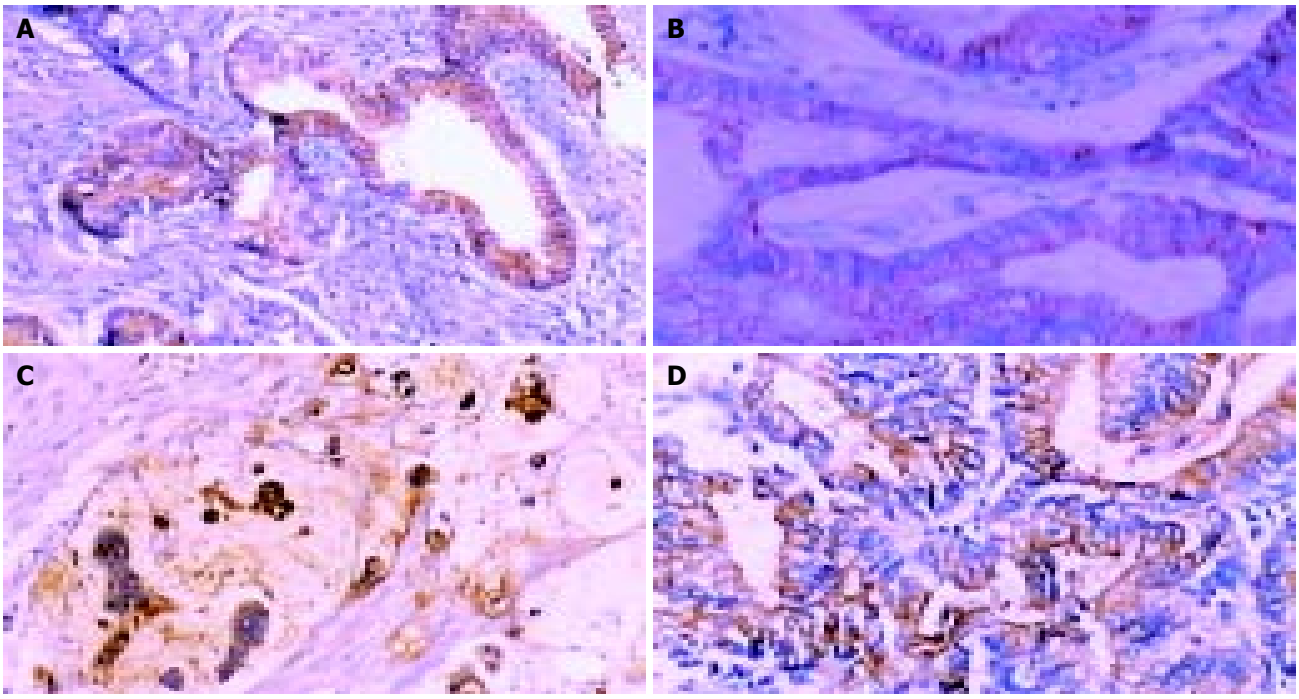

Figure 1 Results of immunohistochemical staining in gastric cancers (original magnification SP ×400). A: MUC5AC expression; B: E-cadherin expression; C: MUC1 expression; D: MUC2 expression.

adenocarcinomas (91%). Moreover, its expression level had significant relationship with patients' age, local lymph nodes involvement and tumor size ($P<0.05$). MUC2 had a positive expression rate of 84%, with the highest expression level in mucinous carcinomas (100%) and lowest expression level in signet-ring cell carcinoma (19%). Furthermore, it also showed significant differences in expression among different types of cancer ($P<0.05$). MUC5AC had a positive expression rate of 40% and the lowest expression level in mucinous carcinoma (14%), but no significant differences in expression levels among different types of cancer were found ($P>0.05$). It expressed mainly in the cytoplasm. E-cadherin had a positive expression rate of 56% with the highest expression in well and moderately differentiated cancers (70%) and the lowest in mucinous type (29%). There was no significant difference of expression level among different types of cancer ($P>0.05$). Its positive expression was on the membrane and in the cytoplasm of cancerous cells. The expression of MUC2, MUC5AC, E-cadherin were not significantly different with regards to clinicopathological characteristics (Table1, Figure1).

Relationship between proteins' expression and prognostic factors

There were significantly positive relationships between MUC1 and MUC2, MUC1 and E-cadherin, MUC2 and E-cadherin ($P<0.05$). According to COX analysis, patients' age, lymph node involvement, types of the cancer and the level of MUC2 expression were the factors related to patients' survival after operation (figures not shown).

DISCUSSION

We confirmed that mucin expression was associated with differentiation characteristics of gastric carcinoma. MUC1 was expressed in most of the studied gastric cancerous specimens (82%), being consistent with other studies[10]. MUC1 expression related to clinical characteristics such as patients' age, tumor size and local lymph nodes involvement. MUC1 expressed higher in older patients with larger tumor or with more ymph nodes involvement. On the other hand, though the expression of MUC1 was not significantly associated with the metastasis and depth of invasion ($P>0.05$), it still had the tendency toward higher expression in advanced stage of cancer. However, we failed to find that MUC1 had the prognostic role in gastric cancer patients, which is different with Ustsunomiya's conclusion[9], but consistent with Reis's conclusion[14]. These contradictory results might be due to our relatively small number of follow-up patients after operation.

MUC2, the intestinal mucin, expressed in most of the studied cases (86%), higher than that in other studies[15], However our result was in accordance with other results concerning its overwhelming expression in mucinous carcinomas[15,16]. Contradictory to some reports that MUC2 indicated good prognosis[9], our study found that MUC2 could predict poor outcome. Our *in vitro* study used anti-sense oligonucleotide of MUC2 to inhibit the growth of gastric cancer cells, while Sternberg used the anti-sense oligonucleotide of MUC2 in colon cells *in vitro* and *in vivo* and found that it decreased the adherence ability of cells to E-selectin and resulted in inhibition of liver metastasis[17]. Both supported our conclusion that MUC2 might contribute to gastric cancer progress.

MUC5AC was thought to be gastric mucin and expressed higher in early stage of cancers than in the advanced stage[18]. MUC5AC rarely expressed in mucinous carcinoma except in one case. Between different sex groups, MUC5AC had significant difference ($P<0.05$).

E-cadherin is a calcium-dependent molecule, and acts as a tumor-inhibitory factor. Some studies have shown that the lower expression level it had, the faster the tumor progressed[12]. But we could not draw a conclusion like this despite the tendency shown at present. While we noted its highest expression in the well and moderately differentiated tubular carcinoma which supported the view on its contribution to tubular structure formation[19].

Although some studies showed that MUC1 expression in gastric cancers was negatively correlated with the expression of E-cadherin[20], we found the positive relationships between them, what's more, the correlation of MUC1, MUC2 and E-cadherin were first studied by us. Both MUC1 and MUC2 might contribute to the progress of gastric cancer, and they might

restrain the role of E-cadherin.

In summary, MUC1 may contribute to gastric cancers progress, larger tumor size and metastasis to lymph nodes, at the same time, it may inhibit E-cadherin. MUC2 had the same role as MUC1,besides, it may be an indicator for prognosis of gastric cancer patients and good marker for mucinous cancers. E-cadherin could not be used a tangible marker to indicate gastric cancers progress but may play a role in the tubular formation. The role of MUC5AC in gastric cancers needs more investigation.

ACKNOWLEDGEMENTS

The authors express their gratitude to Dr. Jie Chen and Dr. Fu-Sheng Liu for their precious advice and suggestions. We thank Mr. Da-Hai Sun for his assistance in preparation of the manuscript.

REFERENCES

1 **Moniaux N,** Escande F, Porchet N, Aubert JP, Batra SK. Structural organization and classification of the human mucin genes. *Front Biosci* 2001; **6:** D1192-1206

2 **Corfield AP**, Myerscough N, Longman R, Sylvester P, Arul S, Pignatelli M. Mucins and mucosal protection in the gastrointestinal tract: new prospects for mucins in the pathology of gastrointestinal disease. *Gut* 2000; **47:** 589-594

3 **Williams SJ,** Wreschner DH, Tran M, Eyre HJ, Sutherland GR, McGuckin MA. Muc13: a novel human cell surface mucin expressed by epithelial and hemopoietic cells. *J Biol Chem* 2001; **276:** 18327-18336

4 **Gendler SJ,** Lancaster CA, Taylor-Papadimitriou J, Duhig T, Peat N, Burchell J, Pemberton L, Lalani EN, Wilson D. Molecular cloning and expression of human tumor–associated polymorphic epithelial mucin. *J Biol Chem* 1990; **265:** 15286-15293

5 **Seregni E,** Botti C, Massaron S, Lombardo C, Capobianco A, Bogni A, Bombardieri E. Structure, function and gene expression of epithelial mucins. *Tumori* 1997; **83:** 625-632

6 **Ho SB,** Shekels LL, Toribara NW, Kim YS, Lyftogt C, Cherwitz DL, Niehans GA. Mucin gene expression in normal, preneoplastic, and neoplastic human gastric epithelium. *Cancer Res* 1995; **55:** 2681-2690

7 **Guyonnet Duperat V,** Audie JP, Debailleul V, Laine A, Buisine MP, Galiegue-Zouitina S, Pigny P, Degand P, Aubert JP, Porchet N. Characterization of the human mucin gene MUC5AC: a consensus cysteine-rich domain for 11p15 mucin genes? *Biochem J* 1995; **305**(Pt 1): 211-219

8 **Berx G,** Staes K, van Hengel J, Molemans F, Bussemakers MJ, van Bokhoven A, van Roy F. Cloning and characterization of the human invasion suppressor gene E-cadherin(CDH1). *Genomics* 1995; **26:** 281-289

9 **Utsunomiya T,** Yonezawa S, Sakamoto H, Kitamura H, Hokita S, Aiko T, Tanaka S, Irimura T, Kim YS, Sato E. Expression of MUC1 and MUC2 mucins in gastric carcinomas: its relationship with the prognosis of the patients. *Clin Cancer Res* 1998; **4:** 2605-2614

10 **Baldus SE,** Zirbes TK, Engel S, Hanisch FG, Monig SP, Lorenzen J, Glossmann J, Fromm S, Thiele J, Pichlmaier H, Dienes HP. Correlation of the immunohistochemical reactivity of mucin peptide cores MUC1 and MUC2 with the histopathological subtype and prognosis of gastric carcinomas. *Int J Cancer* 1998; **79:** 133-138

11 **Reis CA,** David L, Carvalho F, Mandel U, de Bolos C, Mirgorodskaya E, Clausen H, Sobrinho-Simes M. Immunohistochemical study of the expression of MUC6 mucin and co-expression of other secrected mucins (MUC5AC and MUC2) in human gastric carcinomas. *J Histochem Cytochem* 2000; **48:** 377-388

12 **Gabbert HE,** Mueller W, Schneiders A, Meier S, Moll R, Birchmeier W, Hommel G. Prognostic value of E-cadherin expression in 413 gastric carcinomas. *Int J Cancer* 1996; **69:** 184-189

13 **Blok P,** Craanen ME, Dekker W, Tytgat GN. Loss of E-cadherin expression in early gastric cancer. *Histopathology* 1999; **34:** 410-415

14 **Reis CA,** David L, Seixas M, Burchell J, Sobrinho-Simoes M. Expression of fully and under-glycosylated forms of MUC1 mucin in gastric carcinoma. *Int J Cancer* 1998; **79:** 402-410

15 **Pinto-de-Sousa J,** David L, Reis CA, Gomes R, Silva L, Pimenta A. Mucins MUC1, MUC2, MUC5AC and MUC6 expression in the evaluation of differentiation and clinico- biological behaviour of gastric carcinoma. *Virchows Arch* 2002; **440:** 304-310

16 **Hanski C,** Hofmeier M, Schmitt-Graff A, Riede E, Hanski ML, Borchard F, Sieber E, Niedobitek F, Foss HD, Stein H, Riecken EO. Overexpression or ectopic expression of MUC2 is the common property of mucinous carcinomas of the colon, pancreas, breast, and ovary. *J Pathol* 1997; **182:** 385-391

17 **Sternberg LR,** Byrd JC, Yunker CK, Dudas S, Hoon VK, Bresalier RS. Liver colonization by human colon cancer cells is reduced by antisense inhibition of MUC2 mucin synthesis. *Gastroenterology* 1999; **116:** 363-371

18 **Reis CA,** David L, Nielsen PA, Clausen H, Mirgorodskaya K, Roepstorff P, Sobrinbo-Simoes M. Immunohistochemical study of MUC5AC expression in human gastric carcinomas using a novel monoclonal antibody. *Int J Cancer* 1997; **74:** 112-121

19 **Correa P,** Shiao YH. Phenotypic and genotypic events in gastric carcinogenesis. *Cancer Res* 1994; **54**(7 Suppl): 1941s-1943s

20 **Tanaka M,** Kitajima Y, Sato S, Miyazaki K. Combined evaluation of mucin antigen and E-cadherin expression may help select patients with gastric cancer suitable for minimally invasive therapy. *Br J Surg* 2003; **90:** 95-101

Edited by Chen WW and Zhu LH **Proofread by** Xu FM

PO Box 2345, Beijing 100023, China
Fax: +86-10-85381893
E-mail: wjg@wjgnet.com www.wjgnet.com

World J Gastroenterol 2004;10(20):3048-3052
World Journal of Gastroenterology
 ISSN 1007-9327

• BRIEF REPORTS •

Effect of resveratrol and in combination with 5-FU on murine liver cancer

Sheng-Li Wu, Zhong-Jie Sun, Liang Yu, Ke-Wei Meng, Xing-Lei Qin, Cheng-En Pan

Sheng-Li Wu, Liang Yu, Ke-Wei Meng, Xing-Lei Qin, Cheng-En Pan, Department of Hepatobiliary Surgery, First Hospital of Xi'an Jiaotong University, Xi'an 710061, Shaanxi Province, China
Zhong-Jie Sun, Department of Hepatobiliary Surgery, People's Hospital of Shaanxi Province, Xi'an 710061, Shaanxi Province, China
Supported by Traditional Chinese Medicine Bureau Foundation of Shaanxi Province, No. 2001-035
Correspondence to: Dr. Sheng-Li Wu, Department of Hepatobiliary Surgery, First Hospital of Xi'an Jiaotong University, Xi'an 710061, Shaanxi Province, China. victorywu2000@163.com
Telephone: +86-29-5324009 **Fax:** +86-29-5323536
Received: 2004-01-15 **Accepted:** 2004-02-12

Abstract

AIM: To study the anti-tumor effect of resveratrol and in combination with 5-FU on murine liver cancer.

METHODS: Transplantable murine hepatoma$_{22}$ model was used to evaluate the anti-tumor activity of resveratrol (RES) alone or in combination with 5-FU *in vivo*. H_{22} cell cycles were analyzed with flow cytometry.

RESULTS: Resveratrol could inhibit the growth of murine hepatoma$_{22}$, after the mice bearing H_{22} tumor were treated with 10 mg/kg or 15 mg/kg resveratrol for ten days, and the inhibition rates were 36.3% (n = 10) and 49.3% (n = 9), respectively, which increased obviously compared with that in control group (85±22 *vs* 68±17, P<0.01). RES could induce the S phase arrest of H_{22} cells, and increase the persentage of cells in S phase from 59.1% (n = 9) to 73.5% (n = 9) in a dose-dependent manner (P<0.05). The enhanced inhibition of tumor growth by 5-FU was also observed in hepatoma$_{22}$ bearing mice when 5-FU was administered in combination with 10 mg/kg resveratrol. The inhibition rates for 20 mg/kg or 10 mg/kg 5-FU in combination with 10 mg/kg resveratrol were 77.4% and 72.4%, respectively, compared with the group of 20 mg/kg or 10 mg/kg 5-FU alone, in which the inhibition rates were 53.4% and 43.8%, respectively (n = 8). There was a statistical significance between the combination group and 5-FU group.

CONCLUSION: RES could induce the S phase arrest of H_{22} cells and enhance the anti-tumor effect of 5-FU on murine hepatoma$_{22}$ and antagonize its toxicity markedly. These results suggest that resveratrol, as a biochemical modulator to enhance the therapeutic effects of 5-FU, may be potentially useful in cancer chemotherapy.

Wu SL, Sun ZJ, Yu L, Meng KW, Qin XL, Pan CE. Effect of resveratrol and in combination with 5-FU on murine liver cancer. *World J Gastroenterol* 2004; 10(20): 3048-3052
http://www.wjgnet.com/1007-9327/10/3048.asp

INTRODUCTION

Liver cancer is common in the world, especially in China[1-10]. Since the introduction of 5-FU for the treatment of liver cancer, the prognosis of liver cancer patients has been greatly improved. However, the serious side effects of 5-FU restrict its extensive clinical application. Searching for some new types of drugs to substitute or combine with 5-FU is necessary. Recently, scientists have found that resveratrol (3,4,5-trihydroxy-trans-stilbene, RES), a kind of phytoalexin found in root extract of the weed *Polygonum cuaspidatum* and in grape skins as well as red wine, has comprehensive pharmacological effects. Studies demonstrated that RES could alter the synthesis and secretion of lipids and lipoproteins by liver cells, block human platelet aggregation and inhibit the synthesis of proaggregatory and proinflammtory eicosanoids by platelets and neutrophils[11-15]. Some reports indicate that RES could prevent tumor growth and metastasis in human lung carcinoma, pancreatic cancer, prostate cancer, bronchial epithelium cancer and breast cancer models[16-20]. The present investigation evaluated the potency of RES and in combination with 5-FU on tumor cell growth and proliferation and on cell cycle distribution in a transplantable murine hepatoma$_{22}$ model.

MATERIALS AND METHODS

Materials

Resveratrol was purchased from Sigma Co (USA), dissolved and sterilized in dimethyl sulfoxide (DMSO) first and then diluted to the required working concentrations in RPMI 1640 (Gibco, USA) containing 100 mL/L calf serum (Sijiqing Co, Hangzhou, China). Mouse hepatocellular carcinoma cell line H_{22} was purchased from the Department of Pathology, Fourth Military Medical University. Male BALB/c mice, 6-8 wk old, weighing 20±2 g, were purchased from the Animal Center of Xi'an Jiaotong University.

Suppressive effect of RES on transplanted liver cancer

H_{22} cells were first subcultured in RPMI 1640 containing 100 mL/L fetal bovine serum, and then washed twice and resuspended in RPMI 1640 culture medium (1×10^{11}/L). About 0.2 mL cell solution (including 2×10^{7} cells) was taken and injected into the right groin of 5 Balb/c mice. After 14 d, when the tumors of 3-5 mm in diameter formed in the right groin of these mice, they were taken out and cut into small pieces of 1 mm^3 under sterile condition. Fifty Balb/c mice were anesthetized using coelio-injection of pentobarbitone (70 mg/kg) and laparotomy was performed. Under sterile condition their middle lobes of liver were punctured to form a 3 mm-long sinus tract and a small piece of tumor tissue was put into each sinus tract. Then these mice were randomly divided into 5 groups: control group, 5-FU group and 3 experimental groups. The experimental groups were injected with RES (dissolved in DMSO and diluted to the working concentration of 25 mmol/L in RPMI 1640 containing 100 mL/L calf serum) at 5, 10 or 15 mg/kg body mass, respectively, while the control group was given the same volume of the solution as for the experimental group without RES and the 5-FU group was injected with 5-FU at 20 mg/kg body mass. Twenty-four hours following liver tumor transplantation, each mouse was injected a corresponding dosage of RES into its abdominal cavity once a day for 10 d. These mice were then

sacrificed on the following day after the last injection. After the maximum diameter and transverse length of tumor were measured, hepatocellular carcinoma tissues were sampled. The tumor volume was calculated by using the formula $V = 1/2$ (maximum diameter×transverse length^2). The suppressive rate of tumor growth was calculated as [(mean V of tumor in control group - mean V of tumor in experimental group)/mean V of tumor in control group]×100%.

H_{22} cell cycle in transplanted liver cancer

Fresh hepatocellular carcinoma tissues with a size of 0.5-0.7 cm^3 were washed twice in saline and then single cells were isolated from sampled tissues using 21 g/L citric acid 5 g/L Tween 20 according to the method of Otto[21]. After this, cells were first washed with PBS(pH 7.4) three times, then adjusted to the density of 1×10^9/L in RPMI 1640, and 0.2 mL cell suspension was taken and stained with 0.2 mL PI compound dye for 20 min at room temperature. Then, cell suspension was centrifuged at 800 r/min for 10 min and washed twice in PBS at pH 7.4. Finally, the cells were added to 1 mL PBS followed by slight shaking at room temperature and cell cycle analysis was performed using flow cytometer (Coulter, Epice Elite, ESP, USA). By using the multicycle software program it was possible to calculate the proportion of H_{22} cells in S and G_2/M phases in tumor.

Synergistic anti-tumor effects of RES and 5-FU

A total of 128 tumor-bearing BALB/c mice were randomly divided into 8 groups: control group, RES group, three 5-FU groups and three experimental groups. The RES group was injected with RES at 10 mg/kg body mass (this dosage was proven to have obvious anti-tumor effect in our preliminary study.) and the 5-FU groups were injected with 5-FU at 5, 10, or 20 mg/kg body mass, respectively, and 3 experimental groups were injected with RES at 10 mg/kg body mass+5-FU at 5, 10, or 20 mg/kg body mass, respectively. The control group was given the same volume of the solution as for the experimental group without RES and 5-FU. Twenty-four hours after liver tumor transplantation, each mouse was injected with a corresponding drug at respective dosage into its abdominal cavity once a day for 10 d. Half of the mice in each group were then sacrificed on the following day after the last injection and the maximum diameter and transverse length of tumor were measured. The tumor tissues of mice treated with various dosages of 5-FU alone or in combination with RES were observed and photographed with an Olympus BH-I microscope. The rest mice were kept on feeding and their survival time and changes of body mass were recorded and their tumor metastasis conditions in lung or abdominal cavity were observed.

Statistical analysis

Student's t test was used to evaluate the significance of the difference between experimental groups and control group, between combination groups and corresponding sole drug groups.

RESULTS

Suppressive effect of RES on transplanted liver cancer and distribution of H_{22} cell cycles

Except 3 Balb/c mice (each in control group, 15 mg/kg RES group and 20.0 mg/kg 5-FU group), all the mice inoculated with hepatocarcinoma cell line H_{22} were successively transplanted with liver cancer. After treatment of the tumour bearing mice with 5, 10 or 15 mg/kg RES for 10 d, the tumour size was reduced from 134±40 mm^3 in control group to 105±14 mm^3, 85±22 mm^3 and 68±17 mm^3 in three experimental groups, the inhibition rate of tumour growth was 21.6 %, 36.3 % and 49.3 %, respectively. The inhibitory effect on the latter 2 therapeutic groups was significant higher than that on control group (P<0.01). Though the inhibition rate of tumour growth of 5-FU was rather high (53.0%), its toxicity was serious and the concrete manifestations included poor ingestion, diarrhea, and decrease in body mass, while the mice in RES groups showed no evident toxicity and were alive at the end of treatment (Table 1).

The cell cycles were analysed using flow cytometer to calculate the number of H_{22} cells in each phase in tumor under the action of various dosages of RES (5, 10, or 15 mg/kg body mass). The results showed that the number of H_{22} cells in S phase increased from 0.60 in control group to 0.75 in 15.0 mg/kg RES group, while the number of H_{22} cells in G_2 phase decreased from 0.11 to 0.00 and the effect was dose-dependent (Table 2, Figure 1).

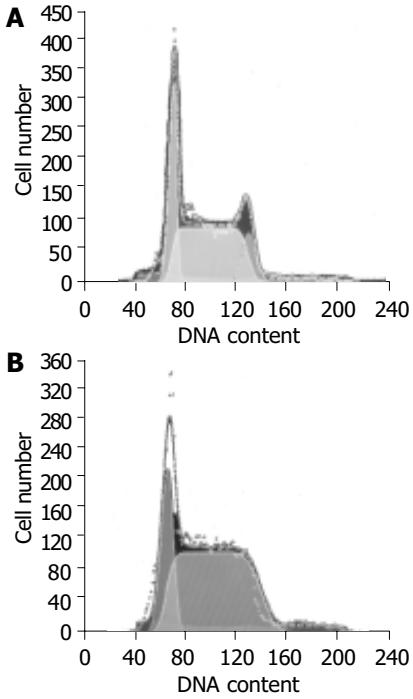

Figure 1 Number of H_{22} cell cycles in transplanted liver cancer of mouse treated with RPMI-1640 (A) or 15.0 mg/kg (B).

Table 1 Suppressive effect of resveratrol on murine transplanted liver cancer (mean±SD)

Group	Dose (mg/kg)	n	Tumor size (mm^3)	Growth inhibitory rate (%)	t value
Control	0.0	9	134±40	-	
5-FU	20.0	9	63±29	53.0	4.36[b]
RES	5.0	10	105±14	21.6	2.16[a]
	10.0	10	85±22	36.6	3.36[b]
	15.0	9	68±17	49.3	4.33[b]

[a]P<0.05, [b]P<0.01, *vs* control.

Table 2 Effect of RES on the number of H_{22} cell cycles in transplanted liver cancer of mouse

Group	Dose (mg/kg)	n	Number of H_{22} cell cycles (%)		
			G0/G1	S	G2/M
Control	0	9	0.29	0.60	0.11
RES	5.0	10	0.30	0.60	0.09
	10.0	10	0.30	0.68[a]	0.02[a]
	15.0	9	0.25	0.75[a]	0.00[a]

[a]P<0.05, *vs* control.

Table 3 Suppressive effect of RES in combination with 5-FU on murine with transplanted liver cancer (mean±SD)

Group	Dose (mg/kg)	*n*	Tumor size (mm^3)		*t* value	Growth inhibitory rate (%)	
			Alone	With 5-FU		Alone	With 5-FU
Control	0	8	128±33				
RES	10.0	8	88±21			31.5	
5-FU	20.0	8	60±12	29±18	4.05[b]	53.4	77.4
	10.0	8	72±17	35±13	4.89[b]	43.8	72.4
	5.0	8	92±19	64±22	2.72[a]	28.4	50.0

[a]$P<0.05$, [b]$P<0.01$, *vs* control.

Table 4 Effect of RES in combination with 5-FU on survival time and body mass of tumor bearing mouse (mean±SD)

Group	Dose (mg/kg)	*n*	Last body mass(g)		*t* value	Survival time (d)		*t* value
			Alone	With 5-FU		Alone	With 5-FU	
Control	0	8	23.6±2.0			17.3±3.3		
RES	10.0	8	23.8±1.2			21.5±5.6		
5-FU	20.0	8	16.5±1.8	20.3±1.3	4.79[b]	32.0±9.7	44.6±11.6	2.34[a]
	10.0	8	19.6±1.8	23.2±2.5	3.25[b]	23.6±5.4	36.3±9.4	3.22[b]
	5.0	8	21.3±1.7	24.5±1.5	3.80[b]	19.5±4.4	30.6±8.0	3.48[b]

[a]$P<0.05$, [b]$P<0.01$, *vs* control.

Suppressive effect of RES in combination with 5-FU on transplanted liver cancer

RES in combination with 5-FU had synergistic suppressive effects on transplanted liver cancer of mouse (Figure 2). When 10 mg/kg RES in combination with 5, 10 or 20 mg/kg 5-FU, the inhibition rate was 50.0%, 72.4%, and 77.4%, respectively. When the group administered 5, 10 or 20 mg/kg 5-FU alone, the inhibition rate was 28.4%, 43.8%, and 53.4%, respectively. There was a statistical significance between the combination group and the 5-FU alone group (Table 3). Morphologic observation showed that more cellular necrosis was found in the combination group than in control group (Figure 3).

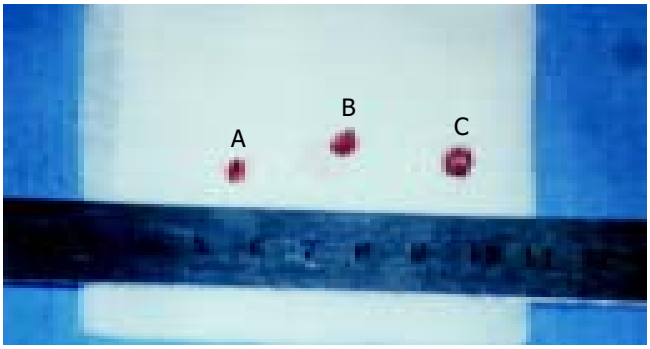

Figure 2 Tumor size of mice treated with 10.0 mg/kg RES+20.0 mg/kg 5-FU (tumor A: 3.5×3.1×2.6 mm) and RPMI-1640 (tumor B: 4.8×4.7×4.2 mm; tumor C: 5.3×5.2×4.8 mm).

Effect of RES in combination with 5-FU on survival time and tumor metastasis

When the mice were administered 10 mg/kg RES in combination with 5, 10 or 20 mg/kg 5-FU, the survival time of tumor bearing mouse was 30.6±8.0 d, 36.3±9.4 d, and 44.6±11.6 d, respectively. When group administered 5, 10 or 20 mg/kg 5-FU alone, the survival time was 19.4±4.4 d, 23.9±5.4 d, and 32.1±9.7 d, respectively (Figure 6). There was a statistical significance between the combination group and the 5-FU alone group. In the beginning of the study, there was no statistical difference in the body mass of mouse among various groups. However, at the end of the investigation, the body mass of mouse in combination group was significantly heavier than that in sole drug group ($P<0.01$), showing that RES might antagonize the toxicity of 5-FU markedly (Table 4). Two Balb/c mice in control group had lung and celiac lymph node metastases, one in 5 mg/kg 5-FU therapeutic group had celiac lymph node metastasis. Except these 3 groups, all the mice inoculated with hepatocarcinoma cell line H_{22} showed no signs of tumor metastasis.

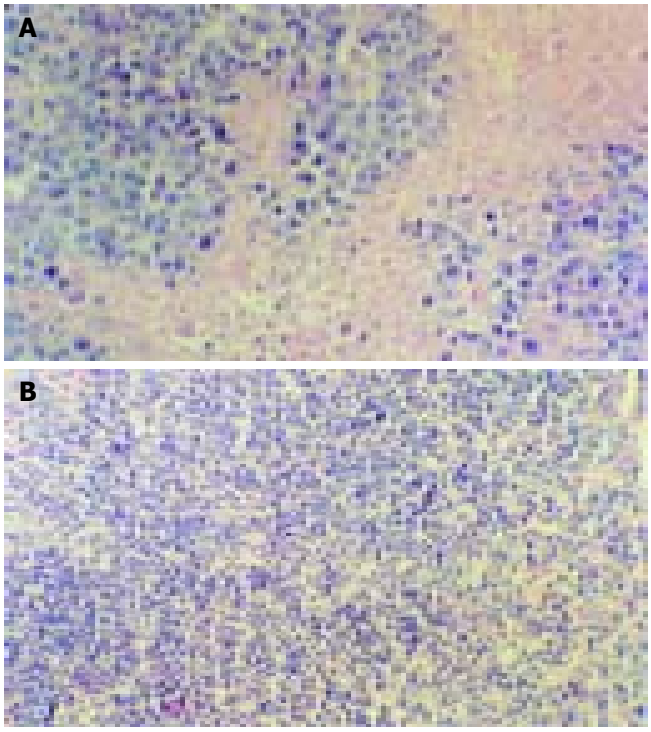

Figure 3 Morphologic observation of tumor tissues of mice treated with RPMI-1640 (A) or 10.0 mg/kg RES+20.0 mg/kg 5-FU(B).

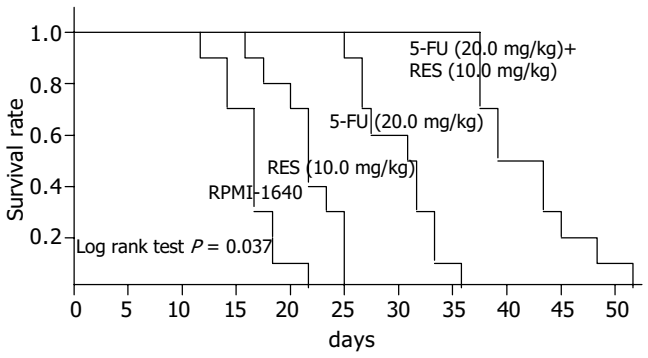

Figure 4 Kaplan-meier curves of survival rates of tumor bearing mice when administered RPMI-1640, 10 mg / kg RES, 20 mg / kg 5-FU, and 5-FU (20.0 mg / kg)+RES (10.0 mg / kg).

DISCUSSION

Great attention has been paid to the chemopreventive activities and low toxicities of dietary polyphenolic compounds like RES[22]. The function of RES might be mediated via different mechanisms in different cells, and the ability of RES to inhibit cellular events associated with tumor initiation, promotion, and progression might be attributed to its anticyclooxygenase activity, inducing apoptosis of tumor cells, antagonism to mutation, antioxidation and anti-free radical activity and effect on cell cycles[23-28]. Ahmad *et al*.[29] proved that resveratrol treatment of human epidermoid carcinoma A431 cells caused an induction of WAF1/p21 inhibiting cyclin D1/D2-cdk6, cyclin D1/D2-cdk4, and cyclin E-cdk2 complexes, thereby imposing an artificial checkpoint at the G1-S transition of the cell cycle, which resulted in a G1 phase arrest of the cell cycle and subsequent apoptotic death of cancer cells. Our previous studies demonstrated that RES could suppress the growth of murine transplanted liver tumor H_{22} and the anti-tumor mechanism of RES might prevent mitosis of tumor cells by suppressing the protein expression of cyclin B1and p34cdc2, thus interfering with the process of tumor cells from S stage to G2/M stage[30,31].

One main role of 5-fluorouracil is to affect the biosynthesis of nucleic acids. Inside cells, 5-FU is converted to 5-fluorouracil deoxynucleotide (5F-dUMP) and inhibits the function of deoxythymidylic acid synthetase, blocks the methylation of uracil deoxyribonucleotide into deoxythymidylic acid, thus affecting the synthesis of DNA. As a result, 5-FU can prevent the tumor cells from splitting and proliferating and its cardinal acting period is S phase. Besides that, after the conversion of 5-FU into 5-fluorouracil uridine (5-FUR) *in vivo*, it also can be added into RNA to interfere with the synthesis of proteins, so it can affect the cells in other phases. Therefore, RES can enhance the anti-tumor effect of 5-FU by inducing the S phase arrest of H_{22} cells, a stage in which 5-FU can exert its max tumor cell killing function, and this synergism was proved in our *in vitro* experiments.

In the present investigation, RES was administered into murine abdomen, its potency on growth and proliferation of H_{22}-innoculated tumors and its synergism with 5-FU were evaluated by measuring the size of hepatoma and examining the distributions of H_{22} cell cycles and observing the survival time of mice. The tumor size was reduced by each dosage of 5, 10 or 15 mg/kg of RES for 10 d. When the larger dosage of RES was applied, the tumor size was significantly reduced, the inhibition rate of tumor growth by 10 or 15 mg/kg reached to 36.3% and 49.3%, respectively (P<0.01). It was also found that RES could induce the S phase arrest of H_{22} cells. RES could increase the persentage of cells in S phase from 59.1% to 73.5% in a dose-dependent manner (P<0.05). The enhanced inhibition of tumor growth by 5-FU was also observed in hepatoma$_{22}$ bearing mice when 5-FU was administered in combination with 10 mg/kg RES. The inhibition rate of 10 mg/kg or 20 mg/kg 5-FU in combination with 10 mg/kg RES was 72.4% and 77.4%, respectively. The inhibition rate was 43.8% and 53.4%, when the group administered 10 mg/kg or 20 mg/kg 5-FU alone. There was a statistical significance between the combination group and the 5-FU alone group (P<0.01). In addition to that, when RES was administrated in combination with a smaller dosage of 5-FU, the therapeutic effect was similar to that of a larger dosage of 5-FU but without severe side effects of 5-FU, therefore the survival time of mice was elongated.

In short, the data suggest that RES can induce the S phase arrest of H_{22} cells and enhance the anti-tumor effect of 5-FU on murine hepatoma$_{22}$ and antagonize its toxicity markedly. Resveratrol, a biochemical modulator to enhance the therapeutic effects of 5-FU, may be potentially useful in cancer chemotherapy.

REFERENCES

1 **Kuang SY**, Jackson PE, Wang JB, Lu PX, Munoz A, Qian GS, Kensler TW, Groopman JD. Specific mutations of hepatitis B virus in plasma predict liver cancer development. *Proc Natl Acad Sci U S A* 2004; **101**: 3575-3580
2 **Kew MC**. Synergistic interaction between aflatoxin B1 and hepatitis B virus in hepatocarcinogenesis. *Liver Int* 2003; **23**: 405-409
3 **Chen HB**, Huang Y, Dai DL, Zhang X, Huang ZW, Zhang QK, Wang HH, Zhang JS, Pan G. Therapeutic effect of transcatheter arterial chemoembolization and percutaneous injection of acetic acids on primary liver cancer. *Hepatobiliary Pancreat Dis Int* 2004; **3**: 55-57
4 **Luo W**, Birkett NJ, Ugnat AM, Mao Y. Cancer incidence patterns among Chinese immigrant populations in Alberta. *J Immigr Health* 2004; **6**: 41-48
5 **Chen JG**, Parkin DM, Chen QG, Lu JH, Shen QJ, Zhang BC, Zhu YR. Screening for liver cancer: results of a randomised controlled trial in Qidong, China. *J Med Screen* 2003; **10**: 204-209
6 **Zou CL**, Chen ZJ, Jin WY, Ni SC, Chen BF, Hu YL. Etiologic fraction and interaction of risk factors for primary hepatocellular carcinoma in Wenzhou, Zhejiang Province. *Zhonghua Yufang Yixue Zazhi* 2003; **37**: 355-357
7 **Tang B**, Kruger WD, Chen G, Shen F, Lin WY, Mboup S, London WT, Evans AA. Hepatitis B viremia is associated with increased risk of hepatocellular carcinoma in chronic carriers. *J Med Virol* 2004; **72**: 35-40
8 **Tang ZY**. Small hepatocellular carcinoma: current status and prospects. *Hepatobiliary Pancreat Dis Int* 2002; **1**: 349-353
9 **Lu W**, Li YH, He XF, Chen Y, Zhao JB. Changes of liver function after transcatheter arterial chemoembolization with use of different dose of anticancer drugs in hepatocellular carcinoma. *Shijie Huaren Xiaohua Zazhi* 2004; **12**: 38-41
10 **Shen BZ**, Liu Y, Li RF, Yang G, Yu YT, Dong BW, Liang P. Effects of intraaterial chemoembolization combined with percutaneous microwave coagulation on hepatocellular carcinoma: a clinical and experimental study. *Shijie Huaren Xiaohua Zazhi* 2003; **11**: 268-271
11 **Afaq F**, Adhami VM, Ahmad N. Prevention of short-term ultraviolet B radiation-mediated damages by resveratrol in SKH-1 hairless mice. *Toxicol Appl Pharmacol* 2003; **186**: 28-37
12 **Fremont L**. Biological effects of resveratrol. *Life Sci* 2000; **66**: 663-673
13 **Sato M**, Ray PS, Maulik G, Maulik N, Engelman RM, Bertelli AA, Bertelli A, Das DK. Myocardial protection with red wine extract. *J Cardiovasc Pharmacol* 2000; **35**: 263-268
14 **Roemer K,** Mahyar-Roemer M. The basis for the chemopreventive action of resveratrol. *Drugs Today* 2002; **38**: 571-580
15 **Zou JG**, Wang ZR, Huang YZ, Cao KJ, Wu JM. Effect of red wine and wine polyphenol resveratrol on endothelial function in hypercholesterolemic rabbits. *Int J Mol Med* 2003; **11**: 317-320
16 **Kimura Y**, Okuda H. Resveratrol isolated from Polygonum cuspidatum root prevents tumor growth and metastasis to

lung and tumor-induced neovascularization in Lewis lung carcinoma-bearing mice. *J Nutr* 2001; **131**: 1844-1849

17 **Narayanan BA**, Narayanan NK, Re GG, Nixon DW. Differential expression of genes induced by resveratrol in LNCaP cells: P53-mediated molecular targets. *Int J Cancer* 2003; **104**: 204-212

18 **Ding XZ**, Adrian TE. Resveratrol inhibits proliferation and induces apoptosis in human pancreatic cancer cells. *Pancreas* 2002; **25**: e71-76

19 **Kuo PL**, Chiang LC, Lin CC. Resveratrol- induced apoptosis is mediated by p53-dependent pathway in Hep G2 cells. *Life Sci* 2002; **72**: 23-34

20 **Banerjee S**, Bueso-Ramos C, Aggarwal BB. Suppression of 7, 12-dimethylbenz(a)anthracene-induced mammary carcinogenesis in rats by resveratrol: role of nuclear factor-kappaB, cyclooxygenase 2, and matrix metalloprotease 9. *Cancer Res* 2002; **62**: 4945-4954

21 **Otto FJ**. High-resolution analysis of nuclear DNA employing the fluorochrome DAPI. *Methods Cell Biol* 1994; **41**: 211–217

22 **Narayanan BA**, Narayanan NK, Stoner GD, Bullock BP. Interactive gene expression pattern in prostate cancer cells exposed to phenolic antioxidants. *Life Sci* 2002; **70**: 1821-1839

23 **Young J**, Barker M, Fraser L, Walsh MD, Spring K, Biden KG, Hopper JL, Leggett BA, Jass JR. Mutation searching in colorectal cancer studies: experience with a denaturing high-pressure liquid chromatography system for exon-by-exon scanning of tumour suppressor genes. *Pathology* 2002; **34**: 529-533

24 **Takahashi M**, Shimomoto T, Miyajima K, Iizuka S, Watanabe T, Yoshida M, Kurokawa Y, Maekawa A. Promotion, but not progression, effects of tamoxifen on uterine carcinogenesis in mice initiated with N-ethyl-N'-nitro-N-nitrosoguanidine. *Carcinogenesis* 2002; **23**: 1549-1555

25 **De la Fuente M**, Victor VM. Anti-oxidants as modulators of immune function. *Immunol Cell Biol* 2000; **78**: 49–54

26 **Falchetti R**, Fuggetta MP, Lanzilli G, Tricarico M, Ravagnan G. Effects of resveratrol on human immune cell function. *Life Sci* 2001; **70**: 81–96

27 **Schneider Y**, Duranton B, Gosse F, Schleiffer R, Seiler N, Raul F. Resveratrol inhibits intestinal tumorigenesis and modulates host-defense-related gene expression in an animal model of human familial adenomatous polyposis. *Nutr Cancer* 2001; **39**: 102–107

28 **Yu C**, Shin YG, Chow A, Li Y, Kosmeder JW, Lee YS, Hirschelman WH, Pezzuto JM, Mehta RG, van Breemen RB. Human, rat, and mouse metabolism of resveratrol. *Pharm Res* 2002; **19**: 1907–1914

29 **Ahmad N**, Adhami VM, Afaq F, Feyes DK, Mukhtar H. Resveratrol causes WAF-1/p21-mediated G(1)-phase arrest of cell cycle and induction of apoptosis in human epidermoid carcinoma A431 cells. *Clin Cancer Res* 2001; **7**: 1466-1473

30 **Holmes-McNary M,** Baldwin AS Jr. Chemopreventive properties of trans-resveratrol are associated with inhibition of activation of the IkappaB kinase. *Cancer Res* 2000; **60**: 3477-3483

31 **Nielsen M**, Ruch RJ, Vang O. Resveratrol reverses tumor-promoter–induced inhibition of gap-junctional intercellular communication. *Biochem Biophys Res Commun* 2000; **275**: 804-809

Edited by Wang XL and Ren SY **Proofread by** Xu FM

PO Box 2345, Beijing 100023, China
Fax: +86-10-85381893
E-mail: wjg@wjgnet.com www.wjgnet.com

World J Gastroenterol 2004;10(20):3053-3055
World Journal of Gastroenterology
 ISSN 1007-9327

• BRIEF REPORTS •

Sentinel lymph node concept in gastric cancer with solitary lymph node metastasis

Li-Yang Cheng, Shi-Zhen Zhong, Zong-Hai Huang

Li-Yang Cheng, Shi-Zhen Zhong, Institute of Clinical Anatomy, First Military Medical University, Guangzhou 510515, Guangdong Province, China
Zong-Hai Huang, Department of General Surgery, Zhujiang Hospital, First Military Medical University, Guangzhou 510282, Guangdong Province, China
Supported by the Natural Science Foundation of Guangdong Province, No. 032204
Correspondence to: Dr. Li-yang Cheng, Department of General Surgery, Guangzhou General Hospital of PLA, 111 Liuhua Road, Guangzhou 510010, Guangdong Province, China. chliyang2001@yahoo.com.cn
Telephone: +86-20-36653547 **Fax:** +86-20-36222275
Received: 2004-02-14 **Accepted:** 2004-02-24

Abstract

AIM: To study the localization of the solitary metastases in relation to the primary gastric cancers and the feasibility of sentinel lymph node (SLN) concept in gastric cancer.

METHODS: Eighty-six patients with gastric cancer, who had only one lymph node involved, were regarded retrospectively as patients with a possible sentinel node metastasis, and the distribution of these nodes were assessed. Thirteen cases with jumping metastases were further studied and followed up.

RESULTS: The single nodal metastasis was found in the nearest perigastric nodal area in 65.1% (56/86) of the cases and in 19.8% (17/86) of the cases in a fairly remote perigastric area. Out of 19 middle-third gastric cancers, 3 tumors at the lesser or greater curvatures had transverse metastases. There were also 15.1% (13/86) of patients with a jumping metastasis to N2-N3 nodes without N1 involved. Among them, the depth of invasion was mucosal (M) in 1 patient, submucosal (SM) in 2, proper-muscular (MP) in 4, subserosal (SS) in 5, and serosa-exposed (SE) in 1. Five of these patients died of gastric cancer recurrence at the time of this report within 3 years after surgery.

CONCLUSION: These results suggest that nodal metastases occur in a random and multidirectional process in gastric cancer and that not every first metastatic node is located in the perigastric region near the primary tumor. The rate of "jumping metastasis" in gastric cancer is much higher than expected, which suggests that the blind examination of the nodal area close to the primary tumor can not be a reliable method to detect the SLN and that a extended lymph node dissection (ELND) should be performed if the preoperative examination indicates submucosal invasion.

Cheng LY, Zhong SZ, Huang ZH. Sentinel lymph node concept in gastric cancer with solitary lymph node metastasis. *World J Gastroenterol* 2004; 10(20): 3053-3055
http://www.wjgnet.com/1007-9327/10/3053.asp

INTRODUCTION

The sentinel lymph node (SLN) which refers to the first lymph node to receive drainage from the primary tumor has been successfully introduced in the patients with breast cancer[1] and malignant melanoma[2] to assess tumor involvement in regional lymph nodes with less morbidity but equal accuracy to complete lymphadenectomy. But the feasibility of sentinel node mapping of gastric carcinoma is still unclear and controversial. To explore the applicability of sentinel node concept to gastric cancer and provide useful information for establishing a novel method to detect sentinel nodes during operation, we retrospectively investigated solitary lymph node metastases that hypothesized to represent sentinel lymph node.

MATERIALS AND METHODS

Patients

Between January 1997 and December 2003, 1 698 patients with gastric cancer underwent gastrectomy with lymph node dissection (more than D1) at the Department of General Surgery, Guangzhou General Hospital of PLA, Nanfang and Zhujiang Hospitals of First Military Medical University. Among them, 86 (5.1%) patients were rolled in this study by the following criteria: (1) the lesion was solitary and limited to one part of the stomach; (2) a curative gastrectomy with ELND was performed; and (3) the histological examination of all resected lymph nodes revealed only one lymph node involved. These patients were subdivided according to the primary site of gastric cancer: 16 upper-third (U) tumors; 19 middle-third (M) tumors; and 51 lower-third (L) tumors. According to the depth of wall invasion, mucosal (M) lesions, submucosal (SM) lesions, proper-muscular (MP) lesions, and subserosal (SS) lesions were observed in 2, 7, 47, and 30 patients, respectively. Regarding their histologic grades, 23 of high-differentiated cases, 55 of middle- differentiated cases, 7 of low- differentiated cases, and 1 of non-differentiated case were proven to have only one lymph node involved. Total gastrectomy, proximal subtotal gastrectomy and distal subtotal gastrectomy were carried out in 29, 6 and 51 cases, respectively.

Methods

The resected specimens and the lymph nodes were stained conventionally with hematoxylin and eosin (HE) and examined by pathologists. The clinicopathological data were evaluated according to the General Rules by the Japanese Research Society for Gastric Cancer[3]. In the present study, to express the group and station number of each lymph node, No. and N were inserted in front of the number, i.e., No. 4 means group 4 lymph node and N1 means station 1 lymph node. If patients were histologically verified to have distant lymph nodes (N2 or N3) involved without perigastric node metastasis (N1), they were defined to have either jumping or skip metastases. If the tumors at the lesser or greater curvatures had metastasized to the lymph nodes located in the opposite curvatures, they were then defined to have transverse metastases. Ten of 13 patients with skip metastases were followed up for 1-5 years until December 2003.

RESULTS

Upper-third (U) tumors

In 13 out of 16 U tumors, the solitary node metastasis was found in perigastric area close to the tumor (N1). In 3 cases, the metastasis was found in N2 area. Among them, 2 nodes were along the left gastric artery (LGA) (No.7), the other 1 along common hepatic artery (CHA) (No.8a).

Middle-third (M) tumors

In 9 out of 19 M tumors, the single node metastasis was found either in the lesser (No.3) or greater curvature (No.4) perigastric area close to the primary tumor. Among them, 2 tumors at the lesser curvature and 1 tumor at the greater curvature had transverse metastases. In 6 cases, the metastasis was found in the remote perigatric area (No.1, 5 and 6), and another 4 cases in the N2 or N3 area (No.7, 8a and 12) were without N1 involvement.

Lower-third (L) tumors

Of 51 patients with L tumors, 34 had the single metastasis in the perigastric node close to the tumor (No.3 and 4), 11 had metastasized to the surprapyloric (No.5) or infrapyloric (No.6), both of which were N1 but somewhat remote from the primary tumor. In the other 6 cases, the metastasis was found in the N2 or N3 area (No.1, 4 s, 7 and 11 p) without N1 involvement.

Invasion and survival of patients with jumping metastasis

Among 13 cases with jumping metastasis, the depth of invasion was M in 1, SM in 2, MP in 4, SS in 5, and SE in 1. Among 6 out of 10 patients who received a follow-up, 5 died of tumor recurrence and 1 of other disease within 3 years after operation. The other 4 were alive at the time of this report for more than 3-5 years after surgery.

Metastasis of tumors

A total of 1376 lymph nodes were harvested in this group of 86 patients with D2-D3 lymphadenectomy. The average number of lymph nodes dissected was 16 in each case. The distribution of the single positive node is shown in Table 1 according to the location of the primary tumor. In total, the single nodal metastasis was found in 65.1% of cases in the nearest perigastric node area, in 19.8% of cases in a fairly remote perigastric area, and in 15.1% of cases in the N2 or N3 area without N1 involvement.

Table 1 Distribution of solitary lymph node metastasis

Location of positive node	Location of primary tumor		
	Upper	Middle	Lower
Right cardial (No1)	2(N1)	1(N1)	1(N2)
Lesser curvature (No3)	7(N1)	7(N1)	20(N1)
Greater curvature (No4d)		2(N1)	14(N1)
Greater curvature (No4s)	2(N1)		1(N3)
Surprapyloric (No5)		2(N1)	5(N1)
Infrapyloric (No6)	2(N1)	3(N1)	6(N1)
Left gastric artery (No7)	2(N2)	2(N2)	3(N2)
Common hepatic artery (No8a)	1(N2)	1(N2)	
Splenic artery (No11p)			1(N2)
Proper hepatic artery (No12)		1(N3)	

No4d and 4 s represent nodes on right and left half of greater curvature respectively; No8a represents nodes on the anterior or upper of CHA; No11p represents nodes on proximal splenic artery.

DISCUSSION

Gastric cancer is generally thought to spread to N1 nodes first, followed by involvement of distant nodes (N2-N3) just as other carcinomas. However, more recent studies have reported that lymph node involvement was noted not only in N1 but also in N2-N3 and that the rate of N2 lymph node metastases in patients with advanced gastric cancers was higher than expected[4,5]. Lymphatic drainage route must be patient-specific and lesion-specific in gastric cancer due to complicated lymphatic streams from the stomach. Our results suggested that although most of the single nodal metastasis was found in the nearest perigastric node area, approximately one quarter of the patients had the first metastasis in a fairly remote perigastric area and up to 15% of patients demonstrated skip metastasis without N1 involvement. To date, to the authors knowledge, there are only 5 retrospective studies on gastric cancer patients with only one lymph node metastasis[6-10]. In these studies, the single nodal metastases were distributed beyond the perigasric area in 12.6-29% of gastric cancer patients, which suggested that the conventional lymphatic routes in stomach that have long been generally accepted should be clarified further. Our present data confirm these results. Among 13 cases with skip metastasis in the current study, most (10/13) of the solitary node metastases were found in No.7, 8, or 12. This result seems to be comparable with other reports, where No.7, 8, 9 and 12 nodes were most commonly involved in patients with skip metastasis[6-10], and suggests that No.7, 8, and 12 to be the most important stations as well as N1[4,5]. In our study, 3 out of 19 mol/L tumors had transverse metastases, which indicates that gastric lymph channels are multidirectional and form complex networks. The survival and depth of invasion in gastric cancer patients with skip metastases presented in this report suggest that if the preoperative examination diagnosed submucosal invasion, then a ELND should be conducted.

Results from these retrospective studies not only demonstrated the feasibility of SLN concept to gastric cancer but also provided useful information for intraoperative sentinel node mapping. That the perigastric nodal area close to the primary tumor is the first site of metastasis in 65.1% of gastric cancers in the present study indicates that the so-called shine-through effect should be considered in sentinel node mapping by radioisotope (RI) method[11]. The high incidence of skip metastasis to N2-N3 nodes suggests that blind examination of the nodal area close to the primary tumor can not be a reliable method to detect the first metastasis[6]. Visualization of dye is useful for real-time observation of lymphatic vessels, but it is difficult to detect multiple sentinel nodes and SLNs in the second or third compartments because vital dye tends to diffuse rapidly from nodal tissue. A probe-guided approach is essential to cover the widespread distribution of SLNs in gastric cancer and is very useful to detect residual SLNs in unexpected areas[12]. Therefore, a combination of the dye and radioguided methods for systemic lymphatic mapping of gastric cancers may be recommended to improve the detection rate and diagnostic accuracy[13,14].

It remains unclear why jumping metastases occurred in these cases. The following reasons could all play some role: (1) N1 involved nodes and occult metastases to N1 nodes may have been missed during the dissection and the routine histopathologic examination, which result in a false skip metastasis. The possible sentinel nodes detected by conventional means might not always be primary portions of any metastasis and true skip metastasis in gastric cancer may be rare[10]; (2) There may have been some aberrant lymphatic drainage patterns in patients with gastric cancer, through which metastasis bypasses lymphatic vessels[7,8,15]; (3) Direct lymphatic flows to distant affected nodes from primary gastric lesions have been found in SLN mapping intraoperatively[16]; (4) Lymphatic flows to the N1 nodes may have been blocked with cancer tissue; (5) The microenvironment in the N1 nodes is sometimes unfit for the

development of metastasis[17]. Free cancer cells may diffuse through regional nodes to distant nodes. In addition, the risk factors associated with skip nodal metastasis may include the stage, depth of invasion, macroscopic classification and pathological type of gastric cancer.

Most surgeons are skeptical about the application of the SLN concept for gastric cancer because of the high incidence of skip metastases and the random process occurring in nodal metastases. However, Kitagawa *et al*.[18,19] have pointed out that the sentinel node for gastrointestinal cancer is not the node necessarily located anatomically closest to the primary lesion and is not necessarily the only one. In those cases with a jumping metastasis to N2-N3 nodes, sentinel nodes in the second or third compartment are considered to be functionally first compartments. Bilchik *et al*.[20] proposed the potential for universal application of sentinel node mapping in solid tumors. Cases with one or two lymph node metastasis examined in these retrospective studies only occupy a little part of patients with gastric carcinoma in which one or more SLNs can be detected in every case theoretically. Then the results from these studies can not represent the real characteristic as to the occurrence of SLN in all gastric cancers. Actual data from sentinel node mapping for gastric cancers, rather than a retrospective analysis of metastatic patterns, are needed to explore the feasibility and validity of sentinel node biopsy in gastric cancer.

REFERENCES

1 **Nieweg OE,** Bartelink H. Implications of lymphatic mapping for staging and adjuvant treatment of patients with breast cancer. *Eur J Cancer* 2004; **40**: 179-181

2 **Kretschmer L,** Hilgers R, Mohrle M, Balda BR, Breuninger H, Konz B, Kunte C, Marsch WC, Neumann C, Starz H. Patients with lymphatic metastasis of cutaneous malignant melanoma benefit from sentinel lymphonodectomy and early excision of their nodal disease. *Eur J Cancer* 2004; **40**: 212-218

3 Japanese Gastric Cancer Association. *Japanese Classification of Gastric carcinoma*. 13th ed. *Tokyo: Kanehara* 1999

4 **Mishima Y,** Hirayama R. The role of lymph node surgery in gastric cancer. *World J Surg* 1987; **11**: 406-411

5 **Maruyama K,** Gunven P, Okabayashi K, Sasako M, Kinoshita T. Lymph node metastases of gastric cancer. General pattern in 1931 patients. *Ann Surg* 1989; **210**: 596-602

6 **Sano T,** Katai H, Sasako M, Maruyama K. Gastric lymphography and detection of sentinel nodes. *Rec Res Cancer Res* 2000; **157**: 253-258

7 **Kosaka T,** Ueshige N, Sugaya J, Nakano Y, Akiyama T, Tomita F, Saito H, Kita I, Takashima S. Lymphatic routes of the stomach demonstrated by gastric carcinomas with solitary lymph node metastasis. *Surg Today* 1999; **29**: 695-700

8 **Ichikura T,** Morita D, Uchida T, Okura E, Majima T, Ogawa T, Mochizuki H. Sentinel node concept in gastric carcinoma. *World J Surg* 2002; **26**: 318-322

9 **Tsuburaya A,** Noguchi Y, Yoshikawa T, Kobayashi O, Sairenji M, Motohashi H. Solitary ly mph node metastasis of gastric cancer as a basis for sentinel lymph node biopsy. *Hepatogastroenterology* 2002; **49**: 1449-1452

10 **Arai K,** Iwasaki Y, Takahashi T. Clinicopathological analysis of early gastric cancer with solitary lymph node metastasis. *Br J Surg* 2002; **89**: 1435-1437

11 **Yasuda S,** Shimada H, Ogoshi K, Tanaka H, Kise Y, Kenmochi T, Soeda J, Nakamura K, Kato Y, Kijima H, Suzuki Y, Fujii H, Tajima T, Makuuchi H. Preliminary study for sentinel lymph node identification with Tc-99m tin colloid in patients with esophageal or gastric cancer. *Tokai J Exp Clin Med* 2001; **26**: 15-18

12 **Kitagawa Y,** Ohgami M, Fujii H, Mukai M, Kubota T, Ando N, Watanabe M, Otani Y, Ozawa S, Hasegawa H, Furukawa T, Matsuda J, Kumai K, Ikeda T, Kubo A, Kitajima M. Laparoscopic detection of sentinel lymph nodes in gastrointestinal cancer: a novel and minimally invasive approach. *Ann Surg Oncol* 2001; **8**(9 Suppl): 86S-89S

13 **Hayashi H,** Ochiai T, Mori M, Karube T, Suzuki T, Gunji Y, Hori S, Akutsu N, Matsubara H, Shimada H. Sentinel lymph node mapping for gastric cancer using a dual procedure with dye-and gamma probe-guided techniques. *J Am Coll Surg* 2003; **196**: 68-74

14 **Tokunaga A,** Okuda T, Tajiri T, Onda M. Intraoperative lymphatic mapping by dye and/or radioactive tracer in early gastric cancer. *J Nippon Med Sch* 2002; **69**: 216-217

15 **Bilchik AJ,** Saha S, Tsioulias GJ, Wood TF, Morton DL. Aberrant drainage and missed micrometastases: the value of lymphatic mapping and focused analysis of sentinel lymph nodes in gastrointestinal neoplasms. *Ann Surg Oncol* 2001; **8**: 82-85

16 **Miwa K,** Kinami S, Taniguchi K, Fushida S, Fujimura T, Nonomura A. Mapping sentinel nodes in patients with early-stage gastric carcinoma. *Br J Surg* 2003; **90**: 178-182

17 **Gervasoni JE Jr,** Taneja C, Chung MA, Cady B. Biologic and clinical significance of lymphadenectomy. *Surg Clin North Am* 2000; **80**: 1632-1673

18 **Kitagawa Y,** Fujii H, Mukai M, Kubota T, Ando N, Watanabe M, Ohgami M, Otani Y, Ozawa S, Hasegawa H, Furukawa T, Kumai K, Ikeda T, Nakahara T, Kubo A, Kitajima M. The role of the sentinel lymph node in gastrointestinal cancer. *Surg Clin North Am* 2000; **80**: 1799-1809

19 **Kitagawa Y,** Kitajima M. Gastrointestinal cancer and sentinel node navigation surgery. *J Surg Oncol* 2002; **79**: 188-193

20 **Bilchik AJ,** Giuliano A, Essner R, Bostick P, Kelemen P, Foshag LJ, Sostrin S, Turner RR, Morton DL. Universal application of intraoperative lymphatic mapping and sentinel lymphadenectomy in solid neoplasms. *Cancer J Sci Am* 1998; **4**: 351-358

Edited by Kumar M **Proofread by** Chen WW and Xu FM

PO Box 2345, Beijing 100023, China
Fax: +86-10-85381893
E-mail: wjg@wjgnet.com www.wjgnet.com

World J Gastroenterol 2004;10(20):3056-3059
World Journal of Gastroenterology
 ISSN 1007-9327

• BRIEF REPORTS •

Cytotoxic T lymphocyte associated antigen-4 gene polymorphisms confer susceptibility to primary biliary cirrhosis and autoimmune hepatitis in Chinese population

Lie-Ying Fan, Xiao-Qing Tu, Qu-Bo Cheng, Ye Zhu, Ralph Feltens, Thomas Pfeiffer, Ren-Qian Zhong

Lie-Ying Fan, Xiao-Qing Tu, Ye Zhu, Ren-Qian Zhong, The center of Clinical Immunology, Changzheng Hospital, Second Military Medical University, Shanghai 200003, China
Qu-Bo Cheng, Department of Laboratory Diagnosis, Traditinal Chinese Medicine Hospital, Guangzhou 501405, Guangdong Province, China
Ralph Feltens, Thomas Pfeiffer, Euroimmun, Medical Laboratory Diagnostic GmbH, Leubeck, Germany
Correspondence to: Lie-Ying Fan, M.D., The Center of Clinical Immunology, Changzheng Hospital, 415 Feng Yang Road, Shanghai 200003, China. flieying@hotmail.com
Telephone: +86-20-636310109 **Fax:** +86-20-33110236
Received: 2003-10-09 **Accepted:** 2003-12-08

Abstract

AIM: To investigate the association between Chinese patients with autoimmune hepatitis (AIH), primary biliary cirrhosis (PBC) and the polymorphisms of cytotoxic T lymphocyte-associated antigen-4 (CTLA-4) gene promoter (-318) and exon 1 (+49).

METHODS: CTLA-4 promoter (-318 T/C) and exon1 (+49A/G) polymorphisms were genotyped via restriction fragment length polymorphism methods in 62 Chinese AIH patients, 77 Chinese PBC patients and 160 healthy controls.

RESULTS: We found a significant association in CTLA-4 gene exon1 49 A/G polymorphism between PBC patients and controls (P = 0.006) and the frequency of G alleles was significantly increased in comparison with controls (P = 0.0046, OR = 1.8). We also found the frequency of C alleles in promoter -318 was significantly increased in AIH patients compared with controls (P = 0.02, OR = 0.41). Although the genotype distribution of the CTLA-4 exon 1-promoter gene was not significantly different between AIH and PBC patients and controls, the occurence of GG-CC was increased in two groups of patients (AIH: 32.3%, PBC: 37.7%, control: 22.5%).

CONCLUSION: Polymorphisms of CTLA-4 gene probably confer susceptibility to AIH and PBC in Chinese population.

Fan LY, Tu XQ, Cheng QB, Zhu Y, Feltens R, Pfeiffer T, Zhong RQ. Cytotoxic T lymphocyte associated antigen-4 gene polymorphisms confer susceptibility to primary biliary cirrhosis and autoimmune hepatitis in Chinese population. *World J Gastroenterol* 2004; 10(20): 3056-3059
http://www.wjgnet.com/1007-9327/10/3056.asp

INTRODUCTION

Autoimmune hepatitis (AIH) is an immune-mediated chronic inflammation of liver tissue. It is characterized by elevated serum transaminase levels, hypergammaglobulinemia, serum autoantibodies, and a good response to immunosuppressive therapy[1,2]. Although its etiology is unknown, genetic factors have been implicated to be involved in its pathogenesis. In previous studies human HLA DRB1*0 301, DRB*0 401 (in Caucasian) and DRB1*0 405 (in Chinese) have been identified as independent determinants of susceptibility to AIH[3,4]. In addition, tumor necrosis factor α (TNF-α) and complement C4 alleles have been associated with AIH[5].

Primary biliary cirrhosis (PBC) is also an immune-mediated chronic disease in which progressive destruction of the bile ducts leads to fibrosis and cirrhosis. It exhibits specific autoantibodies and disorder of liver function. Twin and family studies suggest that there is a genetic component in PBC[6,7]. The genetic typing of HLA class II and III alleles revealed a highly significant increase of HLA DRw8 and C4A-Q0 alleles in patients with PBC compared with controls, and the HLA DRB1*0 801-DQA1*0 401-DQB1*0 402 haplotype was considered to represent a maker of disease progression[8]. Polymorphism of the interleukin 1 (IL-1) and vitamin D receptor genes have been reported to be associated with PBC[8,9]. These genes, however, are neither necessary nor sufficient to cause AIH or PBC.

Cytotoxic T lymphocyte antigen-4 (CTLA-4) is involved in the regulation of T cells and is a member of the same family of cell surface molecules as CD28[10]. CTLA-4 antigen is only expressed on activated T cells, which binds to B7 molecules on antigen-presenting cells. CTLA-4-B7 binding delivers negative signals to T cells affecting T cell proliferation, cytokine production, and immune responses. Breakdown in the B7-CD28/CTLA-4 pathway could alter T-cell response and lead to autoimmune diseases[11]. Many studies have shown that specific CTLA-4 gene polymorphisms confer susceptibility to several autoimmune diseases, such as Graves' disease, insulin-dependent diabetes mellitus[12,13]. However, studies on the polymorphisms within CTLA-4 exon 1 (+49) and promoter (-318) gene in rheumatoid arthritis, multiple sclerosis and AIH have shown conflicting results in different ethnicis[14-20].

In this study, we investigated whether the polymorphisms of CTLA-4 exon 1 (+49) and promoter (-318) genes were associated with susceptibility to AIH and PBC in the Chinese population.

MATERIALS AND METHODS

Patients and controls

Blood samples were obtained from 62 patients with autoimmune hepatitis (40 females; mean age: 50 years with range 16-76 years) and 77 patients with PBC (68 females; mean age: 51.34 years, range 32-79 years). AIH cases included 44 patients with antinuclear antibodies (titer >1:100), 15 patients with antismooth muscle antibodies, 4 patients with antibodies against soluble liver antigen/liver pancreas antigen, and 2 patients with anti-liver/kidney microsomal antibodies. The diagnosis of AIH was based on the revised criteria defined by the International Autoimmune Hepatitis Group. Patients with PBC were positive for antimitochondrial antibody (titer >1:1000) and type M2 antimitochondrial antibody, and had abnormal liver function test, in which 10 patients had liver biopsy. Control group consisted of 160 healthy blood donors (100 females).

DNA preparation

Blood samples from all subjects were obtained for DNA extraction. Blood was collected in EDTA tubes and DNA was extracted using the method of proteinase K treatment and phenol/choroform extraction.

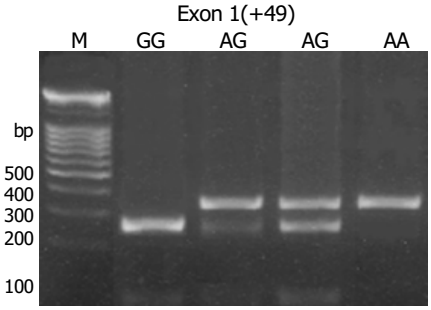

Figure 1 Gel electrophoresis of the products of BbvI restriction analysis.

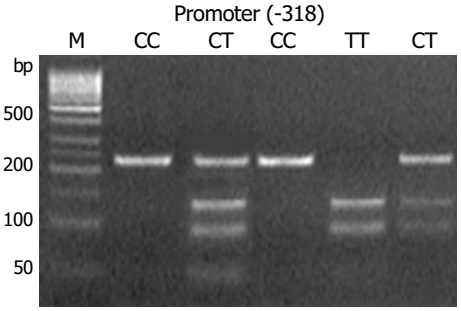

Figure 2 Gel electrophresis of the products of Tru9 I restriction analysis.

Polymorphism typing of CTLA-4 exon 1 (+49) and promoter (-318)

CTLA-4 exon 1 +49 polymorphism was defined using a polymerase chain reaction-restriction fragment length polymorphism (PCR-RFLP) with BbvI restriction enzyme. PCR was carried out using a forward primer 5'-CCACGGCTTCCTTTCTCGTA-3' and a reverse primer 5'-AGTCTCACTCACCTTTGCAG-3'. Using a MJ PTC-200 Peltier thermal cycler samples were subjected to initial denaturation for 2 min at 95 ℃, 40 cycles at 94 ℃ for 30 s, for denaturing, 45 s at 50 ℃ for annealing and 30 s at 72 ℃ for extension. *A* 327 bp fragment containing +49 A/G polymorphism in exon 1 of CTLA-4 was amplified. The substitution created a Bbv I restriction site in G allele. Amplified products were incubated at 65 ℃ for 2 h using 2 U of Bbv I per reaction. Digested products were electrophoresed on a 2.0% agarose gel. Digested G allele yielded fragments of 244 bp and 84 bp, and an allele yielded a 327 bp fragment (Figure 1).

The CTLA-4 promoter polymorphism at position -318 was defined using PCR-RFLP and Tru9 I restriction enzyme. To amplify the target DNA in CTLA-4 promoter, PCR was performed with the forward primer 5'-AAATGAATTGGACTGGATGGT-3' and reverse primer 5'-TTACGAGAAAGGAAGCCGTG-3'. *A*247 bp fragment was amplified. The following conditions were applied: initial denaturation for 2 min at 95 ℃, followed by 40 cycles (at 94 ℃ for 40 s, at 60 ℃ for 45 s, 60 ℃, at 72 ℃ for 30 s), and a final extension for 2 min at 72 ℃. PCR fragments with thymine at position -318 were cut into three fragments (21, 96 and 130 bp), whereas fragments with cytosine at the same position only had the restriction site at 21 bp (Figure 2).

Statistical analysis

Hardy-Weinberg equilibrium was tested by calculating the χ^2 for goodness of fit. Frequencies of the genotypes, alleles and phenotypes were analyzed by using chi-square test. Statistical significance was defined as $P<0.05$. The odds ratio (OR) was calculated to measure the strength of the association observed. Calculation was made by using the Internet programs from www.myatt.demon.co.uk/epicalc.htm.

RESULTS

Samples from 62 cases of AIH, 77 cases of PBC and 160 control subjects were successfully genotyped for CTLA-4 exon 1 +49 and promoter -318 polymorphisms. Allelic variation at the +49 site of CTLA-4 exon 1 was significantly associated with PBC ($P = 0.006$). Compared with controls, the frequency of G alleles was increased in patients with PBC (PBC, 70.1%, controls, 56.6%, $P = 0.0046$, OR = 1.8). Although G allele was more frequent in AIH patients (62.9%), the distribution of alleles and phenotype at the +49 site were not associated with AIH (Table 1).

In CTLA-4 promoter (-318) polymorphisms between AIH, PBC patients and controls, CC genotypes occurred more frequently than TT genotypes wasless frequently in patients than in controls, but the distribution of genotypes was not significantly different between AIH, PBC patients and controls ($P>0.05$). Compared with controls, the frequency of C alleles was significantly increased (PBC, 93.6%, controls, 85.6%, $P = 0.02$, OR = 0.41) in patients with AIH (Table 2). The genotype distribution of CTLA-4 exon 1-promoter gene had no significant difference between PBC patients and controls ($\chi^2 = 13.02$, $P = 0.07$), but the frequency of GG-CC was increased in patients with PBC (PBC, 37.7%, controls, 22.5%). The frequency of GG-CC was also higher in AIH patients (32.3%), but the genotype distribution of CTLA-4 exon 1-promoter gene did not reach statistical

Table 1 CTLA-4 exon 1 +49 polymorphism in patients with AIH, PBC and controls

	Control (%)	AIH (%)	*P*	PBC (%)	*P*
Genotype frequencies			0.4		0.006
A / A	23 (14.4)	6 (9.7)		6 (7.8)	
A / G	93 (58.1)	34 (54.8)		34 (44.2)	
G / G	44 (27.5)	22 (35.5)		37 (48.0)	
Allele frequencies[1]			0.22		0.0046
A	139 (43.4)	46 (37.1)		46 (29.9)	
G	181 (56.6)	78 (62.9)		108 (70.1)	
Phenotype frequencies[2]			0.32		0.035
A positive	116 (72.5)	40 (64.5)		40 (51.9)	
G positive	137 (85.6)	56 (90.3)		71 (92.2)	

[1]Odds ratio for G allele (AIH) = 1.3, 95% CI = 0.85-1.99; Odds ratio for G allele (PBC) = 1, 95% CI = 1.20-2.72, [2]Odds ratio for G phenotype (AIH) = 1.27, 95% CI = 0.79-2.05; Odds ratio for G phenotype (PBC) = 1.65, 95% CI = 1.03-2.63.

Table 2 CTLA-4 promoter –318 polymorphism in patients with AIH, PBC and controls

	Control (%)	AIH (%)	*P*	PBC (%)	*P*
Genotype frequencies			0.10		0.55
C / C	122 (76.3)	54 (87.1)		3 (81.8)	
C / T	30 (18.8)	8 (12.9)		12 (15.6)	
T / T	8 (5.0)	0 (0)		2 (2.6)	
Allele[(1)]			0.02		0.23
C	274 (85.6)	116 (93.6)		138 (89.6)	
T	46 (14.4)	8 (6.5)		16 (10.4)	
Phenotype frequencies[(2)]			0.11		0.39
C positive	152 (95.0)	62 (100)		75 (97.4)	
T positive	38 (23.8)	8 (12.9)		14 (18.2)	

[1]Odds ratio for C allele (AIH) = 0.41, 95% CI = 0.19-0.90; Odds ratio for C allele (PBC) = 0.69, 95% CI = 0.38-1.26, [2]Odds ratio for C phenotype (AIH) = 0.52, 95% CI = 0.23-1.17; Odds ratio for C phenotype (PBC) = 0.75, 95% CI = 0.38-1.46.

difference between AIH patients and controls ($\chi^2 = 6.82$, $P = 0.45$) (Table 3).

Table 3 CTLA-4 exon 1- promoter genotypes in patients with AIH, PBC and controls

	Control	AIH[(1)]	PBC[(2)]
AA-CC	12 (7.5)	4 (6.5)	4 (5.2)
AA-CT	7 (4.4)	2 (3.2)	1 (1.3)
AA-TT	4 (2.5)	0 (0)	1 (1.3)
AG-CC	70 (43.8)	30 (48.4)	30 (39.0)
AG-CT	19 (11.9)	4 (6.5)	3 (3.9)
AG-TT	4 (2.5)	0 (0)	1 (1.3)
GG-CC	36 (22.5)	20 (32.3)	29 (37.7)
GG-CT	8 (5.0)	2 (3.2)	8 (10.4)
Total	160 (100)	62 (100)	77 (100)

[1]AIH *vs* controls: $\chi^2 = 6.82$, $P = 0.45$; [2]PBC *vs* controls: $\chi^2 = 13.02$, $P = 0.07$.

DISCUSSION

CTLA-4 is essentially a costimulatory receptor that controls activation of T cells. In contrast to CD28, CTLA-4 delivers negative signals to T cells. CTLA-4 gene is located on chromosome 2q33 and three CTLA-4 gene polymorphisms in exon 1(adenine or guanine at position) and in promoter -318, and a microsatellite (AT) n marker at position 642 of the 3'-untranslated region of exon 3[21,22]. The polymorphism, A/G variation at position +49 (+49*A/G) in the first exon of the gene leads to the change of threonine to alanine in the leader peptide. Recently, several independent studies reported a reduced inhibitory function of CTLA-4 in individuals with certain CTLA-4 genotypes[12,23]. Kouki studied the CTLA-4 expression and T cell proliferative responses in patients with Graves's disease and healthy controls genotyped for +49*A/G. They found a correlation of +49*G/G genotype with reduced inhibitory function of CTLA-4, and suggested that this particular polymorphism was the actual disease-associated allele[24]. Maurer also got the same result[25]. A similar effect on CTLA-4 function has been suggested for the second polymorphism[26]. Wang showed that -318T allele was associated with a higher promoter activity than -318C alleles. The presence of -318T alleles may thus contribute to up regulation of the expression of CTLA-4, and consequently represents one mechanism to inhibit exaggerated immune activity.

Studies on the CTLA-4 polymorphisms in autoimmune liver diseases have shown conflicting results on the relations between the polymorphisms of CTLA-4 exon 1 +49 and AIH[18,20,27]. Agarwal indicated that CTLA-4 G allele at exon 1 +49 was more common in European Caucasoid patients with type 1 AIH and represented a second susceptibility allele, and there might be synergy between HLA-DRB1*0 301 and GG genotype in terms of disease risk. Djilali-Saiah found that the presence of +49GG predisposed to AIH type 1 in Canada children. However, Bittencourt found no associations between AIH (type 1 and type 2) and exon 1 CTLA-4 gene polymorphisms at position 49 in the Brazilian population.

In our study, we found that the frequency of -318C alleles was significantly increased in AIH patients compared with the control subjects, and GG-CC genotype occurred more frequently in CTLA-4 exon 1-promoter gene. It is therefore possible that the -318C allele and GG-CC genotype of CTLA-4 may contribute to susceptibility to Chinese patients with AIH. To our knowledge, this is the first report concerning an association of CTLA-4 promoter -318 polymorphism with AIH. In addition, we found a strong association between CTLA-4 exon 1 (+49) polymorphism and PBC, the GG genotype confers susceptibility to PBC in Chinese population. This result was coincident with Agarwal and colleague's conclusion[19]. Likewise, the GG-CC genotype occurred more frequently compared with control subjects.

AIH and PBC are two autoimmune diseases of unknown pathogenesis. There is a general agreement that induction involves $CD4^+$ T cells in the pathogenesis of AIH, but it is still not clear whether the liver damage was due to direct T cell cytotoxicity or involved autoantibodies, either through complement-mediated or antibody-dependent (ADCC) cytotoxic reactions[28]. T cell respones would certainly participate in the pathogenesis of PBC, as judged by histochemical staining of tissue samples, and by analyzing T cell lines that proliferate in the presence of putative mitochondrial autoantigens[29]. So we speculate that the single nucleotide polymorphism (SNP) of CTLA-4 (exon 1 +49 and promoter -318), and the interaction between these two SNPs may alter the inhibitory effect of CTLA-4 on T cells, and it may be an important factor in the pathogenesis of autoimmune hepatitis and primary biliary cirrhosis.

Besides CTLA-4 exon 1 (+49) and promoter (-318) polymorphisms, the CTLA-4 (AT) n microsatellite within the 3'-untranslated region of exon 3 was also a good candidate gene of autoimmune disease[21]. Previous studies demonstrated that AT-rich tracks might contribute to mRNA instability[30,31]. If the size of CTLA-4 AT tract limited the accumulation of CTLA-4 mRNA, down-regulation of CTLA-4 expression might account for the increase in the risk of an autoimmune disease. Several studies found that CTLA-4 (AT) n polymorphism was associated with Graves'disease and rheumatoid arthritis[32,33]. Since it may be involved in mRNA stability, futher studies are needed to determine the relations between CTLA-4 (AT) n polymorphism and autoimmune liver diseases.

In summary, this study showed a strong association between CTLA-4 exon 1 polymorphism (G-carrying genotypes) and PBC, and a significant association between CTLA-4 promoter -318C allele and AIH. In addition, we found that GG-CC genotype of CTLA-4 exon 1-promoter seemed to be susceptible to Chinese patients with AIH and PBC.

REFERENCES

1 **Krawitt EL,** Wiesner RH, Nishioka M. Autoimmune liver diseases. Second edition. The netherlands: *Elsevier Science B.V* 1998: 343-360

2 **Krawitt EL,** Wiesner RH, Nishioka M. Autoimmune liver diseases. Second edition. The netherlands: *Elsevier Science B.V* 1998: 361-380

3 **Czaja AJ**, Strettell MD, Thomson LJ, Santrach PJ, Moore SB, Donaldson PT, Williams R. Associations between alleles of the major histocompatibility complex and type 1 autoimmune hepatitis. *Hepatology* 1997; **25**: 317-323

4 **Qiu D**, Ma X. Relationship between type I autoimmune hepatitis and alleles of HLA-DRB1 in Chinese patients of Shanghai area. *Zhonghua Ganzangbing Zazhi* 2002; **10**: 347-349

5 **Czaja AJ**, Cookson S, Constantini PK, Clare M, Underhill JA, Donaldson PT. Cytokine polymorphisms associated with clinical features and treatment outcome in type 1 autoimmune hepatitis. *Gastroenterology* 1999; **117**: 645-652

6 **Jones DE**, Watt FE, Metcalf JV, Bassendine MF, James OF. Familial primary biliary cirrhosis reassessed: a geographically-based population study. *J Hepatol* 1999; **30**: 402-407

7 **Brind AM**, Bray GP, Portmann BC, Williams R. Prevalence and pattern of familial disease in primary biliary cirrhosis. *Gut* 1995; **36**: 615-617

8 **Donaldson P**, Agarwal K, Craggs A, Craig W, James O, Jones D. HLA and interleukin 1 gene polymorphisms in primary biliary cirrhosis: associations with disease progression and disease susceptibility. *Gut* 2001; **48**: 397-402

9 **Vogel A**, Strassburg CP, Manns MP. Genetic association of vitamin D receptor polymorphisms with primary biliary cirrhosis and autoimmune hepatitis. *Hepatology* 2002; **35**: 126-131

10 **Thompson CB**, Allison JP. The emerging role of CTLA-4 as an immune attenuator. *Immunity* 1997; **7**: 445-450

11 **Tivol EA**, Schweitzer AN, Sharpe AH. Costimulation and autoimmunity. *Curr Opin Immunol* 1996; **8**: 822-830

12 **Vaidya B**, Imrie H, Perros P, Young ET, Kelly WF, Carr D, Large DM, Toft AD, McCarthy MI, Kendall-Taylor P, Pearce SH. The cytotoxic T lymphocyte antigen-4 is a major Graves' disease locus. *Hum Mol Genet* 1999; **8**: 1195-1199

13 **Nistico L**, Buzzetti R, Pritchard LE, Van der Auwera B, Giovannini C, Bosi E, Larrad MT, Rios MS, Chow CC, Cockram CS, Jacobs K, Mijovic C, Bain SC, Barnett AH, Vandewalle CL, Schuit F, Gorus FK, Tosi R, Pozzilli P, Todd JA. The CTLA-4 gene region of chromosome 2q33 is linked to, and associated with, type I diabetes. Belgian Diabetes Registry. *Hum Mol Genet* 1996; **7**: 1075-1080

14 **Gonzalez-Escribano MF**, Rodriguez R, Valenzuela A, Garcia A, Garcia-Lozano JR, Nunez-Roldan A. CTLA4 polymorphisms in Spanish patients with rheumatoid arthritis. *Tissue Antigens* 1999; **53**: 296-300

15 **Lee YH**, Choi SJ, Ji JD, Song GG. No association of polymorphisms of the CTLA-4 exon 1 (+49) and promoter (-318) genes with rheumatoid arthritis in the Korean population. *Scand J Rheumatol* 2002; **31**: 266-270

16 **Bocko D**, Bilinska M, Dobosz T, Zoledziewska M, Suwalska K, Tutak A, Gruszka E, Frydecka I. Lack of association between an exon 1 CTLA-4 gene polymorphism A (49) G and multiple sclerosis in a Polish population of the Lower Silesia region. *Arch Immunol Ther Exp* 2003; **51**: 201-205

17 **Kantarci OH**, Hebrink DD, Achenbach SJ, Atkinson EJ, Waliszewska A, Buckle G, McMurray CT, de Andrade M, Hafler DA, Weinshenker BG. CTLA4 is associated with susceptibility to multiple sclerosis. *J Neuroimmunol* 2003; **134**: 133-141

18 **Agarwal K**, Czaja AJ, Jones DE, Donaldson PT. Cytotoxic T lymphocyte antigen-4 (CTLA-4) gene polymorphisms and susceptibility to type 1 autoimmune hepatitis. *Hepatology* 2000; **31**: 49-53

19 **Agarwal K**, Jones DE, Daly AK, James OF, Vaidya B, Pearce S, Bassendine MF. CTLA-4 gene polymorphism confers susceptibility to primary biliary cirrhosis. *J Hepatol* 2000; **32**: 538-541

20 **Bittencourt PL**, Palacios SA, Cancado EL, Porta G, Carrilho FJ, Laudanna AA, Kalil J, Goldberg AC. Cytotoxic T lymphocyte antigen-4 gene polymorphisms do not confer susceptibility to autoimmune hepatitis types 1 and 2 in Brazil. *Am J Gastroenterol* 2003; **98**: 1616-1620

21 **Deichmann K**, Heinzmann A, Bruggenolte E, Forster J, Kuehr J. An Mse I RFLP in the human CTLA4 promoto. *Biochem Biophys Res Commun* 1996; **225**: 817-818

22 **Polymeropoulos MH**, Xiao H, Rath DS, Merril CR. Dinucleotide repeat polymorphism at the human CTLA4 gene. *Nucleic Acids Res* 1991; **19**: 4018

23 **Donner H**, Rau H, Walfish PG, Braun J, Siegmund T, Finke R, Herwig J, Usadel KH, Badenhoop K. CTLA4 alanine-17 confers genetic susceptibility to Graves'disease and to type 1 diabetes mellitus. *J Clin Endocrinol Metab* 1997; **82**: 143-146

24 **Kouki T**, Sawai Y, Gardine CA, Fisfalen ME, Alegre ML, DeGroot LJ. CTLA-4 gene polymorphism at position 49 in exon 1 reduces the inhibitory function of CTLA-4 and contributes to the pathogenesis of Graves'disease. *J Immunol* 2000; **165**: 6606-6611

25 **Maurer M**, Loserth S, Kolb-Maurer A, Ponath A, Wiese S, Kruse N, Rieckmann P. A polymorphism in the human cytotoxic T-lymphocyte antigen 4 (CTLA4) gene (exon 1 +49) alters T-cell activation. *Immunogenetics* 2002; **54**: 1-8

26 **Wang XB**, Zhao X, Giscombe R, Lefvert AK. A CTLA-4 gene polymorphism at position -318 in the promoter region affects the expression of protein. *Genes Immun* 2002; **3**: 233-234

27 **Djilali-Saiah I**, Ouellette P, Caillat-Zucman S, Debray D, Kohn JI, Alvarez F. CTLA-4/CD 28 region polymorphisms in children from families with autoimmune hepatitis. *Hum Immunol* 2001; **62**: 1356-1362

28 **Krawitt EL,** Wiesner RH, Nishioka M. Autoimmune liver diseases. Second edition. The netherlands: *Elsevier Science B.V*. 1998: 35-48

29 **Krawitt EL,** Wiesner RH, Nishioka M. Autoimmune liver diseases. Second edition. *Amsterdam: Elsevier* 1998: 49-69

30 **Shaw G**, Kamen R. A conserved AU sequence from the 3'untranslated region of GM-CSF mRNA mediates selective mRNA degradation. *Cell* 1986; **46**: 659-667

31 **Jackson RJ**. Cytoplasmic regulation of mRNA function: the importance of the 3'untranslated region. *Cell* 1993; **74**: 9-14

32 **Hadj Kacem H**, Kaddour N, Adyel FZ, Bahloul Z, Ayadi H. HLA-DQB1 CAR1/CAR2, TNFα IR2/IR4 and CTLA-4 polymorphisms in Tunisian patients with rheumatoid arthritis and Sjögren's syndrome. *Rheumatology* 2001; **40**: 1370-1374

33 **Kotsa K**, Watson PF, Weetman AP. A CTLA-4 gene polymorphism is associated with both Graves disease and autoimmune hypothyroidism. *Clin Endocrinol* 1997; **46**: 551-554

Edited by Zhang JZ and Wang XL **Proofread by** Xu FM

PO Box 2345, Beijing 100023, China
Fax: +86-10-85381893
E-mail: wjg@wjgnet.com www.wjgnet.com

World J Gastroenterol 2004;10(20):3060-3061
World Journal of Gastroenterology
 ISSN 1007-9327

• BRIEF REPORTS •

Diagnostic and surgical therapeutic features of extrahepatic bile duct carcinoma without jaundice

Hui-Huan Tang, Shi Chang, Xian-Wei Wang, Yun Huang, Xue-Jun Gong, Jun Zhou

Hui-Huan Tang, Shi Chang, Xian-Wei Wang, Yun Huang, Xue-Jun Gong, Jun Zhou, Department of Surgery, Xiangya Hospital of Central South University, Changsha 410008, Hunan Province, China
Correspondence to: Shi Chang, Department of Surgery, Xiangya Hospital of Central South University, Changsha 410008, Hunan Province, China. changshi@medmail.com.cn
Telephone: +86-731-4327468
Received: 2003-11-12 **Accepted:** 2003-12-08

Abstract

AIM: To analyze the diagnostic and therapeutic features of extrahepatic bile duct carcinoma (EBDC) without jaundice.

METHODS: Between 1985 and 1999, 101 patients underwent surgery for EBDC in Xiangya Hospital. These patients were divided into two groups: 84 jaundiced patients and 17 non-jaundiced patients according to preoperative serum total bilirubin levels. The clinical manifestations, laboratory findings, location, pathology and surgical resectability of the tumors were compared between the two groups.

RESULTS: The laboratory parameters such as hemoglobin, serum albumin ALB, AKP, γ-GT, and sonography appearance were similar between the two groups, and there was no significant difference in tumor location, pathological type and resectability. However, the number of non-jaundiced patients associated with chololithiasis was significantly greater than that of jaundiced patients ($P = 0.008$).

CONCLUSION: The presence of jaundice is not a reliable criterion for the prediction of the resectability and the extent of tumor progression in extrahepatic bile duct carcinoma. Decreased levels of blood hemoglobin and serum albumin, elevated levels of AKP and γ-GT, and /or abnormal sonography may be suggestive. Biopsy of a stenotic or thickened bile duct is strongly recommended for a correct diagnosis before the appearance of jaundice.

Tang HH, Chang S, Wang XW, Huang Y, Gong XJ, Zhou J. Diagnostic and surgical therapeutic features of extrahepatic bile duct carcinoma without jaundice. *World J Gastroenterol* 2004; 10(20): 3060-3061
http://www.wjgnet.com/1007-9327/10/3060.asp

INTRODUCTION

Primary carcinoma of the extrahepatic bile duct is an uncommon malignant tumor, with reported incidence rate of about 0.01-0.46%. About 2% of patients who died of cancer were autopsied to have this disease[1-4]. Jaundice is generally thought to be the most important factor in the diagnosis of this disease, but there are still few cases seeking doctors' consultation before jaundice appears[5-9]. Those patients could be underdiagnosed or misdiagnosed because of atypical clinical symptoms. In this study, the diagnostic and therapeutic features of bile duct carcinoma without jaundice were compared with those with jaundice.

MATERIALS AND METHODS

From January 1984 to December 1999, two hundred and thirty-nine patients who were diagnosed as extrahepatic bile duct carcinoma were admitted to Xiangya Hospital. One hundred and one were operated and the diagnosis was confirmed by pathology. Patients with carcinomas of gallbladder, intrahepatic bile duct and ampulla of Vater were excluded from the study. The patients under studies consisted of 58 males and 43 females, aged 27 to 76 years (an average age of 61.7 years).

According to the level of serum total bilirubin (STB), the patients were divided into non-jaundiced group (17 patients, STB $\leqslant$ 2.0 mg/dL at the time of diagnosis) and jaundiced group (84 patients, STB>2.0 mg/dL). Clinical data included symptoms, laboratory results, imaging findings, pathological results, treatments and resectabilities.

Statistical analysis

The difference between the two groups was compared using chi-square analysis and Student's *t* test. $P<0.05$ was considered statistically significant.

RESULTS

Symptoms and signs

Fifteen (88.2%) patients in the non-jaundiced group had anorexia or/and vomiting, abdominal pain compared with 63 (75.0%) in the jaundiced group. Eight (47.1%) patients in the non-jaundiced group and fifty-seven (67.9%) patients in the jaundiced group were found to show positive signs in liver, spleen or gallbladder enlargement. (Table 1).

Laboratory examination

The patients showed no difference in the levels of abnormal serum albumin, alkaline phosphates (AKP), γ-glutamyltranspeptidase (γ-GT), except STB level (Table 2).

Image examination

All patients in the non-jaundiced group underwent sonography. The results showed segmental stenosis of extrahepatic bile duct, thickening of the bile duct wall, and dilatation of intra- or extra-hepatic bile duct proximal to the stenosis. Sixty-seven out of 78 patients showed stenosis or neoplastic space-occupying lesions within the extrahepatic bile duct.

Operation findings

During the operation, 59 patients had neoplasms located in the upper extrahepatic bile duct while 8 in the middle and 34 in the lower. There was no difference with regard to localization of the tumor between the two groups.

Pathological features

All patients were proved to have adenocarcinoma. The patients were categorized into three different grades by the degree of differentiation. The results showed that there was no difference between the patients with or without jaundice.

Treatment

Radical resection, biliary bypass, external drainage or biopsy

were performed according to the surgical findings. There was no difference in tumor resectability between the two groups (P>0.05, Table 3).

Table 1 Symptoms and signs

Symptom	Non-jaundiced		Jaundiced		P value
	No.	%	No.	%	
Abdominal discomfort	15	88.2	63	75.0	>0.05
Liver or gallbladder palpable	8	47.1	57	67.9	>0.05
Cholelithiasis 11	64.7	26	31.0	<0.05[a]	

No significant difference was found between the two groups in the clinical symptoms and signs. In the non-jaundice group, the rate of combined cholelithiasis was obviously higher than in the jaundice group.

Table 2 Laboratory data

	Non-jaundiced		Jaundiced		P value
	No.	%	No.	%	
Descending of HB	8	47.1	45	53.6	>0.05
Ascending of AKP	8	72.7	56	86.2	>0.05
Ascending of γ-GT	4	66.7	28	93.3	>0.05
Descending of ALB	4	23.5	39	47.0	>0.05

No significant difference was found between the two groups in laboratory data.

Table 3 Tumor location, pathological type, treatment

	Non-jaundiced		Jaundiced		P value
	No.	%	No.	%	
Upper	11	64.7	48	57.1	
Location middle	0	0.0	8	9.6	>0.05
Lower	6	35.3	28	33.3	
Good	6	35.3	48	57.1	
Differential mild	8	47.1	27	32.1	>0.05
Poor	3	17.7	9	10.8	
Biopsy	3	17.7	8	9.5	
Treatment drainage	9	52.9	43	51.2	>0.05
By pass	0	0.0	1	1.2	
Radical	5	29.4	32	38.1	

No significant difference was found between the two groups in tumor locations, pathological types and treatment methods.

DISCUSSION

Jaundice is the early and main manifestation of extrahepatic bile duct carcinoma. It has been reported to be the initial sign in 83-97% of patients[5-9]. However, there are few patients coming to hospital before the appearance of jaundice. In the present study 16.8% of the patients with EBDC were diagnosed before the presence of jaundice. These patients were likely to be neglected during busy outpatient service. We found that, there were still some clues to the diagnosis of bile duct carcinoma for these patients without jaundice. Some laboratory parameters, such as hemoglobin, serum albumin, AKP and γ-GT may be suggestive.

Sonography is almost the first tool for the diagnosis of extrahepatic bile duct carcinoma because it is non-invasive and less expensive. Ninety-five of the patients underwent sonography in our study, of whom 84 (88.4%) had positive findings, such as duct stenosis, thickness of the bile duct wall or space-occupying lesions within the duct. The results were in accordance with those documented in the literature[10-12].

The relationship between choledocholithiasis and bile duct carcinoma is still unclear. As reported, 6-37% of extrahepatic bile duct carcinomas were associated with bile duct stones[13]. In the present study the number of patients who suffered from choledocholithiasis in the non-jaundiced group was significantly higher than that in the jaundiced group (P<0.05). Two factors may contribute to this finding. First, for patients with bile duct stones, the clinical manifestations were so typical that the doctor would pay more attention to the biliary system. Second, during the operation for choledocholithiasis, we usually took the whole layer of bile duct wall for biopsy whenever there was stenosis, sclerosis or nodular change in the bile duct. Eight patients were diagnosed by this means and radical resection was performed.

It was reported that extrahepatic bile duct carcinoma without jaundice occurred in the early stage of the disease. The tumor was well differentiated and the resection rate was usually high[8]. However, there was no difference between the two groups in our study. The radical resection rate was 29.4% in the non-jaundiced group and 38.1% in the jaundiced group (P>0.05). Liver and/or intrabdominal lymph node metastases were found in 12 patients without jaundice. We suggest that the presence of jaundice cannot be taken as the major criterion to predict the tumor resectability or the extent of tumor progression.

ACKNOWLEDGEMENT

We are grateful to Professor Zhong-Shu Yan for his assistance in preparing this manuscript.

REFERENCES

1 **Helling TS**. Carcinoma of the proximal bile duct. *J Am Coll Surg* 1994; **178**: 97-106
2 **de Groen PC**, Gores GJ, LaRusso NF, Gunderson LL, Nagorney DM. Biliary tract cancers. *N Engl J Med* 1999; **341**: 1368-1378
3 **Chamberlain RS**, Blumgart LH. Hilar cholangiocarcinoma: a review and commentary. *Ann Surg Oncol* 2000; **7**: 55-66
4 **Tsujino K**, Landry JC, Smith RG, Keller JW, Williams WH, Davis LW. Definitive radiation therapy for extrahepatic bile duct carcinoma. *Radiology* 1995; **196**: 275-280
5 **Chung C**, Bautista N, O'Connell TX. Prognosis and treatment of bile duct carcinoma. *Am Surg* 1998; **64**: 921-925
6 **Miyazaki M**, Ito H, Nakagawa K, Ambiru S, Shimizu H, Shimizu Y, Kato A, Nakamura S, Omoto H, Nakajima N, Kimura F, Suwa T. Aggressive surgical approaches to hilar cholangiocarcinoma: hepatic or local resection? *Surgery* 1998; **123**: 131-136
7 **Suzuki M**, Takahashi T, Ouchi K, Matsuno S. The development and extension of hepatohilar bile duct carcinoma. A three-dimensional tumor mapping in the intrahepatic biliary tree visualized with the aid of a graphics computer system. *Cancer* 1989; **64**: 658-666
8 **Sugiyama M**, Atomi Y, Kuroda A, Muto T. Bile duct carcinoma without jaundice: clues to early diagnosis. *Hepatogastroenterology* 1997; **44**: 1477-1483
9 **Tamada K**, Sugano K. Diagnosis and non-surgical treatment of bile duct carcinoma: developments in the past decade. *J Gastroenterol* 2000; **35**: 319-325
10 **Choi BI**, Lee JH, Han MC, Kim SH, Yi JG, Kim CW. Hilar Cholangiocarcinoma: comparative study with sonography and CT. *Radiology* 1989; **172**: 689-692
11 **Chou FF**, Sheen-Chen SM, Chen YS, Chen MC, Chen CL. Surgical treatment of cholangiocarcinoma. *Hepatogastroenterology* 1997; **44**: 760-765
12 **Looser C**, Stain SC, Baer HU, Triller J, Blumgart LH. Staging of hilar cholangiocarcinoma by ultrasound and duplex sonography: a comparison with angiography and operative findings. *Br J Radiol* 1992; **65**: 871-877
13 **Schoenthaler R**, Phillips TL, Castro J, Efird JT, Better A, Way LW. Carcinoma of the extrahepatic bile ducts. The university of california at san francisco experimence. *Ann Surg* 1994; **219**: 267-274

Edited by Wang XL **Proofread by** Xu FM

PO Box 2345, Beijing 100023, China
Fax: +86-10-85381893
E-mail: wjg@wjgnet.com www.wjgnet.com

World J Gastroenterol 2004;10(20):3065-3069
World Journal of Gastroenterology
 ISSN 1007-9327

• BRIEF REPORTS •

Choledochal cysts in pregnancy: Case management and literature review

De-Quan Wu, Long-Xian Zheng, Qiu-Shi Wang, Wen-Hua Tan, Shuang-Jiu Hu, Pei-Ling Li

De-Quan Wu, Long-Xian Zheng, Qiu-Shi Wang, Department of Surgery, the Second Affiliated Hospital of Harbin Medical University, Harbin 150086, Heilongjiang Province, China
Wen-Hua Tan, Shuang-Jiu Hu, Pei-Ling Li, Department of Obstetrics and Gynecology, the Second Affiliated Hospital of Harbin Medical University, Harbin 150086, Heilongjiang Province, China
Correspondence to: Professor De-Quan Wu, Department of Surgery, the Second Affiliated Hospital of Harbin Medical University, 157 Baojian Road, City of Harbin, Harbin 150086, Heilongjiang Province, China. zhenglxhrbmu@hotmail.com
Telephone: +86-451-86605411
Received: 2004-02-14 **Accepted:** 2004-02-21

Abstract

AIM: To evaluate the diagnosis, management principles and long-term results of congenital choledochal cysts in pregnancy.

METHODS: Three adult patients were diagnosed as choledochal cysts in pregnancy from 1986 to 1989 and their long-term results were evaluated.

RESULTS: The first patient had a Roux-en-Y cysto-jejunostomy with T-tube external drainage and died of septic shock and multi-organ failure 25 d after operation. In the second patient, 4 wk after percutaneous trans-choledochal cyst was drained externally with a catheter under US guidance, four weeks later the patient delivered vaginally, and had a cysto-jejunostomy 3 mo after delivery, and lived well without any complications for 15 years after operation. The third patient received Roux-en-Y cysto-jejunostomy after a vertex delivery by induced labor at 28 wk gestation, and demonstrated repetitively intermittent retrograde cholangitis within 10 years, and then died of well-differentiated congenital cholangioadenocarcinoma one month after re-operation with exploratory biopsy at the age of 36.

CONCLUSION: More conservative approaches such as external drainage of choledochal cyst should be considered for pregnant patients with high risk, complete excision of choledochal cyst during hepaticojejunostomy or modified hepaticojejunostomy is highly recommended at the optimal time.

Wu DQ, Zheng LX, Wang QS, Tan WH, Hu SJ, Li PL. Choledochal cysts in pregnancy: Case management and literature review. *World J Gastroenterol* 2004; 10(20): 3065-3069
http://www.wjgnet.com/1007-9327/10/3065.asp

INTRODUCTION

Choledochal cysts in pregnant women represent a diagnostic and therapeutic challenge to a broad spectrum of the medical profession. Not only the rare association, but also the clinical signs and symptoms are obscured by physiological changes that occur during pregnancy. As a result, diagnosis is often delayed until patients present with life-threatening complications. We reported our experiences in managing three cases of choledochal cyst in pregnant patients.

MATERIALS AND METHODS

Three adult patients were diagnosed as choledochal cyst in pregnancy from 1986 to 1989 and their long-term results were studied retrospectively (Tables 1, 2).

RESULTS

A 27-year-old primigravida (patient No.1) at 20-wk gestation presented with jaundice, dark urine, nausea, anorexia, vomiting, intermittent upper abdominal pain, fever and weight loss during the past three months and was admitted to our hospital in February, 1986. Physical examination demonstrated a palpable 12 cm×10 cm mass in the upper right quadrant of the abdomen, a tender protuberant abdomen due to her pregnant state, and fullness in the right upper quadrant. Laboratory evaluation data are shown in Table 2. Ultrasound examination showed a cystic lesion, 12 cm×9 cm×10 cm at the right upper quadrant with a connection to tubular structure, and dilated intrahepatic ducts in both lobes of liver. Impressive diagnosis was gestation with a type IV choledochal cyst. Perioperative fluid therapy and transfusion were administered. A Roux-en-Y cysto-jejunostomy was performed for the choledochal cyst with T-tube external drainage in the proximal part of the cyst. Five hundred milliliter bile was drained from T-tube post-surgery and documented everyday. The patient was afebrile with normal vital signs, flatus was released on d 3 and 10 postoperation. Progressive nausea, vomiting, anorexia, occurred with aggravated jaundice, hypokalemia (2.8 mEq/L), serum electrolyte disturbance and hypoalbuminemia, and then developed to retrograde bile duct infection. The primigravida lost, her consciousness on day 19 postoperation. She was diagnosed as incipient (threatened) abortion, and died of septic shock and multi-organ failure on the 25th d postoperation.

Patient No.2 was a 23-year-old primigravida at 36-wk G1P1 gestation with choledochal cyst. She had intermittent upper abdominal pain, progressive nausea, anorexia, vomiting and abdominal tenderness in the upper right quadrant and epigastric burning during the past several weeks. She was admitted to our hospital in February 1987. Physical examination demonstrated a nontender protuberant abdomen due to her pregnant state, and fullness in the right upper quadrant. Her skin and sclera were slightly jaundiced. Sonographic evaluation of the right upper quadrant demonstrated an oval-shaped, 15 cm×16 cm×3 cm cystic mass arising from the portal hepatic separated from the gallbladder, and diffuse dilatation of intrahepatic left ductal system. Clinical diagnosis was a type IV choledochal cyst with gestation (G1P1). Laboratory evaluation data are shown in Table 2. Percutaneous trans-choledochal cyst operation was performed on the patient with a catheter placed for external drainage under the abdominal ultrasonography guidance. About 3000 mL sap green bile was excreted from the cyst, and then about 600 mL sap green bile was excreted daily. Gradually, her clinical conditions were improved and remained stable and her pregnancy progressed without problems. She delivered vaginally 4 wk later without

Table 1 Information in 3 patients diagnosed as choledochal cysts in pregnancy

Patients					Treatment		Complication		Survival time (postoperation)	Prognosis (postoperation)
No.	Age(yr)	Type	Size (cm)	Chief Complaints	Initial operation	Final operation	Early	Late		
1	27	IV	12×9×10	Abdominal pain Jaundice Abdominal mass	Roux-en-Y cystojejunostomy with T-tube external drainage		Septic shock and multi-organ failure		25 d	died
2	23	IV	15×16×3	Abdominal pain Jaundice	Plasement and fixation of a catheterization	Roux-en-Y cystojejunostomy			15 yr	survived
3	26	I	20×20×20	Jaundice Abdominal mass	Roux-en-Y cystojejunostomy	Exploratory biopsy	Retrograde cholangitis	Intermittent recurrence of Retrograde cholangitis Cholangioadenocarcinoma	10 yr	died

Table 2 Analysis of pre-operation laboratory values for 3 patients

Parameters	Normal range	Patient No. 1	Patient No. 2	Patient No. 3
Total bilirubin (μmol/L)	1.6-20.6	59	57	26
Direct bilirubin (μmol/L)	0-6.4	8.0	8.7	8.1
Alkaline phosphatase (U/L)	35-150	171	63	110
r-GT (U/L)	0-60	51	58	26
Aspartate aminotranferase (U/L)	0-40	37	37	37
Alanine aminotranferase (U/L)	0-40	5	11	102
Total protein (g/L)	60-85	40	67	55
Albumin (g/L)	35-55	18	39	32
Globin (g/L)	-	22	25	23
Potassium (mmol/L)	3.5-5.5	1.9	4.2	4
Sodium (mmol/L)	135-145	134	128	139
Chloride (mmol/L)	101-111	89.3	96.9	105
Hemoglobin (g/L)	120-160	74	150	122
Erythrocyte (10^{12}/L)	3.5-5.5	2.4	4.81	3.9
Hemoleukocyte (10^9/L)	3.5-10	5.8	4.4	9.7
Platelet (10^9/L)	100-300	92	177	128

complications. As choledochal cyst was extensively attached to the surrounding tissues, it was dissected using cysto-jejunostomy 3 mo after delivery. Choledochal cyst was histologically confirmed. The patient was discharged from hospital 40 d postoperation and was well without any complications for 15 years.

Patient No.3, a 26-year-old multiparous woman at 28-wk gestation with choledochal cyst was admitted to our hospital in July 1989. Her chief complaint was jaundice and she had a palpable mass in the upper right quadrant of the abdomen during the past 20 d. On examination, the patient was afebrile with normal vital signs with skin and her sclera slightly jaundicised. She had a soft palpable 8 cm×10 cm mass in the upper right quadrant of the abdomen without tenderness. Laboratory evaluation data are shown in Table 2. Ultrasound examination showed a large cyst of 20 cm×20 cm×20 cm at the right upper quadrant connected to tubular structure. The patient gave a vertex delivery by induced labor at 28-wk gestation on the second day of admission. Following treatment with prophylactic antibiotics, the patient received Roux-en-Y cysto-jejunostomy on d 8 after delivery. The patient had 4 or 5 times of recurrence of intermittent retrograde cholangitis annually for 10 years, lasting for about 20 d each time, and relieved after a few days of conservative antibiotics. However, the patient was not re-operated due to the extensive adherence with surrounding tissues, and died of well differentiated congenital mucinous cholangioadenocarcinoma proved at the age of 36 years.

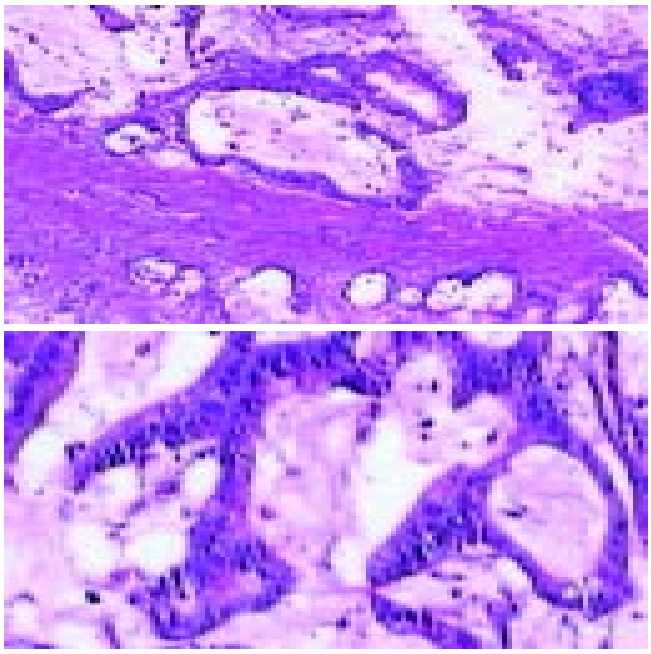

Figure 1 High-columnar or flat carcinoma cells with darkly stained nuclei and variation in size and shape arranged in irregular glandular pattern with intra- and extra-glandular mucin (hematoxylin and eosin, 40×10).

DISCUSSION

Choledochal cyst is a focal dilatation of the biliary tract. Although rare in adulthood, it is diagnosed more frequently with the advances in biliary imaging techniques[1]. Of the numerous descriptions and classifications of choledochal cyst, the most practical is the classification proposed by Alonso-Lej 1 and modified by Todani[1] in 1977 (Table 3). The major point of this classification is that the gallbladder is not usually distended and arises from a small cystic duct, not at the upper end of the cyst[2].

Table 3 Todani modification of the Alonso-Lej, classification system of choledochal cyst

Type I	Fusiform dilation of the extrahepatic bile duct
Type II	Single saccular dilation or diverticulum of the extrahepatic bile duct
Type III	Dilation of the intraduodenal portion of the bile duct
Type IVa	Combined intra-and extrahepatic dilation of the bile duct
Type IVb	Multiple dilations of the extrahepatic bile duct
Type V	Isolated or diffuse intrahepatic biliary dilation (Caroli's disease when associated with hepatic fibrosis)

Since the first pathological description of a choledochal cyst by Vatero in 1723 and the first clinical report by Douglas in 1852, the aetiology of this abnomality has been controversial[3]. It is unclear whether choledochal cyst is congenital, or acquired. In 1936 Yotsuyanagi[3] suggested that choledochal cysts arose from inequality in the vacuolization of the biliary tract in early embryonic life. The common channel theory proposed by Babbitt[3] in 1969 is most widely accepted, which was based on an abnomality of the pancreaticobiliary junction and the formation of an abnormally long common channel (greater than 15 mm) outside the control of the sphincters of Boyden. This configuration permits pancreatic enzymes to reflux into the common bile duct. The pancreatic enzymes then lead to persistent inflammation, epithelial denudation, thinning of the bile duct wall and distal obstruction, then eventually cyst formation. The incidence of choledochal cysts was reported as 1 in 13 000 to 1 in 2 million patients[3,4]. It affects females 4 times as often as males, and more common in Asians and presents mainly in infancy and childhood (60%)[1]. It is necessary to classify the type of cysts and to recognize the presence of an abnomal pancreaticobiliary duct junction, visualization of both the biliary tree and pancreatic duct. Thus, direct cholangiography, especially ERCP, is beneficial. But intraoperative cholangiography is not sensitive enough to detect the presence of an abnomal pancreaticobiliary duct junction. Radiographic visualization of both the biliary tree and pancreatic duct prior to surgery is helpful for surgical manipulation and complete excision of the cyst[5-8]. Other pathologic features of choledochal cysts include acute and chronic mucosal inflammation, mucosal dysplasia, and absence of smooth or elastic fibers. A true mucosal lining may be hard to find, or it is usually cuboidal or columnar and frequently ulcerated if it is present. The cyst wall varies from 1 to 10 mm in thickness. Mucus-producing glands are rarely seen. There is usually a large amount of fibrosis, some of which may be involved in luminal stenoses. The bile is often very thick, and sometimes less pigmented than normal. Biliary calculi are uncommon. Pathologic complications include biliary obstruction, cholangitis, hepatic abscess, rupture, or development of cancer. Cholelithiasis due to choledochal cysts is unusual[2,9].

Clinical manifestations are nonspecific and variable. The most common symptoms are abdominal pain and jaundice. If untreated, the condition may be fatal due to ascending cholangitis, biliary cirrhosis or diffuse peritonitis following rupture of the cyst. Malignancy might also develop in the cyst and occur in pregnant women[10]. Choledochal cyst in pregnancy is rare but poses a threat to both the mother and fetus. The maternal complications include cholangitis, pancreatitis, peritonitis and even malignancy. The fetal complications include fetal loss and preterm labor. Most reported cases were diagnosed when women presented with symptoms. It has been suggested that pregnancy may exacerbate the symptoms due to hormonal effect, compression by the gravid uterus and increase in intraabdominal pressure during pregnancy and postpartum. The cyst might be asymptomatic during the first pregnancy[11,12], as demonstrated in our third patient. Asymptomatic cysts discovered on routine US could be observed with serial US examinations[11].

Diagnosis of choledochal cysts during pregnancy is difficult. Radiologic imaging, ultrasound, computed tomography, cholangiography and biliary scintigraphy, could clinch the diagnosis[1,12-15]. Although ultrasonography is a common useful investigation, difficulty may arise during pregnancy due to distortion of the normal abdominal anatomy and gravid uterus. Furthermore, ultrasound examination cannot demonstrate anatomic details of the biliary tree. Due to exposure of the fetus to ionizing radiation, contrast and ionizing imagings, such as CT or ERCP, should be avoided in pregnancy[11,12,16]. Magnetic resonance imaging (MRI) could provide clear visualization of the relations between the choledochal cyst and biliary tree and of the extent and size of the choledochal cyst. Therefore, MRI is the investigation of choice in doubtful cases[12,17]. To improve the management of this potentially serious condition in pregnancy, both clinicians and radiologists should be aware of this possibility in women with a right upper quadrant mass.

Concerning the optimal time of treatment, conservative management is commonly adopted during pregnancy. Once the diagnosis has been established, surgery is the only option for treatment[11,12]. Surgical time is critical during pregnancy and the operative risk to the fetus and mother has to be balanced against the likelihood of cyst-related complications[11,12]. Any patient who presents with a symptomatic or rapidly enlarging choledochal cyst or with cyst-related complications during pregnancy should undergo urgent treatment. Unfortunately, surgery during pregnancy has been associated with high fetal and maternal morbidity and mortality rate[1,11,12,15]. Therefore, other more conservative approaches might have to be adopted until surgery could be performed under optimal conditions. Percutaneous cyst decompression might be done to relieve symptoms of pain and jaundice[1,11,12,15,16]. In addition, antibiotics should be administered for treatment of cholangitis or for long-term prophylaxis, and the need for subsequent definitive cyst surgery should not be obviated[11,12]. An operation should ideally be performed in the second trimester when the risk of surgery and anesthesia is lowest. When symptoms occur in the first trimester, surgery should be postponed unless the life of the mother is in danger, while in the third trimester, early cesarean section should be performed when amniocentesis indicates that the fetus is sufficiently mature. At the same time, a temporizing or definitive cyst operation could be undertaken as necessary[1,11,12]. Definitive surgery depends on the cyst type and associated hepatobiliary pathology. Definitive surgical excision of the cyst can avoid postpartum complication and non-cyst excision may induce long-term complications.

Early reports suggested that internal or external drainage of a choledochal cyst by choledochocystojejunostomy or T-tube choledochocystomy was a satisfactory treatment, but with a longer follow-up it has become clear that complications such as suppurative cholangitis, lithiasis, pancreatitis, secondary biliary cirrhosis, portal hypertention and intrahepatic abscess occurred in up to 40 percent of cases[3,4,9,15]. This is similar as our results. The increased risk of bile duct carcinoma in

choledochal cysts has been well characterized[3,4,9,10,14,15]. The reported incidence of biliary tract carcinoma in choledochal cysts varied from 2.5% to 17.5%, significantly higher than that found in the general population, which was from 0.01% to 0.05%[3,4,9,10,14,15]. The incidence of cancer in patients with a choledochal cyst and in those undergone enteric drainage without cyst excision was much higher than that of carcinoma of the bile ducts in the general population. The age-related incidence of cyst-associated cancer has been shown to increase from 0.7 % in the first decade of life to 14.3 % after 20 years of age. It means the favorable outcome in congenital choladochal cyst patients was due to earlier diagnosis[3,4,9,10,14,15].

Kasai *et al*.[3] reported firstly the increased incidence of carcinoma in choledochal cysts and advocated primary cyst excision. The advances in diagnostic and therapeutic procedures and increased operative experience have lowered the mortality rate to 0-7%[3,4,9,10,14,15]. Roux-en-Y choledocho-jejunostomy has replaced choledochoduodenostomy as the preferred operative procedure because of the high morbidity rate of cholangitis and the frequent need for reoperation later[3, 4,9,15].

Excision of types I, II and IV choledochal cysts is now widely accepted because of the lower incidence of postoperative complications. In contrast to cyst enterostomy, cyst excision with hepaticojejunostomy had satisfactory results. Although the occurrence of intrahepatic cholangiocarcinoma after the excision of a type I cyst has been reported[18,19], but cyst excision is the primary choice of treatment for type I cysts. Type III cysts require adequate drainage and generally can be managed by endoscopic sphincterotomy and cannot be undertaken, operative sphincteroplasty with transduodenal cyst excision might be attempted[5]. Sphincteroplasty either endoscopically or surgically has been found to be satisfactory[20]. Treatment for type IV cysts is still controversial. Either excision of the extrahepatic cyst alone[5] or total cyst excision including hepatectomy[21] has been recommended. Concerning type V cysts, some authors recommended hepatic resection for unilobar Caroli's disease[1].

Complete excision of the extrahepatic bile duct from the hepatic hilum to the pancreaticobiliary duct junction has become the choice of treatment for types I and IV cysts[3-5,9,11,19,21-23]. However, it should be mentioned that since complete excision seems to be difficult in some patients, pancreaticoduodenectomy or hepatic resection should then be considered. In such cases, the distal choledochus is resected just above the pancreaticobiliary duct junction with the aid of preoperative ERCP and intraoperative US to avoid injuring the pancreatic duct. In the hepatic hilum, the hepatic duct must be resected at the hilum, and hepaticojejunostomy with a wide opening by plastic of both the hepatic ducts is necessary.

The reason why the three patients turned out quite different was their different clinical conditions. Our first Patient's situation was not quite good in peri-operation, she had a progressive nausea, vomiting, anorexia, fever, weight loss, and anemia with skin and her sclera slightly jaundicized, hypoalbuminemia, as well as disturbed blood electrolytes. Although the patient received fluid therapy and transfusion in peri-operation, the volume of blood was not enough to improve her clinical conditions within a short period of time, such as anemia, hypoalbuminemia. Gentamicin sulfate 240 000 iu one time per day could not prevent occurrence of retrograde bile duct infection, and the patient died of septic shock and multi-organ failure on day 25 postoperation.

Choledochal cyst in our No. 2 patient was drained externally with a catheter under the abdominal ultrasonography guidance, and she delivered safely. As the choledochal cyst was extensively infused with surrounding tissues, a cysto-jejunostomy was performed 3 mo after delivery. The patient's general condition was good. In our study, the No.3 patient developed a malignant tumor, because she did not receive re-operation for complete cyst excision, hepatojejunostomy or modified hepatojejunostomy for treatment of repeated occurrence of intermittent retrograde cholangitis, which could be treated or avoided by early diagnosis and early complete cyst excision[3,4,9,10,14,15], which are very important for the treatment of congenital choladochal cyst patients. Although cyst excision did not completely eliminate the risk of intrahepatic cholangiocarcinoma after the excision of a type I cyst[3-5,9-11,14,15,18-22], but it significantly decreased the incidence of bile duct carcinoma. Thus, laparotomy during pregnancy should be avoided if possible and non-cyst excision cases should be explored to remove the cyst completely in the optimal surgical time.

Although choledochal cysts rarely occur in pregnancy, clinicians need to be aware of the condition. Inappropriate therapy may be catastrophic for both mother and child. This is why we recommend that patients should be admitted to a specialized hospital once the diagnosis is established. Complete excision of choledochal cyst with Roux-en-Y hepaticojejunostomy or modified Roux-en-Y hepaticojejunostomy is the choice of treatment for types I, II and IV choledochal cysts in non-pregnant adult patients; whereas in pregnancy, a more conservative approach should be adopted until the time when the surgical risk is lowest. Percutaneous external drainage of choledochal cyst under the abdominal ultrasonography guidance is indicated, if a complication of cystic rupture occurs. Complete excision of choledochal cyst with hepaticojejunostomy or modified hepaticojejunostomy is helpful in avoiding late complications such as retrograde cholangitis, biliary tract carcinoma, and is the most ideal choice of treatment for types I, II, IV choledochal cysts in pregnant adult patients, and is therefore highly recommended.

REFERENCES

1 **Crittenden SL**, McKinley MJ. Choledochal cyst- clinical features and classification. *Am J Gastroenterol* 1985; **80**: 643-647
2 **Meyers WC**, Jones RS. Textbook of liver and biliary surgery. *J B Lippincott Company* 1990: 312-318
3 **Benhidjeb T**, Munster B, Ridwelski K, Rudolph B, Mau H, Lippert H. Cystic dilatation of the common bile duct: surgical treatment and long-term results. *Br J Surg* 1994; **81**: 433-436
4 **Chijiiwa K**, Koga A. Surgical management and long-term follow-up of patients with choledochal cysts. *Am J Surg* 1993; **165**: 238-242
5 **Scudamore CH**, Hemming AW, Teare JP, Fache JS, Erb SR, Watkinson AF. Surgical management of Choledochal cysts. *Am J Surg* 1994; **167**: 497-500
6 **Sugiyama M**, Atomi Y, Kuroda A. Pancreatic disorders associated with anomalous pancreaticobiliary junction. *Surgery* 1999; **126**: 492-497
7 **Sugiyama M,** Atomi Y. Anomalous pancreaticobiliary junction without congenital choledochal cyst. *Br J Surg* 1998; **85**: 911-916
8 **Tagge EP**, Tarnasky PR, Chandler J, Tagge DU, Smith C, Hebra A, Hawes RH, Cotton PB, Othersen HB Jr. Multidisciplinary approach to the treatment of pediatric pancreaticobiliary disorders. *J Pediatr Surg* 1997; **32**: 158-164
9 **Yamataka A**, Ohshiro K, Okada Y, Hosoda Y, Fujiwara T, Kohno S, Sunagawa M, Futagawa S, Sakakibara N, Miyano T. Complications after cyst excision with hepaticoenterostomy for choledochal cysts and their surgical management in children versus adults. *J Pediatr Surg* 1997; **32**: 1097-1102
10 **Binstock M**, Sondak VK, Herd J, Reimnitz C, Lindsay K, Brinkman C, Roslyn JJ. Adenocarcinoma in a choledochal cyst during pregnancy: A case report and guidelines for management. *Surgery* 1988; **103**: 588-592
11 Hewitt **PM**, Krige JEJ, Bornman PC, Terblanche J. Choledochal cyst in pregnancy: A therapeutic dilemma. *J Am Coll Surg* 1995; **181**: 237-240
12 **Fok WY,** Yip SK, Leung TN, Leung KF, Chui AKK. Large choledochal cyst present through 2 pregnancies. A case report. *J*

Reprod Med 2003; **48**: 482-484
13 **Beattie GJ,** Keay S, Muir BB, Boddy K. Acute pancreatitis with pseudocyst formation complicating pregnancy in a patient with a co-existent choledochal cyst. *Br J Obstet Gynaecol* 1993; **100:** 957-959
14 **Bismuth H**, Krissat J. Choledochal cystic malignancies. *Ann Oncol* 1999; **10**(Suppl 4)**:** S94-98
15 **Hopkins NFG,** Benjamin IS, Thompson MH, Williamson RCN. Complications of choledochal cysts in adulthood. *Ann R Coll Surg Engl* 1990; **72:** 229-235
16 **Russell JGB**, Taylor V, Torrance B. Ultrasonic diagnosis of choledochal cyst in pregnancy. *Br J Radiol* 1976; **49**: 425-426
17 **Shanley DJ**, Gagliardi JA, Daum-Kowalski R. Choledochal cyst complicating pregnancy: antepartum diagnosis with MRI. *Abdom Imaging* 1994; **19**: 61-63
18 **Kinoshita H**, Nagata E, Hirohashi K, Saki K, Kobayashi Y. Carcinoma of the gallbladder with an anomalous connection between the choledochus and the pancreatic duct. Report of 10 cases and review of the literature in Japan. *Cancer* 1984; **54**: 762-769
19 **Todani T**, Watanabe Y, Toki A, Urushihara N, Sato Y. Reoperation for congenital choledochal cyst. *Ann Surg* 1988; **207**: 142-147
20 **Venu RP**, Geenen JE, Hogan WJ, Dodds WJ, Wilson SW, Stewart ET, Soergel KH. Role of endoscopic retrograde cholangiopancreatography in the diagnosis and treatment of choledochocele. *Gastroenterology* 1984; **87**: 1144-1149
21 **Todani T**, Narusue M, Watanabe Y, Tabuchi K, Okajima K. Management of congenital choledochal cyst with intrahepatic involvement. *Ann Surg* 1978; **187**: 272-280
22 **Hara H**, Morita S, Ishibashi T, Sako S, Otani M, Tanigawa N. Surgical treatment for congenital biliary dilatation, with or without intrahepatic bile duct dilatation. *Hepatogastroenterology* 2001; **48**: 638-641
23 **Bose SM,** Lobo DN, Singh G, Wig JD. Bile duct cysts: presentation in adults. *Aust N Z J Surg* 1993; **63**: 853-857

Edited by Wang XL and Ren SY **Proofread by** Xu FM

PO Box 2345, Beijing 100023, China
Fax: +86-10-85381893
E-mail: wjg@wjgnet.com www.wjgnet.com

World J Gastroenterol 2004;10(20):3070-3072
World Journal of Gastroenterology
 ISSN 1007-9327

• BRIEF REPORTS •

Clinical significance of preoperative regional intra-arterial infusion chemotherapy for advanced gastric cancer

Cheng-Wu Zhang, Shou-Chun Zou, Dun Shi, Da-Jian Zhao

Cheng-Wu Zhang, Shou-Chun Zou, Dun Shi, Da-Jian Zhao, Department of General Surgery, Zhejiang Provincial People's Hospital, Hangzhou 310014, Zhejiang Province, China
Correspondence to: Cheng-Wu Zhang, Department of General Surgery, Zhejiang Provincial People's Hospital, Hangzhou 310014, Zhejiang Province, China. zcw1989@sina.com
Telephone: +86-571-85239988
Received: 2003-10-30 **Accepted:** 2003-12-16

Abstract

AIM: Preoperative intra-arterial infusion chemotherapy could increase the radical resection rate of advanced gastric cancer, but its effect on the long-term survival has not been assessed. This study was designed to evaluate the clinical significance of preoperative intra-arterial infusion chemotherapy for advanced gastric cancer.

METHODS: Clinicopathological data of 91 patients who underwent curative resection for advanced gastric cancer were collected. Among them, 37 patients undertaken preoperative intra-arterial infusion chemotherapy were used as the interventional chemotherapy group, and the remaining 54 patients as the control group. Eleven factors including clinicopathological variables, treatment procedures and molecular biological makers that might contribute to the long-term survival rate were analyzed using Cox multivariate regression analysis.

RESULTS: The 5-year survival rate was 52.5% and 39.8%, respectively, for the interventional group and the control group ($P<0.05$). Cox multivariate regression analysis revealed that the TNM stage ($P<0.001$), preoperative intra-arterial infusion chemotherapy ($P = 0.029$) and growth pattern ($P = 0.042$) were the independent factors for the long-term survival of patients with advanced gastric cancer.

CONCLUSION: Preoperative intra-arterial infusion chemotherapy plays an important role in improving the prognosis of advanced gastric cancer.

Zhang CW, Zou SC, Shi D, Zhao DJ. Clinical significance of preoperative regional intra-arterial infusion chemotherapy for advanced gastric cancer. *World J Gastroenterol* 2004; 10 (20): 3070-3072
http://www.wjgnet.com/1007-9327/10/3070.asp

INTRODUCTION

Gastric cancer is one of the most common cancers in China. Despite recent advances in experimental researches, early diagnosis and surgical techniques, the outcome of patients with gastric carcinoma is still far from satisfaction. Surgery remains the mainstay of potentially curative treatment, but the survival rates of patients with advanced gastric cancer are poor. A number of studies have investigated whether intravenous chemotherapy after a resection could improve the survival rate, but the results were different and disputable[1,2]. Preoperative regional intra-arterial infusion chemotherapy could increase the radical resection rate of advanced gastric cancer. However, there are few reports about the influence of preoperative intra-arterial chemotherapy on the long-term survival of patients with advanced gastric carcinomas after curative resections. In the current study, we analyzed retrospectively the clinicopathologic data of 91 patients with advanced gastric cancers undergone curative surgeries during recent years. To investigate the effect of preoperative intra-arterial chemotherapy on the prognosis of advanced gastric cancer, the Cox model of proportional hazards was utilized to identify the independent variables affecting the long-term survival of patients with gastric carcinomas.

MATERIALS AND METHODS

Clinicopathologic materials

The study comprised 91 patients who underwent curative resection for advanced gastric cancer from June 1984 to June 1992 at our hospital. All patients received follow-ups for 3 to 220 mo (mean time 57.1±23.8 mo) and their clinicopathologic data were well-provided. There were 69 males and 22 females,their ages ranged from 25 to 73 years with a mean age of 54.9±12.9 years. The tumor staging for each gastric cancer was evaluated according to the new TNM classification system of UICC[3], and there were 27 patients with stageII, 49 with stage III and 15 with stage IV. Of the 91 cases, 2 had well- differentiated adenocarcinomas, 48 had moderately differentiated adenocarcinomas and 41 had poorly differentiated adenocarcinomas. Thirty-one were negative for lymphatic vessel invasions and 60 were positive for lymphatic vessel invasions. For venous vessel invasion of tumor, 78 cases were negative and 13 were positive. The tumor growth pattern was defined according to Ming classification. There were 40 patients with expansive types and 51 with infiltrative types. Expressions of CD44 splice variants v6(CD44V6) and E-cadherin(E-CD) and proliferating cell nuclear antigen(PCNA) in all the 91 resected gastric carcinomous tissue specimens were detected by streptavidin-peroxidase immunohistochemistry. Of the patients, 37 patients undergone preoperative regional intra-arterial infusion chemotherapy were used as the interventional chemotherapy group and the remaining 54 patients as the control group. All the patients received systemic chemotherapy after surgeries. The clinicopathologic parameters of the two groups were analyzed and compared.

Preoperative intra-arterial infusion chemotherapy

Preoperative intra-arterial infusion chemotherapy was performed via transfemoral artery route using the Seldinger's approach before surgery. Celiac axis angiogram was initially carried out to document the visceral arterial anatomy and the arterial supply of tumor, and the digital subtraction technique was utilized in the study. According to the results of angiogram, the main blood supplying arteries of gastric cancer were detected and superselective catheterization of these arteries was performed. Then, chemotherapy drugs were administered via the placed catheter. Protocols of chemotherapy were FAP (5-FU 1.0 g+ADM 30-50 mg+DDP 40-60 mg) or FMP (5-FU 1.0 g+MMC 8-10 mg+DDP 40-60 mg). Preoperative interventional

chemotherapy was performed one or two times for each patient, and the interval time ranged from 10 to 14 d. Surgery was carried out two weeks after interventional chemotherapy. Of the 37 patients who underwent interventional chemotherapy, 31 received chemotherapy one time and 6 received two times.

Statistical analysis

The eleven variables observed including gender, age, preoperative intra-arterial infusion chemotherapy, TNM stage classification, differentiation grade, growth pattern, lymphatic vessel and venous vessel invasion, expressions of CD44V6 and E-CD, PCNA labeling index (PCNA LI), were stored in a computer, and analyses were performed using the SPSS 9.0 for Windows. Survival rates were calculated using life table method and the differences among the groups of patients were measured by Log rank test. Univariate analysis was performed first, and the variables found by univariate analysis significantly associated with survival rates were subjected to multivariate analyses using the Cox model of proportional hazards. $P<0.05$ was considered statistically significant.

RESULTS

Comparison of pathological parameters between two groups

The differences of pathological parameters were not significant between two groups ($P>0.05$, Table 1).

Comparison of immunohistochemistry results between two groups

The expressions of CD44V6 and E-CD and PCNA were not significantly different between two groups ($P>0.05$, Table 2).

Comparison of postoperative complications and survival rates between two groups

No death occurred due to surgery in this study. One wound infection and 1 pneumonic infection were found in the interventional chemotherapy group, whereas 2 pneumonic infections and 1 abdominal cavity infection occurred in the control group after surgery. The incidence of postoperative complications was not significantly different between two groups ($P>0.05$). The 5-year survival rate of the interventional chemotherapy group and the control group was 52.5% and 39.8%, respectively, and the difference between the two groups was significant ($P<0.05$).

Univariate and multivariate analyses of prognostic factors

The results of univariate analysis demonstrated that the factors including gender, age and tumor cellular differentiation grade were not associated with postoperative survival rate ($P>0.05$). The variables significantly correlated with survival rates were TNM stage, growth pattern of tumor, lymphatic vessel and venous vessel invasion, intra-arterial infusion chemotherapy, expressions of CD44V6 and E-CD, PCNA LI ($P<0.05$). These factors were subjected to multivariate analyses using the Cox model of proportional hazards. These analyses identified three independent prognostic variables which were TNM stage, preoperative interventional chemotherapy and growth pattern of tumor, according to influence strength (Table 3). The survival predicting equation ($\chi^2 = 37.63$, $P<0.001$) was obtained, it suggested the foundation of the equation be reasonable.

Table 3 Independent prognostic variables identified by Cox proportional hazard model

Variables	SE	Wald	df	Sig	R	Exp(B)
TNM stage	0.1220	16.3113	1	0.0001	0.1753	1.6304
Interventional chemotherapy	0.2501	4.7491	1	0.0285	0.0681	1.6981
Growth pattern	0.2607	4.0105	1	0.0417	0.0711	1.6953

DISCUSSION

Preoperative chemotherapy was initiated in the 1980s as an auxiliary therapy for malignant neoplasms[4]. It has been considered that preoperative chemotherapy could reduce activities of tumor cells, contract volumes of tumors, decrease iatrogenic diffusion of tumor cells during surgery, and improve curative resections for tumors. It was reported that serum concentration of chemotherapy drugs in abdominal organs by local intra-arterial infusion was nearly ten times as high as by systemic chemotherapy[5]. Kosaka *et al*.[6] investigated the therapeutic efficacy of intra-arterial infusion chemotherapy for advanced gastric cancer, and found that the response rate of tumors to intra-arterial infusion chemotherapy was significantly higher than that to systemic infusion chemotherapy. Liu[7] reported that the overall response rate to preoperative interventional chemotherapy was 72.8% for gastric carcinomas, and it was revealed that preoperative intra-arterial infusion chemotherapy exerted its effect by introducing apoptosis of cancer cells, restraining tumor cell proliferation and promoting pathological necrosis of tumors[8]. Tao *et al.* also demonstrated that preoperative regional artery chemotherapy showed inhibitory actions on growth of gastric cancer cells mainly through inhibiting proliferation and inducing the apoptosis of tumor cells[9]. Our previous study also showed that preoperative intra-arterial infusion chemotherapy could dramatically improve the rate of radical resection for gastric cancer. However, the

Table 1 Comparison of pathological parameters between two groups

Groups	TNM stage			Differentiation grade			Growth pattern		Lymphatic vessel invasion		Venous vessel invasion	
	II	III	IV	Well	Moderately	Poorly	Expensiv	Infiltrative	Negative	Positive	Negative	Positive
Interveytional	11	12	6	1	19	17	15	22	14	23	32	5
Control	16	29	9	1	29	24	25	29	17	37	46	8
	$P>0.05$			$P>0.05$			$P>0.05$		$P>0.05$		$P>0.05$	

Table 2 Comparison of immunohistochemistry results between two groups

Groups	Expression of CD44V6				Expression of E-CD				PCNA LI (%)
	-	+	++	+++	-	+	++	+++	
Interventional	8	14	5	10	11	13	9	4	63.8±17.6
Control	16	12	8	18	17	18	13	6	64.7±18.0
	$P>0.05$				$P>0.05$				$P>0.05$

influence of preoperative intra-arterial infusion chemotherapy on the prognosis of patients with gastric cancer has been controversial. Masuyama *et al.*[10] concluded that preoperative intra-arterial infusion chemotherapy might prevent local and lymph node metastases, but it could not improve the survival of gastric cancer patients. Whereas Shchepotin *et al.*[11] reported superselective intra-arterial chemotherapy conferred a highly significant survival advantage compared to control or systemic intravenous chemotherapy for advanced nonresectable gastric cancer. This study demonstrated that the 5-year survival rate of preoperative interventional chemotherapy group was significantly higher than that of the control group, and there was no statistical difference between the incidences of postoperative complications of the two groups. It is suggested that preoperative intra-arterial infusion chemotherapy is both effective and safe for patients with advanced gastric cancer.

Among the prognostic factors of gastric cancer, the influence of clinical modalities on the prognosis of patients has been the focus of studies on gastric cancer. It has been proved that the most important prognostic variable for gastric cancer is curative resection of tumor[12]. In the current study, all patients underwent curative resections of tumors. Furthermore, the clinicopathologic parameters of the two groups were not significantly different. This makes it possible to evaluate the effect of other therapeutic modalities on the prognosis of patients with advanced gastric cancers. As is shown in this article, among the seven variables significantly associated with the survival of patients with gastric cancer by univariate analysis, TNM stage was the most important independent prognostic factor by multivariate analyses using the Cox model of proportional hazards. It was consistent with previous reports[13]. The results of our study also revealed that preoperative intra-arterial infusion chemotherapy and growth pattern of tumors were the independent prognostic variables affecting long-term survival of gastric cancer patients, suggesting that preoperative intra-arterial infusion chemotherapy is of great importance in improving the prognosis of patients with advanced gastric cancers after undergoing curative resections.

In summary, the results of the present study revealed that preoperative intra-arterial infusion chemotherapy was one of the independent prognostic variables of patients with advanced gastric cancer. Therefore, preoperative intra-arterial infusion chemotherapy in combination with curative resection would have important clinical values in improving the prognosis of patients with advanced gastric carcinoma.

REFERENCES

1 **Hermans J**, Bonenkamp JJ, Boon MC, Bunt AM, Ohyama S, Sasako M, Van de Velde CJ. Adjuvant therapy after curative resection for gastric cancer: meta-analysis of randomized trials. *J Clin Oncol* 1993; **11:** 1441-1447

2 **Janunger KG,** Hafstrom L, Nygren P, Glimelius B. A systematic overview of chemotherapy effects in gastric cancer. *Acta Oncol* 2001; **40**: 309-326

3 **Yoo CH**, Noh SH, Kim Y, Min JS. Comparison of prognostic significance of nodal staging between old (4th edition) and new (5th edition) UICC TNM classification for gastric carcinoma. *World J Surg* 1999; **23**: 492-497

4 **Leong T**, Michael M, Foo K, Thompson A, Lim Joon D, Weih L, Ngan S, Thomas R, Zalcberg J. Adjuvant and neoadjuvant therapy for gastric cancer using epirubicin / cisplatin / 5-fluorouracil (ECF) and alternative regimens before and after chemoradiation. *Br J Cancer* 2003; **89**: 1433-1438

5 **Tokairin Y,** Maruyama M, Baba H, Yoshida T, Kure N, Nagahama T, Ebuchi M. Pharmacokinetics of "subselective" arterial infusion chemotherapy. *Gan To Kagaku Ryoho* 2001; **28:** 1795-1798

6 **Kosaka T**, Ueshige N, Sugaya J, Nakano Y, Akiyama T, Tomita F, Saito H, Kita I, Takashima S. Evaluation of intra-arterial infusion chemotherapy for advanced gastric cancer. *Gan To Kagaku Ryoho* 1998; **25:** 1288-1291

7 **Liu FK.** The interventional therapy for advanced gastric cancer before and after operation. *Zhongguo Shiyong Waike Zazhi* 2001; **21**: 403

8 **Dong XC**, Li B, Li YP. Effect of preoperative intra-arterial chemotherapy on apoptosis and p53 expression of gastric cancer. *Aizheng* 2002; **21**: 1078-1080

9 **Tao HQ,** Zou SC. Effect of preoperative regional artery chemotherapy on proliferation and apoptosis of gastric carcinoma cells. *World J Gastroenterol* 2002; **8:** 451-454

10 **Masuyama M,** Taniguchi H, Takeuchi K, Miyata K, Koyama H, Tanaka H, Higashida T, Koishi Y, Mugitani T, Yamaguchi T. Recurrence and survival rate of advanced gastric cancer after preoperative EAP-II intra-arterial infusion therapy. *Gan To Kagaku Ryoho* 1994; **21:** 2253-2255

11 **Shchepotin IB,** Chorny V, Hanfelt J, Evans SR. Palliative superselective intra-arterial chemotherapy for advanced nonresectable gastric cancer. *J Gastrointest Surg* 1999; **3**: 426-431

12 **Allgayer H,** Heiss MM, Schildberg FW. Prognostic factors in gastric cancer. *Br J Surg* 1997; **84:** 1651-1664

13 **Hermanek P**, Wittekind C. News of TNM and its use for classification of gastric cancer. *World J Surg* 1995; **19:** 491-495

Edited by Wang XL and Xu FM

PO Box 2345, Beijing 100023, China
Fax: +86-10-85381893
E-mail: wjg@wjgnet.com www.wjgnet.com

World J Gastroenterol 2004;10(20):3073-3075
World Journal of Gastroenterology
 ISSN 1007-9327

• BRIEF REPORTS •

Levels of plasma des-γ-carboxy protein C and prothrombin in patients with liver diseases

Xiao-Fan He, Zhi-Bin Wen, Min-Juan Liu, Hui Zhang, Qun Li, Shi-Lin He

Xiao-Fan He, Zhi-Bin Wen, Hui Zhang, Shi-Lin He, Haemostasis Physiology Laboratory, Department of Physiology, Xiangya Medical College, Central South University, Changsha 410078, Hunan Province, China
Min-Juan Liu, Second Affiliated Hospital of Guangzhou Medical College, Guangzhou 510260, Guangdong Province, China
Qun Li, Xiangya Hospital, Central South University, Changsha 410008, Hunan Province, China
Supported by the National Natural Science Foundation of China NO.C39600197, the Foundation of Education Ministry of China for Outstanding Youth Scholars, NO.2001:39
Correspondence to: Zhi-Bin Wen, Haemostasis Physiology Laboratory, Department of Physiology, Xiangya Medical College, Central South University, Changsha 410078, Hunan Province, China. wenzhibin2002@yahoo.com.cn
Telephone: +86-731-2355053 **Fax:** +86-731-2650668
Received: 2004-02-28 **Accepted:** 2004-04-29

Abstract

AIM: To study the plasma des-γ-carboxy protein C activity, antigen and prothrombin levels in patients with liver diseases and their clinical significance.

METHODS: Plasma protein C activity (PC:C) was detected by chromogenic assay and antigen (PC:Ag) and des-γ-carboxy protein C (DCPC) were detected by ELISA. Total prothrombin and unabsorbed prothrombin in plasma were detected by ecarin chromogenic assay.

RESULTS: Compared with the control, the levels of PC:C and PC:Ag in patients with hepatocellular carcinoma (HCC) and liver cirrhosis (LC) were lower (PC:C: 104.65±23.0%, 62.50±24.89%, 56.75±20.14%, PC:Ag: 5.31±1.63 μg/mL, 2.28±1.15 μg/mL, 2.43±0.79 μg/mL, $P<0.05$). The levels of PC:Ag in patients with acute viral hepatitis (AVH) also was lower (2.98±0.91 μg/mL, $P<0.01$), but PC:C was close to the control (93.76±30.49%, $P>0.05$). The levels of DCPC in patients with HCC were remarkably higher (0.69±0.29 μg/mL, 1.18±0.63 μg/mL, 0.45±0.21 μg/mL, $P<0.05$) and its average was up to 50% of total PC:Ag. But those of DCPC in patients with AVH were not significantly different from the control. The levels of total prothrombin were lower in patients with LC, but higher in patients with HCC. The levels of unabsorbed prothrombin were predominantly higher than those of other groups.

CONCLUSION: PC:C and PC:Ag in patients with liver diseases (except PC:C in AVH) were lower. The total prothrombin was lower in patients with LC. The higher level of unabsorbed prothrombin may be used as a scanning marker for HCC. DCPC may be used as a complementary marker in the diagnosis of HCC.

He XF, Wen ZB, Liu MJ, Zhang H, Li Q, He SL. Levels of Plasma des-γ-carboxy protein C and prothrombin in patients with liver diseases. *World J Gastroenterol* 2004; 10(20): 3073-3075
http://www.wjgnet.com/1007-9327/10/3073.asp

INTRODUCTION

Protein C is a plasma glycoprotein of M_r 62 000 and is synthesized and degraded in the liver. There is 2-6 mg/L PC of plasma in healthy person, with about 72-139% biological activity. No difference in the content of protein C between males and females was found, but protein C shows an increased trend towards increasing age (with an average increase of 4% every 10 years). Thrombin formed during coagulation is responsible for conversion of protein C to activated protein C (APC). This activation takes place on the surface of endothelial cells and monocytes by compound thrombin with thrombomodulin[1]. Because protein C is a vitamin K-dependent plasma protein, it is highly homologous in structure to factors X, IX, VII and prothrombin. Many studies have demonstrated that there are changes of factors X, IX, VII and prothrombin in patients with liver diseases, and des-γ-carboxy (abnormal) prothrombin is a useful tumor marker in the diagnosis of hepatocellula carcinoma[2-4]. But up to now, few reports are available about the association between PC and liver diseases. Therefore, in the present study we not only reported the changes of PC and prothrombin in liver diseases, but also explored the relationship between des-γ-carboxy protein C (DCPC) and HCC.

MATERIALS AND METHODS

Clinical data

Fifty-three patients (33 males and 20 females, aged 20-81 years) were included in this study. Of them, 18 patients with hepatocellular carcinoma (HCC) , 20 with liver cirrhosis (LC) , 15 with acute viral hepatitis (AVH). They were from The Second Affiliated Hospital of Guangzhou Medical College and the Xiangya Hospital of Central South University. HCC and LC were diagnosed by clinical, pathological and ultrasonic examinations. AVH was diagnosed by clinical and immunological/RT-PCR examinations. Twenty healthy volunteers (10 males and 10 females, aged 25-65 years) were enrolled as the control group.

Materials

Blood sampling and preparation of plasma (for PC:C, PC:Ag assay) were as follows. Blood was drawn into 0.13 mol/L sodium citrate (9/1,v/v), plasma (for DCPC, prothrombin assay) was obtained by drawing blood (9vol) into 0.1 mol/L sodium oxalate (9/1, 1v/v) , and centrifugation at 4 000 r/min for 10 min. All were snap frozen and stored at -40 ℃.

PC activity (PC:C) and PC antigen (PC:Ag) kits were purchased from Shanghai Sun Biotech Company. Vials containing 50 U of ecarin were provided by Sigma Company. Chromogenic substance S2238 was obtained from American Diagnostica Inc. (ADI). $Bacl_2$, Tris, and others were of analytical grade and purchased from Shanghai Reagent Factory. ELX800 enzyme-linked immunosorbent detector was from America BIO-Tek Instruments Inc.

Methods

PC:C assay PC:C was detected by chromogenic assay (SH Sun Bio CO kits). Excessive actvator was put into the diluted human plasma, PC was activate and convert it into activated protein C

(APC). Then chromozym APC was hydrolyzed, and PNA was released. PNA levels are determined by measuring the sample solution absorbances at 405 nm and comparing against those of standard curves generated using a PC:C. The assay procedures performed according to the instructions of the manufacturer.

PC:Ag assay PC:Ag was determined by ELISA (SH Sun Bio CO. kits). Murine PC antibody was used as capture antibody and an enzyme-linked antibody fragment that specifically recognizes bound hPC as detection antibody. After plasma PC bound to capture antibody and detection antibody, the substrate was hydrolyzed by enzyme and chromagenic reaction occurred. The sample absorbance at 492 nm was proportional to the concentrations of plasma PC. The assay procedures were performed according to the manufacturer's instructions.

DCPC assay A total of 40 μL of 1 mol/L $BaCl_2$ was added into 500 μL of normal reference plasma or pending measured plasma. The mixture was surged for 30 min at 4 ℃. After centrifuged for 5 min,collect the supernatant was collected. Then the supernatant was absorbed by barium salt again and collected. The level of PC:Ag in the supernatant was measured by ELISA.

Prothrombin assay Ecarin could activate γ-carboxylated and des-γ-carboxylated prothrombin into thrombin and then thrombin amidolyse chromozym P. The absorbance at 405 nm was proportional to the concentration of γ-carboxylated and des-γ-carboxylated Prothrombin. Levels of prothrombin in plasma reflected the total prothrombin and those in plasma absorbed by $Bacl_2$ reflect the unabsorbed prothrombin.

Statistical analysis

Results were expressed as mean±SD. One way analysis of variance and Newman-keuls test were used for comparisons of the mean value in various groups. *P* values less than 0.05 was considered statistically significant.

RESULTS

PC:C and PC:Ag in liver diseases

Compared with the control, the levels of PC:C and PC:Ag in patients with hepatocellular carcinoma (HCC) and liver cirrhosis were lower ($P<0.05$). PC:Ag in acute viral hepatitis (AVH) also was lower, but PC:C was close to the control ($P>0.05$) (Table 1).

Table 1 The levels of PC:C and PC:Ag in patients with liver diseases (mean±SD)

	n	PC:C (%)	PC:Ag (μg/mL)
Control	20	104.65±23.0	5.31±1.63
Hepatocellular carcinoma	18	62.50±24.89[a]	2.28±1.15[b]
Liver cirrhosis	20	56.75±20.14[a]	2.43±0.79[b]
Acute viral hepatitis	15	93.76±30.49	2.98±0.91[b]

[a]$P<0.05$, [b]$P<0.01$ *vs* control group.

DCPC in liver diseases

As shown in Table 2, the difference of DCPC between acute viral hepatitis group and control group was not statistically significant ($P<0.01$). But DCPC in patients with HCC was remarkably higher than those in patients with acute viral hepatitis and the control ($P<0.01$).

Prothrombin in liver diseases

In contrast to the control, the levels of total prothrombin was lower in patients with liver cirrhosis ($P<0.05$). There was no significant difference in plasma prothrombin between acute viral hepatitis and control groups ($P>0.10$). But the level of total prothrombin in patients with HCC was markedly higher than that in other groups ($P<0.01$). The levels of unabsorbed prothrombin in patients with HCC were predominantly higher than those in the other groups ($P<0.01$).

Table 2 The levels of DCPC in patients with liver diseases (mean±SD)

	n	Total PC:Ag (μg/mL)	DCPC:Ag (μg/mL)	DCPC:Ag Total PC:Ag
Control	15	5.23±1.95	0.69±0.29	13.19%
Hepatocellular carcinoma	15	2.33±1.21	1.18±0.63[b]	50.64%[b]
Acute viral hepatitis	15	2.98±0.91	0.45±0.21	15.10%

[b]$P<0.01$ *vs* control and acute viral hepatitis groups.

Table 3 The levels of prothrombin in patients with liver diseases (mean±SD)

	n	Total prothrombin (%)	Unabsorbed prothrombin (%)
Control	20	101.99±12.29	0.30±0.18
Hepatocellular carcinoma	18	220.61±67.95[b]	2.87±0.89[b]
Liver cirrhosis	10	85.33±6.99[a]	0.95±0.45[a]
Acute viral hepatitis	15	99.05±14.97	1.09±0.36[a]

[a]$P<0.05$, [b]$P<0.01$ *vs* control groups.

DISCUSSION

Vitamin K-dependent zymogens, prothrombin, factor VII, IX , protein C and protein S are synthesized in the liver. It is understandable that the liver diseases are associated with thrombosis and/or hemorrhage. In the present investigation, we observed that the levels of total prothrombin decreased in patients with liver cirrhosis and increased in patients with HCC. The results are consistent with previous reports[5].

Prior to secretion into plasma, all the vitamin K-dependent proteins undergo post-transtional modifications by a vitamin K-dependent carboxylase that converts several specific glutamic acid residuces to γ-carboxyglutuminic acid (Gla). Gla residues are located in N-terminal of the mature proteins and contribute to the ability of these proteins to bind to Ca^{2+} and offer metal ions such as Ba^{2+}, *etc*. Ca^{2+} binding induces conformational changes leading to expression of membrane -binding phoepholipid, which is a key step to bring about biological activities. Therefore, des-γ-carboxylated proteins can not bind to divalent ions and lose their procoagulant or anticoagulant activities. Our data showed that after plasma was absorbed by barium salt, the levels of unabsorbed prothrombin from plasma of patients with HCC was very high and lower in patients with acute viral hepatitis and liver cirrhosis, and less in healthy volunteers. This fact further suggested that high levels of unabsorbed prothrombin in plasma could be used a scanning marker of HCC. It is due to unabsorbed prothrombin essentially reflecting des-γ-carboxy prothrombin(DCP). Recent studies demonstrated that DCP could not only differentiate HCC from nonmalignant chronic liver diseases, but also indicate prognosis for HCC[3,4]. Because the assay of unabsorbed prothrombin is more economical and simpler than the determination of DCP, it maybe spread in clinic, especially in the developing countries.

The activation of protein C is catalyzed by a compound of α-thrombin and the endothelial cell surface protein thrombomodulin. In contrast to other vitamin K- dependent coagulation factors, activated protein C (APC) functions as an anticoagulant by proteolytic inactivation of factor Va and VIIIa. APC also promotes

fibrinolytic response by forming compounds with plasminogen activator inhibitor-1 and by diminishing the activation of thrombin-activatable fibrinolysis inhibitor via inhibition of thrombin generation. Thus the deficiency of protein C is associated with thrombosis[6,7]. Previous reports demonstrated that the levels of protein C from plasma in patients with liver diseases were lower[8,9]. Our data showed that PC:C in patients with hepatocellular carcinoma and liver cirrhosis was lower than control group ,and the descendant degree was proportional to the damaged degree (unpublished data). Thus, the results provided further evidence for the association of protein C and liver diseases. However, PC:Ag in acute viral hepatitis (AVH) was also lower, but PC:C was close to the control , the reason is unknown. Protein C inhibitors synthesized in liver can specifically inactivate APC. Perhaps the decrease of protein C inhibitors in liver disease is one of the causes. In addition, the decrease of coagulation factors and some drugs may be partly responsible for it.

Because protein C is one of the vitamin K-dependent proteins synthesized in the liver, its biological functions are also dependent on complete Gla domain. Yashiikawa *et al*. reported that the impaired vitamin K-dependent γ-carboxylation in patients with HCC involved not only prothrombin, but also protein C[10]. Our data showed that the levels of DCPC in patients with HCC were surprisingly high, almost up to 50% of total protein C. This fact shows that the high level of DCPC from plasma can be used as a complemental tumor marker of HCC. As surgical removal or reduction in tumor was with chemotherapy is associated with reduction or elimination of the abnormal prothrombin (des-γ-carboxy prothrombin , DCP), the tumor itself is responsible for the production of DCP. We believe that DCPC may have the same production process like DCP. Up to date, it is still unknown why tumor cells of HCC make so many DCP and DCPC as well as des-γ-carboxy proteins. Because vitamin therapy can not reduce the concentration of DCP and DCPC, the production of des-γ-carboxy protein is not due to vitamin K deficiency. Its specific mechanisms remain unclear.

It is becoming increasingly clear that there is an interaction network between coagulation and inflammation and natural anticoagulants have strong anti-inflammatory effects[11,12]. Animal experiments indicated that protein C and activated protein C inhibits could inhibit DIC and improve survival rate[11-13]. Clinical trials could demonstrated that recombinant human activated protein C (rhAPC) could attenuate systemic inflammatory response syndrome and reduces mortality in patients with severe sepsis[14-16]. Therefore, it may be beneficial when an appropriate dose of protein C or rhAPC is given to the patients with liver diseases especially HCC to prevent and treat sepsis and DIC.

REFERENCES

1 **Esmon CT.** The protein C pathway. *Chest* 2003; **124**(3 Suppl): 26S-32S

2 **Liebman HA,** Furie BC, Tong MJ, Blanchard RA, Lo KJ , Lee SD, Coleman MS, Furie B. Des-γ-carboxy (abnomal) prothrombin as a serum marker of primary hepatocellular carcinoma. *N Engl J Med* 1984; **310**: 1427-1431

3 **Marrero JA,** Su GL,Wei W, Emick D, Conjeevaram HS, Fontana RJ, Lok AS. Des-gamma carboxyprothrombin can differentiate hepatocellular carcinoma from nonmalignant chronic liver disease in American patients. *Hepatology* 2003; **37**: 1114-1121

4 **Nagaoka S,** Yatsuhashi H, Hamada H, Yano K, Matsumoto T, Daikoku M, Arisawa K, Ishibashi H, Koga M, Sata M, Yano M. The Des-γ-carboxy prothrombin index is a new prognostic indicator for hepatocellular carcinoma. *Cancer* 2003; **98**: 2671-2677

5 **Furie B,** Furie BC. The molecular basis of blood coagulation. *Cell* 1988; **53**: 505-518

6 **Castellino FJ.** Gene targeting in hemostasis: protein C. *Front Biosci* 2001; **6**: D807-819

7 **Esmon CT.** Protein C anticoagulant pathway and its role in controlling microvascular thrombosis and inflammation. *Crit Care Med* 2001; **29**(7 Suppl): S48-51

8 **Shimada M,** Matsumata T, Kamakura T, Suehiro T, Itasaka H, Sugimachi K. Changes in regulating blood coagulation in hepatic resection with special references to soluble thrombomodulin and protein C. *J Am Coll Surg* 1994; **178**: 65-68

9 **Kloczko J,** Mian M, Wojtukiewicz MZ, Babiuch L, Bielawiec M, Galar M. Plasma protein C as a marker of hepatocellular damage in alcoholic liver disease. *Haemostasis* 1992; **22**: 340-344

10 **Yoshikawa Y,** Sakata Y, Toda G, Oka H. The acquired vitaminK-dependent γ-carboxylation deficiency in hepatocellular carcinoma involves not only prothrombin, but also protein C. *Hepatology* 1988; **8**: 524-530

11 **He SL.** Coagulation-inflammatiory network: anti-inflammatory effect of natural coagulation inhibitors. *Chin J Thromb Hemost* 2001; **7**: 147-149

12 **Esmon CT.** Role of coagulation inhibitors in inflammation. *Thromb Haemost* 2001; **86**: 51-56

13 **Taylor FB,** Chang A, Esmon CT, D'Angelo A, Vigano-D'Angelo SV, Blick KE. Protein C prevents the coagulopathic and lethal effects of *E.coli* infusion in the baboon. *J Clin Invest* 1987; **79**: 918-925

14 **Bernard GR,** Vincent JL, Laterre PF, LaRosa SP, Dhainaut JF, Lopez-Rodriguez A, Steingrub JS, Garber GE, Helterbrand JD, Ely EW, Fisher CJ Jr. Efficacy and safety of recombinant human activated protein C for severe sepsis. *N Engl Med* 2001; **34**: 699-709

15 **Griffin JH,** Zlokovic B, Fernandez JA. Activated protein C: potential therapy for severe sepsis, thrombosis, and stroke. *Semin Hematol* 2002; **39**: 197-205

16 **Vincent JL,** Angus DC, Artigas A, Kalil A, Basson BR, Jamal HH, Johnson G, Bernard GR. Effects of drotrecogin alfa (activated) on organ dysfunction in the PROWESS trial. *Crit Care Med* 2003; **31**: 834-840

Edited by Chen WW and Wang XL **Proofread by** Xu FM

PO Box 2345, Beijing 100023, China
Fax: +86-10-85381893
E-mail: wjg@wjgnet.com www.wjgnet.com

World J Gastroenterol 2004;10(20):3076-3077
World Journal of Gastroenterology
 ISSN 1007-9327

• CASE REPORT •

Fasciola hepatica infestation as a very rare cause of extrahepatic cholestasis

Ahmet Dobrucali, Rafet Yigitbasi, Yusuf Erzin, Oguzhan Sunamak, Erdal Polat, Hakan Yakar

Ahmet Dobrucali, Yusuf Erzin, Division of Gastroenterology, Cerrahpasa Medical Faculty, Istanbul University, Turkey
Rafet Yigitbasi, Oguzhan Sunamak, Division of General Surgery, Cerrahpasa Medical Faculty, Istanbul University, Turkey
Erdal Polat, Hakan Yakar, Division of Microbiology and Parasitology, Cerrahpasa Medical Faculty, Istanbul University, Turkey
Correspondence to: Dr. Yusuf Erzin, Hurriyet Cad. 9/1, 34 810 Florya-Istanbul, Turkey. dryusuf@doruk.net.tr
Telephone: +90-532-2655008 **Fax:** +90-212-5307440
Received: 2004-01-02 **Accepted:** 2004-01-17

Abstract

Fasciola hepatica, an endemic parasite in Turkey, is still a very rare cause of cholestasis worldwide. Through ingestion of contaminated water plants like watercress, humans can become the definitive host of this parasite. Cholestatic symptoms may be sudden but in some cases they may be preceeded by a long period of fever, eosinophilia and vague gastrointestinal symptoms. We report a woman with cholangitis symptoms of sudden onset which was proved to be due to *Fasciola hepatica* infestation by an endoscopic retrograde cholangiography.

Dobrucali A, Yigitbasi R, Erzin Y, Sunamak O, Polat E, Yakar H. Fasciola hepatica infestation as a very rare cause of extrahepatic cholestasis. *World J Gastroenterol* 2004; 10(20): 3076-3077
http://www.wjgnet.com/1007-9327/10/3076.asp

CASE REPORT

A 40-year old woman with no prior complaints was admitted to our emergency unit due to fever, chills, nausea, vomiting and persistent right-upper quadrant pain for one week. She was born at the East of Turkey and in her medical history she had a cesarean section five years ago and was operated for inguinal hernia one year ago. She was a non-smoker and had no prior medication.

On her physical examination, she was pale but not jaundiced and had a body temperature of 36.8 ℃. She was normotensive with a regular pulse of 92 per minute. She had a mild mid-systolic murmur on the aortic valve, but no additional pathologic heart sounds or murmurs on major arteries were noted. All peripheric pulses were palpable. Auscultation of the lungs revealed no pathology. She had a cesarean section incision and another right lower quadrant incision due to hernia repair. Her bowel sounds were hyperactive on auscultation of the abdomen and she had a prominent right subcostal tenderness, but no liver or spleen enlargements were noted on palpation.

Her complete blood count was: hematocrit 30%, mean corpuscular volume 75 fl (normal, 80-95 fl), white blood cells 8 700/mm^3 (normal, 4 000-10 000) with 15% eosinophils on peripheral smear, platelets 169 000 /mm^3 (normal, 100 000-450 000). The erythrocyte sedimentation rate was 45 mm/h, C reactive protein (CRP) level was 75 mg/L (normal, 0-5). Her complete blood chemistry was normal but alanine aminotransferase (ALT) level was 74 U/L (normal, 5-37), aspartate aminotransferase (AST) level was 93 U/L (normal, 5-37), alkaline phosphatase level (ALP) was 266 U/L (normal, 32-155), gamma glutamyl transferase (GGT) level was 319 U/L (normal, 7-49). Total bilirubin level and urinalysis were normal.

A chest x-ray and plain abdominal radiograph revealed no pathology. In suspicion of gallstone disease, an ultrasonographic examination was performed and it showed a normal liver parenchyma but two hyperechogen solid lesions measuring 9 mm×9 mm and 7 mm×8 mm in the 7th segment of the right lobe. The gallbladder wall was normal but besides sludge multiple, milimetric, intraluminal echogenic particles were noted. Intrahepatic bile ducts were normal but there was a slight enlargement of the common bile duct (11 mm).

Still in suspecion of cholangitis due to gallstone, ceftriaxone 2 g/d i.v. was empirically started and the patient was referred to our endoscopy unit for endoscopic retrograde cholangiopancreatography (ERCP). After its selective cannulation, the common bile duct was filled with contrast agent and a slight enlargement and multiple, mobile, oval shaped filling defects were noted. Intrahepatic bile ducts were proved to be normal (Figure 1). After sphincterotomy, balloon extraction was performed and five *Fasciola hepatica* worms were noted. All of them were captured and taken out via a dormia basket (Figure 2, 3). After this interesting finding the patient's stool examination disclosed the parasites' ova (Figure 4) and an indirect hemaglutination test proved to be positive in 1/1 320 titer.

Figure 1 Multiple oval shaped filling defects on cholangiogram.

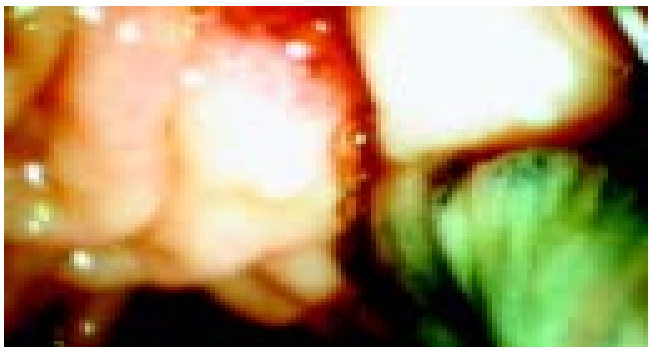

Figure 2 *Fasciola hepatica* next to papilla of Vater after sphincterotomy and balloon extraction.

After extraction of the worms the patient's symptoms

rapidly regressed and her liver enzymes returned to normal levels, then she was put on bithionol treatment 30 mg/kg every other day for 15 doses.

Figure 3 Adult flukes measuring 2.5 cm×1.5 cm in diameter.

Figure 4 Ova of *Fasciola hepatica* (×40).

DISCUSSION

A variety of liver flukes, including *Fasciola hepatica* may colonize the biliary tree where they lay their eggs, which can give rise to the formation of gallstones by serving as nidus for them. Living or dead worms may occlude the bile ducts causing obstruction and sometimes cholangitis.

Fascioliasis is primarily a common disease of livestock animals as cattle and sheep with humans serving only occasionally as accidental hosts. This zoonotic disease is common in Africa, Western Europe and Latin America[1]. In a recent study from the East of Turkey, its seroprevalance was reported to be 2.78% independent of age, educational and socioeconomical status[2].

Two stages have been described in human *fascioliasis*, namely an acute phase which coincides with hepatic invasion and a chronic phase due to the presence of flukes in the bile ducts[3]. The metasercariae for this parasite encyst on freshwater plants such as wild watercress and human consumption of aquatic plants harvested from contaminated areas lead to infection. Then developing larvae penetrate the gut wall and enter the peritoneal cavity. After a period of migration for 6 to 9 wk, the young flukes penetrate the capsule of the liver and they mature in the biliary tree and begin to pass their eggs. In the acute phase, the patient may have prolonged fevers, right upper quadrant pain, liver enlargement and eosinophilia which can be easily misdiagnosed. These symptoms abate with the chronic phase. Once the flukes enter the bile ducts, they may cause symptoms due to cholestasis and cholangitis[4].

Although the definitive diag nosis for *fascioliasis* can be made by detecting the parasite eggs in stool or duodenal aspirates, egg detection rate is not so high because of the low egg production rate of the parasite. Immunoserological tests become the cornerstone for the diagnosis of *fascioliasis* especially in early stage or ectopic infections[5] but an ELISA test provides more rapid and reliable results[6].

Although some parts of our country are endemic areas for human *fascioliasis*, this diagnosis was not suspected prior to give its full term (ERCP) as it is still a very rare cause of biliary obstruction. As usual[7], sphincterotomy and balloon extraction rapidly alleviated symptoms in our patient.

Unlike other liver flukes, therapeutic failure was common in patients with *Fasciola hepatica* treated with piraziquantel so bithionol or triclabendazole has been the treatment of choice for this parasitic infection[8]. The use of bithionol with the recommended dose of 30-50 mg/kg every other day for 10-15 doses or repeated doses has resulted in cure of acute and prolonged *fascioliasis*[9]. Triclabendazole, another effective and safe drug for *fascioliasis*, has been found to be able to eradicate the parasite with a single oral dose of 10 mg/kg[10]. Our patient was put on bithionol treatment 30 mg/kg every other day for 15 doses and no major side effects were noted.

We report this patient to draw attention to the latter that *fascioliasis* should be kept in mind in patients with cholestasis and preceeding vague gastrointestinal symptoms especially in endemic areas of the world.

REFERENCES

1 **Mas-Coma MS,** Esteban JG, Bargues MD. Epidemiology of human fascioliasis: a review and proposed new classification. *Bull World Health Organ* 1999; **77**: 340-346

2 **Kaplan M,** Kuk S, Kalkan A, Demirdag K, Ozdarendeli A. Fasciola hepatica seroprevalence in the Elazig region. *Mikrobiyol Bul* 2002; **36**: 337-342

3 **Barrett-Conner E.** Fluke infections. In: Braude AI, editor. Infectious diseases and medical microbiology, 2nd ed. *Philadelphia, PA: W. B Saunders* 1986: 979-982

4 **King CH,** Mahmoud AAF. Schistosoma and other trematodes. In: Gorbach SL, Bartlett JG, Blacklow NR, editors. Infectious diseases. *Philadelphia, PA: W.B. Saunders* 1992: 2015-2021

5 **Harinasuta T,** Pungpak P, Keystone JS. Trematode infections. Opisthorchiasis, clonorchiasis, fascioliasis. *Infect Dis Clin North Am* 1993; **7**: 699-716

6 **Shaheen HI,** Kamal KA, Farid Z, Mansour N, Boctor FN, Woody JN. Dot-enzyme-linked immunosorbent assay (dot-ELISA) for the rapid diagnosis of human fascioliasis. *J Parasitol* 1989; **75**: 549-552

7 **el-Newihi HM,** Waked IA, Mihas AA. Biliary complications of Fasciola hepatica: the role of endoscopic retrograde cholangiography in management. *J Clin Gastroenterol* 1995; **21**: 309-311

8 **Pearson RD.** Parasitic diseases: Helminths. In: Yamada T, Alpers DH, Kaplowitz N, Laine L, Owyang C, Powell DW, editors. Textbook of gastroenterology, 4th ed. *Philadelphia, PA: Lippincott Williams Wilkins* 2003: 2608-2625

9 **Bacq Y,** Besnier JM, Duong TH, Pavie G, Metman EH, Choutet P. Successful treatment of acute fascioliasis with bithionol. *Hepatology* 1991; **14**: 1066-1069

10 **Loutan L,** Bouvier M, Rojanawisut B, Stalder H, Rouan MC, Buescher G, Poltera AA. Single treatment of invasive fascioliasis with triclabendazole. *Lancet* 1989; **2**: 383

Edited by Wang XL **Proofread by** Xu FM

PO Box 2345, Beijing 100023, China
Fax: +86-10-85381893
E-mail: wjg@wjgnet.com www.wjgnet.com

World J Gastroenterol 2004;10(20):3078-3079
World Journal of Gastroenterology
 ISSN 1007-9327

• CASE REPORT •

Common bile duct obstruction due to fibrous pseudotumor of pancreas associated with retroperitoneal fibrosis: A case report

Mei-Fen Zhao, Yu Tian, Ke-Jian Guo, Zhi-Gang Ma, Hai-Hui Liao

Mei-Fen Zhao, Yu Tian, Ke-Jian Guo, Zhi-Gang Ma, Hai-Hui Liao, Department of General Surgery, First Affiliated Hospital, China Medical University, Shenyang 110001, Liaoning Province, China
Correspondence to: Dr. Mei-Fen Zhao, Department of General Surgery, First Affiliated Hospital, China Medical University, Shenyang 110001, Liaoning Province, China. zhaomeifen@medmail.com.cn
Telephone: +86-24-81677066 **Fax:** +86-24-81677066
Received: 2003-12-19 **Accepted:** 2004-01-12

Abstract

One 63-year-old woman, who presented with cholestatic jaundice due to common bile duct compression produced by primary retroperitoneal fibrosis, is studied. The patient was operated six years ago because of hydronephrosis, when the disease was first diagnosed. Magnetic resonance cholangiopancreatography (MRCP) revealed the presence of extrahepatic bile duct obstruction, which once was considered to be pathognomonic of pancreatic cancer. CT-scan demonstrated the change of retroperitoneal fibrosis around left kidney, atrophy of right kidney, and obstruction of extrahepatic bile duct (pancreatic head). An explorative laparotomy was performed, and the retroperitoneum and pancreas were grayish-white and hard, the fibrotic pancreatic head compressed the common bile duct. Bile duct stricture was managed by Rouxen-Y hepatocholangio-jejunostomy. To the best of our knowledge, few similar cases of retroperitoneal fibrosis have been reported.

Zhao MF, Tian Y, Guo KJ, Ma ZG, Liao HH. Common bile duct obstruction due to fibrous pseudotumor of pancreas associated with retroperitoneal fibrosis: A case report. *World J Gastroenterol* 2004; 10(20): 3078-3079
http://www.wjgnet.com/1007-9327/10/3078.asp

INTRODUCTION

Retroperitoneum is one of the most complex regions of human anatomy as it contains a variety of organs and structures from different systems, in particular those belonging to the urinary and digestive tracts and the vascular systems. Primary retroperitoneal fibrosis (Ormond's disease) is a rare disorder typically with an insidious clinical course, characterized by the presence of dense, grayish-white plaques centered around the abdominal aorta in this space. The peak incidence of this uncommon disease is between the ages of 40 and 60 years and mostly in men[1]. Most commonly, it causes fibrous encasementb of the ureters and subsequent obstructive hydronephrosis. Atypical sites of involvement include the duodenum, colon, urinary bladder, mesentery, small intestine and epidural space. Typically, mass effect from the enlarging fibrosis plaque leads to compromise of surrounding structures. For example, extrinsic compression can lead to small and large bowel obstruction, vena cava stasis, and arterial insufficiency in lower extremities.

In this report, we describe an unusual case of this rare disorder, which presented with obstructive jaundice caused by the compression of common bile duct due to the involved diffusive pancreatic fibrosis. To the best of our knowledge, few similar cases of Ormond's disease have been reported.

CASE REPORT

One 63-year-old woman was sent to our hospital because of jaundice, slight loss of weight and anorexia in October 2003. The patient was operated six years ago because of hydronephrosis, when the Ormond's disease was first diagnosed. After operation, no corticosteroid was administrated and no reopening of the ureter was observed up to the admission to our hospital. Her antihypertensive medications included *Fufangluobuma* (TCM compound) and metoprolol.

The patient had been jaundiced for 9 d before sent to our hospital, and had no stigmata of chronic liver disease. Physical examination revealed a slight cachectic state. Abdominal examination was unremarkable without signs of ascites, and the liver edge was not palpable below the right costal margin. Patient had no fever and alcohol or drug abuse. Laboratory tests revealed a normal red and white blood cell counts. Erythrocyte sedimentation rate (ESR) was 120 mm/h in the first hour (normal 0-32), C-reactive protein (CRP) 0.4 mg/dL (normal <1 mg/dL). Blood urea nitrogen, creatinine level and amylase were normal. Total bilirubin was 278.3 μmol/L (normal 2-20 μmol/L), direct bilirubin 237.1 μmol/L (normal 0-3.4 μmol/L), alkaline phosphatase 326 U/L (normal 15-128 U/L), aspartate aminotransferase (AST) 27 U/L (normal 1-38 U/L), and alanine aminotranferase (ALT) 40 U/L (normal 1-41 U/L). Hepatitis and human immunodeficiency viruses were negative. Abdominal ultrasonography showed an enlarged pancreatic head and dilated intra- and extra- hepatic ducts. Additionally, cholecystolithiasis was detected. CT-scan demonstrated the change of retroperitoneal fibrosis around the left kidney, atrophy of right kidney, and obstruction of extra-hepatic bile duct (pancreatic head). The pancreatic head was slightly enlarged, but the enhanced scan showed that the density of the whole pancreas was homogeneous. Also gallbladder stones were found (Figure 1). Subsequent MRCP revealed the interruption of extrahepatic bile duct (Figure 2).

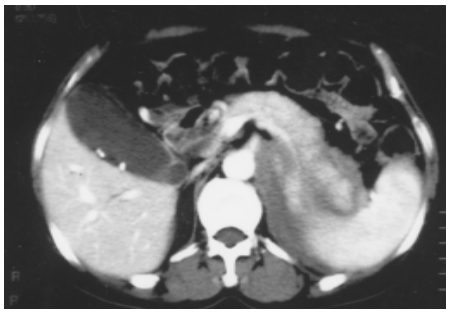

Figure 1 CT-scan demonstrated the change of retroperitoneal fibrosis around left kidney, atrophy of right kidney. The density of the whole pancreas was homogeneous.

A presumptive diagnosis of pancreatic cancer or cholangiocarcinoma was made and an explorative laparotomy was performed. We found that the retroperitoneum and pancreas

were grayish-white, and the consistency of them was hard (Figure 3). The fibrotic pancreatic head compressed the common bile duct. Then the gallbladder was resected and a Rouxen-Y hepatocholangio-jejunostomy was constructed. Adjacent lymph nodes were not enlarged or malignant. The patient recovered fully after surgery.

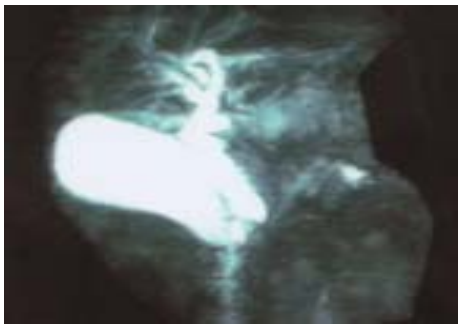

Figure 2 MRCP revealed the interruption of extrahepatic bile duct.

Figure 3 Retroperitoneum and pancreas were grayish-white and hard.

DISCUSSION

Ormond's disease is a rare disorder characterized by transformation of normal fat tissue into a retractile fibrosis mass. Although the etiology of this chronic process is still unclear, the proposed mechanism is thought to be an autoimmune disorder secondary to the development of antibodies produced against ceroid, a polymer of oxidized lipid and protein[2,3]. This hypothesis is based upon the finding of association between atherosclerotic plaques of the aorta and retroperitoneal fibrosis[4,5]. It is thought that inflammatory antigens like ceroid pass through the adventitia into the periaortic fatty tissue and produce a periaortic and periarterial fibrosis[6-8]. In addition, several pharmacological substances have been cited as possible causative agents of retroperitoneal fibrosis[3]. Methysergide is the only drug that has been proved to cause retroperitoneal fibrosis[2]. Other suspected causative drugs include β-adrenergic blockers, antihypertensives, analgesics[3]. The medications of this patient included metoprolol, which is a kind of β-adrenergic blocker, but we were not able to identify the exact etiologic agent of this disease.

The presentation of retroperitoneal fibrosis in this patient was unique for two reasons. Ormond's disease often manifests clinically by constriction and compression of ureters, blood vessels and nerves. This patient had had an initial manifestation of Ormond's disease affecting left ureter before this admission. Uncommonly, upon this admission she presented with clinical manifestation of obstructive jaundice, which was due to the compression of portions of the common bile duct. There have been only 9 reports of retroperitoneal fibrosis with cholestatic jaundice due to compression of the distal part of the common bile duct by fibrotic pancreatic head[9-15]. A second distinctive feature of this Ormond's disease case was the direct involvement of the pancreas, which has not previously been highlighted and led to diagnostic difficulty. Obstructive jaundice due to the retroperitoneal fibrosis of pancreas head is easy to mimicking the carcinoma of pancreas. In some authors' opinion, sclerosing pancreatitis due to retroperitoneal fibrosis as this patient has been classified into the new clinical entity-"autoimmune related pancreatitis" or "autoimmune pancreatitis".

Management of retroperitoneal fibrosis includes surgical relief of extrinsically compressed or encased structures, deep tissue biopsies to confirm the diagnosis and to exclude the malignant variant, and the use of corticosteroids (and other immunosuppressants) to prevent further progression of the disease[2]. There is no definitive duration or dosage of corticosteroids recommended for the therapy of this disease. This patient did not take corticosteroids.

In conclusion, this atypical retroperitoneal fibrosis illustrates that this disease involves the pancreas, and diffusive pancreatic fibrosis (sclerosing pancreatitis) can affect the common bile duct to manifest the initial symptom of cholestatic jaundice. Additionally, surgeons should pay attention to this condition mimicking pancreatic carcinoma or cholangiocarcinoma.

REFERENCES

1 **Meier P**, Gilabert C, Burnier M, Blanc E. Retroperitoneal fibrosis, an unrecognized inflammatory disease. Clinical observations and review of the literature. *Nephrologie* 2003; **24**: 173-180
2 **Kottra JJ**, Dunnick NR. Retroperitoneal fibrosis. *Radiol Clin North Am* 1996; **34**: 1259-1275
3 **Buff DD**, Bogin MB, Faltz LL. Retroperitoneal fibrosis. A report of selected cases and a review of the literature. *N Y State J Med* 1989; **89**: 511-516
4 **Mitchinson MJ**. Retroperitoneal fibrosis revisited. *Arch Pathol Lab Med* 1986; **110**: 784-786
5 **Martina B**. Chronic periaortitis-a new interpretation of Ormond's disease. *Urol Res* 1990; **18**: 165-167
6 **Amis ES Jr**. Retroperitoneal fibrosis. *Am J Roentgenol* 1991; **157**: 321-329
7 **Hughes D**, Buckley PJ. Idiopathic retroperitoneal fibrosis is a macrophage-rich process. Implications for its pathogenesis and treatment. *Am J Surg Pathol* 1993; **17**: 482-490
8 **Martina FB**, Nuech R, Gasser TC. Retroperitoneal fibrosis and chronic periaortitis: a new hypothesis. *Eur Urol* 1993; **23**: 371-374
9 **Renner IG**, Ponto GC, Savage WT 3rd, Boswell WD. Idiopathic retroperitoneal fibrosis producing common bile duct and pancreatic duct obstruction. *Gastroenterology* 1980; **79**: 348-351
10 **Remedios D**, Coppen M, Bradbeer J, Theodossi A. Chronic periaortitis presenting as common bile duct obstruction. *Gut* 1991; **32**: 713-714
11 **Laitt RD**, Hubscher SG, Buckels JA, Darby S, Elias E. Sclerosing cholangitis associated with multifocal fibrosis: a case report. *Gut* 1992; **33**: 1430-1432
12 **Cappell MS**. Obstructive jaundice due to retroperitoneal fibrosis involving the head of the pancreas. *J Clin Gastroenterol* 1994; **18**: 53-56
13 **Chutaputti A**, Burrell MI, Boyer JL. Pseudotumor of the pancreas associated with retroperitoneal fibrosis: a dramatic response to corticosteroid therapy. *Am J Gastroenterol* 1995; **90**: 1155-1158
14 **Pereira-Lima JC**, Kromer MU, Adamek HE, Riemann JF. Cholestatic jaundice due to Ormond's disease (primary retroperitoneal fibrosis). *Hepatogastroenterology* 1996; **43**: 992-994
15 **Dejaco C**, Ferenci P, Schober E, Kaserer K, Fugger R, Novacek G, Gangl A. Stenosis of the common bile duct due to Ormond's disease: case report and review of the literature. *J Hepatol* 1999; **31**: 156-159

Edited by Chen WW **Proofread by** Zhu LH and Xu FM